

The Interaction of Automatic Transmission Fluid Additives with Copper

Bethan Lora May Warren

Submitted in accordance with the requirements for the degree of
Doctor of Philosophy

THE UNIVERSITY OF LEEDS
School of Mechanical Engineering

September 2018

The candidate confirms that the work submitted is her own and that appropriate credit has been given where reference has been made to the work of others.

This copy has been supplied on the understanding that it is copyright material and that no quotation from the thesis may be published without proper acknowledgement.

The right of Bethan Lora May Warren to be identified as Author of this work has been asserted by her in accordance with the Copyright, Designs and Patents Act 1988.

© 2018 The University of Leeds and Bethan Lora May Warren.

Acknowledgements

I would like to start by thanking Lubrizol for their funding for this project, it has been a pleasure working with you. In particular I wish to thank Michael Gahagan and Greg Hunt who have overseen this project and have given very useful advice throughout. Greg, I am especially grateful for the monthly meetings which were very encouraging and helped keep everything on track. Nathan, Lynette and Will, thank you for putting up with the countless emails asking for data and results, your help was invaluable.

I also wish to thank my Leeds supervisors, Ardian Morina and Anne Neville who have helped to guide this project over the past three years. Your countless proof reads of this thesis, as well as your help and encouragement have been greatly appreciated.

I would like to thank all those at Kings Church Selby who have supported me through the past few years, your prayers have been invaluable. I would particularly like to thank my cell group for your encouragement each week, especially when I felt things could be going better, your kind words did not go unnoticed.

Finally I wish to thank my wonderful husband, David Warren, for all his help and support in the final stages of writing this thesis.

Abstract

In recent years there has been an increase in the number of cars using automatic transmissions and in these systems the control units are often placed in contact with the Automatic Transmission Fluid (ATF). It is therefore important that the additives present in the ATF do not adversely interact with the transmission components, particularly those which are copper-based, such as the solenoids.

There is currently very little literature on copper corrosion in oil based systems particularly when looking specifically at the interaction between ATFs and copper. This study looks at the interaction of some common ATF additives with copper surfaces. This is achieved through the combination of simple immersion tests, conducted on coupons, and resistance tests, carried out on wires. The coupons allow detailed analysis of the surface by FTIR, SEM and XPS. The wire tests monitor the resistance of a thin copper wire which can be directly related to the radius and indicate when there is loss of material. This allows the corrosion of the wire to be monitored in situ which is not achievable through immersion tests.

The study looked at the standard ASTM D130 rating method as a basis for attributing corrosion to coupons after they had been immersed in a test fluid. It was found that this rating did not really correlate with any other measures of corrosion such as weight change, amount of copper in the used test fluid or radius change measured using the copper wire resistance test. It was concluded that whilst this test may be suitable for screening large numbers of fluids it provides little information on the actual corrosion taking place on the surface and in some instances film formation can be identified as corrosion.

The study showed that increasing the temperature at which testing took place did not always speed up the corrosion process. In one instance increasing the temperature

slowed the rate of reaction but in most cases increasing the temperature changed the mechanism of corrosion. The most extreme case of this was with the thiadiazole-based corrosion inhibitor which showed good inhibition until 150 °C when it broke down and caused pitting on the copper surface.

The wire tests were able to show which additives protected the copper from corrosion, which gave constant corrosion, and the effect of combining additives. An antagonism was seen at 120 °C between dispersant 1 and a mix of antiwear, antioxidant and friction modifier. Detergent 2 combined with a mix of antiwear, antioxidant and friction modifier at 150 °C was also antagonistic.

SEM images of the surfaces of coupons tested in full formulation fluids were able to be compared with those tested in single additives and simple mixtures to give information on which of the additives were causing the observed surface structure. This worked well for formulations where the additives were at similar levels to those tested individually but not for those where the concentration of additives was much lower. For each of the individual additives tested a mechanism of interaction with the copper surface has also been proposed.

Contents

Acknowledgements	iii
Abstract	iv
List of Tables	x
List of Figures	xiii
List of Abbreviations	xxiv
1 Introduction	1
1.1 Research Objectives	2
1.2 Thesis Outline	3
2 Background information	5
2.1 ATF composition	5
2.1.1 Base oil	6
2.1.2 Additives with surface activity	7
2.1.2.1 Dispersants	8
2.1.2.2 Detergents	8
2.1.2.3 Corrosion inhibitors	9
2.1.2.4 Friction modifiers	10
2.1.2.5 Antiwear additives	10
2.1.3 Additives which modify physical properties of oil	11
2.1.3.1 Viscosity modifiers	11
2.1.3.2 Pour point depressants	12
2.1.3.3 Antifoam	12
2.1.4 Antioxidants	13
2.1.5 ATF additive interactions	14
3 Literature Review	16
3.1 Corrosion	16
3.1.1 General or uniform corrosion	17
3.1.2 Pitting corrosion	19
3.1.3 Crevice corrosion	21
3.1.4 Intergranular corrosion	21
3.1.5 Dealloying	22
3.1.6 Passivity	23
3.2 Copper corrosion	24
3.2.1 Common copper corrosion products	24
3.2.2 Copper oxidation and passivation	25

3.2.3	Effect of alloying and microstructure	26
3.2.4	Rates of copper corrosion and passivation	27
3.3	Corrosion in oil based systems	27
3.4	Copper protection by corrosion inhibitors	36
3.5	Methods of monitoring corrosion	41
3.5.1	Gravimetric techniques	43
3.5.1.1	Thermogravimetric analysis (TGA)	44
3.5.1.2	Quartz Crystal Microbalance (QCM) technique	44
3.5.2	Electrical resistance techniques	45
3.5.3	Industry standard ASTM D130 testing	47
3.6	Characterising corroded surfaces	48
3.6.1	Surface morphology	49
3.6.1.1	Optical microscopy	49
3.6.1.2	Scanning Electron Microscopy (SEM)	50
3.6.1.3	Back Scattered Electron (BSE) images	52
3.6.2	Chemical Characterisation	53
3.6.2.1	Energy Dispersive X-ray spectroscopy (EDX or EDS)	54
3.6.2.2	Fourier Transform Infrared (FTIR) Spectroscopy	55
3.6.2.3	Raman Spectroscopy	57
3.6.2.4	X-Ray Photoelectron Spectroscopy (XPS)	57
3.7	Summary	58
4	Methodology	60
4.1	General Materials	61
4.2	Full formulation coupon immersion testing	63
4.2.1	Materials	63
4.2.2	Method	65
4.2.2.1	End of test	66
4.3	Wire testing	66
4.3.1	Materials	66
4.3.2	Method	67
4.3.2.1	End of test	68
4.3.3	Calculation of radius from resistance	68
4.3.4	Start length determination	70
4.3.5	The impact of current on copper wire corrosion	72
4.4	Wire-coupon testing	74
4.4.1	Materials	74
4.4.2	Method	75
4.4.2.1	End of test	76
4.4.3	Repeatability of tests	76
4.5	Analysis techniques	79
4.5.1	ICP-AES analysis	79
4.5.2	FTIR microscopy	80
4.5.3	Scanning Electron Microscopy (SEM), Energy Dispersive X-ray spectroscopy (EDX) and Focused Ion Beam (FIB)	80
4.5.4	XPS	81
4.5.5	White Light Interferometry (WLI)	82

5	Results of full formulation testing	83
5.1	Rating of copper squares	83
5.2	Weight change of copper coupons	84
5.3	Amount of copper in end of test fluid	86
5.4	Level of sulfur in formulation	87
5.5	FTIR-ATR analysis	90
5.6	SEM analysis	96
5.6.1	Full formulation samples showing flaking	97
5.6.2	Full formulation samples showing surface spheres	98
5.6.3	Full formulation samples showing porous surfaces	100
5.6.4	Full formulation samples showing small particles	103
5.6.5	Full formulation samples which are relatively featureless	108
5.7	Variation of additive levels	109
5.7.1	Dispersants tested alone in base oil	111
5.7.2	Dispersant variations of formulation -779	112
5.7.3	Dispersant variations of formulation -794	114
5.7.4	Dispersant and corrosion inhibitor variations for formulation -776	116
5.7.5	Dispersant variations of full formulation -793	117
5.7.6	Corrosion inhibitor variation of formulation -810	118
5.8	Summary	119
6	Initial wire testing	121
6.1	Choice of full formulation fluids for wire tests	121
6.2	Wire test results	123
6.2.1	Wire-coupon initial tests with varying time periods - wire results	125
6.2.2	Wire-coupon initial tests with varying time periods - coupon results	129
6.3	Effect of temperature on radius change	131
6.4	Summary	132
7	Wire and coupon analysis for additives tested at different temperatures	133
7.1	Base oil	134
7.2	Corrosion inhibitor 1	138
7.3	Corrosion inhibitor 2	143
7.4	Dispersant 1	147
7.5	Dispersant 2	151
7.6	Detergent 1	155
7.7	Detergent 2	158
7.8	Antioxidant (AO), Antiwear (AW), and Friction Modifier (FM) mix	162
7.9	Antioxidant	166
7.10	Antiwear	168
7.11	Friction modifier	171
7.12	Corrosion inhibitor 2 + Antiwear (AW)	173
7.13	Summary	176
8	Comparisons of additive mixtures to their component additives	178
8.1	Change in rating	178
8.2	ICP levels of additive combinations	182
8.3	Radius change of copper wires tested in solutions of additive combinations	186
8.4	XPS and SEM results for selected combinations	188
8.5	XPS and SEM results for 120 °C samples	190

8.6	XPS and SEM results for 150 °C samples	199
8.7	Summay	207
9	Film progression	208
9.1	Surface changes of copper tested in individual additives	209
9.2	Surface changes of copper tested with simple additive mixtures	212
9.3	Copper level in test fluids measured using ICP-AES	214
9.4	Summary	218
10	Predicting full formulation behaviour from simple additive mixture re- sults	219
10.1	Comparison of results from full formulations and simple additive mixtures	220
10.2	Summary	227
11	Discussion	228
11.1	Evaluation of the ASTM D130 standard test method and the wire resis- tance test	228
11.2	Correlation of full formulation results to the additives present in their formulations	233
11.3	Correlating the radius loss of copper wires to other test results	238
11.3.1	Comparing the amount of copper lost to the amount measured in the end of test fluid	244
11.4	Effect of temperature	246
11.5	Mechanisms of surface interactions	251
11.5.1	Corrosion inhibitor 1	254
11.5.1.1	Corrosion inhibitor 1 with other additives	260
11.5.2	Corrosion inhibitor 2	262
11.5.2.1	Corrosion inhibitor 2 with other additives	264
11.5.3	Dispersant 1	266
11.5.3.1	Dispersant 1 with other additives	269
11.5.4	Dispersant 2	270
11.5.4.1	Dispersant 2 with other additives	271
11.5.5	Detergent 1 and detergent 2	272
11.5.6	Antioxidant, Antiwear and Friction Modifier	273
11.6	Interactions in full formulations	275
12	Conclusions and Future Work	278
12.1	Conclusions	278
12.1.1	ASTM D130 standard test method and wire resistance tests	278
12.1.2	Effect of temperature	279
12.1.3	Mechanisms of surface interactions	280
12.2	Future research	280
12.2.1	Concentration effects	281
12.2.2	Static versus non-static testing	281
12.2.3	Multiple interactions	281
12.2.4	Alloying effects	282
A	XPS analysis of coupons tested in individual additives	283
A.1	Base oil	284
A.2	Corrosion inhibitor 1	286
A.3	Corrosion inhibitor 2	288

A.4	Dispersant 1	290
A.5	Dispersant 2	292
A.6	Detergent 1	294
A.7	Detergent 2	296
A.8	Antioxidant, antiwear, friction modifier mixture	298
A.9	Corrosion inhibitor 2 + antiwear	300
A.10	Antioxidant	302
A.11	Antiwear	304
A.12	Friction modifier	306
B	Radius changes	308
B.1	Additives at 120 °C	309
B.2	Additives at 150 °C	316
	Bibliography	323

List of Tables

2.1	Composition of generic ATF [4, 6, 11, 12]	6
2.2	Base oil categories [2, 6, 14]	6
3.1	Copper strip rating descriptions [84, 87]	30
3.2	Surface sensitive analytical techniques and information obtainable by using them [24, 127]	49
4.1	Structures of individual additives used for testing	62
4.2	Concentration (wt%) of additives in full formulation fluids; fluids which have been shaded were not used for wire testing	64
4.3	Levels of additives, wt%, in second batch of full formulation fluids after changes to corrosion inhibitor and dispersant levels	65
4.4	Structures and concentrations of individual additives tested, the concentrations were the same as listed when additives were combined	75
4.5	Images of samples tested at 130 °C for 1 week, with the exception of sample 4 which was tested for 2 weeks	77
4.6	SEM images of the sample surfaces tested in base oil, dispersant 1, or the AO, AW, FM mix for 1 week, except for sample 4 which was tested for 2 weeks. Each of the scale bars represent 30 μm	77
4.7	Standard deviation of wires in each fluid calculated at specified time points	78
4.8	Spin-orbit component parameters used for peak fitting	81
5.1	Formulations grouped by FTIR similarities for all coupons run	95
5.2	BSE and coupon images for full formulation fluids showing surfaces that flake	97
5.3	Formulations of samples which show flaking surfaces and amount of copper measured in end of test fluid	98
5.4	BSE and coupon images for full formulation fluids showing distinct surface spheres	99
5.5	Formulations of samples which show distinct surface spheres and amount of copper measured in end of test fluid	100
5.6	BSE and coupon images for full formulation fluids showing porous or pitted surfaces	100
5.7	Formulations of samples which show porous surfaces and amount of copper measured in end of test fluid	102
5.8	BSE and coupon images for full formulation fluids showing small particles on the surface	104
5.9	Formulations of samples which show small surface particles and amount of copper measured in end of test fluid	107
5.10	BSE and coupon images for full formulation fluids showing featureless surfaces	108

5.11	Formulations of samples with featureless surfaces and amount of copper measured in end of test fluid	108
5.12	Levels of additives, wt%, in original full formulation fluids and the subsequent changes in corrosion inhibitor and dispersant levels	110
6.1	Sample grouping for SEM surface appearance, FTIR similarities, and ASTM rating	122
6.2	Reminder of full formulations for samples 779, 780, 806 and 811	125
6.3	Percentage weight change of copper coupons tested in full formulation fluids 779, 780, 806, and 811	129
7.1	Images of end of test copper coupons after immersion in base oil at 110 °C, 120 °C, 130 °C and 150 °C. All coupons were the same height and approximately 1.5 cm in width	134
7.2	Images of end of test copper coupons after immersion in corrosion inhibitor 1 at 110 °C, 120 °C, 130 °C and 150 °C, with repeats at 120 °C and 150 °C. All coupons were the same height and approximately 1.5 cm in width	139
7.3	Images of end of test copper coupons after immersion in corrosion inhibitor 2 at 110 °C, 120 °C, 130 °C and 150 °C, with repeats at 120 °C and 150 °C. All coupons were the same height and approximately 1.5 cm in width	143
7.4	Images of end of test copper coupons after immersion in dispersant 1 at 110 °C, 120 °C, 130 °C and 150 °C, with repeats at 120 °C and 150 °C. All coupons were the same height and approximately 1.5 cm in width	147
7.5	Images of end of test copper coupons after immersion in dispersant 2 at 110 °C, 120 °C, 130 °C and 150 °C, with repeats at 120 °C and 150 °C. All coupons were the same height and approximately 1.5 cm in width	151
7.6	Images of end of test copper coupons after immersion in detergent 1 at 110 °C, 120 °C, 130 °C and 150 °C, with repeats at 120 °C and 150 °C. All coupons were the same height and approximately 1.5 cm in width	155
7.7	Images of end of test copper coupons after immersion in detergent 2 at 110 °C, 120 °C, 130 °C and 150 °C, with repeats at 120 °C and 150 °C. All coupons were the same height and approximately 1.5 cm in width	159
7.8	Images of end of test copper coupons after immersion in a mixture of friction modifier, antioxidant, and antiwear at 110 °C, 120 °C, 130 °C and 150 °C. All coupons were the same height and approximately 1.5 cm in width	162
7.9	Images of end of test copper coupons after immersion in antioxidant at 120 °C and 150 °C, with repeats. All coupons were the same height and approximately 1.5 cm in width	166
7.10	Images of end of test copper coupons after immersion in antiwear additive at 120 °C and 150 °C, with repeats. All coupons were the same height and approximately 1.5 cm in width	170
7.11	Images of end of test copper coupons after immersion in friction modifier at 120 °C and 150 °C, with repeats. All coupons were the same height and approximately 1.5 cm in width	172
7.12	Images of end of test copper coupons after immersion in a mixture of corrosion inhibitor 2 with antiwear at 110 °C, 120 °C, 130 °C and 150 °C. All coupons were the same height and approximately 1.5 cm in width	174

8.1	Images of samples and their ratings for both individual and combined additives tested at 120 °C	180
8.2	Images of samples and their ratings for both individual and combined additives tested at 150 °C	181
8.3	Amount of copper in end of test fluid (ppm), as determined by ICP, for individual additives and combined additives at 120 °C	182
8.4	Amount of copper in end of test fluid (ppm), as determined by ICP, for individual additives and combined additives at 150 °C	182
8.5	Synergies (+/yellow) and antagonisms (-/red) seen for rating (+/-) and copper levels (colour)	186
8.6	Radius change (μm) for the additive combinations with synergies (yellow shading) and antagonisms (red shading) identified from radius change results	187
8.7	Concentration and structure of additives used for tests after which coupons were analysed using XPS	189
8.8	Peak positions (eV) for high resolution spectra of all samples analysed at 120 °C	196
8.9	Peak assignments for high resolution spectra of all samples analysed at 150 °C	204
9.1	Images and ratings of coupons after different immersion periods in specified additives	210
9.2	BSE images of the coupon surfaces after immersion for different time periods in specified additives	211
9.3	Images and ratings and BSE image of coupons after 3 hours and 100 hours immersion in specified additives	213
10.1	Full formulation additive levels for samples which showed spheres on their surface, along with the additive combination corrosion inhibitor 1 and the AO, AW, FM mix	221
10.2	Amount of copper in the end of test fluid for formulations which showed spheres on their surface	221
10.3	Full formulation additive levels for samples with high levels of corrosion inhibitor 1 and the simple additive combinations they were matched with	224
10.4	Additive breakdown of formulation -793 and the simple additive combinations which matched the surface	225
10.5	Additive breakdown of formulation -793 and the simple additive combinations which matched the surface	226
10.6	Full formulations that did not show similarities in their SEM images with those of the simple additive combinations	227
11.1	Formulations grouped by rating for all full formulation coupons run	234
11.2	Formulations grouped according to correlations seen in Figure 11.5	240

List of Figures

2.1	Generic structure of a surface-active additive	7
2.2	Schematic showing the interaction of dispersant with particulates in oil .	8
2.3	Structure of detergent molecule with calcium carbonate core	9
2.4	Metal surface with corrosion inhibitor molecules forming a protective layer	10
2.5	Effect of viscosity modifier on viscosity of oil	12
2.6	Direction of interaction between additives of different classes [18]	15
3.1	Illustration of general corrosion adapted from [28]	17
3.2	Typical cross sectional shapes of pits [28]	19
3.3	Self-Propagating mechanism occurring in a corrosion pit with rapid dissolution of metal, M, within the pit with oxygen reduction on adjacent surfaces [33]	20
3.4	Illustration of crevice corrosion adapted from [28]	21
3.5	Illustration of intergranular corrosion adapted from [28]	22
3.6	Schematic diagram showing surface diffusion mechanism [45]	23
3.7	Schematic showing the change in copper with plated tin layers [7]	25
3.8	Prototype layout (left) of thin film corrosion sensors with different thicknesses of copper on a glass substrate, fabricated prototype covered with protective lacquer (right) [81]	28
3.9	S % concentration on the copper strip versus S concentration in mg l ⁻¹ of sulfur (left) and elthylmercaptan (right) [87]	31
3.10	Sulfur concentration at surface versus concentration in iso-octane, also indicating test ratings [26]	32
3.11	SEM of copper surface after testing in 10 mg l ⁻¹ of elemental sulfur (left) 25 mg l ⁻¹ elemental sulfur (centre) and 10 mg l ⁻¹ ethylmercaptan (right) [87, 89]	33
3.12	Sulfide film thickness versus time of immersion in hydrocarbon solution containing 20 ppm sulfur at 100 °C [88]	33
3.13	Depth profiles of components of a film formed on copper after exposure to a hydrocarbon solution containing 20 ppm sulfur for 3 hours at 100 °C [88]	34
3.14	Amount of dissolved copper at temperature ranging between 90 °C and 150 °C over 2000 hours in ATF A (left) and ATF B (right) [11]	35
3.15	Model of film growth due to copper diffusion through the reaction layer [11]	36
3.16	Basic structures of azole compound inhibitors. Left to right; benzotriazole, thiazole, imidazole and 1,2,4-triazole	38
3.17	Schematic showing the adsorption of inhibitor onto a metal surface, where Inh represents the inhibitor molecules [92]	38

3.18	Schematic illustration of outer layer growth of BTAH film on inner layer of Cu(I)BTA complex [97]	39
3.19	Model of the interaction mechanism of DMTD with a copper surface [111]	40
3.20	Schematic diagram of the adsorption and decomposition of 2-mercapto-5-methyl-1, 3, 4-thiadiazole adlayers on gold by chemical vapour deposition [113]	41
3.21	Schematic diagram of the possible interactions occurring at the surface .	42
3.22	Schematic showing measurement of corrosive material loss from copper film, where A and B are electrodes measuring the sacrificial metal film [81]	46
3.23	Thickness loss of copper foil with time, exposed to sulfur vapour at 140 °C [124]	46
3.24	Schematic of different signals emitted from a specimen on interaction with an incident electron beam [134]	50
3.25	Contrast differences in secondary electron images when accelerating voltage is varied [134]	51
3.26	SEM images of copper surface exposed to sodium sulfide at different temperatures: a) 20 °C, b) 40 °C, c) 60 °C, d) 80 °C [135]	52
3.27	Cross sectional BSE images of copper exposed to sulfur vapour: a) 80 °C, b) 110 °C, c) 140 °C, d) 80–140 °C [124]	53
3.28	Schematic showing how characteristic X-rays are produced after the interaction of incident electrons [134]	54
3.29	Regions of fundamental vibration of some characteristic groups [138] . .	55
3.30	Schematic diagram showing the ejection of a core electron after excitation with an X-ray beam	58
4.1	Schematic of each of the three different test methods used throughout the study	61
4.2	(A) Copper wire wrapped around former; (B) Beakers in bath connected to control system	67
4.3	Graph showing temperature of oil and length of wires immersed in different additives with time	71
4.4	Base oil and formulation 811 with currents of 5 mA, 10 mA, 15 mA, and 20 mA passed through	73
4.5	Amount of copper in end of test fluid as measured by ICP-AES	73
4.6	Schematic of wire-square test, beaker setup	75
4.7	Radius changes of wires immersed in base oil, dispersant 1, or the AO, AW, FM mix, with lines denoting where standard deviation was calculated	79
5.1	Digital brightness ratings plotted against the ASTM rating with an image of the corresponding sample	83
5.2	Percentage weight change of copper coupons	85
5.3	The amount of copper in the end of test fluid as determined by ICP-AES, for full formulation fluids run for 4 weeks at 120 °C	86
5.4	Average weight change of copper coupon and amount of copper measured with ICP-AES in the end of test fluid	87
5.5	Sulfur level in each formulation plotted against (A) ASTM rating of the copper square, and (B) the copper level in the end of test fluid, highlighting the level of corrosion inhibitor 1	88
5.6	Sulfur level in each formulation plotted against (A) ASTM rating of the copper square, and (B) the copper level in the end of test fluid, highlighting the level of dispersant 2	89

5.7	Sulfur level in each formulation plotted against (A) ASTM rating of the copper square, and (B) the copper level in the end of test fluid, highlighting the level of dispersant 1	89
5.8	FTIR spectra and images for coupons -779, -794, and -795	91
5.9	FTIR spectra and images for coupons -778, -797, and -807	92
5.10	FTIR spectra and images for coupons -776, -796, -806, and -810	92
5.11	FTIR spectra and images for coupons -780, -783, and -792	93
5.12	FTIR spectra and images for coupons -777, -782, and -811	93
5.13	FTIR spectra and images for coupons -781 and -798	94
5.14	FTIR spectra and images for coupons -793, -799, -808, and -809	94
5.15	EDX spectrum of sample -782	103
5.16	SEM and cross-sectional analysis of sample -776	107
5.17	Amount of copper in the end of test fluid as determined by ICP-AES for dispersant variations for dispersants dissolved in base oil alone	111
5.18	SEM images of the surfaces of samples immersed in base oil and dispersant mixtures	112
5.19	Amount of copper in the end of test fluid as determined by ICP-AES for dispersant variations based on the full formulation -779	113
5.20	SEM images of the surfaces of samples immersed in dispersant variations of the full formulation -779	114
5.21	Amount of copper in the end of test fluid as determined by ICP-AES for dispersant variations based on the full formulation -794	115
5.22	BSE images of the surfaces of samples immersed in dispersant variations of the full formulation -794	115
5.23	Amount of copper in the end of test fluid as determined by ICP-AES for full formulation -776 and variations involving corrosion inhibitors 1 and 2, and dispersant 2	116
5.24	BSE images of the surfaces of samples immersed in variations of the full formulation -776	117
5.25	Amount of copper in the end of test fluid as determined by ICP-AES for full formulation -793, with and without dispersant present	118
5.26	BSE images of the surfaces of samples immersed in variations of the full formulation 793, with and without dispersants	118
5.27	Amount of copper in end of test fluid for formulation -810, and corrosion inhibitor variation	119
6.1	Radius change of copper wire immersed in full formulation fluids at 130 °C, formulations giving less than 1 μm radius change	124
6.2	Radius change of copper wire immersed in full formulation fluids at 130 °C, formulations giving more than 1 μm radius change	124
6.3	Change of radius of a copper wire at 130 °C immersed in 811, stopped at various time points	127
6.4	Change of radius of a copper wire at 130 °C immersed in 806, stopped at various time points	127
6.5	Change of radius of a copper wire at 130 °C immersed in 779, stopped at various time points	128
6.6	Change of radius of a copper wire at 130 °C immersed in 780, stopped at various time points	128
6.7	Images of coupons after testing for different lengths of time, placed in order of increasing time	129

6.8	Amount of copper in the test fluid at 130 °C, measured once cool using ICP-AES	130
6.9	Differences in the change in radius for formulations run at different temperatures	131
7.1	End of test BSE images of coupon surface after immersion in base oil at various temperatures	135
7.2	End of test BSE images of wire surfaces after testing in base oil at specified temperatures	136
7.3	Change in radius of copper wires immersed in base oil at 110 °C, 120 °C, 130 °C and 150 °C	136
7.4	The amount of copper in the end of test fluid as determined using ICP-AES for base oil alone	137
7.5	Atomic concentration of C, O, N, S and Cu on sample surface tested in base oil at 120 °C and 150 °C determined by XPS	138
7.6	End of test BSE images of coupon surface after immersion in corrosion inhibitor 1 at various temperatures	139
7.7	End of test BSE images of wire surfaces after testing in corrosion inhibitor 1 at specified temperatures	140
7.8	Radius change of copper wires immersed in 0.5 wt% corrosion inhibitor 1 at 110 °C, 120 °C, 130 °C and 150 °C, including repeats at 120 °C and 150 °C	141
7.9	The amount of copper in the end of test fluid as determined using ICP-AES for corrosion inhibitor 1	142
7.10	Atomic concentration of C, O, N, S and Cu on sample surface tested in corrosion inhibitor 1 at 120 °C and 150 °C determined by XPS	142
7.11	End of test BSE images of coupon surface after immersion in corrosion inhibitor 2 at various temperatures	144
7.12	End of test BSE images of wire surfaces after testing in corrosion inhibitor 2 at specified temperatures	144
7.13	Radius change of copper wires immersed in 0.5 wt% corrosion inhibitor 2 at 110 °C, 120 °C, 130 °C and 150 °C, including repeats at 120 °C and 150 °C	145
7.14	The amount of copper in the end of test fluid as determined using ICP-AES for corrosion inhibitor 2	146
7.15	Atomic concentration of C, O, N, S and Cu on sample surface tested in corrosion inhibitor 2 at 120 °C and 150 °C determined by XPS	147
7.16	End of test BSE images of coupon surface after immersion in dispersant 1 at various temperatures	148
7.17	End of test BSE images of wire surfaces after testing in dispersant 1 at specified temperatures	149
7.18	Radius change of copper wires immersed in 5 wt% dispersant 1 at 110 °C, 120 °C, 130 °C and 150 °C, including repeats at 120 °C and 150 °C	149
7.19	The amount of copper in the end of test fluid as determined using ICP-AES for dispersant 1	150
7.20	Atomic concentration of C, O, N, S and Cu on sample surface tested in dispersant 1 at 120 °C and 150 °C determined by XPS	150
7.21	End of test BSE images of coupon surface after immersion in dispersant 2 at various temperatures	152
7.22	End of test BSE images of wire surfaces after testing in dispersant 2 at specified temperatures	153

7.23	Radius change of copper wires immersed in 5 wt% dispersant 2 at 110 °C, 120 °C, 130 °C and 150 °C, including repeats at 120 °C and 150 °C	153
7.24	The amount of copper in the end of test fluid as determined using ICP-AES for dispersant 2	154
7.25	Atomic concentration of C, O, N, S and Cu on sample surface tested in dispersant 2 at 120 °C and 150 °C determined by XPS	154
7.26	End of test BSE images of coupon surface after immersion in detergent 1 at various temperatures	156
7.27	End of test BSE images of wire surfaces after testing in detergent 1 at specified temperatures	156
7.28	Radius change of copper wires immersed in 0.5 wt% detergent 1 at 110 °C, 120 °C, 130 °C and 150 °C, including repeats at 120 °C and 150 °C	157
7.29	The amount of copper in the end of test fluid as determined using ICP-AES for detergent 1	158
7.30	Atomic concentration of C, O, N, S and Cu on sample surface tested in detergent 1 at 120 °C and 150 °C determined by XPS	158
7.31	End of test BSE images of coupon surface after immersion in detergent 2 at various temperatures	160
7.32	End of test BSE images of wire surfaces after testing in detergent 1 at specified temperatures	160
7.33	Radius change of copper wires immersed in 0.5 wt% detergent 2 at 110 °C, 120 °C, 130 °C and 150 °C, including repeats at 120 °C and 150 °C	161
7.34	The amount of copper in the end of test fluid as determined using ICP-AES for detergent 2	161
7.35	Atomic concentration of C, O, N, S and Cu on sample surface tested in detergent 2 at 120 °C and 150 °C determined by XPS	162
7.36	End of test BSE images of coupon surface after immersion in a mixture of friction modifier, antioxidant, and antiwear at various temperatures	163
7.37	End of test BSE images of wire surfaces after testing in the AO, AW, FM mix at specified temperatures	164
7.38	Radius change of copper wires immersed in a mixture of 0.65 wt% friction modifier, 0.33 wt% antioxidant, and 0.165 wt% antiwear at 110 °C, 120 °C, 130 °C and 150 °C	164
7.39	The amount of copper in the end of test fluid as determined using ICP-AES for the friction modifier, antioxidant, and antiwear mixture	165
7.40	Atomic concentration of C, O, N, S and Cu on sample surface tested in the AO, AW, FM mix at 120 °C and 150 °C determined by XPS	165
7.41	End of test BSE images of coupon surface after immersion in antioxidant at various temperatures	166
7.42	Radius change of copper wires immersed in 0.33 wt% antioxidant at 120 °C and 150 °C, with repeats	167
7.43	Atomic concentration of C, O, N, S and Cu on sample surface tested in antioxidant at 120 °C and 150 °C determined by XPS	168
7.44	Radius change of copper wires immersed in 0.165 wt% antiwear additive at 120 °C and 150 °C, with repeats	169
7.45	End of test BSE images of coupon surface after immersion in antiwear additive at various temperatures	170
7.46	Atomic concentration of C, O, N, S and Cu on sample surface tested in antiwear at 120 °C and 150 °C determined by XPS	171

7.47	Radius change of copper wires immersed in 0.65 wt% friction modifier at 120 °C and 150 °C, with repeats	172
7.48	End of test BSE images of coupon surface after immersion in friction modifier at various temperatures	173
7.49	Atomic concentration of C, O, N, S and Cu on sample surface tested in friction modifier at 120 °C and 150 °C determined by XPS	173
7.50	End of test BSE images of coupon surface after immersion in a mixture of corrosion inhibitor 2 with antiwear at various temperatures	174
7.51	Radius change of copper wires immersed in a mixture of 0.05 wt% corrosion inhibitor 2 with 0.165 wt% antiwear at 110 °C, 120 °C, 130 °C and 150 °C	175
7.52	The amount of copper in the end of test fluid as determined using ICP-AES for corrosion inhibitor 2 with antiwear	176
7.53	Atomic concentration of C, O, N, S and Cu on sample surface tested in corrosion inhibitor 2 and antiwear at 120 °C and 150 °C determined by XPS	176
8.1	Amount of copper in the end of test fluid for combinations which showed synergies	183
8.2	Amount of copper in the end of test fluid for combinations which showed antagonisms	184
8.3	Radius changes for dispersant 2 and detergent 1, individually and combined at 150 °C	188
8.4	Radius changes for dispersant 1 and the AO, AW, FM mix, individually and combined at 120 °C	188
8.5	High resolution XPS copper scans for samples run at 120 °C containing corrosion inhibitor 1, corrosion inhibitor 2, dispersant 1, and dispersant 2	191
8.6	High resolution XPS nitrogen scans for samples run at 120 °C containing corrosion inhibitor 1, corrosion inhibitor 2, dispersant 1, and dispersant 2	194
8.7	High resolution XPS sulfur scans for samples run at 120 °C containing corrosion inhibitor 1, corrosion inhibitor 2, dispersant 1, and dispersant 2	197
8.8	SEM images of coupons tested at 120 °C in corrosion inhibitor 1, corrosion inhibitor 2, dispersant 1, dispersant 2, and their combinations	198
8.9	High resolution XPS copper scans for samples run at 150 °C containing corrosion inhibitor 1, corrosion inhibitor 2, dispersant 1, and dispersant 2	200
8.10	High resolution XPS nitrogen scans for samples run at 150 °C containing corrosion inhibitor 1, corrosion inhibitor 2, dispersant 1, and dispersant 2	202
8.11	High resolution XPS sulfur scans for samples run at 150 °C containing corrosion inhibitor 1, corrosion inhibitor 2, dispersant 1, and dispersant 2	205
8.12	SEM images of coupons tested at 150 °C in corrosion inhibitor 1, corrosion inhibitor 2, dispersant 1, dispersant 2, and their combinations	206
9.1	Amount of copper in end of test fluid after different time periods for fluids containing corrosion inhibitor 1	215
9.2	Amount of copper in end of test fluid after different time periods for fluids containing corrosion inhibitor 2	216
9.3	Amount of copper in end of test fluid after different time periods for fluids containing dispersant 1	217
9.4	Amount of copper in end of test fluid after different time periods for fluids containing dispersant 2	218

10.1	SEM images of full formulation samples showing spheres on the surface along with the corrosion inhibitor 1 and AO, AW, FM mix sample surface	220
10.2	SEM images of the surfaces of full formulation samples and simple additive combination samples which contained corrosion inhibitor 1 at 0.5 wt%	223
10.3	SEM images of sample -793 and the simple additive mixtures it was matched with	224
10.4	SEM images of sample -796 and the simple additive mixtures it was matched with	225
10.5	SEM images of sample -798 and all the simple additive mixtures it was matched with	226
11.1	Coupons tested for 1000 hours in two different ATFs by Rathgeber et al. [11]	230
11.2	The radius loss of copper wires after approximately 300 hours plotted against the coupon rating for wire-coupon tests conducted in individual additives and simple additive mixtures across all temperatures	231
11.3	Schematic of samples containing no corrosion inhibitor 2 and their corresponding levels of corrosion inhibitor 1 and dispersant 2 showing that higher levels of corrosion inhibitor 1 and dispersant 2 lead to flaking of the surface film on the sample	235
11.4	The effect of dispersant in fully formulated fluids on (A) the level of copper in the end of test fluid, and (B) the ASTM rating	236
11.5	Radius loss of copper wire plotted against the amount of copper measured at the end of the coupon immersion test for full formulation fluids	239
11.6	Weight change for the coupons at each specified time point in the experiment at 130 °C, recorded as a percentage of the start weight of the coupon	241
11.7	Similarities between the amount of copper in the test fluid and the changes in radius of the copper wire for the experiment carried out at 130 °C	242
11.8	Amount of copper in the end of test fluid and the change in radius of the copper wire for all individual additives tested at temperatures between 110 °C and 150 °C	243
11.9	Amount of copper in the end of test fluid and the change in radius of the copper wire for all additive combinations tested at temperatures of 120 °C and 150 °C	244
11.10	Copper levels in end of test fluids determined by ICP-AES against the calculated level of copper determined from weight loss of coupons and radius loss of wire	246
11.11	Copper in end of test fluid for tests carried out in fluids containing individual additives	247
11.12	Radius loss of copper wire immersed in test fluids containing individual additives at different temperatures	248
11.13	Graph showing how the temperature effects the change in radius of wire tested in the AO, AW, FM mix	249
11.14	Graph showing estimation of corrosion with time at different temperatures [151]	250
11.15	Schematic diagram showing base oil interaction with copper surface as temperature increases	252
11.16	Radius change of copper wires tested at 110 °C	253
11.17	Radius change of copper wires tested at 120 °C	253

11.18	Radius change of copper wires tested at 130 °C	254
11.19	Radius change of copper wires tested at 150 °C	254
11.20	Proposed mechanism, by Ling et al., of the interaction of DMTD with a copper surface [111]	255
11.21	Mechanism proposed by Hipler et al. of the interaction of DMTD with a gold surface [113]	256
11.22	White light interferometry images of two pits found on the surface of a coupon tested in corrosion inhibitor 1 at 150 °C	257
11.23	First derivative of TGA against temperature for corrosion inhibitor 1 with and without the presence of copper	257
11.24	Corrosion inhibitor 1 sulfur XPS spectra at 120 °C and 150 °C	259
11.25	Corrosion inhibitor 1 copper XPS spectra at 120 °C and 150 °C	259
11.26	Schematic diagram of corrosion inhibitor 1 interaction with copper surface above and below 150 °C	260
11.27	Radius change of copper wires tested at 150 °C in corrosion inhibitor 1 alone, the AO, AW, FM mix alone, and a combination of both, with repeats	262
11.28	Schematic diagram of corrosion inhibitor 2 interaction with copper surface	264
11.29	Radius changes of copper wires immersed in corrosion inhibitor 2 and dispersant 1 alone and combined, at 120 °C (left) and 150 °C (right)	265
11.30	SEM images showing improvement of surface when corrosion inhibitor 2 is combined with dispersant 1 at 120 °C (top line) and 150 °C (bottom line)	265
11.31	Structure of dispersant 1	266
11.32	Radius change of wire immersed in dispersant 1 at various temperatures	267
11.33	Schematic of dispersant interaction with surface	271
11.34	Copper coupons tested at 120 °C in dispersant 1, dispersant 2 and a combination of both	272
11.35	Copper coupons tested at 150 °C in base oil alone or with the presence of detergent	272
11.36	Radius change for AO, AW, FM mix and antioxidant, antiwear, and friction modifier independently at 120 °C	274
11.37	Radius change for AO, AW, FM mix and antioxidant, antiwear, and friction modifier independently at 150 °C	274
A.1	XPS analysis of three different areas of a coupon tested in base oil at 120 °C	284
A.2	XPS analysis of three different areas of a coupon tested in base oil at 150 °C	285
A.3	XPS analysis of three different areas of a coupon tested in corrosion inhibitor 1 at 120 °C	286
A.4	XPS analysis of three different areas of a coupon tested in corrosion inhibitor 1 at 150 °C	287
A.5	XPS analysis of three different areas of a coupon tested in corrosion inhibitor 2 at 120 °C	288
A.6	XPS analysis of three different areas of a coupon tested in corrosion inhibitor 2 at 150 °C	289
A.7	XPS analysis of three different areas of a coupon tested in dispersant 1 at 120 °C	290
A.8	XPS analysis of three different areas of a coupon tested in dispersant 1 at 150 °C	291
A.9	XPS analysis of three different areas of a coupon tested in dispersant 2 at 120 °C	292

A.10	XPS analysis of three different areas of a coupon tested in dispersant 2 at 150 °C	293
A.11	XPS analysis of three different areas of a coupon tested in detergent 1 at 120 °C	294
A.12	XPS analysis of three different areas of a coupon tested in detergent 1 at 150 °C	295
A.13	XPS analysis of three different areas of a coupon tested in detergent 2 at 120 °C	296
A.14	XPS analysis of three different areas of a coupon tested in detergent 2 at 150 °C	297
A.15	XPS analysis of three different areas of a coupon tested in the antioxidant, antiwear, friction modifier mixture at 120 °C	298
A.16	XPS analysis of three different areas of a coupon tested in the antioxidant, antiwear, friction modifier mixture at 150 °C	299
A.17	XPS analysis of three different areas of a coupon tested in corrosion inhibitor 2 + antiwear at 120 °C	300
A.18	XPS analysis of three different areas of a coupon tested in corrosion inhibitor 2 + antiwear at 150 °C	301
A.19	XPS analysis of three different areas of a coupon tested in antioxidant at 120 °C	302
A.20	XPS analysis of three different areas of a coupon tested in antioxidant at 150 °C	303
A.21	XPS analysis of three different areas of a coupon tested in antiwear at 120 °C	304
A.22	XPS analysis of three different areas of a coupon tested in antiwear at 150 °C	305
A.23	XPS analysis of three different areas of a coupon tested in friction modifier at 120 °C	306
A.24	XPS analysis of three different areas of a coupon tested in friction modifier at 150 °C	307
B.1	Radius change data for additive combinations, and their individual additives at 120 °C for fluids containing corrosion inhibitor 1, with repeats where they were carried out	309
B.2	Radius change data for additive combinations, and their individual additives at 120 °C for fluids containing corrosion inhibitor 2, with repeats where they were carried out	310
B.3	Radius change data for additive combinations, and their individual additives at 120 °C for fluids containing dispersant 1, with repeats where they were carried out	311
B.4	Radius change data for additive combinations, and their individual additives at 120 °C for fluids containing dispersant 2, with repeats where they were carried out	312
B.5	Radius change data for additive combinations, and their individual additives at 120 °C for fluids containing detergent 1, with repeats where they were carried out	313
B.6	Radius change data for additive combinations, and their individual additives at 120 °C for fluids containing detergent 2, with repeats where they were carried out	314

B.7	Radius change data for additive combinations, and their individual additives at 120 °C for fluids containing the AO, AW, FM mix, with repeats where they were carried out	315
B.8	Radius change data for additive combinations, and their individual additives at 150 °C for fluids containing corrosion inhibitor 1, with repeats where they were carried out	316
B.9	Radius change data for additive combinations, and their individual additives at 150 °C for fluids containing corrosion inhibitor 2, with repeats where they were carried out	317
B.10	Radius change data for additive combinations, and their individual additives at 150 °C for fluids containing dispersant 1, with repeats where they were carried out	318
B.11	Radius change data for additive combinations, and their individual additives at 150 °C for fluids containing dispersant 2, with repeats where they were carried out	319
B.12	Radius change data for additive combinations, and their individual additives at 150 °C for fluids containing detergent 1, with repeats where they were carried out	320
B.13	Radius change data for additive combinations, and their individual additives at 150 °C for fluids containing detergent 2, with repeats where they were carried out	321
B.14	Radius change data for additive combinations, and their individual additives at 150 °C for fluids containing the AO, AW, FM mix, with repeats where they were carried out	322

List of Abbreviations

AO	Antioxidant
ASTM	American Society for Testing and Materials
ATF	Automatic Transmission Fluid
ATR	Attenuated Total Reflectance
AW	Antiwear
BSE	Backscattered Electron
BTA⁻	Benzotriazole (dissociated hydrogen)
BTAH	Benzotriazole (with hydrogen attached)
DMTD	Dimecapthiadiazole
DSC	Differential Scanning Calorimetry
EDX	Energy Dispersive X-ray Spectroscopy
FIB	Focussed Ion Beam
FM	Friction modifier
FTIR	Fourier Transform Infrared spectroscopy
FWHM	Full Wave Half Maximum
ICP-AES	Inductively Coupled Plasma – Atomic Emission Spectroscopy
IR	Infrared
PIB	polyisobutylene
PIBSA	polyisobutylene succinic anhydride
PMA	Polymethacrylate
ppm	parts per million
QCM	Quartz Crystal Microbalance
SBP2L	Special Boiling Point (ID number)
SEM	Scanning Electron Microscopy
TGA	Thermogravimetric Analysis
XPS	X-ray Photoelectron Spectroscopy
ZDDP	Zinc dialkyldithiophosphate

1: Introduction

In recent years electronics have become more commonplace in vehicle driving systems as many automotive manufacturers strive to reduce emissions and improve the overall environmental performance of cars. Governmental restrictions on emissions means that greater efficiency is key, with a move towards greater electrification, with electric hybrid vehicles the most likely next step. Conservative estimates would see 20% of all passenger vehicle miles travelled in plug-in hybrid vehicles by 2050 [1]. Partly due to these changes vehicles are undergoing electrification, with sensors introduced to aid the driver or alert them to specific goings on in the car. In 2010 around 25% of passenger cars had automatic transmissions and they are becoming increasingly popular across the globe, thanks to their efficiency and ease of driving [2, 3].

Automatic transmissions use sophisticated electronic devices in order to change gear [2]. These devices must be very reliable, lasting for many years, and work in much harsher conditions than similar devices in household appliances. The electronics of these systems are often housed within the transmission casing and as a result come in to contact with the Automatic Transmission Fluid (ATF) which can contain additives which may interact with the components, as well as subjecting them to temperatures in the region of 80 °C to 120 °C [4] .

ATFs play an important role in keeping the transmission running smoothly and, as with other lubricants, have a specific set of roles which include [2, 5, 6]:

- Lubricating, cleaning and protecting a number of moving parts, for example gears and bearings
- Removal of excess heat away from the torque converter and during clutch engagement
- Acting as a hydraulic control medium to activate clutch systems

As in manual transmissions the gears and other moving parts must be kept lubricated in order to prevent wear and reduce friction. ATFs however have added complications in that they must not interfere with the electronics placed in contact with them, whilst also being routinely subject to more severe working conditions than manual transmission fluids [4, 7]. Many manufacturers specify long drain intervals for ATFs and in some cases they are required to be fill-for-life fluids and so the fluid would not be changed over the lifespan of the transmission. As such ATFs are highly specialised lubricants and considered the most complex driveline fluid, due to the number of functions they must perform [2, 8].

Before being introduced to the transmission the compatibility of the ATF with a number of different materials must be tested, to ensure it will not damage any of the components or seals present. The electronic systems present in automatic transmissions which control the gear changes consist of components with a high copper content. It is therefore crucial that copper is not corroded by the ATF or else there may be situations where components, such as solenoids fail.

At present an industry standard test, the ASTM D130, is used to visually evaluate the ATF interaction with copper. Although able to quickly screen a large number of fluids this visual inspection gives no information on the interaction of the ATF with the surface.

1.1 Research Objectives

The aim of this study is to understand how common ATF additives interact with copper surfaces using both static and in situ techniques. The objectives of this study are as follows

1. **To determine how individual additives and simple mixtures interact with copper surfaces**
 - Conduct copper wire tests to determine radius loss, and therefore corrosion, caused by each additive
 - Use a variety of surface analysis techniques to analyse the surface of coupons tested in each additive to determine differences between the surfaces

2. **To understand how fully formulated fluids interact with copper surfaces**
 - Conduct static coupon tests and in situ wire tests and compare results to those obtained from the individual additives to determine if the behaviour of individual additives is mimicked in formulations
3. **To determine if individual additives and simple mixtures can be used to provide information about full formulation results**
 - Compare full formulation results with those of individual additives and simple additive mixtures
 - Determine if the results can explain the behaviour seen in full formulation fluids

1.2 Thesis Outline

- Chapter Two: Background information and theory relevant to this study is presented
- Chapter Three: Literature review on methods of monitoring corrosion, types of corrosion common to copper and corrosion of metals in oil based systems is presented
- Chapter Four: Experimental and surface analysis techniques are explained alongside a description of the materials used for testing
- Chapter Five: Results from coupons tested in full formulations are presented
- Chapter Six: Results of initial wire tests in full formulations are presented
- Chapter Seven: Results of coupons and wires tested in individual additives tested across a range of temperatures is presented
- Chapter Eight: Individual additive results are compared to those of simple combinations
- Chapter Nine: Results which look at the progression of surface film formation with time are shown
- Chapter Ten: Comparisons of full formulation results with those of the individual additive and simple mixtures are presented
- Chapter Eleven: Overall discussion of results from chapters five to ten

- Chapter Twelve: Main conclusions from this work are presented and an outline of possible future studies is given

2: Background information

As more vehicles undergo electrification greater thought has to be given to the fluids the electrical components come into contact with. This not only helps to protect the components but also prolong the life of the fluid.

This study focuses on the interaction of Automatic Transmission Fluids (ATFs) with copper. It shall look at the surface corrosion of copper and how common ATF additives affect this. This chapter aims to provide some background information on the composition of ATFs.

2.1 ATF composition

All transmission fluids are comprised of two main components: base oil and an additive package. Additive packages, and therefore ATFs, incorporate a number of different chemistries in order to achieve their desired performance and enhance certain qualities [2, 9].

Lubricant additives can perform their required function either at the surface or in the bulk fluid; they can also be grouped into three basic categories [2]:

1. Compounds which have surface activity (dispersants, detergents, corrosion inhibitors, friction modifiers, antiwear additives);
2. Compounds which modify a physical property (viscosity modifiers, pour point depressants, antifoams);
3. Compounds which reduce oil degradation (antioxidants).

Table 2.1 details the amount of each additive likely to be present in a generic ATF formulation and the main functional groups present in each of these components. Common chemical structures of the additives, along with their function, are given in subsequent

sections. It is possible for additives to have more than one functionality but for simplicity the function which is most recognised shall be used [10].

Table 2.1: Composition of generic ATF [4, 6, 11, 12]

Component	Content (wt%)	Component functional groups
Base oil	60–95	Mineral or synthetic oil
Dispersant/Detergent	2–10	Succinimide, sulfonate, phosphate
Corrosion inhibitor	0.03–1	Carboxylate, sulfonate, alkyl amine, phosphate
Friction modifier	0.2–2	Carboxylic ester, phosphoric acid, organic polymer
Antiwear	0.1–1	Sulfurized olefin, mercaptobenothiazole, phosphate
Viscosity modifier	2–20	Olefin copolymer, polymethylmethacrylate
Antifoam	0.005–0.1	Silicone
Antioxidant	0.3–2	ZDDP, amine and phenol derivatives

2.1.1 Base oil

Base oil is the starting point to making any lubricant, as it makes up the majority of the fluid [2, 9, 13]. Base oil is a mineral or synthetic oil into which additives are added in order to enhance or add properties. In order to achieve the best performance in a finished lubricant, the base oil must be carefully selected for the conditions under which it is expected to operate [3, 10].

Base oils are split into five main groups each of which have slightly different characteristics as summarised in Table 2.2.

Table 2.2: Base oil categories [2, 6, 14]

	Category	Sulfur (%)	Saturates (%)	Viscosity index
Mineral oil	Group I	> 0.03	< 90	80–120
	Group II	< 0.03	> 90	80–120
	Group III	< 0.03	> 90	> 120
Synthetic oil	Group IV	Polyalphaolefins		
	Group V	All other base oils not in the above categories. Examples: silicone, phosphate ester		

Mineral oils are refined from crude oil whilst synthetic base oils are produced from chemical reactions [2, 9, 15]. The way that the crude oil is refined gives the differences between groups I, II and III. Group I is solvent refined which is simple to undertake

making them the cheapest of the base oils. Group II base oils are hydrocracked which gives them a higher saturation level than group I and therefore they are more resistant to oxidation [16]. Group III oils are more severely hydrocracked than group II making them purer and increasing the viscosity index [6, 13].

Synthesised base oils are split into two groups but contain a wide variety of base oils. Group IV base oils are synthesised and are exclusively polyalphaolefin molecules which have a broad temperature range. As these are made in a lab they are generally free from impurities. Group V incorporates any other base oils such as silicone, phosphate ester, polyalkylene glycol etc. all of which are synthesised. They are often the most expensive of the base oils and therefore are rarely used alone, instead they are added to cheaper base oils to improve the properties, particularly as they have excellent high temperature resistance [6].

2.1.2 Additives with surface activity

ATF additives which have surface activity are dispersants, detergents, corrosion inhibitors, friction modifiers and antiwear additives. All surface active compounds are comprised of polar and non-polar constituents. The basic structure for a simple surface-active additive is shown in Figure 2.1. There are three groups present in the additive: a polar group, a connecting group, and a non-polar group [10].

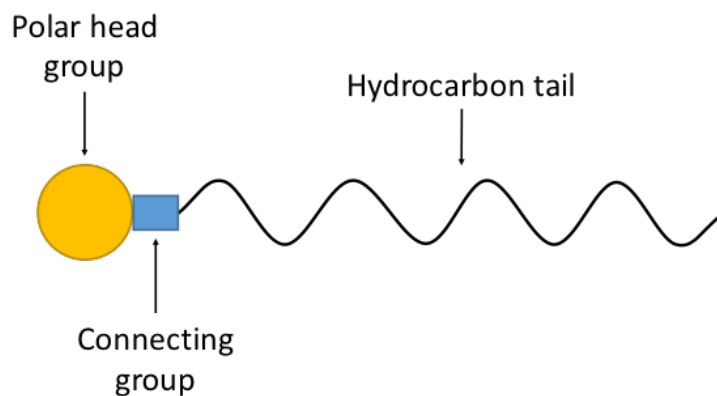


Figure 2.1: Generic structure of a surface-active additive

The polar group is normally the head group and often contains oxygen, nitrogen or sulfur, depending on the activity it is required to have. The connecting group, very simply, links the polar head with the non-polar tail. The tail is a long hydrocarbon chain,

which may be linear or branched, and can be of varying molecular weights depending on the function the additive should perform.

2.1.2.1 Dispersants

Dispersants play an important role in keeping the transmission clean. As oil undergoes oxidation, polar products are formed. Oil is a non-polar fluid and so there is a tendency for the polar products to try and separate from the bulk; as such these particles naturally agglomerate together and drop out of solution. The polar head groups on dispersant additives interact with these polar particulates, resulting in two benefits.

The first benefit is the size of the dispersant molecules prevent the particles from agglomerating due to steric hindrance. The second is that the long hydrocarbon chains have a high affinity for the bulk oil and so they help to keep the particles suspended, minimising the amount of deposit [10, 17]. A schematic showing how dispersants work is shown in Figure 2.2.

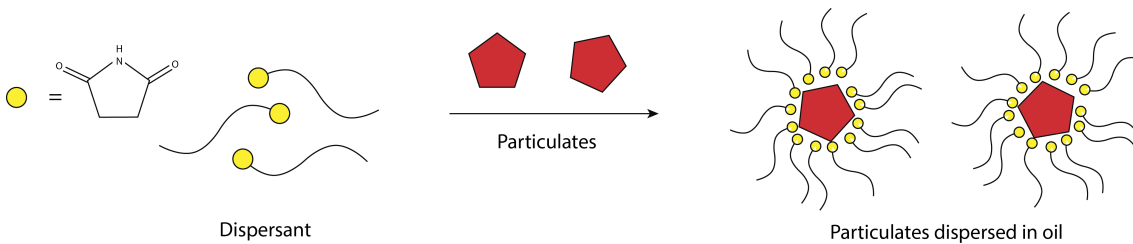


Figure 2.2: Schematic showing the interaction of dispersant with particulates in oil

Dispersant head groups are most often oxygen or nitrogen based [10]. An example of a common dispersant would be polyisobutylene succinic anhydride (PIBSA) reacted with polyamines to produce polyisobutylene succinimides. Choosing different molecular weight PIBSA and different polyamines means it is possible to modify dispersants of this kind to target specific particulate contaminants [2, 6].

2.1.2.2 Detergents

Detergents are similar to dispersants in that they are able to suspend particles in the bulk fluid but they also provide a secondary role, namely neutralising acid. During the degradation of oil, acids, both organic and inorganic, may be formed. These acids can then attack the transmission surfaces, causing corrosion [10].

Detergents contain a basic core which acts to neutralise any acid formed during decomposition of the lubricant, thereby helping to prevent corrosion by acid attack. The core is normally a metal carbonate, prepared by reacting metal oxides or hydroxides with a neutral detergent and carbon dioxide [2]. Magnesium and calcium metals are most commonly used.

The basic core is surrounded by oil soluble chains, with polar head groups, which help to suspend the core in the fluid. These oil soluble chains also help to suspend neutralised products, although they are less effective than dispersants as they generally have a lower molecular weight. A schematic diagram showing the structure of a calcium carbonate core, stabilised with sulfonate head group chains, is shown in Figure 2.3.

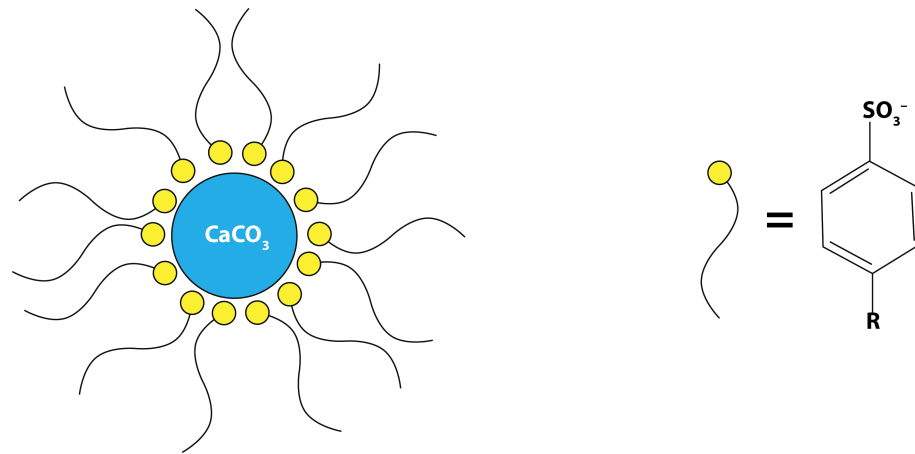


Figure 2.3: Structure of detergent molecule with calcium carbonate core

2.1.2.3 Corrosion inhibitors

Corrosion inhibitors are molecules which react with the metal surfaces inside the transmission, by physical or chemical absorption, to create a protective barrier, preventing water, oxygen or other corrosive products from reaching the metal. It is also possible to have corrosion inhibitors which react with oxidation products in the fluid, similar to detergents, preventing them from interacting with the metal surface.

The polar corrosion inhibitor head groups often contain sulfur and/or nitrogen. The molecules are designed to interact with the metal surface and form a continuous surface film, where each of the molecules packs together covering the surface as depicted in Figure 2.4 [2]. The general mechanisms of corrosion protection shall be covered in greater detail in the literature review.

Effective corrosion inhibitors for copper surfaces have been found to be heterocycles containing sulfur and/or nitrogen [9].

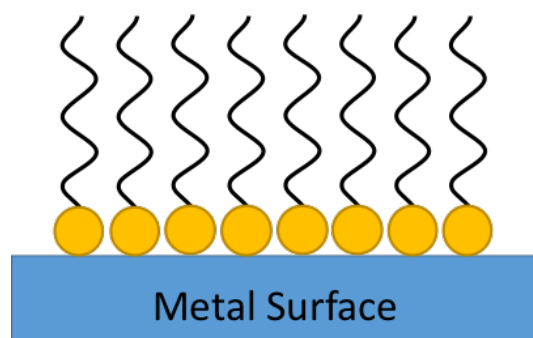


Figure 2.4: Metal surface with corrosion inhibitor molecules forming a protective layer

2.1.2.4 Friction modifiers

Friction modifiers, as their name suggests, modify friction. They work by adsorbing onto surfaces and forming low resistance films, thereby reducing the friction between two surfaces [10]. They are generally formed of long hydrocarbon chain molecules with polar head groups. As the polar head group is designed to adsorb onto the metal surface, the type of head group that is chosen can affect how well the additive interacts with the surface. The length of the tails and any branching affect the overall solubility of the additive. Unlike in engines, where the aim is often to reduce the friction of moving parts to minimise energy loss, automatic transmission systems want to control the amount of friction in order to improve the drivability of the car [2]. Common friction modifiers include amines, amides, alcohols, esters and fatty acids.

2.1.2.5 Antiwear additives

Antiwear additives react chemically with the metal surface to create a surface film. When two surfaces come into contact, the chemically formed film is removed in preference to the metal surface, therefore providing protection from wear [10]. Typical antiwear additives are organic in nature and can contain zinc, phosphorous, sulfur, boron or chlorine [2]. Zinc dialkyldithiophosphate (ZDDP) is a very well-studied antiwear additive as it became widely used after its discovery in the 1940s. As well as functioning as an antiwear additive it was found that it had antioxidant properties [10, 14, 16, 18] which helped to

prevent the formation of peroxides this in turn minimised the formation of organic acids and so also reduced corrosion in bearings.

2.1.3 Additives which modify physical properties of oil

2.1.3.1 Viscosity modifiers

The viscosity of a lubricating oil is very important, but the viscosity of lubricants changes with temperature. As this is the case it is necessary to consider the operating temperature of the fluid, as well as if it is required to start at low temperatures [10]. At low temperatures oil is viscous; as the temperature increases the fluid's viscosity decreases. At high temperatures the lubricant may become so thin as to be ineffective at lubricating the transmission, whilst if it is too thick at low temperatures it may not be pumped effectively, leaving areas with low lubricant supply [9]. Viscosity modifiers are added to an oil to try and minimise the viscosity change with temperature. As gear oils have been required to become more fuel-efficient there has been a move to thinner viscosities with greater temperature spans [3].

Long polymeric molecules, such as polymethacrylate (PMAs) or styrene/diene copolymers, are used to modify the viscosity of lubricants. They work by increasing the viscosity of the oil at all temperatures. At low temperatures the polymer molecules coil into relatively small ball-like shapes; at higher temperatures they uncoil, forming much straighter molecules and so contribute to an increase in viscosity as they interact to a greater extent with the base oil [6, 9, 10].

The viscosity increase at high temperatures is much greater than the increase at low temperatures, therefore the viscosity change is lessened overall. This allows acceptable low temperature viscosities to be found and the oil will not thin as much at high temperatures, providing protection and lubrication to the transmission. A simplified plot of this effect can be seen in Figure 2.5.

One problem encountered with some viscosity modifiers is that they can be broken down into polymers with smaller chain lengths, limiting their effectiveness at increasing oil viscosity at high temperatures. Viscosity modifiers with differing architectures, such as branched chains, star shape or brushes, have been found to improve this problem [2].

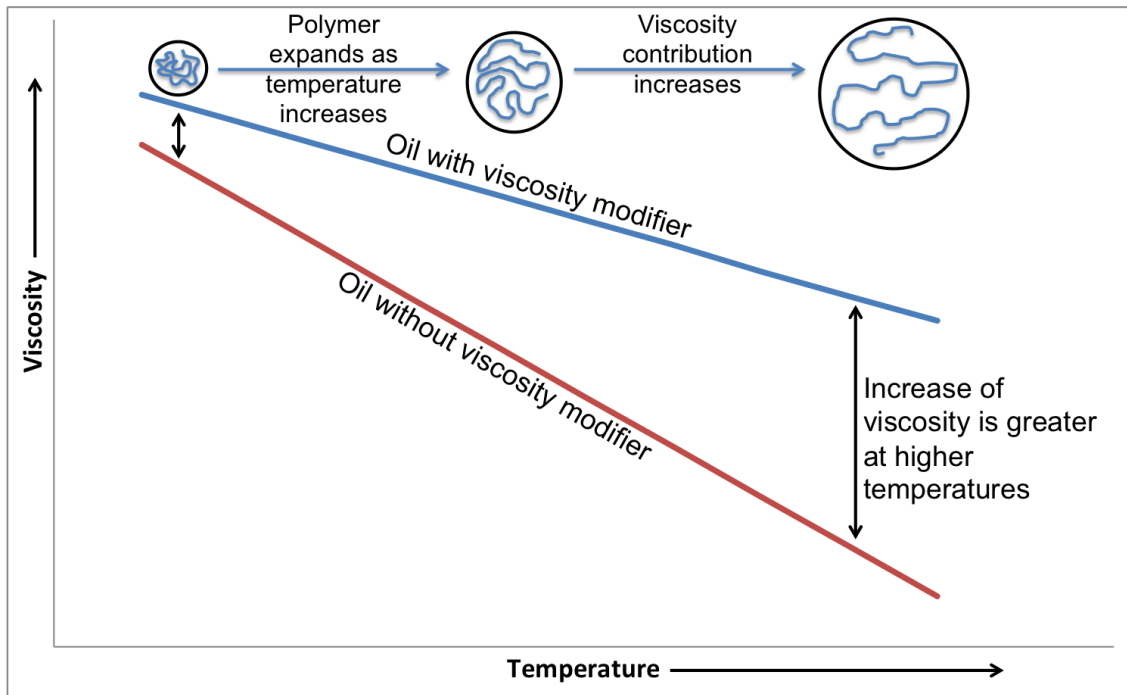


Figure 2.5: Effect of viscosity modifier on viscosity of oil

2.1.3.2 Pour point depressants

Pour point depressants are similar in ways to viscosity modifiers, with polyacrylates and polymethacrylates commonly used. The pour point of a lubricant is the lowest temperature at which it will flow [10]. Mineral oils can contain some dissolved wax, which crystallises at low temperatures and prevents flow. The addition of polymers of high molecular weight can interfere with the crystallisation process and so move the pour point to lower temperatures. It should be noted that synthetic oils do not require the addition of pour point depressants as they contain no wax [9].

It is important that the pour point is below the minimum operating temperature of the transmission, otherwise in the middle of winter the lubricant would not flow and so cause damage.

2.1.3.3 Antifoam

Very simply, foam can be considered to be bubbles of air surrounded by thin layers of oil. These bubbles are introduced as oil is pumped quickly around the transmission, trapping air. This is an undesirable property as it can lead to changes in the fluid characteristics, as well as increased oxidation [10]. Silicone is often added as an antifoam additive as it

has a very low surface tension, meaning that when the silicone interacts with the surface of the bubble it causes the walls to thin to such an extent that the bubble bursts [9].

2.1.4 Antioxidants

Oxidation of lubricants is bad as it causes thickening, sludge and varnish; all of which are undesirable and affect the lubrication. It can be exacerbated by a number of factors such as temperature, aeration (which increases the amount of dissolved oxygen), and catalysis caused by the presence of metal ions. Copper is generally considered to be an oxidation promoter, and is added to oxidation stability tests to accelerate the process [14].

The process of oxidation is complex but can be summarised into three main stages [2, 14] initiation, propagation and termination:

1. **Initiation** marks the start of the oxidation process and is summarised in Equation 2.1. A carbon chain is broken down to form a free radical, either by heat or the presence of a catalyst.



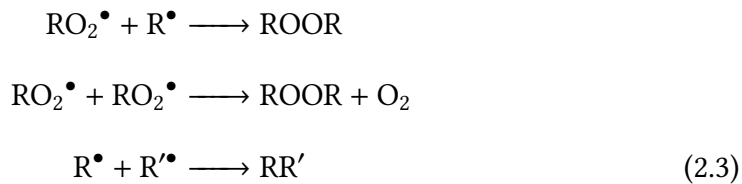
Copper has been found to be a good catalyst for oxidation. In a transmission both heat and copper are present, so there is the potential for oxidation to occur more readily than in other environments.

2. **Propagation** is the ongoing reaction of free radicals. Some potential reactions are shown in Equation 2.2. Reactions with oxygen, dissolved in the oil, or further hydrocarbon chains preserve the free radical and so continue to react further.



3. **Termination** involves the reaction of two radicals with each other, leading to the formation of stable products and the elimination of the radicals. Equation 2.3

shows a number of different termination reactions that could occur.



Antioxidants are added to lubricants to minimise the impact of oxidation. There are two main types of antioxidant; primary and secondary. Primary antioxidants donate hydrogen to radicals in order to prevent propagation. In order to be successful, the radicals must be able to react more readily with the antioxidant than the hydrocarbons [14].

Secondary antioxidants decompose peroxide molecules to less reactive alcohols. ZDDPs are very effective antioxidants but, due to new regulations limiting their use, alternatives are being sought.

2.1.5 ATF additive interactions

As with many lubricants ATFs are comprised of a base oil and an additive package. This additive package contains an array of different additives which each help to suppress or enhance specific functionalities of the oil as explained above. Many additives are chemically active compared to the base oil and interact both with surfaces and each other.

In 1989 Spikes [18] collated a paper showing the current knowledge on what were considered to be practically important additive interactions. Figure 2.6 shows a table of the interactions identified between different classes of additives.

Additives may interact directly in the fluid, potentially limiting their performance. They may react with each other at a surface, or one may react only once another has already formed a surface film. On the other hand, if one additive interacts more quickly with a surface than another, it may prevent the second additive from functioning at all as it has masked the surface. He suggests that interactions normally occur between two additives, with three additive interactions less likely [18]. What is not addressed is what

	VI-IMPROVER	POURPOINT DEPRESSANT	DETERGENT DISPERSANT	OXIDATION INHIBITOR	CORROSION INHIBITOR	ANTIWEAR	EXTREME PRESSURE	ANTI-FOAM
VI-IMPROVER	☐ (+)	○	○	○	○ (+)	○	○	○ (-)
POURPOINT DEPRESSANT	☐	○	○	○	○	○	○	○
DETERGENT DISPERSANT	☐	+	+	+	-	-	-	○ (-)
OXIDATION INHIBITOR	☐	+	+	(+)	○	○	○	○
CORROSION INHIBITOR	☐	-	-	-	○	○	○	○
ANTIWEAR	☐	-	-	-	+	○	○	○
EXTREME PRESSURE	☐	-	-	-	+	○	○	○
ANTI-FOAM	☐	-	-	-	-	-	○	☐

+ = synergism
 - = antagonism
 ○ = no influence

Figure 2.6: Direction of interaction between additives of different classes [18]

would happen if one additive reacted with several other additives individually and all of these additives were combined. That is, additive A interacts with additives B and C. B and C do not interact. What would happen if additives A, B and C were combined?

The only way to truly understand how additives interact would be to understand their mechanisms fully [18].

3: Literature Review

The main focus of this study is the interaction of copper with a number of common ATF additives. Literature which looks at corrosion of copper in oil based environments is lacking, particularly with regards to ATFs. This literature study will therefore address the corrosion of copper in all environments. Copper corrosion and corrosion prevention is most often studied in aqueous or atmospheric environments and so these studies shall be used to try and understand the types of corrosion most common to copper and how they are prevented.

This literature review will systematically look at corrosion and its different forms. The basics of copper corrosion and how it is affected by various parameters, such as temperature or alloying, and how it is commonly monitored.

The literature will then focus on corrosion, primarily of copper, in oil based systems. This will be followed by how copper is protected from corrosion in various environments. Finally methods of monitoring corrosion and characterising corroded surfaces shall be investigated.

3.1 Corrosion

Corrosion is primarily a surface phenomenon [19, 20] which is unpredictable in its growth [21] and differs with material, temperature, humidity and pH; to name but a few variables [22]. It can be described as the deterioration of a material through interaction with its environment. The term corrosion is used whether this interaction is desirable, and in some cases deliberate, such as the formation of oxidation products on the surface of alloys forming a protective passivation layer; or if it is undesirable and adversely affects the properties that wish to be preserved [23]. In either case it describes

a reaction that takes place between a metal and its environment, either by chemical or electrochemical processes [23–26].

Electrochemical corrosion requires a metal to dissolve in an electrolyte, forming metal cations, implying electron transfer between the metal and the environment.

Chemical corrosion occurs when a metal reacts without the presence of an electrolyte, for example, oxidation at high temperatures [24, 27].

Corrosion is widely studied due to the importance of knowing the durability of materials used in different circumstances; to build structures or make circuitry for example [23, 27]. Despite the material being the same the corrosion may differ with the exact environment. For example a bridge in a wet cold climate may corrode differently to the same structure placed in a hot dry climate. This means that materials are often tested for the specific conditions they may be used in. This can be complicated by the fact that there are many different types of corrosion [28], some of which are more prevalent in different environments.

Corrosion may be seen by the naked eye, for example general corrosion, it may need specific inspection tools to be identified, such as intergranular corrosion, or it may be identified through microscopic examination, in the case of cracking [24, 28].

The degree of localisation can be an important factor of corrosion, as highly localised corrosion can cause more serious failure and can be much harder to detect [28, 29]. Some common corrosion types are discussed below.

3.1.1 General or uniform corrosion

General corrosion is the most common form of corrosion which extends over a very large – if not the whole – area of an exposed surface, with the depth of corrosion similar across the affected area [24].



Figure 3.1: Illustration of general corrosion adapted from [28]

The term general or uniform corrosion can actually refer to several different specific types of corrosion, each of which exhibit uniform material loss of the surface. Atmospheric corrosion is the most common, galvanic corrosion is electrochemical in nature, and high-temperature corrosion is particularly important in industrial environments. All are types of general corrosion but can also show other corrosion forms such as pitting [26, 29].

Uniform corrosion is usually easy to detect unless it is hidden from sight, such as inside a pipeline. Despite this, its effects are often quite predictable, although the rate of corrosion will vary depending on the material and environment [28]. Good estimations on the rate of uniform corrosion can be achieved by carrying out relatively simple corrosion tests, such as immersion tests or electrochemical tests in the environment of interest [24]. Techniques which use the mass loss of coupons to determine corrosion rate generally assume uniform corrosion of the surface [30], although further examination by microscope can show the presence of other types of corrosion such as pitting or crevice corrosion.

Rates of corrosion for common materials in common environments are often well documented and are used to inform material choices for specific applications. Due to this a corrosion allowance is often built into the product, an industrial plant for example, and is based on the expected corrosion rate of the material and the required service life of the item [31].

Uniform corrosion can often be prevented to a large extent by the addition of protective coatings, or the use of corrosion inhibitors, which form a protective layer on the surface. In some cases corrosion products which form on the surface of the corroding material act as a protective layer and prevent or minimise further corrosion. For example Rodriguez et al. [32] found that the corrosion rate of copper in an atmospheric environment decreased with time due to the formation of a protective patina on the surface.

3.1.2 Pitting corrosion

Pitting corrosion is the most common type of localised corrosion [28]. It can be highly localised and is characterised by the formation of cavities on the metal surface. Pits are normally well defined but their shapes can vary widely, as depicted in Figure 3.2 [24, 28, 29].

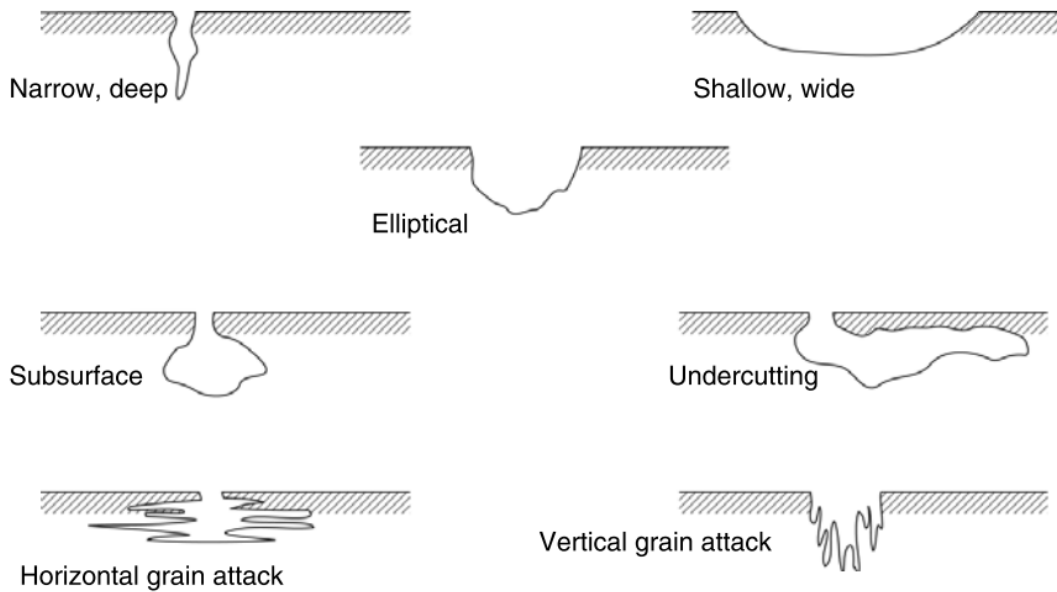


Figure 3.2: Typical cross sectional shapes of pits [28]

Pits which have irregularities in their walls could indicate the presence of a second type of corrosion. The occurrence of pitting on clean surfaces often indicate the break-down of inhibitor protection, or the end of passivity. A small number of pits spaced apart often means penetration will be more rapid than when pits are closely spaced and numerous; as the number of pits increases the rate of penetration decreases [28, 29, 33]. Due to the nature of pit propagation once a pit is formed the local environment changes with metal dissolution causing a build up of positive charge inside the pit which then attracts negative ions into it causing further dissolution of the metal; this process is self propagating and is illustrated in Figure 3.3 [29, 33] for a metal in a sodium chloride aqueous solution. Pitting can be particularly problematic in stagnant fluids where no movement, such as a convection current, is present to move the build-up of corrosive ions [28, 29].

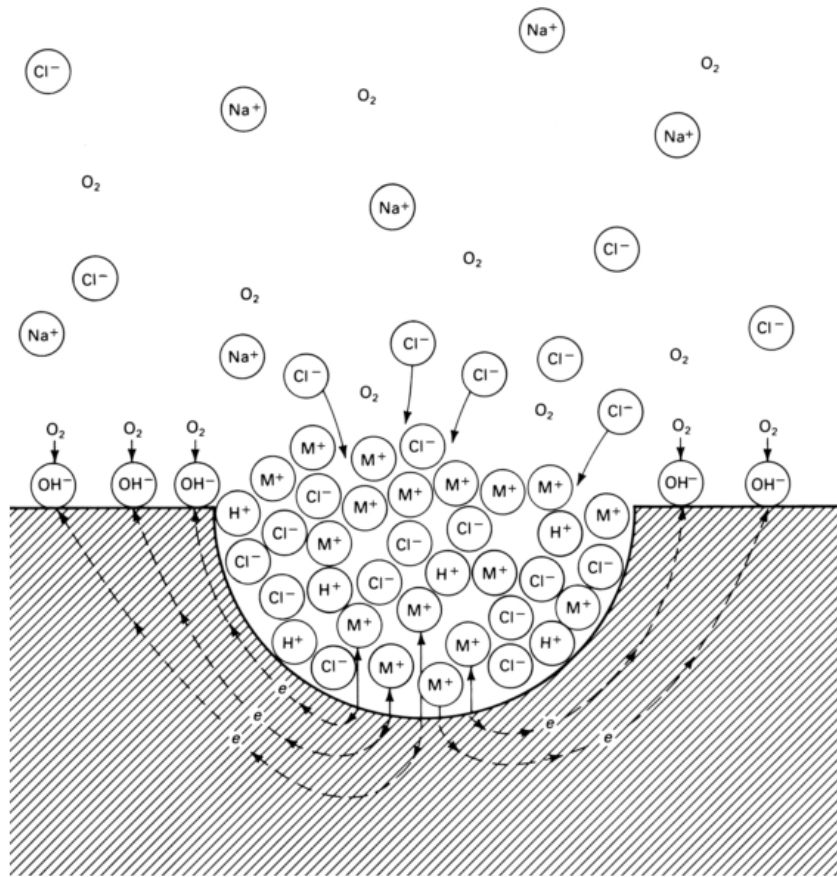


Figure 3.3: Self-Propagating mechanism occurring in a corrosion pit with rapid dissolution of metal, M, within the pit with oxygen reduction on adjacent surfaces [33]

Commonly Cl^- is associated with pitting, due to its prevalence in natural water systems, but other anions such as SO_4^{2-} and ClO_4^- can also promote corrosion [24, 34]. Temperature is reported to be a critical factor in pitting corrosion [33, 35, 36]

Vasquez Moll et al. [37] studied copper electrodes immersed in NaOH solutions with the addition of Na_2S . They found that there was formation of a thin Cu_2S layer on top of which another copper sulfide layer was formed, resulting in a thick adherent complex copper sulfide film. When this layer broke it gave a poorly adhered CuS layer and resulted in pitting of the copper underneath. These processes were dependant on the concentration of Na_2S .

Corrosion inhibitors such as sodium mercaptobenzotriazole have been used to prevent the pitting of copper pipes in water according to Bharucha and Baker [38]. Benzotriazole was also reported to have the same effect by Cotton and Scholes [39].

Pits can be difficult to detect as they show very little weight loss, are generally small in size and when well-spaced can often be overlooked, particularly if some general

corrosion is also present [28, 29]. Li and Li [22] found that the roughness of a surface could affect pitting with rougher surfaces giving greater corrosion rates and higher number of pits than smoother surfaces. In-depth study of localised corrosion is difficult as there is no way of predicting where the sites will occur [40]. However it is thought that corrosion is more likely to start from grain boundaries.

3.1.3 Crevice corrosion

Pitting which occurs at a site between two mating surfaces is termed crevice corrosion. It may be observed between metals which are the same, or different, or it may occur under a scale or surface deposit [28, 41]. Figure 3.4 shows an illustration of crevice corrosion between two adjoining materials. This material could be another piece of metal or solder, a coating or a solid deposit [29].

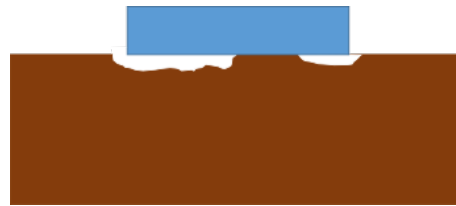


Figure 3.4: Illustration of crevice corrosion adapted from [28]

In an aqueous environment the gap formed between the surface and the adjoining material must be sufficient to allow solution to enter but small enough to maintain a different environment to the bulk. The smaller the gap between the two surfaces the more severe the corrosion is likely to be [29, 41].

The mechanism of crevice corrosion is the same as that presented for pitting corrosion in Figure 3.3. Both pitting and crevice corrosion can be more problematic as they can lead to premature failure of a structure with little weight loss, making them more difficult to detect [29]

3.1.4 Intergranular corrosion

Intergranular corrosion is also a type of localised corrosion, with preferential corrosion at grain boundaries. It occurs when the corrosion rate at the grain-boundaries is faster than that of the grain interior [29]. A difference in chemical composition caused by

alloying elements or impurities can cause a difference in corrosion potential between the grains. This in turn causes preferential corrosion at the boundary regions [28]. An illustration of intergranular corrosion can be seen in Figure 3.5.

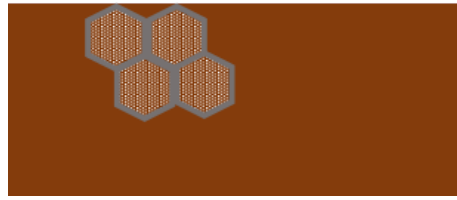


Figure 3.5: Illustration of intergranular corrosion adapted from [28]

Intergranular corrosion can be accompanied by weight loss that accelerates with time as the grains are detached from the bulk and fall out due to the intergranular corrosion spreading in all directions around them [29, 42, 43].

Zhu and Lei [44] found that the initial processing and therefore morphology of a 70Cu-30Ni alloy affected the severity of intergranular corrosion seen after the samples had been immersed in seawater. They reported that corrosion had a preference to proceed on the grain boundaries. The grain boundaries are deficient in the elements that help to form a protective corrosion layer on the surface, in this case nickel, as such the layer takes longer to form at these sites and so corrosion is more prevalent.

3.1.5 Dealloying

Where alloys are composed of metals of very different electrochemical potentials, the most active metal can be selectively removed by electrochemical dissolution. This is known as *dealloying* of which dezincification is a well-known phenomenon and is the removal of zinc from Cu-Zn alloys. Two main theories try to explain this phenomenon. The first is selective dissolution whereby zinc is selectively dissolved, without the involvement of copper. The second is dissolution-redeposition where both zinc and copper are dissolved, followed by the copper being plated back onto the surface [45].

Forty [46] proposed a method of surface diffusion where the less noble element is removed and the remaining element restructures itself to form islands which then grow to form an interconnected structure. This is shown schematically in Figure 3.6 [45].

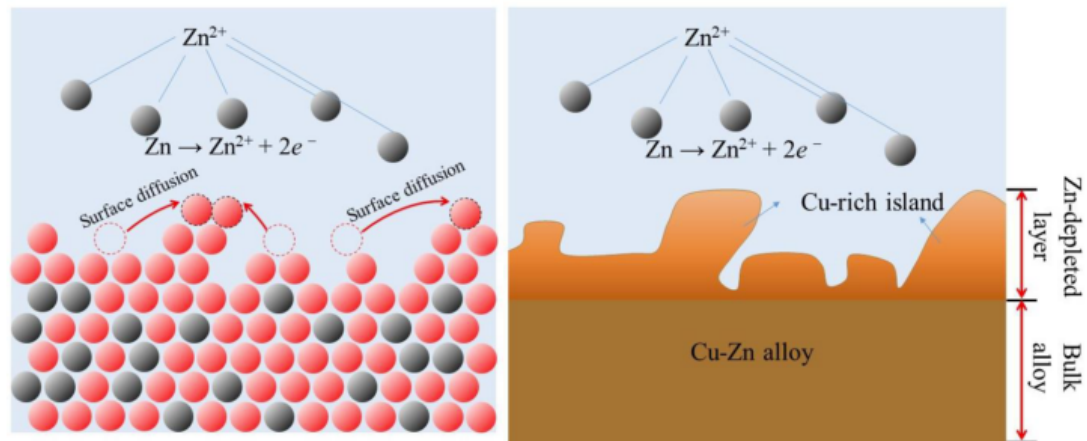


Figure 3.6: Schematic diagram showing surface diffusion mechanism [45]

This removal of one element weakens the material as it makes it porous and brittle, therefore likely to fail without warning [28, 29].

For simplification purposes the copper chosen to be used in this study is 99.99 % pure and so should not exhibit dealloying.

3.1.6 Passivity

Metal alloys which are considered to be corrosion resistant are often called passive. Passive surfaces remain relatively unchanged with time, even when the surface may be expected to undergo corrosion [24]. Passivity is reached when diffusion limits are reached or corrosion products have formed a surface layer; such as the formation of an oxide film [47]. The film does not have to be thick to be effective, and can vary from a few nanometres to several hundred nanometres depending on the metal and environment [47]. Different alloys can have varying passivity. For example Virtanen et al [48] found the Cu-Al10-Sn5 alloy in neutral solutions to be passive due to the formation of a film rich in aluminium oxide. Breakdown of the passive film can lead to general, pitting or crevice corrosion [24]. Breakdown often occurs when there is a change in the environment, for example a change in pH.

3.2 Copper corrosion

Copper and its alloys are materials used in a wide range of applications, from roofing tiles to water pipes, but most recently in modern applications involving electronics [34, 49–51]. When any metal is used the mechanical, physical and chemical properties must be considered so it can be decided if the material will be able to fulfil the specified function. Mechanical and physical properties are easy to deduce as they are constant; chemical properties are dependant on the environment in which the metal is placed and therefore may differ from one application to another [23, 52].

Due to such an array of uses there are extensive studies on the corrosion and protection of copper and its alloys under conditions in which they are commonly used. Aqueous [52–59] and atmospheric [32, 60–64] corrosion is widely studied, but fewer studies have been carried out looking at corrosion in oil based systems. Studies conducted in oil based systems are often related to transformer fluids [25, 65–69] rather than motor lubricants such as ATFs.

Literature has been found in order to see what types of corrosion are common with copper and how it is protected under such conditions.

3.2.1 Common copper corrosion products

The corrosion products formed on copper will vary dramatically depending on the environment [23].

Atmospheric corrosion usually occurs when water is present on the metal surface producing a small electrochemical cell. This means that many atmospheric corrosion products contain oxides and hydroxides [47]. Pollutants in the air can lead to other corrosion products.

Fiaud et al. [70] exposed copper to air + H₂O + H₂S to investigate the effects of atmospheric pollution. Analysis of the surface produced Cu₂S, Cu₂O and CuO. The addition of SO₂ had little effect on the corrosion products formed. Demirkan et al. [50] also found that exposing copper to highly corrosive gases generally leads to the formation of Cu₂S on top of the copper with a layer of Cu₂O between them. This Cu₂S

layer was found to flake and became worse with increasing test length. Both of these tests were carried out under laboratory settings.

Rodríguez et al. [32] also looked at atmospheric corrosion of copper but in corrosion stations placed around Las Palmas in Gran Canaria. The copper surface formed more complex films comprised of Cu_2O , $\text{CuCl}_2 \cdot 3\text{Cu}(\text{OH})_2$, $\text{Cu}_4(\text{OH})_6\text{SO}_4$ and $\text{Cu}_3(\text{OH})_4\text{SO}_4$. Some of these formed a protective patina, which were also identified by Schlesinger et al. [71] as present on historical copper and bronze monuments.

Aqueous corrosion can give similar results but ultimately depends on the ions present in the solution. Cu_2O and CuO are common but the presence of Cl ions can lead to incorporation of CuCl and competitive adsorption of chlorine and oxygen species [53]. Aqueous corrosion is often studied with the use of electrochemical techniques and in many cases looks at the addition of inhibitors to the solution to prevent corrosion.

Tests using alloys can be much more complicated as they can undergo processes such as denickelification, producing a layer of nickel on the surface as well as copper oxide [44]. In order to prevent corrosion in certain environments the copper can be plated. Some copper alloys are plated with tin which begins as several distinct layers but eventually is reacted into Cu_3Sn which can crack and expose the copper [72], a schematic of this transformation is shown in Figure 3.7.

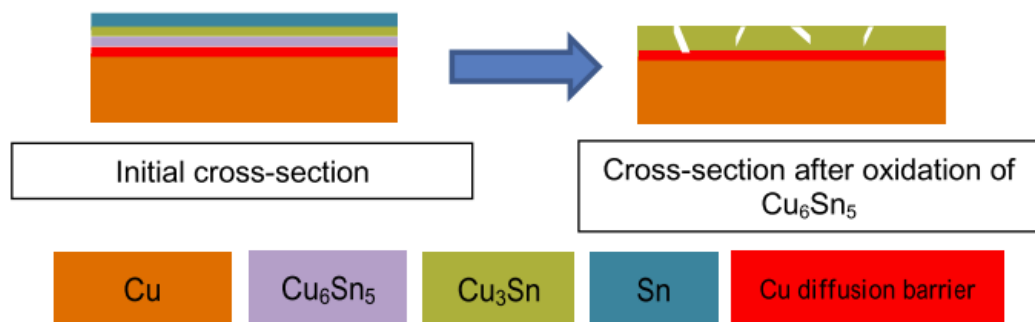


Figure 3.7: Schematic showing the change in copper with plated tin layers [7]

3.2.2 Copper oxidation and passivation

Oxidation is considered a form of corrosion. Copper is readily oxidised to CuO and Cu_2O at low temperatures (below $200\text{ }^\circ\text{C}$). This degrades the copper's electrical properties [73].

Alloying or placing an oxidation resistant layer on the surface are both used to try and reduce copper oxidation.

Oxidation is a very rapid process in its initial stages, forming a stable film in minutes. This happens to many metals at room temperature; and in the case of copper, iron and barium for example can occur at much lower temperatures [74]. Copper oxidises readily in air to form CuO and Cu₂O, depending on the temperature and pressure. Most often a multilayered system is reported where there is an outer layer of CuO and an inner layer of Cu₂O on the bulk Cu [61].

Zhi Hu et al. [60] found that the copper oxide grain size was larger when it was grown under wet conditions (50 % H₂O in N₂).

Passivation describes the corrosion resistance of a material. In some instances it is the corrosion of a metallic surface in its environment to a point where corrosion is no longer observed. More often in literature it is used to describe the interaction of a surface with particular molecules, such as inhibitors, which protect the metal from corrosion. Many studies look at the passivation of copper through interaction with inhibitors. Grillo et al. [75, 76] look at the passivation of copper using benzotriazole, one of the most common inhibitors for copper, as discussed later.

It is possible for a passive layer to break down and this can then lead to other forms of corrosion, such as pitting.

3.2.3 Effect of alloying and microstructure

Alloying of copper can be carried out to modify its properties or to try and prevent oxidation. For copper which is to be used in electronic applications the effect of alloying on conductivity must be considered. Alloying copper with chromium, titanium, palladium or aluminium can reduce the oxidation rate at the expense of increasing the resistance [73].

The alloy composition and microstructure can have a strong influence on which type of corrosion a material may undergo. The alloy composition and microstructure of the metal can effect how likely it is for the material to undergo pitting corrosion [33]. The grain structure is particularly important when considering intergranular corrosion. The

alloy composition is more important when considering selective attack of one metal in an alloy [44]. Dezincification of brass is a good example of this, where zinc is dissolved out of the alloy without any visible signs of damage to the surface, study under a microscope would show a porous structure [28].

3.2.4 Rates of copper corrosion and passivation

The rate of corrosion of any material is not a constant easily identified value. The corrosion rate will depend on the exact environment of the material; the temperature, concentration and pH of any solution, level of oxygen, prevailing wind etc. Some corrosion is measured over a period of months, or years, such as the environmental corrosion studied by Rodriguez et al. [32] which corrodes at a rate of 2 μm a year, but this can slow in subsequent years due to the formation of a protective patina on the surface. Alternatively it can be studied over a series of hours or days.

The formation of a film can decrease the rate at which corrosion occurs; if the process is diffusion controlled the thicker the film the longer the diffusion takes and the slower the corrosion. A breakdown in passivation can accelerate the corrosion process that had, until that point, been non-existent.

Many different factors can influence the corrosion rate. Li and Li [22] showed that the corrosion rate increased with an increase in surface roughness.

Temperature also plays an important role in the rate of corrosion [20, 69, 77]. Corrosion is a thermodynamic process which requires energy to react the metal with its surrounding environment. An increase in temperature can accelerate corrosion by providing the system with more energy.

3.3 Corrosion in oil based systems

Oil based corrosion is particularly important in engines and transmissions [5, 78] as well as other systems where oil is used, such as in transformers where it is used as an insulating fluid. [67, 69, 79]. Regardless of the application it is important to know how the metal will corrode in such an environment and what can be done to prevent it.

Knowing what makes an oil corrosive is a good place to start. Unlike in aqueous systems, charge is not carried by the fresh oil. Instead the formation of acids or other oxidised species as the oil degrades can carry this charge [25].

Oils undergo thermal and oxidative degradation during service, the degree of which depends upon the specific running conditions [80]. Sensors which can monitor properties of the oil or lubricant can give an indication about the extent of deterioration. Viscosity or IR-adsorption are two such properties which could be monitored [81]. The corrosivity of the lubricants could be considered most important in this instance as it has a direct impact on the corrosion of engine or transmission parts. Measuring the corrosive species in large volumes of oil can be problematic so often the effect caused by those corrosive species is measured. Agoston et al. [81] developed thin film copper sensors to monitor the corrosion of engine oils by measuring the changing resistance of the films, as seen in Figure 3.8.

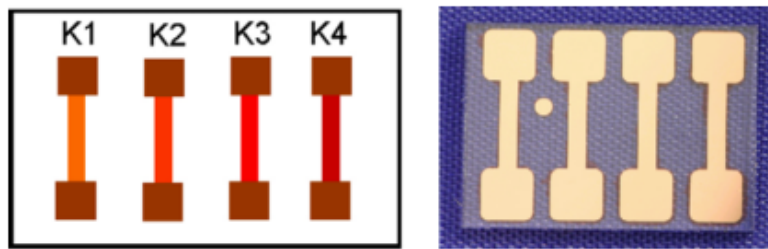


Figure 3.8: Prototype layout (left) of thin film corrosion sensors with different thicknesses of copper on a glass substrate, fabricated prototype covered with protective lacquer (right) [81]

They found that corrosion does not occur at a constant rate. They attribute this to passivation effects occurring on the copper surface which slow down the corrosion over time. The tests were conducted in engine oils, which contain corrosion inhibitors, and these are designed specifically to react with the surface to form a barrier and prevent corrosion. The inhibitors chemically react with the copper surface which the sensors detect as corrosion as there is a change in the copper. Once this layer has been formed the rate of corrosion decreases dramatically. They also saw that corrosion products could form on the copper surface and act as a barrier to other corroding species [81].

As well as oxidation, other reactions can lead to the formation of nitrogen oxides, organic nitrates, organic sulfones, sulfoxides and the formation of SO_x . The oxidation of

sulfur species can in extreme cases form sulfuric acid, which is highly corrosive to copper [80]. Temperature, oxygen availability and, in the case of transformer oils, electric field can all influence the reaction of sulfur with copper [69]. Kalantar and Levin [25] found that the presence of acids and peroxides increased the dissolution of copper into the base oil, whereas model nitrogen compounds helped to passivate the copper surface decreasing this effect.

Copper is an active oxidation catalyst for the degradation of many oils [82] and is added to some laboratory bench tests to enhance the rate of oil degradation. Cu_2O films can be soluble in oil and so catalyse the oil degradation process [11, 82, 83]. This means consideration must not only be given to how to protect the copper surface from corrosion but also how to prevent the accelerated oxidation of oil by copper [25].

Before any lubricant is put into use it is tested to see that it performs the functions required of it but also does not adversely interact with any other materials it may come into contact with. The ASTM D130 test is the standard test method used by industry to measure the corrosiveness to copper by petroleum products [26, 84, 85]. This is a simple visual test which attributes the colour of the test piece to a level of corrosion, using an arbitrary scale which is described in Table 3.1. The corrosion standards were formed by exposing a series of copper strips to a solution of elemental sulfur in *n*-heptane or *n*-centane in increasing time intervals with the results placed in order and numbered [86].

It was thought that these copper strips covered the entire range from no corrosion to black and scaly. Colour changes were attributed to light interference through a thin copper sulfide film which increased in thickness as the time interval, and also rating, increased. A study by Kashima and Nose [86] did not find this to be the case. Tests conducted by Reid and Smith [26] with different concentrations of elemental sulfur found ratings of 1a or 4a however there did not appear to be any transition through the ratings, rather samples showed both 1a and 4a areas. This suggests that the test may not be too sensitive and highly subjective. It has been suggested that copper strips rated 1a to 3a differ only in film thickness with the change in colours due to interference effects.

Table 3.1: Copper strip rating descriptions [84, 87]

Rating	Designation	Visual description
1a	Slight tarnish	Light orange, very similar to freshly polished strip
1b		Dark orange
2a	Moderate tarnish	Claret red
2b		Lavender
2c		Multi-coloured with lavender blue and/or silver overlaid on claret red (no green)
2d	Dark tarnish	Sliver
2e		Brassy or gold
3a		Magenta overcast on brassy strip
3b		Multi-coloured with red and green showing (peacock), no grey
4a	Corrosion	Transparent black, dark grey or brown with peacock green barely showing
4b		Graphite or lustreless black
4c		Glossy or jet black

Kashima and Nose [86] used electron diffraction to look at the surface films and found that the composition of the film was often Cu_2O for lower rated samples with Cu_2S over layers and only at higher ratings was Cu_2S found alone. The colour change was attributed to a change in the thickness of copper oxide films in the lower portion of the scale 1a–3a, rather than copper sulfide films as was originally proposed during the development of the test. At higher ratings, the formation of cuprous sulfide and cupric sulfide contributed to the colour. They also determined that the degree of corrosion shown in the ratings was not linear.

Although useful for screening large numbers of fluids quickly, the ASTM D130 does not identify the cause of the test failure [26]. The actual depth of the film or degree of corrosion were not considered to be relevant when the ASTM D130 test method was developed [86].

Corrosion in oil is often attributed to sulfur species, which naturally occur in crude oil and are not fully removed on refining [13]. Many studies focus specifically on corrosion caused by different sulfur compounds [26, 66, 69, 70, 85, 87–91].

A number of studies have analysed the surface of copper strips which have undergone the ASTM D130 test to see if correlations can be found between the ratings and analytical results [26, 85, 87, 89]. García-Antón et al. [87] studied the corrosivity of

different sulfur compounds to copper using the ASTM D130 test coupled with SEM and EDX in order to visualise the surface and determine the amount of sulfur present.

All tests were conducted in synthetic naphtha with increasing concentrations of sulfur compounds. Elemental sulfur showed a linear relationship between the amount of sulfur on the copper surface and the amount dissolved in solution. Ethylmercaptan also showed a linear relationship between the sulfur in solution and on the copper surface. No other mercaptans tested showed corrosion and no sulfur was detected on the surface, concluding that the corrosiveness of mercaptans decreases with increasing molecular weight. These relationships can be seen in Figure 3.9 for the elemental sulfur (left) and ethylmercaptan (right). Interestingly elemental sulfur in synthetic naphtha only showed 4a ratings, although the colour intensity increased with sulfur concentration. Ethylmercaptan in synthetic naphtha progressed through the rating system, which are indicated on the graph.

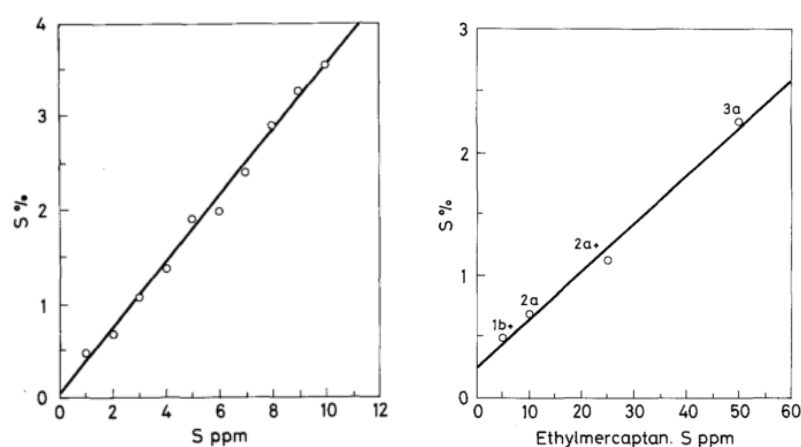


Figure 3.9: S % concentration on the copper strip versus S concentration in mg l^{-1} of sulfur (left) and ethylmercaptan (right) [87]

Reid and Smith [26] showed that the amount of sulfur present at the surface was not proportional to the test rating. A failed test piece tested in elemental sulfur had a surface concentration of 3.7 % sulfur. 1-propanethiol had a sulfur concentration of 13.8 % at the surface but had a 1a pass rating. The surface ratings and concentrations of sulfur at the surface for these tests are shown in Figure 3.10.

Elemental sulfur can react with mercaptans to produce hydrogen sulfide or disulfide, depending on their relevant concentrations. [85]

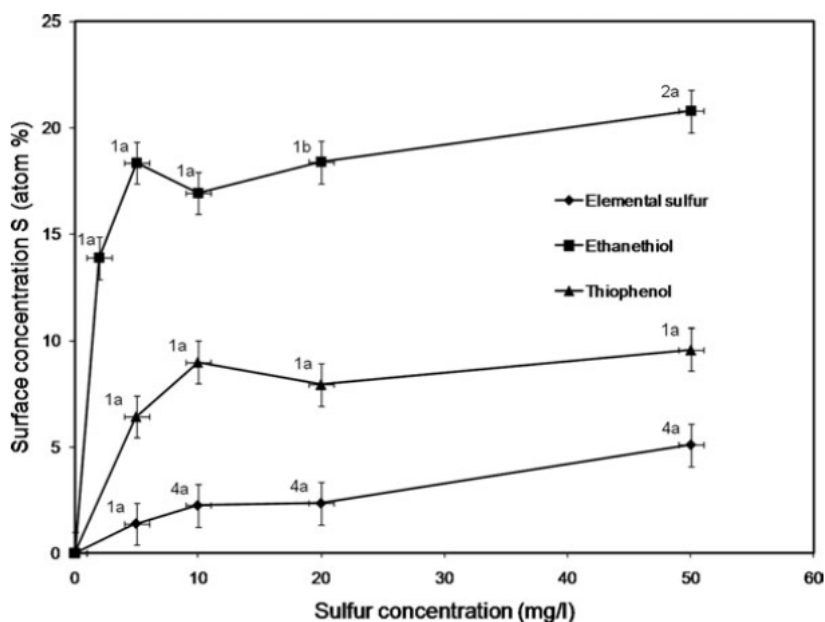
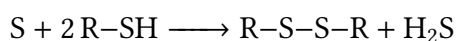


Figure 3.10: Sulfur concentration at surface versus concentration in iso-octane, also indicating test ratings [26]



Some mercaptans have been shown to produce an inhibitor effect as they absorb onto copper and so avoid attack by elemental sulfur. Low concentrations of mercaptans in solution with elemental sulfur appeared to show an inhibitor effect but at higher concentrations the corrosion of the copper was increased. Of the sulfur compounds tested diphenyl disulfide was the best inhibitor of elemental sulfur corrosion on copper [85]. A different study, conducted by Reid and Smith [26], showed that diphenyl disulfide was an effective inhibitor, except when combined with propanethiol. Surface analysis showed that when the two compounds were in solution together the diphenyl disulfide only formed a partial film leaving the remaining surface exposed to attack from propanethiol, although this did not cause a test failure.

SEM images of the surface tested with elemental sulfur showed a distribution of nodules, thought to be copper sulfide. The number of nodules increased with the sulfur concentration. Ethylmercaptan formed a uniform surface film, very different to the

elemental sulfur as seen in Figure 3.11 [87, 89].

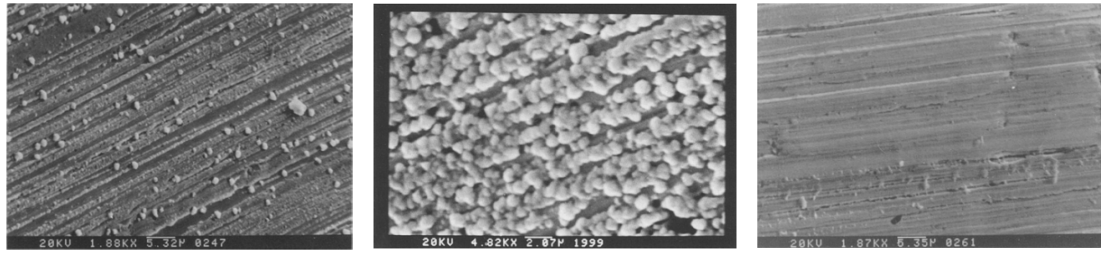


Figure 3.11: SEM of copper surface after testing in 10 mg l^{-1} of elemental sulfur (left) 25 mg l^{-1} elemental sulfur (centre) and 10 mg l^{-1} ethylmercaptan (right) [87, 89]

Schreifels et al. [88] studied films formed on copper exposed to hydrocarbons with and without the addition of elemental sulfur. Films were grown by exposing the copper to the fluid for different periods of time. The thickness of the film was estimated using sputtering rates from depth profiling. The film thickness was found to increase very quickly over 0.75 hours, which can be seen in Figure 3.12. Growth then slowed considerably as transport of copper through the film becomes difficult due to the increased thickness. This is a little difficult to see in the figure due to a non-linear x -axis.

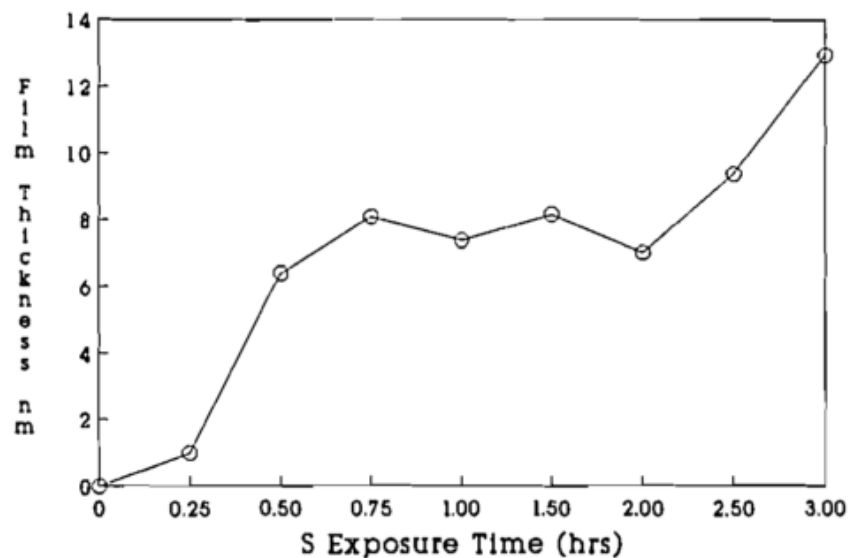


Figure 3.12: Sulfide film thickness versus time of immersion in hydrocarbon solution containing 20 ppm sulfur at $100 \text{ }^\circ\text{C}$ [88]

When copper was tested in hydrocarbon alone no sulfur was detected, suggesting that the sulfur level in the fluid was negligible. Analysis of the copper surface tested in hydrocarbon containing dissolved elemental sulfur showed S, C, O and Cu in various

relative concentrations changing with respect to the immersion period. The film was sputtered and the relative intensity of each of the elements measured.

The topmost outer layer of the film consisted of carbon and oxygen which quickly decreased in intensity. The amount of sulfur detected rose dramatically as the carbon and oxygen concentration diminished, the amount of copper rose steadily throughout the film before the bulk was reached. The amount of copper and sulfur was reported to be closely linked as one increased the other seemed to decrease. This can be seen in Figure 3.13 but is slightly more pronounced for the sulfur line. This change in intensity indicates that the film is not purely Cu_2S but rather the ratio of copper and sulfur changes slightly through the layer with the part closest to the bulk copper having the lowest sulfur ratio, therefore most likely to be Cu_2S . XPS analysis of the film suggested that copper was in the +2 oxidation state, indicating that the outermost part of the film was more likely to be Cu^{2+} , and therefore CuS .

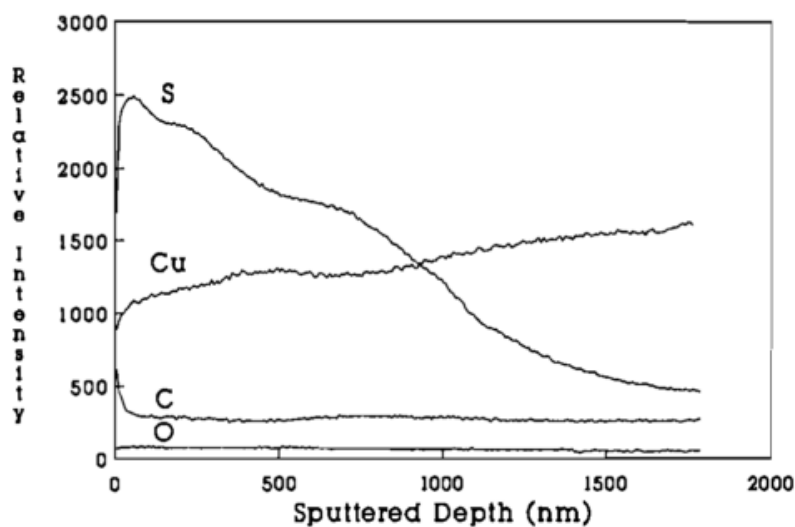


Figure 3.13: Depth profiles of components of a film formed on copper after exposure to a hydrocarbon solution containing 20 ppm sulfur for 3 hours at 100 °C [88]

Rathgeber et al. [11] acknowledges the difficulties of testing metals in ATF fluids stating that accelerated tests particularly those using elevated temperatures could lead to a change in the failure mechanism. Arrhenius behaviour is often assumed during corrosion testing which directly relates the temperature and the rate constant. It is assumed that when the temperature is increased the rate of reaction will increase, this is only true if the reaction mechanism does not change with elevated temperatures.

Rathgeber et al. [11] wanted to verify the influence of temperature on copper corrosion the amount of copper dissolved in the test fluid increased with both time and temperature for the two commercial ATFs studied by Rathgeber et al. and can be seen in Figure 3.14.

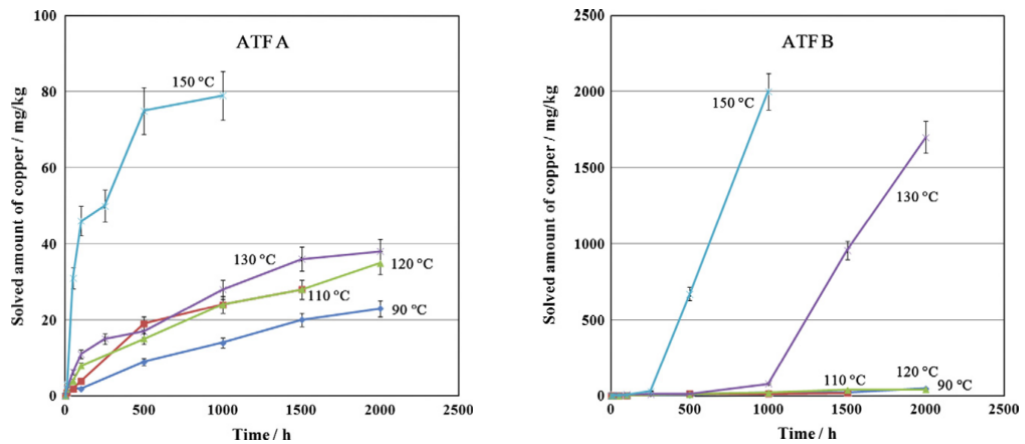


Figure 3.14: Amount of dissolved copper at temperature ranging between 90 °C and 150 °C over 2000 hours in ATF A (left) and ATF B (right) [11]

ATF A shows a steady increase of copper, with the reaction at 150 °C accelerating the dissolution of copper dramatically. Rathgeber et al. [11] suggest that the reaction is likely to be diffusion-controlled as the corrosion rate appears to decrease with time. The amount of copper in ATF B appears very different, with the amount of copper measured at 130 °C and 150 °C increasing abruptly after 1000 hours and 250 hours respectively. As the increase is almost linear they suggest the corrosion is reaction-controlled, although further study led them to believe that the reaction is actually diffusion controlled whilst the surface film remains intact.

Examining the samples showed that ATF A gave a robust reaction layer whilst ATF B did not and the reaction layer began to chip. This chipping corresponded to the large increases seen in the dissolved copper level. The surface layers formed were analysed by XPS and seemed to be mainly copper and sulfur, although other inorganic copper compounds were likely to be present. Rathgeber et al. [11] state that as the Gibbs free energy for the formation of Cu_2O is greater than that for Cu_2S and there is also a lack of di-oxygen in the fluids then copper (I) sulfide is the dominant component of the surface layer. They propose the film formation reaction shown in Figure 3.15, where copper diffuses through the reaction layer and reacts with sulfur compounds on the interface with the ATF (labelled as Interface II). They propose that this is most likely as the sulfur

present is bonded in heterocyclic compounds, for example, and is therefore chemically stable so it would be unlikely for the sulfur to separate and diffuse through the reaction layer and react at the inner interface (labelled Interface I). Rathgeber et al. do point out that although their model proposes atomic copper is diffusing through the reaction layer they do not think that it is freely diffusing and the real situation is likely to be more complex.

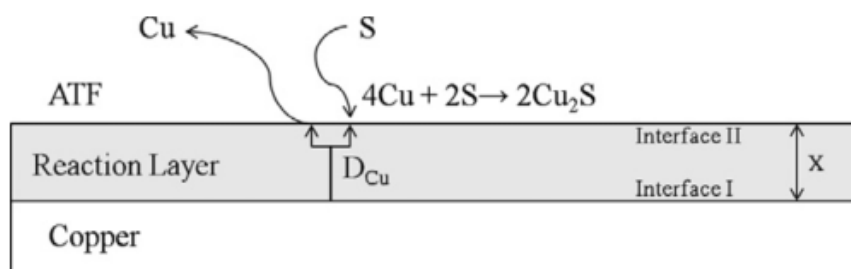


Figure 3.15: Model of film growth due to copper diffusion through the reaction layer [11]

The diffusion of copper through the reaction layer is also suggested by Schreifels et al. [88] where Cu_2S was found closest to the bulk copper and CuS found at the top of the film, with the rate of growth of the film proportional to the thickness, as would be expected for a diffusion-controlled reaction.

3.4 Copper protection by corrosion inhibitors

Corrosion inhibitors are compounds which prevent or minimise corrosion, when present in low concentrations. The protection of metals and alloys is of high importance due to their vast array of uses across diverse fields [49], consequently a wide range of inhibitors have been used for several decades [34]. The study of corrosion not only looks at how it takes place in particular environments but also how it can be prevented. Minimising the production of corrosive species is one way to minimise corrosion, using corrosion inhibitors is another [92, 93].

Corrosion inhibitors can work in two ways;

- Interacting with corrosive species in the fluid and either transforming them into non-corrosive species, or complexing with them to prevent them from interacting with the surface
- Absorbing onto the surface of the metal and forming a protective layer which stops corrosive species from attacking the surface

Polar groups, such as nitrogen, oxygen and sulfur, present in organic compounds or as functional groups on heterocyclic compounds are reported to inhibit copper corrosion [34, 49, 92, 94]. Inhibition of these compounds is attributed to adsorption of the organic species to the copper surface.

In many cases tests are carried out to look at how effective inhibitors are for particular surfaces in particular environments. As a result the precise mechanisms regarding how corrosion inhibitors work is often not known [93].

In order for inhibitors to be effective they must have a high affinity for the metal surface but in order to be delivered they must also be soluble in the medium surrounding the metal [92]. For film forming inhibitors the size, chemical structure, aromaticity and ability of the compound to cross-link all affect the efficiency. In order to understand inhibitors better information regarding the number of adsorption sites, the molecular dimensions and interaction with a metal surface is useful [34].

The presence of inhibitor films has been studied using surface enhanced raman spectroscopy [95, 96], electrochemical quartz crystal microbalance [57, 97], electrochemical impedance spectroscopy [49, 57, 97], secondary ionisation mass spectrometry [57] and XPS [66, 98] to name but a few. Each technique has been used to provide new information, such as how the inhibitor is adsorbed onto the surface, the properties of the film and the reaction kinetics.

One of the most common copper corrosion inhibitors, which has been well-known since the 1950s, is benzotriazole (BTAH) [34, 39, 49, 57, 66, 68, 69, 75, 93, 95–108], although similar heterocyclic compounds, such as thiazole, imidazole and triazole along with their derivatives [94] are also used to protect copper, primarily in aqueous environments. Basic structures of the compounds are given in Figure 3.16.

The ability of heterocyclic molecules to protect copper from corrosion comes from

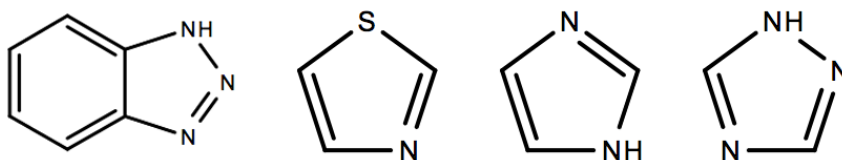


Figure 3.16: Basic structures of azole compound inhibitors. Left to right; benzotriazole, thiazole, imidazole and 1,2,4-triazole

their ability to form polymer-like films on the surface [49]. Figure 3.17 shows how inhibitor molecules adsorb to a metal surface forming a protective layer.

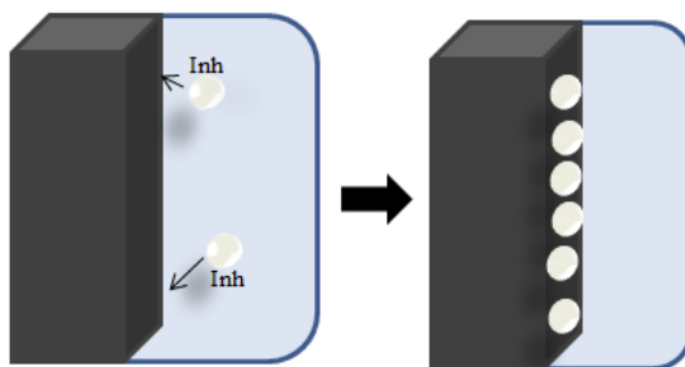


Figure 3.17: Schematic showing the adsorption of inhibitor onto a metal surface, where Inh represents the inhibitor molecules [92]

Benzotriazole was already established as a corrosion inhibitor for copper when it was discovered that the protected metal could be exposed to a new environment and retain its protection [39, 98]. The films formed from aqueous solutions or after exposure to vapour of BTAH were not easily washed off and so it is thought that there is more permanent chemical bond formed.

Evidence suggests that the film is polymeric in nature and so the simplest explanation of protection is that a continuous film is formed [39, 57, 95]. Cotton and Scholes [39] suggest that a continuous film is unrealistic and instead the film is more likely to reinforce the protection offered by cuprous oxides films normally present on the surface, particularly where there are defects. Holm et al. [57] and Fang et al. [109] showed that an oxide layer was not needed for absorption to occur and BTAH would form a film on both Cu and Cu₂O surfaces.

Bayoumi et al. [97] studied the kinetics of BTAH growth on a copper surface. They identified a period of initial very fast growth which was attributed to the formation of a

Cu(I)BTA complex, a slower second period of growth was attributed to growth of BTAH on top of this complex until a plateau was reached, as indicated in Figure 3.18.



Figure 3.18: Schematic illustration of outer layer growth of BTAH film on inner layer of Cu(I)BTA complex [97]

Over the years several theories have been presented to try and explain how the BTAH molecule bonds with the copper surface. One of the more prevalent theories is that one of the nitrogen atoms bonds covalently to a copper atom and another of the nitrogens then binds coordinatively with the next copper, producing a polymeric like layer [39, 57, 110]. This structure has never been conclusively proved [75, 96, 100], although most theories suggest that the main bonding occurs between the copper and nitrogen atoms.

The protection of corrosion inhibitors in aqueous media are most frequently studied. Oil based studies are less common but can often be found in relation to corrosion prevention in transformer insulating oil, where corrosive sulfur is often the cause of failure [66]. Temperature and operating load are also important factors when considering the failure mechanism [69].

Wan et al. [66] studied corrosion prevention of copper windings in transformer oils with and without the inhibitor irgamet 39, which is a benzotriazole molecule with a branched carbon chain to aid solubility in oil. They concluded that the addition of the inhibitor prevented the corrosion of the copper caused by sulfur, but the amount present was an important consideration. BTAH is known to complex with copper and they found excess inhibitor coordinated with copper ions dissolved in the oil and enhanced the catalytic activity, leading to degradation of the insulating oil.

Qian and Su [69] also found that BTAH was able to prevent corrosion, caused by sulfur in insulating oils, at a variety of temperatures.

Thiadiazole derivatives are also popular corrosion inhibitors for copper [27, 49, 94, 111–115]. Like other effective inhibitors they are also based on heterocyclic rings and

have two carbon, two nitrogen and one sulfur atom, along with two double bonds; this means there are several different isomers that can be used.

One benefit of thiadiazoles is that they are considered to be non-toxic, making them an eco-friendly choice in place of some other inhibitors [27, 34].

The inhibitive action of thiadiazoles is thought to be due to their adsorption onto the surface, creating a barrier to corrosive species [27, 94]. However Luo et al. [112] suggest that corrosion inhibition is also due to scavenging the active sulfur in the fluid.

There have been some reports that the inhibition efficiency increases with concentration [115], but decreases with temperature [27, 94].

The exact interaction with the surface is uncertain [58] but Ling et al. [111] proposed that the molecules could interact with the copper surface in such a way as to create a continuous adsorbed polymer chain, as shown in Figure 3.19.

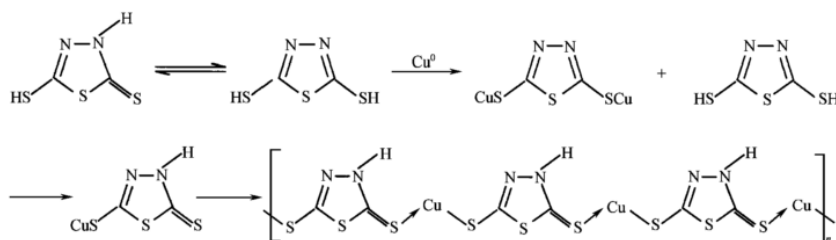


Figure 3.19: Model of the interaction mechanism of DMTD with a copper surface [111]

Hipler et al. [113] propose a different mechanism, but what is interesting is that they observed the breakdown of the thiadiazole molecule at higher temperatures. Their adsorption model is shown in Figure 3.20. It should be noted that the thiadiazole molecule has slightly different side chains and was deposited using vapour deposition.

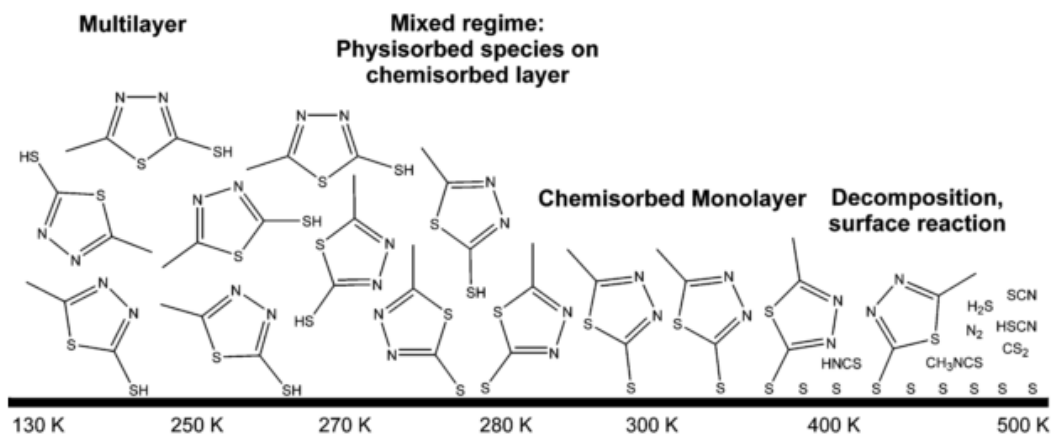


Figure 3.20: Schematic diagram of the adsorption and decomposition of 2-mercapto-5-methyl-1,3,4-thiadiazole adlayers on gold by chemical vapour deposition [113]

3.5 Methods of monitoring corrosion

Corrosion monitoring at its simplest can be described as collecting data on the rate of material degradation [30]. In some circumstances, however, information regarding the build up of protective films or surface layers is desired.

There are many methods which can be used to monitor corrosion. Some are able to follow the corrosion in-situ, whilst others rely on changes measured at the end of test or at specific time intervals, to provide information on the corrosion that is occurring. Testing may be carried out in a laboratory, field test or service test.

In a laboratory, conditions can be carefully controlled in order to identify the effect of specific factors on corrosion behaviour. Often accelerated testing is used, where the severity of a particular factor is increased in order to speed up corrosion. Such results should be carefully considered as the results can be very different to those which would occur under normal use [43].

Service tests are carried out on real components as opposed to sample specimens and are often used after other tests have been carried out in order to confirm results [43]. For example a period of laboratory testing may be conducted to provide information on the corrosion likely to occur in an engine from a series of different oils. Once the best oil has been determined from the laboratory tests a service test would be conducted to ensure that the results seen in the laboratory were the same as those seen in service.

Field tests are a step up from service tests and are carried out on real components in their actual working environment.

As field and service tests can be very costly laboratory tests are most commonly conducted. These also allow many different factors to be varied and analysed to provide better understanding of the mechanisms taking place. There are a wide range of tests commonly used to monitor corrosion such as; the weight change of samples; the colour of a corroded surface; the elements or functional groups present on a surface or in a fluid; or the electrical impedance of a system. Some surface analysis techniques can have their limitations as they give a picture of the surface only at one point whilst corrosion is a dynamic process [116]. For many surface analysis techniques the sample must be removed from the corrosive environment and in most cases placed into a vacuum. This can cause changes to the surface structure [19].

The techniques chosen will depend on what specifically is to be measured and how fast the corrosion process occurs. If the reaction is slow then static monitoring can be more effective with data collected every few hours, days, or even months. Fast changes are better monitored in situ if possible.

A number of different monitoring techniques shall be examined to try and identify those most suitable for studying the interaction between ATF additives and copper surfaces.

We shall begin by considering what is likely to occur at the surface of the copper, of which there are three main options; dissolution of copper into solution, formation of a film or corrosion deposit on the copper surface, or a combination of both. These are shown schematically in Figure 3.21.

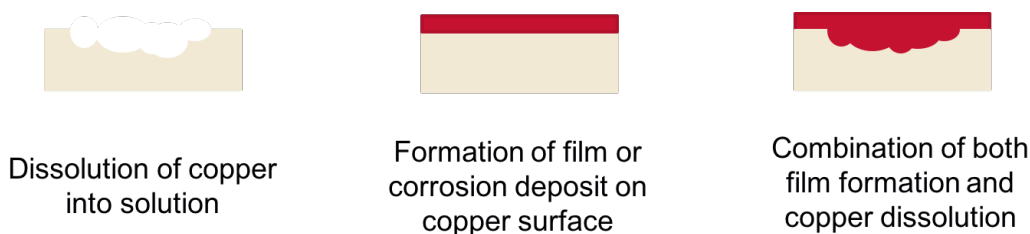


Figure 3.21: Schematic diagram of the possible interactions occurring at the surface

When considering monitoring techniques these three options should be taken into account to determine if the technique would be able to give meaningful information.

3.5.1 Gravimetric techniques

Measuring the weight change of samples in corrosive environments using highly sensitive balances is widely used to monitor degradation [34, 117]. This can work well for samples that have significant weight loss and are cleaned thoroughly before weighing [118].

If copper dissolution was the only thing occurring at the surface then it is possible that weight loss could be detected if the corrosion was severe enough.

If formation of a film or corrosion deposit were to occur it may be possible to detect a weight gain, provided that the film was not removed when cleaning the sample. Interestingly Ohajianya and Abumere [62] were able to calculate the thickness of Cu_2O on copper by using the density and weighing the sample before and after the removal of the Cu_2O film. This technique appeared to work well but for use in other situations you would need to know the exact nature of the film and its density in order to be able to calculate the thickness.

If a combination of both film formation and dissolution were to occur this could be more difficult to detect, particularly if the material lost were similar in weight to that gained, giving no overall weight change.

It could be difficult to tell which of these may be occurring at the surface particularly as any film or deposit formed on the surface would want to be retained for further analysis.

It can be difficult to study small weight changes, or changes which happen in very specific environments, using conventional balances. Thermogravimetric analysis (TGA) and quartz crystal microbalance (QCM) techniques can be used to study small changes in weight.

3.5.1.1 Thermogravimetric analysis (TGA)

TGA can be used for several different measurements. A sensitive microbalance can be used to record the weight of the sample with time, whilst it is held in a specific environment. The temperature can be varied with time or held constant, and the technique is often used to study oxidation or high temperature corrosion [117]. The atmosphere is also closely controlled and a number of different gases can be used, such as oxygen, nitrogen or hydrogen.

As well as looking at the weight change in solid samples TGA can also be used to look at the stability of oils [80] as the weight loss indicates when specific molecules begin to evaporate. In ATF formulations this could be used to see when specific additives, for example the antioxidant, begin to evaporate [119].

Some of the processes which can be studied using TGA are oxidation rate, surface adsorption, or desorption [117]. Although many different processes are able to be probed, the sample size is limited for TGA with samples less than 1 g, and with precision of around 0.1 μg .

This study is interested in the interaction of copper surfaces immersed in ATF fluids and so TGA analysis is not the right technique to use.

3.5.1.2 Quartz Crystal Microbalance (QCM) technique

QCM is able to measure changes in the order of nanograms and was originally used to measure thin film deposition. QCMs work by passing a current through a quartz single-crystal, causing it to oscillate. The oscillating frequency changes depending on the mass of the absorbed surface film [97].

The technique can be used in a vacuum, in air or in a liquid, however the viscosity of the fluid affects the crystal oscillation, with higher viscosities giving less oscillation [117]. This is potentially problematic for tests carried out in oils as they tend to have higher viscosities.

In order to study surface interactions it is possible to coat the crystal with copper, which would be most useful for this study as interactions between ATF additives and copper are being investigated. QCM can be used to monitor the build up of deposit on a

surface, caused by degradation of an oil [120]; the dissolution of the metal surface into solution; or the build up of different inhibitor films on the surface [34].

The equations which are used to interpret QCM results [49, 117] often assume that the film formed on the surface is rigid, however a dissipation technique can be used that looks at films which are not fully rigid. This may be required as the molecules present in an ATF often have long carbon chains to make them soluble and if these were absorbed onto the surface the film is unlikely to be rigid.

Although QCM results can show very precise changes to a surface, when monitoring adsorption or corrosion in-situ often ideal solutions are studied, with only one molecule present. The difficulties in monitoring molecules with long non-rigid tails in oil means that this technique is probably not right for this study.

3.5.2 Electrical resistance techniques

Techniques which monitor changes in the electrical resistance of conductive materials in corrosive environments have been used for several decades. As the material undergoes corrosion, the cross-sectional area decreases and this change will be measured as an increase in the resistance [118, 121]. These probes are simple to use and give changes in real time with results that are simple to interpret.

This technique is similar in ways to an immersion test, in that the material is simply exposed to the environment. It differs in that the information gathered can show whether or not the corrosion rate is constant [121], which is assumed in immersion tests. The assumption made during electrical resistance tests is that corrosion is uniform; non-uniform corrosion can only be seen through visual inspection of the probe, which is encouraged.

Conventional electrical resistance probes can sense a minimal thickness loss of 1 μm according to Brossia [121]. A newer technique introduced by Hunt and Gahagan [116, 122, 123] measures the resistance change of thin wires and appears able to detect changes of 0.2 μm .

It is not only wires that can be used to measure corrosion. Agoston et al. [81] proposed a method for determining the resistance change of a thin copper film, a schematic

of which is shown in Figure 3.22. This test was demonstrated in both laboratory and field testing using a variety of oils.

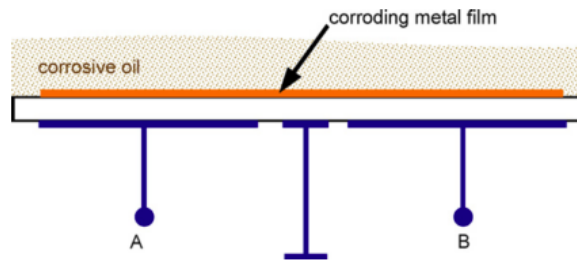


Figure 3.22: Schematic showing measurement of corrosive material loss from copper film, where A and B are electrodes measuring the sacrificial metal film [81]

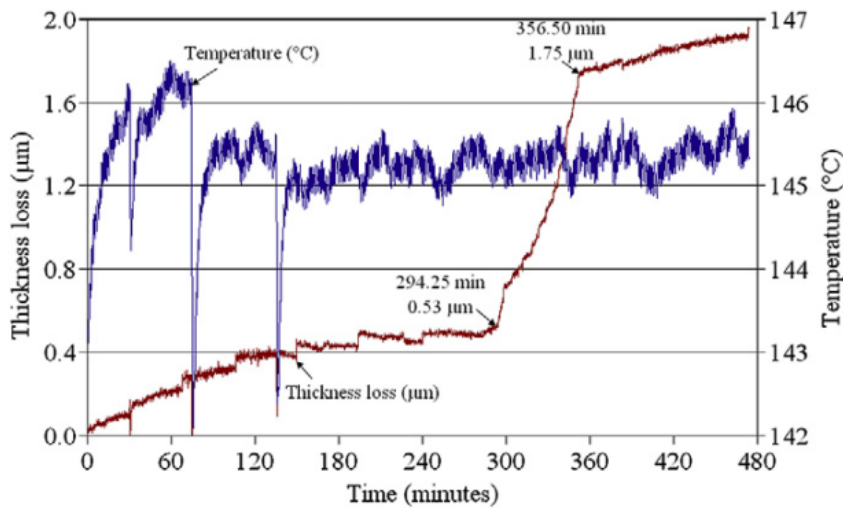


Figure 3.23: Thickness loss of copper foil with time, exposed to sulfur vapour at 140 °C [124]

A similar technique was employed by Thethwayo et al. [124] who were able to see distinct changes in the corrosion rate of copper foils exposed to sulfur vapour, as shown in Figure 3.23. They attributed the sudden change in rate to cracking of the corrosion product which exposed fresh copper to the corrosive gas.

As electrical resistance probes measure the current passing through the sensing element, they can be used in many different corrosive environments and, unlike electrochemical techniques, the environment does not have to be able to carry a charge [121]. This makes it an ideal technique for monitoring corrosion in oil based environments which are close to real life transmission environments.

Thinking back to the three proposed interactions, dissolution of copper could be measured easily and in-situ giving more information than a static measurement at the end of the test. If film formation were to occur this would not be easily detected, unless the film were conductive. This method is likely to give the best results regarding material loss and so could be coupled with other techniques focusing on film formation.

Electrical resistance looks to be a good way of measuring the material loss from copper in an oil based environment. If wires are used the surface area may present difficulties in analysing the surface and so another method should also be used. A simple immersion test could be run in conjunction with the resistance tests to allow a better surface for analysis. The industry standard ASTM test may be a good starting point.

3.5.3 Industry standard ASTM D130 testing

In industry a test to measure the corrosiveness of a lubricant to copper was first introduced in 1921, with the current edition of the standard test method approved in November 2012 [125]. The “standard test method for corrosiveness to copper from petroleum products by copper strip test” (ASTM D130) [84] is used to determine how corrosive a lubricant is likely to be when in contact with a copper surface.

The ASTM D130 can be used with a wide variety of different petroleum products from aviation gasoline to lubricating oil. The document states that crude oil contains sulfur compounds, which, depending on their chemical type, can be corrosive to metal. As the corrosivity is dependent on the chemical nature of the sulfur, corrosiveness is not necessarily related to sulfur content [84]. Ultimately this test looks at how sulfur corrodes the copper surface. This seems appropriate for products which could still contain sulfur, however, lubricants are often made from base oils which contain less than 0.03 % sulfur, most of which is unlikely to be elemental and therefore would not corrode the copper. Despite this, the ASTM D130 is the main test used to look at the compatibility of ATFs with copper [78].

The ratings are taken at the end of a three-hour test and the rating is purely visual, so there is no way of knowing if the colour perceived is due to removal of the copper or a build-up of protective film. The ratings are non-numerical and although pass rates

are set it is not possible to know how much worse one rating is from another. The test can also be subjective depending on the person rating, consequently all raters must be specially trained, however this does not get rid of all variation as differences in lighting can also impact the results. The test is quick to run and can be used to screen a large number of fluids for further development, but due to the lack of information obtainable it is not the most robust test to monitor corrosion.

Reid and Smith [26], as previously discussed, used the ASTM D130 method alongside XPS analysis to determine the concentration of sulfur present on the surface of copper strips immersed in solutions containing different types of sulfur. They concluded that the rating achieved was not directly related to the concentration of sulfur present in either the solution or on the surface.

As this is the standard test required in the industry it would be interesting to run alongside other test methods. The ASTM D130 does not give a numerical result however it is able to place the samples in order of the severity of corrosion seen, it would be interesting to see if the results of the electrical resistance technique would place the samples in the same order.

As the ASTM D130 test is run using coupons it would be possible to analyse the surface using various analytical techniques.

3.6 Characterising corroded surfaces

There is no single technique that can provide all the desired information about a corroded surface. Many techniques can be used to analyse corrosion products and features, choosing the correct ones depends on the specific situation [126].

Analytical techniques can be placed into two main groups, those which look at the surface morphology, and those which allow chemical identification and composition of the surface. Different information is available from each technique, a number of which have been summarised in Table 3.2.

3.6.1 Surface morphology

There are a number of techniques which can be used to visualise and image surfaces. These techniques can use an array of different particles, for example, photons, electrons or ions, to visualise the surface of a sample. In order to completely analyse a sample multiple techniques would need to be used [127].

Table 3.2: Surface sensitive analytical techniques and information obtainable by using them [24, 127]

Analytical technique	Target information	Depth of analysis
Surface morphology		
Optical microscopy	Macroscopic surface structure	Visible surface
Scanning electron microscopy (SEM)	Microscopic surface structure	Sub μm
Backscattered electron images (BSE)	Microscopic surface structures with contrast possible between different atomic weights	Sub μm
Chemical identification and composition		
Energy dispersive X-ray spectroscopy (EDX)	Elemental identification of the surface species	1 μm
X-ray diffraction (XRD)	Crystallinity of corrosion products	10 μm
Fourier transform infra-red spectroscopy (FTIR)	Identification of molecular vibrational structure and bonding interactions with the surface	Few μm
Raman spectroscopy	Identification of vibrational structure of molecules adsorbed on the surface	Few μm
X-ray photoelectron spectroscopy (XPS)	Elemental identification of top surface species, electronic structure, chemical bonding and elemental depth profiling	3 nm

3.6.1.1 Optical microscopy

Optical microscopy is possibly one of the simplest techniques that could be used to look at a surface. It is a magnification technique which allows us to view structures below the resolving power of the human eye [128] with practical magnification up to around

1500x. Although it is a simple technique it is able to identify if the surface is uniform and pick out places of interest for further analysis.

Optical microscopy uses only light to image a sample and as such it is a non-destructive analytical technique, with little to no sample preparation required. Optical microscopy is often used as a reference technique to visually inspect the surface, before and after other techniques are used, for any damage caused.

Corrosion is often identifiable using optical microscopy, particularly when it covers a significant area of the surface [24]. However Frankel [36] and Zhou [45] mention the use of video microscopy to follow the evolution of corrosion pits.

Optical microscopy is a readily available technique however it is used in many studies as a way of checking samples rather than analysing them in great detail, for example checking for scratches or the presence of uniform layers [11, 65, 97, 99, 129]. It is also used as a means of examining the surface when using another analytical method, such as Raman spectroscopy [130, 131] or FTIR microscopy [132].

3.6.1.2 Scanning Electron Microscopy (SEM)

Scanning electron microscopy (SEM) is a widely-used surface analytical technique [11, 50, 56, 87, 89, 124, 133]. In order to create an image a beam of incident electrons is fired at the sample where it penetrates into the surface. This interaction leads to a number of different emission signals which can be seen in the form of a schematic diagram in Figure 3.24.

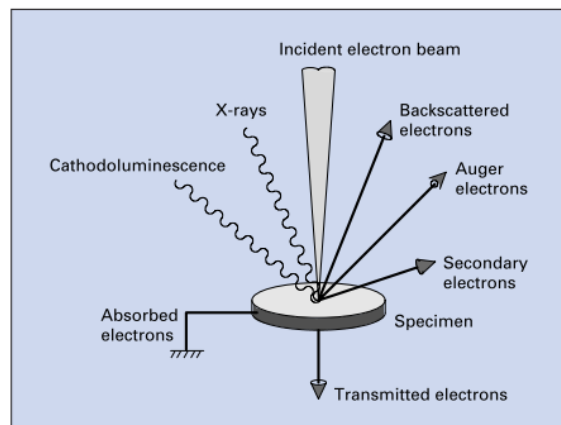


Figure 3.24: Schematic of different signals emitted from a specimen on interaction with an incident electron beam [134]

Of these different emissions secondary electrons are used to image the sample as they are most sensitive to the surface structure. Care must be taken when setting the accelerating voltage of the electron beam; the higher the voltage the greater the beam penetration.

Greater penetration minimises the contrast of the surface, making images less clear. This can be clearly seen in Figure 3.25 where accelerating voltages of 10 kV, 3 kV and 1 kV (left to right) have been used to image a surface. The surface imaged at 10 kV has become translucent and at 3 kV the edges of the plate structures are very bright. The clearest image is given when an accelerating voltage of 1 kV is used [134].

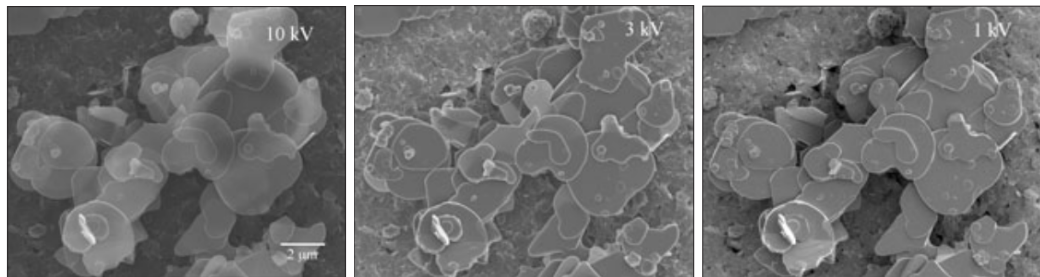


Figure 3.25: Contrast differences in secondary electron images when accelerating voltage is varied [134]

When the incident electron beam interacts with the sample it is important that the sample is able to conduct the electrons. Non-conducting samples can give problems with charge build up, where a large negative charge accumulates, distorting the image or leading to bright areas. In order to prevent charge building up, the sample should be conductive. If the sample is non-conductive it can be coated with a conductive layer thin film, such as gold or carbon [128]. Using a low accelerating voltage can also help to minimise charge build up.

In some ways SEM is similar to optical microscopy, both are imaging techniques used to look at the topography of a surface. However SEM has a greater depth of field, meaning surfaces with irregularities can often be easier to image [134]. Greater magnification limits are also possible, due to the use of electrons, with 5,000x–100,000x being a typical operating range, but it is possible to achieve magnification of up to 300,000x [127, 128].

Kong et al. [135] used SEM to look at the surface morphology of copper after reaction with SH^- . The images, shown in Figure 3.26, show how the porosity of the surface layer

changes with temperature which helped to explain the differences in corrosion rate.

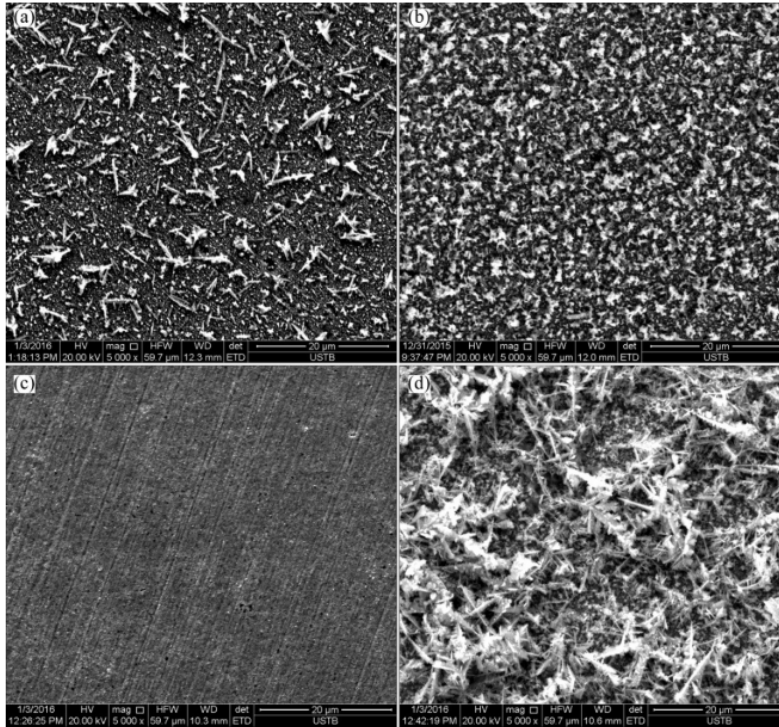


Figure 3.26: SEM images of copper surface exposed to sodium sulfide at different temperatures: a) 20 °C, b) 40 °C, c) 60 °C, d) 80 °C [135]

It is also possible to make very accurate size measurements with an SEM, this can often be useful in determining the size of pits formed during corrosion, for example.

One other advantage of SEM over other high magnification techniques is that sample preparation is often minimal, provided the sample is vacuum compatible and fits inside the instrument sampling chamber. However, the interaction between the beam and the surface can lead to damage, particularly with higher beam energies. This means that care must be taken if other techniques are to be used to characterise the surface after SEM has taken place.

3.6.1.3 Back Scattered Electron (BSE) images

As can be seen from Figure 3.24 the incident electron beam used in SEM emits not only the secondary electrons used for surface imaging but also backscattered electrons. Backscattered electrons have a higher energy than secondary electrons and therefore give information from deeper in the sample [128, 134].

The amount of electrons scattered is directly proportional to the atomic number of the scattering element, meaning that BSE images can visually show variation in atomic

number [134]. Larger heavier elements scatter electrons more readily and so appear brighter than smaller lighter elements. This makes BSE imaging suitable for looking at compositional differences, such as alloys for example.

Thethwayo and Garbers-Craig [124] used BSE to study cross sections of corrosion products formed on the surface of copper. The difference in brightness allowed them to more easily identify the different copper-sulfur layers formed, although the elements present were identified with the use of XRD. Figure 3.27 shows images of the cross sections taken after the copper had been exposed to sulfur vapour.

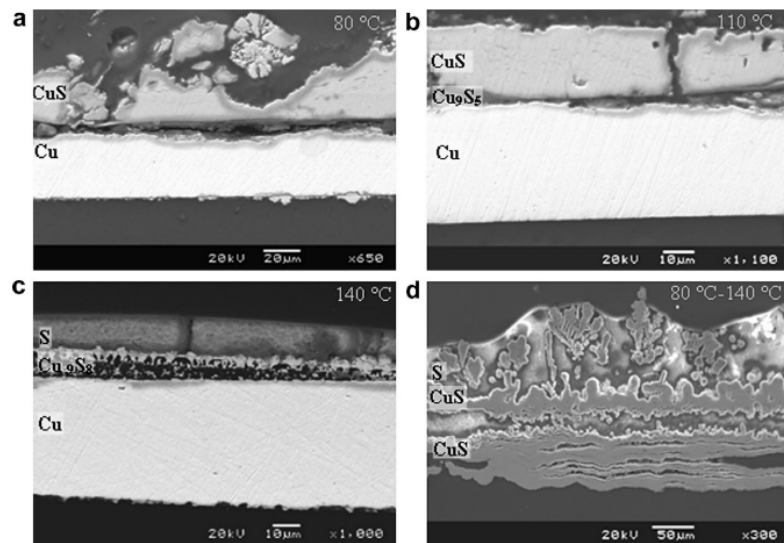


Figure 3.27: Cross sectional BSE images of copper exposed to sulfur vapour: a) 80 °C, b) 110 °C, c) 140 °C, d) 80–140 °C [124]

3.6.2 Chemical Characterisation

Although the surface morphology can give us information such as there is a deposit present, or pitting has occurred, it is not enough to simply look at a surface. Being able to chemically characterise a surface can provide valuable information about how it has corroded, or interacted, with a solution. Knowing the make-up of any film formation or deposit can begin to help identify mechanisms of surface interaction. A number of techniques which can be used to look at chemical composition are listed in Table 3.2 and detailed below.

3.6.2.1 Energy Dispersive X-ray spectroscopy (EDX or EDS)

One benefit of SEM is that due to the interaction of the electron beam with the surface several different signals are emitted, as shown previously in Figure 3.24. This can allow the surface to be imaged, as has already been shown, but it can also allow some chemical characterisation to take place. EDX systems are often integrated into SEM instruments and so can be conducted in conjunction with imaging, with no additional sample preparation required [127, 128].

Elements give out characteristic X-rays when excited with the electron beam. The value of the X-rays corresponds to the discrete energy levels that make up an element's atomic shells. On excitation electrons can be promoted into higher energy levels; when they return to their original state they emit X-rays corresponding to the difference between the two energy levels [24, 134]. This principle is illustrated in Figure 3.28.

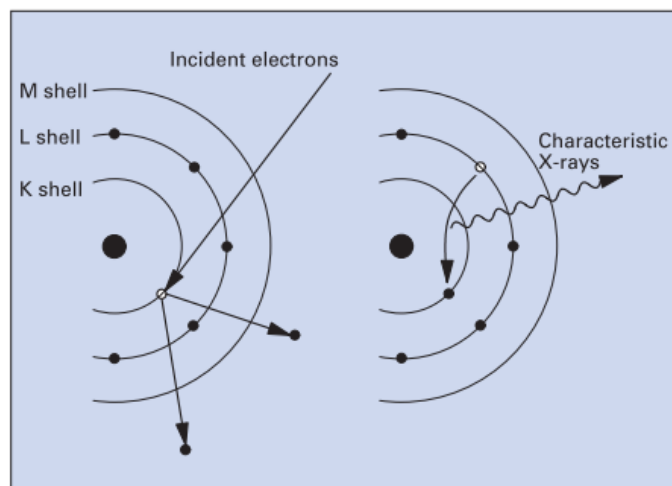


Figure 3.28: Schematic showing how characteristic X-rays are produced after the interaction of incident electrons [134]

Software is available to make the process of assigning peaks easier as it automatically assigns the energy levels to an element. Some user discretion is advised however, as these assignments can be wrong. An example of this would be the misidentification of sulfur (peak at 2.307) with molybdenum (peak at 2.293) or lead (peak 2.342) [136]. If an element seems unlikely given the history of the sample then it may be possible that another element has a similar energy level.

EDX is very useful for elemental mapping as it is possible to scan across the surface, resulting in a distribution map of specific elements. It should be noted that low molecular

weight elements cannot be detected; for the best detectors this is normally anything below boron in the periodic table [19].

EDX analysis was used by Zhu and Lei to identify the elements present in corrosion films formed on 70Cu–30Ni alloys immersed in seawater [44]. Other papers have shown the interaction of corrosion inhibitors with copper surfaces using EDX [34, 114].

3.6.2.2 Fourier Transform Infrared (FTIR) Spectroscopy

FTIR is a non-destructive, fast technique, making it ideal for studying potentially delicate, thin films. FTIR works by measuring the intensity of an infrared beam before and after it interacts with a sample [127, 137]. Functional groups on the surface absorb specific wavelengths, which cause them to vibrate, and so these wavelengths are missing from the returning beam. The absorption is dependent on the atoms and types of bond present, but the sensitivity is variable and depends on the change in dipole of a molecule when it is vibrating [127, 138]. The vibrations for each bond are well documented and the wavenumber can easily be looked up in reference tables, although some knowledge of the bonding that is likely to be present is useful as different bonds can have similar vibrational frequencies. An example of this can be seen in the simple reference regions in Figure 3.29.

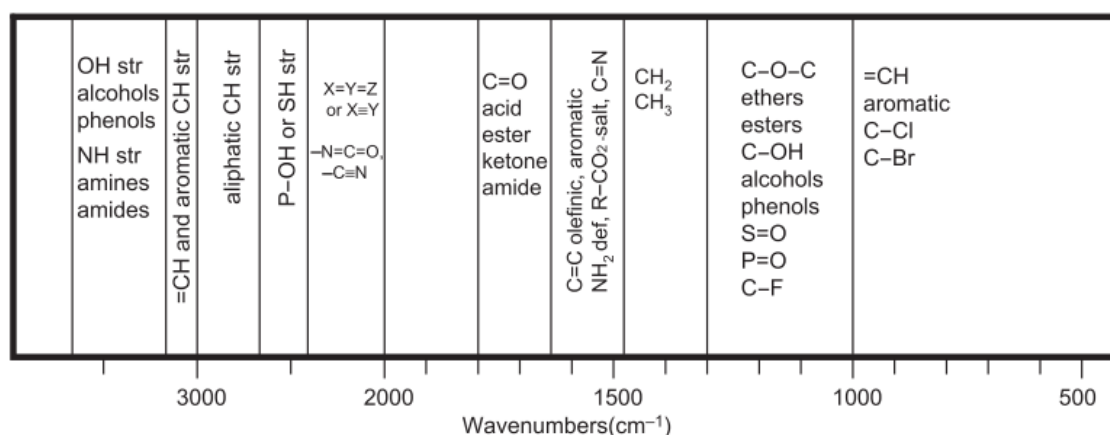


Figure 3.29: Regions of fundamental vibration of some characteristic groups [138]

There are a number of different FTIR methods, each of which suit samples in different phases. For solid samples, attenuated total reflectance (ATR) is the most popular technique as minimal pre-treatment is required. The sample is placed in contact with the crystal surface, through which the IR beam is passed; as the beam bounces through the

crystal it interacts with the sample, which absorbs specific wavelengths. For this to be successful, good contact needs to be made between the sample and the crystal. Although this method is very good, surface roughness can affect the spectrum which is often the case when looking at corroded samples.

FTIR microscopy is probably the best method for looking at corroded surfaces. It allows very specific areas of the surface to be analysed and the distribution of functional groups across the surface to be studied. It works by reflectance: the IR beam is directed onto the surface and is reflected back again where it is detected in the same way as the other techniques, giving information about the frequencies absorbed by the sample surface. Oelichmann [132] explains how infrared microscopy can be used to great effect to analyse polymer laminate films. Whilst Antonijevic and Radovanovic [49] list a number of different studies which used FTIR spectroscopy to characterise corrosion inhibitors and their adsorption onto copper surfaces.

Hegazy et al. [139] used FTIR to analyse the spectra of quaternary ammonium inhibitors, whilst many other papers use it to look at other inhibitors [66, 94, 140] or monitor oil [65, 141]. If the additives proposed in this study gave distinct FTIR spectra it would be interesting to use this technique to see if it possible to identify which additives are present on the surface and how uniform they may be. Vogt et al. [104] used FTIR spectroscopy in situ to monitor the adsorption of BTAH onto a copper surface.

As already mentioned in order for molecules to be IR active they must undergo a change in dipole upon vibration. Sometimes molecules show a change in polarisation upon vibration, meaning they are not IR active but instead are Raman active [138]. Generally, peaks which appear strong in IR spectra are weak, or do not appear at all, in Raman spectra and vice versa. This makes FTIR and Raman spectroscopy complementary techniques, which when used together can give very useful information regarding the functional groups present in molecules.

3.6.2.3 Raman Spectroscopy

Raman spectroscopy is a technique, complementary to FTIR, which helps to identify different chemical functionalities present in a sample. Monochromatic light, usually provided by a laser, is directed at the sample which then scatters the light either elastically (no loss of energy) or inelastically (loss or gain of energy) [137, 138]. Raman spectroscopy measures inelastically scattered light from a sample: the increase or decrease in energy in comparison to the incident light gives information relating to the molecular structure.

Different chemical bonds vibrate with specific frequencies, so it is possible to identify species from the energy difference between the incident and scattered light. Raman spectroscopy can be used for studying a layer of molecules on the surface of a sample as it does not penetrate very deeply, therefore measuring the surface rather than the bulk material [137]. Although Raman spectroscopy is considered to be a non-destructive technique, care should be taken with the power of the excitation laser as this can cause excessive sample heating and result in burning the film being analysed.

A number of studies use surface-enhanced Raman spectroscopy to analyse surface films or follow the build up of a surface film with time [53, 111, 131, 142]. Chan et al. [53] specified that in order to detect Cu_2O the surface layer had to be in the region of 40 Å. This could mean that very thin surface films may not be able to be measured using this technique. Procaccini et al. [52] mention that identification of CuO is difficult due to its low intensity, particularly compared to Cu_2O .

3.6.2.4 X-Ray Photoelectron Spectroscopy (XPS)

XPS is a surface sensitive technique which can be used to identify elements, and their chemical states [19]. This is achieved by bombarding the sample with X-rays which in turn excites core electrons, causing them to be emitted from the sample. The kinetic energy of the emitted electron is equal to the energy of the incident X-ray minus the ionisation energy, which was required to eject the electron from the core. A simplified schematic of this process is shown in Figure 3.30. High ionisation energies result in low kinetic energies and vice versa. Since every element has characteristic ionisation

energies associated with it, the presence of a specific element and also its oxidation state can be identified [127].

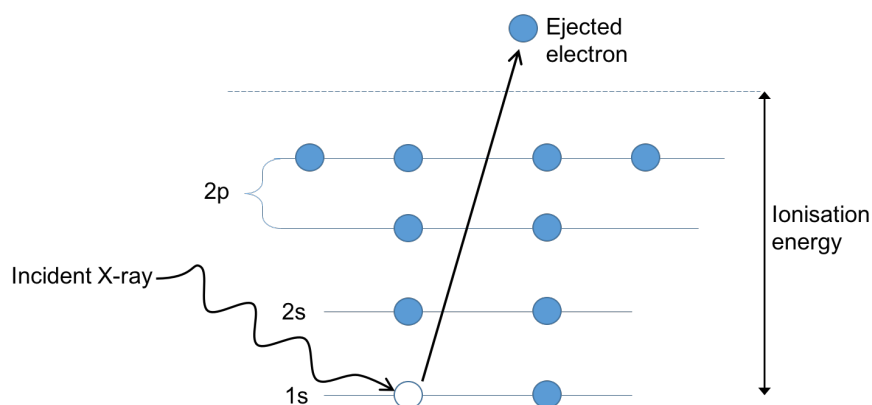


Figure 3.30: Schematic diagram showing the ejection of a core electron after excitation with an X-ray beam

Unlike some other techniques it is possible to determine the composition of both a surface film and the bulk substrate without the need for etching, provided that the film is very thin, in the region of 1 or 2 nm [126]. Although some damage will be caused to the surface through interaction with the beam the damage is far less than some other techniques, particularly when compared to those which would involve etching to give the same compositional information [19, 126].

Many studies use XPS [45, 50, 71, 88] as it is able to provide information not only on the elements present but also their binding state. For example Kong et al. [135] use XPS to determine the presence of both CuS and Cu₂S in their surface film. Whilst Finšgar [99] used XPS at various angles to study surface films with greater sensitivity.

3.7 Summary

As can be seen from this literature review there is extensive research on the corrosion of copper and how best to inhibit it in a variety of different environments.

Research that has been conducted in oil based systems often studies the effect of different sulfur compounds on copper corrosion. Studies which look at the interaction of additives, specifically those commonly found in ATF, with copper surfaces are lacking. Corrosion inhibition is well documented in aqueous systems. The same types of inhibitors can be used in ATF formulations, with the addition of carbon tails to aid the

dissolution into oil. Research regarding their interaction in oil based systems is again lacking.

This study shall look at how copper corrosion is affected by different common ATF additives, specifically how they interact with the copper surface across a range of temperatures. This shall be achieved using two main methods.

Immersion testing similar to that of the ASTM D130 method shall be conducted on coupons in order to analyse and characterise the surface. Electrical resistance testing shall be used to determine dissolution of the copper occurring at the surface. These techniques shall be used to conduct testing with both fully formulated fluids and individual additives. A systematic study will then look at how the additives interact with each other when placed in simple two and three component mixtures, in order to try and begin to understand the more complex interactions taking place in fully formulated fluids.

4: Methodology

Three main experimental setups were used to investigate the corrosiveness of ATFs to copper. An experimental method shall be given in forthcoming sections for each of these test setups:

- Full formulation coupon immersion testing;
- Copper wire tests;
- Copper wire-coupon tests used for individual additive and combination additive testing.

Immersion tests were initially carried out on copper coupons using a matrix of model full formulations. However the limited amount data available from these tests coupled with the complexity of the formulations meant it was difficult to find evidence as to which additives may be contributing towards corrosion. More information regarding when corrosion was happening, how quickly it occurred and whether it varied throughout the duration of the test was desired.

To address this need wire tests were conducted on a selection of the full formulations. Although more data was able to be obtained, and it was possible to follow the corrosion in-situ, the formulations were still complex and it was not possible to determine which of the additives was causing the observed effects. The wires were also very small and awkward to handle meaning that it was difficult and impractical to carry out detailed surface analysis.

As the coupons allowed analysis to be carried out and the wires gave in situ information about corrosion the two tests were combined. In order to simplify the fluids single additives and simple 2 and 3 component mixtures were studied. From this test setup information could be obtained regarding how each of the individual additives interacted with the copper surface particularly with regards the films that were formed and the

corrosion that could be expected.

After establishing how each of the additives interacted on their own simple mixtures of the additives were made to investigate how the additives behaved in combination with each other. This allowed synergies and antagonisms to be identified. Understanding how the additives behaved on their own and as simple mixtures then allowed comparison of the results with those obtained for the full formulations. Where the formulations were simple enough the additives causing the effects seen on the surface could be identified.

A schematic diagram showing the three different test setups is shown in Figure 4.1. While all tests were conducted in glass beakers the quantity of fluid present and the method of heating used for the coupon immersion tests was different to those used for the wire and wire-coupon tests. Further details are given in subsequent sections.

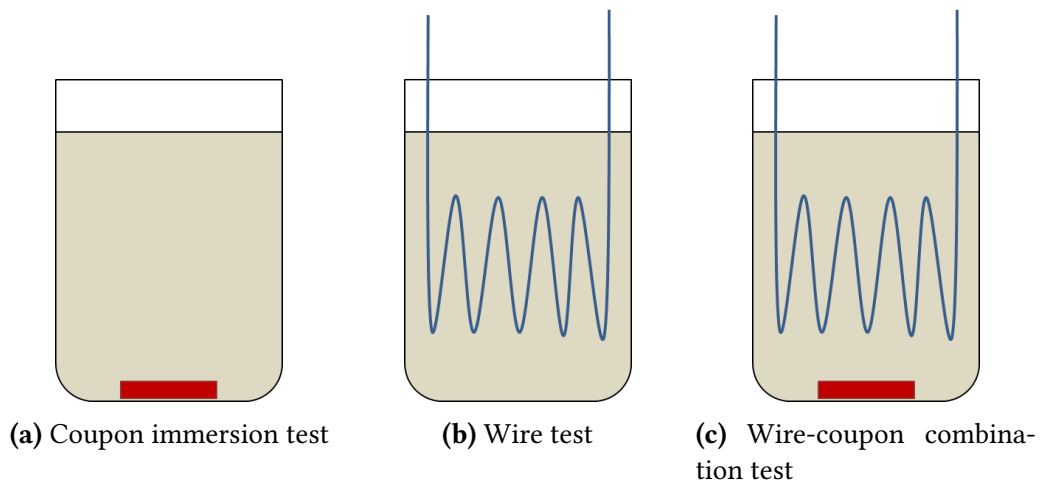


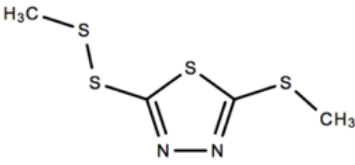
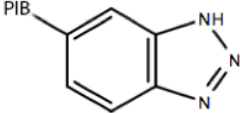
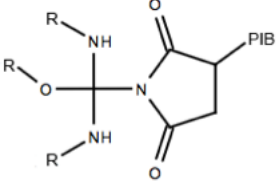
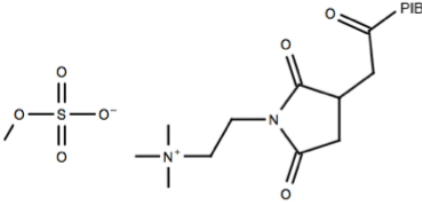
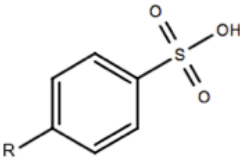
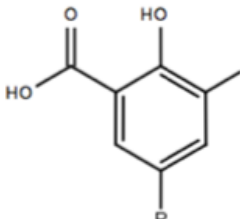
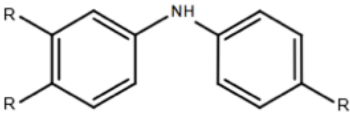
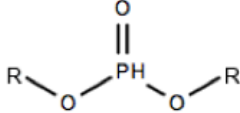
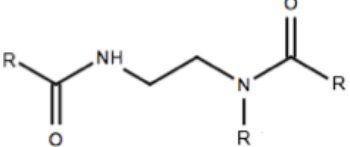
Figure 4.1: Schematic of each of the three different test methods used throughout the study

4.1 General Materials

All fluids used in this study were comprised of a combination of up to nine different common ATF additives. The additives used are presented in Table 4.1 along with an idealised structure of each of the molecules.

No additive was used neat, base oil was used to dissolve the additives and any mixtures. The base oil used throughout this study is a Group III base oil containing < 1% of shear stable polymethacrylate (PMA). The concentration of each of the additives was partly dependent upon their solubility limit, but the concentration levels studied were

Table 4.1: Structures of individual additives used for testing

Additive	Structure
Corrosion inhibitor 1	
Corrosion inhibitor 2	
Dispersant 1	
Dispersant 2	
Detergent 1	
Detergent 2	
Antioxidant	
Antiwear	
Friction modifier	

generally reflective of the levels found in traditional ATF formulations. Details of the concentrations used can be found in each of the following sections.

For cleaning, polishing, and rinsing, SBP2L solvent was used. This solvent comprised of C6–C10 paraffins and cycloparaffins with low levels of aromatics, and was used as purchased from Shell. This solvent was used as the ASTM D130 test method, which this study is partly based around, specifies the use of a volatile hydrocarbon solvent. Much of the testing was carried out in the Lubrizol laboratories where this solvent is commonly used as an alternative to heptane and was therefore the best choice of solvent .

Copper strips of 99.95% purity, purchased from Metaspec USA, were cut into approximately 1.5 cm lengths, to make coupons, and polished using cotton wool, wetted with SBP2L, and silicon carbide grit with an average diameter of 115 μm . This gave a surface with an Ra value of approximately 0.4 μm . Coupons were polished by hand for approximately 3 minutes per side until a fresh copper surface was seen and visible signs of tarnish had been removed. Polished coupons were rinsed with SBP2L and weighed using Mettler Toledo scales, with an accuracy of 0.1 mg.

Weighed coupons were placed into the pre-measured test fluid as quickly as possible to minimise oxidation of the surface. This allowed a clean surface to be produced which was similar to those found in transmissions in real-life applications.

At the end of the test the copper coupons were studied using a variety of different surface analytical techniques. These techniques shall be listed at the end of each experimental test method, but the details for the technique shall be given in Section 4.5.

4.2 Full formulation coupon immersion testing

4.2.1 Materials

Copper coupons were polished and rinsed as described in Section 4.1. For the initial investigation 22 different fully formulated model ATFs were used. Each formulation was comprised of up to nine different common ATF additives, the structures of which are provided in Table 4.1. Details of the concentration levels of each additive in each of these initial formulations can be seen in Table 4.2. The formulations were blended by Lubrizol

Table 4.2: Concentration (wt%) of additives in full formulation fluids; fluids which have been shaded were not used for wire testing

Sample number	Corrosion inhibitor 1	Corrosion inhibitor 2	Dispersant 1	Dispersant 2	Detergent 1	Detergent 2	Antioxidant	Antiwear	Friction Modifier
-776	0.03	0	0	5	0.2	0	0.33	0.11	1.2
-777	0.03	0.026	5	0	0.1	0	0.06	0.22	1.2
-778	0.5	0.013	2.5	2.5	0	0	0.06	0.11	1.2
-779	0.5	0.026	0	0	0	0	0.6	0.11	0.65
-780	0.5	0	0	2.5	0	0.4	0.06	0.22	1.2
-781	0.5	0.026	5	0	0	0.4	0.33	0.22	0.1
-782	0.03	0	0	0	0	0	0.06	0.165	0.1
-783	0.5	0	0	5	0.1	0.4	0.6	0.11	0.1
-792	0.265	0	2.5	2.5	0	0	0.6	0.22	0.1
-793	0.03	0.026	3.33	1.67	0.2	0	0.6	0.11	0.1
-794	0.265	0.026	0	0	0.2	0.4	0.06	0.11	1.2
-795	0.5	0	2.5	0	0.2	0	0.6	0.22	1.2
-796	0.03	0	2.5	2.5	0.2	0.4	0.06	0.22	0.65
-797	0.5	0.026	2.5	2.5	0.2	0.4	0.6	0.165	1.2
-798	0.265	0.013	2.5	2.5	0.1	0.2	0.33	0.165	0.65
-799	0.5	0	5	0	0.2	0.2	0.06	0.11	0.1
-806	0.03	0	5	0	0	0.4	0.6	0.11	1.2
-807	0.03	0.013	0	0	0.2	0.4	0.6	0.22	0.1
-808	0.03	0.026	0	5	0	0.2	0.6	0.22	1.2
-809	0.03	0.026	1.67	3.33	0	0.4	0.06	0.11	0.1
-810	0.5	0.026	0	5	0.2	0	0.06	0.22	0.1
-811	0	0.026	5	0	0	0.4	0.33	0.22	0.25

and each fluid had a three-digit number associated with it which was retained for ease of reference. This number became the sample number but has no other significance.

After the initial period of testing more formulations were requested. These new fluids were based on a number of the existing formulations but varied the level of corrosion inhibitor and dispersant in order to look at the impact of these particular additives. The dispersants were also dissolved alone in base oil to provide comparison information. The fluids were chosen as they showed particularly high or low levels of corrosion, as is discussed in the results Section 5.7. Details of these formulations can be seen in Table 4.3

Table 4.3: Levels of additives, wt%, in second batch of full formulation fluids after changes to corrosion inhibitor and dispersant levels

Sample number	Corrosion inhibitor 1	Corrosion inhibitor 2	Dispersant 1	Dispersant 2	Detergent 1	Detergent 2	Antioxidant	Antiwear	Friction Modifier
Base oil	0	0	0	0	0	0	0	0	0
Dispersant 1	0	0	5	0	0	0	0	0	0
Dispersant 2	0	0	0	5	0	0	0	0	0
Mix of both dispersants	0	0	2.5	2.5	0	0	0	0	0
-860	0.5	0.026	0	5	0	0	0.6	0.11	0.65
-861	0.5	0.026	5	0	0	0	0.6	0.11	0.65
-862	0.5	0.026	2.5	2.5	0	0	0.6	0.11	0.65
-661	0.265	0.265	2.5	2.5	0.2	0.4	0.06	0.11	1.2
-663	0.265	0.265	0	5	0.2	0.4	0.06	0.11	1.2
-859	0.03	0	0	0	0.2	0	0.33	0.11	1.2
-863	0.5	0	0	5	0.2	0	0.33	0.11	1.2
-864	0.03	0.026	0	0	0.2	0	0.33	0.11	1.2
-660	0.03	0.026	0	0	0.2	0	0.6	0.11	0.1
-865	0	0.026	0	5	0.2	0	0.06	0.22	0.1

4.2.2 Method

The test fluids were blended, by Lubrizol, to the concentrations defined in Table 4.2 and 4.3 and used as received.

The basic premise of the ASTM D130 test method of placing a copper coupon into a fluid, leaving it at an elevated temperature, then rating the coupon was used as a basis for these immersion tests.

A cleaned copper coupon was placed into a clean 250 mL tall form beaker, to which 100 mL of test fluid was added. The beaker was covered with a watch glass and placed into a convection oven, pre-heated to 120 °C, and left for 4 weeks. Each test fluid was run in triplicate and placed randomly throughout the oven, to prevent any sample sets being sat in a hotspot. These parameters gave a wide range of ratings, therefore allowing good differentiation between samples.

4.2.2.1 End of test

At the end of the test the beakers were removed from the oven and allowed to cool. The oil was drained and a small portion sent for ICP-AES analysis, as described in Section 4.5.1. The copper coupon was rinsed with SBP2L, reweighed and rated against the ASTM D130 standards. This rating method can be highly subjective depending on who is rating the sample and the lighting conditions used; to eliminate this subjectivity, all samples in this study were rated in a light box by myself. Where it was possible to give the surface one of two ratings, in these instances the higher, more severe rating was given.

In order to see if there was a less biased scale that could be applied, a 'digital brightness scale' was used. This involved taking two reference coupons, a freshly polished copper strip and one that was completely blackened, along with the test piece of interest. These three copper pieces were placed together on a flatbed scanner and a greyscale image taken. Software was then used to digitally rate the sample against the references, where the blackened copper had a score of 0 and the clean copper had a score of 100.

The coupons were also examined using FTIR microscopy and SEM.

4.3 Wire testing

4.3.1 Materials

Temper annealed copper wire of 99.9% purity with a 64 μm diameter was used as purchased from Advent Research Materials.

3D-printed nylon moulds were used to suspend the wires in the fluid; these shall be referred to as *formers*. They consisted of a central shaft, which was partially hollow from the middle up; the lower part of the shaft had two sets of spindles which pointed outwards. A disc-like area was on the top of the shaft, with two holes which connectors could be placed through. Two connectors were securely attached to the top disc. One end of the wire was passed up through the hollow shaft and soldered to one of the connectors; the other end of the wire was passed around the spindles, which contained shallow grooves so the wire did not slip. Once all the spindles had wire wound around

them, the wire was passed back up through the hollow shaft and soldered to the other connector. This allowed approximately 1 metre of wire to be held securely. The wire was always threaded by myself to allow consistency and was never pulled tightly in order to minimise any tension. An image of a wired former in fluid can be seen in Figure 4.2a.

A total of 16 samples were chosen from the initial sample fluid matrix, these were: base oil, -776, -778, -779, -780, -782, -783, -792, -794, -795, -796, -798, -806, -808, -810 and -811. These fluids have been highlighted as the non-shaded cells in Table 4.2. The reason for choosing these samples is detailed in the results section 6.1.

4.3.2 Method

1 m of copper wire was wound around a nylon former, as described above in section 4.3.1. A wired former was placed into a clean beaker containing approximately 400 mL of the test fluid. An image of the prepared former can be seen in Figure 4.2a.



Figure 4.2: (A) Copper wire wrapped around former; (B) Beakers in bath connected to control system

The beakers containing test fluid and a wired former were placed into a metal rack that held nine beakers, allowing them to be placed into the oil bath at the same time. After placing the beakers in the rack the connection points at the top of each former were attached to a control system which passed 1 mA of current through the wire and measured its resistance. The control system was capable of monitoring nine different wires at once; an image of the oil bath setup can be seen in Figure 4.2b.

A stabilisation period of 5 minutes was run to determine the resistance in the connecting wires, before connecting the experimental copper wire into the circuit. The rack – which held the beakers containing the test fluid and wires, attached to the control system – was then placed into a pre-heated oil bath and the resistance of the wire recorded every 10 seconds for varying periods of time. The temperature and time was dependant on the exact test run and details are given in the sections where this test was used.

4.3.2.1 End of test

At the end of the test the rack, containing the beakers, was removed from the oil bath; ensuring all beakers were removed at the same time. The beakers were allowed to cool until it was possible to handle them at which point the fluid was drained and a small portion sent for ICP-AES analysis. The wires were unwound from the formers and placed in clean polythene bags for storage, until required for analysis. The resistance data collected from the test was analysed and used to calculate the radius change of each wire.

4.3.3 Calculation of radius from resistance

Throughout the wire experiment the resistance of the copper wire was recorded. The radius change of the wire is directly related to the resistance; so rather than looking at the change in resistance data it is possible to convert the results to look at the radius of the wire. This allows the radius change of the wire to be monitored [116, 122, 123].

The first thing to note is that the resistance was recorded every 10 seconds, meaning that over the course of an average 2 week experiment, over 120,000 data points were collected for a single wire. Such a quantity of data was often difficult to work with as it made calculations very slow. For this reason the data was down-sampled.

Every six data points were averaged, which was equivalent to averaging the data collected in one minute; both the resistance data for a wire and the temperature were averaged in this way. It was these averaged values that were then used in subsequent calculations.

The resistance of the copper wire used in these experiments is governed by Ohm's law, shown in Equation 4.1, where R = resistance in Ω ; ρ_{Cu_T} = resistivity of copper in Ωm , at temperature T ; l = length of wire in m; and r = radius of copper wire in m.

$$R = \frac{\rho_{Cu_T} l}{\pi r^2} \quad (4.1)$$

In order for Equation 4.1 to be used the resistivity of the wire must first be calculated [143]. As resistivity is temperature dependant; it was calculated for every data point using Equation 4.2, where $\rho_{Cu_{20}}$ = resistivity of copper at 20 °C; T = temperature at a given point; α = coefficient of thermal expansion of copper; and ρ_{Cu_T} = resistivity of copper to be calculated at temperature T .

$$\rho_{Cu_T} = \rho_{Cu_{20}} + \alpha(T - 20)\rho_{Cu_{20}} \quad (4.2)$$

The values of α and $\rho_{Cu_{20}}$ are constants, but for reference the values used in these calculations were $\alpha = 3.86 \times 10^{-3} \text{ }^\circ\text{C}^{-1}$ and $\rho_{Cu_{20}} = 1.68 \times 10^{-8} \text{ } \Omega\text{m}$.

It is important to take resistivity changes into account, particularly when comparing differences in corrosion at higher temperatures.

Each wire differed slightly in length and during heating some thermal expansion will also take place. In order to compare values obtained for different wires, the length was normalised to 1.01 m.

In order to try and account for the thermal expansion, the start length of the wire was calculated 1 hour after being placed in the heated oil bath. After this point changes in the resistance were assumed to account for changes to the radius, rather than the length.

The start length of the wire was calculated using Equation 4.3, which is a rearrangement of Equation 4.1, where R = resistance in Ω ; r = radius of copper wire, in m (3.2×10^{-5} m in the initial calculation); ρ_{Cu_T} = the calculated resistivity of copper in Ωm , at temperature T for the data point at 1 hour; and l = length of wire, in m.

$$l = \frac{R\pi r^2}{\rho_{Cu_T}} \quad (4.3)$$

Once the start length had been calculated it was possible to normalise the length to 1.01 m. This normalisation had to be applied to all of the resistance data using Equation 4.4, where R = resistance in Ω ; l = length of wire, in m; and R_{norm} = resistance values, in Ω , normalised to 1.01 m.

$$R_{\text{norm}} = \frac{1.01}{l} \times R \quad (4.4)$$

Having adjusted the resistance data to be normalised to a length of 1.01 m, it was then possible to calculate the radius of the wire at each point using Equation 4.5, which is another rearrangement of Equation 4.1, where r_{norm} = radius of the copper wire, in m; ρ_{Cu_T} = resistivity of copper, in Ωm , at temperature T ; and R_{norm} = normalised resistance values, in Ω .

$$r_{\text{norm}} = \sqrt{\frac{\rho_{\text{Cu}_T} \times 1.01}{\pi R_{\text{norm}}}} \quad (4.5)$$

In order to allow easier comprehension the radius is presented in μm .

4.3.4 Start length determination

The length of the wire was normalised to 1.01 m as explained in Section 4.3.3 above, so that all of the wires could be compared independently of length, where radius was the only factor changing. In order to do this elongation of the wire was also taken into account. It was possible to calculate the length of wire wound around each of the formers, assuming that the radius remained at $32 \mu\text{m}$ and the only expansion of the wire was in its length.

In order to do this the resistivity of copper was calculated, using Equation 4.2 above, for the temperature at each time point. This was followed by calculation of the length using Equation 4.3. The calculated length of a number of wires immersed in different additives can be seen in Figure 4.3; the temperature of the oil is also plotted.

It can be seen that the temperature begins at 20°C and then rises rapidly to around 145°C , after which there was a slight dip followed by a gradual increase to 150°C ; the temperature at which the experiment was conducted.

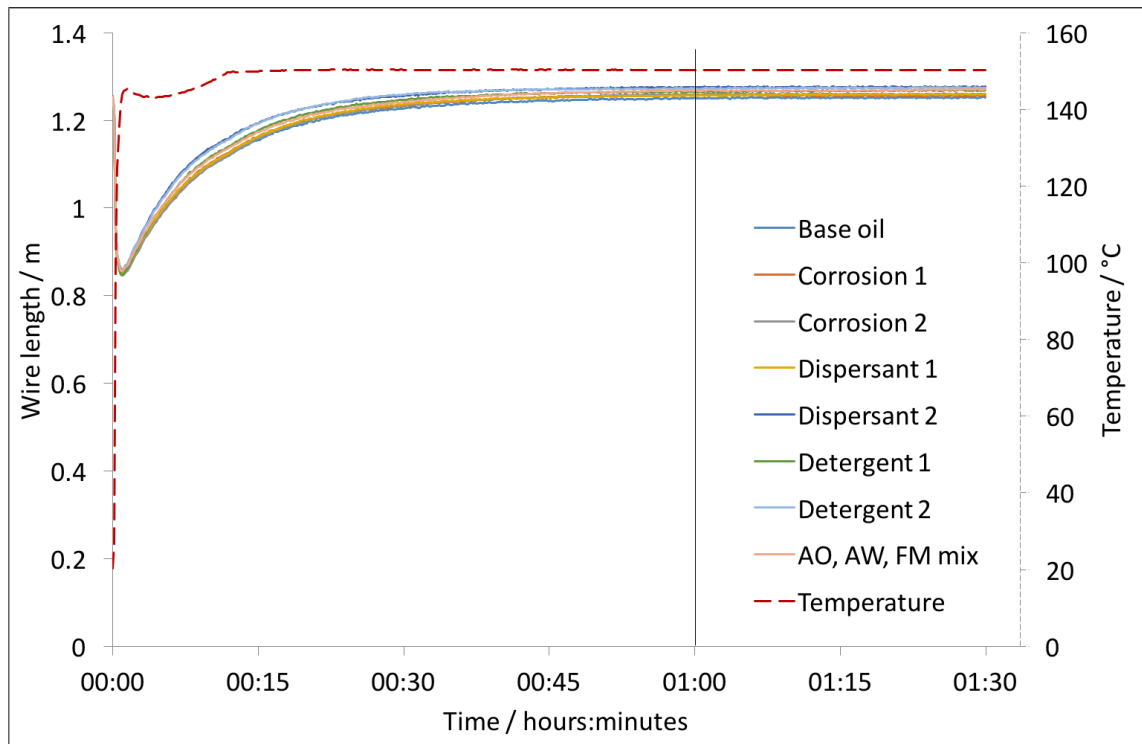


Figure 4.3: Graph showing temperature of oil and length of wires immersed in different additives with time

It took almost 15 minutes for the oil to reach the desired temperature. It should be noted that the temperature probe is placed in the rack containing the beakers of additives and is lifted into the oil bath at the start of the experiment; the temperature measured was the temperature of the oil in the oil bath.

The length of each of the wires was approximately 1.24 m at the start of the experiment. This dropped rapidly in the first minute and then slowly increased with time. The length of the wire tracked the change in temperature but the slow increase arose from the lag between the temperature of the oil in the bath and the temperature of the additive in the beakers, and therefore also the temperature of the wires. Due to this lag it was decided that although the data would be collected, no data before 1 hour would be used in calculations of radius change.

This time point is marked in Figure 4.3 and is the point at which it was decided elongation of the wire had finished and further changes were attributed to radius changes.

4.3.5 The impact of current on copper wire corrosion

During the running of experiments two different control units available at Lubrizol were used. The first had a fixed current of 1 mA which gave very good resolution; the second had variable current control and was able to deliver a range of currents from 1 mA to 20 mA, but the resolution on this unit was poorer compared to the other control unit.

The fixed current control unit was used for initial wire testing but this system then became unavailable for use. Lubrizol were only able to offer the variable control units for the remainder of the study and so a short experiment was carried out to see if the resolution was able to be improved.

Initial tests with the variable control unit found that running at 1 mA, to replicate the tests carried out on the fixed control unit, gave very noisy results, particularly when the changes being measured were small. This was due to the control unit running at the lowest possible current and having a lower resolution. Some studies have been conducted which show that passing a high current through a wire will heat it and initiate a reaction, in the case of Barcroft [144] a 24 V circuit was used to heat the wire to an average temperature of 568 °C.

It was thought that running the wire experiment at a higher current should decrease the amount of noise in the data, but it was unknown if this would have an impact on the reactions taking place at the wire surface. The impact on noise and surface reactions by varying the current was investigated.

In order to see the impact different currents had on the radius change, four tests containing base oil were set up, each with a constant current of either 5 mA, 10 mA, 15 mA or 20 mA. Five beakers containing sample -811 were set up; four of them as above, while the fifth had 15 mA of current passed through it for 2 hours at the start of the experiment and then the current was stopped, but the wires remained connected so as not to disturb the setup. A current of 15 mA was then passed through the wire again for the final hour and a half of the test. This was to see if actively passing current impacted the radius change of the wire, which could suggest a change in the reactions at the surface.

As can be seen in Figure 4.4 there was no difference seen between any of the currents

measured, other than a reduction of noise in the data as the current was increased. The wire that had no current passed through showed the same radius decrease as that which had a constant current passed through it.

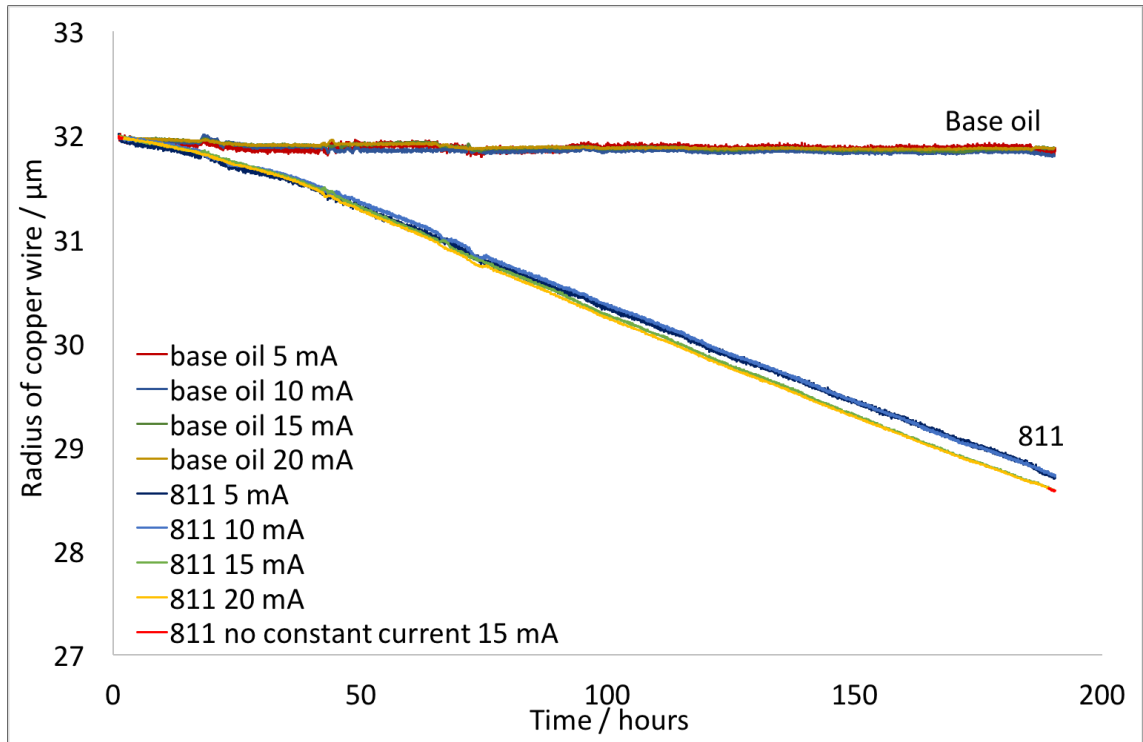


Figure 4.4: Base oil and formulation 811 with currents of 5 mA, 10 mA, 15 mA, and 20 mA passed through

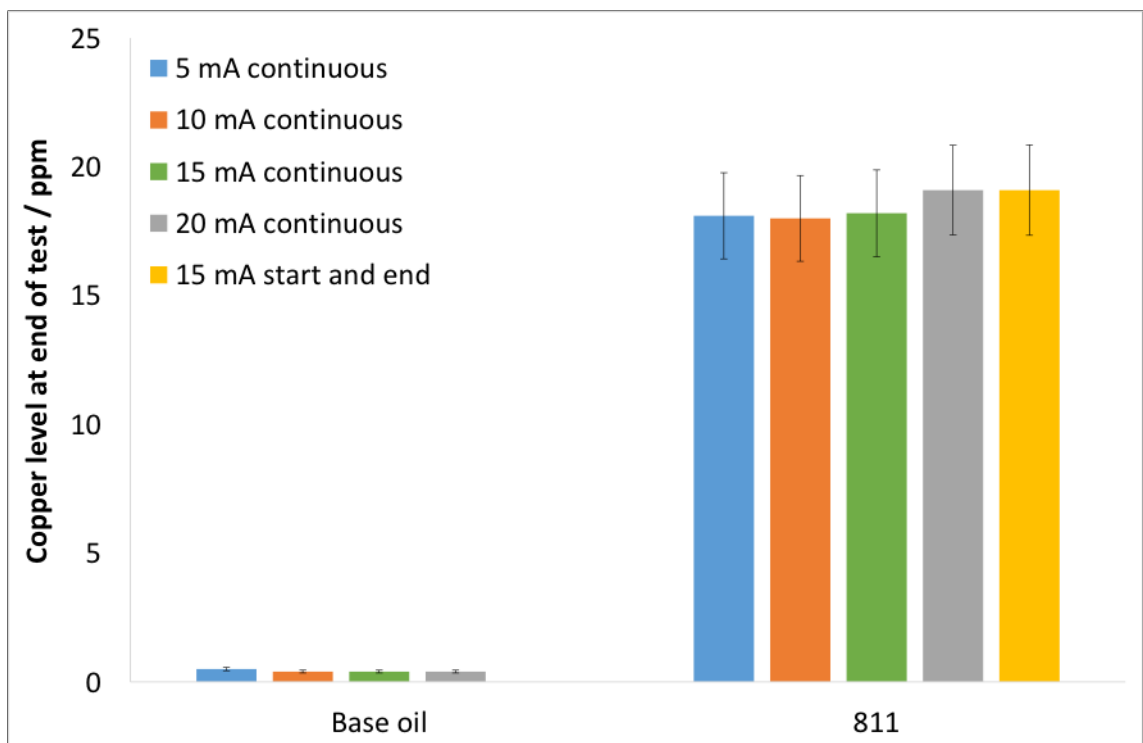


Figure 4.5: Amount of copper in end of test fluid as measured by ICP-AES

The amount of copper in the end of test fluid was also measured to make sure that passing a current through the wire did not have an effect on how much copper leached into the fluid. There was no difference in the amount of copper measured for any of the different currents used, as seen in Figure 4.5. There was also no difference seen for the experiment where no current was actively passed through the wire for the majority of the experiment.

It was concluded that the current had no impact on the corrosion of the copper wire at the levels tested and a current of 15 mA was chosen for future experiments as this gave smaller amounts of noise in the data without running at the limit of the control unit.

4.4 Wire-coupon testing

The wire-coupon tests combined both the immersion tests and the wire tests in the same beaker. This enabled study of the interaction of copper with test fluids using two different methods; the process could be followed in-situ using the wires, and incorporation of the coupon allowed easier analysis of the surface using standard techniques.

As well as being used to test some full formulations this method was primarily used to study the individual additives, and simple 2- or 3-additive mixtures.

4.4.1 Materials

Temper annealed copper wire of 99.9% purity with a 64 μm diameter was used as purchased from Advent Research Materials. Copper coupons were polished, as described in Section 4.1, rinsed and weighed. Individual additives, combinations of these additives and full formulations were all tested using this method and information about the particular test fluids used is given in relevant sections.

Where individual additives were studied they were used at the concentrations outlined in Table 4.4, with the structures given in Section 4.1.

Where additives were combined, the same concentration as the additive alone was used. For example, a mixture of the antioxidant, antiwear and friction modifier used

additive concentrations of 0.33 wt%, 0.165 wt% and 0.65 wt% respectively, the same as when the additives were tested separately.

Table 4.4: Structures and concentrations of individual additives tested, the concentrations were the same as listed when additives were combined

Additive	Concentration/ wt%
Corrosion inhibitor 1	0.5
Corrosion inhibitor 2	0.05
Dispersant 1	5
Dispersant 2	5
Detergent 1	0.5
Detergent 2	0.5
Antioxidant	0.33
Antiwear	0.165
Friction modifier	0.65

4.4.2 Method

400mL of test fluid was measured into clean beakers. A clean, rinsed, and weighed copper coupon was placed into each beaker as soon as it had been prepared, in order to minimise oxidation. 1 m of 64 μm diameter copper wire was wound around a former, as before, and placed into a beaker containing test fluid and a copper coupon. A schematic of this setup can be seen in Figure 4.6.

The same method of stabilisation was run as with the wire tests, however 15 mA of current was used to monitor the resistance of the wire. This method was run over different periods of time, as specified within the results sections.

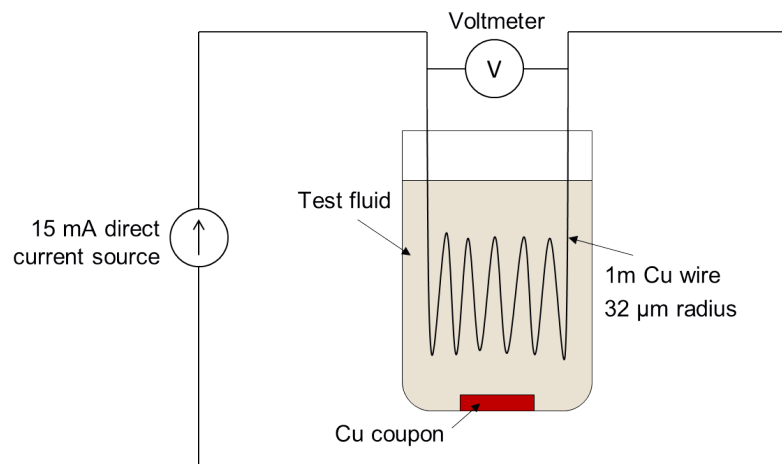


Figure 4.6: Schematic of wire-square test, beaker setup

4.4.2.1 End of test

At the end of the test the beakers were removed from the oil bath – using the rack to allow them all to be removed at once – and allowed to cool until they could be handled. The fluid was then drained, with a small portion sent for ICP-AES analysis. The coupon was rinsed, and re-weighed once dry, before being placed in a clean polythene bag for storage until further analysis was carried out. The wire was unwound from the former and placed in a separate clean polythene bag. These bags were clearly labelled and used to identify and store the samples.

SEM was used to image the surface of the coupons and some were also analysed using FTIR microscopy or sent for XPS analysis. The resistance data collected from the wires throughout the test were analysed and converted into the radius of the wire using the method presented in Section 4.3.3.

4.4.3 Repeatability of tests

The tests were run for a minimum of 1 week, with most tests being run for a two week period. Due to the length of time taken to run, and the number of test fluids, it was not possible to repeat every experiment; for this reason the repeatability and error of the tests were calculated. In order to calculate this the wire-coupon test was set up with three sets of three different fluids.

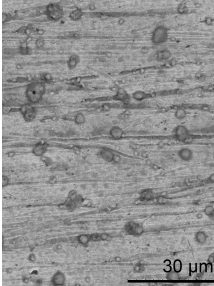
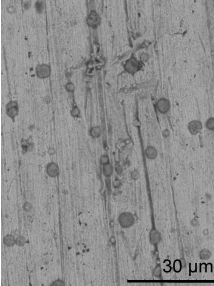
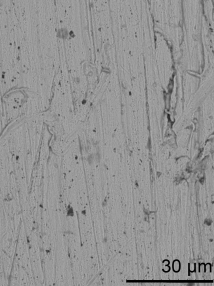
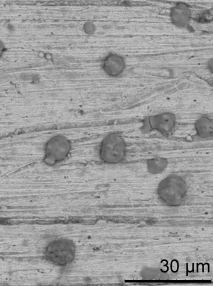
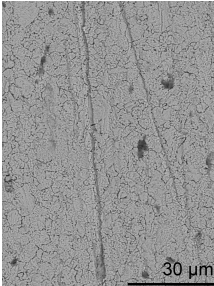
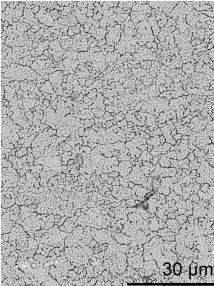
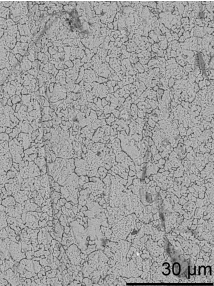
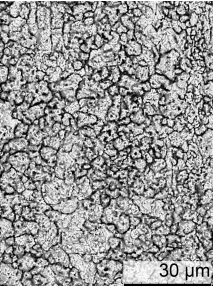
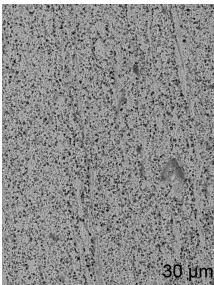
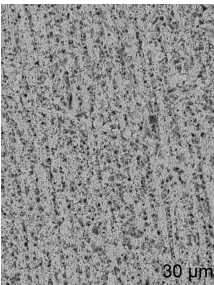
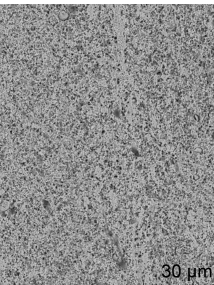
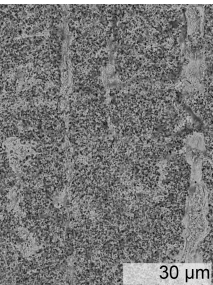
Three beakers containing base oil, three containing dispersant 1, and three containing a single mix of AO, AW and FM were set up, before being tested at 130 °C for 1 week. A subsequent test carried out at 130 °C for 2 weeks had the initial week's wire data taken and compared to these; this data was also used in the calculation. The weight change, sample colour and SEM surface image of this extended test were compared to those of the 1 week tests but could not be used to show repeatability due to the increased test length.

Table 4.5 shows images of the coupons tested in each fluid. Sample 4 in all cases is an image of the test coupon after 2 weeks and so it cannot be directly compared; it is interesting, however, that the sample is very similar in all cases to the samples tested for 1 week and is just a little darker.

Table 4.5: Images of samples tested at 130 °C for 1 week, with the exception of sample 4 which was tested for 2 weeks

	Sample 1	Sample 2	Sample 3	Sample 4
Base oil				
dispersant 1				
AO, AW, FM mix				

Table 4.6: SEM images of the sample surfaces tested in base oil, dispersant 1, or the AO, AW, FM mix for 1 week, except for sample 4 which was tested for 2 weeks. Each of the scale bars represent 30 μm

	Sample 1	Sample 2	Sample 3	Sample 4
Base oil				
dispersant 1				
AO, AW, FM mix				

The same can be said for the images in Table 4.6. If we look at samples 1–3 tested in the AO, AW, FM mix they all show small holes on the surface; sample 4 (which is after 2 weeks) shows the same holes but they appear deeper and there are small areas

of what could be a deposit on the surface. If we compare samples tested in dispersant 1, samples 1–3 show the beginning of intergranular corrosion; sample 4 again shows these crevices to be deeper and more defined. The samples tested in base oil show spherical deposits on the surface in the case of samples 1 and 2, while sample 3 appears to be lacking in deposit, although smaller particles are visible in some areas. Sample 4 shows the same deposit but the particles are larger.

The 1 week test sample (1–3) show good repeatability in both the surface colour and the SEM images of the surfaces.

Repeatability is how well results agree when they are obtained using the same method and equipment, under the same conditions, by the same operator and is determined using Equation 4.6 [145].

$$\text{Repeatability} = 2.8 \times \text{standard deviation} \quad (4.6)$$

Standard deviation of the radius measurements calculated from the wire was calculated at 4 different points: 5 hours, 50 hours, 83 hours and 150 hours. The standard deviation increased slightly with time for each of the additives tested, and was also greater for additives which had larger radius changes measured overall.

Figure 4.7 shows the calculated wire radius for each of the wires tested and shows the points where the standard deviation was calculated. Table 4.7 shows the calculated standard deviation in each fluid at the specified time points.

Table 4.7: Standard deviation of wires in each fluid calculated at specified time points

Time / hours	Base oil	dispersant 1	AO, AW, FM mix
5	0.0175	0.0090	0.0451
50	0.0137	0.0277	0.1135
83	0.0179	0.0249	0.1593
150	0.0308	0.0499	0.1552

The greatest standard deviation value is 0.159 (AO, AW, FM mix; 50 hours) making the repeatability 0.446. This means that for any test carried out under these conditions there should be no change greater than 0.446 from the measured value. It is likely that the repeatability is better than this, as the average standard deviation for base oil is 0.02, therefore repeatability is 0.06. For dispersant 1 the average standard deviation is 0.03, so

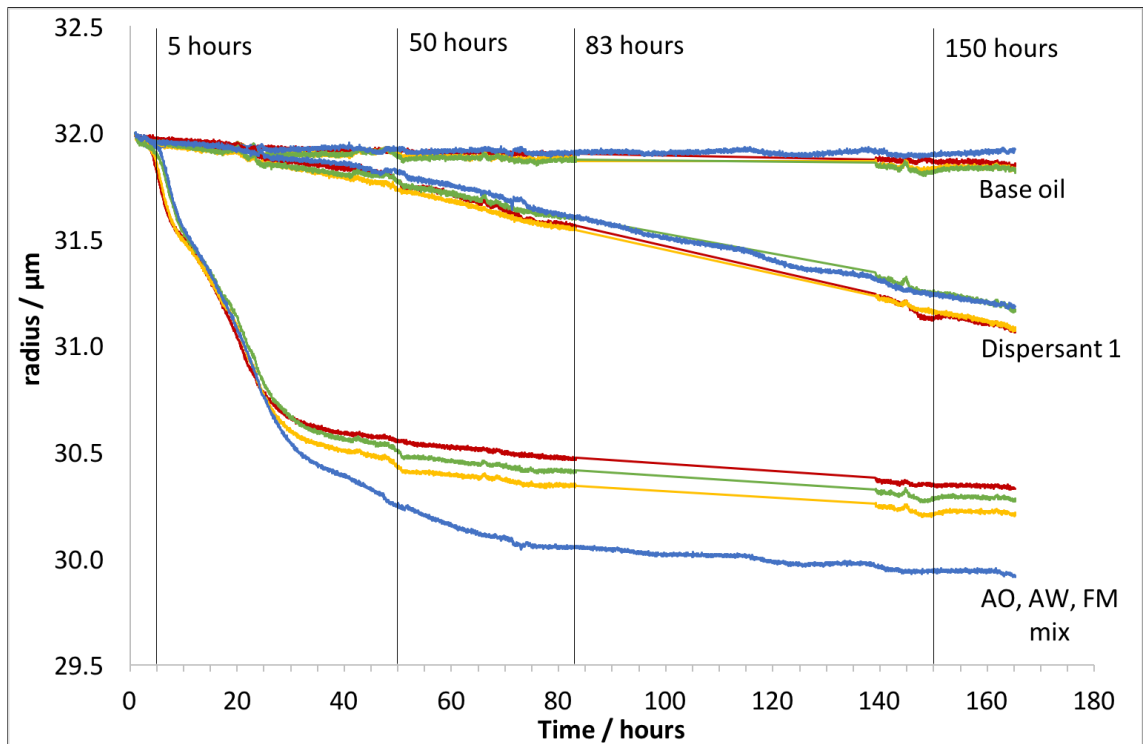


Figure 4.7: Radius changes of wires immersed in base oil, dispersant 1, or the AO, AW, FM mix, with lines denoting where standard deviation was calculated

the repeatability is 0.08 and for the AO, AW, FM mix the repeatability is 0.33, calculated from an average standard deviation of 0.12.

From this we can calculate the standard error using Equation 4.7, giving a value of 0.223.

$$\text{standard error} = \frac{\text{standard deviation}}{\sqrt{\text{number of results}}} \quad (4.7)$$

4.5 Analysis techniques

A number of different analysis techniques were used to examine the used test fluid and also the copper coupons and wires. These techniques are detailed in the following subsections.

4.5.1 ICP-AES analysis

After each experiment around 25 mL of the used test fluid was poured out of the test beaker, before the remaining fluid was disposed of, and sent for elemental analysis using

inductively coupled plasma atomic emission spectroscopy (ICP-AES) in order to determine the amount of copper present. This was performed on site by Lubrizol. Samples were diluted in white spirit followed by placement on rollers for several hours to ensure homogeneity. A Perkin Elmer ICP-AES system was used following the ASTM D5185 test method for used oils. This test method determines the quantity of 22 different elements in a lubricating fluid. In this study the amount of copper detected is used as a measure of corrosion. The amount of sulfur detected was also used for some correlation determination as described in Chapter 5.4. The values determined for other elements were not used in this study.

The ICP-AES measurement uncertainty differs by element and for copper is $0.12x^{0.91}$ where x is the ppm value of the copper present.

4.5.2 FTIR microscopy

FTIR (Fourier transform infrared) microscopy analysis was conducted with a Perkin Elmer FTIR and attached microscope with $100\ \mu\text{m}^2$ aperture, with the scan set to $500\text{--}4000\ \text{cm}^{-1}$ with a minimum of three spectra taken at random points across the surface. These spectra were compared to ensure a uniform surface film. The main functional group peaks were determined for each spectra with reference primarily to ‘Infrared and Raman Spectroscopy’ [138].

4.5.3 Scanning Electron Microscopy (SEM), Energy Dispersive X-ray spectroscopy (EDX) and Focused Ion Beam (FIB)

Coupons were removed from the test fluid, rinsed with SBP2L and then stored in clean polythene bags until required. The samples were removed from the bags and attached to an SEM analysis stub using carbon sticky tabs. Care was taken to only handle the coupons by the edge but no other preparation was undertaken before placing the samples into the machine.

The surface films were investigated with a Hitachi TM3030 scanning electron microscope operating in backscattering electron mode with an accelerating voltage of 5 kV or 15 kV.

EDX analysis was carried out using a Carl Zeiss EVO MA15 SEM with Oxford instruments AZtecEnergy EDX system, which was located in the Leeds electron microscopy and spectroscopy centre. Sample preparation involved attaching the coupon to an SEM stub and applying a small amount of carbon paint to the sides to ensure good conductivity of the sample surface.

A FEI Helios G4 CX DualBeam - High resolution monochromated FEGSEM with precise Focused Ion Beam (FIB) was used to mill a small hole in the sample surface. Once cleaned the side of the hole was imaged using EDX as specified above.

4.5.4 XPS

After testing, coupons were placed in clean polythene bags for transfer between the laboratories in Lubrizol and the University of Leeds. The coupons were kept for up to 4 weeks before being sent for XPS analysis. Before being sent the coupons were rinsed with SBP2L, dried with nitrogen, and wrapped loosely in clean Al foil. The samples were packaged in bubble wrap and placed in a padded envelope to be sent for analysis at NEXUS (National EPSRC XPS Users' Service). Surfaces were thought to be stable and not adversely affected by the transfer.

The chemical analysis of the surface was performed using X-ray photoelectron spectroscopy (XPS) by the staff at NEXUS, without further modification to the surface. Subsequent analysis was carried out by the author using CasaXPS.

All peaks were calibrated to the adventitious carbon peak at 284.8. Peak positions were determined using the CasaXPS software with Gaussian-Lorentzian peak fitting and a Shirley background. A full width half maximum (FWHM) in the region of 1.6–1.8 was aimed for, and peaks added or subtracted until both a good fit was achieved and the FWHM value was within the specified range.

Sulfur and copper have spin-orbit coupled peaks so in order to fit them the parameters outlined in Table 4.8 were used.

Table 4.8: Spin-orbit component parameters used for peak fitting

Element	Δ / eV	ratio
Sulfur	1.16	0.511
Copper	19.75	0.508

4.5.5 White Light Interferometry (WLI)

White light interferometry is a non-contact surface analysis technique. In this study an NPFLEX by Bruker Corporations UK was used to take 3D surface topography measurements. Vision64 software was then used to quantify the height, depth and volume of pits seen.

5: Results of full formulation testing

After the full formulation immersion tests were complete the copper coupons were removed, rinsed and rated. The weight change of the coupons was also recorded and the amount of copper in the end of test fluid determined using ICP-AES. Each test fluid was run three times and the data presented is the average of these three runs.

5.1 Rating of copper squares

The rated coupons were a wide variety of colours, some of which did not match the ASTM standards very well. As well as the ASTM rating a digital brightness rating was also given to each of the coupons.

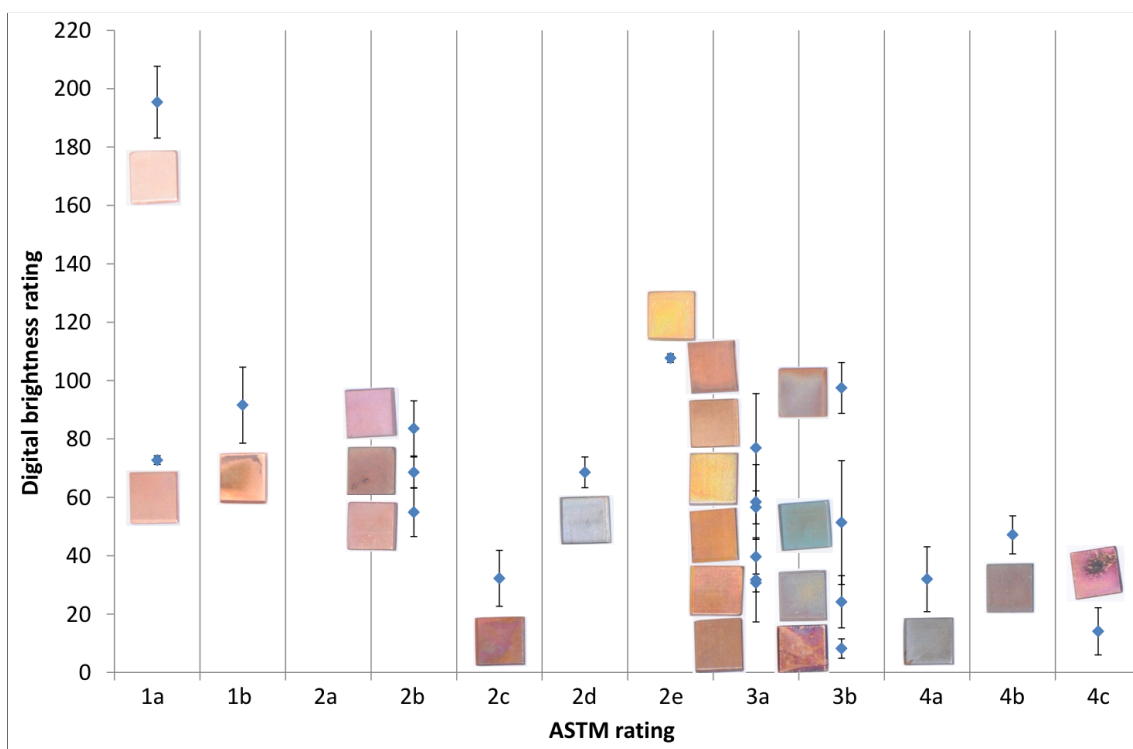


Figure 5.1: Digital brightness ratings plotted against the ASTM rating with an image of the corresponding sample

Figure 5.1 shows the digital brightness rating, y -axis, plotted against the ASTM rating of the sample, x -axis. An image of the corresponding sample is also shown.

From this figure it can be seen that there is a very weak correlation between the ASTM rating and the digital brightness rating. Generally higher rated ASTM samples are darker and therefore have lower digital brightness values. From the images of the samples it is also easy to see how subjective the ASTM rating can be, for example the 4 samples rated as 3b have a variety of colours on their surface, ranging from turquoise to something close to maroon. One problem with the digital brightness rating is that it takes an average of the surface, so if a sample is not a uniform colour it can be biased towards the brighter or dimmer colour. The sample with ASTM rating 1a and a brightness of 195 poses another issue with the digital brightness rating. The rating references span from 0 (black) to 100 (clean copper), a rating of 195 is brighter than the clean reference.

5.2 Weight change of copper coupons

The copper coupons were cut in house by Lubrizol to approximately 1 cm, as a result each of the coupons is a slightly different weight. Rather than calculating the difference in weight between the start and end of the test, the weight change is calculated as a percentage of the initial starting weight. A positive number signifies weight gain where as a negative number signifies weight loss.

Figure 5.2 plots the weight change for each of the copper coupons, tested in full formulation fluids for 4 weeks at 120 °C, against their ASTM rating. As the fluids were tested 3 times, each with a different coupon, the weight change presented is an average of the weight change of the three coupons. The standard deviation is also plotted, in many cases it is very small, but for a number of sample the standard deviation was very large. Inspection of these samples often showed a poorly adhered film which had flaked off from one of the samples, or in other cases a localised deposit build up on one of the coupons which was not so pronounced on the others, and so the standard deviation increased for these samples.

Almost all of the samples show weight change of less than $\pm 0.5\%$ the original weight of the coupon. It can be seen from Figure 5.2 that the weight change is often very small

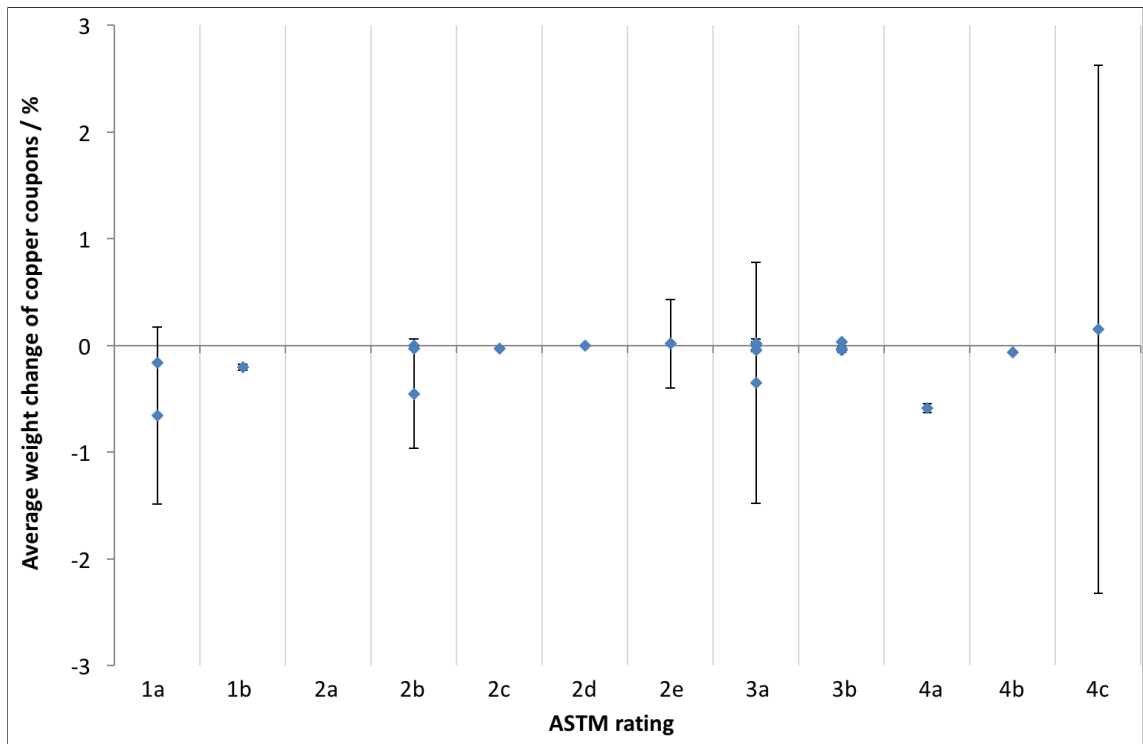


Figure 5.2: Percentage weight change of copper coupons

and there is no distinction between the weight change of mid-rated samples; for example most of the samples rated 2b to 3b show very little weight change.

It is interesting to note that coupons which would be considered to have good ASTM ratings, those with 1a and 1b ratings in Figure 5.2, seem to show greater weight loss than those with higher ratings. The sample which showed a rating of 4c shows a weight gain over the period of the test. It also has a very large error associated with it. With reference back to Figure 5.1 it can be seen that the sample with the 4c rating is predominantly pink with a large black deposit in the centre. As mentioned these samples were run in triplicate and the other coupons run in this fluid had varying levels of coverage by the black deposit. This variation in coverage accounts for the large error in the average weight change.

It is assumed that weight gain is due to the build up of a film or deposit on the surface whilst weight loss is thought to be related to the amount of copper dissolved into the solution. Greater weight loss would be detrimental as it would be indicative of more copper in the fluid which is known to accelerate the degradation of ATFs.

Samples which show little change in weight are more interesting. They may not be corroding or may have corrosion and film formation occurring at a similar rate therefore

showing no weight change; there is no way of knowing which without looking at other measurements, such as the amount of copper in the test fluid.

5.3 Amount of copper in end of test fluid

The amount of copper detected in the end of test fluid for each of the full formulations can be seen in Figure 5.3, plotted against the ASTM rating of the coupon. For clarification the multiple points in each rating correspond to different test fluids which gave that particular rating. There is no clear correlation between the rating and copper level as determined by ICP-AES.

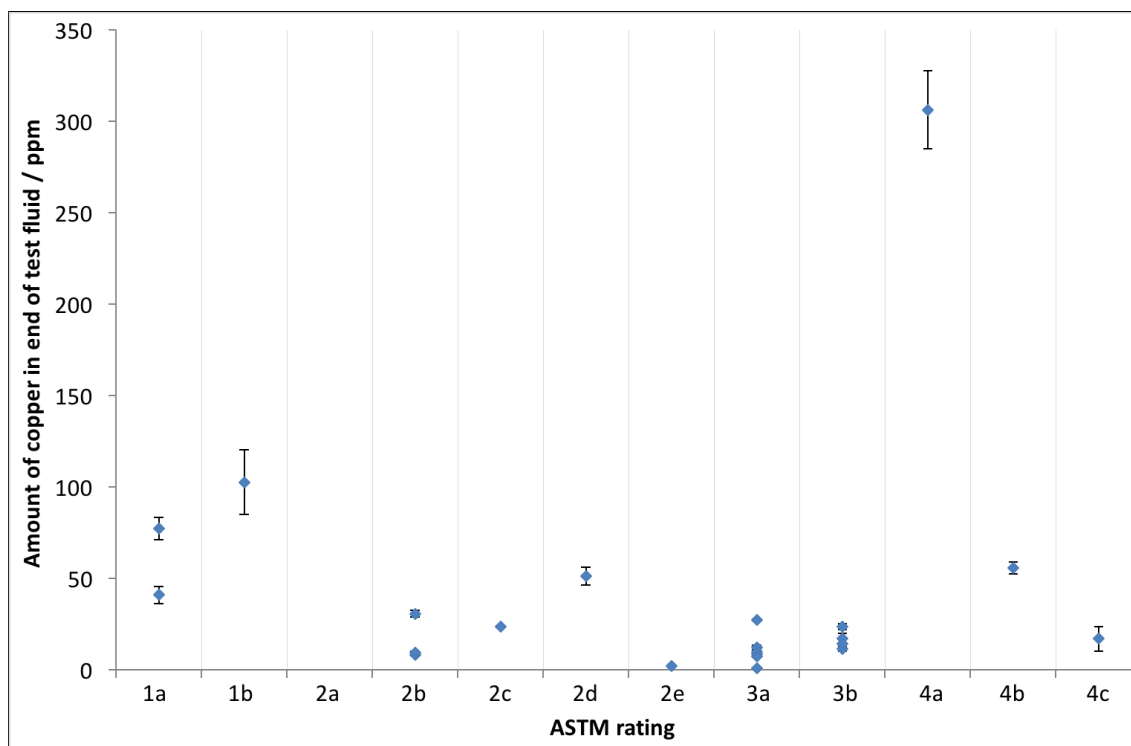


Figure 5.3: The amount of copper in the end of test fluid as determined by ICP-AES, for full formulation fluids run for 4 weeks at 120 °C

It would seem logical that the weight change of the copper coupons should relate to the amount of copper in the end of test fluid, with greater weight loss leading to more dissolved copper. This can be seen in Figure 5.4. It is possible to plot a trend line through the majority of the data with the exception of four data points, highlighted in red. On closer inspection, these four points showed very different values for the weight change of the copper squares for each of the three test runs, as indicated by the large error bars, and as such the weight change data for these samples could be considered anomalous.

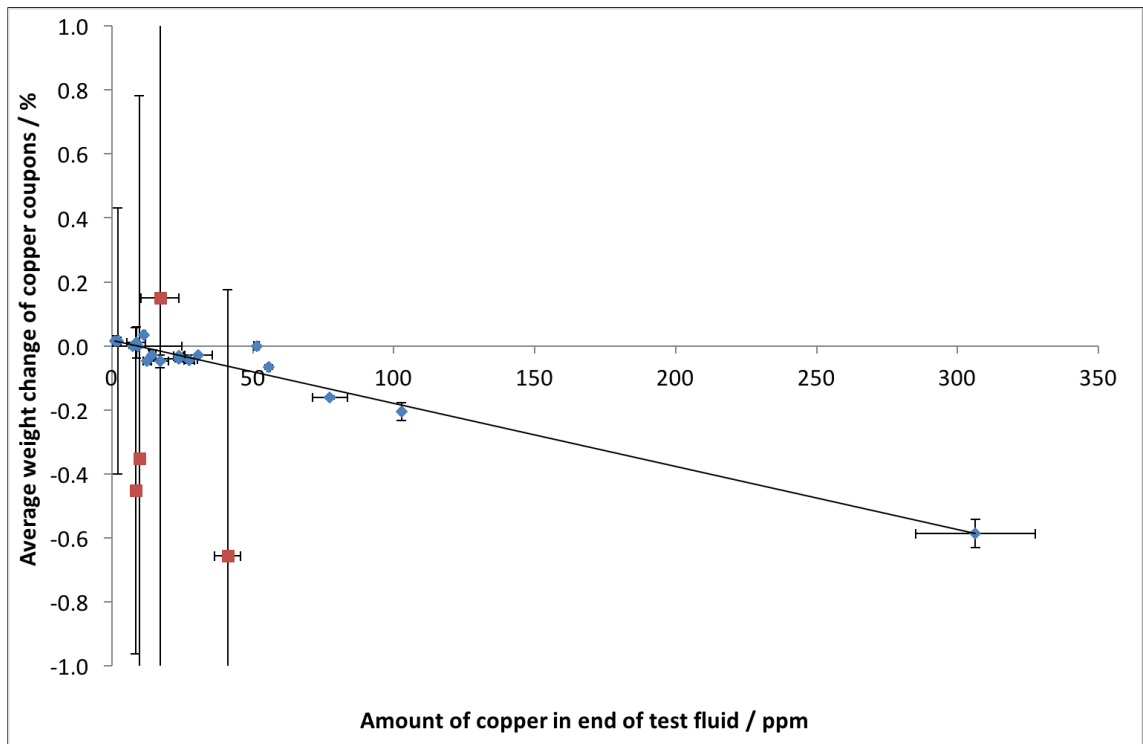


Figure 5.4: Average weight change of copper coupon and amount of copper measured with ICP-AES in the end of test fluid

A weak correlation was found between the ASTM rating and digital brightness rating. No clear correlation could be seen between the ASTM rating and the weight change of the copper coupons or the amount of copper in the end of test fluid. However a correlation was seen between the weight change of the copper coupons and the amount of copper in the end of test fluid. It was wondered if there were any other measurable quantities that would give a correlation with the ASTM rating of the coupons. A number of other ways to analyse and group the samples were found which are presented in the following sections.

5.4 Level of sulfur in formulation

Corrosion to the copper coupons can be assessed either by using the ASTM rating or by looking at the amount of copper in the end of test fluid. The ASTM D130 standard test method suggests that the significance and use of the test is to measure the impact of different sulfur species on the corrosion of copper [84]. Three of the additives used in the formulations contain sulfur; these are corrosion inhibitor 1, dispersant 2 and dispersant 1.

It is documented in literature that the corrosivity of sulfur is dependant on the chemical state it is in. Elemental sulfur is highly corrosive, but sulfur contained within hydrocarbon chains is less corrosive, often determined by the size of the molecule, with larger molecules being the least corrosive [26, 85, 87, 89].

It was wondered if there was any correlation between the amount of sulfur in the formulation and the ASTM rating or copper level in the end of test fluid; and particularly if one additive contributed to more corrosive formulations.

In order to test this theory the amount of sulfur in the start of test fluid was measured using ICP-AES for each formulation, this was then plotted on two separate graphs against the ASTM rating and the amount of copper in the end of test fluid. In order to tell if the different additives were showing any correlations the graphs were coloured by the concentration of additive present. Figures 5.5, 5.6 and 5.7 show the plots highlighting the sulfur contribution from corrosion inhibitor 1, dispersant 2 and dispersant 1 respectively.

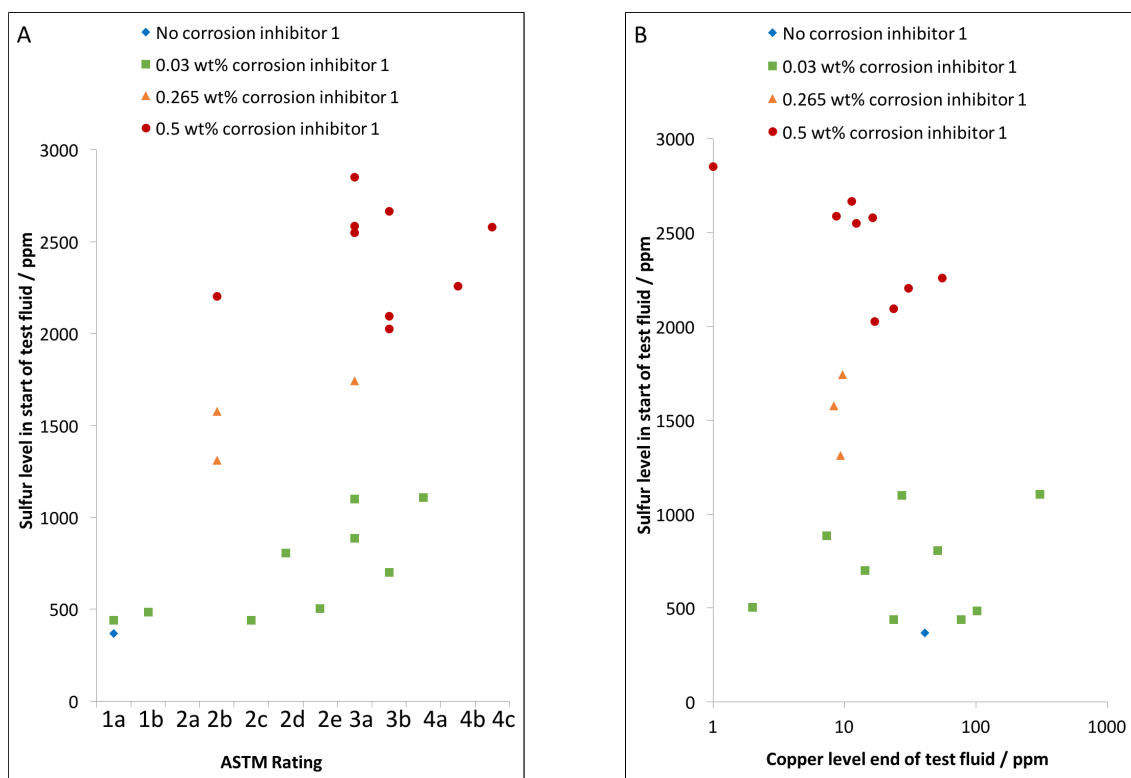


Figure 5.5: Sulfur level in each formulation plotted against (A) ASTM rating of the copper square, and (B) the copper level in the end of test fluid, highlighting the level of corrosion inhibitor 1

No correlations were found for any of the additives; all that can be concluded is that the majority of the sulfur contribution comes from corrosion inhibitor 1, Figure 5.5.

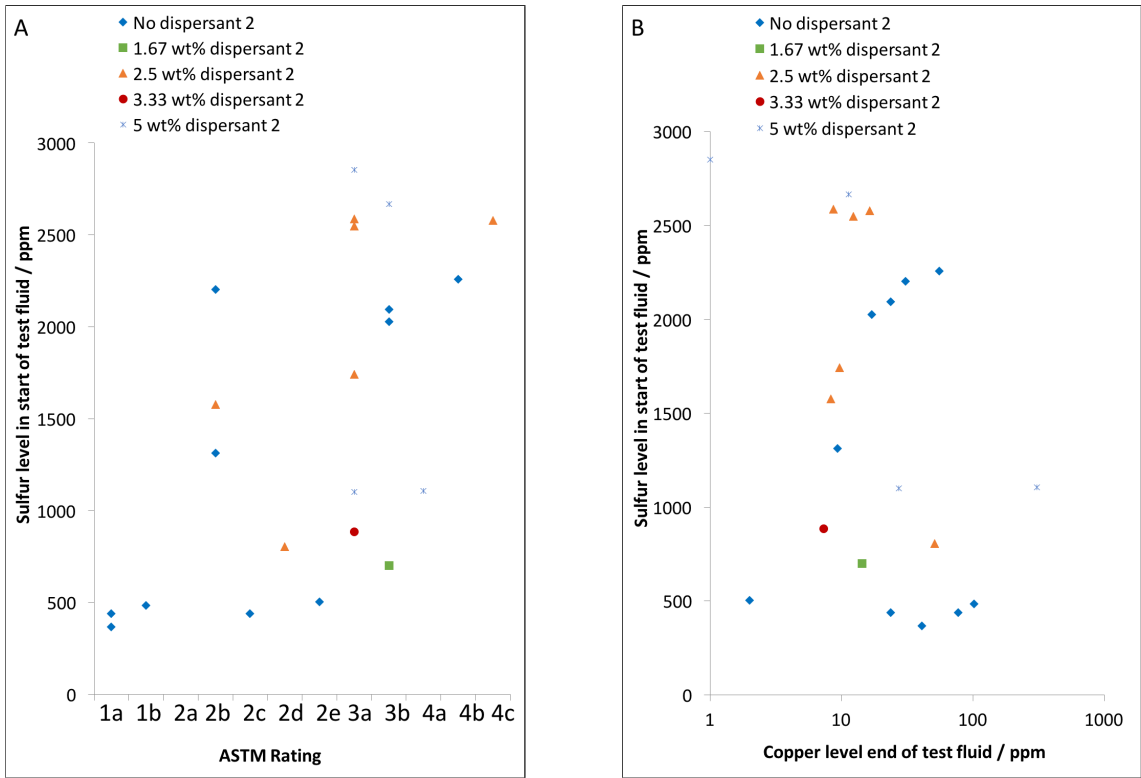


Figure 5.6: Sulfur level in each formulation plotted against (A) ASTM rating of the copper square, and (B) the copper level in the end of test fluid, highlighting the level of dispersant 2

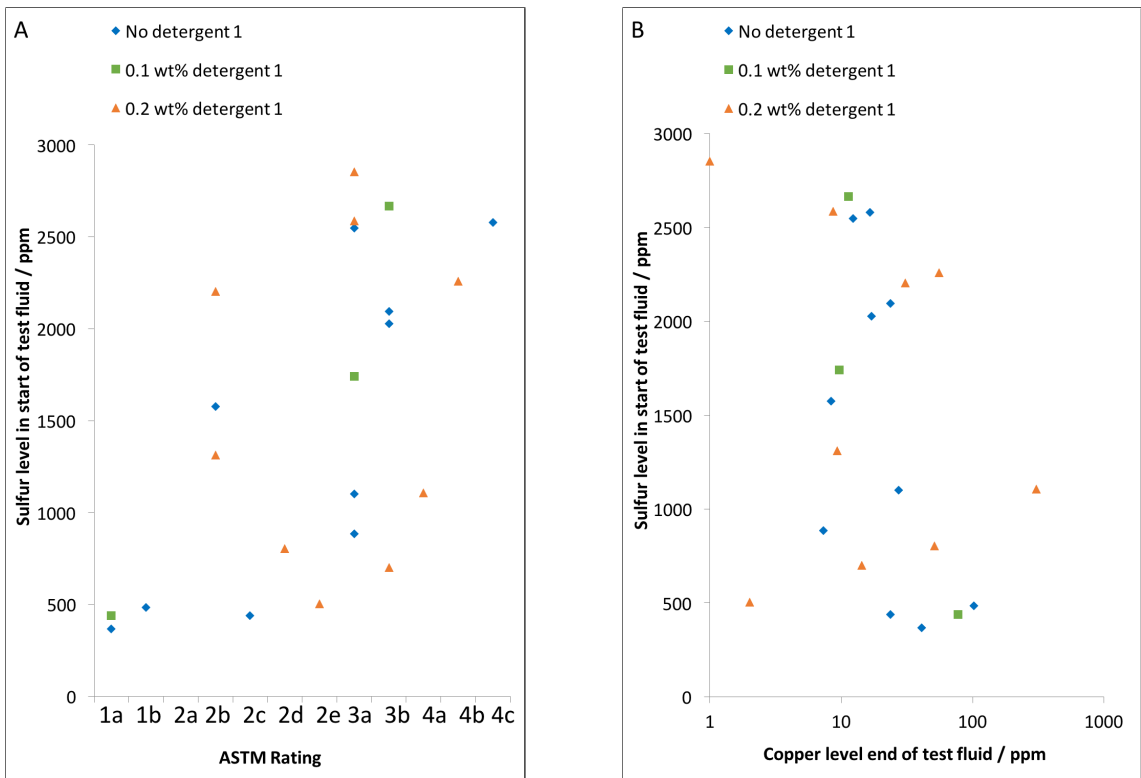


Figure 5.7: Sulfur level in each formulation plotted against (A) ASTM rating of the copper square, and (B) the copper level in the end of test fluid, highlighting the level of dispersant 1

It could be argued that a very weak correlation can be seen in the sulfur level against ASTM rating, when highlighted for corrosion inhibitor 1 as generally samples containing higher concentrations of the additive give poorer ASTM ratings.

5.5 FTIR-ATR analysis

FTIR-ATR spectra were taken of all the copper coupon surfaces. The spectra were able to be grouped based on similarities in the peaks which can be seen in Figures 5.8–5.14. Spectra which showed many of the same sets of peaks were classed as being similar, this is much easier to see visually in any of the Figures 5.8–5.14. As the FTIR spectra showed samples with similar surface functional group chemistry the formulations for the samples were inspected to see if any had additives at levels which were the same within these groups. The formulations are shown in Table 5.1 and are grouped and shaded by FTIR similarity.

All of the FTIR spectra taken show a noisy peak at 2300 cm^{-1} which was practically impossible to eliminate and is believed to come from CO_2 in the air. As all spectra were taken using a reflectance method through air it was not possible to completely eliminate the peak.

Almost all of the FTIR spectra show C-H alkane peaks centring around 2900 cm^{-1} . The base oil is primarily an alkane and many of the additives contain long alkane chains to make them soluble. It is therefore unsurprising that alkane peaks are detected.

Figure 5.8 has peaks relating to branched alkanes. These are most likely to arise from the PIB chains, which are included on some of the additive molecules to make them oil soluble. The C–N group from an aliphatic amine indicates that the nitrogen is not part of a ring structure. From the additive structures given in the methodology section (Table 4.1) it would seem that dispersant 1 is an obvious choice for these functional groups however when the additives present in the formulation are studied, Table 5.1, it can be seen that there is no dispersant 1 in either formulation -779 or -794, therefore cannot be the source of the peaks. Taking into account the additives present in all of the formulations the peaks are most likely from the interaction of friction modifier with the surface.

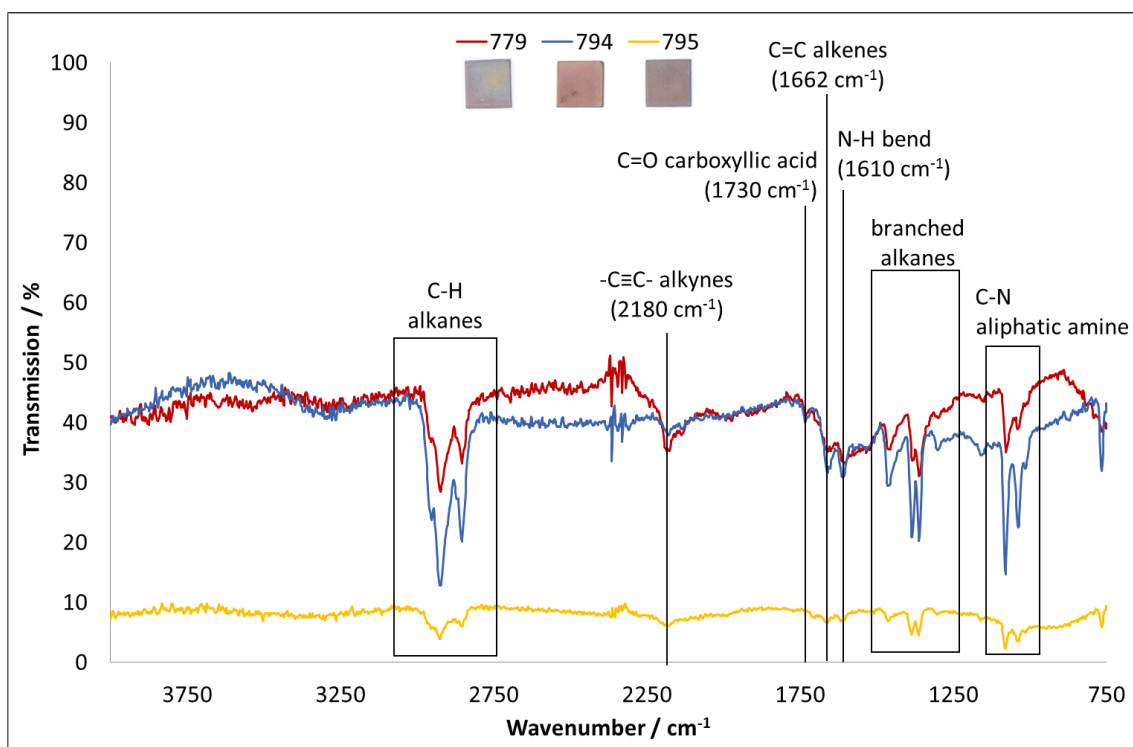


Figure 5.8: FTIR spectra and images for coupons -779, -794, and -795

What is unclear is why these peaks do not appear in all spectra given that friction modifier is present in all of the formulations.

Figure 5.9 has only four main peaks. The C-H alkane peaks are not useful in determining which additives may be present on the surface as all additives have long alkane chains in order to make them oil soluble. The N=C=S and ring structure vibrations would suggest that corrosion inhibitor 1 is most likely responsible for the peaks seen. The lower intensity of the peaks for -807 could be due to the fact that less corrosion inhibitor 1 is present in the formulation; 0.03 wt% compared to 0.5 wt%. This raises a question about why these particular formulations show these peaks and if they do arise from corrosion inhibitor 1 why the peaks do not appear in other FTIR spectra.

The peaks seen in Figure 5.10 and Figure 5.11 do not match as precisely as those seen in other groupings, however they are sufficiently similar to be grouped together. It is difficult to conclude which additives may be causing the peaks as with the exception of corrosion inhibitor 1, antioxidant, antiwear and friction modifier none of the other additives appear in all of the formulations within each group.

Although the peaks are well aligned the same is true of the group -777, -782 and -811 for which the spectra can be seen in Figure 5.12. The peaks do not obviously relate to an

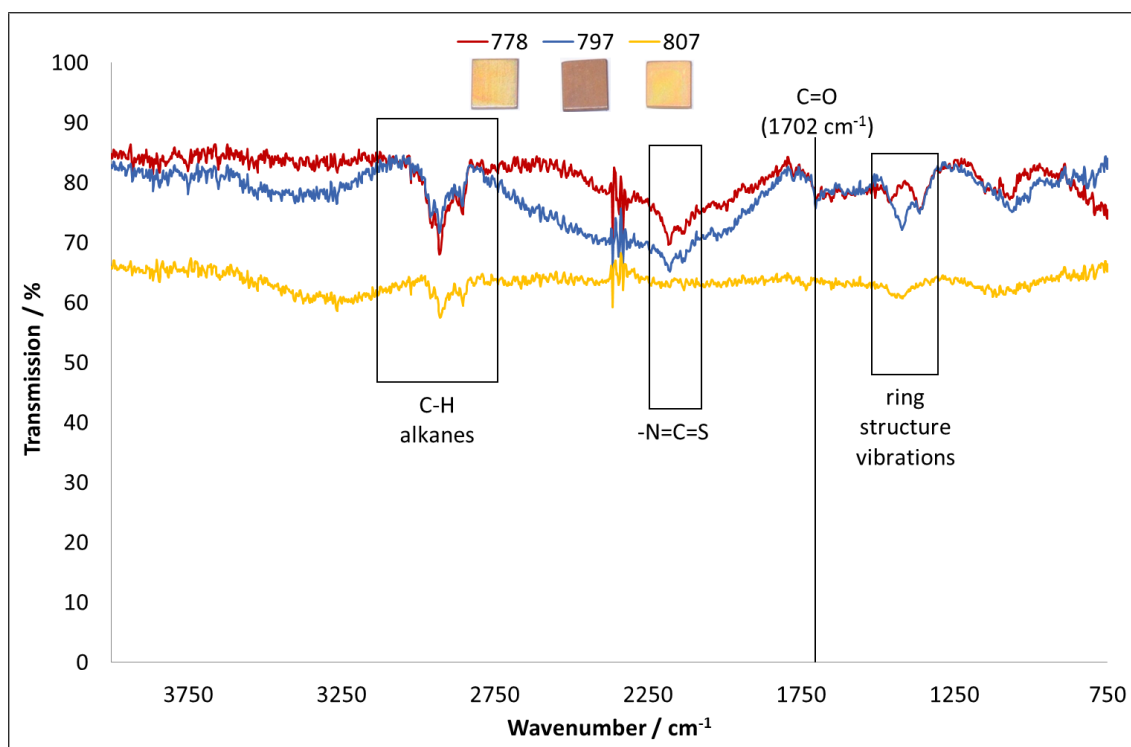


Figure 5.9: FTIR spectra and images for coupons -778, -797, and -807

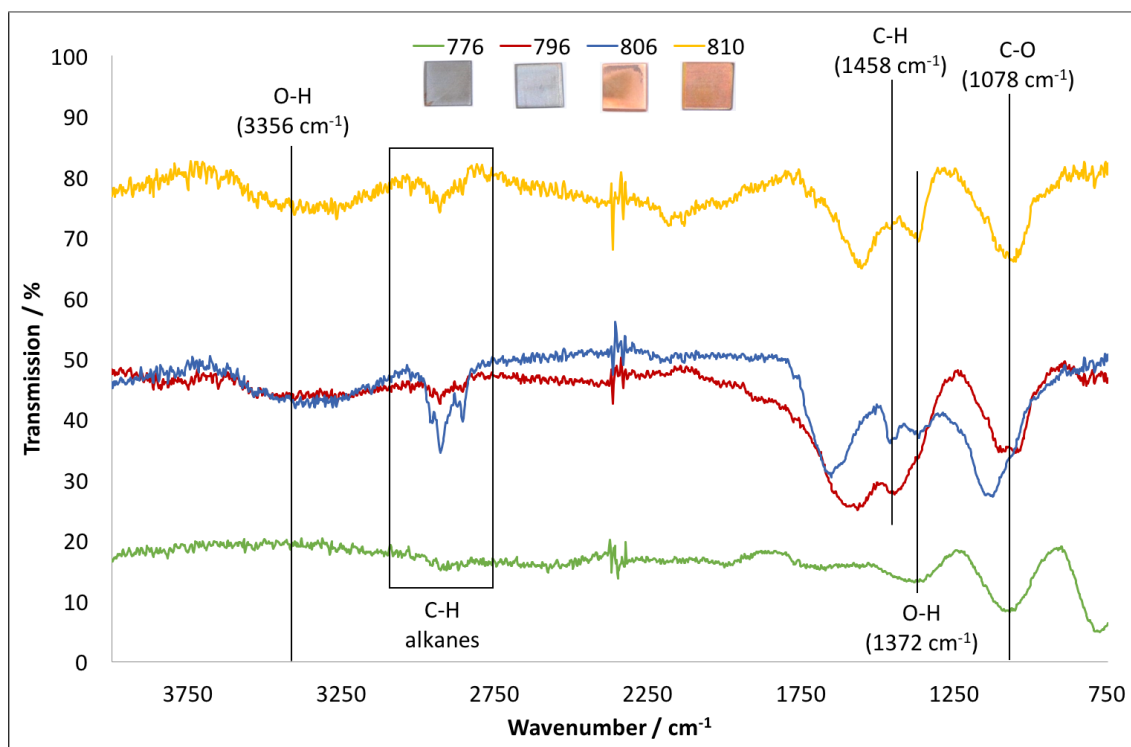


Figure 5.10: FTIR spectra and images for coupons -776, -796, -806, and -810

additive which is present in all three formulations.

The final two groupings show no distinguishable peaks. It could be that the peaks are not IR active or it is possible that the films were too thin to detect. The grouping of -781 and -798 showed alkane peaks but the other peaks in the spectra were too broad

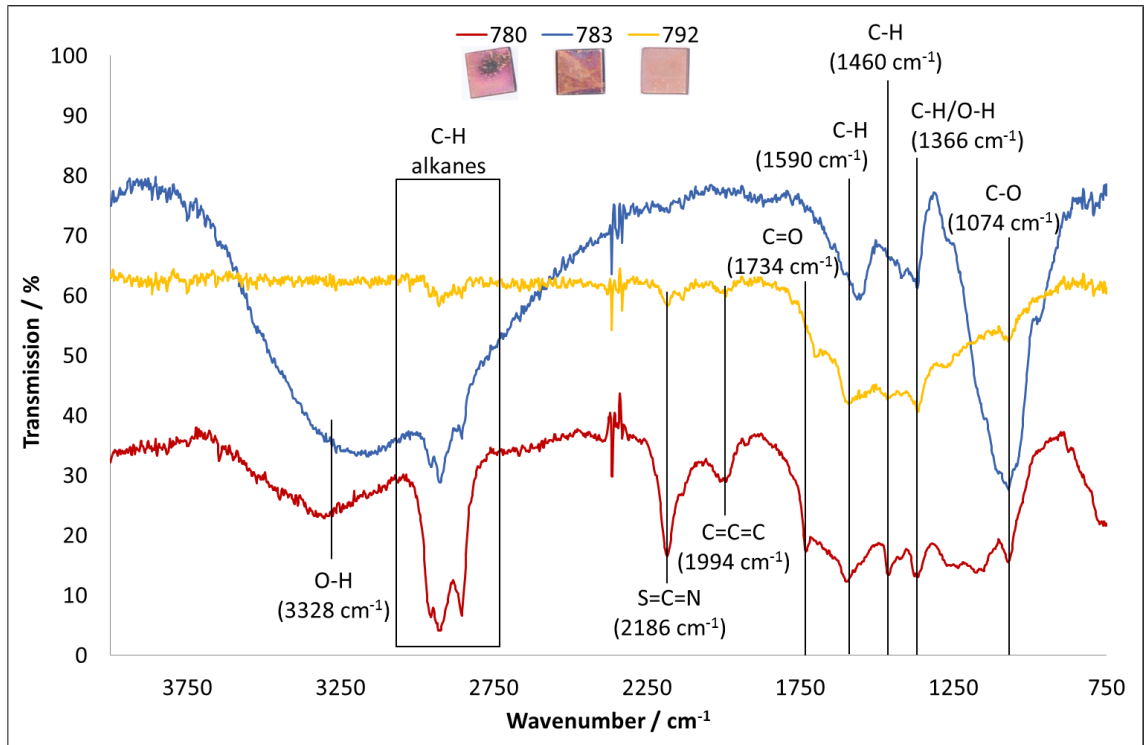


Figure 5.11: FTIR spectra and images for coupons -780, -783, and -792

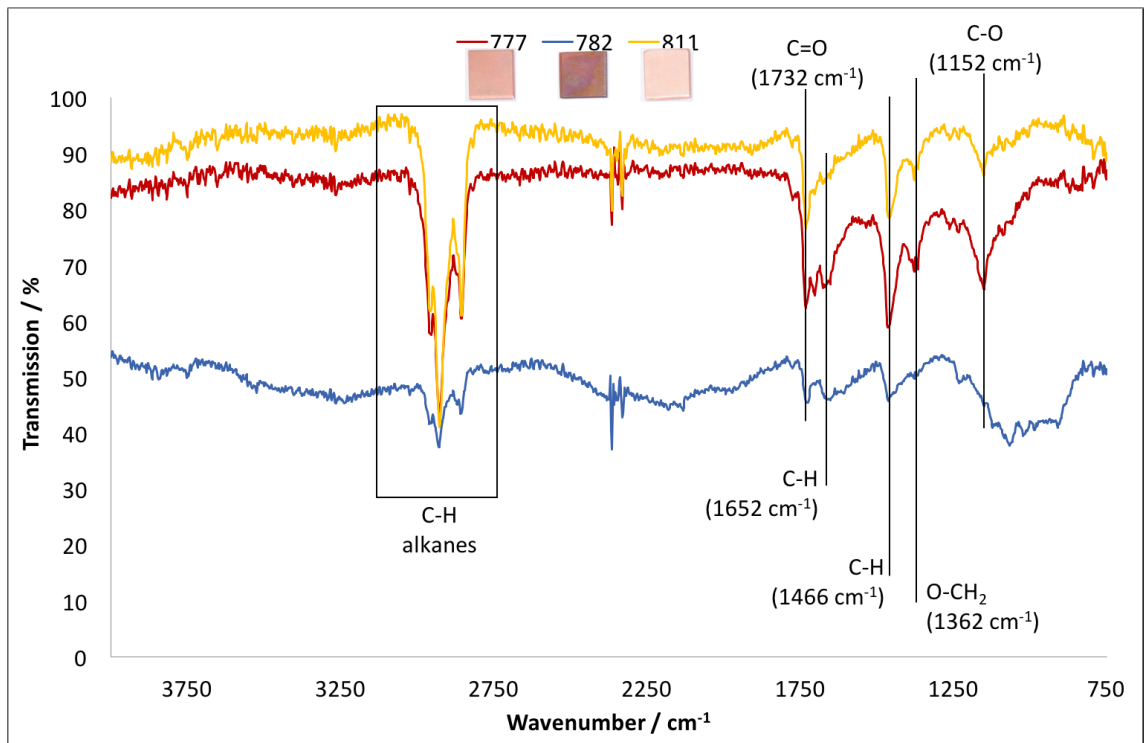


Figure 5.12: FTIR spectra and images for coupons -777, -782, and -811

and weak for identification, as can be seen in Figure 5.13.

Figure 5.14 shows no peaks were present in a group of samples. The reason for this is unknown given that the surface showed a change in colour suggesting the presence of a film on the surface.

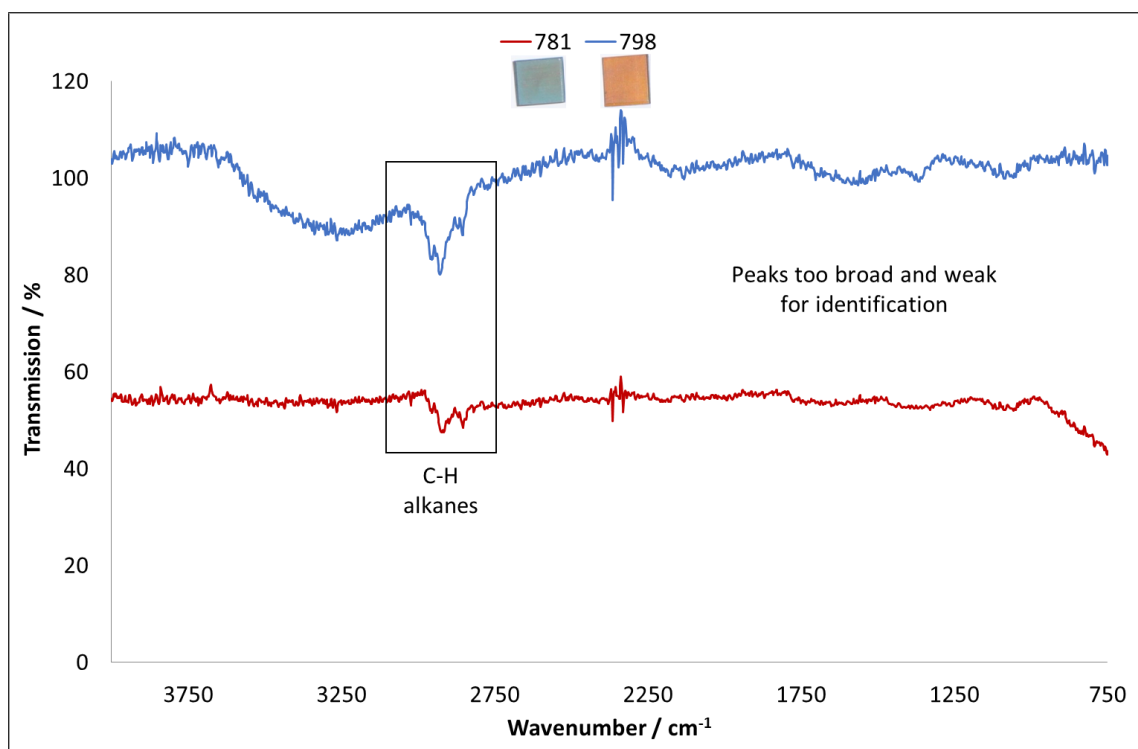


Figure 5.13: FTIR spectra and images for coupons -781 and -798

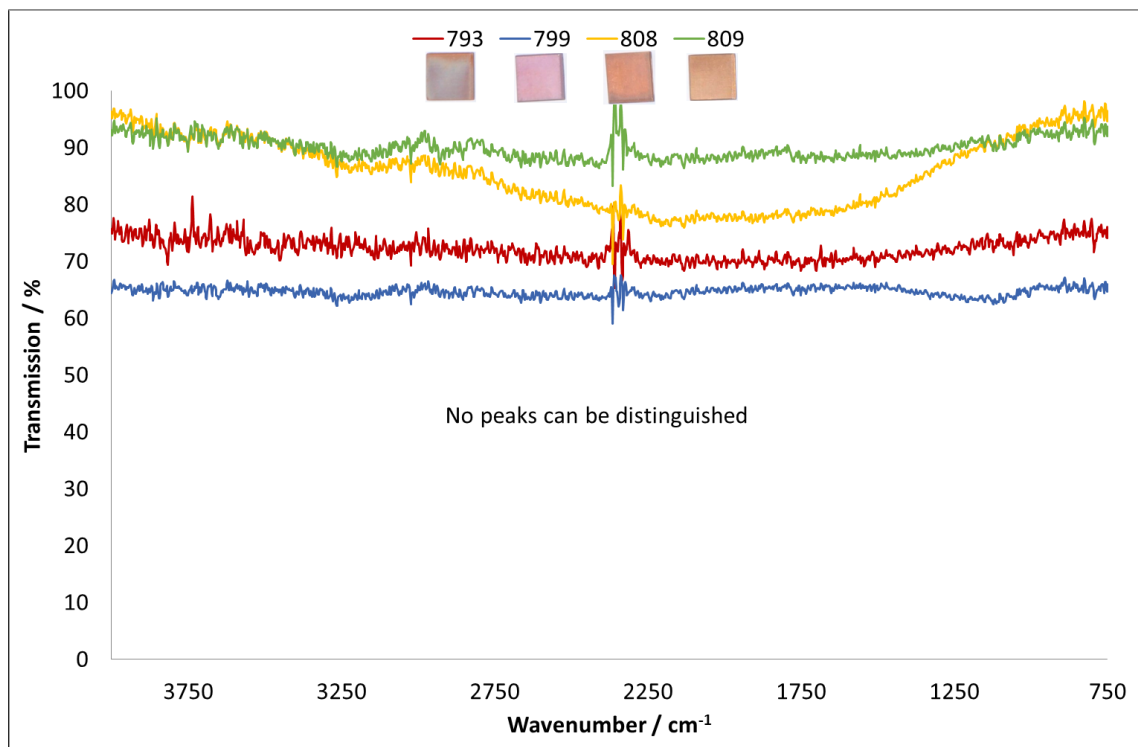


Figure 5.14: FTIR spectra and images for coupons -793, -799, -808, and -809

Table 5.1 shows the additives and their respective concentrations in each of the formulations, grouped according to the similarity of their FTIR spectra.

The peaks in the FTIR spectra have been examined alongside the additives present in the formulations in order to try and determine which may be causing the peaks that are

seen. In many cases it has not been possible to determine which additives are causing the peaks seen.

If the peaks are disregarded and instead the formulations within each grouping is examined due to their complexity it is not possible to find any clear trends as to why it is possible to group certain samples together based on their FTIR spectra. It is also interesting that samples with the same rating are not often grouped together, in terms of FTIR spectra.

Table 5.1: Formulations grouped by FTIR similarities for all coupons run

Sample number	Concentration of Additive (wt%)								
	Corrosion inhibitor 1	Corrosion inhibitor 2	Dispersant 1	Dispersant 2	Detergent 1	Detergent 2	Antioxidant	Antiwear	Friction Modifier
-779	0.5	0.026	0	0	0	0	0.6	0.11	0.65
-794	0.265	0.026	0	0	0.2	0.4	0.06	0.11	1.2
-795	0.5	0	2.5	0	0.2	0	0.6	0.22	1.2
-778	0.5	0.013	2.5	2.5	0	0	0.06	0.11	1.2
-797	0.5	0.026	2.5	2.5	0.2	0.4	0.6	0.165	1.2
-807	0.03	0.013	0	0	0.2	0.4	0.6	0.22	0.1
-796	0.03	0	2.5	2.5	0.2	0.4	0.06	0.22	0.65
-806	0.03	0	5	0	0	0.4	0.6	0.11	1.2
-810	0.5	0.026	0	5	0.2	0	0.06	0.22	0.1
-776	0.03	0	0	5	0.2	0	0.33	0.11	1.2
-777	0.03	0.026	5	0	0.1	0	0.06	0.22	1.2
-782	0.03	0	0	0	0	0	0.06	0.165	0.1
-811	0	0.026	5	0	0	0.4	0.33	0.22	0.25
-780	0.5	0	0	2.5	0	0.4	0.06	0.22	1.2
-783	0.5	0	0	5	0.1	0.4	0.6	0.11	0.1
-792	0.265	0	2.5	2.5	0	0	0.6	0.22	0.1
-781	0.5	0.026	5	0	0	0.4	0.33	0.22	0.1
-798	0.265	0.013	2.5	2.5	0.1	0.2	0.33	0.165	0.65
-793	0.03	0.026	3.33	1.67	0.2	0	0.6	0.11	0.1
-799	0.5	0	5	0	0.2	0.2	0.06	0.11	0.1
-808	0.03	0.026	0	5	0	0.2	0.6	0.22	1.2
-809	0.03	0.026	1.67	3.33	0	0.4	0.06	0.11	0.1

5.6 SEM analysis

For each of the copper samples tested in the fully formulated fluids BSE images were taken of each of the surfaces, using an accelerating voltage of 5 kV and 15 kV as some features were picked up by one or the other due to the difference in the electron escape depth. Where similarities could be seen between certain samples they were grouped, which yielded some interesting results. There were 5 main surface features identified, into which the samples were grouped. The groups that were identified are labelled as:

Flaking samples showed clear areas of flaking, where surface layers and lower layers could be seen (Table 5.2)

Spheres samples had clear spherical objects on the surface (Table 5.4)

Porous surfaces had areas that were porous or pitted (the size and shape of the pits was not distinguished and all samples were grouped together) (Table 5.6)

Small particles samples were often quite featureless but showed small particles on the surface (Table 5.8)

Featureless samples contained no real identifying features on the surface, other than polishing marks or scratches (Table 5.10)

Many of the samples could be placed into more than one of the categories and grouped as such; this was done to allow better analysis of what may be causing distinct surface features. Where samples appear in more than one category images from different areas of the surface may be shown to help emphasise the particular feature.

As well as imaging the surface EDX spectra were also taken for each of the samples. In all instances oxygen, carbon, sulfur and copper were detected as would be expected given the elements present in the additives. There was little to distinguish between the samples and for this reason the EDX spectra are not shown.

5.6.1 Full formulation samples showing flaking

Table 5.2 shows BSE images of samples which showed flaking on their surfaces. The images on the left were taken using a 5 kV accelerating voltage, which helps to highlight the very top of the surface layers whilst the images on the right were taken using a 15 kV accelerating voltage. This allows a little more penetration into the surface and helps to highlight more detail. These samples show clear formation of a surface layer which is poorly adhered and has cracked and flaked.

Table 5.2: BSE and coupon images for full formulation fluids showing surfaces that flake

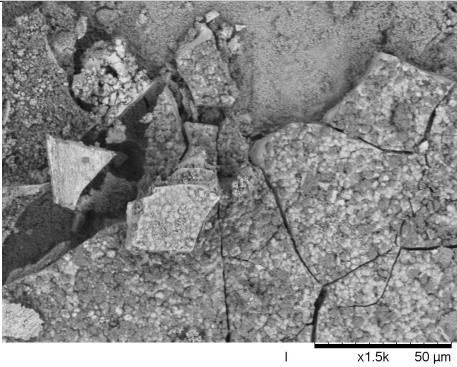
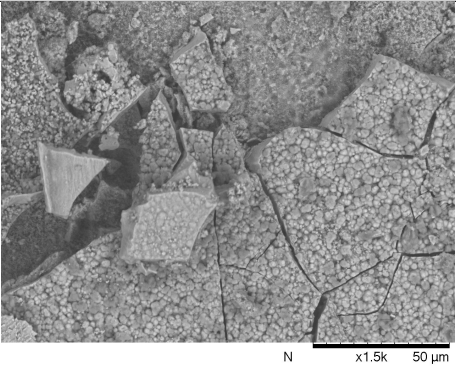
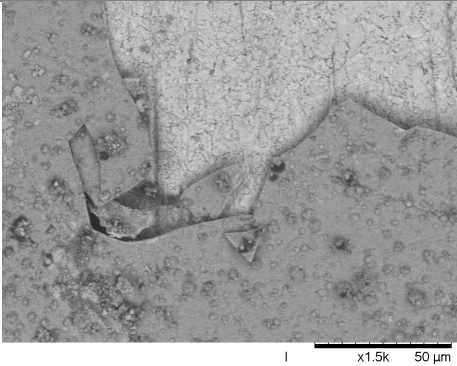
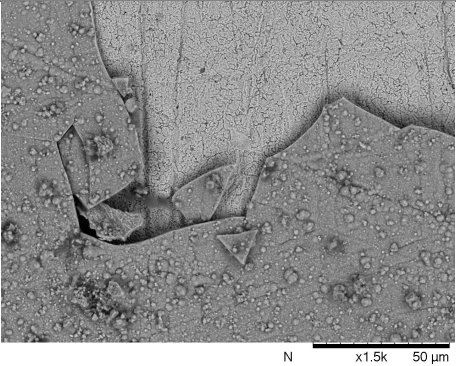
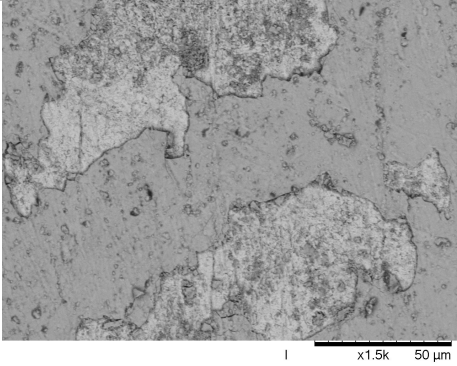
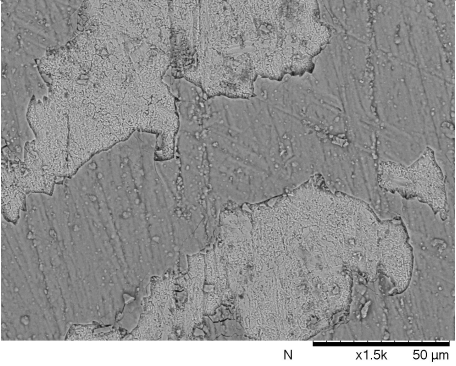
Sample	5 kV	15 kV
 -780		
 -783		
 -792		

Table 5.3 shows the additives present in each of the formulations and their respective concentrations. Corrosion inhibitor 2 is not present in any of the formulations which is the only similarity between them. Sample -792 has a thinner top layer this could be due

to the presence of dispersant 1, the lack of detergent 2 or a combination of both. It is very difficult to pinpoint which additives may be causing the flaking to occur.

These three samples have low amounts of copper in their end of test fluids, which are shown in the shaded column of Table 5.3. The values, although low, are not considered to be similar.

Table 5.3: Formulations of samples which show flaking surfaces and amount of copper measured in end of test fluid

Sample number	Concentration of Additive (wt%)									Copper level (ppm)
	Corrosion inhibitor 1	Corrosion inhibitor 2	Dispersant 1	Dispersant 2	Detergent 1	Detergent 2	Antioxidant	Antiwear	Friction Modifier	
-780	0.5	0	0	2.5	0	0.4	0.06	0.22	1.2	17
-783	0.5	0	0	5	0.1	0.4	0.6	0.11	0.1	11
-792	0.265	0	2.5	2.5	0	0	0.6	0.22	0.1	8

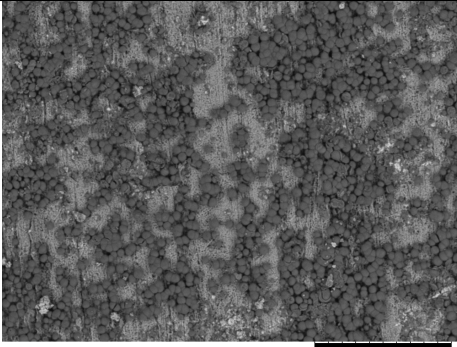
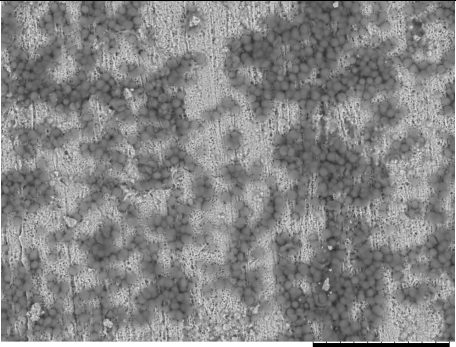
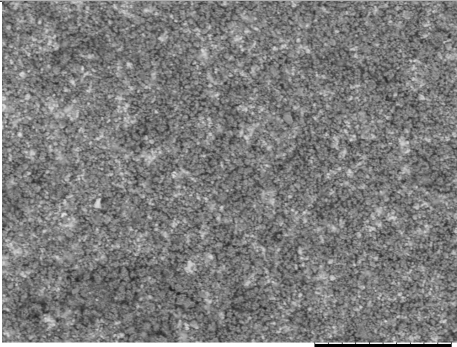
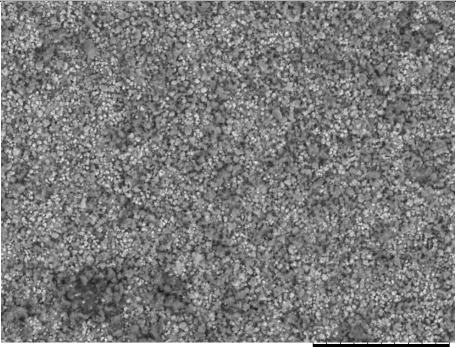
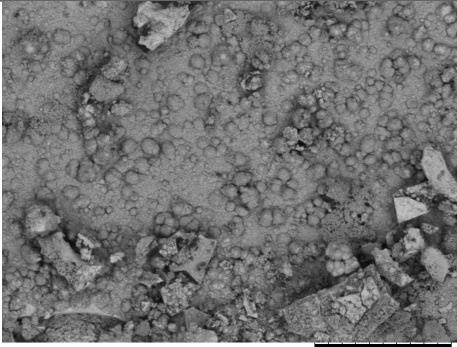
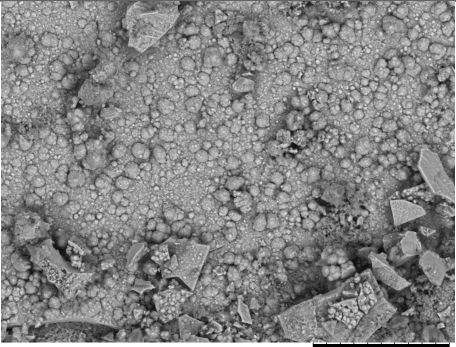
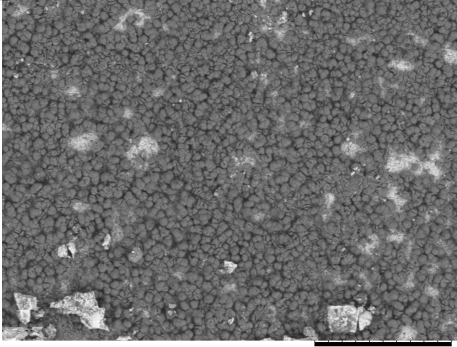
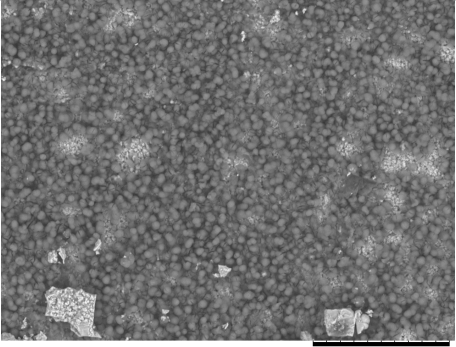
5.6.2 Full formulation samples showing surface spheres

The spherical morphology seen on the surface of the samples in Table 5.4 looks like there has been nucleation and growth of a corrosion product. The size and density of the spheres varies between the samples.

Table 5.5 shows the formulation of each of the sample fluids which gave spheres on the copper surface. All of the fluids contain 0.5 wt% corrosion inhibitor 1 but then differ in the remaining additives. It is very difficult to suggest which additives may be causing the density or size of the spheres to vary.

Sample -780 has the smallest and most densely packed spheres, whilst -779 has the least dense spheres. Sample -783 appears to have the spheres joining and forming a continuous layer, with various sized spheres, whereas for the other samples the spheres are mostly one size and do not seem to be amalgamating. It is possible that the presence of corrosion inhibitor 2 in -779 is causing the spheres to be less dense.

Table 5.4: BSE and coupon images for full formulation fluids showing distinct surface spheres

Sample	5 kV	15 kV
 -779		
 -780		
 -783		
 -795		

The copper level in the end of test fluid for sample -795 is 56 ppm, much higher than for the other samples in this group. It is possible that this is caused by the presence of dispersant 1 although further tests would be needed to confirm this.

From these full formulations it is not possible to draw meaningful conclusions about the influence of each additive on the formation of surface spheres.

Table 5.5: Formulations of samples which show distinct surface spheres and amount of copper measured in end of test fluid

Sample number	Concentration of Additive (wt%)									Copper level (ppm)
	Corrosion inhibitor 1	Corrosion inhibitor 2	Dispersant 1	Dispersant 2	Detergent 1	Detergent 2	Antioxidant	Antiwear	Friction Modifier	
-779	0.5	0.026	0	0	0	0	0.6	0.11	0.65	17
-780	0.5	0	0	2.5	0	0.4	0.06	0.22	1.2	17
-783	0.5	0	0	5	0.1	0.4	0.6	0.11	0.1	11
-795	0.5	0	2.5	0	0.2	0	0.6	0.22	1.2	56

5.6.3 Full formulation samples showing porous surfaces

Surfaces which showed pores or pitting on their surface were placed into this next category. The size and shape of the pits was not defined and all were grouped together.

Sample -808 had the largest and most distinct pits whilst the pores on sample -809 were the smallest, a higher magnification image is used in order to show the pores. Sample -806 was possibly the hardest to define as it appears to have an uneven surface with shallow wide pits.

Table 5.6: BSE and coupon images for full formulation fluids showing porous or pitted surfaces

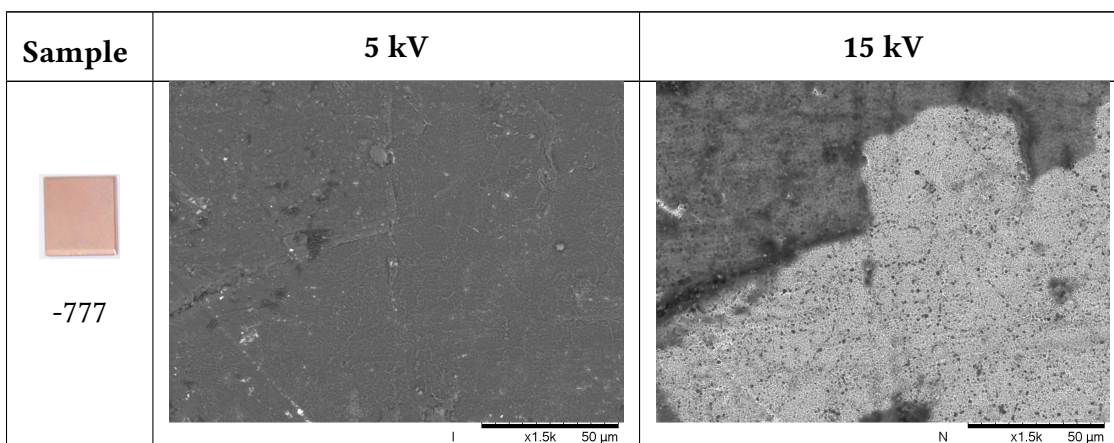


Table 5.6 cont.

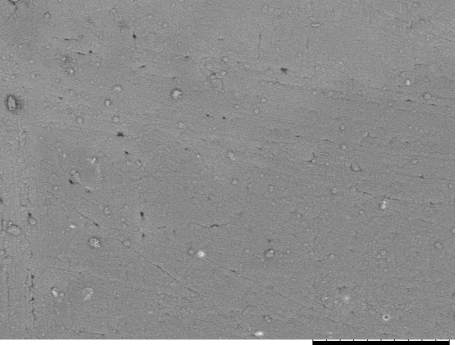
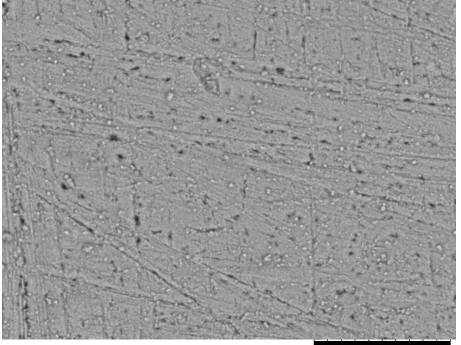
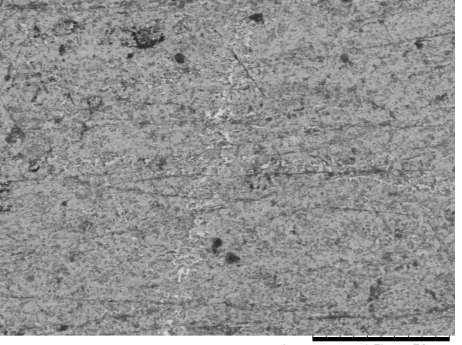
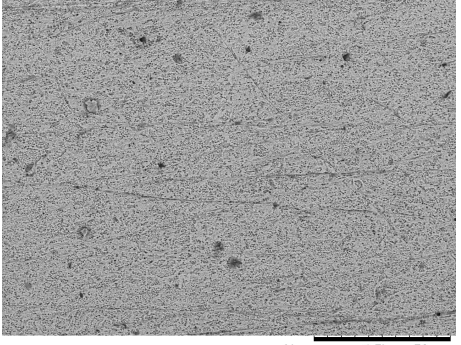
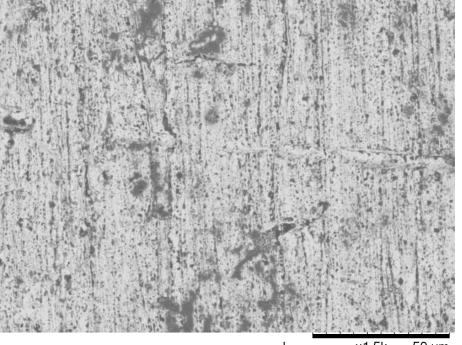
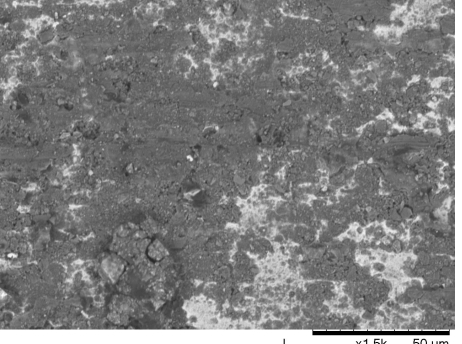
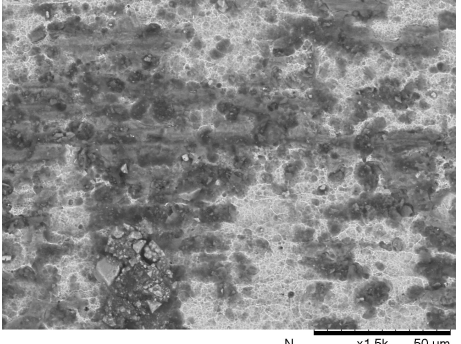
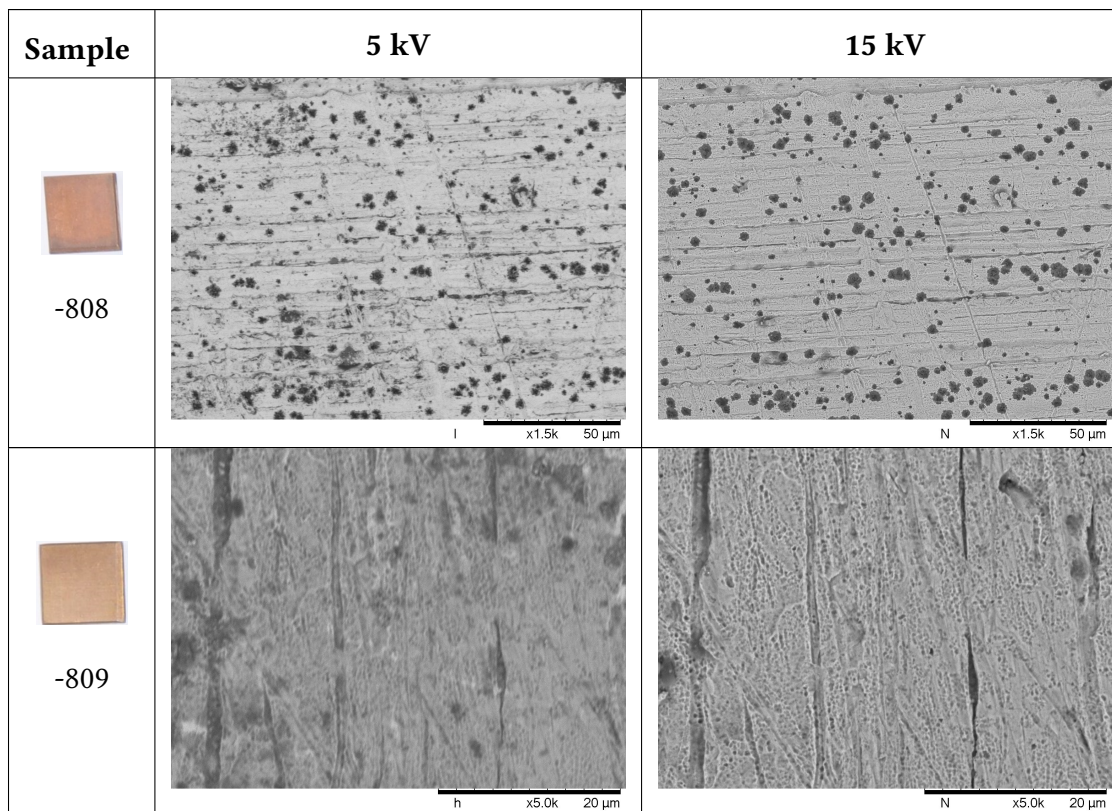
Sample	5 kV	15 kV
 -782	 I x1.5k 50 μm	 N x1.5k 50 μm
 -793	 I x1.5k 50 μm	 N x1.5k 50 μm
 -799	 I x1.5k 50 μm	 N x1.5k 50 μm
 -806	 I x1.5k 50 μm	 N x1.5k 50 μm

Table 5.6 cont.



Note that a higher magnification (x5k) is shown for sample 809 as the porosity of the surface was not easily seen at the magnification normally used (x1.5k)

The formulations of these sample fluids are shown in Table 5.7. With the exception of sample -799 the fluids all contain 0.03 wt% corrosion inhibitor 1.

Table 5.7: Formulations of samples which show porous surfaces and amount of copper measured in end of test fluid

Sample number	Concentration of Additive (wt%)									Copper level (ppm)
	Corrosion inhibitor 1	Corrosion inhibitor 2	Dispersant 1	Dispersant 2	Detergent 1	Detergent 2	Antioxidant	Antiwear	Friction Modifier	
-777	0.03	0.026	5	0	0.1	0	0.06	0.22	1.2	77
-782	0.03	0	0	0	0	0	0.06	0.165	0.1	24
-793	0.03	0.026	3.33	1.67	0.2	0	0.6	0.11	0.1	14
-799	0.5	0	5	0	0.2	0.2	0.06	0.11	0.1	31
-806	0.03	0	5	0	0	0.4	0.6	0.11	1.2	103
-808	0.03	0.026	0	5	0	0.2	0.6	0.22	1.2	27
-809	0.03	0.026	1.67	3.33	0	0.4	0.06	0.11	0.1	7

The difference in the size and shape of the pits on different surfaces makes comparisons between the formulations even more difficult. The amount of copper measured in the end of test fluid also varies widely between the samples so no meaningful conclusions can be drawn from the additives present in the different formulations.

Sample -782 did however show the presence of phosphorous in its EDX spectra which was not seen in any of the other samples. The spectra is shown in Figure 5.15. The antiwear molecule is the only one to contain phosphorous. The fact that it appears on the surface of sample -782 but not others is likely due to its formulation. It contains only corrosion inhibitor 1, antioxidant, antiwear and friction modifier. The antiwear has the highest concentration of the molecules present and so it is unsurprising that it should be detected on the surface. There are no other formulations where so few additives are present and this may explain why it is not seen on any of the other surfaces.

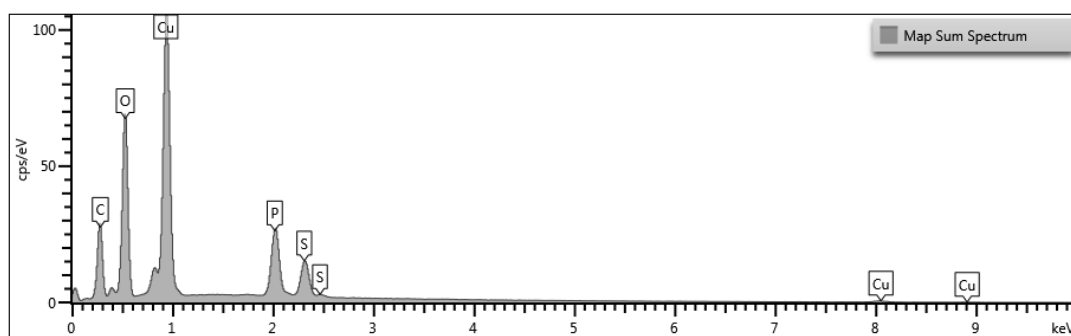


Figure 5.15: EDX spectrum of sample -782

5.6.4 Full formulation samples showing small particles

Samples which showed small particles on their surfaces are shown in Table 5.8, whilst Table 5.9 shows the concentrations of additives present in each of the sample formulations.

The amount of copper measured in the end of test fluid for each of the samples is also given in Table 5.9 and varies from 1 ppm to 306 ppm so there is no correlation between the amount of copper measured and the formation of small particles on the surface of the coupon.

Table 5.8: BSE and coupon images for full formulation fluids showing small particles on the surface

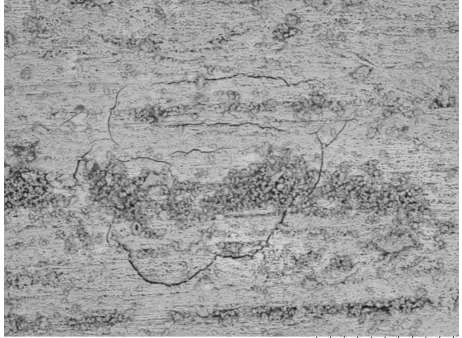
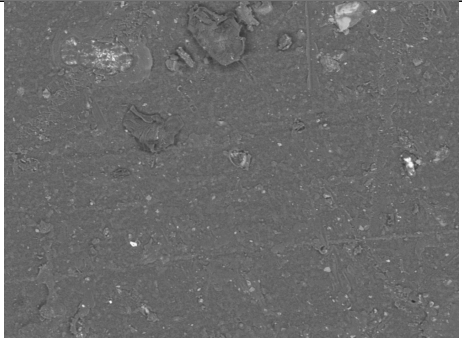
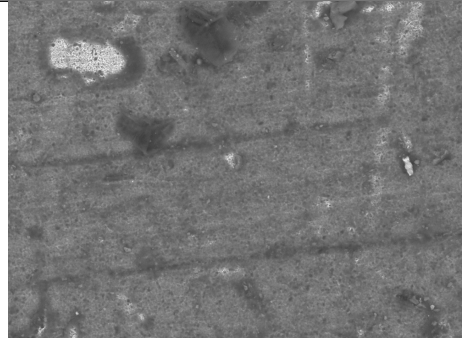
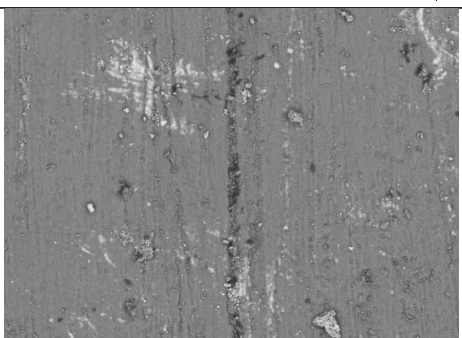
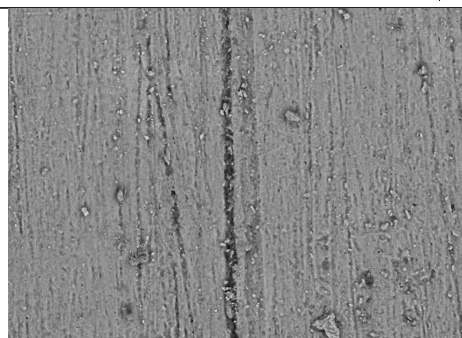
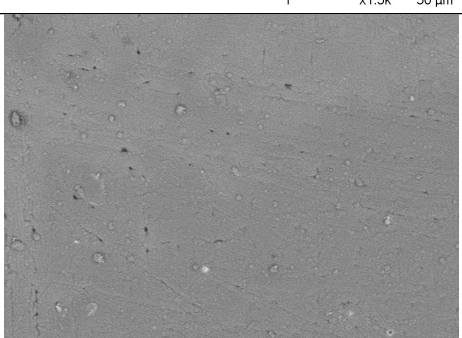
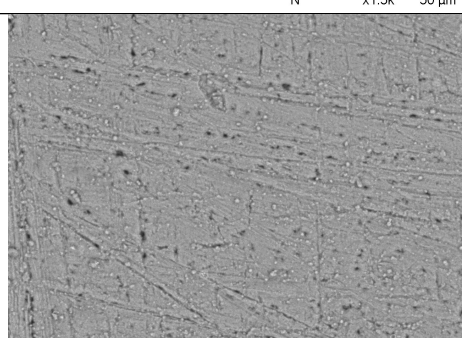
Sample	5 kV	15 kV
 -776	 I x1.5k 50 μm	 N x1.5k 50 μm
 -777	 I x1.5k 50 μm	 N x1.5k 50 μm
 -778	 I x1.5k 50 μm	 N x1.5k 50 μm
 -782	 I x1.5k 50 μm	 N x1.5k 50 μm

Table 5.8 cont.

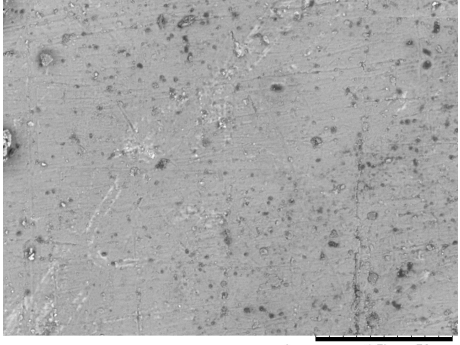
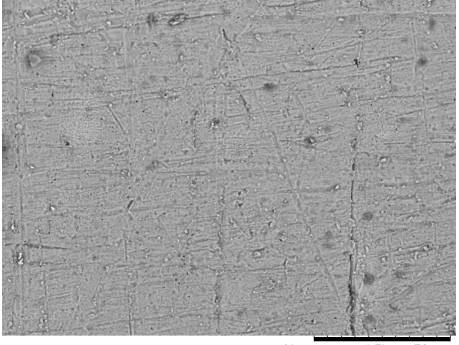
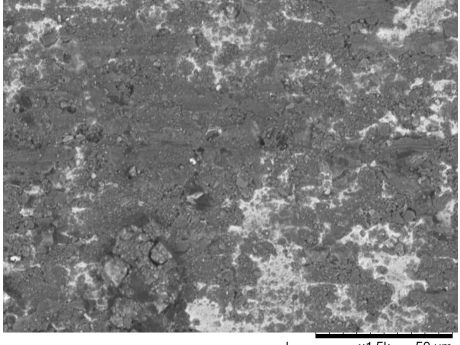
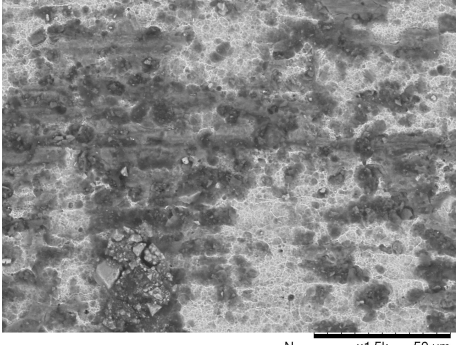
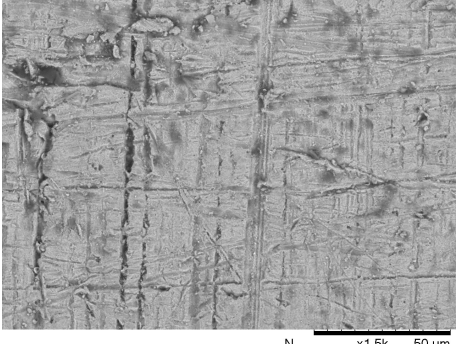
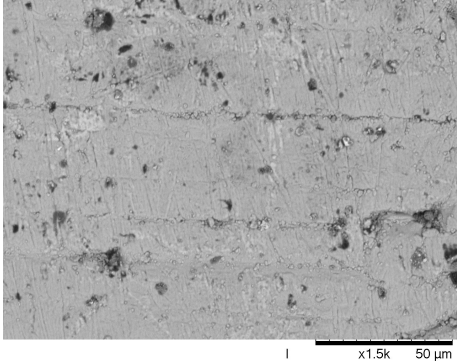
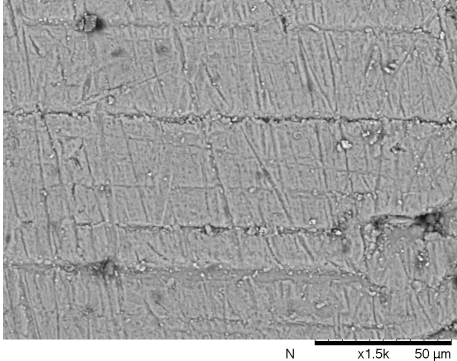
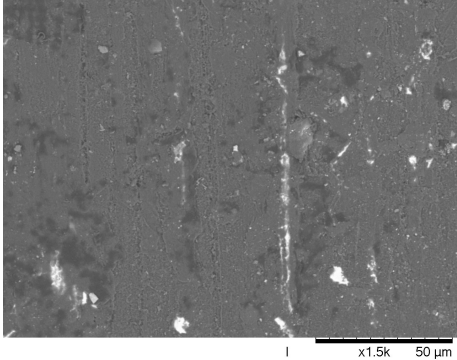
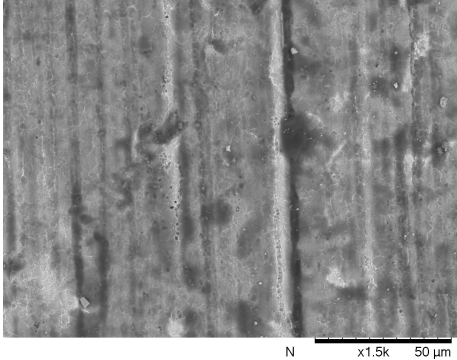
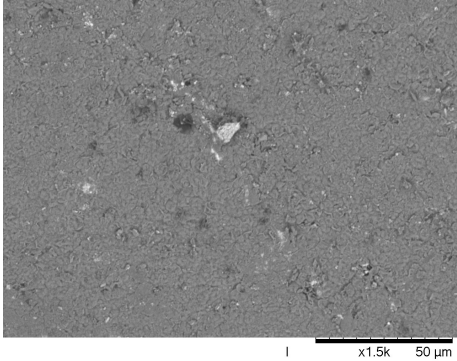
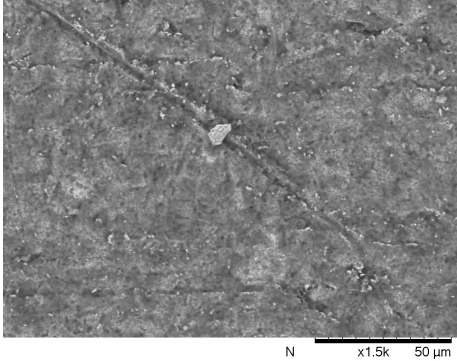
Sample	5 kV	15 kV
 <p data-bbox="352 499 413 533">-797</p>	 <p data-bbox="754 629 927 651">I x1.5k 50 μm</p>	 <p data-bbox="1244 629 1417 651">N x1.5k 50 μm</p>
 <p data-bbox="352 871 413 904">-798</p>	 <p data-bbox="754 1001 927 1023">I x1.5k 50 μm</p>	 <p data-bbox="1244 1001 1417 1023">N x1.5k 50 μm</p>
 <p data-bbox="352 1238 413 1272">-806</p>	 <p data-bbox="754 1373 927 1395">I x1.5k 50 μm</p>	 <p data-bbox="1244 1373 1417 1395">N x1.5k 50 μm</p>
 <p data-bbox="352 1610 413 1644">-807</p>	 <p data-bbox="754 1744 927 1767">I x1.5k 50 μm</p>	 <p data-bbox="1244 1744 1417 1767">N x1.5k 50 μm</p>

Table 5.8 cont.

Sample	5 kV	15 kV
 -810		
 -811		
 -794		

794 is an unusual sample that could be classified on its own as the surface appears to be formed from particles that have agglomerated together to form a layer across the surface; this is seen most easily in the 5 kV image.

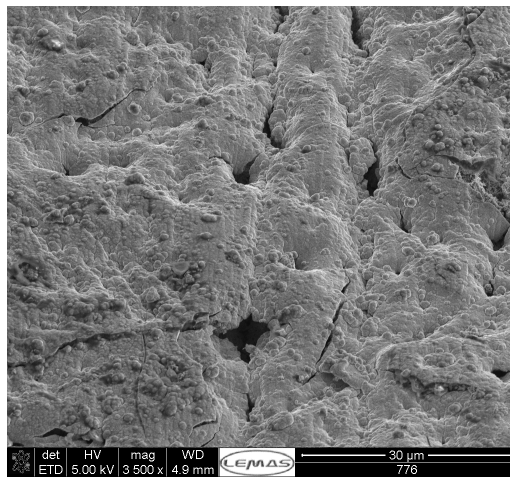
It is possible that these samples could have been further divided by the quantity, size or density of particles but this had no additional benefit in determining which additives were causing the surface features and so all samples were grouped together.

Sample -776 was unusual in that it showed small particles but also some cracking along the surface, which did not seem to be present in other samples. In order to investigate this further a focussed ion beam (FIB) was used to mill a small hole in the surface to gain a cross-sectional view. This cross-section can be seen in Figure 5.16b.

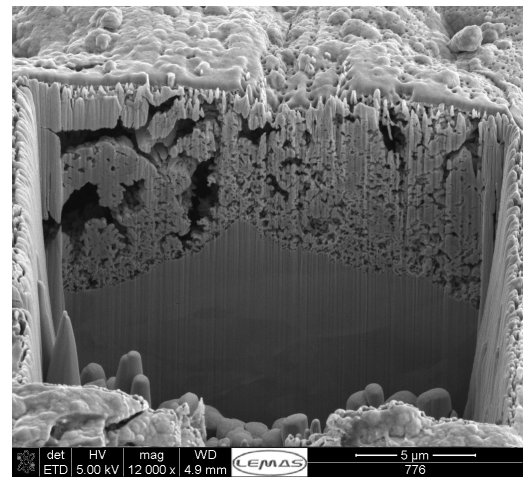
The cross section shows the bulk copper underneath a porous region up to 7 μm

Table 5.9: Formulations of samples which show small surface particles and amount of copper measured in end of test fluid

Sample number	Concentration of Additive (wt%)									Copper level (ppm)
	Corrosion inhibitor 1	Corrosion inhibitor 2	Dispersant 1	Dispersant 2	Detergent 1	Detergent 2	Antioxidant	Antiwear	Friction Modifier	
-776	0.03	0	0	5	0.2	0	0.33	0.11	1.2	306
-777	0.03	0.026	5	0	0.1	0	0.06	0.22	1.2	77
-778	0.5	0.013	2.5	2.5	0	0	0.06	0.11	1.2	12
-782	0.03	0	0	0	0	0	0.06	0.165	0.1	24
-797	0.5	0.026	2.5	2.5	0.2	0.4	0.6	0.165	1.2	9
-798	0.265	0.013	2.5	2.5	0.1	0.2	0.33	0.165	0.65	10
-806	0.03	0	5	0	0	0.4	0.6	0.11	1.2	103
-807	0.03	0.013	0	0	0.2	0.4	0.6	0.22	0.1	2
-810	0.5	0.026	0	5	0.2	0	0.06	0.22	0.1	1
-811	0	0.026	5	0	0	0.4	0.33	0.22	0.25	41
-794	0.265	0.026	0	0	0.2	0.4	0.06	0.11	1.2	9



(a) SEM surface image



(b) FIB cross-section

Figure 5.16: SEM and cross-sectional analysis of sample -776

thick. EDX was carried out on the cross section and indicated that the porous layer was mainly comprised of copper and sulfur.

5.6.5 Full formulation samples which are relatively featureless

Two samples did not seem to obviously fit within these categories and so were classified as being featureless, as shown in Table 5.10. The additives present in the formulations can be seen in Table 5.11.

Table 5.10: BSE and coupon images for full formulation fluids showing featureless surfaces

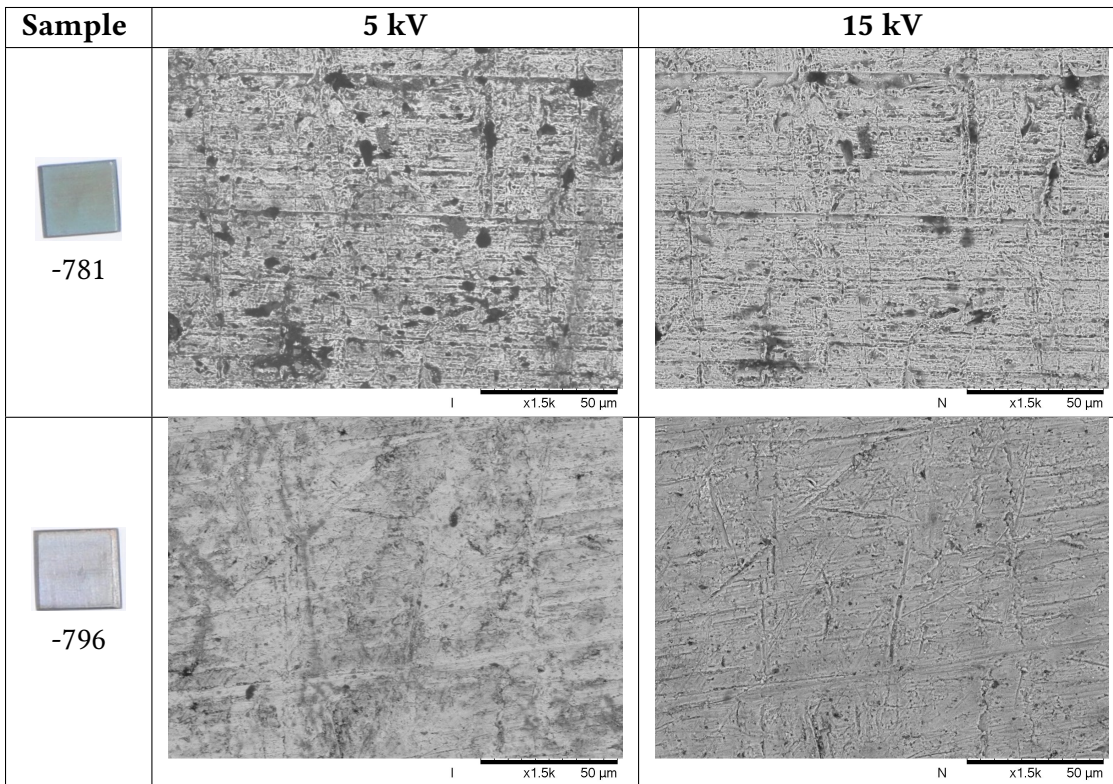


Table 5.11: Formulations of samples with featureless surfaces and amount of copper measured in end of test fluid

Sample number	Concentration of Additive (wt%)									Copper level (ppm)
	Corrosion inhibitor 1	Corrosion inhibitor 2	Dispersant 1	Dispersant 2	Detergent 1	Detergent 2	Antioxidant	Antiwear	Friction Modifier	
-781	0.5	0.026	5	0	0	0.4	0.33	0.22	0.1	24
-796	0.03	0	2.5	2.5	0.2	0.4	0.06	0.22	0.65	51

All of the samples were grouped based on the appearance of their BSE images and the formulations within these groups compared. Due to the complexities of the formulations

it was not possible to draw any useful conclusions from similarities, with one exception. The group which had flaking surfaces were found to have meaningful similarities. They were found to contain no corrosion inhibitor 2 and when all samples containing no corrosion inhibitor 2 were analysed flaking occurred in those which contained higher levels of corrosion inhibitor 1 and dispersant 2. Although it was possible to identify which additives may be causing the flaking other trends, such as the amount of copper in the end of test fluid or the ASTM rating, were not found.

5.7 Variation of additive levels

From studying the formulations present in each of the above groups, it was seen that dispersant 2 and the presence and lack of corrosion inhibitors caused flaking. It was thought that these additives may have the biggest impact on the interaction of the fluid with the copper surface. In order to test this theory 5 fully formulated fluids were chosen and their dispersant and corrosion inhibitor levels changed. The original fluids and their variations are detailed in Table 5.12. In order to emphasise the changes made the differences from the original fluid are highlighted. As well as studying fully formulated fluids the dispersants were also studied individually.

In order to see the effect on the surface in more detail each group of variations shall be presented in turn, for some only 1 variation was looked at whilst for others all 4 variations were carried out.

Table 5.12: Levels of additives, wt%, in original full formulation fluids and the subsequent changes in corrosion inhibitor and dispersant levels

Sample number	Variation	Corrosion inhibitor 1	Corrosion inhibitor 2	Dispersant 1	Dispersant 2	Detergent 1	Detergent 2	Antioxidant	Antiwear	Friction Modifier
Base oil	No dispersant	0	0	0	0	0	0	0	0	0
dispersant 1	dispersant 1	0	0	5	0	0	0	0	0	0
dispersant 2	dispersant 2	0	0	0	5	0	0	0	0	0
Mix of both dispersants	Both dispersants	0	0	2.5	2.5	0	0	0	0	0
-779	No dispersant	0.5	0.026	0	0	0	0	0.6	0.11	0.65
-860	dispersant 2	0.5	0.026	0	5	0	0	0.6	0.11	0.65
-861	dispersant 1	0.5	0.026	5	0	0	0	0.6	0.11	0.65
-862	Both dispersants	0.5	0.026	2.5	2.5	0	0	0.6	0.11	0.65
-794	No dispersant	0.265	0.265	0	0	0.2	0.4	0.06	0.11	1.2
-661	Both dispersants	0.265	0.265	2.5	2.5	0.2	0.4	0.06	0.11	1.2
-663	dispersant 2	0.265	0.265	0	5	0.2	0.4	0.06	0.11	1.2
-776	dispersant 2	0.03	0	0	5	0.2	0	0.33	0.11	1.2
-859	No dispersant	0.03	0	0	0	0.2	0	0.33	0.11	1.2
-863		0.5	0	0	5	0.2	0	0.33	0.11	1.2
-864		0.03	0.026	0	0	0.2	0	0.33	0.11	1.2
-793	Both dispersants	0.03	0.026	3.33	1.67	0.2	0	0.6	0.11	0.1
-660	No dispersant	0.03	0.026	0	0	0.2	0	0.6	0.11	0.1
-810		0.5	0.026	0	5	0.2	0	0.06	0.22	0.1
-865		0	0.026	0	5	0.2	0	0.06	0.22	0.1

5.7.1 Dispersants tested alone in base oil

In order to look at the impact of the dispersants the impact of base oil alone needed to be understood. Figure 5.17 shows the amount of copper in the end of test fluid for the base oil (no dispersant present) and also for base oil containing the amount of dispersant specified in Table 5.12. The base oil alone shows a small amount of copper in the end of test fluid. This is increased with the addition of dispersant 1 and dispersant 2 individually. When both dispersants are present together another increase is seen. However, the amount of copper in the end of test fluid is still fairly low compared to other values seen for the fully formulated fluids tested previously. This would suggest that although the presence of dispersant can increase the amount of copper in the end of test fluid the interaction of other additives must also play a part in increasing the copper levels in full formulations.

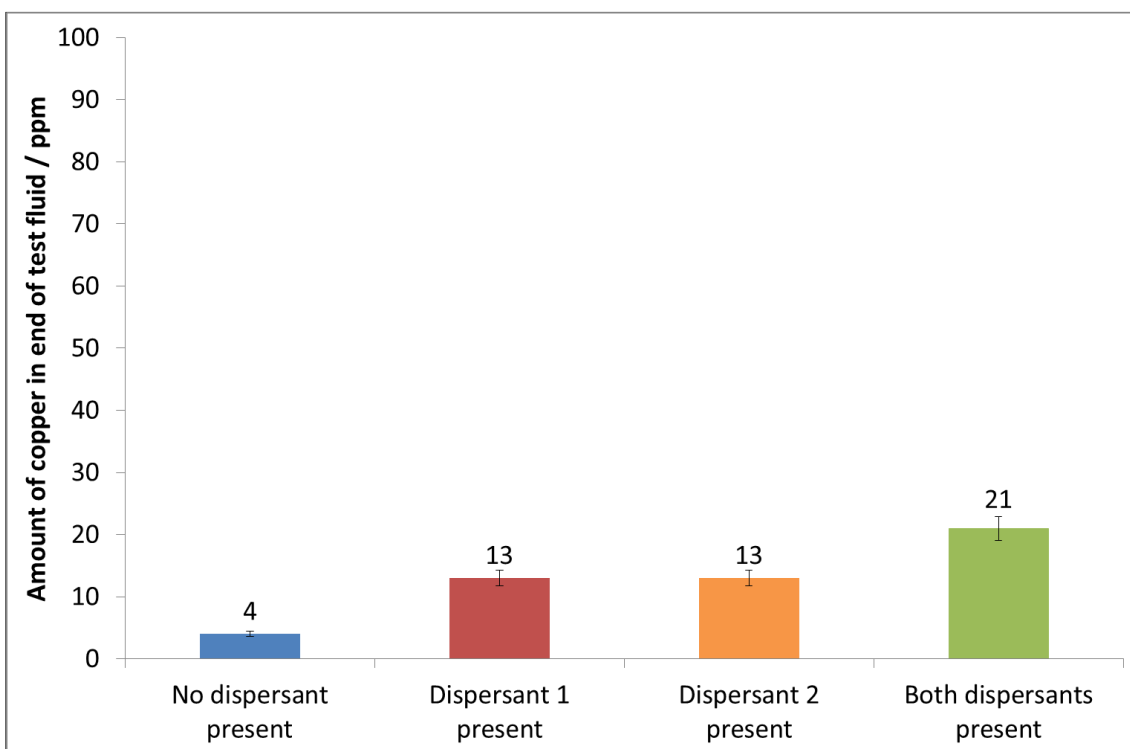


Figure 5.17: Amount of copper in the end of test fluid as determined by ICP-AES for dispersant variations for dispersants dissolved in base oil alone

SEM images of the sample surfaces can be seen in Figure 5.18. When no dispersant is present it looks as if small particles are deposited on the surface, however when dispersant is present individually it looks as if a film is formed on the surface, and in the case of dispersant 2 this film appears crystalline in structure with defined edges. When both

dispersants are present a more porous structure is seen. This porosity could explain the higher level of copper in the end of test fluid.

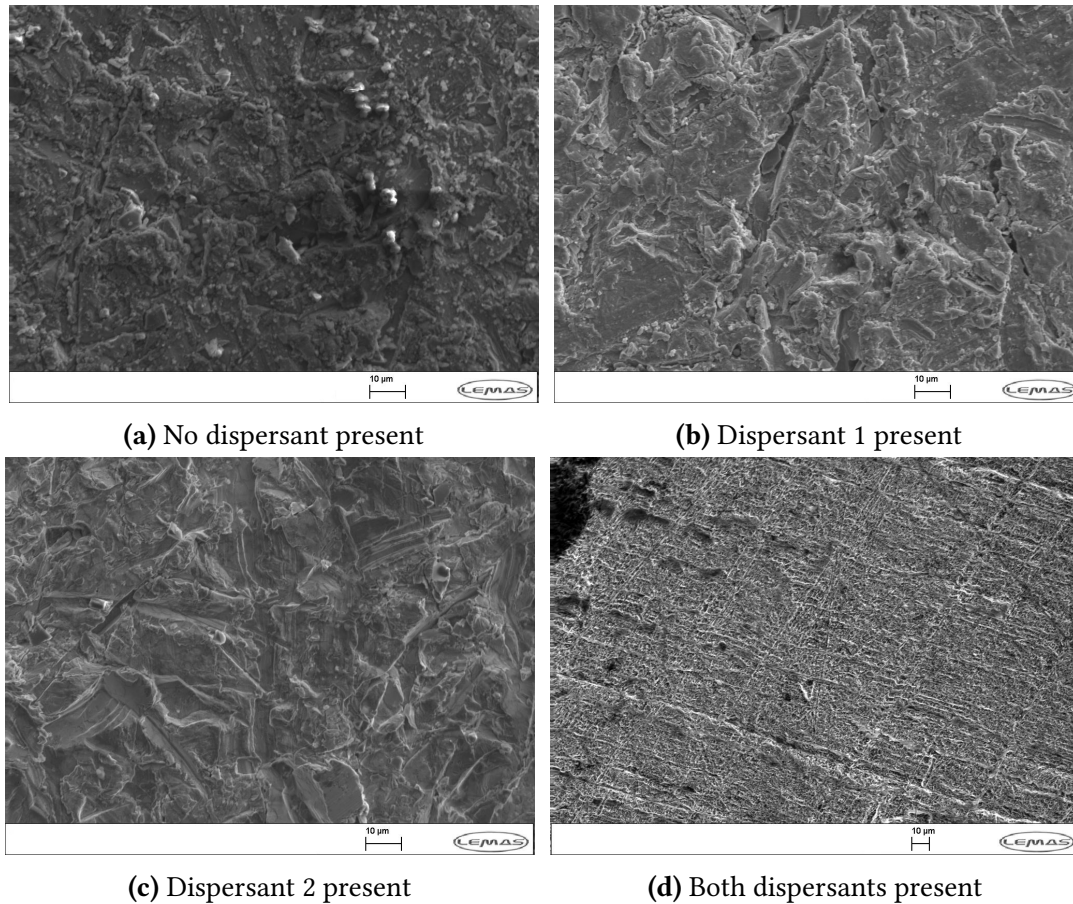


Figure 5.18: SEM images of the surfaces of samples immersed in base oil and dispersant mixtures

5.7.2 Dispersant variations of formulation -779

Formulation -779 originally contained both corrosion inhibitors and no dispersant. It was the only formulation tested with all permutations of dispersant present. The changes to the formulation are stated in Table 5.12.

Figure 5.19 shows the amount of copper in the end of test fluid for each variation; with each bar of the chart representing one change. With no dispersant present the formulation has 17 ppm of copper in the end of test fluid, on the addition of either dispersant individually the amount of copper increases, with a greater increase seen for dispersant 2. Interestingly the addition of both dispersants gives an increase in the copper level above the formulation with no dispersant but below the variations containing the dispersants individually. This is in contrast to when the dispersants

were tested in base oil alone as in that instance the mix of both dispersants gave the highest amount of copper in the end of test fluid. The difference could be due to the concentration of each additive individually; the total level of dispersant is equal to 5 wt% in each instance and so the combination contains 2.5 wt% of each dispersant. If the two dispersants interact competitively then a lower concentration could affect the amount of copper seen in the end of test fluid.

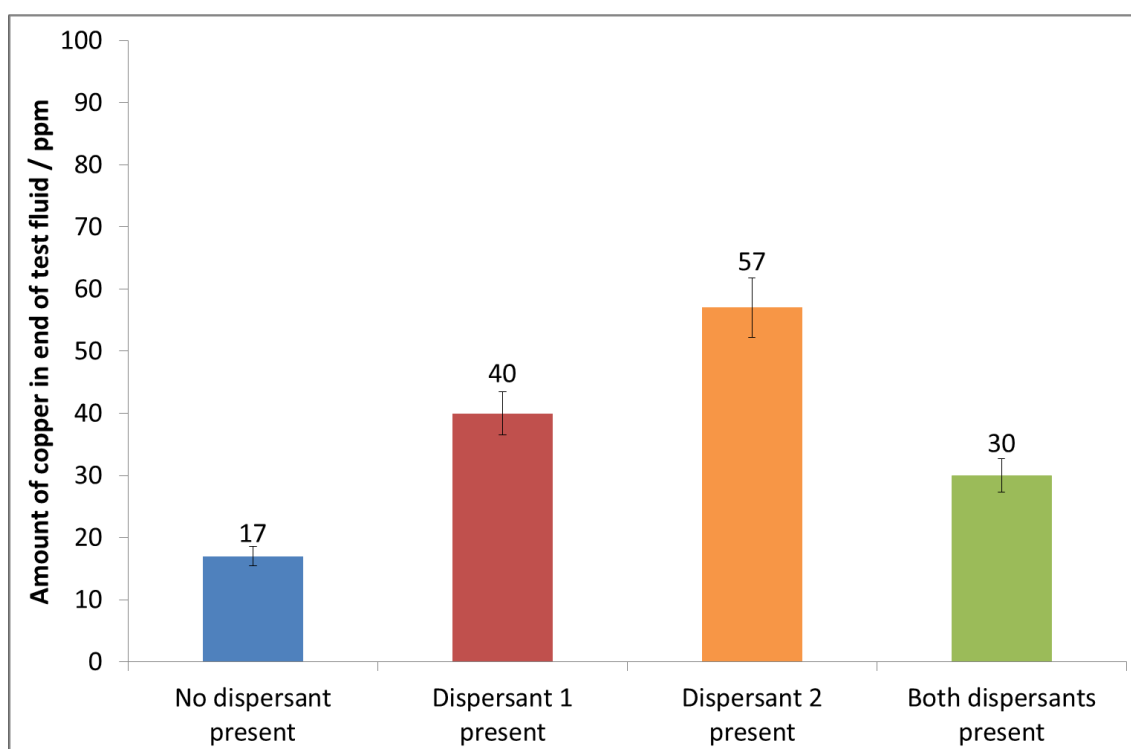


Figure 5.19: Amount of copper in the end of test fluid as determined by ICP-AES for dispersant variations based on the full formulation -779

Figure 5.20 shows the surface of samples which have been tested in variations of formulation -779. When no dispersant is present small spherical deposits can be seen on the surface. When dispersant 1 is present these spherical structures can no longer be seen but it is clear that there is some sort of deposit present. Interestingly when dispersant 2 is present, there are very many spherical structures covering the entire surface but they are much larger and have a more interesting structure, in that they are not like solid spheres but rather spheres that have split open. When both dispersants are present the surfaces is covered in what appears to be very many patches, in some ways a mixture of both dispersants with a deposit similar to that of dispersant 1 but in clear circular type arrangements, like dispersant 2.

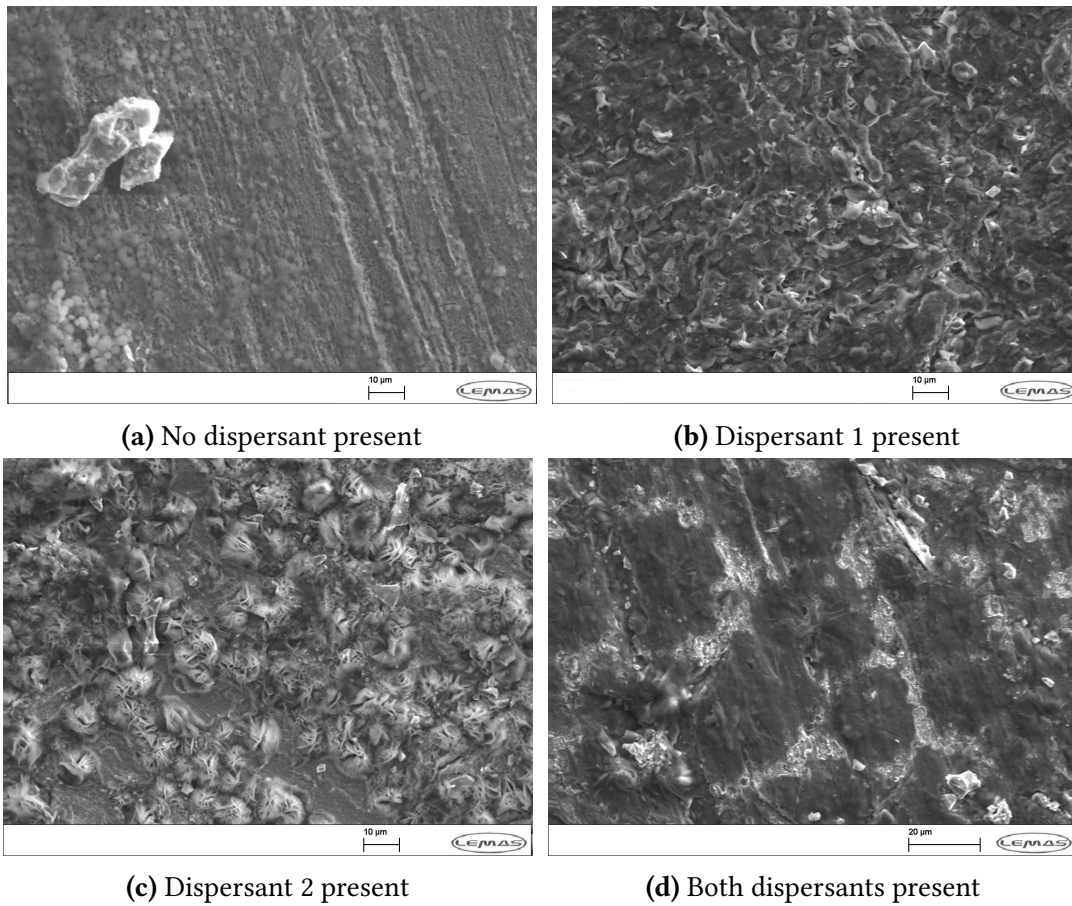


Figure 5.20: SEM images of the surfaces of samples immersed in dispersant variations of the full formulation -779

5.7.3 Dispersant variations of formulation -794

Formulation -794 had no dispersant present initially, but equal levels of corrosion inhibitors 1 and 2. It had a low level of copper in the end of test fluid and it was chosen to see if the copper level increased with the addition of dispersant. Figure 5.21 shows the amount of copper in the end of test fluid for variations of the formulation -794. As seen for -779 the amount of copper increases with the presence of dispersant 2 but is not quite as high when both dispersants are present.

SEM images of the surfaces of these formulation variations can be seen in Figure 5.22. When no dispersant is present a film or similar is clearly present on the surface, which appear to be patches which have grown and agglomerated together. When dispersant 2 is present the surface appears to be porous; this may help to explain the increased copper level in the end of test fluid. When both dispersants are present there are clear circular objects which have not agglomerated across the entire surface.

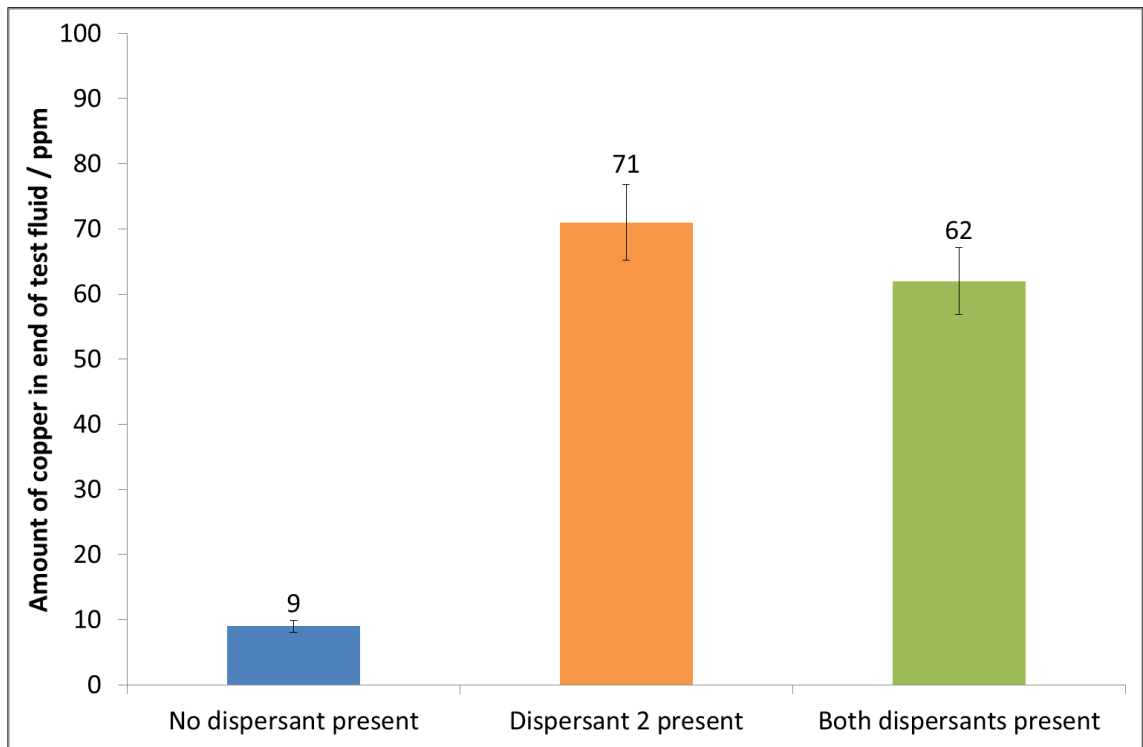
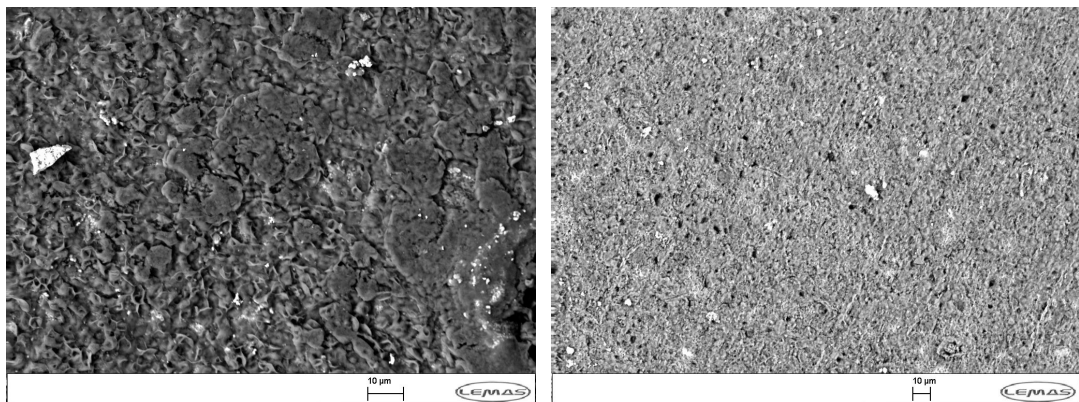
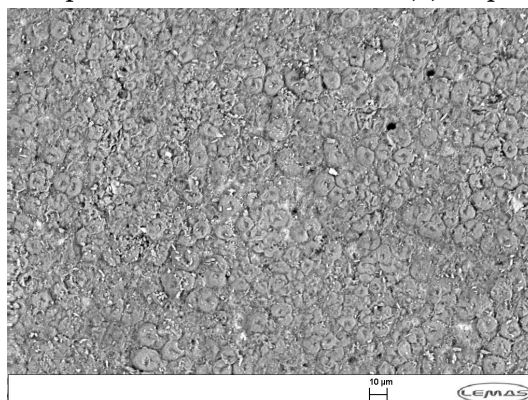


Figure 5.21: Amount of copper in the end of test fluid as determined by ICP-AES for dispersant variations based on the full formulation -794



(a) No dispersant present

(b) Dispersant 2 present



(c) Both dispersants present

Figure 5.22: BSE images of the surfaces of samples immersed in dispersant variations of the full formulation -794

5.7.4 Dispersant and corrosion inhibitor variations for formulation -776

Formulation -776 had the highest level of copper in the end of test fluid for any of the formulations tested and for this reason it was chosen to be studied. It contained a low level of corrosion inhibitor 1 and a high level of dispersant 2 in its original formulation. Dispersant 2 was removed from the formulation to create one variation and the level of corrosion inhibitor was varied to provide 2 other variations as it was the impact of dispersant and corrosion inhibitor that was investigated.

The amount of copper in the end of test fluid for formulation -776 and its variations can be seen in Figure 5.23, each bar of the chart represents one change to the original formulation and more details can be found in Table 5.12.

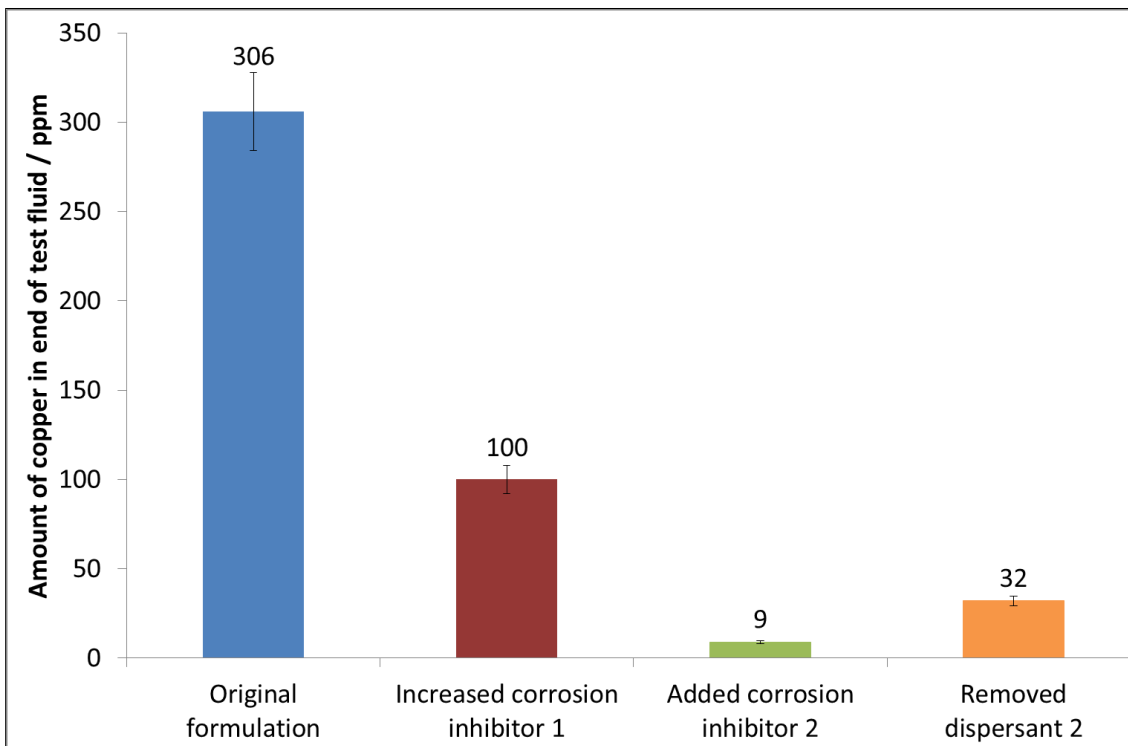


Figure 5.23: Amount of copper in the end of test fluid as determined by ICP-AES for full formulation -776 and variations involving corrosion inhibitors 1 and 2, and dispersant 2

All variations significantly reduce the amount of copper in the end of test fluid. The addition of corrosion inhibitor 2 has the greatest effect whilst simply increasing the amount of corrosion inhibitor 1 has the least effect.

SEM images of the sample surfaces are shown in Figure 5.24. The original formulation shows many holes and cracks on the surface. Increasing the amount of corrosion inhibitor 1 gets rid of much of this and a fuzzy layer is seen across the surface. Removal of dispersant 2 gives much smaller holes across the surface and practically eliminates the cracks seen in the full formulation.

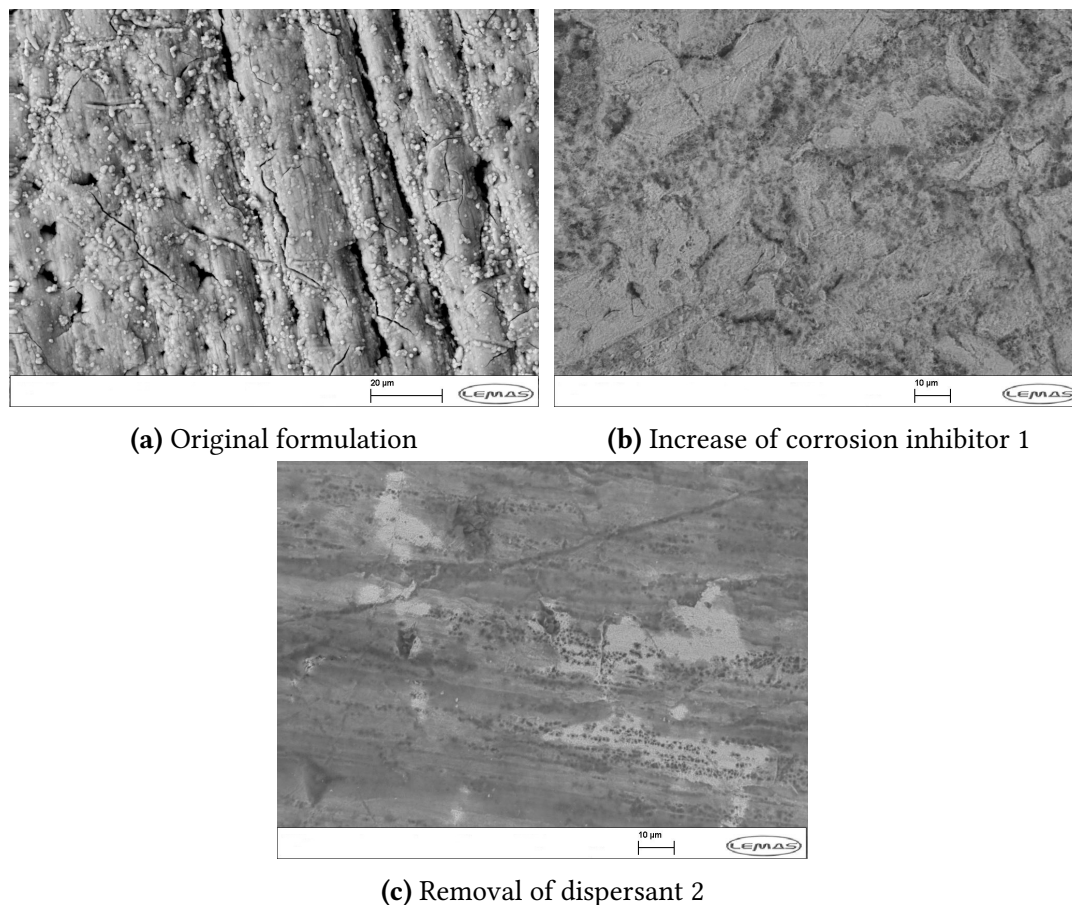


Figure 5.24: BSE images of the surfaces of samples immersed in variations of the full formulation -776

5.7.5 Dispersant variations of full formulation -793

Unlike the other formulations to this point the presence of both dispersants in formulation -793 gives a fractionally lower amount of copper in the end of test fluid than when no dispersant is present. This formulation is unusual in that the dispersants are not present in equal amounts; dispersant 1 is at 3.33 wt% and dispersant 2 at 1.67 wt%, giving a total of 5 wt% as for the other formulations.

SEM images of the surfaces, Figure 5.26, show that with no dispersant the surface is slightly porous whereas when both dispersants are present this is not the case.

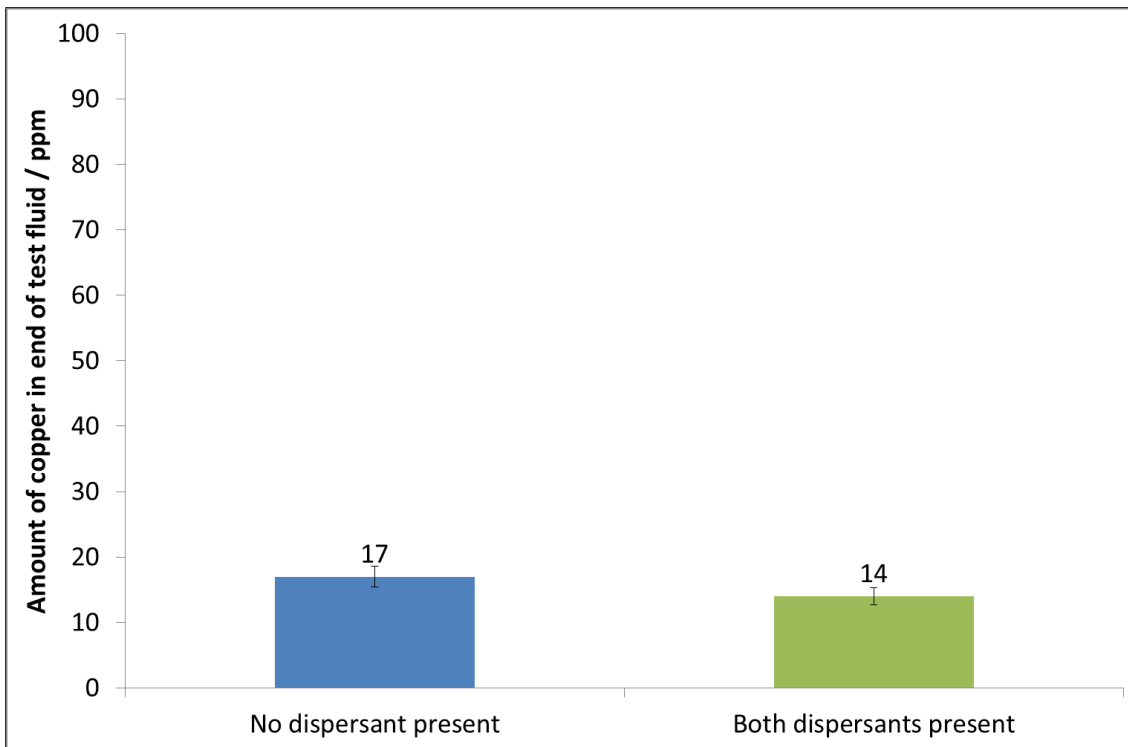


Figure 5.25: Amount of copper in the end of test fluid as determined by ICP-AES for full formulation -793, with and without dispersant present

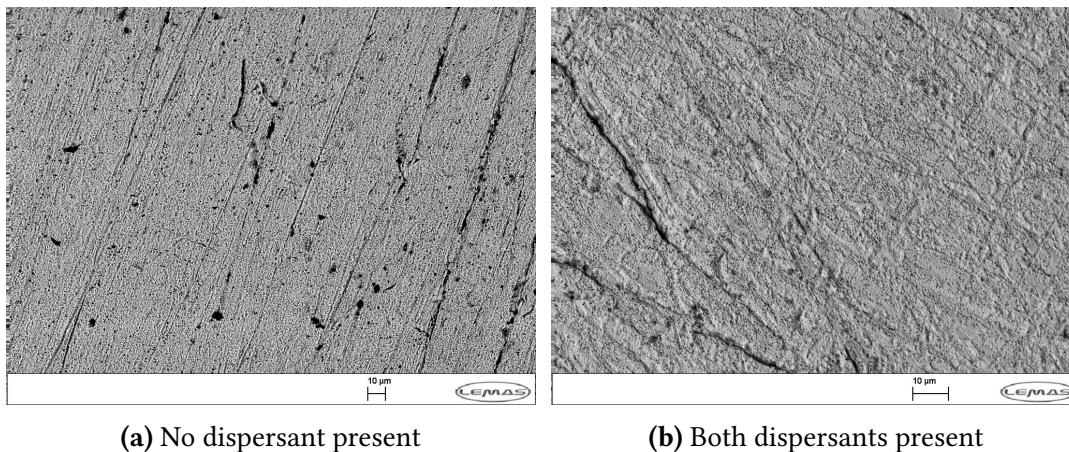


Figure 5.26: BSE images of the surfaces of samples immersed in variations of the full formulation 793, with and without dispersants

5.7.6 Corrosion inhibitor variation of formulation -810

One other variation was carried out to look at the impact of corrosion inhibitors; this lack of variations was partly due to time constraints. The variation took formulation -810, which had practically no copper in the end of test fluid, only 1 ppm was detected. This formulation initially contained both corrosion inhibitors. Corrosion inhibitor 1 was removed, leaving only corrosion inhibitor 2 present. The amount of copper in the end of test fluid did not rise significantly, with only 3 ppm of copper detected. This suggests

that corrosion inhibitor 2 is a very efficient corrosion inhibitor. These results for the amount of copper in the end of test fluid can be seen in Figure 5.27.

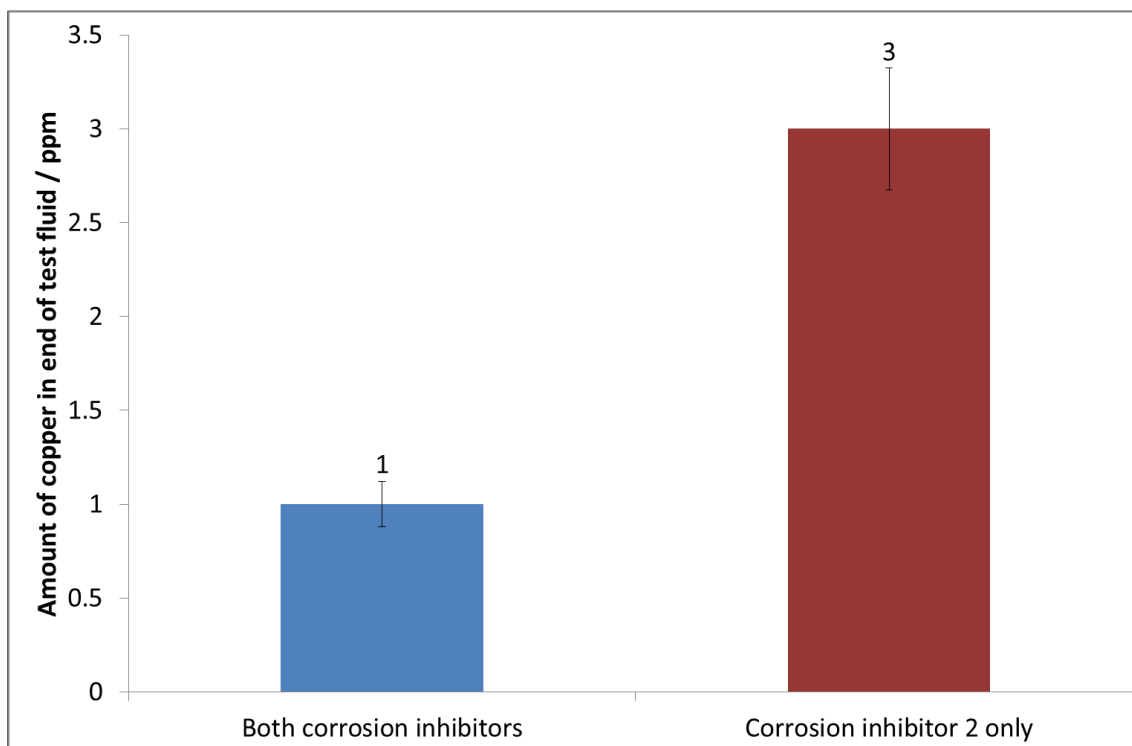


Figure 5.27: Amount of copper in end of test fluid for formulation -810, and corrosion inhibitor variation

From these variation experiments it has been possible to see that the addition of dispersants to a formulation generally increases the amount of copper in the end of test fluid. The corrosion inhibitor variations were not as thorough owing to time constraints but it appears that corrosion inhibitor 2 may be more effective than corrosion inhibitor 1. For a better understanding of the impact of the additives they shall all be studied individually.

5.8 Summary

This section has focussed on the testing of full formulation fluids. A number of different observations have been identified from the testing carried out.

- The ASTM rating cannot easily be quantified. The digital brightness rating assigned to test coupons did not always match the ASTM rating, particularly when the samples were not a uniform colour.

- The weight change of samples is very small and in cases where films are formed, and removed, the weight change can differ dramatically between repeat samples.
- The ASTM rating does not correlate with the weight change of the coupons, and mid ratings often show very little weight change.
- The amount of copper measured in the end of test fluid does not correlate with the ASTM rating, poorer ratings do not always have higher copper levels.
- With a few exceptions there is a fairly good correlation between the weight change of the coupons and the amount of copper measured in the corresponding end of test fluid.
- The amount of sulfur present in the formulation has no correlation with the ASTM rating or the amount of copper in the end of test fluid.
- Similarities could be found between different FTIR spectra, allowing them to be grouped according to the peaks present, however no similarities could be found in the corresponding formulations.
- SEM images of the coupon surfaces could also be grouped according to similarity, 5 main groups were identified, only one gave significant results. The group which showed flaking were found to have no corrosion inhibitor 2 present. Expanding the selection to all samples which contained no corrosion inhibitor 2 it was found that those which flaked had high levels of corrosion inhibitor 1 and dispersant 2.
- The levels of corrosion inhibitor and dispersant were varied in a number of the formulations. Generally speaking the presence of dispersant increased the amount of copper measured in the end of test fluid. Increasing the amount of corrosion inhibitor decreased the amount of copper in the end of test fluid.

6: Initial wire testing

Carrying out only immersion testing, as in the previous chapter, cannot tell us anything about how corrosion may be progressing. Conventional electrochemical techniques will not work, due to the low conductivity of the fluids, so a new technique was used, based on work by Hunt and Gahagan [116, 122, 123]. This involved measuring the change in resistance of a thin copper wire when it is placed into an ATF fluid. The change in resistance can be converted into a change in radius and give an idea of how corrosion may be affecting the wire with time, as detailed in Section 4.3.3.

6.1 Choice of full formulation fluids for wire tests

As full formulation fluids were available from the initial tests conducted these were used to test whether the wire resistance method was a viable option for measuring the corrosion of copper in ATFs. Due to limited space, and time constraints not all fluids could be tested using the wire method. Therefore the initial 24 samples were narrowed down to 15 full formulation fluids plus the base oil alone; 16 fluids in total.

A range of fluids which gave a variation of coupon properties and end of test copper levels were chosen from the initial samples. As discussed in the full formulation testing chapter it was possible to group the samples by SEM surface appearance, FTIR similarities and ASTM rating. These groupings are summarised in Table 6.1. The sample numbers refer to the numbers assigned to each of the full formulations. Information regarding the make up of these formulations can be found in the methodology section.

At least one sample was chosen from each of the groupings; particularly if it had a unique feature. The level of copper in the end of test fluid was also taken into consideration when selecting samples.

Table 6.1: Sample grouping for SEM surface appearance, FTIR similarities, and ASTM rating

Category	Group	Samples
SEM surface appearance	Flaking	780, 783, 792
	Spheres	779, 780, 783, 795
	Porous	777, 793, 799, 806, 808, 809
	Small particles	776, 777, 778, 782, 794, 797, 798, 806, 807, 810, 811
	Featureless	781, 796
FTIR similarities	<i>Based on visual inspection of spectra</i>	779, 794, 795
		776, 796, 806, 810
		777, 782, 811
		781, 798
		780, 783, 792
		778, 797, 807
		793, 799, 808, 809
ASTM rating colour	1a	777, 811
	1b	806
	2a	
	2b	792, 794, 799
	2c	782
	2d	796
	2e	807
	3a	778, 797, 798, 808, 809, 810
	3b	779, 781, 783, 793
	4a	776
	4b	795
	4c	780

The 16 samples chosen for testing using the wire method were selected as follows:

1. Base oil, with diluent oil: to see effect of base oil only on copper
2. 776: worst Cu level and very poor rating, also have distinctive features, cracks and spots, FIB showed porous structure
3. 810: very low Cu level
4. 780: flaking is very distinctive and pink and black layers visible on surface
5. 792: flaking apparent but layer still seems adhered to surface
6. 783: flaking shows multilayers and colour rating is varied across surface
7. 782: showed phosphorous in EDX
8. 796: SEM featureless but high Cu level

9. 795: distinctive circular features with small flakes sometimes seen deposited on surface
10. 808: large pits
11. 794: surface appears distinct from others with agglomerated features
12. 779: spherical objects spread across surface with possible small pitted features
13. 798: featureless, low ASTM rating
14. 778: mid ASTM rating and chosen from FTIR group with no other samples yet chosen

These 14 samples were selected as described and their formulations were then examined to see if all levels of additive had been covered. None of these 14 fluids had a high level of dispersant 1. Comparing the remaining samples which had high dispersant 1 levels led to the choice of the following samples:

15. 806: high dispersant 1 and high Cu level
16. 811: high dispersant 1, low Cu level and less formulation overlap than other potential samples of this type

These 16 samples were run using the wire test method described in Section 4.3 at 130 °C for 210 hours.

6.2 Wire test results

The results of the wire tests are presented below. However, placing all of the samples on one graph makes it difficult to see individual data sets; therefore the data has been split into two graphs. Figure 6.1, shows samples which have very small changes to their radius; less than 1 μm over the duration of the test. Figure 6.2 shows those with greater changes; over 1 μm . Note the significant differences in the y -axis scale.

As the wire tests could be grouped by those which gave less than 1 μm change in radius and those which gave more the formulations were investigated to see if there were any similarities within these two groups. However there was no clear correlation between their formulations and the radius change of the wire.

Measuring the change in the radius of a thin copper wire appears to be a good test method with distinguishable results between the fluids. However at this stage it is still

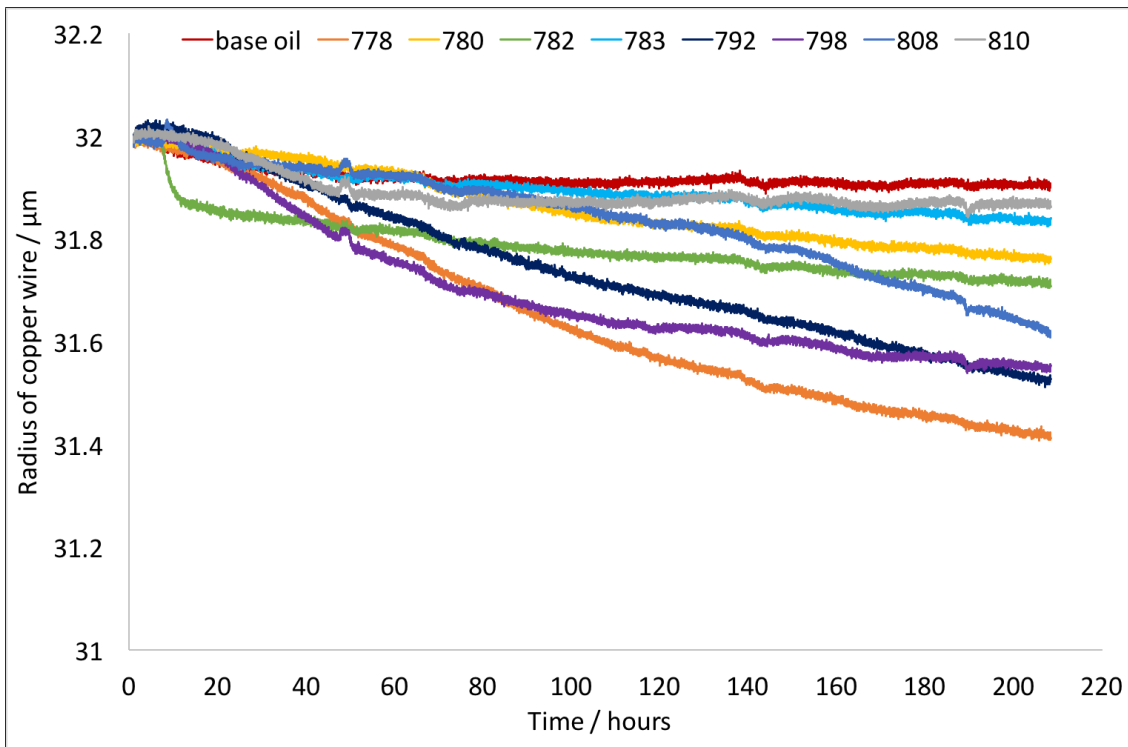


Figure 6.1: Radius change of copper wire immersed in full formulation fluids at 130 °C, formulations giving less than 1 μm radius change

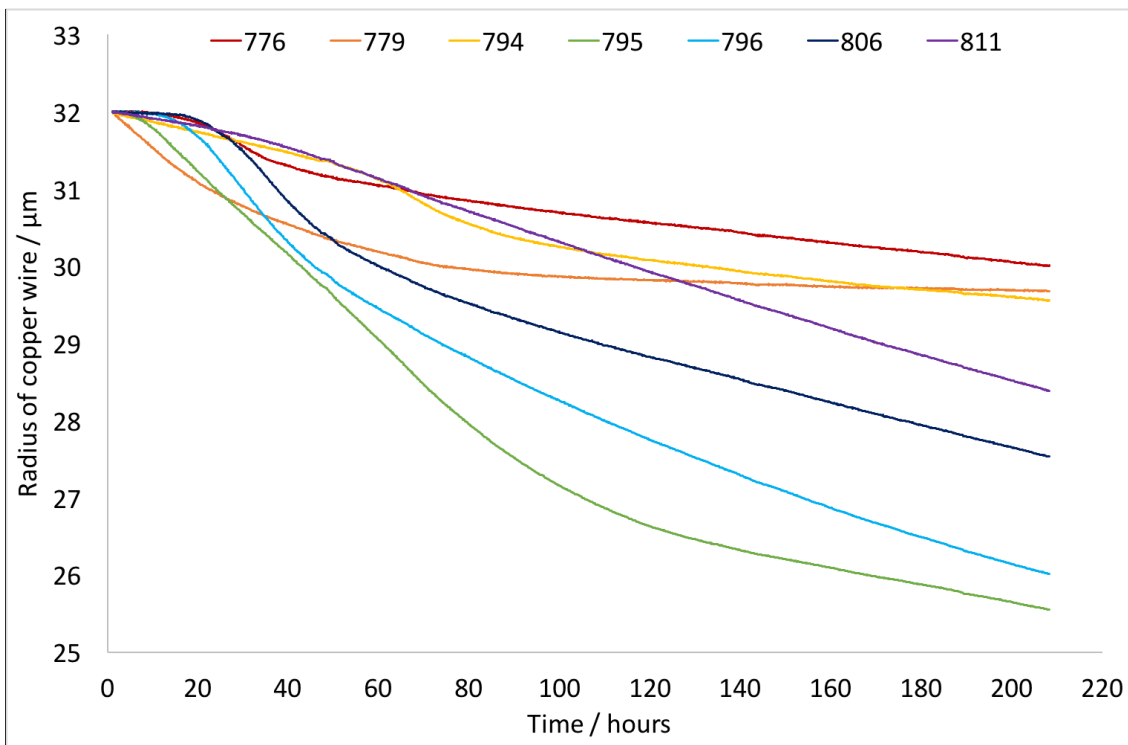


Figure 6.2: Radius change of copper wire immersed in full formulation fluids at 130 °C, formulations giving more than 1 μm radius change

not possible to identify which additives are causing the greatest corrosion, or which are contributing to stable passivating film formation. The test method enables us to follow corrosion in-situ therefore individual additives could be studied. This would give an idea

of how they may interact with the copper and if this interaction remains the same for the duration of the experiment or if there are different stages of interaction, for example an induction period followed by a period of corrosion.

6.2.1 Wire-coupon initial tests with varying time periods - wire results

As the wires are small and difficult to conduct surface analysis on and the immersion testing does not give in-situ data, the two tests could be combined to give a coupon that is easy to analyse at the end of the test, whilst also giving an idea of how the corrosion progresses throughout the experiment. To see if this is feasible and also whether the coupon shows the same corrosion progression as the wire a new experiment was devised.

The wire-coupon test, described in Section 4.4, placed a copper coupon into the bottom of a beaker containing the wire test. Four of the full formulation fluids already tested, 779, 780, 806 and 811 and the two corrosion inhibitors as individual additives were used as test fluids. Eight separate wire-coupon beakers of each fluid were set up so that they could be removed at different time points; after 3, 21, 27, 45, 52, 72, 97 and 170 hours. As a reminder the formulations of these samples can be found in Table 6.2.

Table 6.2: Reminder of full formulations for samples 779, 780, 806 and 811

Sample number	Concentration of Additive (wt%)								
	Corrosion inhibitor 1	Corrosion inhibitor 2	Dispersant 1	Dispersant 2	Detergent 1	Detergent 2	Antioxidant	Antiwear	Friction Modifier
-779	0.5	0.026	0	0	0	0	0.6	0.11	0.65
-780	0.5	0	0	2.5	0	0.4	0.06	0.22	1.2
-806	0.03	0	5	0	0	0.4	0.6	0.11	1.2
-811	0	0.026	5	0	0	0.4	0.33	0.22	0.25

Once the experiment had finished and the data was analysed, two significant problems were found to have occurred. The first was the noise caused by some equipment. Lubrizol have 4 oil baths setup for testing, two of them have fixed settings, allowing only

1 mA of current to be passed; the resolution on these setups is very good. The other two have variable current settings; in order to make the experiments the same a current of 1 mA was passed through the wires, this is at the bottom end of what the equipment can achieve and as such the resolution is worse, resulting in very noisy data. This led to an investigation into whether using different currents affected the radius change measured, as detailed in the methodology Section 4.3.5.

The second problem arose with the sensitivity of the experimental setup. From the data it can be seen that there are large spikes in the data. These correspond to when samples were removed from the oil bath or, to a lesser extent, when the fume hood sash was raised. This meant that any future testing had to be carried out in one go without interference to the fume cupboard or beakers.

The data collected for the experiments which stopped at different time points was plotted on the the same graph as the original radius change data measured for that sample. Due to the low resolution of the data from the variable control units and the spikes in the data caused by interference the data is not very good. When the radius change was large it was easy to see that the experiments stopped at different times follow the same trend as the original data, even when the resolution was poor. This can be seen for formulation 811 in Figure 6.3, 806 in Figure 6.4 and 779 in Figure 6.5. Formulation 780, shown in Figure 6.6, had little change in the radius to begin with and where the experiment has been stopped there have been sharp jumps in the data, this does not overlay well with the original uninterrupted experimental data.

The two corrosion inhibitors which were run have very noisy data with sharp jumps in several places. It is not possible from this data to tell what impact the corrosion inhibitor had on the corrosion of the copper wire. The data for these fluids is not shown as further testing was carried out on solutions containing only corrosion inhibitor and more useful information was obtained from those tests.

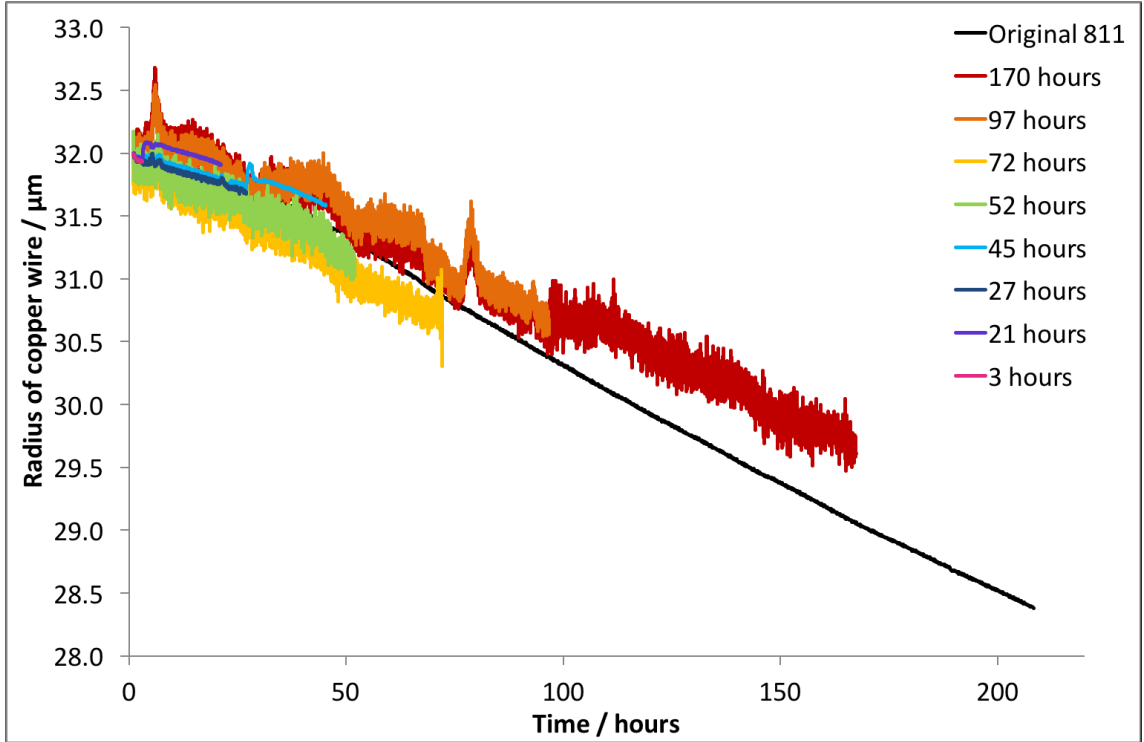


Figure 6.3: Change of radius of a copper wire at 130 °C immersed in 811, stopped at various time points

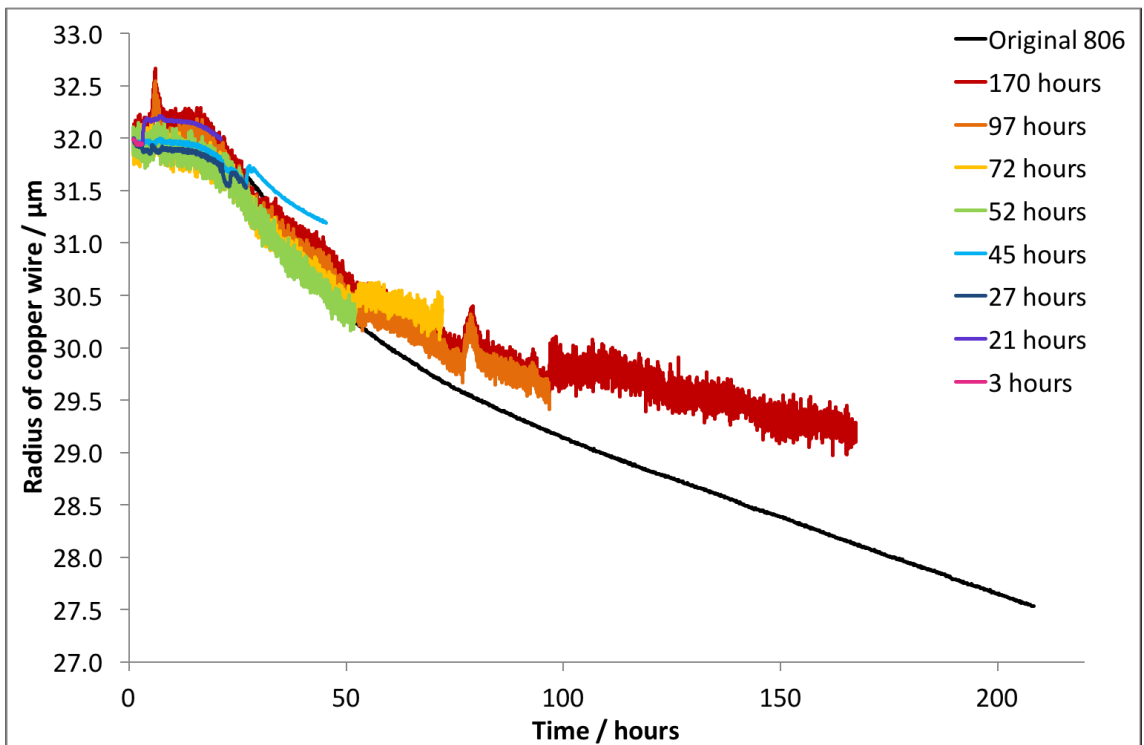


Figure 6.4: Change of radius of a copper wire at 130 °C immersed in 806, stopped at various time points

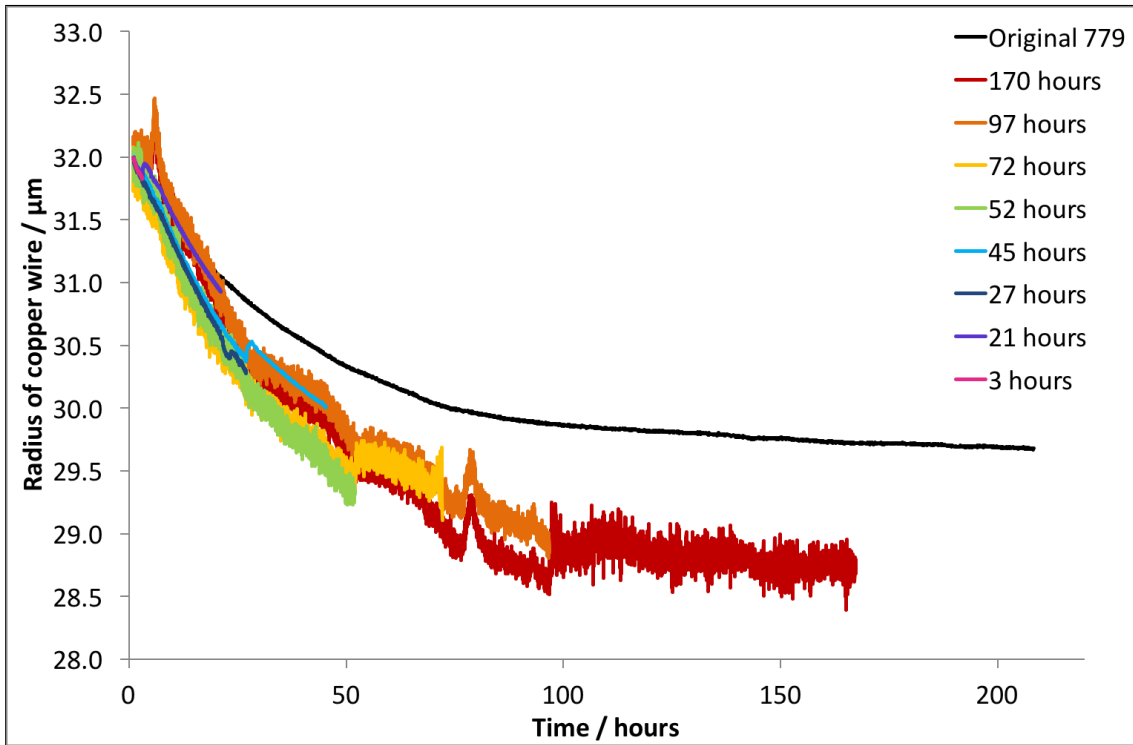


Figure 6.5: Change of radius of a copper wire at 130 °C immersed in 779, stopped at various time points

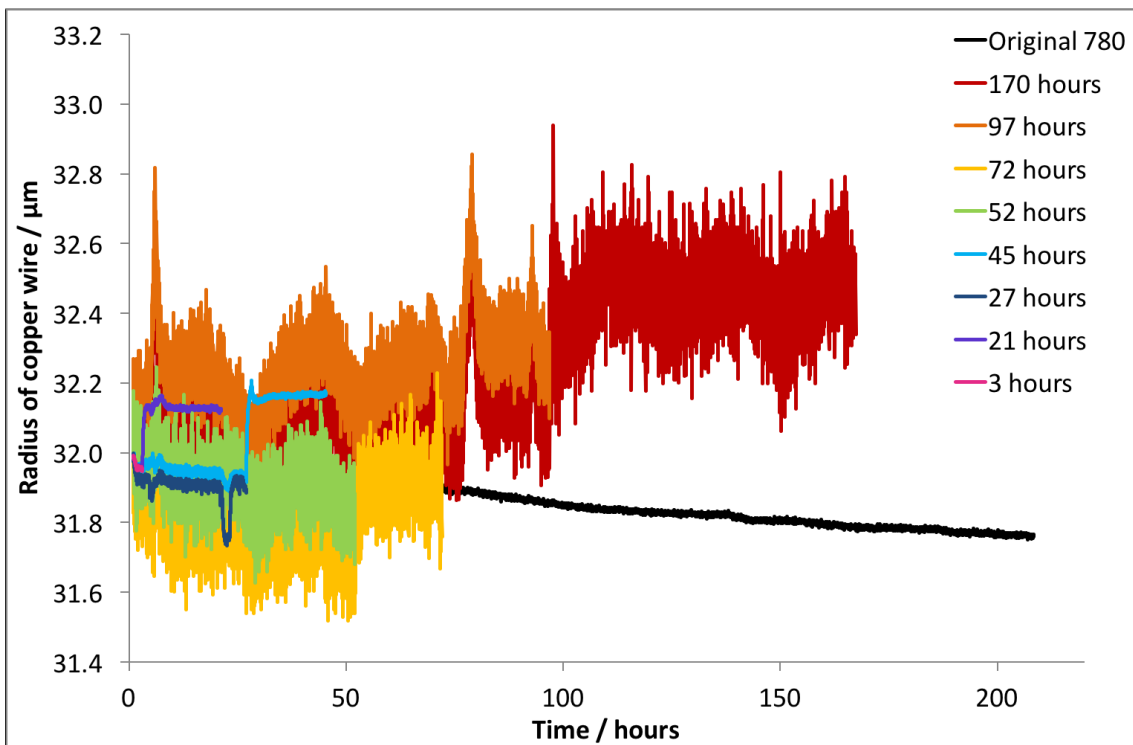


Figure 6.6: Change of radius of a copper wire at 130 °C immersed in 780, stopped at various time points

6.2.2 Wire-coupon initial tests with varying time periods - coupon results

As well as measuring the change in radius of the wires each of the beakers also had a copper coupon in the bottom that was weighed and visually analysed, in the same manner as the previous immersion tests. Table 6.3 shows the change in weight of the coupons, as a percentage of their starting weight, where positive numbers indicate a weight gain. It is interesting that samples tested in 779 and 780 show fluctuation in their weight change, whilst coupons tested in 806 and 811 generally show a steady decrease in weight over time.

Table 6.3: Percentage weight change of copper coupons tested in full formulation fluids 779, 780, 806, and 811

Formulation number	Weight change of coupon / % difference from start weight							
	3 hours	21 hours	27 hours	45 hours	52 hours	72 hours	97 hours	170 hours
779	0.004	0.007	0.007	0.004	-0.008	0	0.018	-0.004
780	0	0.007	0.012	0	0	0.004	-0.015	-0.027
806	-0.012	-0.020	-0.038	-0.046	-0.059	-0.088	-0.106	-0.186
811	0.004	-0.008	-0.008	-0.010	-0.026	-0.027	-0.038	-0.056

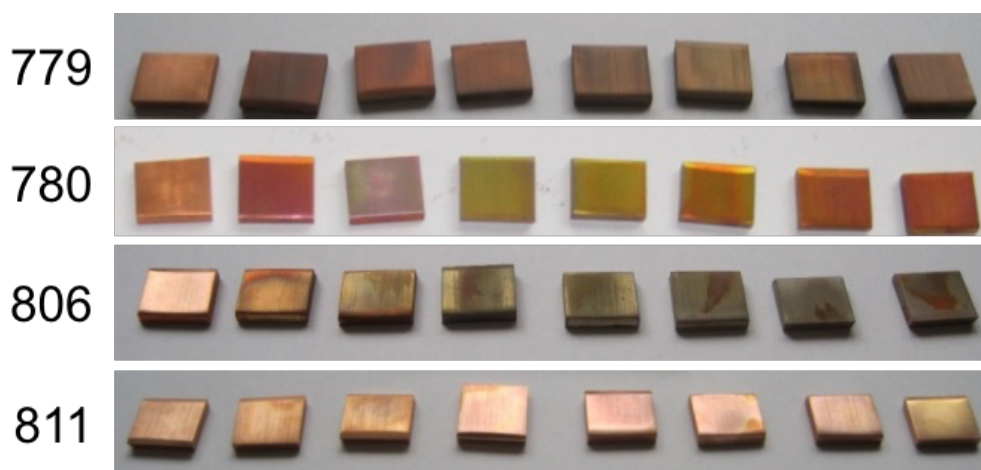


Figure 6.7: Images of coupons after testing for different lengths of time, placed in order of increasing time

Figure 6.7 shows how the colour of the coupon surface changes with increasing experiment time, in the case of fluid 780 a nice progression through the rating system is seen. Coupons tested in fluid 806 however show that the rating initially gets worse but remains constant for the rest of the test. The rating of samples tested in fluid 811 appear

to get better with time initially, whilst samples in 779 remain largely the same regardless of the test duration.

The amount of copper in the test fluid was measured using ICP-AES. This picks up any copper leached into solution by the coupon or the wire, as both are present in the beaker. It is far more representative of the corrosion occurring at the surface than the weight change or rating. Figure 6.8 shows how the amount of copper increases throughout the test for each of the fluids.

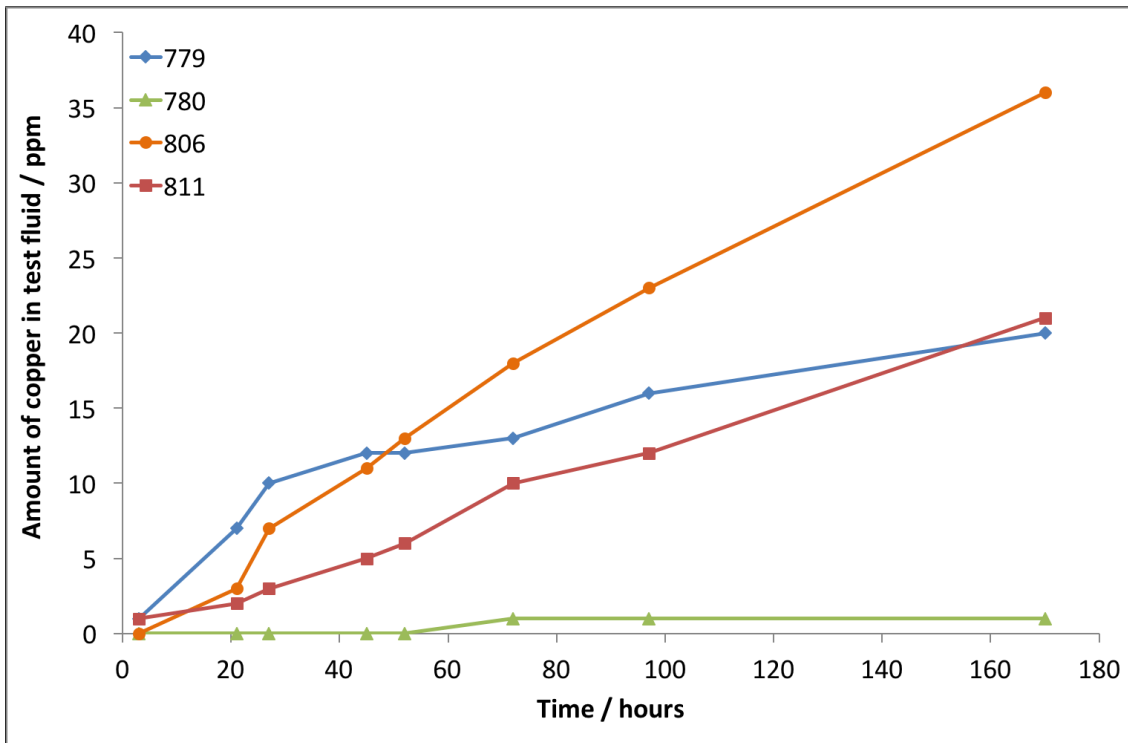


Figure 6.8: Amount of copper in the test fluid at 130 °C, measured once cool using ICP-AES

It is clear from running the experiments which removed beakers at specified time periods that the wires are sensitive to changes in the surrounding environment but it seems that left undisturbed they can give a very interesting insight into the way corrosion progresses. In order to determine if it would be possible to use this method to look at how corrosion changes with temperature the same four fluids were run at 150 °C, along with the base oil and formulation 795 which was run previously in the initial wire tests.

6.3 Effect of temperature on radius change

Figure 6.9 plots the results for the change in radius of a copper wire run at 130 °C and 150 °C for formulations 779, 780, 806, 811, 795 and the base oil alone. The first thing to note is that the radius change does not always get worse when the temperature is increased.

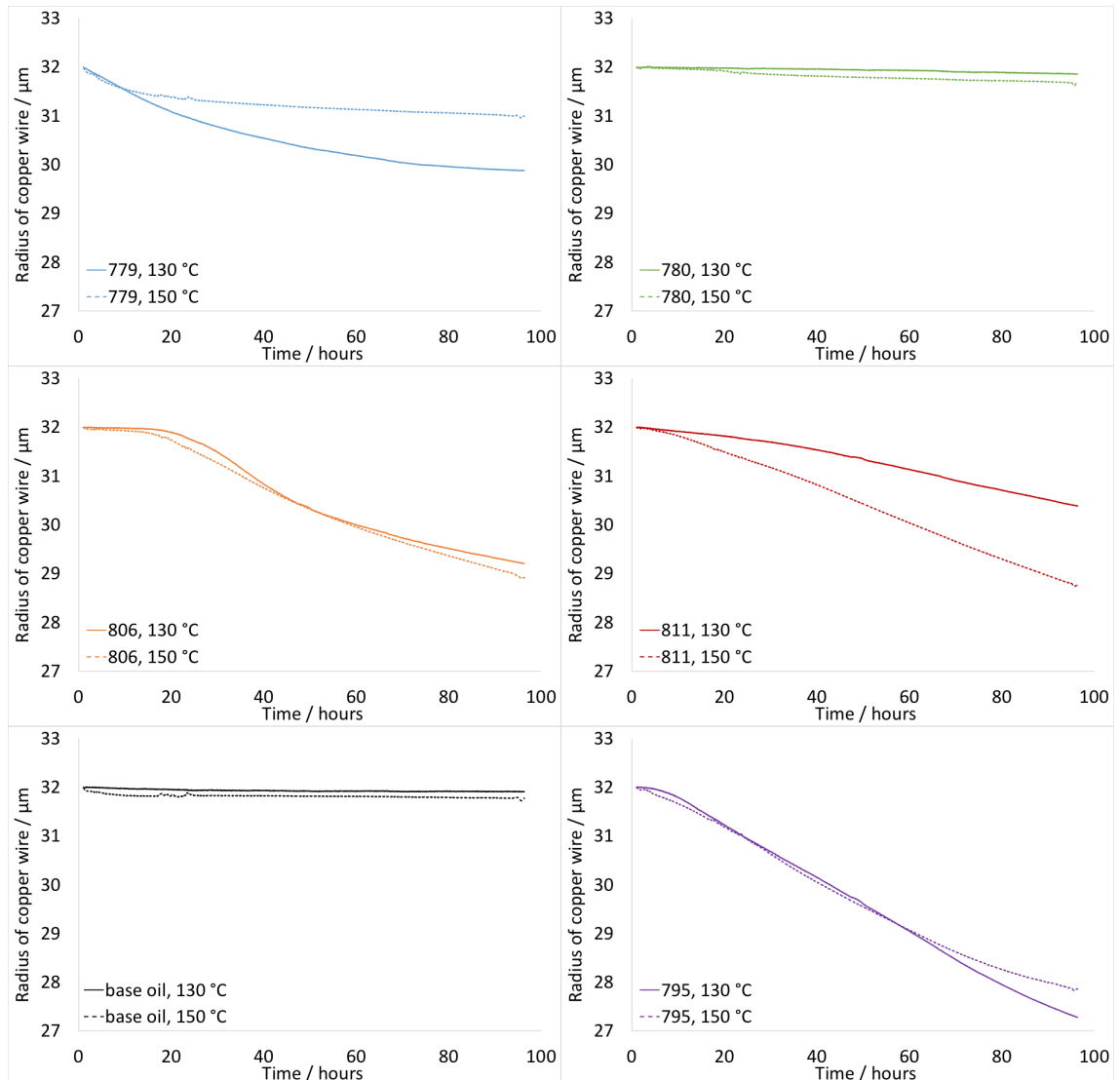


Figure 6.9: Differences in the change in radius for formulations run at different temperatures

Formulation 779 (blue) run at 150 °C gives a smaller change in radius compared to when run at 130 °C. This is something which should be given important consideration as the ASTM D130 tests are run at 150 °C in the hope of accelerating the corrosion that would be seen at lower temperatures, but in this instance the elevated temperature leads to better results.

In the instance of 811 (red) the radius change is worse at 150 °C than 130 °C which is what would normally be expected.

It is also interesting to note that for most of the other formulations tested at both 130 °C and 150 °C the change in the radius of the wire is very similar, with no significant differences between the two temperatures and raising the temperature does not appear to accelerate the test.

As the formulations are so complex and only a limited number have been run there is no way of knowing what is causing the change in the corrosion behaviour. The fact that some show a greater radius change at elevated temperatures, whilst others show what could be considered to be an improvement is also difficult to understand for such a small set of fluids. For this reason the additives were run individually to try and better understand how changes in temperature affect them.

6.4 Summary

- Wire testing allows a way to monitor the corrosion of a copper wire in situ without the use of additional electrolytes.
- The wires are sensitive to changes in the environment, such as opening the fume hood sash or removing beakers from the oil bath where other tests are still running. Knowing this, future tests shall be run without interference.
- The weight change of copper coupons does not always show a continuous trend, with some fluctuating in weight with time.
- Generally the longer the coupon is immersed in test fluid the higher the ASTM rating. However some samples do not change much throughout the experiment, retaining the same rating at 170 hours as they had at 21 hours.
- The amount of copper in the end of test fluid seems to be a better indicator of corrosion than the ASTM rating, increasing with time where corrosion is observed.
- Increasing the temperature of the test fluid does not always accelerate the corrosion. In some instances fluids tested at 150 °C performed better, with regards the radius change of a wire, than when tested at 130 °C.

7: Wire and coupon analysis for additives tested at different temperatures

As full formulation testing was unable to provide insight at this time into how certain additives interact with copper surfaces individual additives were tested using the copper wire-coupon test.

Nine different additives were investigated, at levels which were expected to be the highest concentration employed in a formulation. Initial thoughts from full formulation testing were that the antioxidant, antiwear and friction modifier were unlikely to do much alone and so the decision was made to create a mixture of these three additives. This thought was quickly determined to be incorrect and so each of the additives were also tested individually although only at 120 °C and 150 °C. It was also thought that the solubility of corrosion inhibitor 2 may be problematic and it would drop out of solution, this did not seem to be the case with the concentration used, however a mixture was also made which combined corrosion inhibitor 2 with the antiwear, as this is sometimes used in formulations to aid solubility. The additives tested, along with their concentrations are outlined in the methodology section, Table 4.4.

ASTM testing is generally carried out at 150 °C but this is far hotter than the transmission is ever likely to get, thanks to temperature sensors which would simply shut the transmission down. A more realistic temperature would be 80°C but at this temperature no significant changes to the surface are seen without testing for a number of days, and most often weeks. As time is an important factor, the tests are heated in the hope of accelerating any interaction allowing them to be run for much shorter time periods.

The additives were tested at 110 °C, 120 °C, 130 °C and 150 °C to identify whether there was a difference in the mechanism between any of the temperatures. The additives were tested using the wire-coupon test method outlined in the methodology, Section 4.4. The results are detailed for each of the individual additives below. XPS analysis was conducted on coupons tested at 120 °C and 150 °C with the atomic concentration for specified elements shown. These results were determined from survey spectra taken for each of the coupons at three separate areas across the surface. The raw data for these spectra can be found in Appendix A.

7.1 Base oil

In order to see what impact different additives have on the corrosion of copper, it must first be understood how the base oil alone interacts with the copper surface.

The copper coupons immersed in base oil at the different test temperatures can be seen in Table 7.1, along with the corresponding rating. The colour is very even for the lower temperatures but at 150 °C it is clear that there is some sort of deposit on the upper half of the coupon. This deposit is shown in the SEM image of the coupon at 150 °C in Figure 7.1.

Table 7.1: Images of end of test copper coupons after immersion in base oil at 110 °C, 120 °C, 130 °C and 150 °C. All coupons were the same height and approximately 1.5 cm in width

110 °C	120 °C	130 °C	150 °C
			
2e	2e	3a	4a

SEM images of the coupon surfaces are shown in Figure 7.1. At 110 °C there is a smooth flat surface with no distinguishing features, at 120 °C some small shadow like areas can be seen but it is unclear what these may be.

At 130 °C we see clear deposit formation in the form of almost spherical structures, with an average diameter of around 10 µm, spread across the entire surface.

At 150 °C the deposit is very different and large particles which appear to be an agglomeration of smaller particles can be seen. Interestingly they did not appear across the entire surface but instead formed a band across the coupon. In places the layer directly underneath this particle band was cracked with small parts flaking off. What was also interesting was that either side of this band was different. On one side of the band there were many small particles, similar to those which seemed to have agglomerated to form the larger particles. On the other side patchy areas, similar to those on the 120 °C sample were seen only they were larger and darker; it was unclear what these areas may be.

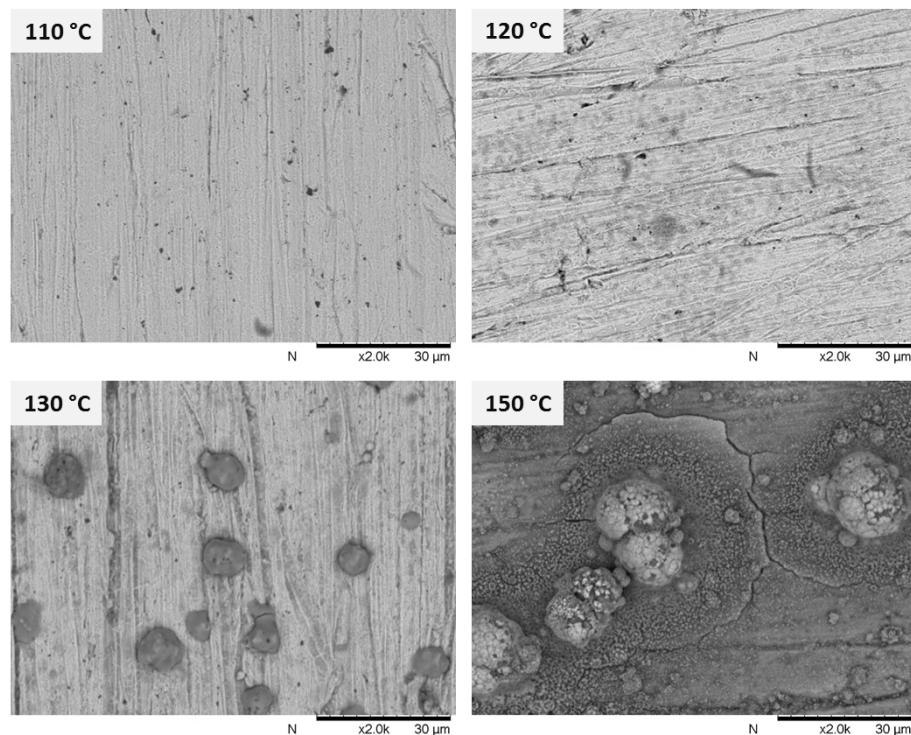
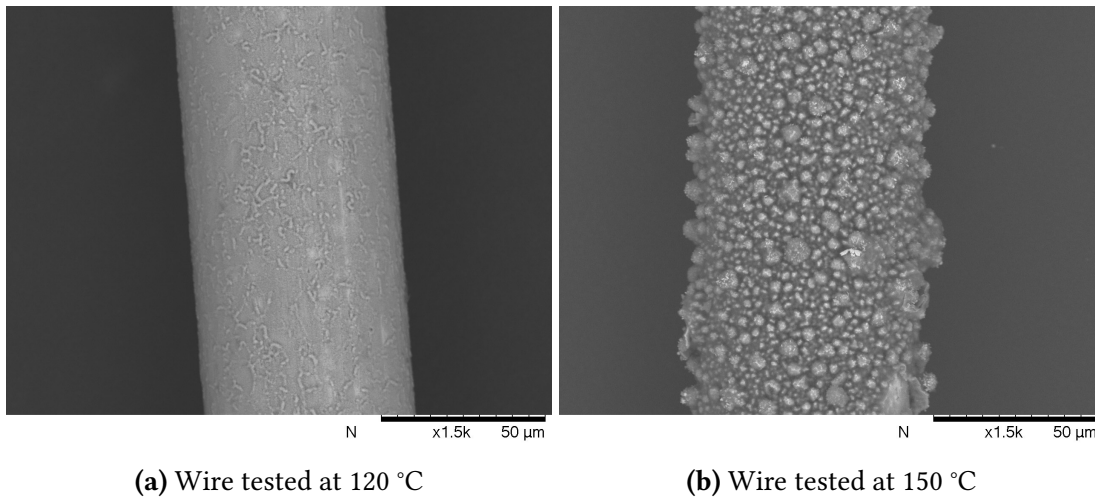


Figure 7.1: End of test BSE images of coupon surface after immersion in base oil at various temperatures

In order to establish if the same interaction was occurring on the surface of the wires SEM images were taken at several points along a random section. Images of the wires tested at 120 °C and 150 °C can be seen in Figure 7.2.

The surface at the wire tested at 120 °C looks similar to the coupon. At 150 °C it is clear that the same deposits are forming on the surface of the wire, as were seen on the coupon. From the images taken of the wires it was possible to determine that the interaction was uniform across the surface.



(a) Wire tested at 120 °C

(b) Wire tested at 150 °C

Figure 7.2: End of test BSE images of wire surfaces after testing in base oil at specified temperatures

Figure 7.3 shows the change in radius for copper wires immersed in base oil at different temperatures. There is very little change in the radius across any of the temperatures. The greatest change is observed at 150 °C but it is still small, less than 0.5 μm .

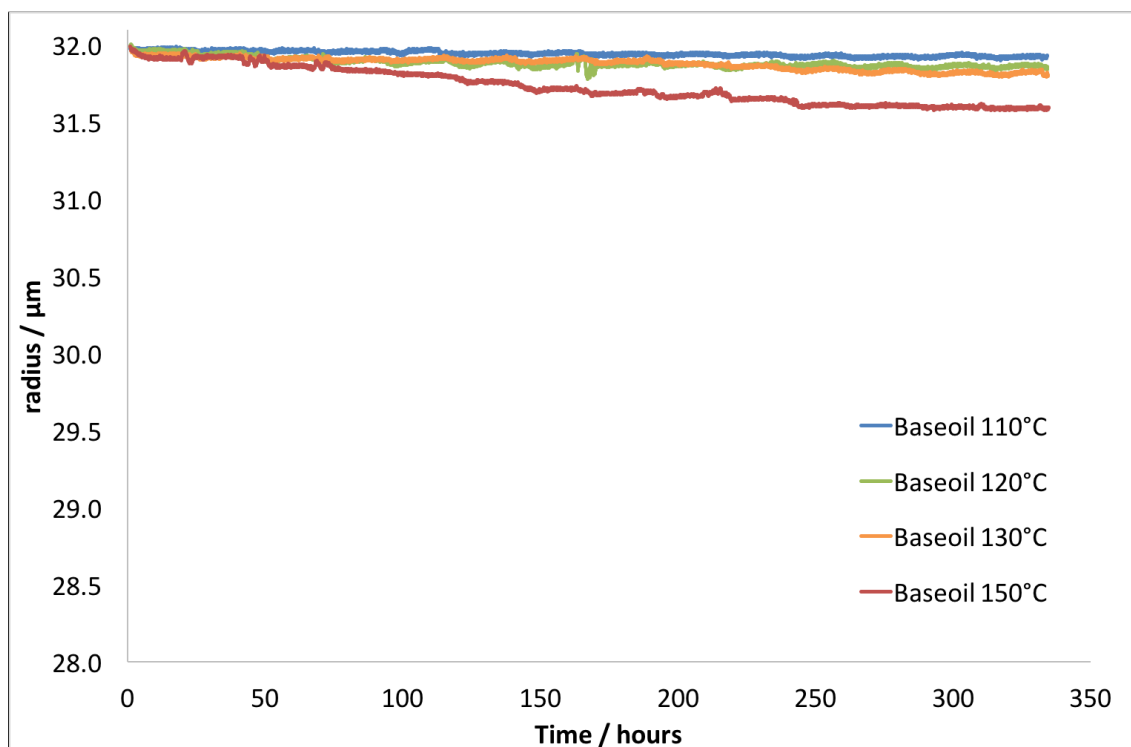


Figure 7.3: Change in radius of copper wires immersed in base oil at 110 °C, 120 °C, 130 °C and 150 °C

From the wire results it would seem that base oil alone is not particularly corrosive towards copper. The SEM images suggest that as the temperature increases the oil is degrading and a deposit is forming on the surface.

The amount of copper in the end of test fluid was determined using ICP-AES and for the base oil, Figure 7.4, it can be seen to increase with increasing temperature. The amount of copper is low in all of the fluids, at 150 °C less than 3 ppm of copper is detected in the end of test fluid. Again this would suggest that base oil alone is not particularly corrosive to the copper surface.

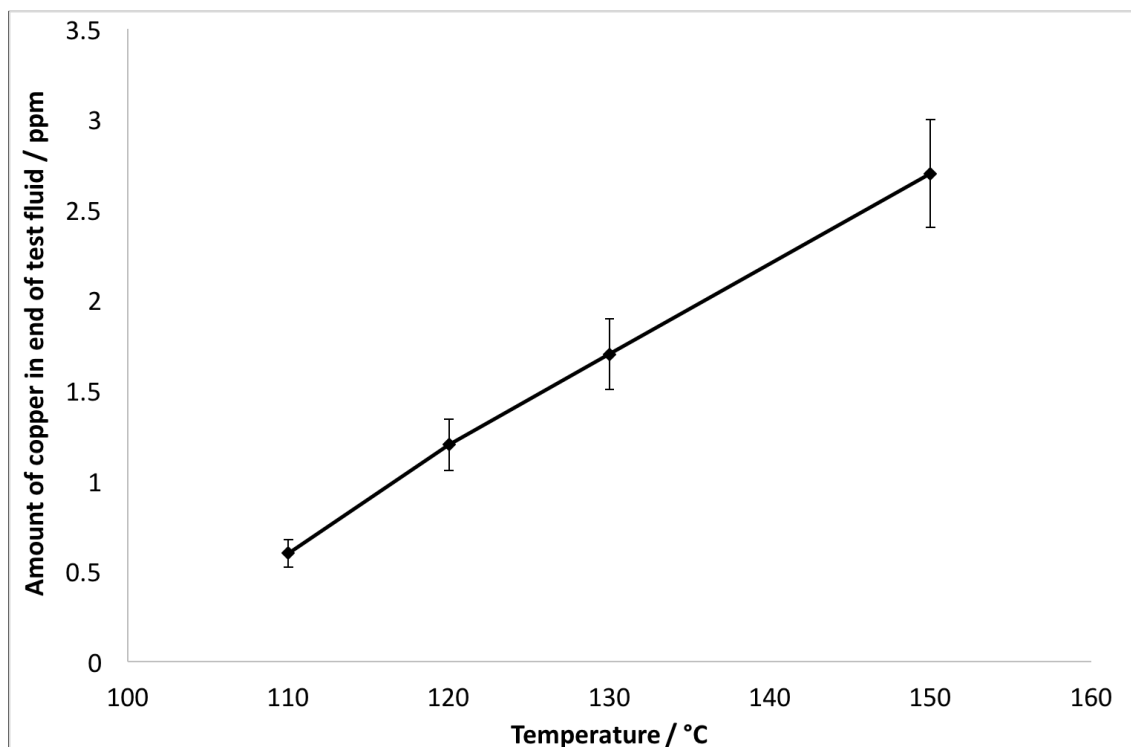


Figure 7.4: The amount of copper in the end of test fluid as determined using ICP-AES for base oil alone

The surface of samples tested in base oil at 120 °C and 150 °C were analysed using XPS and the results for the atomic concentration of specific elements can be seen in Figure 7.5. At both temperatures the results are very similar. The surface analysis shows over 70 % carbon with the remainder being primarily oxygen.

There are small amounts of nitrogen and sulfur present in the XPS analysis, both of these are likely to be from surface contamination as although the surfaces are kept clean in a polythene bag they are exposed to the atmosphere.

It is also possible that handling could cause some cross contamination as the sample was sent to NEXUS for analysis. The coupons were cleaned with SBP2L before being packaged and sent but would have been handled by the analysts and not cleaned again before testing. Knowing that there is a small amount of N and S detected when the

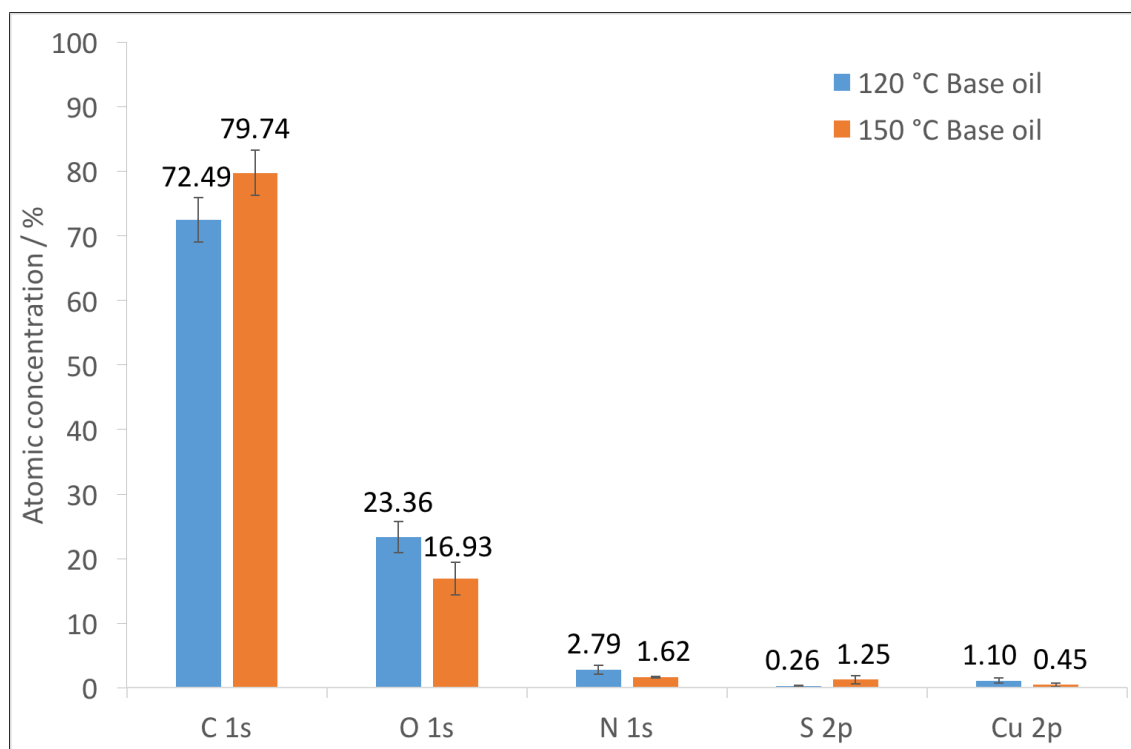


Figure 7.5: Atomic concentration of C, O, N, S and Cu on sample surface tested in base oil at 120 °C and 150 °C determined by XPS

base oil is tested alone analysis of the surfaces tested in the presence of additives can be compared against these levels to see if any presence of N or S is likely to be coming from this contamination or from the additive interacting with the surface.

Very little copper is detected on the surface at either 120 °C or 150 °C, suggesting that the surface layer is unlikely to contain copper and is of sufficient thickness that the XPS analysis does not pick up the bulk copper below. XPS has an analysis depth of around 3 nm [127] so the film is likely to be no thinner than this.

7.2 Corrosion inhibitor 1

0.5 wt% of corrosion inhibitor 1 in base oil was used for testing. Images of the coupons at each of the test temperatures can be seen in Table 7.2, with their corresponding ratings. All of the coupons between 110 °C and 130 °C are rated as 3b; at 150 °C the surface becomes a 4c rating and in the first experiment the film began to flake off. This was not seen during the repeat testing, however the surface rating was equally poor.

Looking at SEM images of the coupon surfaces, shown in Figure 7.6, 110 °C, 120 °C, and 130 °C samples were very similar, with little to distinguish on the surface except

Table 7.2: Images of end of test copper coupons after immersion in corrosion inhibitor 1 at 110 °C, 120 °C, 130 °C and 150 °C, with repeats at 120 °C and 150 °C. All coupons were the same height and approximately 1.5 cm in width

	110 °C	120 °C	130 °C	150 °C
Original	 3b	 3b	 3b	 4c
Repeat		 3b		 4c

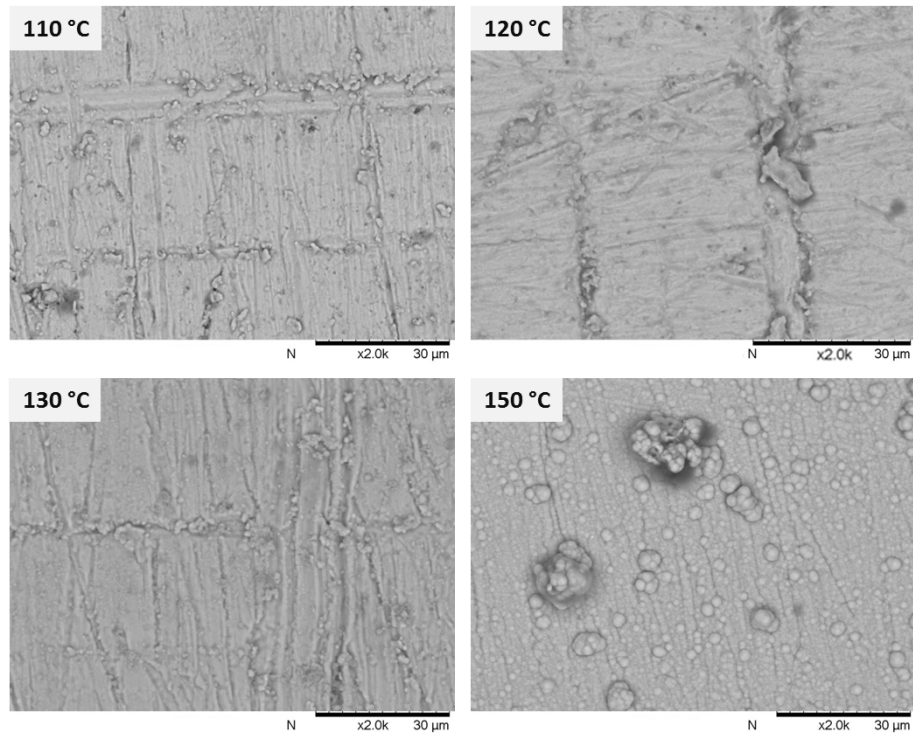


Figure 7.6: End of test BSE images of coupon surface after immersion in corrosion inhibitor 1 at various temperatures

small particles building up in polishing marks.

At 150 °C this was very different with a clear film formation on the surface made up of many particles fusing together. Sometimes larger particles were found on top of the film, which did not seem to have been incorporated. As can be seen from the original coupon image in Table 7.2 there was an area which had flaked off, SEM imaging of the exposed copper looked slightly porous as if the copper had been corroded away, this

image is not shown.

SEM images of the wires, shown in Figure 7.7 showed similar particles agglomerated on the surface of the wire at 150 °C as seen on the coupon, although the particles are slightly smaller on the wire. At 120 °C the wire surface appeared a little more porous than the coupon surface, however polishing marks can be seen on the coupon surface which may mask any small holes, as the wire surface was flatter these pores are more noticeable.

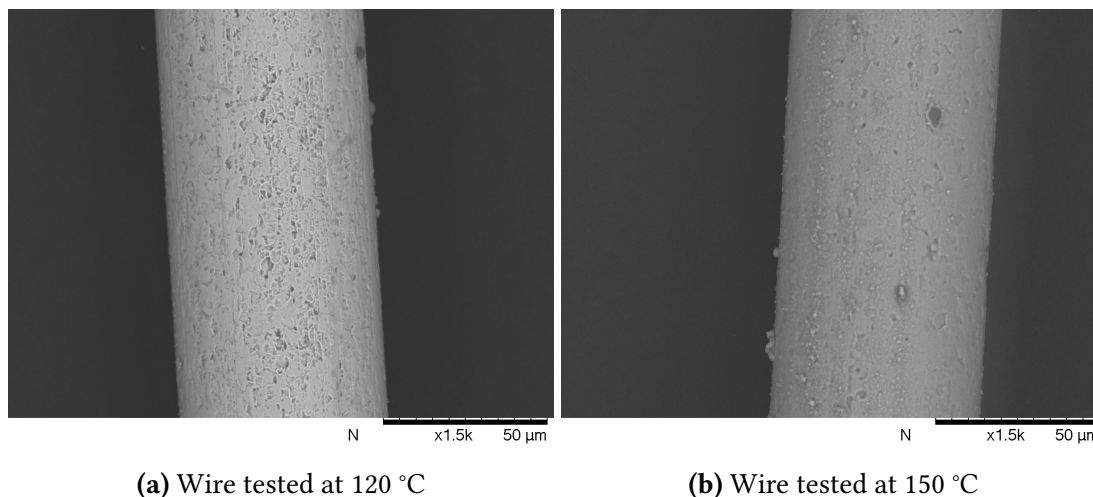


Figure 7.7: End of test BSE images of wire surfaces after testing in corrosion inhibitor 1 at specified temperatures

Figure 7.8 shows how the radius of thin copper wires change over time when immersed in corrosion inhibitor 1 at different temperatures, with repeats at 120 °C and 150 °C. At temperatures between 110 °C and 130 °C there appears to be little change in the radius of the wire.

At 150 °C very different behaviour is seen. The initial 50 hours are very similar to the changes seen at lower temperatures but then a slightly more rapid change is seen for the next 80 hours or so. At around 130 hours the radius of the wire decreases from around 31.5 μm to 0 μm in the space of 30 minutes. This very rapid decrease suggests localised corrosion and on inspection of the wire at the end of the test, it was found to be broken in 11 different places, 7 places on the repeat.

The amount of copper in the end of test fluid, at each of the temperatures, was determined using ICP-AES and can be seen in Figure 7.9. The level of copper in the fluid at the end of test is below 2 ppm for all temperatures. This is very low and suggests

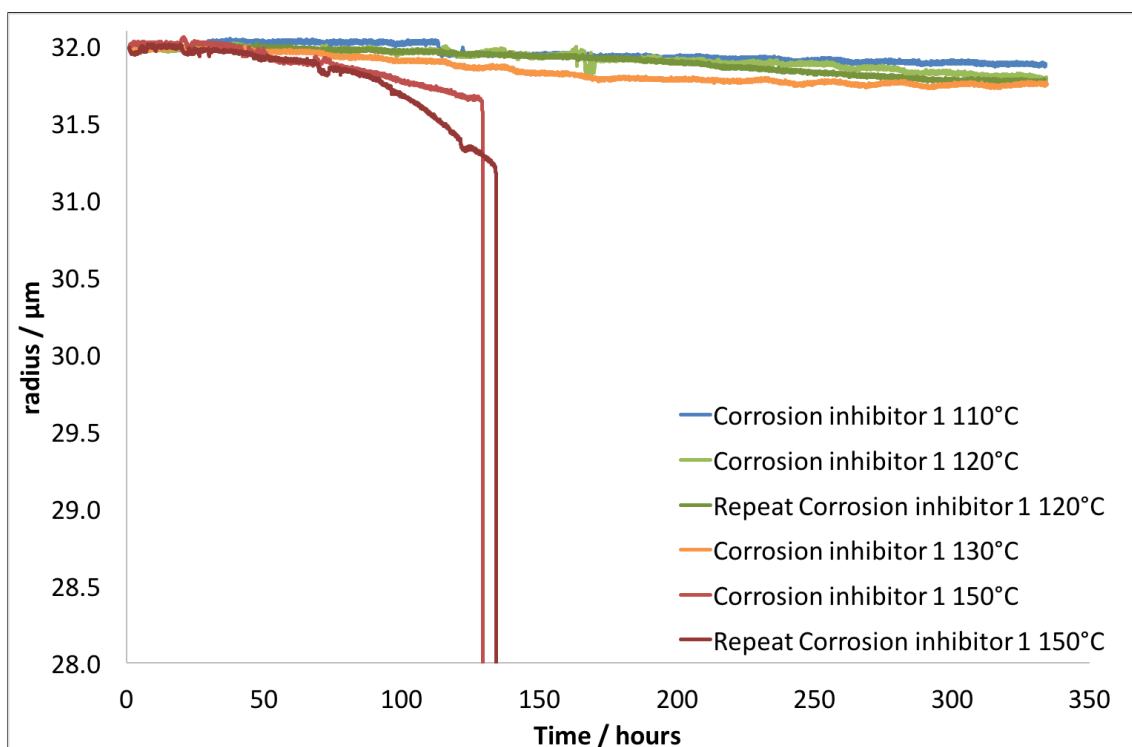


Figure 7.8: Radius change of copper wires immersed in 0.5 wt% corrosion inhibitor 1 at 110 °C, 120 °C, 130 °C and 150 °C, including repeats at 120 °C and 150 °C

little removal of copper resulting from corrosion. What is interesting is that whilst there is a huge decrease in the radius of the copper wire measured at 150 °C there is no real increase in the amount of copper in the end of test fluid for 150 °C. Instead it is very similar to that measured for 130 °C. This again would suggest highly localised corrosion, with very narrow deep pits likely.

The atomic concentration of specified elements was determined on the surface of the 120 °C and 150 °C samples using XPS. Corrosion inhibitor 1 contains carbon, sulfur and nitrogen so if it is present on the surface the levels of these elements should be higher than the levels measured for the samples tested in base oil alone.

The 120 °C sample tested in corrosion inhibitor 1 contains around 4.2 % nitrogen. This is slightly higher than the 2.8 % measured with base oil alone. Similarly 3.8 % sulfur was measured on the surface when corrosion inhibitor 1 was present compared to 0.3 % for the base oil alone. The increase in both of these elements indicates that corrosion inhibitor 1 is present on the surface and forms a protective layer.

The 150 °C sample tested in corrosion inhibitor 1 is different. Nitrogen is measured at 1.75 %, this is very similar to the 1.62 % measured on the surface of the sample tested

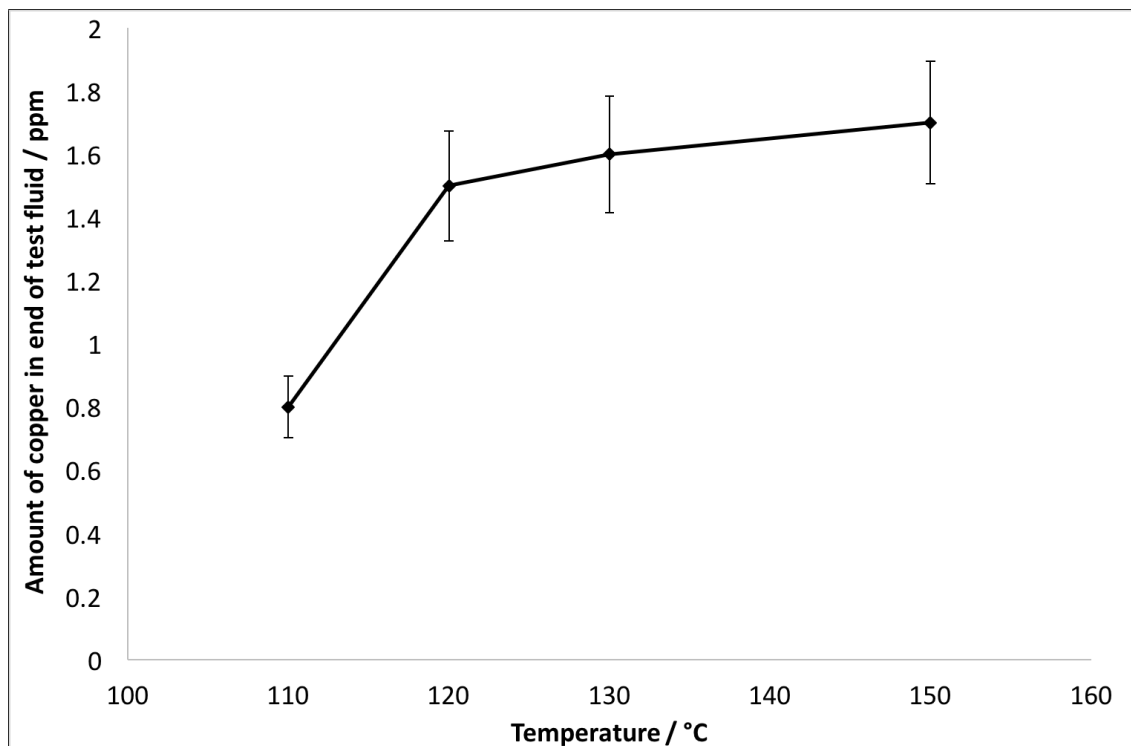


Figure 7.9: The amount of copper in the end of test fluid as determined using ICP-AES for corrosion inhibitor 1

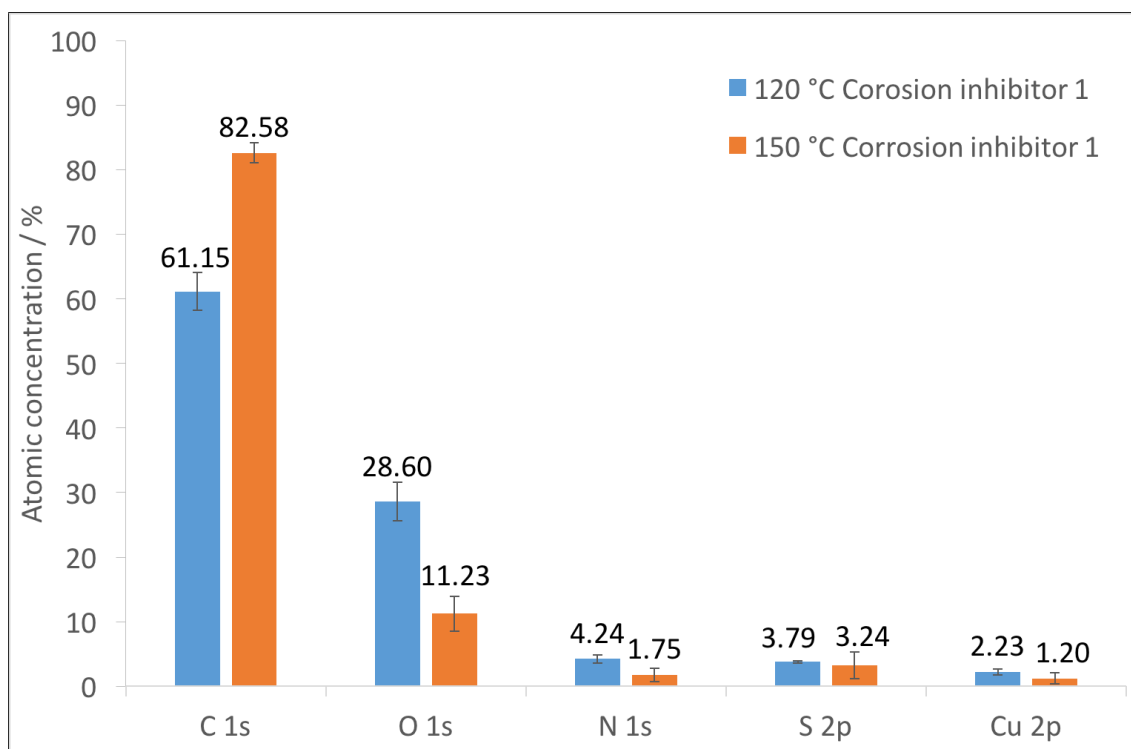


Figure 7.10: Atomic concentration of C, O, N, S and Cu on sample surface tested in corrosion inhibitor 1 at 120 °C and 150 °C determined by XPS

in base oil alone. This would suggest that there is no nitrogen on the surface coming from corrosion inhibitor 1. The sulfur level is measured at 3.2 %, higher than the base oil level of 1.3 %. This increased sulfur level would suggest some interaction between

the corrosion inhibitor and the surface but this seems to be in disagreement with the nitrogen level.

From the wire tests it can be seen that at 150 °C there is a rapid decrease in the radius of the wire. It is also known that certain sulfur species can be highly corrosive towards copper. Given the XPS results show an increased sulfur level but no nitrogen, it is possible that corrosion inhibitor 1 is breaking down to give sulfur species which are corrosive.

7.3 Corrosion inhibitor 2

Corrosion inhibitor 2 was tested at a concentration of 0.05 wt%. Table 7.3 shows images of copper coupons after immersion in corrosion inhibitor 2 at different temperatures, along with their ratings. The 150 °C original sample was unfortunately damaged during removal from a test before it was photographed and so the scratches and dullness were not formed from the immersion test; the repeat image is much more representative of what the sample originally looked like.

Table 7.3: Images of end of test copper coupons after immersion in corrosion inhibitor 2 at 110 °C, 120 °C, 130 °C and 150 °C, with repeats at 120 °C and 150 °C. All coupons were the same height and approximately 1.5 cm in width

	110 °C	120 °C	130 °C	150 °C
Original	 1b	 3a	 3a	 3a
Repeat		 3a		 3a

Figure 7.11 shows SEM images of the surface of the coupons at each of the test temperatures. The surface is very similar in all cases except that some small particles can be seen at 150 °C.

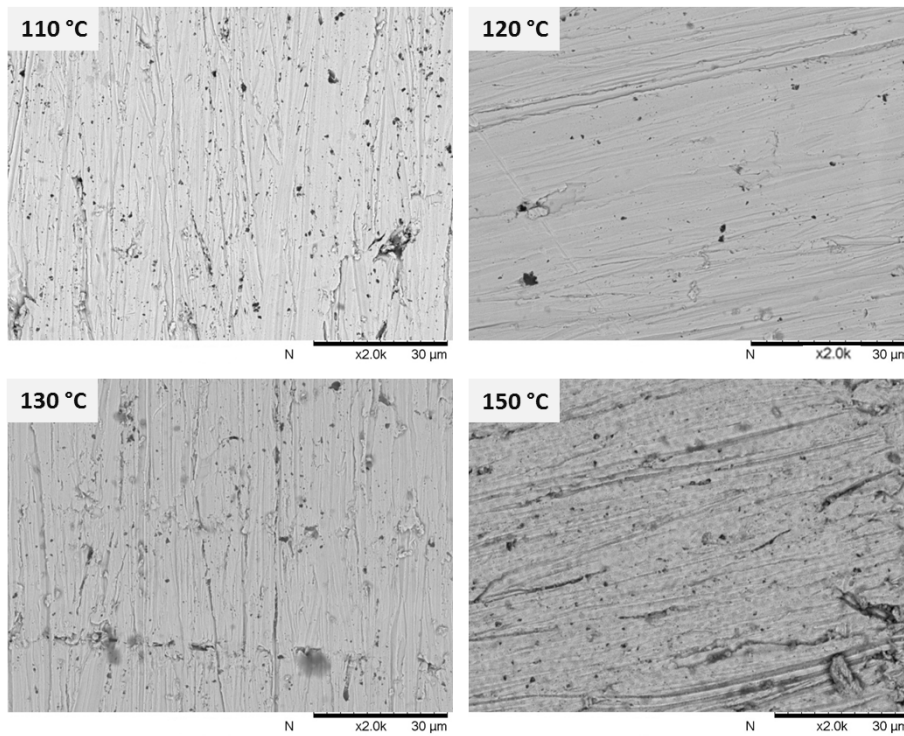
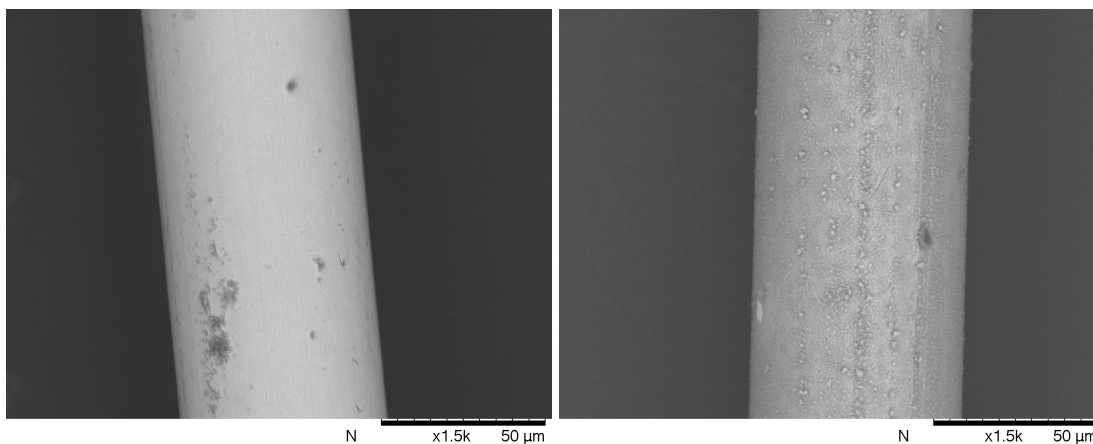


Figure 7.11: End of test BSE images of coupon surface after immersion in corrosion inhibitor 2 at various temperatures

SEM images of the wires tested at 120 °C and 150 °C can be seen in Figure 7.12. At 120 °C nothing can be distinguished on the surface of the wire, similar to the coupon at the same temperature. At 150 °C small particles can be seen on the surface, these were also present on the coupon but are more difficult to see.



(a) Wire tested at 120 °C

(b) Wire tested at 150 °C

Figure 7.12: End of test BSE images of wire surfaces after testing in corrosion inhibitor 2 at specified temperatures

Figure 7.13 shows the radius change for copper wires immersed at different temperatures. There is no difference in the radius change at any of the temperatures tested,

suggesting that at all temperatures tested corrosion inhibitor 2 provides good corrosion protection to the surface.

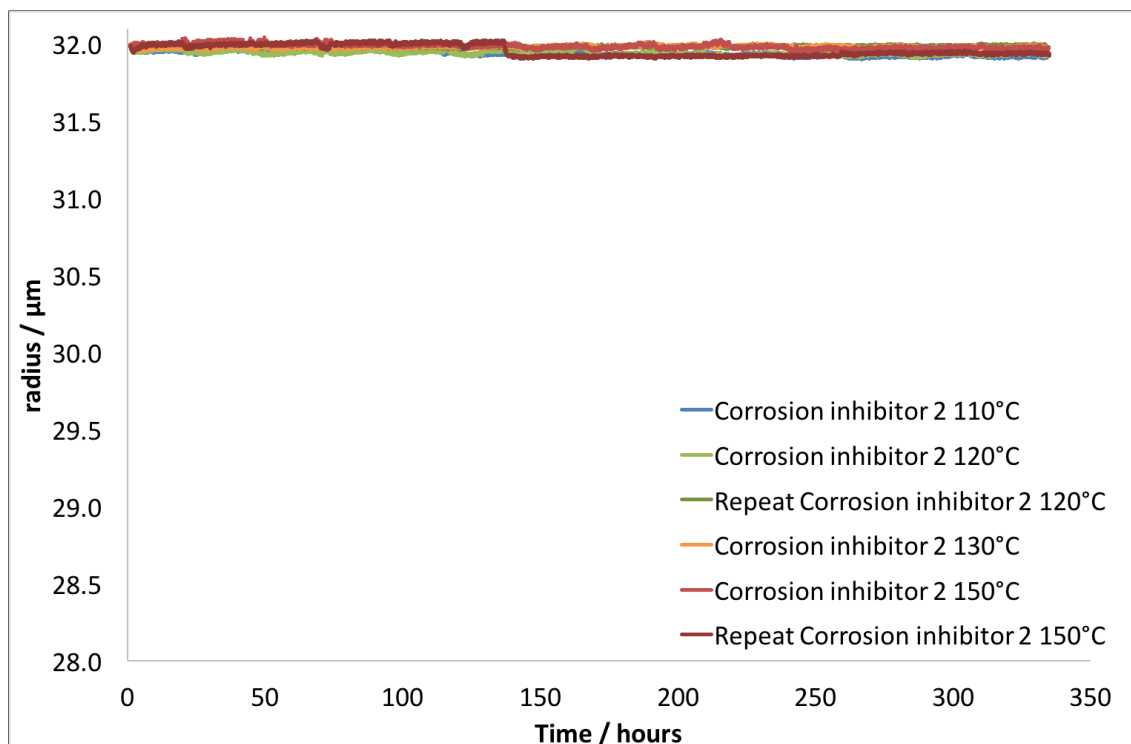


Figure 7.13: Radius change of copper wires immersed in 0.5 wt% corrosion inhibitor 2 at 110 °C, 120 °C, 130 °C and 150 °C, including repeats at 120 °C and 150 °C

There is very little copper measured in the end of test fluid, as seen in Figure 7.14. There is less than 0.5 ppm of copper across all temperatures as measured by ICP-AES. This supports the wire test results that corrosion inhibitor 2 provides good corrosion protection to the copper.

At 130 °C no copper is measured in solution using ICP-AES, this is most likely due to the instrument not being sensitive enough to detect copper below 0.1 ppm. The very small amount of copper in the fluid across all temperatures is very good as copper is known to accelerate degradation of lubricating fluids. It is clear that the interaction of corrosion inhibitor 2 with the copper surface does not allow copper to be pulled in to solution.

The atomic concentration of specific elements on the surface of samples at 120 °C and 150 °C can be seen in Figure 7.15 and are very similar at both temperatures.

Corrosion inhibitor 2 contains only carbon and nitrogen. If there is an interaction between the copper surface and the inhibitor an increase in the nitrogen level, compared

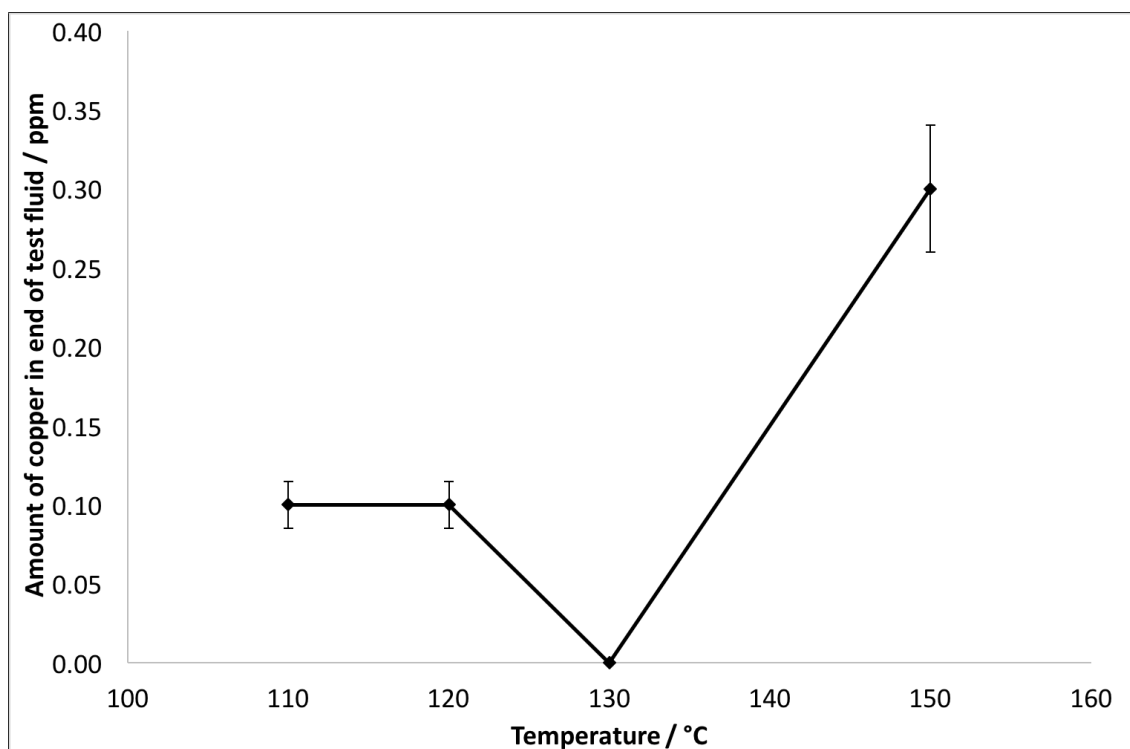


Figure 7.14: The amount of copper in the end of test fluid as determined using ICP-AES for corrosion inhibitor 2

to the base oil samples, would be expected. The base oil levels of nitrogen measured 2.8 % and 1.6 % for the 120 °C and 150 °C samples respectively; and 3.2 % and 3.8 % for the corrosion inhibitor 2 samples at 120 °C and 150 °C respectively. This increase suggests that there is an interaction between the inhibitor and the surface. The sulfur level remains the same for both the corrosion inhibitor 2 samples and the base oil samples confirming that the increase in nitrogen is from the inhibitor and not contamination.

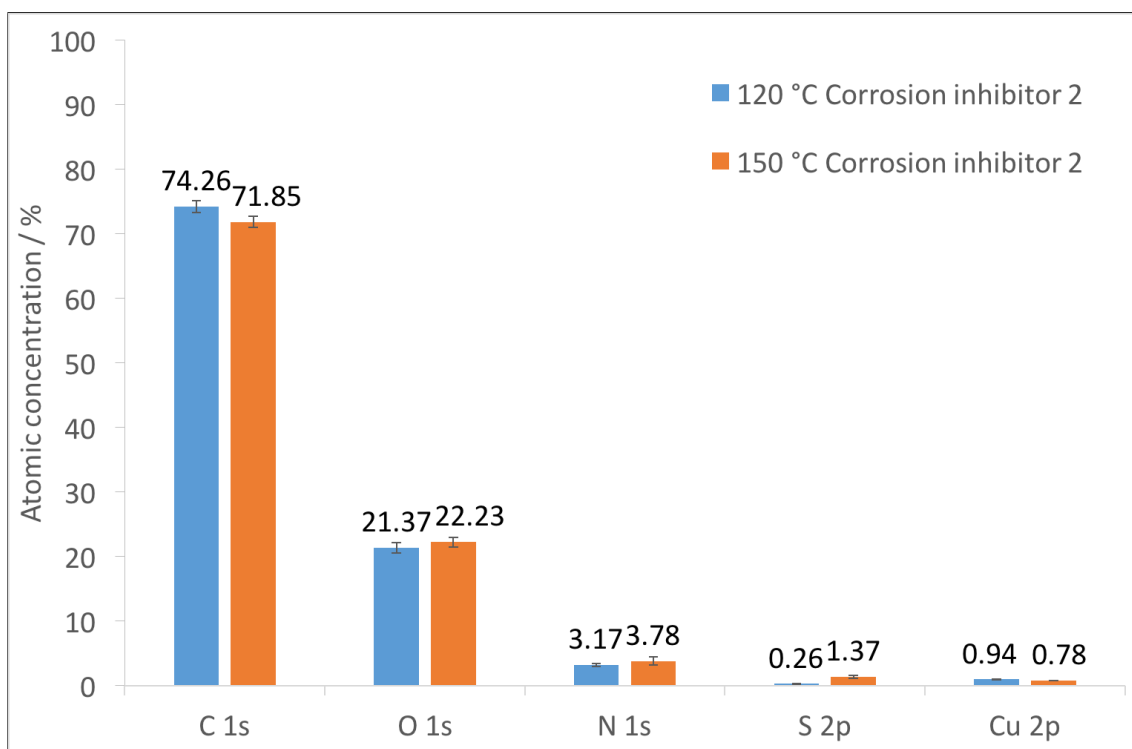


Figure 7.15: Atomic concentration of C, O, N, S and Cu on sample surface tested in corrosion inhibitor 2 at 120 °C and 150 °C determined by XPS

7.4 Dispersant 1

Dispersant 1 was tested at 5 wt% concentration and images of the coupons tested at each temperature are shown in Table 7.4. There were slight discrepancies between the original and repeat samples, but the ratings were generally poor and gave dull surfaces.

Table 7.4: Images of end of test copper coupons after immersion in dispersant 1 at 110 °C, 120 °C, 130 °C and 150 °C, with repeats at 120 °C and 150 °C. All coupons were the same height and approximately 1.5 cm in width

	110 °C	120 °C	130 °C	150 °C
Original	 4a	 4a	 4a	 4c
Repeat		 2b		 3b

SEM images of the surfaces, seen in Figure 7.16, shows etching of the surface at all temperatures above 120 °C. At 150 °C there did seem to be a thin film present on the surface, however it was very patchy and often cracked or flaking away from the surface. This film formation did not appear to be present at any of the other temperatures tested.

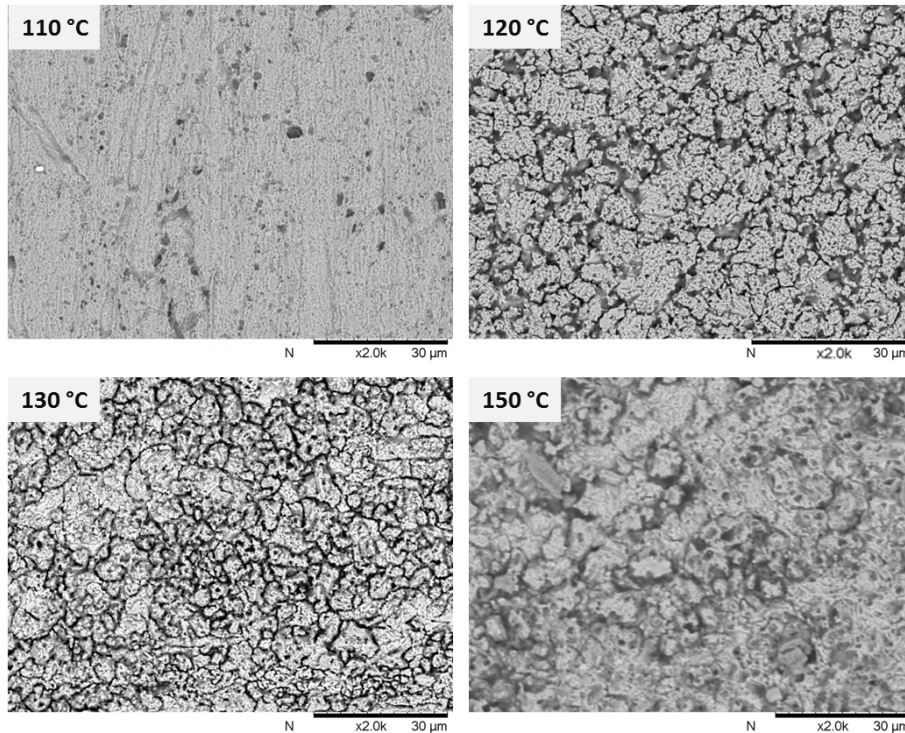


Figure 7.16: End of test BSE images of coupon surface after immersion in dispersant 1 at various temperatures

Figure 7.17 shows SEM images of the wires tested in dispersant 1 at 120 °C and 150 °C. The etching seen on the surface of the coupon at 120 °C is also present on the surface of the wire. The wire at 150 °C is interesting as it shows a flaking layer on the surface, which is not well adhered. The wires were not rinsed at all after testing, unlike the coupons. It is thought that rinsing the coupon may have removed this surface layer. Some of the layer may be present on the coupon surface but it is more difficult to see as the image looks straight down on the surface, whereas because the wire is curved the flaking layer is more noticeable.

The change in radius for the copper wires at each temperature can be seen in Figure 7.18, including repeat test data at 120 °C and 150 °C. The repeat wire testing varied slightly to the original but did give the same trend in both instances.

The amount of copper measured in the end of test fluid increased significantly with

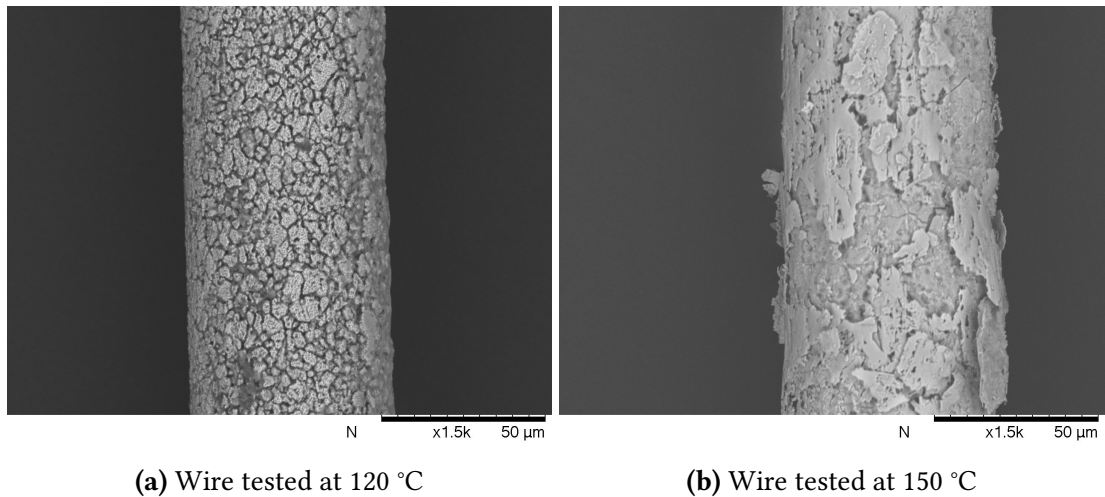


Figure 7.17: End of test BSE images of wire surfaces after testing in dispersant 1 at specified temperatures

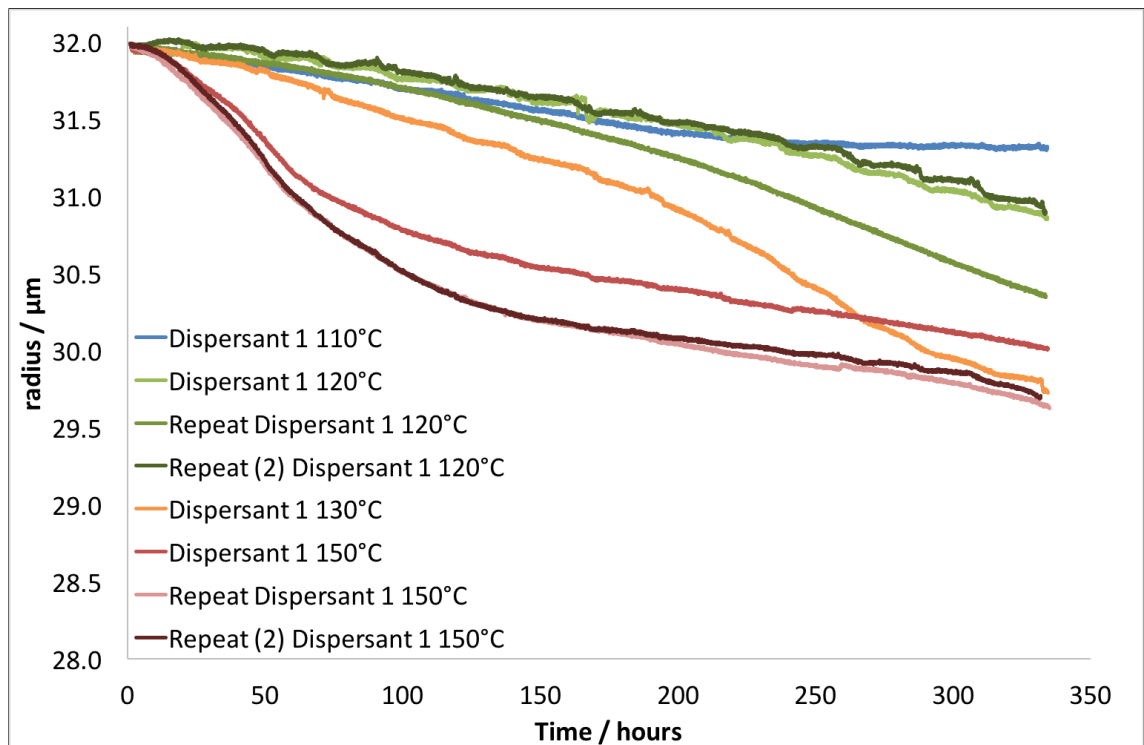


Figure 7.18: Radius change of copper wires immersed in 5 wt% dispersant 1 at 110 °C, 120 °C, 130 °C and 150 °C, including repeats at 120 °C and 150 °C

increasing temperature, as determined using ICP-AES and can be seen in Figure 7.19. This coincides with the porous nature of the surface seen with SEM imaging. It would appear that the copper is being dissolved into the additive solution, probably aided by the nature of the dispersant, keeping particles in suspension.

Results of XPS analysis carried out on the surface of the samples tested in dispersant 1 at 120 °C and 150 °C can be seen in Figure 7.20. The levels are very similar to those measured for the samples tested in base oil alone. There are slight changes in the oxygen

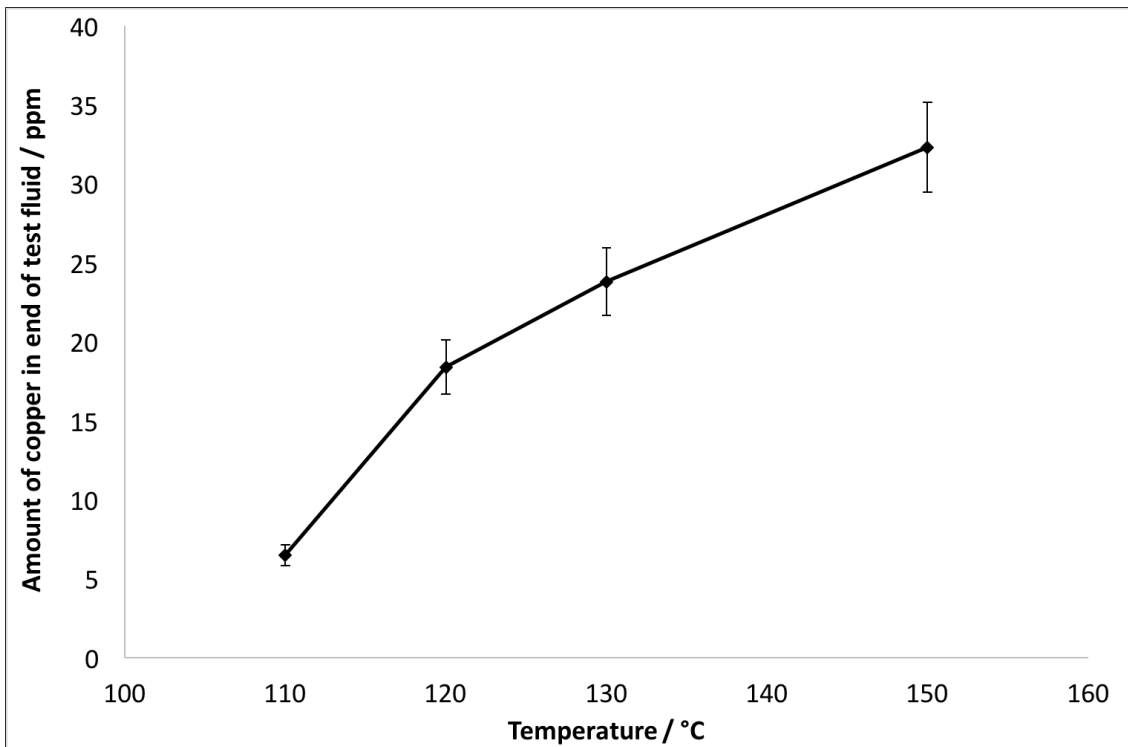


Figure 7.19: The amount of copper in the end of test fluid as determined using ICP-AES for dispersant 1

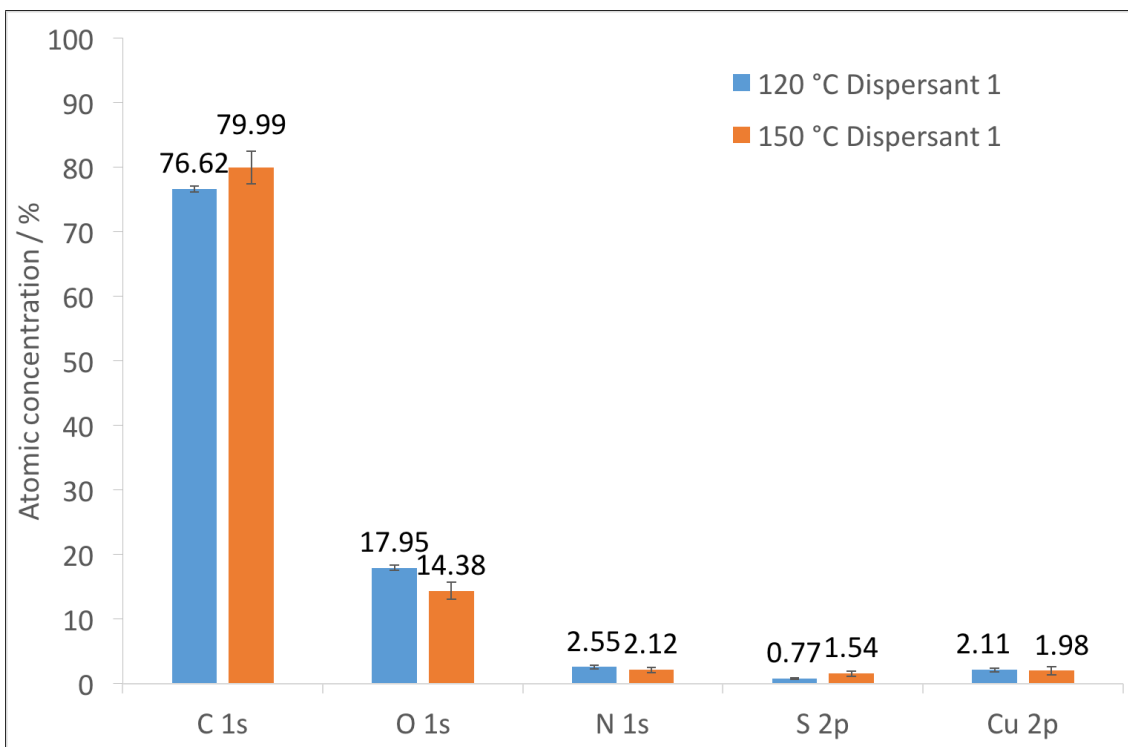


Figure 7.20: Atomic concentration of C, O, N, S and Cu on sample surface tested in dispersant 1 at 120 °C and 150 °C determined by XPS

and copper levels. The oxygen levels measured on the dispersant 1 samples are lower than those measured on the base oil samples whilst the copper levels are higher for the dispersant 1 samples. This could be due to the dispersant removing material from the

surface and not forming a film. The lack of a film would help to explain why the copper level is slightly higher, the decrease in oxygen compared to the base oil samples is a little harder to justify but could be due to a less copper-oxygen bonding.

7.5 Dispersant 2

Dispersant 2 was tested at 5 wt% concentration. Table 7.5 shows images of the coupons at the end of the test for each temperature. At 120 °C, 130 °C and 150 °C the samples are similar in colour, if not quite in appearance. At 130 °C and the repeat of 120 °C there appears to be some exposed copper, however this did not appear to occur when rinsing, as in the case of some of the other additives. Instead it appears to be uneven or differing corrosion across the surface, leading to different colours.

Table 7.5: Images of end of test copper coupons after immersion in dispersant 2 at 110 °C, 120 °C, 130 °C and 150 °C, with repeats at 120 °C and 150 °C. All coupons were the same height and approximately 1.5 cm in width

	110 °C	120 °C	130 °C	150 °C
Original	 3a	 4b	 4a	 4a
Repeat		 4a		 4a

SEM images of the sample surfaces, in Figure 7.21, show what appears to be some sort of porous corrosion. At 110 °C small pits appear to cover the surface, which appear to be larger at 120 °C. At 130 °C the two areas seen in the SEM image show the difference between the colours seen in the images in Table 7.5. There appeared to be a slight film build up which was not present across the entire surface, leaving some areas exposed. At 150 °C there is more of a film on the surface but it seems to be patchy.

Figure 7.22 shows SEM images of the wire at 120 °C and 150 °C. At 120 °C the wire shows a flaking layer, under which the surface appears to be etched, this can be seen on

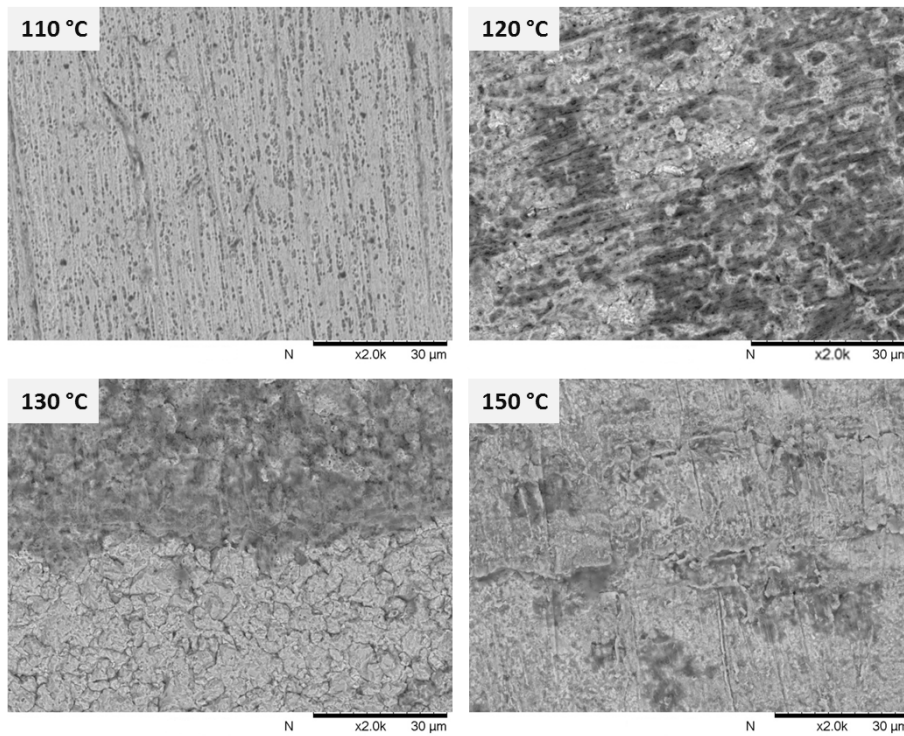


Figure 7.21: End of test BSE images of coupon surface after immersion in dispersant 2 at various temperatures

the coupon surface but is more similar to that seen at 130 °C. The fact that the wires are not cleaned could explain the difference with the 120 °C coupon; cleaning the coupon is likely to have removed any film formed on the surface.

At 150 °C the wire surface appears to show the formation of a film, as there are a number of cracks in it, but it is much better adhered than the film seen at 120 °C. The coupon does not show quite the same surface structure as the wire but they both show a flat surface with few other features. Both the wire and the coupon look better at 150 °C than at 120 °C.

Changes in the radius of copper wires at different temperatures can be seen in Figure 7.23, including repeats for 120 °C and 150 °C. There is a difference between the shapes of the plots for the different temperatures tested and the repeat data overlays well with the original. At 120 °C, for example, the radius change increases with time after 200 hours whilst at 150 °C the rate of change slows after this point. These changes shall be reviewed further in the discussion.

The amount of copper in the end of test fluid is shown in Figure 7.24, for experiments containing dispersant 2. There is an increase in the amount of copper present with increasing temperature; however it is not as severe as for dispersant 1. There is a large

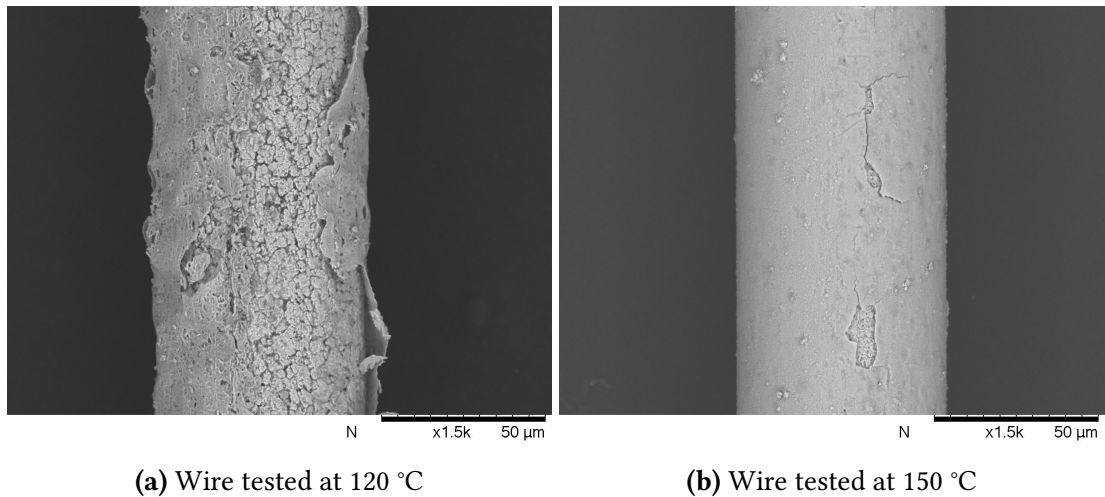


Figure 7.22: End of test BSE images of wire surfaces after testing in dispersant 2 at specified temperatures

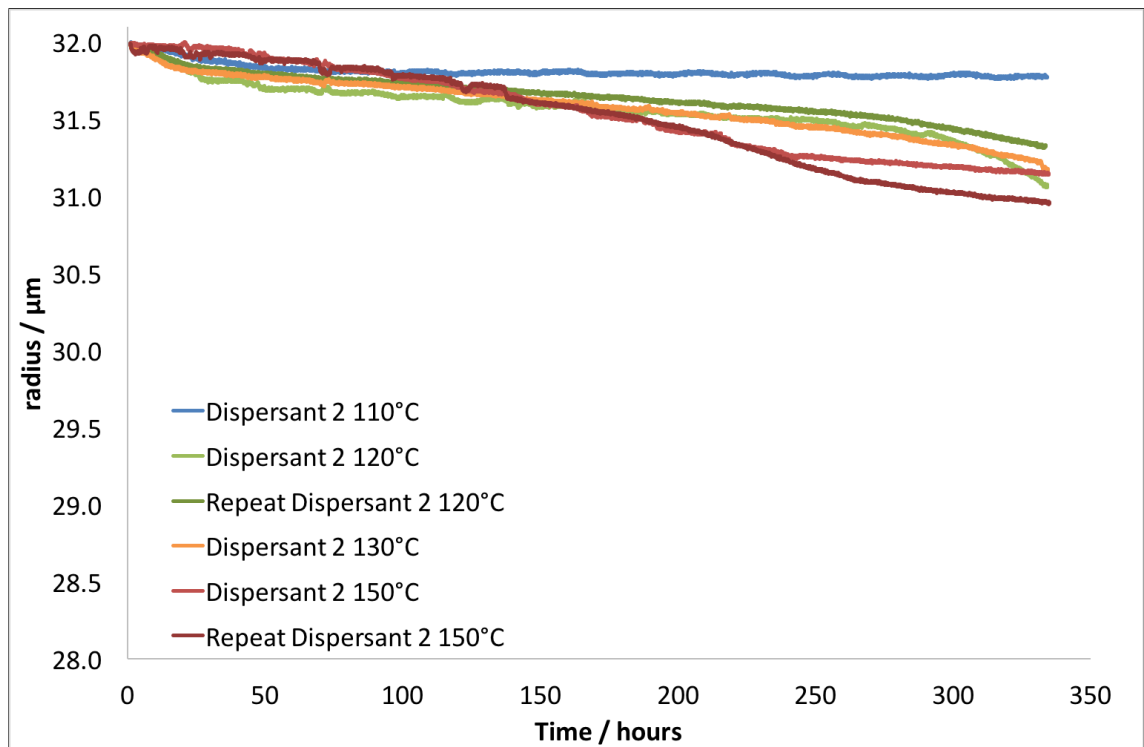


Figure 7.23: Radius change of copper wires immersed in 5 wt% dispersant 2 at 110 °C, 120 °C, 130 °C and 150 °C, including repeats at 120 °C and 150 °C

increase between 110 °C and 120 °C but the increase is not so great between 120 °C and 150 °C.

Figure 7.25 shows the elemental composition of the 120 °C and 150 °C sample surfaces determined using XPS analysis. There is a decrease in the amount of oxygen present, compared to the base oil samples. The nitrogen level at both temperatures is very similar to the corresponding base oil samples which would suggest that the dispersant does not interact with the surface. At 120 °C the sulfur level at 1.85 % is higher than the 0.26 %

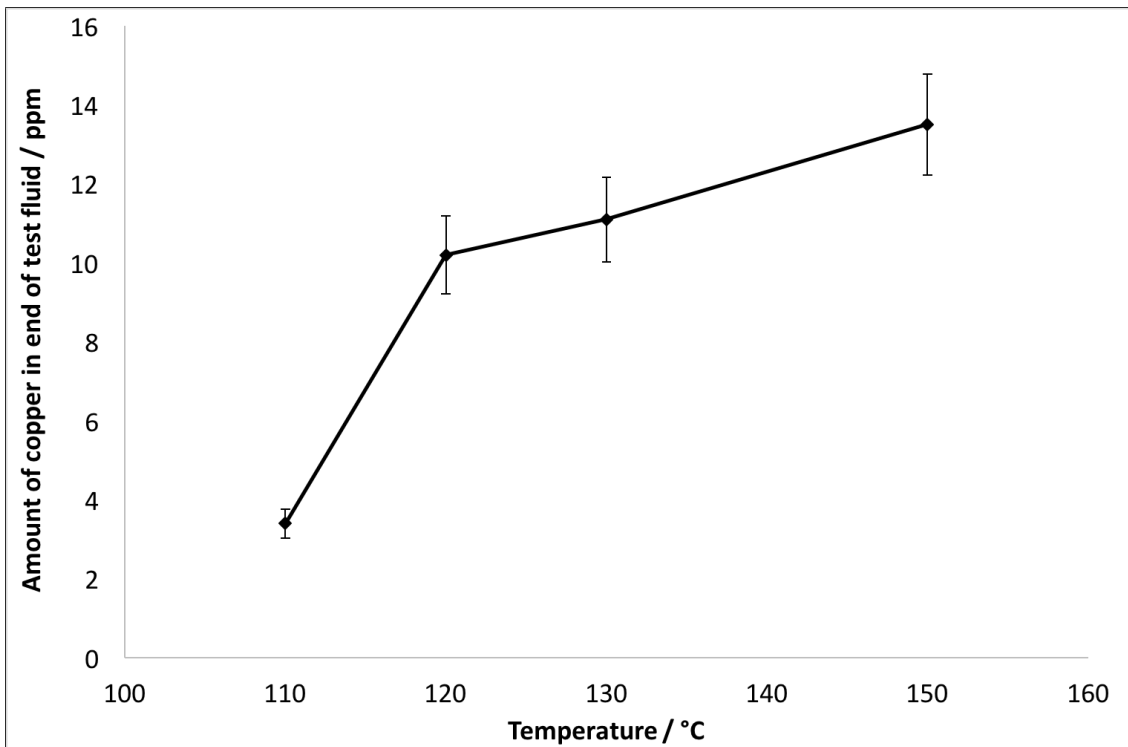


Figure 7.24: The amount of copper in the end of test fluid as determined using ICP-AES for dispersant 2

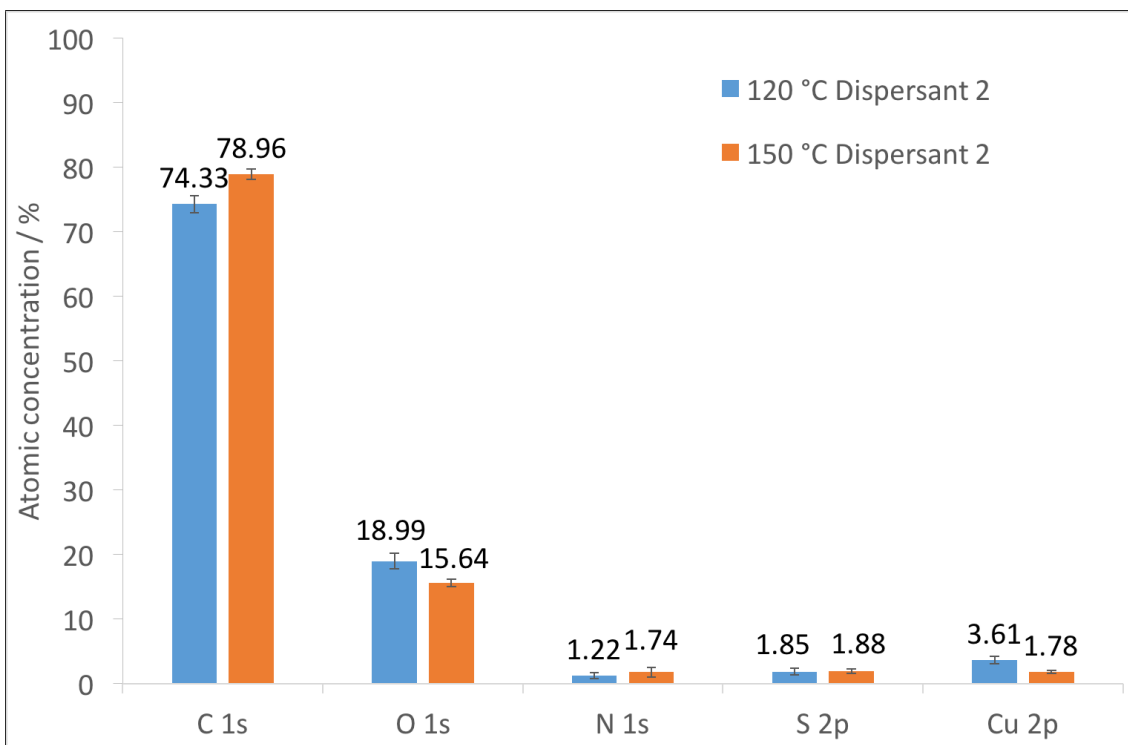


Figure 7.25: Atomic concentration of C, O, N, S and Cu on sample surface tested in dispersant 2 at 120 °C and 150 °C determined by XPS

measured for the base oil sample which could come from interaction of the stabilising sulfate group with the surface, the increase is not as noticeable at 150 °C.

The copper level is slightly higher for the dispersant 2 samples than the base oil

suggesting if there is any film is present on the surface it is thinner than the base oil film.

7.6 Detergent 1

Detergent 1 was tested at a concentration of 0.5 wt%, with Table 7.6 showing images of the samples at each temperature. The difference in rating between the original and repeat coupons shows how subjective some of the ratings can be; particularly between the 1b and 3a ratings at 120 °C.

Table 7.6: Images of end of test copper coupons after immersion in detergent 1 at 110 °C, 120 °C, 130 °C and 150 °C, with repeats at 120 °C and 150 °C. All coupons were the same height and approximately 1.5 cm in width

	110 °C	120 °C	130 °C	150 °C
Original	 1b	 1b	 1b	 2d
Repeat		 3a		 4a

The repeat coupon at 150 °C is rated 4a due to the darker colour that was present diagonally across the centre, although it is mainly the same colour as the original coupon. This shows how imperfections on the surface can affect the rating, possibly giving an unfairly biased result.

SEM images of the surface, Figure 7.26, do not show anything particularly significant. There appears to be a thin film present at all temperatures, but is most notable at 130 °C where a small area has been accidentally scratched off.

SEM images of the wires tested at 120 °C and 150 °C can be seen in Figure 7.27. The surface of the wire and the coupon tested at 120 °C look very similar. At 150 °C the wire can be seen to show some etching underneath a surface layer. This surface layer looks

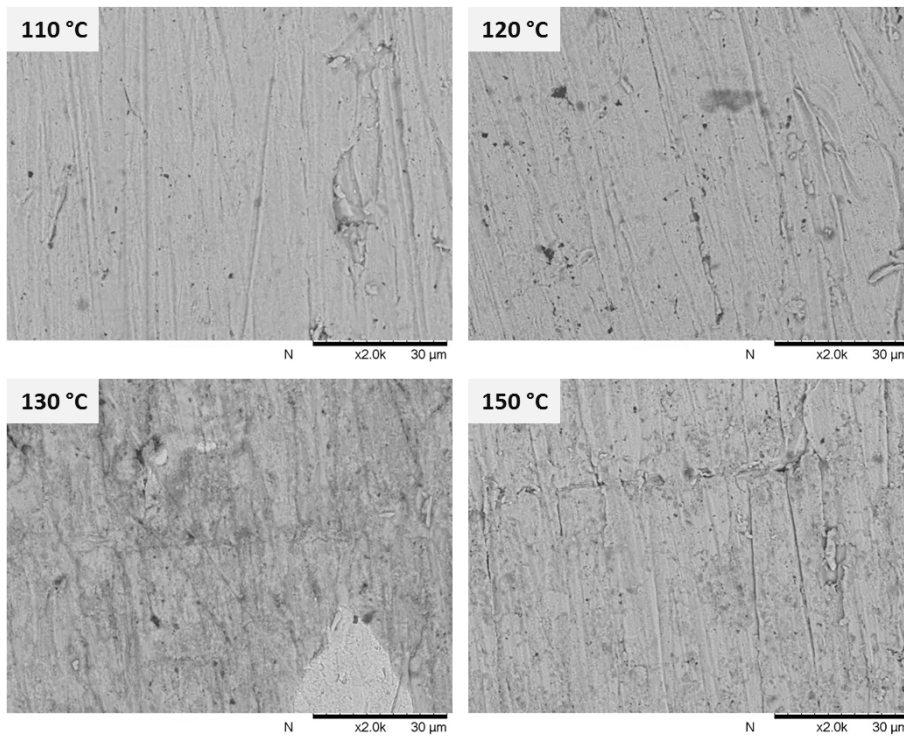
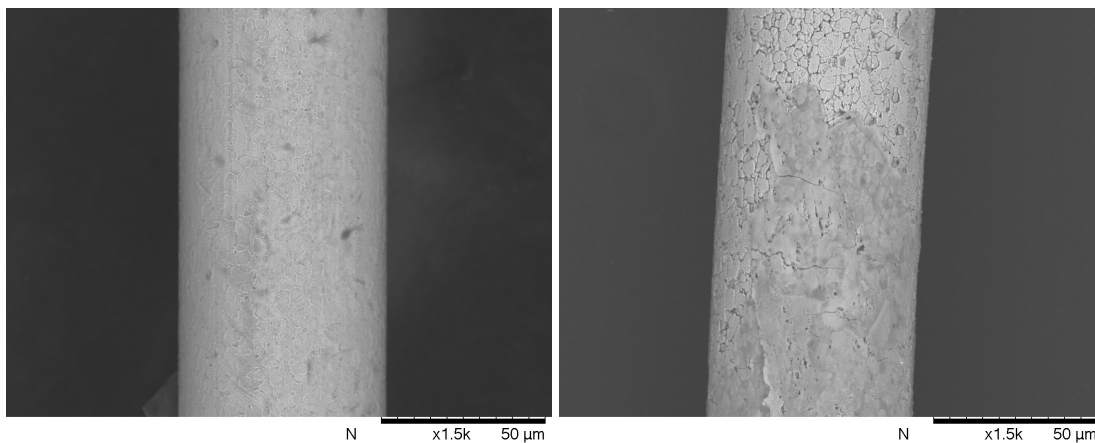


Figure 7.26: End of test BSE images of coupon surface after immersion in detergent 1 at various temperatures

similar to the coupon surface and so it is likely that the surface covering on the wire was removed during handling as it otherwise appears well adhered to the surface. This is interesting to see and helps to explain the reduction in radius seen in Figure 7.28 which could otherwise not be explained by looking at the coupon image alone.



(a) Wire tested at 120 °C

(b) Wire tested at 150 °C

Figure 7.27: End of test BSE images of wire surfaces after testing in detergent 1 at specified temperatures

Figure 7.28 shows the results of the change in radius of wires tested at different temperatures. There is good agreement with the repeat data at 120 °C and 150 °C which

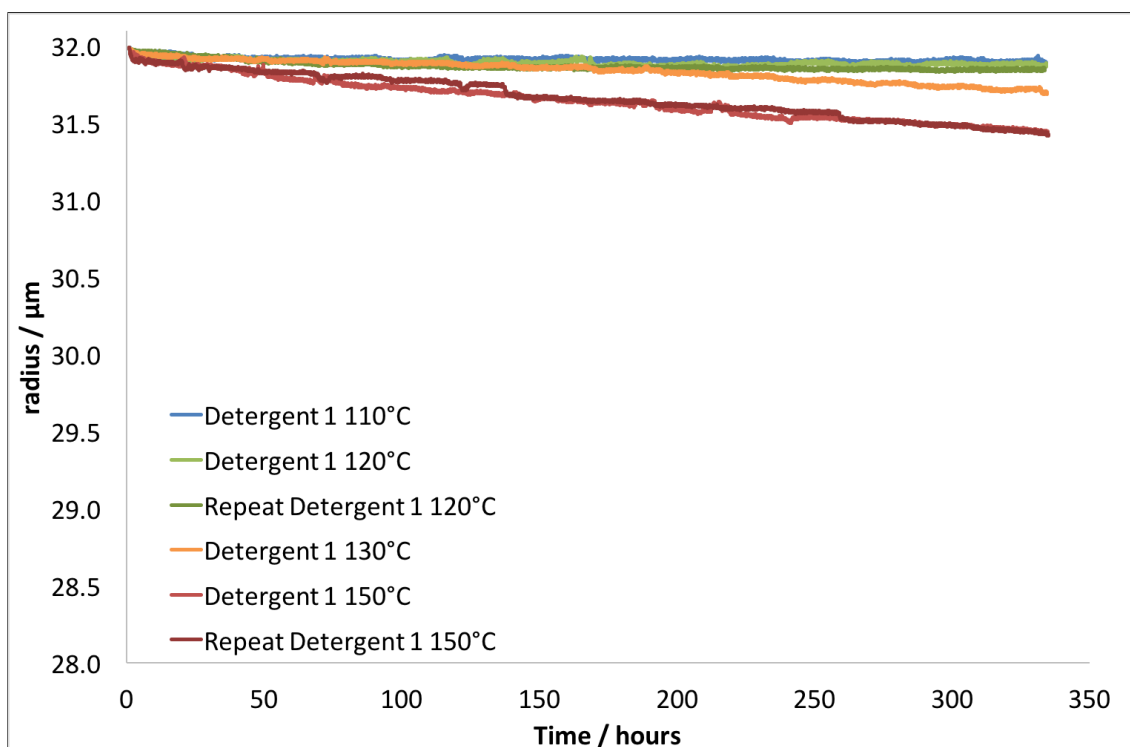


Figure 7.28: Radius change of copper wires immersed in 0.5 wt% detergent 1 at 110 °C, 120 °C, 130 °C and 150 °C, including repeats at 120 °C and 150 °C

has also been included. There is little change in the radius particularly at the lower temperatures, although it does appear that at 150 °C the radius is steadily decreasing, with no plateau observed within the timeframe of the experiment. Even so the radius change in 350 hours was around 0.5 μm, which is not considered to show serious corrosion. This change in radius can be rationalised with Figure 7.27 where etching of the copper can be seen on the wire surface.

The amount of copper in the end of test fluid for detergent 1 is low for all temperatures tested, as seen in Figure 7.29. There is a small amount of copper measured at 130 °C and 150 °C, which seems to correspond to the decrease in the wire radius measured for those temperatures. The level of copper is below 3 ppm in all cases which is very good and therefore shows there is minimal corrosion.

XPS results can be seen in Figure 7.30. The atomic concentration of a number of specific elements on the surface of samples tested at 120 °C and 150 °C are shown. The values are similar to those measured on samples tested in base oil, therefore it is likely that the detergent has minimal interaction with the copper surface.

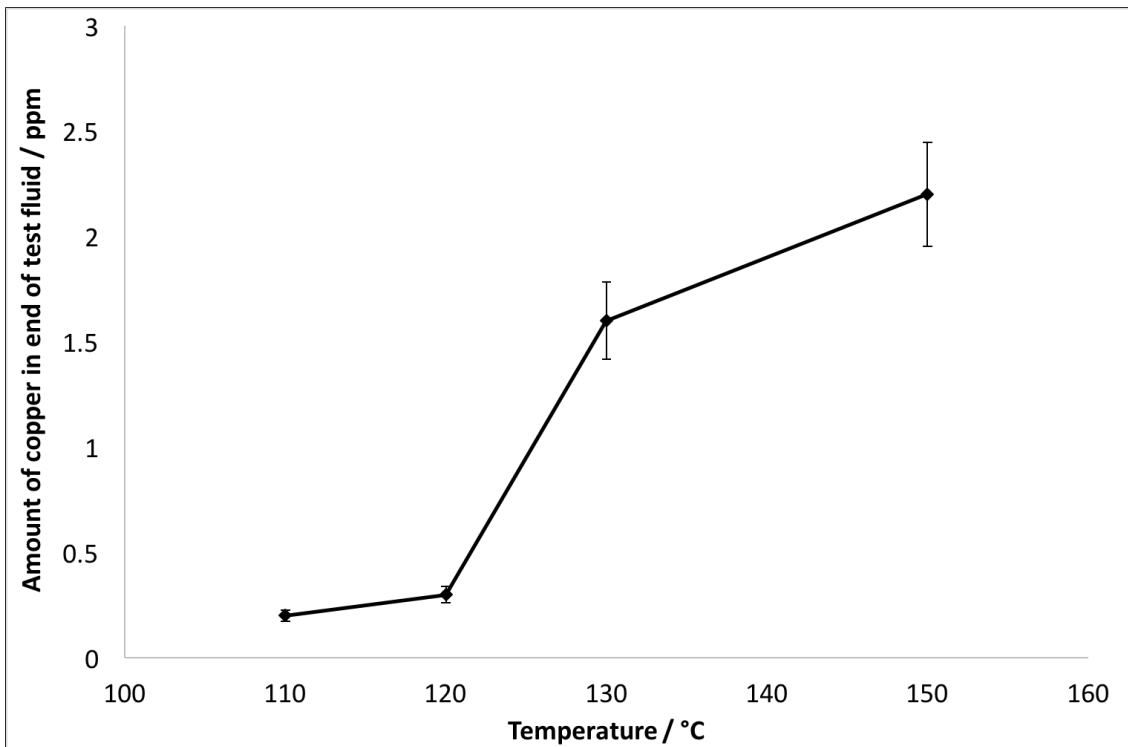


Figure 7.29: The amount of copper in the end of test fluid as determined using ICP-AES for detergent 1

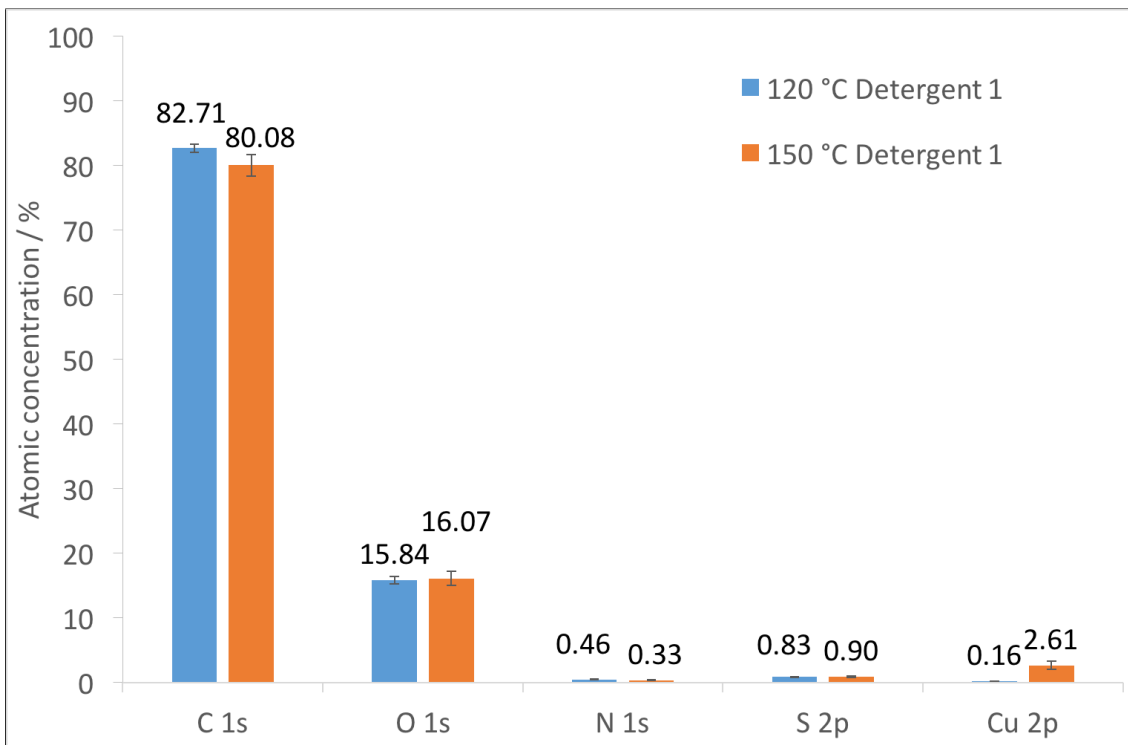


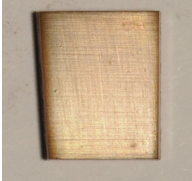
Figure 7.30: Atomic concentration of C, O, N, S and Cu on sample surface tested in detergent 1 at 120 °C and 150 °C determined by XPS

7.7 Detergent 2

Tests carried out in detergent 2 were conducted at 0.5 wt% concentration. Images of the coupon surfaces can be seen in Table 7.7, where there appears to be some discrepancy

between the original and repeat coupon rating at 150 °C.

Table 7.7: Images of end of test copper coupons after immersion in detergent 2 at 110 °C, 120 °C, 130 °C and 150 °C, with repeats at 120 °C and 150 °C. All coupons were the same height and approximately 1.5 cm in width

	110 °C	120 °C	130 °C	150 °C
Original	 3b	 2e	 1b	 3a
Repeat		 2e		 1b

This discrepancy is partly due to difficulties in matching the colours on the coupons with the colours of the standard ratings. It is interesting to note that the ratings do not appear to get worse with increasing temperature; actually they do not show any trend at all.

SEM images (Figure 7.31) show thin film formation at all temperatures with little to distinguish between the temperatures below 130 °C. At 150 °C there are some small particles present which are likely to be from an increase in the film thickness.

Figure 7.32 shows SEM images of wires tested in detergent 1 at 120 °C and 150 °C. Both surfaces look very similar to the respective coupon surface, so we can assume that the same mechanism is occurring on both the wire and the coupon.

The change in radius of wires tested in the presence of detergent 2 can be seen in Figure 7.33. There is very little change in the radius of the wire at any of the temperatures tested. At 150 °C where a small change is seen this decrease occurs at the start of the test and remains constant for the remainder of the experiment.

There is very little copper detected in the end of test fluid, as determined by ICP-AES, below 2 ppm across all temperatures tested, as seen in Figure 7.34. This shows that detergent 2 has little interaction with the copper surface and does not contribute to the corrosion of copper at these temperatures over the given time period.

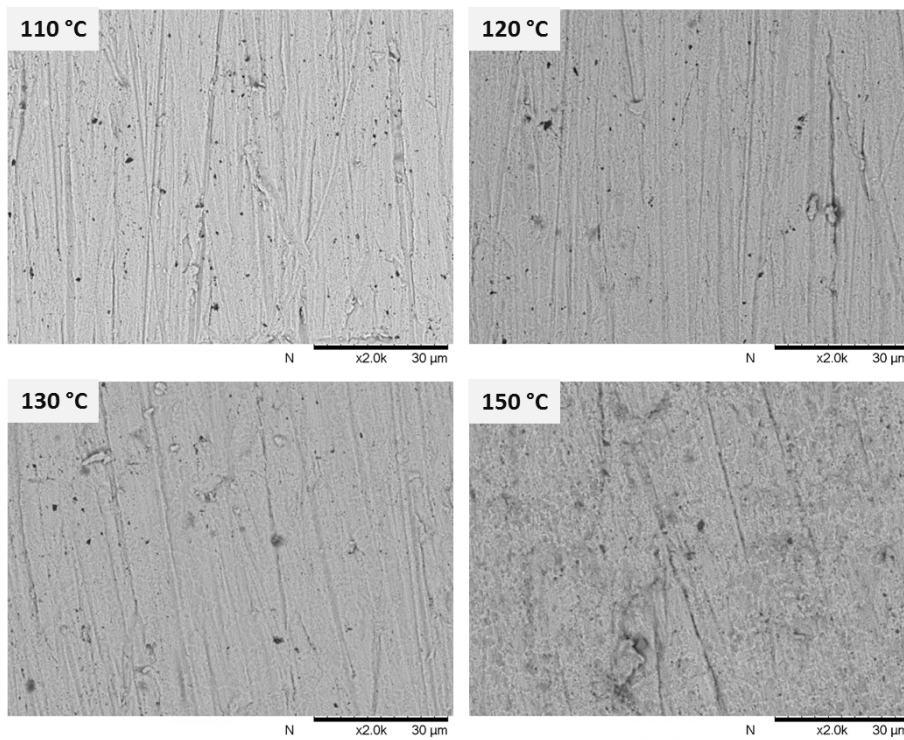
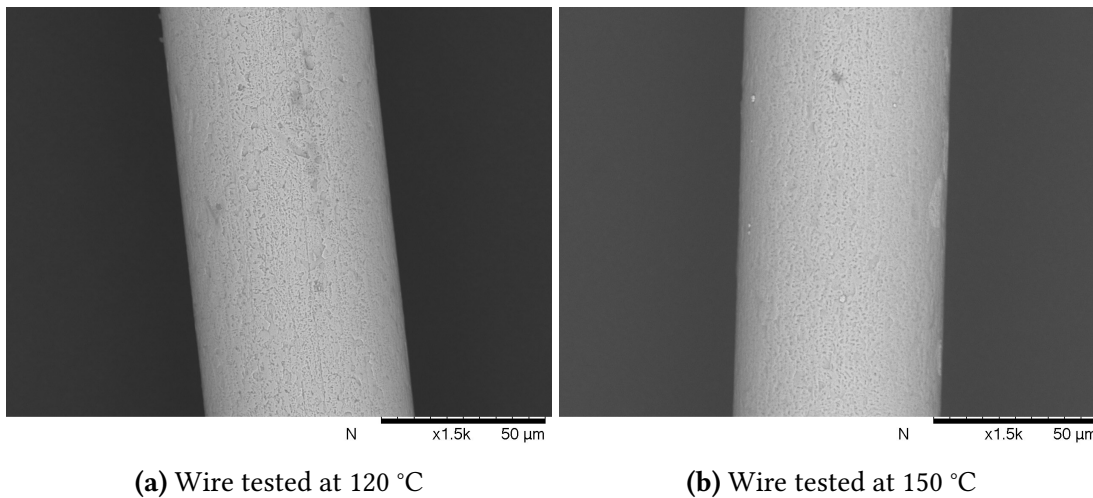


Figure 7.31: End of test BSE images of coupon surface after immersion in detergent 2 at various temperatures



(a) Wire tested at 120 °C

(b) Wire tested at 150 °C

Figure 7.32: End of test BSE images of wire surfaces after testing in detergent 1 at specified temperatures

XPS results for samples tested in detergent 2 can be seen in Figure 7.35. The level of carbon differs between the 120 °C and 150 °C samples, with higher carbon levels seen at the lower temperature. The reverse is seen in the oxygen levels.

The carbon and oxygen levels also differ significantly from those measured on the surface of coupons tested in base oil. This would suggest some interaction with the detergent is possibly occurring. Detergent 2 is comprised of carbon and oxygen molecules and so changes in these elements may be expected on the surface, however it is not

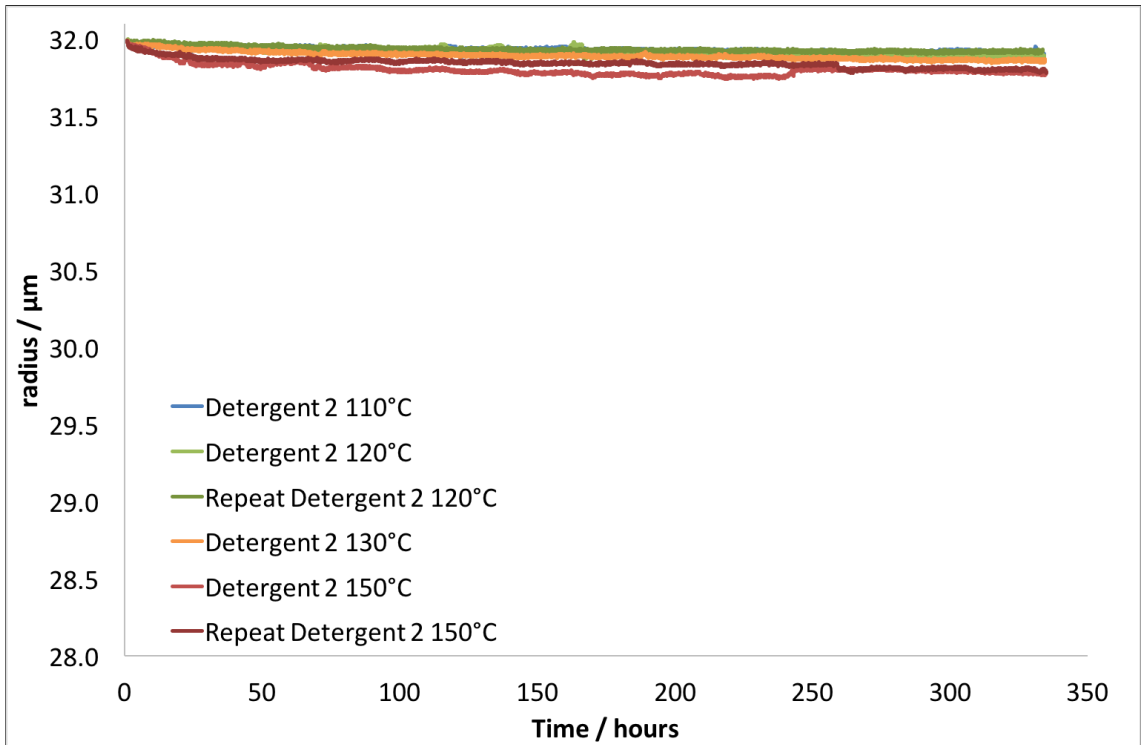


Figure 7.33: Radius change of copper wires immersed in 0.5 wt% detergent 2 at 110 °C, 120 °C, 130 °C and 150 °C, including repeats at 120 °C and 150 °C

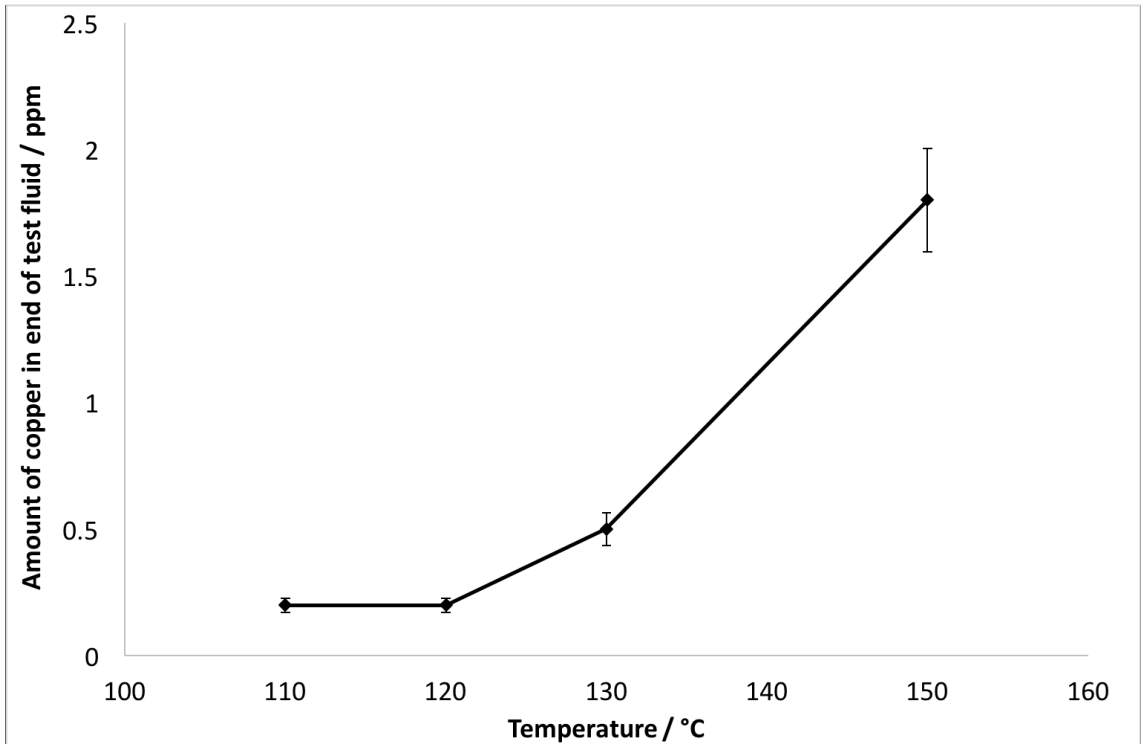


Figure 7.34: The amount of copper in the end of test fluid as determined using ICP-AES for detergent 2

clear why at one temperature the levels should increase and at the other temperature decrease.

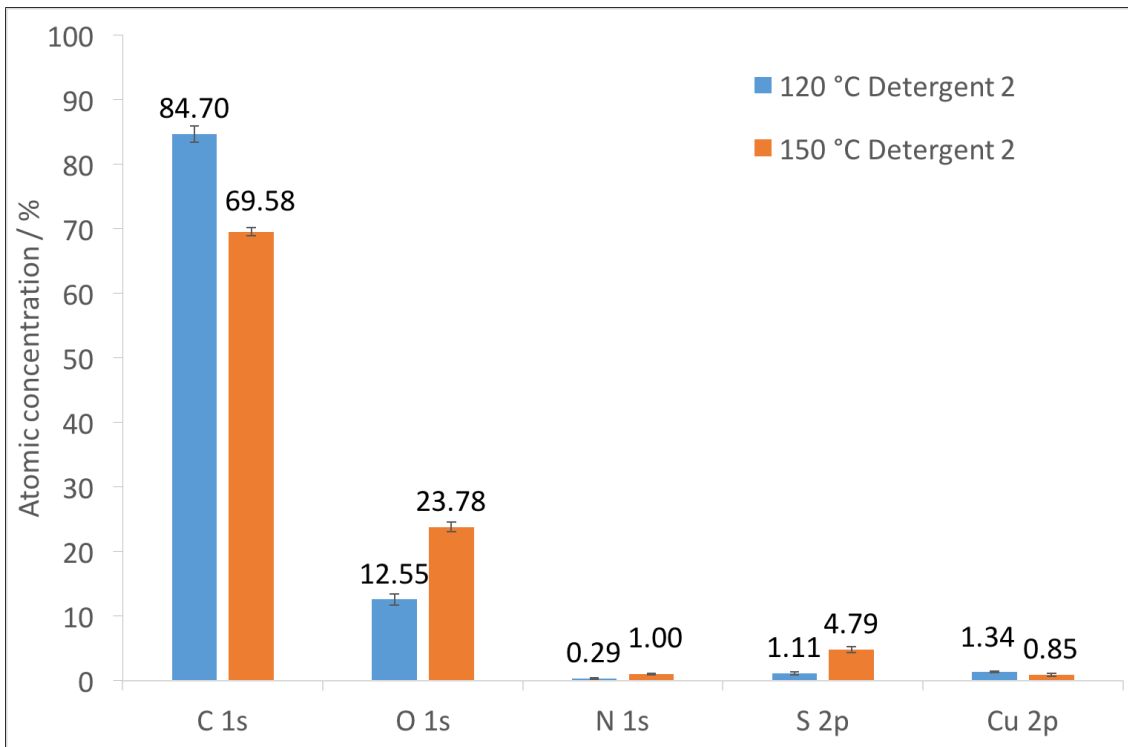


Figure 7.35: Atomic concentration of C, O, N, S and Cu on sample surface tested in detergent 2 at 120 °C and 150 °C determined by XPS

7.8 Antioxidant (AO), Antiwear (AW), and Friction Modifier (FM) mix

Coupons and wires were tested in a mixture of antioxidant, 0.33 wt%, antiwear, 0.165 wt% and friction modifier, 0.65 wt%, which shall be abbreviated to AO, AW, FM mix. Table 7.8 shows images of coupons at the the end of the experiment for the different temperatures tested.

Table 7.8: Images of end of test copper coupons after immersion in a mixture of friction modifier, antioxidant, and antiwear at 110 °C, 120 °C, 130 °C and 150 °C. All coupons were the same height and approximately 1.5 cm in width

110 °C	120 °C	130 °C	150 °C
			
4b	4b	4a	2e

The rating appears to improve with increasing temperature with the 150 °C sample having the best rating. This is also mirrored in the SEM images of the surface in Figure 7.36, where the surface at 150 °C appears to have fewer, smaller, holes than the surfaces at lower temperatures.

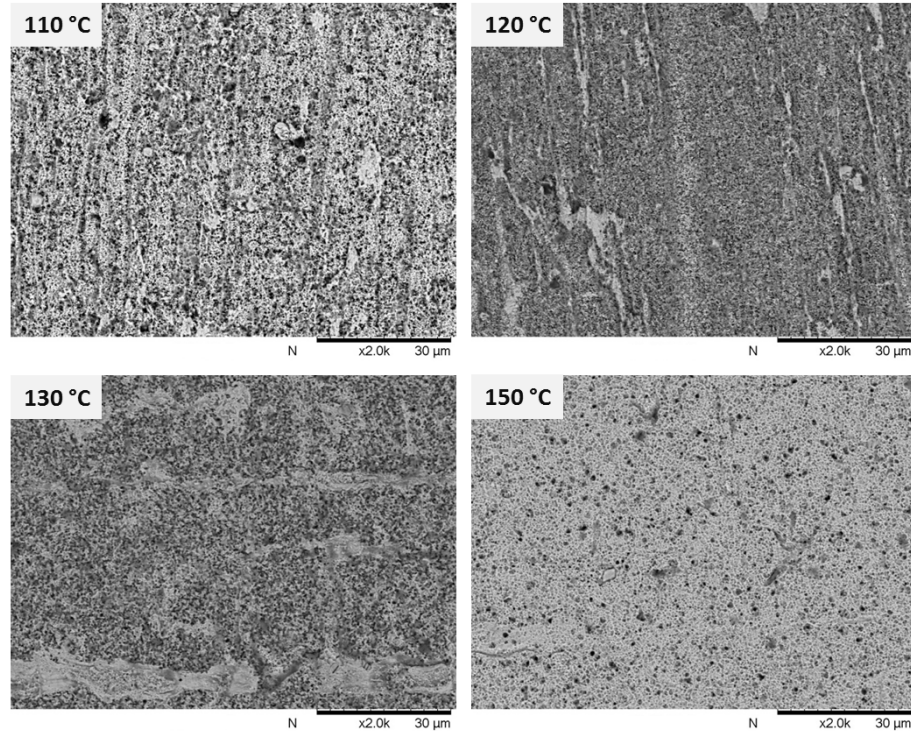
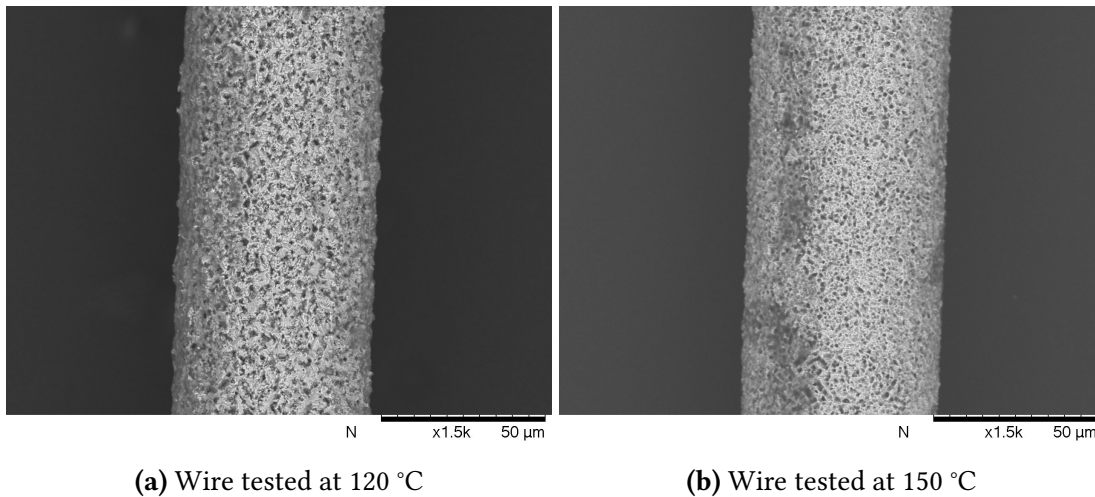


Figure 7.36: End of test BSE images of coupon surface after immersion in a mixture of friction modifier, antioxidant, and antiwear at various temperatures

SEM images of the wire surfaces tested at 120 °C and 150 °C can be seen in Figure 7.37. Both wires are covered in small holes or pits. The surface of the wire at 150 °C looks very similar to that of the coupon surface at the same temperature. The wire at 120 °C looks slightly different to that of the 120 °C coupon. The holes on the wire are larger than those seen on the coupon. The coupon also has small ‘islands’ which look as if they are un-corroded surface. It is not clear why the wire and coupon should show a difference but both show evidence of corrosion in the form of small pits.

Radius changes for wires immersed in a mixture of friction modifier, antioxidant and antiwear mixture can be seen in Figure 7.38. Unlike the other additives the change in radius seems to be smaller with increasing temperature, with the exception of 110 °C.

The amount of copper measured in the end of test fluid, Figure 7.39 is unusual as there is no clear pattern to it. It does not increase or decrease consistently with temperature. The 110 °C – 130 °C trend does follow that of the radius change to a point.



(a) Wire tested at 120 °C

(b) Wire tested at 150 °C

Figure 7.37: End of test BSE images of wire surfaces after testing in the AO, AW, FM mix at specified temperatures

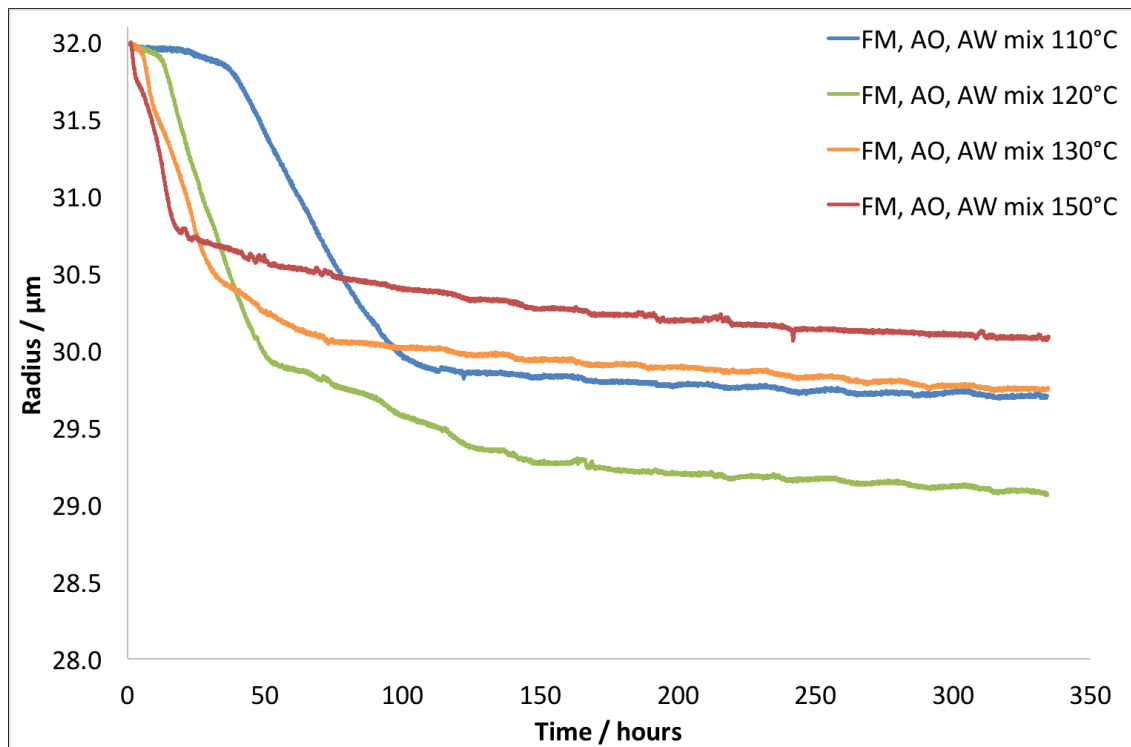


Figure 7.38: Radius change of copper wires immersed in a mixture of 0.65 wt% friction modifier, 0.33 wt% antioxidant, and 0.165 wt% antiwear at 110 °C, 120 °C, 130 °C and 150 °C

Assuming a decrease in radius leads to an increase in copper in the end of test fluid then according to the radius data the 110 °C and 130 °C samples should have roughly equal ICP values for copper, which they do. The 120 °C sample has a lower radius, therefore should have a higher copper level by ICP, which it does. What does not follow is the 150 °C sample, which having a smaller radius change should mean a lower ICP copper value than the 110 °C sample, but this is not the case.

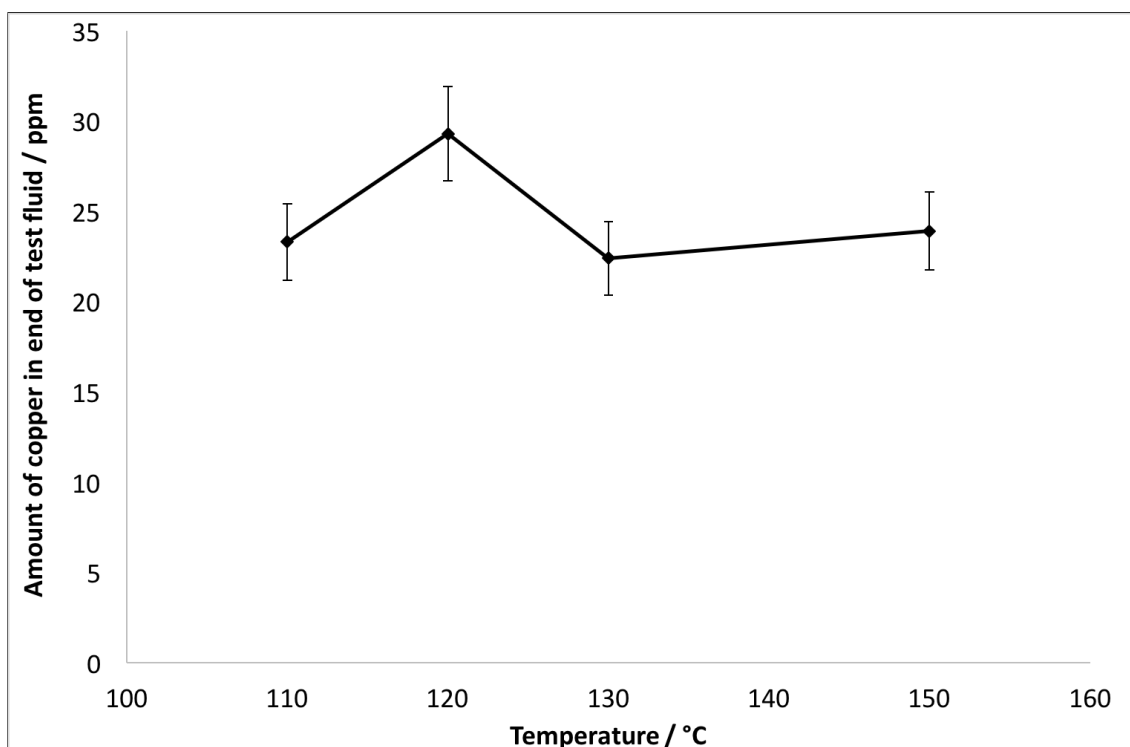


Figure 7.39: The amount of copper in the end of test fluid as determined using ICP-AES for the friction modifier, antioxidant, and antiwear mixture

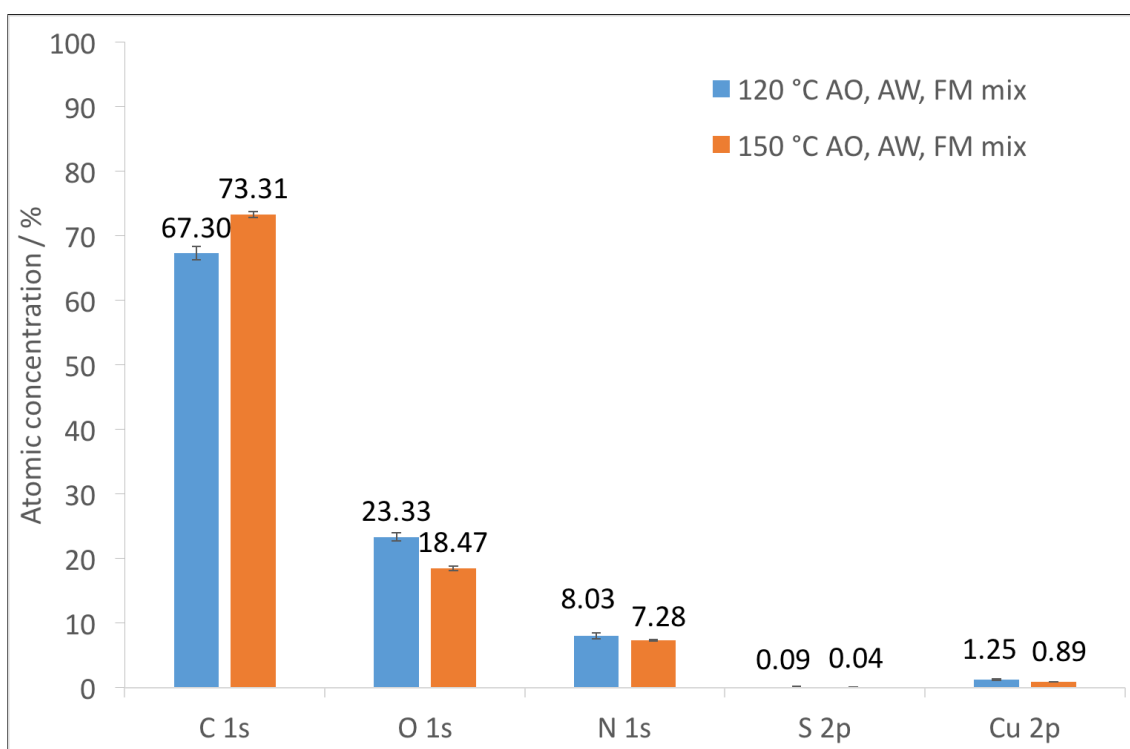


Figure 7.40: Atomic concentration of C, O, N, S and Cu on sample surface tested in the AO, AW, FM mix at 120 °C and 150 °C determined by XPS

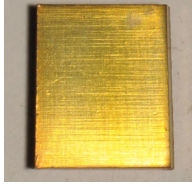
XPS analysis has been used to identify the atomic concentration of specific elements on the surface and can be seen in Figure 7.40. The amount of nitrogen is higher than that measured for the base oil samples. The antioxidant and friction modifier molecules

contain nitrogen and so it is likely that they are interacting with the surface, increasing the amount of nitrogen detected. From this mix it is not possible to tell whether the nitrogen is coming from the antioxidant or the friction modifier or indeed both.

7.9 Antioxidant

The antioxidant alone was tested at a concentration of 0.33 wt% and images of the coupons and their ratings can be seen in Table 7.9. Interestingly they are the same at both 120 °C and 150 °C.

Table 7.9: Images of end of test copper coupons after immersion in antioxidant at 120 °C and 150 °C, with repeats. All coupons were the same height and approximately 1.5 cm in width

	120 °C	150 °C
Original	 2e	 2e
Repeat	 2e	 2e

SEM images of the surfaces, seen in Figure 7.41 also show the surfaces to be very similar at both temperatures.

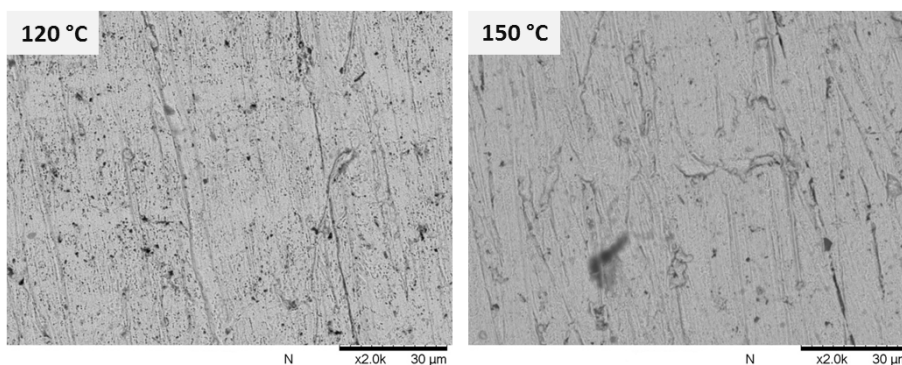


Figure 7.41: End of test BSE images of coupon surface after immersion in antioxidant at various temperatures

The radius changes of wires immersed in the antioxidant test fluid at 120 °C and 150 °C can be seen in Figure 7.42, along with repeat data. There is very little change in the radius for either temperature and the only real difference appears to be that at 150 °C there is a slight decrease in the initial 10 hours or so followed by a plateau for the remainder of the test.

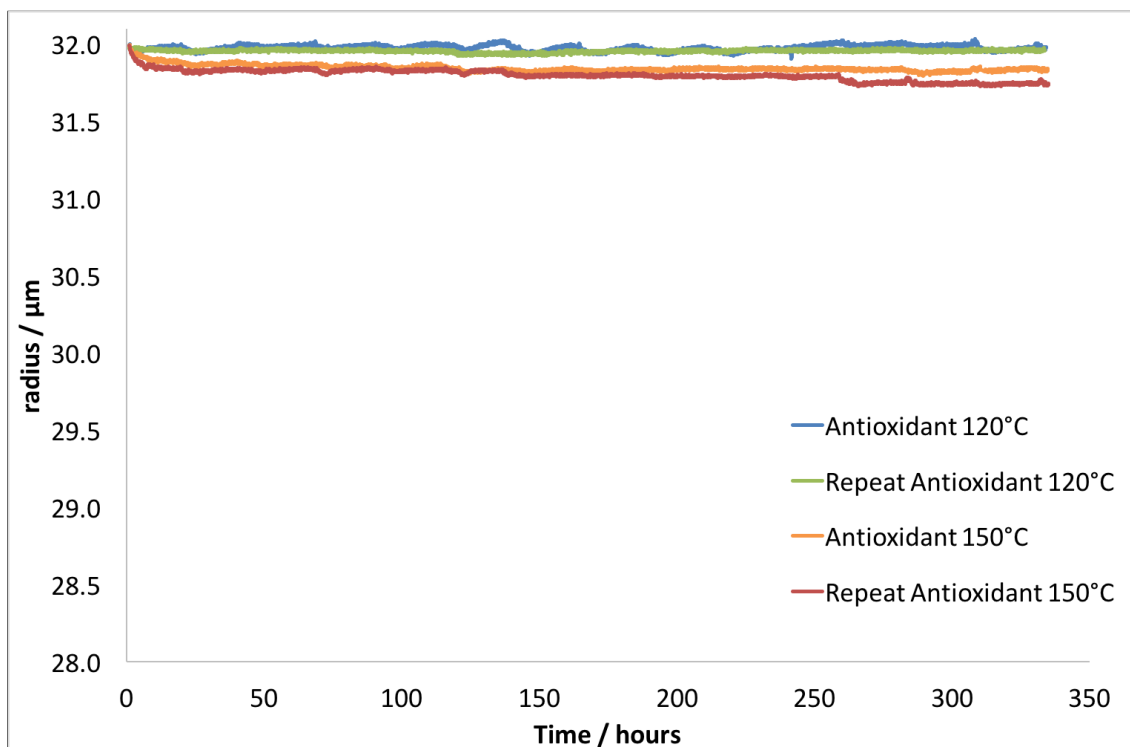


Figure 7.42: Radius change of copper wires immersed in 0.33 wt% antioxidant at 120 °C and 150 °C, with repeats

Figure 7.43 shows the atomic concentration of specific elements determined from XPS. Compared to the results from the base oil samples there are several differences.

The amount of nitrogen, oxygen and copper measured is higher than for the samples tested in the antioxidant than in base oil. The antioxidant molecule has two phenyl groups attached to a central nitrogen. We can assume that the molecule is attaching to the copper surface from the amount of nitrogen measured. The amount of carbon is reduced compared to the base oil samples and this is likely to be due to the arrangement of the antioxidant molecules on the surface; they will take up more room than straight carbon chains which would be interacting in the case of the base oil alone.

The increased oxygen level compared to the base oil alone may also be due to the space taken up by the antioxidant, if they are spaced apart, due to the size of the side

group chains, but carbon chains from the base oil cannot pack between them it is possible that on exposure to the atmosphere oxygen will bond to available copper sites.

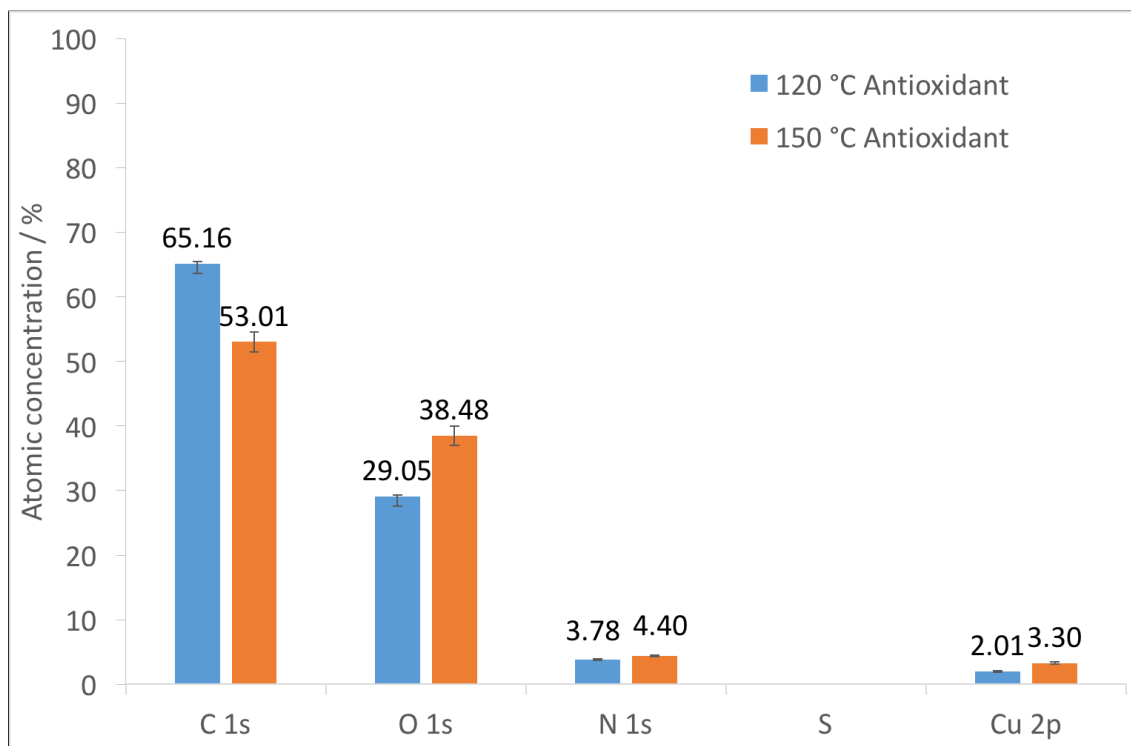


Figure 7.43: Atomic concentration of C, O, N, S and Cu on sample surface tested in antioxidant at 120 °C and 150 °C determined by XPS

7.10 Antiwear

Testing of the antiwear, at 0.165 wt%, was interesting, as can be seen in the radius change data in Figure 7.44. At both 120°C and 150°C there are sudden breaks in the data, however the repeats do appear to sit nicely over the top of one another. Only one test ran for the entire test duration, which was the repeat of 150 °C. Inspection of the broken wires at the end of the test showed that breakages occurred in the gaseous phase. For this reason these results were thought not to be a true representation of the reaction of the antiwear molecule with the copper surface. Even the test that did not break was considered unreliable as it was not known if the measured decrease in the radius was due to interaction of corrosive components in the gas phase and therefore not representative of the wire in the liquid phase.

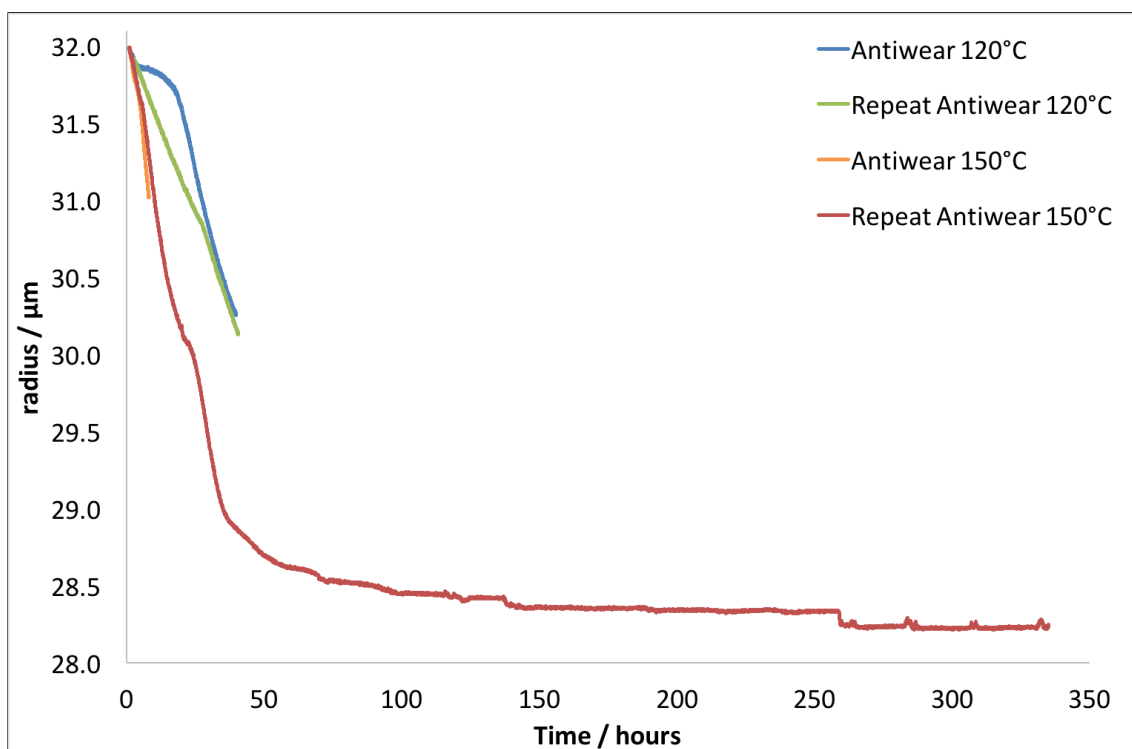


Figure 7.44: Radius change of copper wires immersed in 0.165 wt% antiwear additive at 120 °C and 150 °C, with repeats

Images of the coupon surfaces at each temperature can be seen in Table 7.10. At 150 °C the coupon is very discoloured with what appears to be a film formed across the surface, this is also seen in the SEM image in Figure 7.45.

At 120 °C there was a thin film formed on the surface which was very easily removed on rinsing. As such the coupons were rinsed in such a way as to try and retain some of this film. The SEM image shows that the film is composed of lots of small particles agglomerated together but it is unclear why it did not adhere to the surface. The copper underneath appears to have been corroded in the sense that no polishing marks can be seen anymore.

XPS analysis of the surfaces can be seen in Figure 7.46. It is difficult to draw conclusions from this set of data. The levels are very similar to those measured for samples tested in base oil, particularly at 150 °C.

At 120 °C the values differ slightly more than those of the base oil samples. There is very little nitrogen on the surface of the antiwear samples, lower than the expected contamination level of the base oil samples. The carbon level is higher and the oxygen level lower than the base oil samples but it is not clear why this may be the case as if the

Table 7.10: Images of end of test copper coupons after immersion in antiwear additive at 120 °C and 150 °C, with repeats. All coupons were the same height and approximately 1.5 cm in width

	120 °C	150 °C
Original	 2b	 4c
Repeat	  2b 2b	 4a

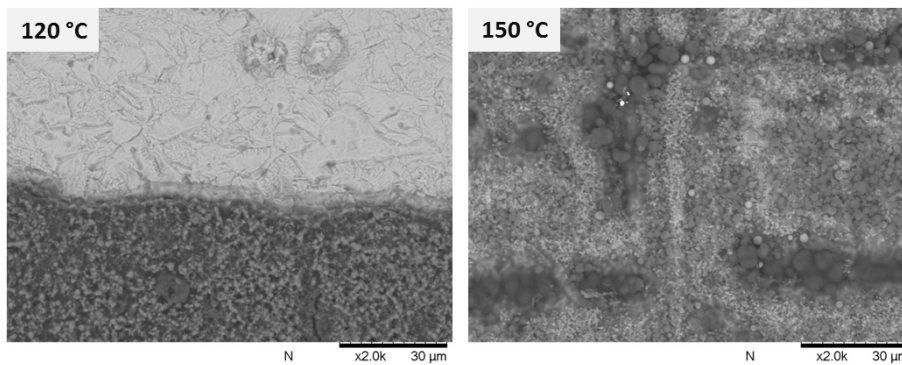


Figure 7.45: End of test BSE images of coupon surface after immersion in antiwear additive at various temperatures

antiwear were to interact with the surface an increase in oxygen is plausible.

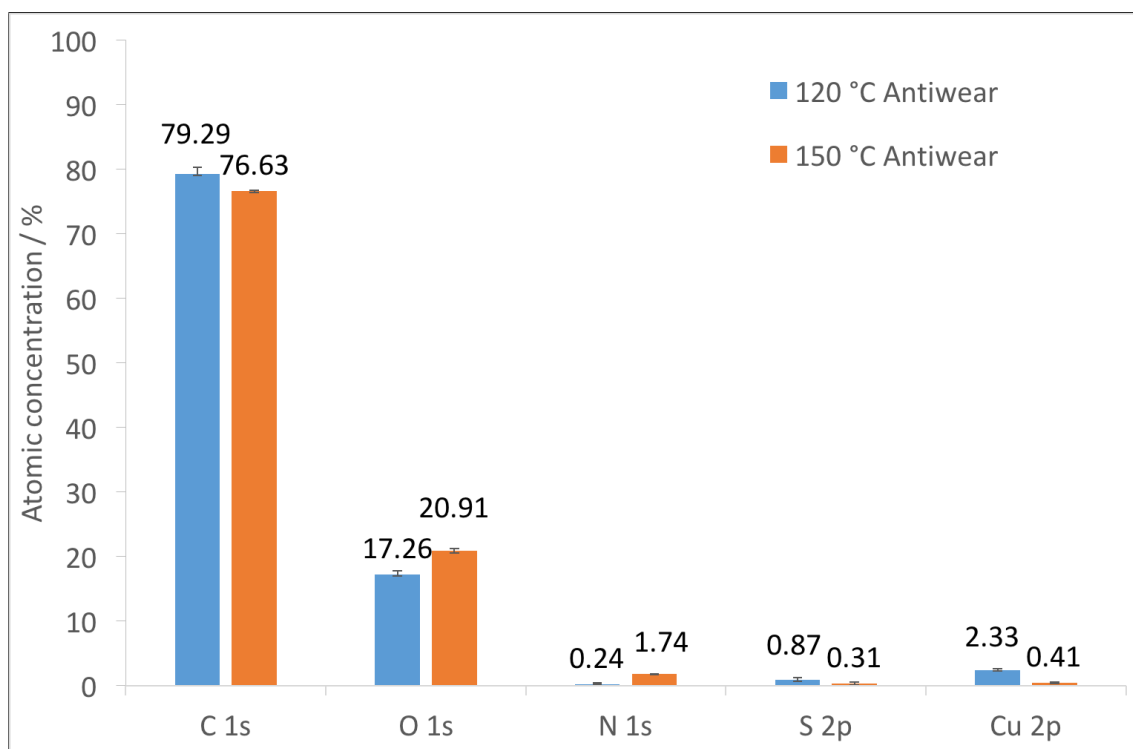


Figure 7.46: Atomic concentration of C, O, N, S and Cu on sample surface tested in antiwear at 120 °C and 150 °C determined by XPS

7.11 Friction modifier

The results of the radius changes of wires tested in 0.65 wt% friction modifier can be seen in Figure 7.47, where the repeat data is very consistent. At 150 °C there appears to be significant radius loss which looks as if it may have continued to decrease had the test been extended. At 120 °C the loss is less but is still steadily decreasing at the end of the 350 hours.

Images of the coupons at the end of the test can be seen in Table 7.11. Although there is a slight difference in the ratings of the coupons at 120 °C the images show them to be very similar in colour; again highlighting the inconsistencies in the ratings. At 150 °C the repeat sample had a surface layer that flaked off, exposing the copper underneath.

SEM images of the surfaces at both 120 °C and 150 °C are surprisingly similar with dark patches of film or deposit on the surface, as seen in Figure 7.48. The difference between them is at 150 °C the patches are larger and closer together.

Results of the XPS analysis of the surface of the samples tested in friction modifier can be seen in Figure 7.49. The amount of nitrogen measured is higher than for the

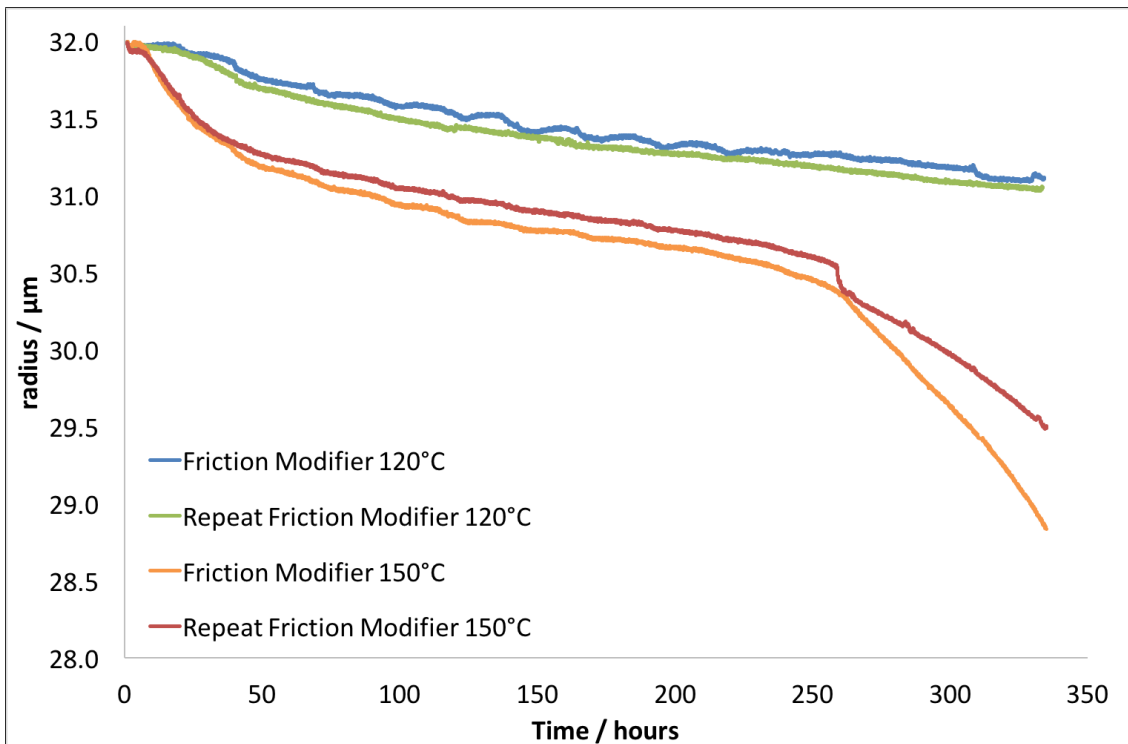


Figure 7.47: Radius change of copper wires immersed in 0.65 wt% friction modifier at 120 °C and 150 °C, with repeats

Table 7.11: Images of end of test copper coupons after immersion in friction modifier at 120 °C and 150 °C, with repeats. All coupons were the same height and approximately 1.5 cm in width

	120 °C	150 °C
Original	 3a	 4c
Repeat	 4a	 4c

samples tested in base oil indicating that the friction modifier molecule interacts with the copper surface, forming a film. The increase in oxygen could also be attributed to this interaction.

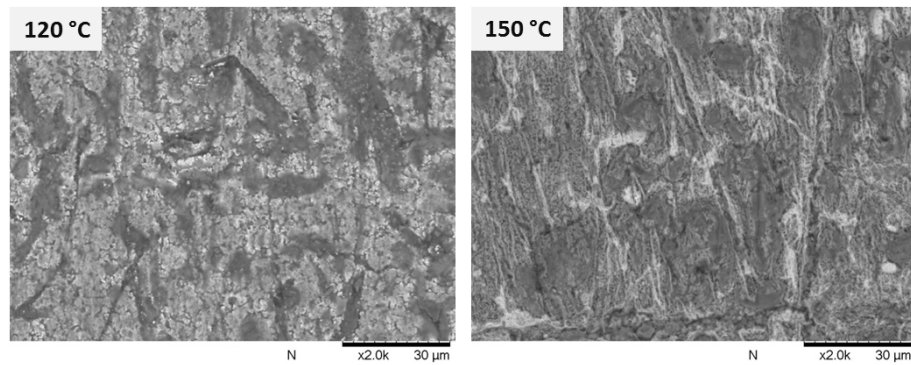


Figure 7.48: End of test BSE images of coupon surface after immersion in friction modifier at various temperatures

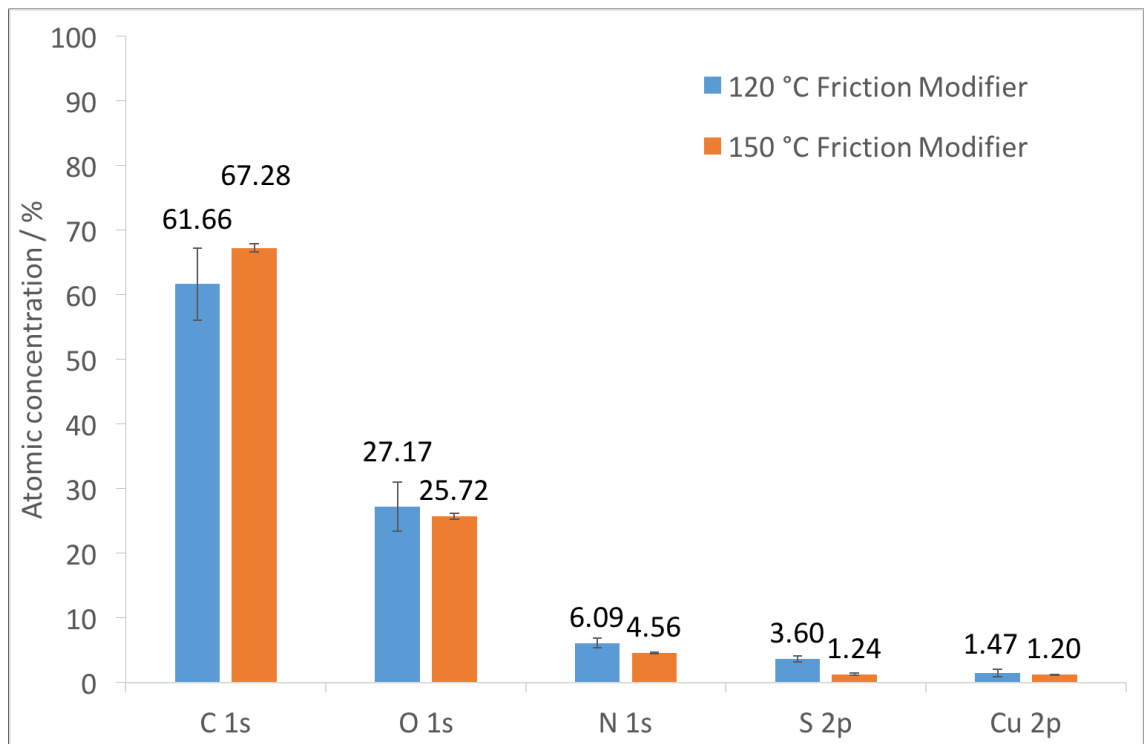


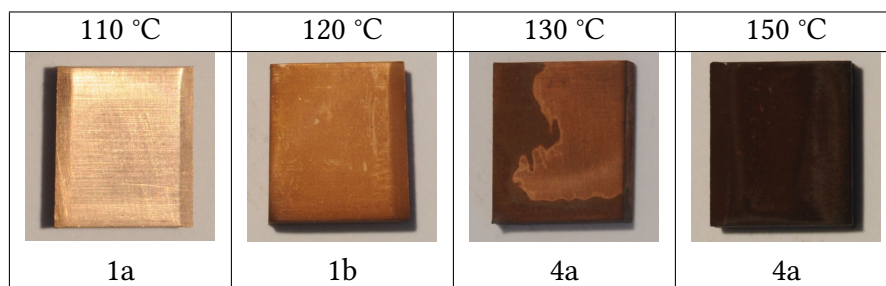
Figure 7.49: Atomic concentration of C, O, N, S and Cu on sample surface tested in friction modifier at 120 °C and 150 °C determined by XPS

7.12 Corrosion inhibitor 2 + Antiwear (AW)

Due to uncertainties about the solubility of corrosion inhibitor 2, a mixture was made which included the antiwear additive. Images of the coupon surfaces at the end of test can be seen in Table 7.12. There is a very significant worsening of the rating with increasing temperature. This is very interesting given that corrosion inhibitor 2 alone gave very good ratings at all temperatures.

Looking at the SEM images of the surfaces (Figure 7.50) from 120 °C upwards there is clear film formation, comprised of small particles that agglomerate together. As the

Table 7.12: Images of end of test copper coupons after immersion in a mixture of corrosion inhibitor 2 with antiwear at 110 °C, 120 °C, 130 °C and 150 °C. All coupons were the same height and approximately 1.5 cm in width



temperature increases the thicker the film appears to become with greater particle agglomeration.

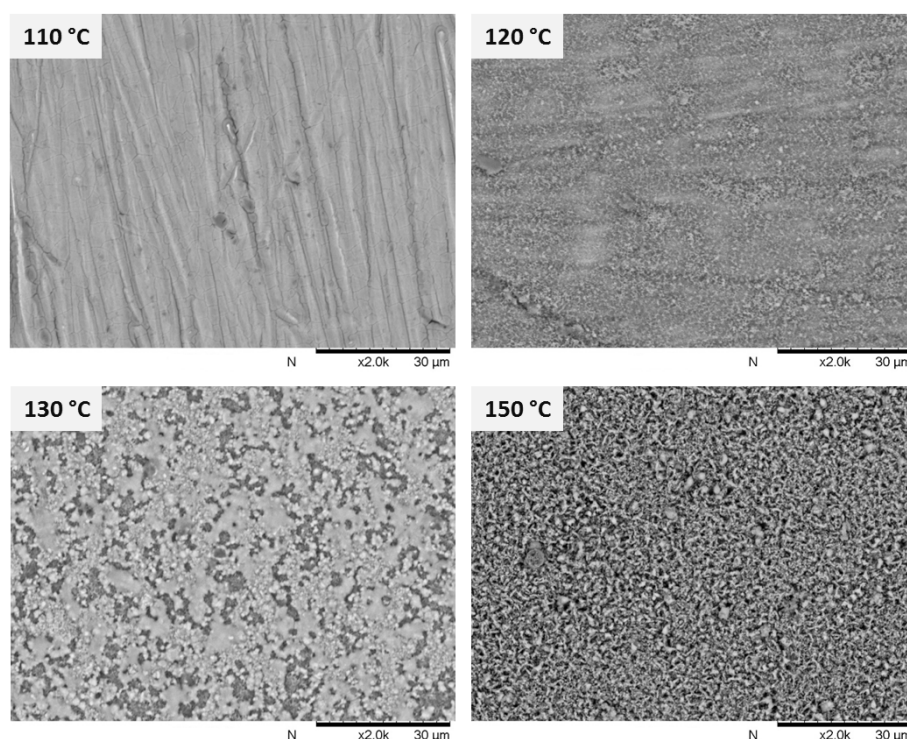


Figure 7.50: End of test BSE images of coupon surface after immersion in a mixture of corrosion inhibitor 2 with antiwear at various temperatures

The results of the change in radius of copper wires tested in the corrosion inhibitor 2/antiwear mixture can be seen in Figure 7.51. Whilst not as good as the corrosion inhibitor alone, which showed no radius change, there is a vast improvement over the antiwear alone, in which the wire broke. The maximum changes to the radius were measured at around 0.5 µm for both 130 °C and 150 °C, which is very good, particularly as the radius change has plateaued at the end of the test so no further change is expected.

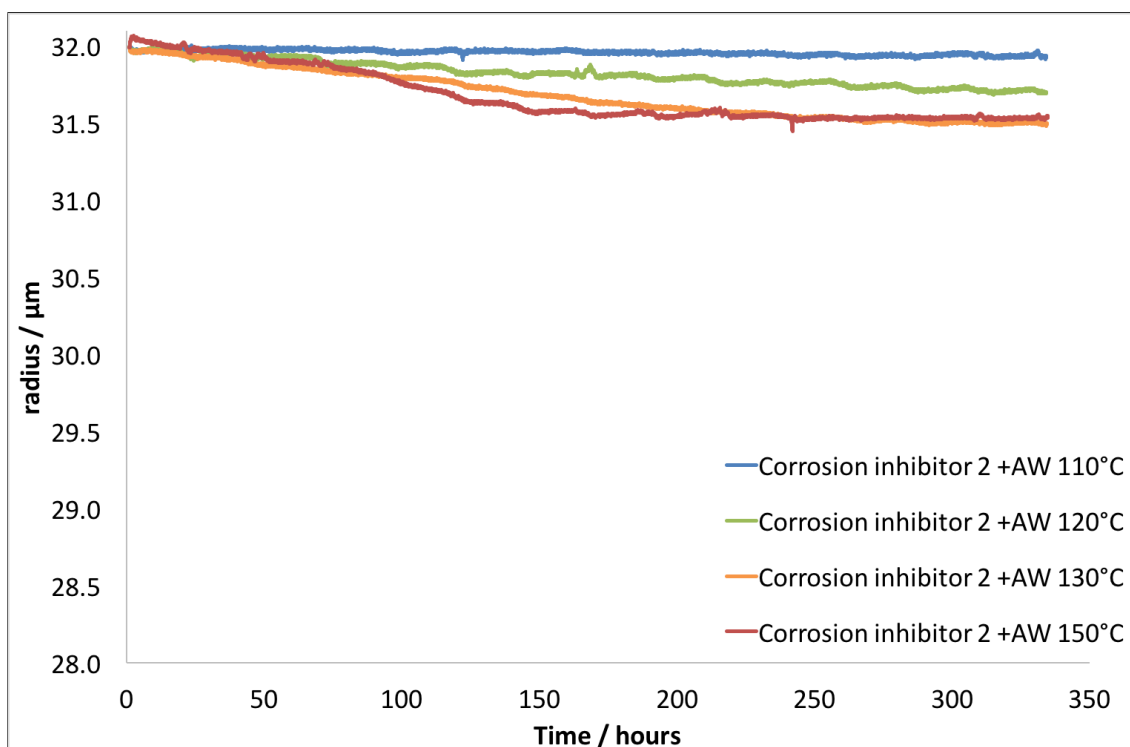


Figure 7.51: Radius change of copper wires immersed in a mixture of 0.05 wt% corrosion inhibitor 2 with 0.165 wt% antiwear at 110 °C, 120 °C, 130 °C and 150 °C

ICP-AES was used to determine the amount of copper in the end of test fluid; the results are plotted in Figure 7.52. The copper level increases slightly between 110 °C and 120 °C but then remains the same, within the margin of error, for the other temperatures. Less than 3 ppm was measured at all temperatures which indicates that little corrosion is taking place.

XPS analysis of the surface at 120 °C and 150 °C was carried out, with the results shown in Figure 7.52. At 120 °C the amount of carbon is lower than for either corrosion inhibitor 2 or the antiwear alone. The amount of oxygen is higher, this could be from greater incorporation of the antiwear into the surface film. The amount of nitrogen is slightly higher than the base oil sample and lower than the corrosion inhibitor 2 sample suggesting that the amount of corrosion inhibitor is not as great at the surface as when it is tested alone.

At 150 °C the values are mainly between the values obtained by each of the additives alone.

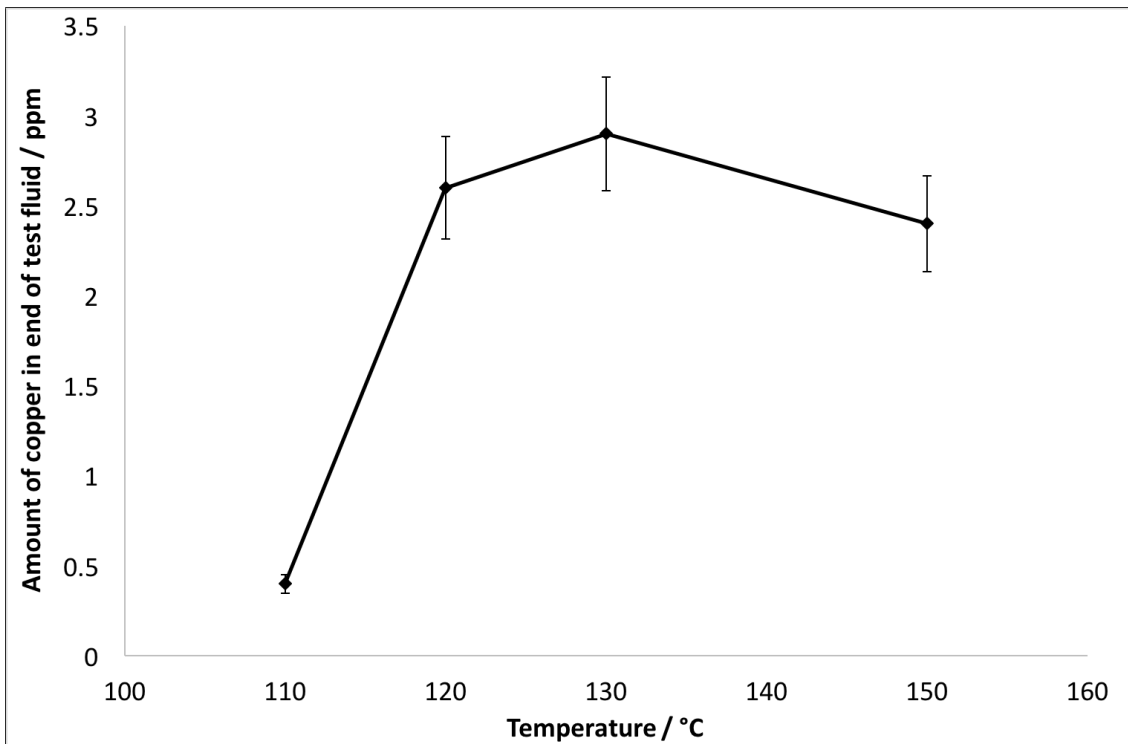


Figure 7.52: The amount of copper in the end of test fluid as determined using ICP-AES for corrosion inhibitor 2 with antiwear

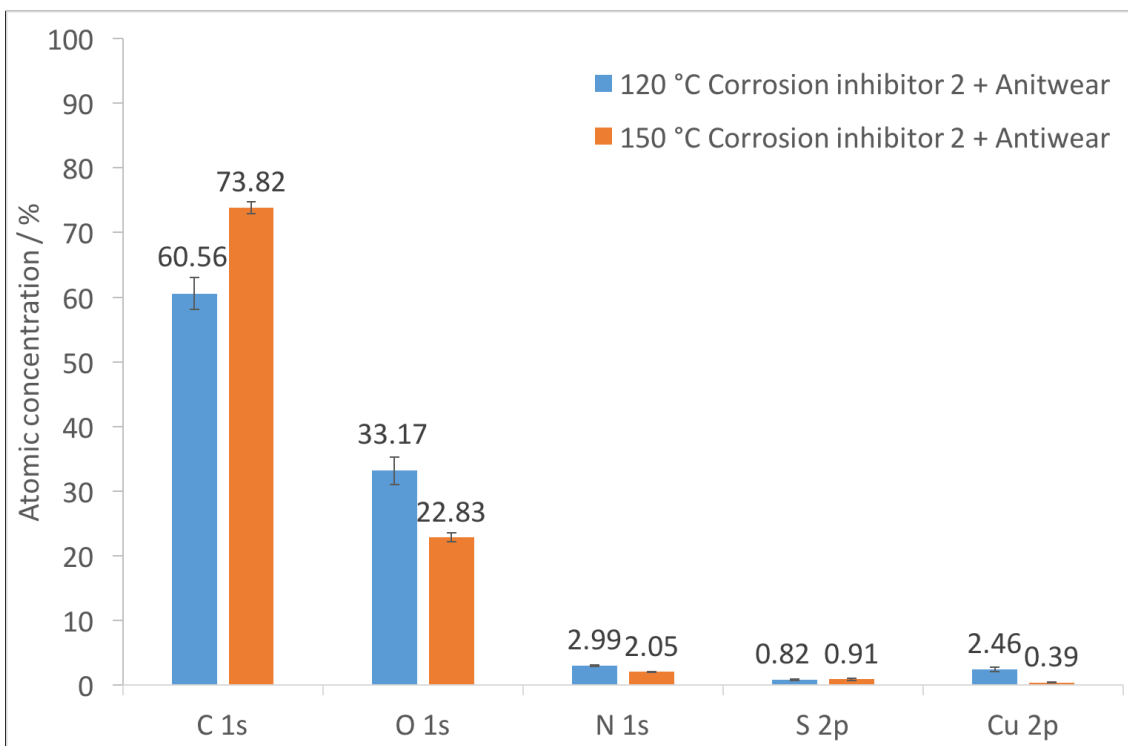


Figure 7.53: Atomic concentration of C, O, N, S and Cu on sample surface tested in corrosion inhibitor 2 and antiwear at 120 °C and 150 °C determined by XPS

7.13 Summary

- Testing the additives individually has given very useful data. It has been possible to see which additives cause corrosion to copper. The severity of this corrosion is

able to be quantified both by the loss of radius of the copper wire and the amount of copper measured in the end of test fluid.

- SEM images of the wires and coupons show the surfaces to be the same. Corrosion was also seen to be uniform along the length of the wire, with the exception of tests conducted at 150 °C in corrosion inhibitor 1 where pitting was observed to break through the wire at several locations.
- Temperature was found to play a significant role in the interaction of corrosion inhibitor 1 with copper. At 150 °C severe corrosion caused the wires to break. This is believed to be caused by the breakdown of the inhibitor to corrosive sulfur species which then causes pitting of the copper.
- Increasing temperature did not simply speed up the corrosion process, in some cases it caused more severe corrosion. Incidentally in the case of the antioxidant, antiwear, friction modifier mix it was found that increasing the temperature improved the corrosion.
- XPS analysis on the copper surfaces gave an indication as to whether the additive was adhering to the surface, as in the case of the corrosion inhibitors, or interacting with it in another way.

8: Comparisons of additive mixtures to their component additives

Seeing how each additive interacts with the surface on its own is useful for determining individual mechanisms of interaction. Additives are, however, seldom present on their own, instead being part of an additive package. As determining many interactions is difficult, knowing how two different additives may interact is the next logical step. Every additive has been combined with every other additive, with the exception of the antioxidant, antiwear and friction modifier which were used together as the mixture that had been previously tested. Although this adds additional complexity as four additives are essentially involved in this particular combination it did give a good idea as to whether addition of other additives made this interaction any better or worse.

8.1 Change in rating

In order to see what effect combining additives has on rating, Table 8.1 shows the ratings and images of each coupon tested in the individual additives and their combinations at 120 °C, whilst Table 8.2 shows the coupon images after testing at 150 °C. Each table has the data duplicated so can be read across or down, meaning that each combination is shown twice. Squares shaded dark grey show the individual additives. Yellow shading indicates synergies, whilst red squares indicate antagonisms. A synergy was defined as the coupon in the additive combination having a better rating than either of the additives tested individually.

In order to more easily compare synergies and antagonisms at both 120 °C and 150 °C the combinations which showed them are recorded below.

Five synergies were seen at 120 °C:

- Corrosion inhibitor 1 and dispersant 1
- Corrosion inhibitor 2 and detergent 2
- Corrosion inhibitor 2 and AO, AW, FM mix
- Dispersant 1 and dispersant 2
- Dispersant 2 and AO, AW, FM mix

Two antagonisms were identified at 120 °C:

- Dispersant 1 and AO, AW, FM mix
- Detergent 2 and AO, AW, FM mix

Five synergies were seen at 150 °C:

- Corrosion inhibitor 2 and detergent 1
- Dispersant 1 and dispersant 2
- Dispersant 1 and detergent 1
- Dispersant 1 and detergent 2
- Detergent 1 and detergent 2

Two antagonisms were identified at 150 °C:

- Corrosion inhibitor 2 and AO, AW, FM mix
- Dispersant 2 and detergent 2

Interestingly synergies and antagonisms seen at 120 °C are not the same as those seen at 150 °C.

Dispersant 1 and dispersant 2 was the only combination that showed a synergy in the rating at both 120 °C and 150 °C.

Table 8.1: Images of samples and their ratings for both individual and combined additives tested at 120 °C

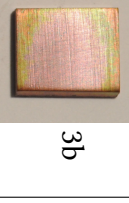
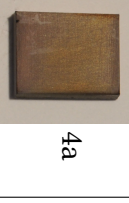
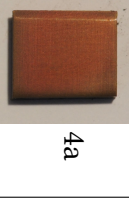
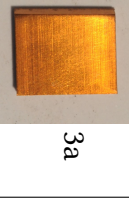
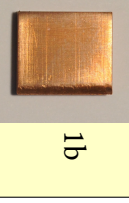
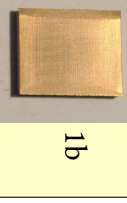
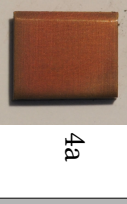
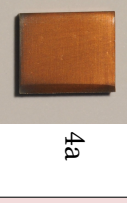
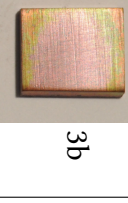
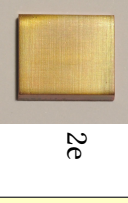
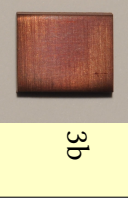
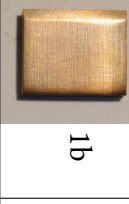
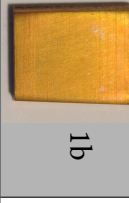
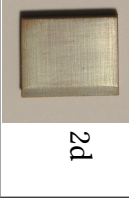
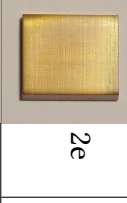
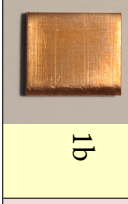
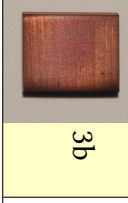
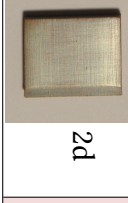
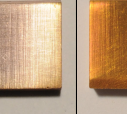
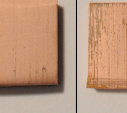
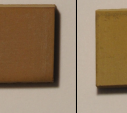
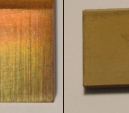
120 °C	Corrosion inhibitor 1	Corrosion inhibitor 2	Dispersant 1	Dispersant 2	Detergent 1	Detergent 2	AO, AW, FM mix
Corrosion inhibitor 1	 3b	 3b	 1b	 3b	 3a	 3a	 4a
Corrosion inhibitor 2	 3b	 3a	 4a	 3a	 1b	 2d	 1b
Dispersant 1	 1b	 4a	 4a	 2b	 2a	 4a	 4b
Dispersant 2	 3b	 3a	 2b	 4b	 2d	 2e	 3b
Detergent 1	 3a	 1b	 2a	 2d	 1b	 2b	 2d
Detergent 2	 3a	 2d	 4a	 2e	 2b	 2e	 4c
AO, AW, FM mix	 4a	 1b	 4b	 3b	 2d	 4c	 4a

Table 8.2: Images of samples and their ratings for both individual and combined additives tested at 150 °C

150 °C	Corrosion inhibitor 1	Corrosion inhibitor 2	Dispersant 1	Dispersant 2	Detergent 1	Detergent 2	AO, AW, FM mix
Corrosion inhibitor 1	 4c	 4a	 3b	 4b	 4c	 4a	 4c
Corrosion inhibitor 2	 4a	 3a	 3b	 3b	 1b	 3a	 4a
Dispersant 1	 3b	 3b	 4c	 2e	 1b	 1b	 4c
Dispersant 2	 4b	 3b	 2e	 4a	 2d	 4c	 4a
Detergent 1	 4c	 1b	 1b	 2d	 2d	 1b	 2e
Detergent 2	 4a	 3a	 1b	 4c	 1b	 3a	 2e
AO, AW, FM mix	 4c	 4a	 4c	 4a	 2e	 2e	 2e

As with the ratings it is interesting to see that the synergies and antagonisms seen are not the same at both temperatures. A number of the synergies show only very small improvements over the individual additive levels and would not be considered to be true synergies, although they have been highlighted as such. An example of this would be at 150 °C corrosion inhibitor 1 has a copper level of 1.7 ppm, detergent 2 a level of 1.8 ppm and combined the copper level is 1.6 ppm the error for each of these values is ± 0.2 ; calculated using $0.12x^{0.91}$ explained in the methodology, Section 4.5.1. Incorporating this error the values would all be considered to be the same.

The antagonisms on the other hand are often extreme with the combined levels significantly higher than either of the individuals. This is a little easier to see with a visual representation of the data. In Figure 8.1 and Figure 8.2 the copper levels of the individual and combined additive mixtures have been plotted showing synergies and antagonisms respectively. For clarity only the combination (green) has been labelled but the first listed additive is ‘additive 1 alone’ (blue) and the second additive listed is ‘additive 2 alone’ (red).

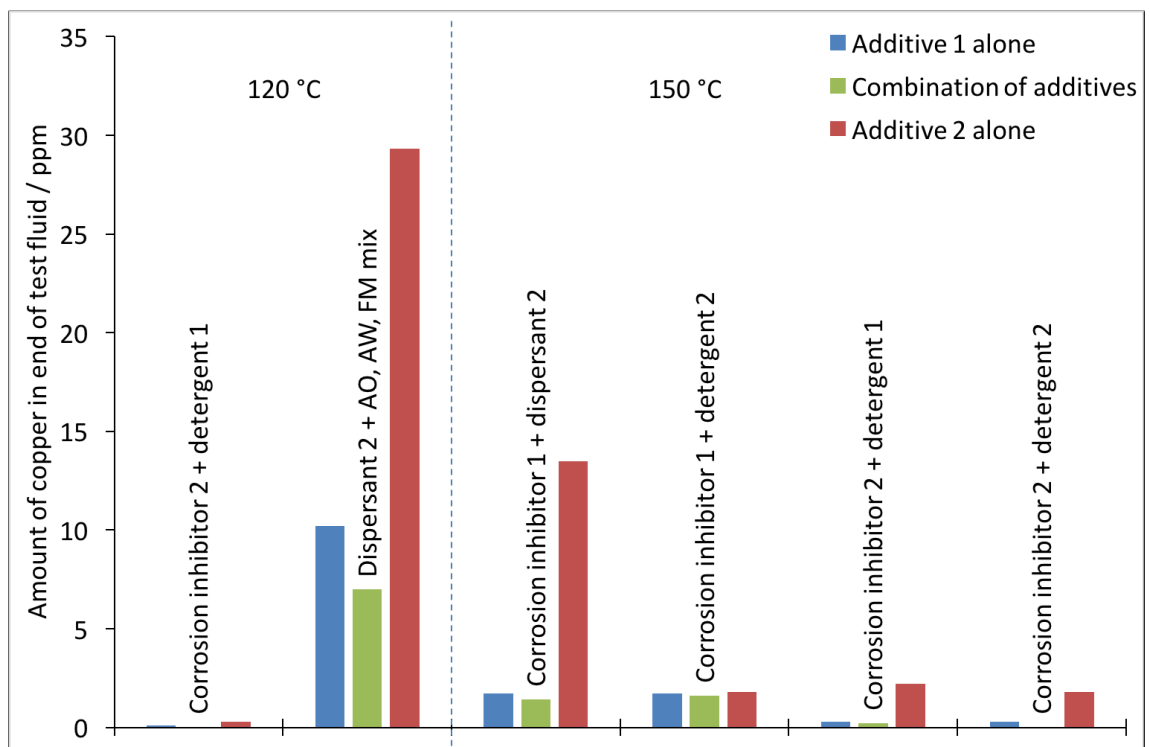


Figure 8.1: Amount of copper in the end of test fluid for combinations which showed synergies

Figure 8.1 shows the amount of copper in the end of test fluids for additive combinations which showed synergies, alongside their individual component additives. Dispersant 2 + AO, AW, FM mix at 120 °C shows a clear decrease in the copper level for the combination. For all of the others the combination gives only a very small decrease compared to at least one of the other additives.

Figure 8.2 shows the antagonistic combinations. The antagonisms are very obvious, with the exception of corrosion inhibitor 1 + detergent 1 at 150 °C which showed only a small increase in copper level compared to its individual component additives.

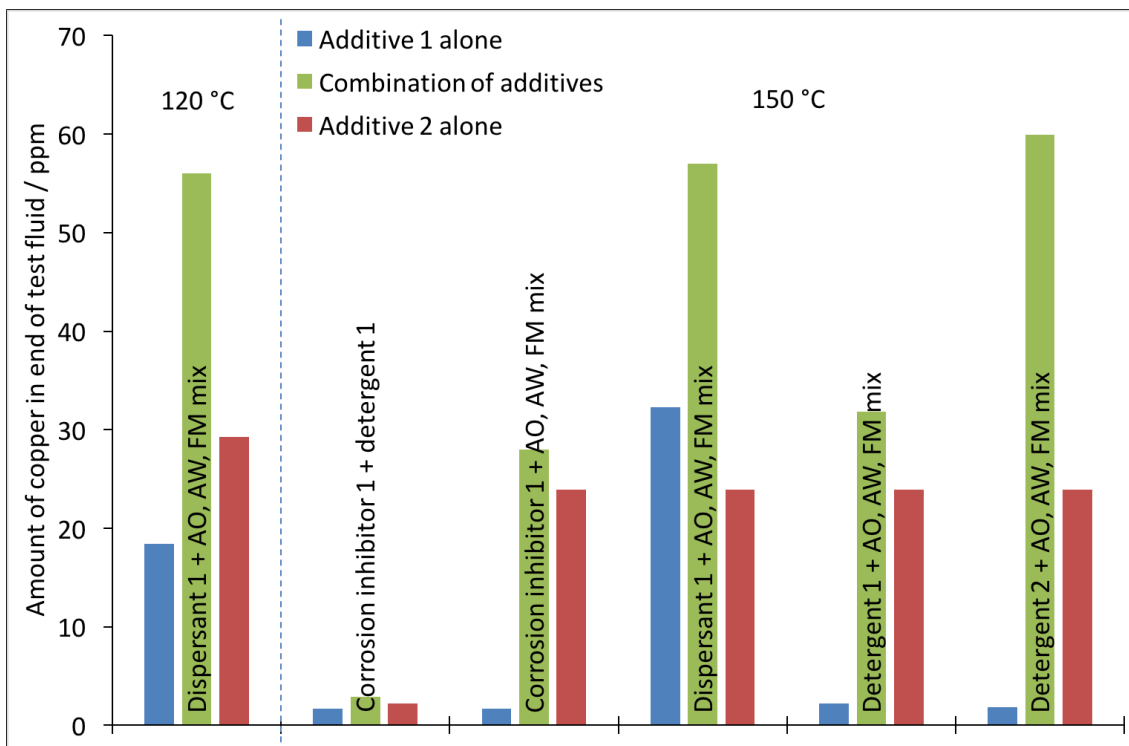


Figure 8.2: Amount of copper in the end of test fluid for combinations which showed antagonisms

As well as the synergies and antagonisms it was found that certain combinations had a dramatic effect on one or other of the additives. For example at 150 °C the addition of corrosion inhibitor 1 to dispersant 1 and dispersant 2 dramatically decreased the amount of copper seen in the end of test fluid compared to the dispersants tested alone.

At 120 °C the copper level for all additives tested in combination with corrosion inhibitor 2 decreased in relation to the other additive alone; this was most noticeable for combinations with dispersant 2 and the AO, AW, FM mix. This decrease was not as great at 150 °C, although there was a big improvement for the combination of corrosion

inhibitor 2 with AO, AW, FM mix and also with dispersant 1 when compared to levels of those additives tested alone.

At 120 °C the amount of copper in the end of test fluid when dispersant 1 was tested alone was 18.4 ppm. Combined with almost all other additives this level dropped. The exception was when combined with the AO, AW, FM mix where the copper level was significantly higher than either additive tested alone. This antagonism can be seen in Figure 8.2. The same trend is found when the combinations were tested at 150 °C with an antagonism seen for the AO, AW, FM mix.

When detergent 1 was combined with the AO, AW, FM mix there was a significant improvement in the level of copper compared to the AO, AW, FM mix alone. Small improvements were generally otherwise made when detergent 1 was combined with other additives at 120 °C.

The AO, AW, FM mix gave high levels of copper in the end of test fluid when tested alone at 120 °C. The addition of any of the additives to the AO, AW, FM mix, with the exception of dispersant 1, showed a reduction in the amount of copper measured in the end of test fluid, compared to the AO, AW, FM mix tested alone, particularly for combinations with corrosion inhibitor 1 and also dispersant 2 where synergies are seen. At 150 °C four antagonisms were identified when the AO, AW, FM mix was combined with either corrosion inhibitor 1, dispersant 1, detergent 1 or detergent 2, as already shown in Figure 8.2.

It is interesting to note that the synergies and antagonisms seen in the ratings are not always the same as those seen with the copper levels. Table 8.5 shows the results for the 120 °C tests in the upper right hand half of the table, whilst the 150 °C results are in the lower left hand half, the diagonal line running through the table separates the 120 °C and 150 °C results. Rating results are indicated with a + or – and the copper level results are shown with shaded squares.

At 120 °C the rating and copper levels for dispersant 1 with the AO, AW, FM mix both show an antagonism, whilst the dispersant 2 with AO, AW, FM mix shows a synergy in both. Other synergies that were seen in the rating were not seen in the copper level results.

Table 8.5: Synergies (+/yellow) and antagonisms (-/red) seen for rating (+/-) and copper levels (colour)

120 °C \ 150 °C	Corrosion inhibitor 1	Corrosion inhibitor 2	Dispersant 1	Dispersant 2	Detergent 1	Detergent 2	AO, AW, FM mix
Corrosion inhibitor 1			+				
Corrosion inhibitor 2						+	+
Dispersant 1				+			-
Dispersant 2			+				+
Detergent 1		+	+				
Detergent 2			+	-	+		-
AO, AW, FM mix		-					

The 150 °C results match even less with only two combinations showing synergies in both sets of results; corrosion inhibitor 2 with detergent 1 and also detergent 1 with detergent 2.

This lack of correlation between the copper level and the rating suggests that the rating is not such a good indicator of corrosion.

8.3 Radius change of copper wires tested in solutions of additive combinations

The radius change of copper wires tested in additive combinations were compared to the radius changes for each of the individual additives it was comprised of. In some instances synergies were seen whilst in other antagonisms were identified. In most cases the radius change of the combination was somewhere between that of the two individual additives. All of the results are shown in Appendix A. Table 8.6 indicates which samples showed synergies and antagonisms at 120 °C and 150 °C. Interestingly only corrosion

inhibitor 1 with dispersant 2 showed a synergy at both 120 °C and 150 °C. Other synergies or antagonisms were only identified at one temperature. This would suggest that there is a difference in the mechanism at each temperature for the combinations where these were identified.

Table 8.6: Radius change (μm) for the additive combinations with synergies (yellow shading) and antagonisms (red shading) identified from radius change results

	120 °C						
150 °C	Corrosion inhibitor 1	Corrosion inhibitor 2	Dispersant 1	Dispersant 2	Detergent 1	Detergent 2	AO, AW, FM mix
Corrosion inhibitor 1	0.21 broken	0.21	0.20	0.13	0.25	0.13	2.68
Corrosion inhibitor 2	0.34	0	0.45	0.02	0.05	0	0.05
Dispersant 1	0.92	1.45	1.14 2.31	1.85	0.65	0.34	8.91
Dispersant 2	0.48	0.45	1.35	0.68 0.85	0.60	0.09	0.73
Detergent 1	0.98	0.07	0.44	0.41	0.13 0.55	0.12	1.00
Detergent 2	0.31	0.03	0.05	1.29	0.25	0.11 0.23	1.28
AO, AW, FM mix	2.01	0.94	0.02	1.52	2.27	6.76	2.93 1.92

An example of an additive combination which showed a synergy was dispersant 2 with detergent 1 at 150 °C, shown in Figure 8.3. In this instance the synergy was only small and followed a similar trace to detergent 1 alone. In this particular case the synergy is actually seen across the entire test period with the combination having a smaller radius change than either of the additives individually.

Figure 8.4 shows an example of one of the antagonisms identified, where dispersant 1 and the AO, AW, FM mix were combined. In the first 50 hours of the test the combined fluid gives a radius change between those of the individual additives after which there is an increase in the rate and the radius of the wire tested in the combination is considerably worse than either of the additives tested alone.

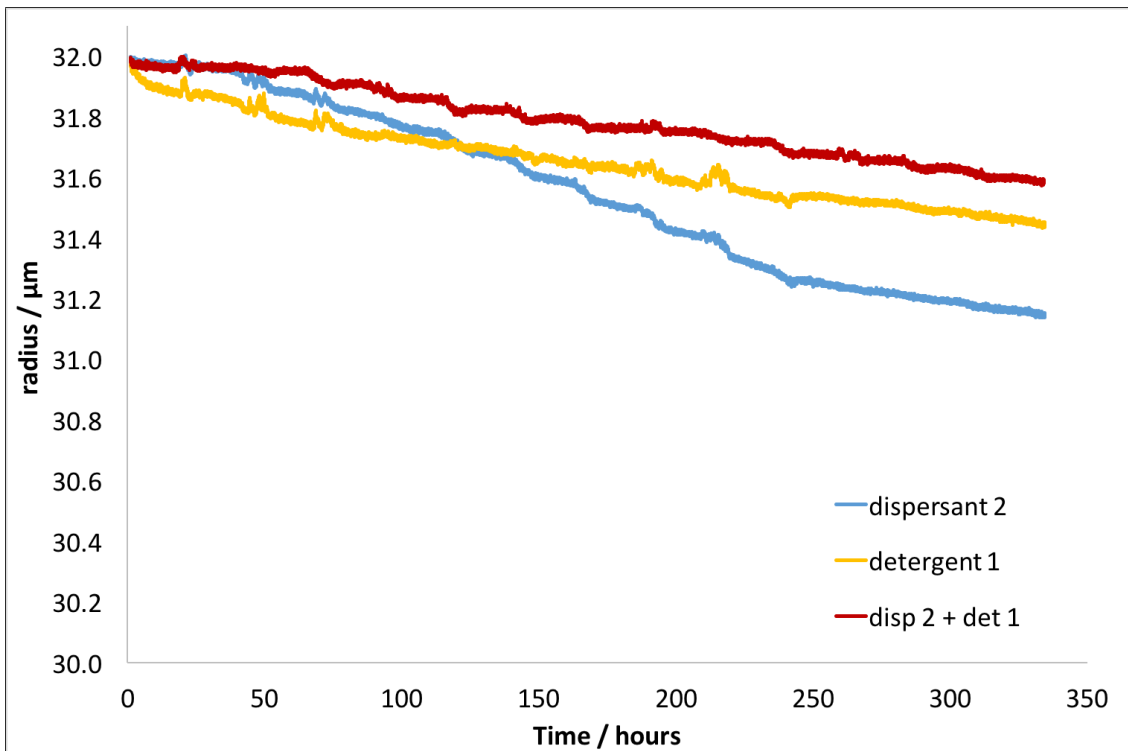


Figure 8.3: Radius changes for dispersant 2 and detergent 1, individually and combined at $150\text{ }^{\circ}\text{C}$

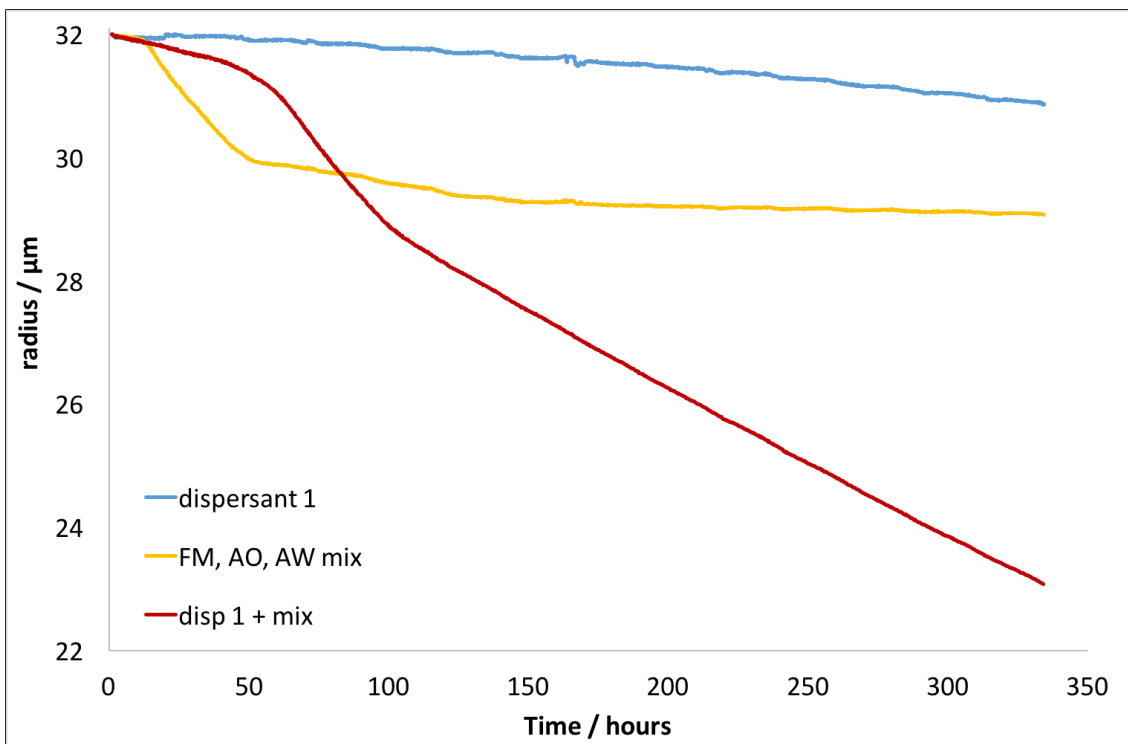


Figure 8.4: Radius changes for dispersant 1 and the AO, AW, FM mix, individually and combined at $120\text{ }^{\circ}\text{C}$

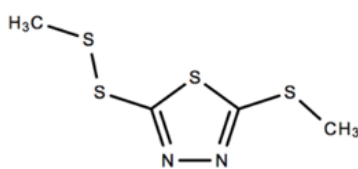
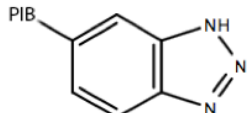
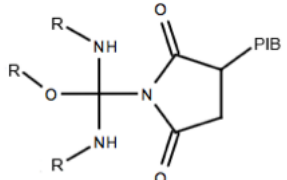
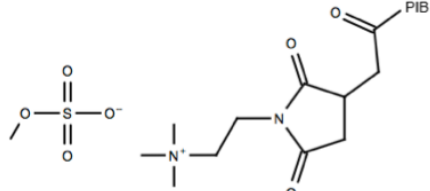
8.4 XPS and SEM results for selected combinations

The wire tests allow us to monitor the reaction between ATF additives and copper in situ, but they are difficult to analyse which is why copper coupons were incorporated into

the tests. SEM allows a visual inspection of the surface but provides no compositional information. A greater understanding of the chemistry of the surface obtained through XPS analysis would be beneficial, but due to the volume of samples it was not possible to test them all.

XPS analysis was conducted on the coupon samples which had been immersed in all combinations of corrosion inhibitor 1, corrosion inhibitor 2, dispersant 1 and dispersant 2. The coupons used were those created during the wire-square tests which ran for around 330 hours at 120 °C and 150 °C. As a reminder the structure of the additives and their concentrations which were used for testing are listed in Table 8.7.

Table 8.7: Concentration and structure of additives used for tests after which coupons were analysed using XPS

Additive	Description	Concentration / wt%
Corrosion inhibitor 1		0.5
Corrosion inhibitor 2		0.05
Dispersant 1		5
Dispersant 2		5

High resolution scans for carbon, nitrogen, oxygen, sulfur and copper have been analysed and are compared for all the individual and combined additives. In the case of sulfur and copper where $2p_{3/2}$ and $2p_{1/2}$ peaks are close, the fitting for both peaks is shown on any graphs but only the $2p_{3/2}$ peaks are listed in tables as these have been used for species identification. Although analysed the XPS carbon spectra are not presented

as there was little variation between them and not a great deal of information could be obtained from them particularly as peaks denoting C–N, C–S and C–O overlap. Similarly the oxygen spectra are not shown as they showed little variation, however the data obtained from these spectra are shown in the tables with the other peak assignments.

High resolution spectra for samples tested at 120 °C are shown in Figures 8.5–8.7, while Figure 8.9–8.11 show the spectra for samples run at 150 °C. All analysis was carried out on the coupon surfaces at the end of test.

8.5 XPS and SEM results for 120 °C samples

Figure 8.5 shows the copper spectra for all samples tested at 120 °C, individual and combined. If we look at all of the samples containing corrosion inhibitor 1 and compare them to corrosion inhibitor 1 alone there are some very interesting differences.

The sample tested in corrosion inhibitor 1 alone shows three main peaks, 932–936 eV, and a satellite feature, around 943 eV. The satellite feature suggests that the copper is in a partial Cu(II) state; as the feature is weak and would be more noticeable if the copper were fully in a Cu(II) state. When corrosion inhibitor 1 is combined with another additive there is a change in the copper XPS spectrum. When combined with corrosion inhibitor 2, there is a change in the intensity of the peaks but otherwise the peaks are the same. The satellite feature remains indicating there is no change in the state of the copper.

When combined with dispersant 1 the overall shape of the peak changes and when fitted slightly different peak positions are seen. Most noticeably when corrosion inhibitor 1 is tested alone a peak corresponding to CuSO₄ is present at 936 eV. When dispersant 1 is also present this peak is replaced with a peak at 933 eV which corresponds to CuO. The satellite feature seen with corrosion inhibitor 1 alone is still present and so the copper is in a Cu(II) state.

Combining corrosion inhibitor 1 with dispersant 2 shows a significant change in the spectrum with only one main peak discernible. There is a loss of the satellite feature at 943 eV meaning that the copper is no longer in a Cu(II) state and so is either in a Cu(0) or Cu(I) state, or a combination of the two.

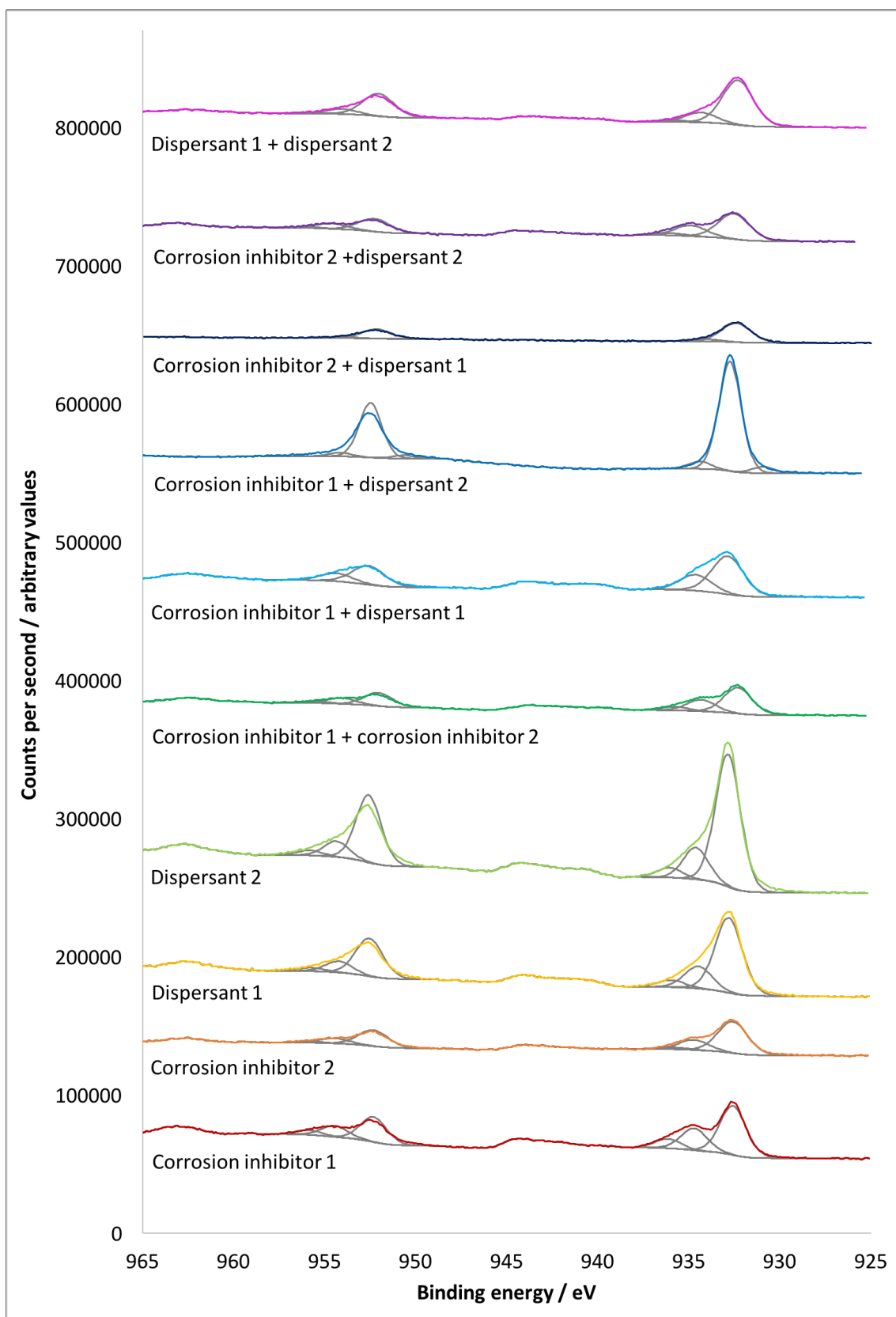


Figure 8.5: High resolution XPS copper scans for samples run at 120 °C containing corrosion inhibitor 1, corrosion inhibitor 2, dispersant 1, and dispersant 2

Corrosion inhibitor 2 tested alone has two main peaks, around 932.5 eV and 935 eV, with a weak satellite feature around 945 eV. The satellite feature indicates the presence

of Cu(II) which would correspond to either CuO or Cu(OH)₂ at 935 eV, while the peak at 932.5 eV indicates the presence of Cu(I) such as Cu₂O [146]. However corrosion inhibitor 2 is a benzotriazole based molecule which in literature is reported to form a complex with copper, such that the copper is in a Cu(I) state. The peak at 932.5 eV may therefore indicate the presence of Cu(I)–BTA bonding as reported by Chadwick and Hashemi [105].

These peaks are also present in the spectra showing the surface tested in a combination of corrosion inhibitor 2 and dispersant 2. There is a slight difference in the spectrum for the combination with corrosion inhibitor 1 as a small sulfate peak is also present at 935.5 eV.

When dispersant 1 is combined with corrosion inhibitor 2 the satellite feature around 945 eV disappears suggesting a loss of Cu(II) this is also shown by the loss of the peak at 935 eV, the remaining peak indicates that Cu(I)–BTA or Cu₂O is the main species.

Dispersant 1 tested alone shows three main peaks in the copper spectrum at 933 eV, 934 eV and 935.5 eV, these most likely correspond to Cu₂O, CuO and CuSO₄ respectively. The satellite feature at 943 eV show that the copper has a significant Cu(II) state. The same peaks are present on the sample tested with a combination of dispersant 1 and dispersant 2 as well as the combination with corrosion inhibitor 1, although with corrosion inhibitor 1 the intensity of the 933 eV peak is less than dispersant 1 alone.

There is a difference seen in the spectrum of dispersant 1 and corrosion inhibitor 2 as only one peak is present and no satellite feature is seen. The lack of satellite feature shows that the state of the copper has changed from being significantly Cu(II), with dispersant 1 alone, to being primarily Cu(I) with the addition of corrosion inhibitor 2.

Tested alone dispersant 2 shows three peaks at 933 eV, 934.5 eV and 936 eV as well as a satellite feature around 943 eV. This satellite feature indicates the copper is in a Cu(II) state and the peak positions indicate the presence of CuSO₄ and CuO or Cu(OH)₂, with the main peak at 933 eV indicating the presence of Cu₂O. These same peaks are present in the combination with dispersant 1. With corrosion inhibitor 2 two of the peaks are present, indicating Cu₂O and CuSO₄ so the copper still has a Cu(II) state.

Dispersant 2 in combination with corrosion inhibitor 1 has no satellite feature so

the copper is primarily in a Cu(I) state, with the peak assigned to Cu_2O , or Cu_2S after consideration of the sulfur spectrum.

All of the peak assignments can be found in Table 8.8.

Figure 8.6 shows all nitrogen high resolution spectral scans for the samples tested at 120 °C. It is difficult to assign the peaks in the nitrogen spectra, however it is easy to see that there are differences. Corrosion inhibitor 1 alone and in combination with corrosion inhibitor 2 show almost identical spectra with two peaks at 399.7 eV and 401.5 eV.

When corrosion inhibitor 1 is combined with dispersant 2 the peak around 399 eV is larger whilst the other decreases in magnitude. As these peaks cannot be definitively assigned it is difficult to say why these differences appear. It is interesting that when combined with dispersant 1 the nitrogen peaks are negligible. Dispersant 1 contains a large amount of nitrogen incorporated into long side chains. If it were to interact with the surface you would expect prominent nitrogen peaks, as none are seen then it can be concluded that dispersant 1, in combination with corrosion inhibitor 1, does not attach itself to the copper surface.

Corrosion inhibitor 2 tested alone is very similar to corrosion inhibitor 1 tested alone, with peaks at 399.9 eV and 401.5 eV, and so it is unsurprising that combining them gives a very similar spectrum. When corrosion inhibitor 2 is combined with dispersant 1 or dispersant 2 the spectrum changes in relation to corrosion inhibitor 2 alone with the peak at 401.5 becoming smaller and in the case of dispersant 1 disappearing altogether.

There is a small nitrogen peak present when dispersant 1 is tested alone. This is also present when it is combined with corrosion inhibitor 2. However when dispersant 1 is combined with corrosion inhibitor 1 or dispersant 2 the nitrogen peaks in the spectra are negligible. This is similar for dispersant 2 tested alone where there is only a small peak. When combined with corrosion inhibitor 1 or 2 the peak is larger, therefore it is likely that the corrosion inhibitor is contributing to this peak, rather than dispersant 2.

The sulfur spectra also show a great number of differences for each additive combination, as seen in Figure 8.7. When corrosion inhibitor 1 is tested alone the main peaks present are at 168 eV. This is likely to be CuSO_4 , a peak in the copper spectra at around 936 eV is also indicative of this species and is present for both corrosion

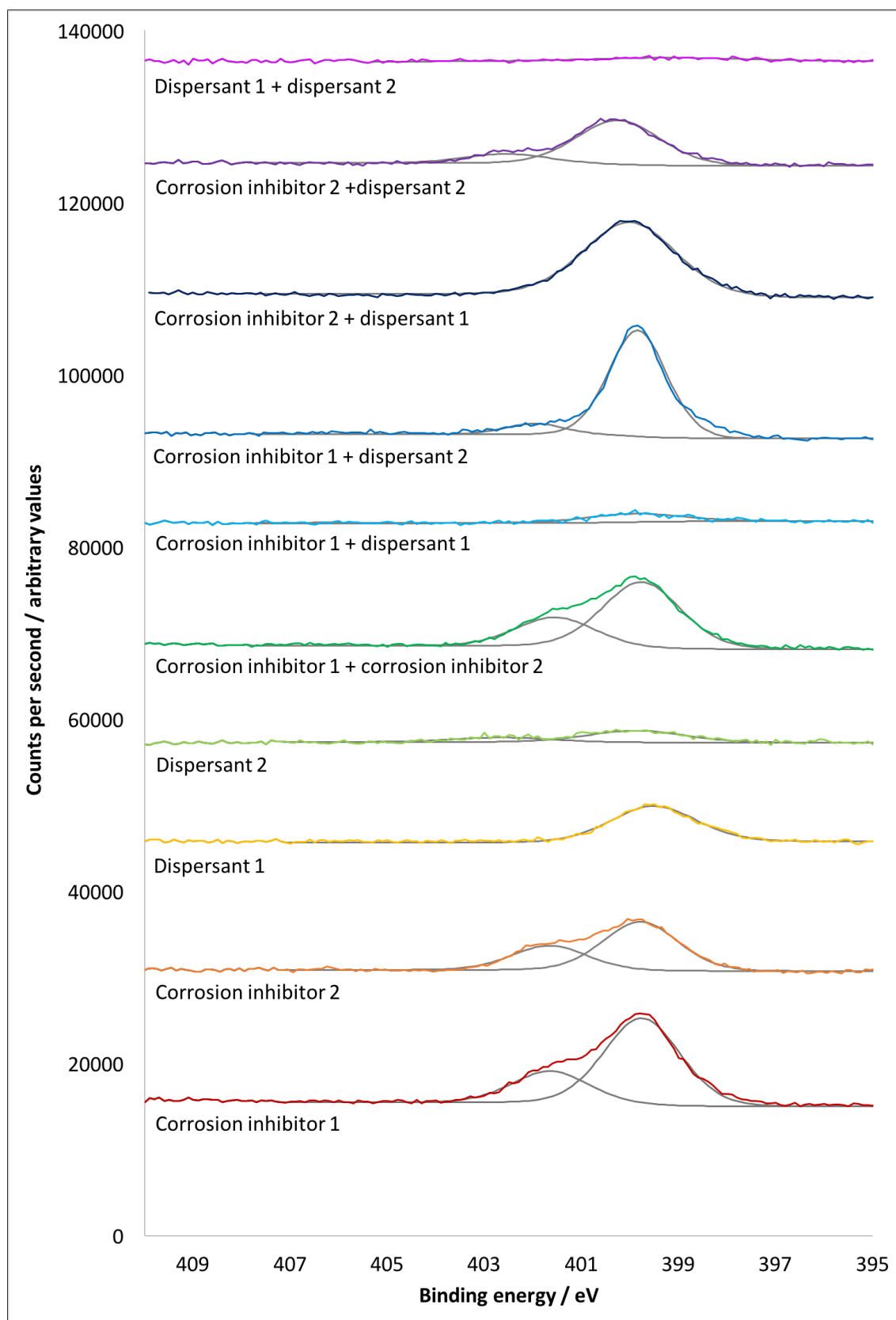


Figure 8.6: High resolution XPS nitrogen scans for samples run at 120 °C containing corrosion inhibitor 1, corrosion inhibitor 2, dispersant 1, and dispersant 2

inhibitor 1 alone and when combined with corrosion inhibitor 2. The sulfur spectra for the combination of corrosion inhibitor 1 with corrosion inhibitor 2 is very similar

to that of corrosion inhibitor 1 alone. This was also the case for the copper spectra and would suggest that when corrosion inhibitor 1 and 2 are combined corrosion inhibitor 1 interacts dominantly with the surface.

When combined with dispersant 1 no sulfur peaks are seen. However when combined with dispersant 2 the amount of CuSO_4 detected is so low as to be negligible, instead 2 other main peaks appear at around 163 eV and 164 eV; these are also present in the samples tested in corrosion inhibitor 1 alone and in combination with corrosion inhibitor 2 but are not as large. These peaks correspond to CuS and S (or thiols). The lack of CuSO_4 is very interesting as dispersant 2 has a sulfate group to balance the charge of the quaternary amine head group yet there is no sulfate peak in the spectrum. It is possible that any sulfate which is formed and would have reacted with the surface is actually kept suspended by the head group of dispersant 2.

Figure 8.7 shows negligible sulfate peaks are seen for corrosion inhibitor 2 alone and in combination with dispersant 1 and 2. When combined with corrosion inhibitor 1 however sulfate and other sulfur species are present on the surface. As corrosion inhibitor 1 contains sulfur it is unsurprising to find some on the surface, the very small sulfate peak in the dispersant 2 spectrum could be caused by surface interaction of the sulfate stabilising head group.

Samples tested in dispersant 1 or with it in the combination show almost negligible sulfur peaks and those present are likely to come from surface contamination.

The sulfur spectrum for dispersant 2 alone shows a small sulfate peak and a peak denoting CuS, which is also the case when combined with dispersant 1. When combined with corrosion inhibitor 2 however the CuS peak disappears. With corrosion inhibitor 1 however the peak for CuS increases significantly and an additional peak denoting S (or thiols) appears. All peak assignments can be found in Table 8.8.

From the 120 °C spectra presented it is possible to begin to hypothesise about the effect of combining samples.

From the spectra which show samples tested in fluids containing corrosion inhibitor 1, in each case the spectra are almost identical for corrosion inhibitor 1 alone and when in combination with corrosion inhibitor 2. This would suggest that corrosion inhibitor 1

Table 8.8: Peak positions (eV) for high resolution spectra of all samples analysed at 120 °C

Peak	Species	Corrosion inhibitor 1	Corrosion inhibitor 2	Dispersant 1	Dispersant 2	Corrosion inhibitor 1 + Corrosion inhibitor 2	Corrosion inhibitor 1 + Dispersant 1	Corrosion inhibitor 1 + Dispersant 2	Corrosion inhibitor 2 + Dispersant 1	Corrosion inhibitor 2 + Dispersant 2	Dispersant 1 + Dispersant 2
Cu 2p_{3/2}	Cu / Cu₂S / CuS / Cu₂O	932.57	932.64	932.79	932.85	932.32	932.59	932.74	932.45	932.54	932.6
	CuO			934.19			933.87				
	Cu(OH)₂	934.75	934.98		934.53	934.27	934.91			935.02	934.16
	CuSO₄	936.12		935.54	935.77	935.46					935.32
N 1s	NH₃ organic			398.45			398.94		398.63		
	C-NH₂ organic	399.78	399.87	399.63	399.89	399.73		399.85	399.91		399.67
	Organic	401.52	401.69			401.45	400.7		400.71	400.25	
	Ammonium salt				402.57			402.16		402.52	
O 1s	CuO					528.98					
	Cu₂O / CuO			530.29	530.21		530	530.61	530.79		530.12
	Cu(OH)₂ / CuCO₃	531.27	531	531.67	531.72	531.35	531.56	531.85	531.73	531.56	531.55
	CuSO₄	532.32	532.16								
	Nitrate Organic C=O	533.51	533.26	533.51	533.55	533.09	533.37	533.58			533.45
S 2p_{3/2}	Cu₂S			162.08	162.07						161.87
	CuS	162.73	162.9			162.74	162.81	162.81	162.16		
	S	164.45		167.76	167.86	164.18	164.39	164.39	167.57		
	SO₂										
	CuSO₄	168.39			168.33	168.18		167.86		168.5	168.16

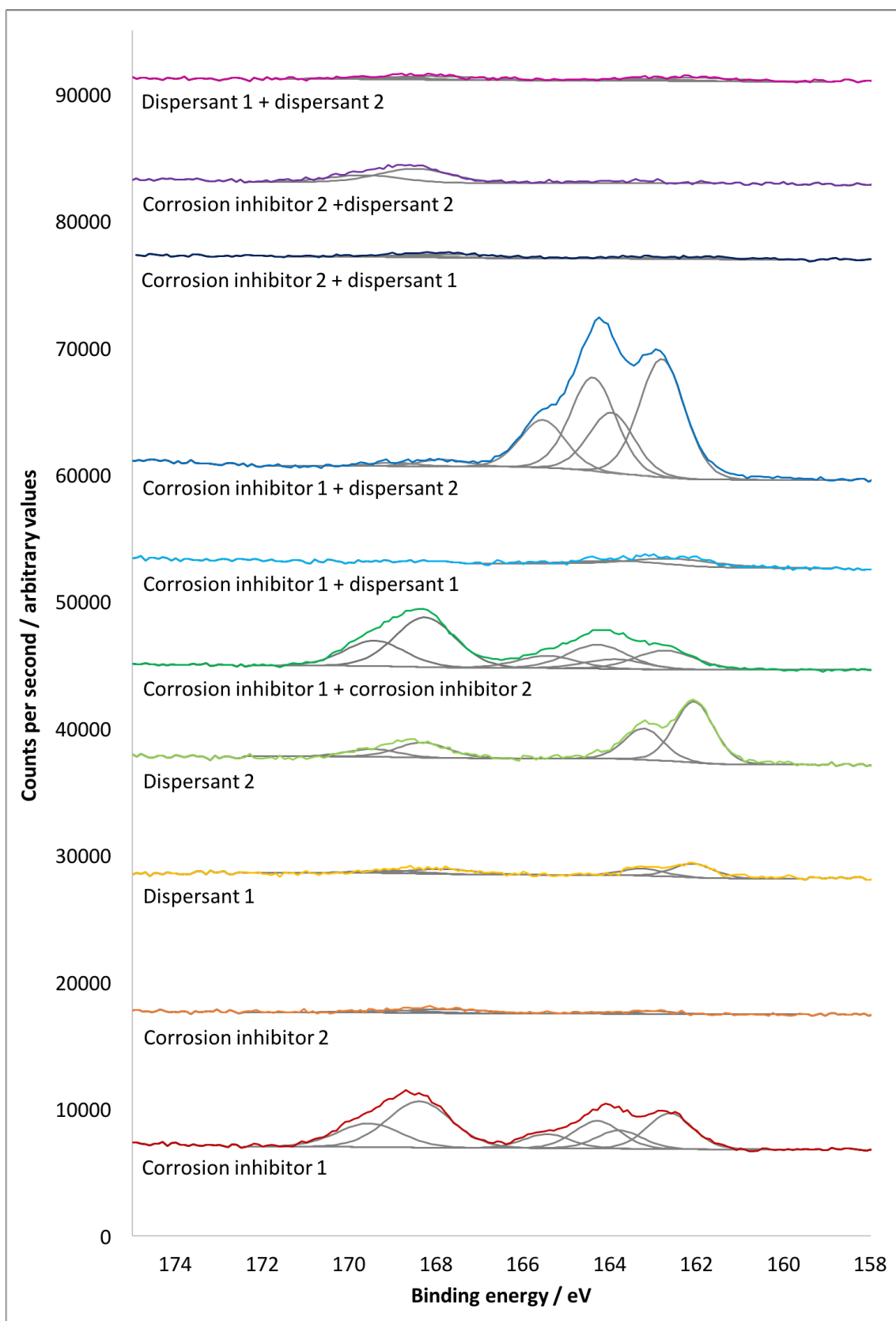
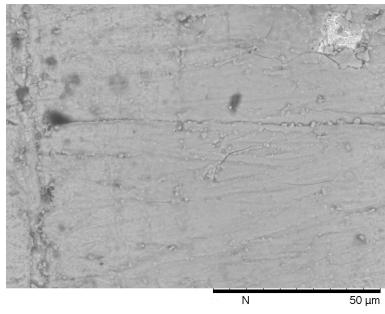
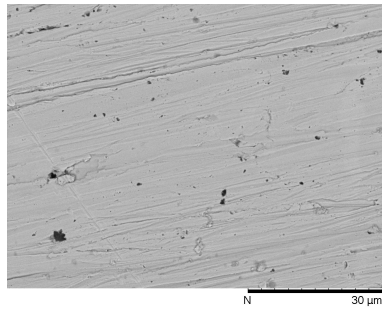


Figure 8.7: High resolution XPS sulfur scans for samples run at 120 °C containing corrosion inhibitor 1, corrosion inhibitor 2, dispersant 1, and dispersant 2

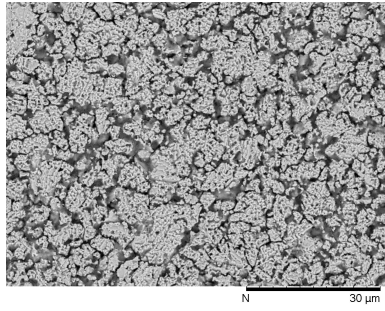
has the dominant interaction and the addition of corrosion inhibitor 2 has little impact.



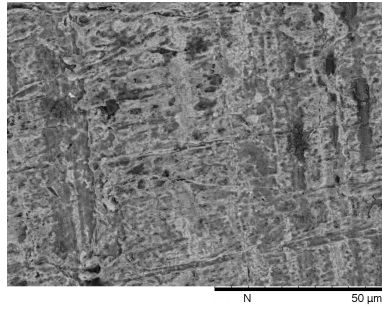
(a) Corrosion inhibitor 1



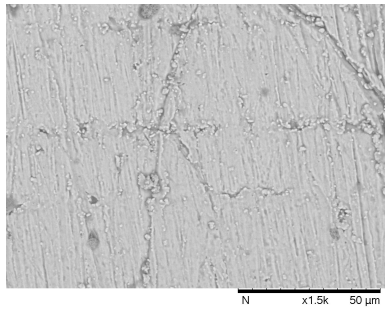
(b) Corrosion inhibitor 2



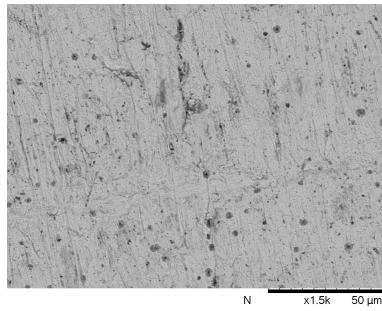
(c) Dispersant 1



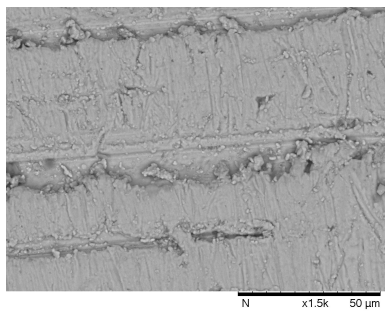
(d) Dispersant 2



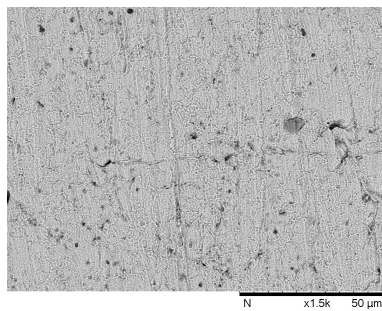
(e) Corrosion inhibitor 1 + corrosion inhibitor 2



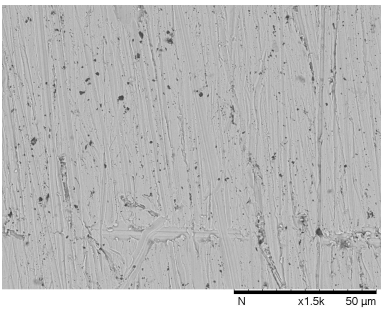
(f) Corrosion inhibitor 1 + dispersant 1



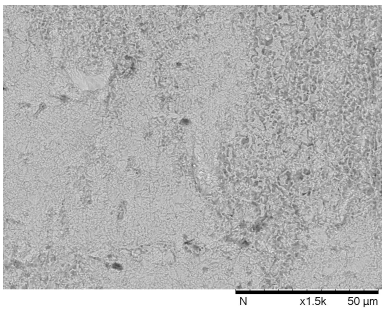
(g) Corrosion inhibitor 1 + dispersant 2



(h) Corrosion inhibitor 2 + dispersant 1



(i) Corrosion inhibitor 2 + dispersant 2



(j) Dispersant 1 + dispersant 2

Figure 8.8: SEM images of coupons tested at 120 °C in corrosion inhibitor 1, corrosion inhibitor 2, dispersant 1, dispersant 2, and their combinations

When combined with dispersant 1 the peaks that were present with corrosion inhibitor 1 alone in the sulfur and nitrogen spectra disappear. The peaks in the copper spectra change with no sulfate detected and more oxide. It is possible that the dispersant prevents interaction of the corrosion inhibitor with the surface and also keeps other by-products of oil degradation from interacting with the surface.

There is also a significant change from the corrosion inhibitor 1 spectra when combined with dispersant 2. The copper changes to a Cu(I) or Cu(0) state when dispersant 2 is present compared to a Cu(II) state for corrosion inhibitor 1 alone. The sulfur spectra shows that the sulfate, present in corrosion inhibitor 1 alone, diminishes significantly on combination with dispersant 2, and peaks denoting CuS and S (or thiols) increase. There is also a change in the nitrogen spectra but as it is difficult to assign these peaks to specific species it is more difficult to understand what has changed in this instance.

SEM images of the coupon surfaces tested at 120 °C in the corrosion inhibitors and dispersants, both individually and combined, are shown in Figure 8.8. The easiest thing to note is that tested alone dispersant 1 shows etching on the surface (c). This is not seen to the same extent in any of the combinations containing dispersant 1 (f, h, j). When combined with either of the corrosion inhibitors small pits can be seen on the surface but appears otherwise protected (f, h). Combined with dispersant 2 the surface does have an etched appearance (j) but it is not to the same extent as dispersant 1 alone.

Combination of corrosion inhibitor 1 with corrosion inhibitor 2 (e) shows a surface very similar to that of corrosion inhibitor 1 alone. This supports the previous hypothesis that when both corrosion inhibitors are combined corrosion inhibitor 1 dominates the interaction.

8.6 XPS and SEM results for 150 °C samples

The same combination of corrosion inhibitors and dispersants were tested at 150 °C. The copper spectra for these samples are shown in Figure 8.9.

Corrosion inhibitor 1 tested alone and in combination with other additives show very similar spectra with a peak around 932.4 eV. There are no satellite features in the spectra and so the copper is in the Cu(I) or Cu(0) state. For the combination of corrosion

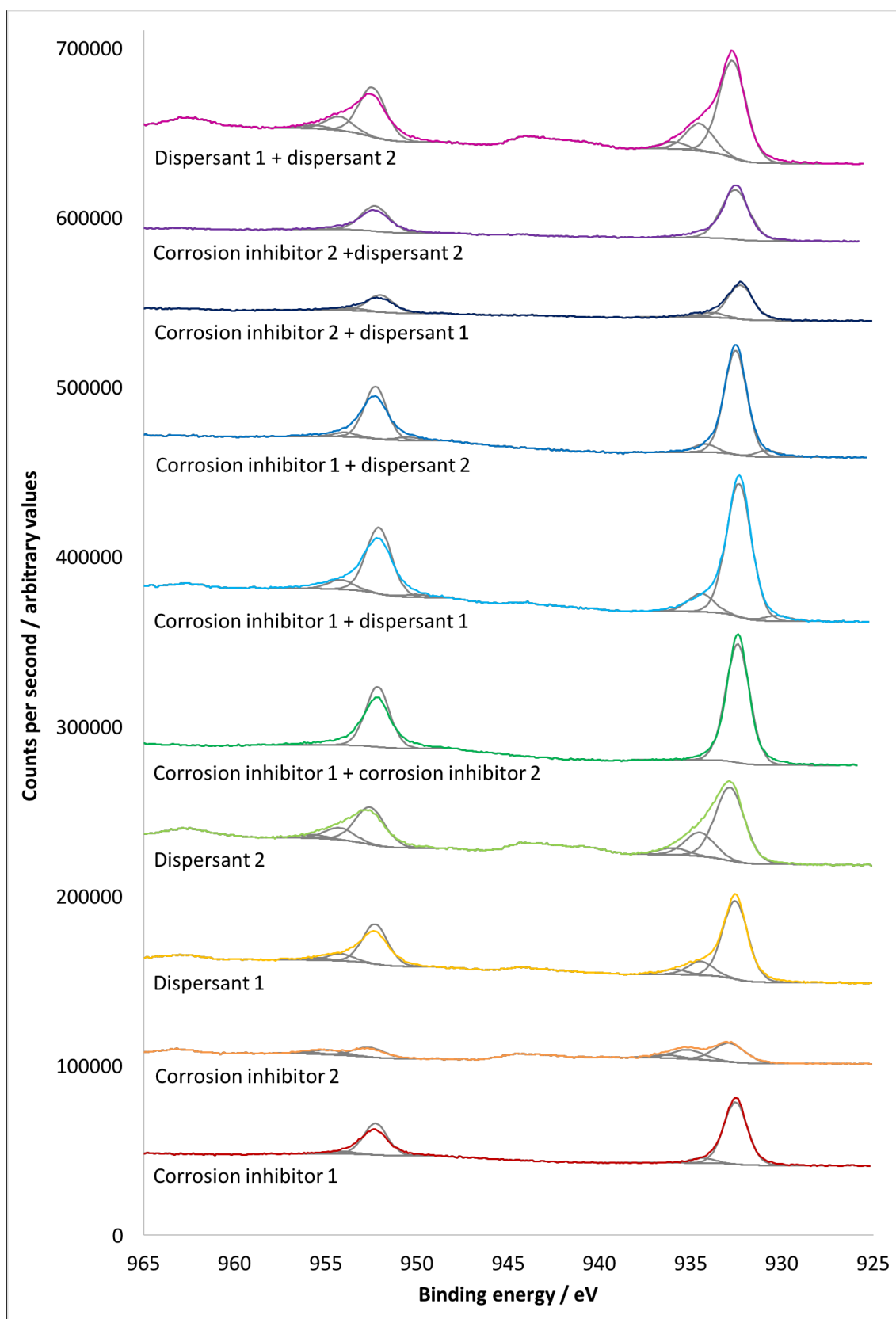


Figure 8.9: High resolution XPS copper scans for samples run at 150 °C containing corrosion inhibitor 1, corrosion inhibitor 2, dispersant 1, and dispersant 2

inhibitor 1 with dispersant 1 there is a small peak at a higher binding energy, around 934.6 eV, suggesting a small Cu(II) contribution, most likely from $\text{Cu}(\text{OH})_2$ or CuO .

There is little difference between the spectra taken at 150 °C and 120 °C for corrosion inhibitor 2 alone and in both cases the copper is in a Cu(II) state as well as Cu(I). At 150 °C the state of the copper changes when corrosion inhibitor 2 is used in combination with other additives. With corrosion inhibitor 1 the copper is in a Cu(I) state, corresponding to Cu₂S or Cu₂O. In combination with dispersant 1 or 2 there is a very small presence of Cu(II), which is not easily visible in Figure 8.9. Primarily though the copper for these combinations is in a Cu(I) state.

Dispersant 1 alone has a main peak at 392.5 eV with smaller minor peaks at 934 eV and 935 eV. The main peak, corresponding to Cu₂O or Cu₂S, is present on the surface of all of the samples but the smaller peaks are not visible in the combination with corrosion inhibitor 2, and are reduced in the combination with corrosion inhibitor 1.

At 150 °C the copper spectrum for dispersant 2 tested alone is very similar to at 120 °C. Three peaks and a satellite feature show that the copper is in a Cu(II) state and this is also the case in combination with dispersant 1. With corrosion inhibitor 2 the satellite feature is much diminished but a small peak at 934.5 eV show there is still some Cu(II) present. This is not the case with corrosion inhibitor 1 as the satellite feature has disappeared and no second peak is visible so the copper is in a Cu(I) state.

The nitrogen spectra obtained for all samples is shown in Figure 8.10. When all samples containing corrosion inhibitor 1 are compared there is only a slight difference between them. Corrosion inhibitor 1 in combination with dispersant 1 has a wider more prominent peak. However as it is difficult to assign nitrogen species it is only really possible to tell that there is a change, rather than what that change is.

A similar thing could be said for the samples containing corrosion inhibitor 2 or dispersant 2. All combinations are very similar to these individual additive tested alone, with the exception of when combined with dispersant 1 where the peak is wider and lacking the second peak around 403 eV.

Dispersant 1 tested alone has two small fitted peaks. Dispersant 1 has a long nitrogen backbone and so could be expected to show significant nitrogen peaks if it were to interact with and stay on the surface, the small peaks suggest this is not the case. When corrosion inhibitor 1 is added the peaks become larger and do not shift much in position.

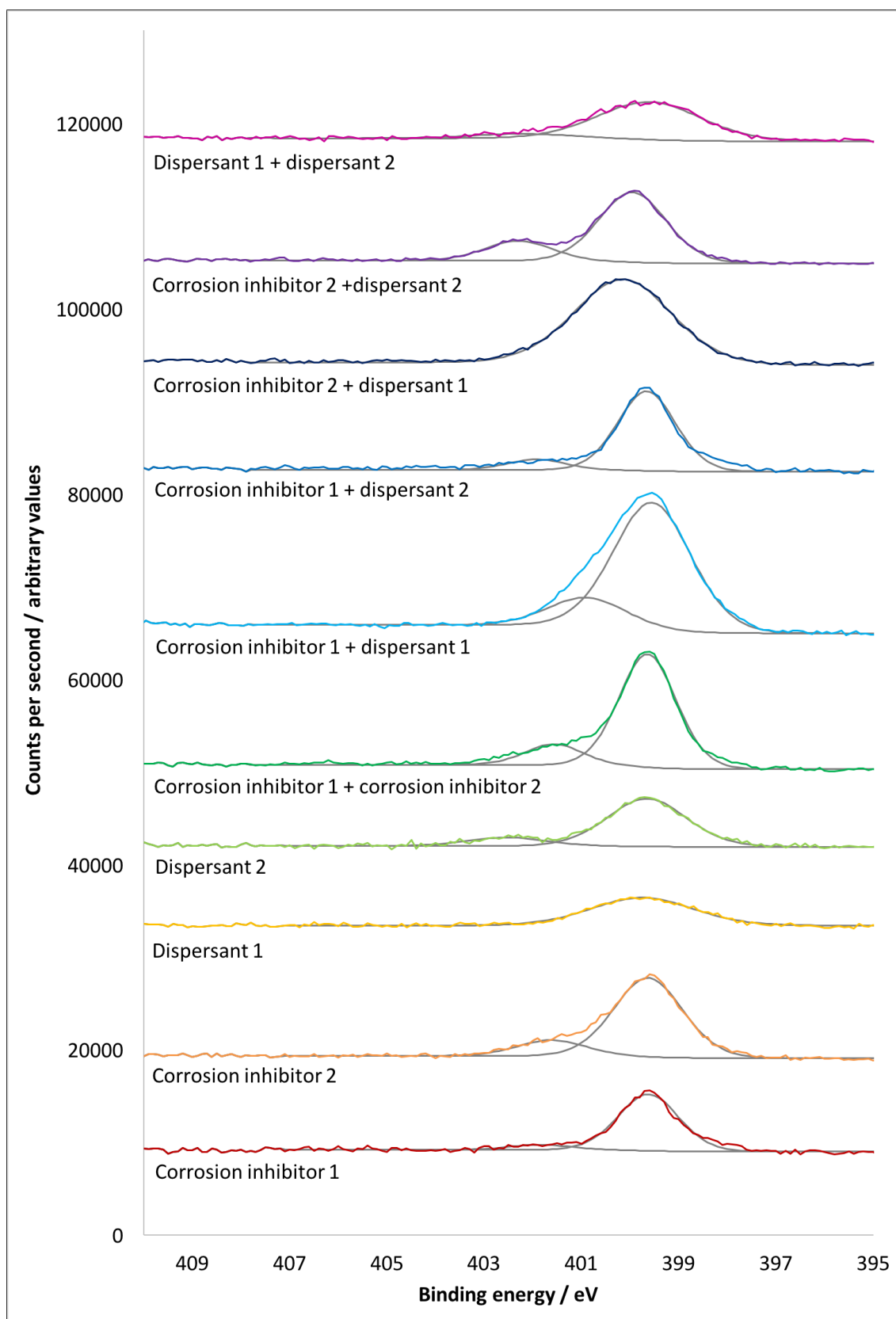


Figure 8.10: High resolution XPS nitrogen scans for samples run at 150 °C containing corrosion inhibitor 1, corrosion inhibitor 2, dispersant 1, and dispersant 2

The increase in nitrogen could be from the corrosion inhibitor interacting with the surface. Dispersant 1 combined with corrosion inhibitor 2 has a slight shift to the peaks

and a peak most likely corresponding to ammonium salt, which is also present in the combination with dispersant 2. The peaks are difficult to ascribe definite species to and are generally classified as being an organic matrix.

The sulfur spectra are shown in Figure 8.11. All of the samples containing corrosion inhibitor 1 show two main peaks fitted at around 162 eV and 164 eV these peaks show the presence of Cu_2S and S (or thiols). When dispersant 1 is present there is also a small but noticeable peak around 168 eV which would correspond with the presence of sulfate. Unlike the spectra at 120 °C where the sulfur differed depending on the combination with corrosion inhibitor 1 all of the samples tested at 150 °C are very similar.

When corrosion inhibitor 2 is tested alone there is a small sulfate peak, this is most likely formed from any sulfur in the base oil or is a contaminant as there is no sulfur present in the additive. There are also small peaks in the spectra of corrosion inhibitor 2 combined with with dispersant 1 and also dispersant 2. In combination with corrosion inhibitor 1 there is a very different spectrum with very little sulfate but large peaks denoting S (or thiols) and Cu_2S .

Dispersant 1 tested alone and in combination with corrosion inhibitor 2 and dispersant 2 show small peaks corresponding to Cu_2S and CuSO_4 . When in combination with corrosion inhibitor 1, the peaks are larger and an additional peak corresponding to S appears. This combination seems to be dominated by interaction from corrosion inhibitor 1 with little influence from the dispersant. This is also true of the dispersant 2 interactions.

All peaks positions (eV) for copper, nitrogen, sulfur and oxygen are given in Table 8.9 for samples tested at 150 °C.

SEM images of the coupon surfaces tested at 150 °C are shown in Figure 8.12. As discussed previously the surface of corrosion inhibitor 1 alone shows a film that has cracked and flaked away from the surface (a). A similar thing is seen in in the combination with dispersant 2 (g). The other corrosion inhibitor 1 combination samples do not show this.

Dispersant 1 (c) and dispersant 2 (d) alone both show corrosion to the surface. When placed in combination with either of the corrosion inhibitors the surface does not appear as severely corroded (f, g, h, i). When both dispersants are tested together there does

Table 8.9: Peak assignments for high resolution spectra of all samples analysed at 150 °C

Peak	Species	Corrosion inhibitor 1	Corrosion inhibitor 2	Dispersant 1	Dispersant 2	Corrosion inhibitor 1 + Corrosion inhibitor 2	Corrosion inhibitor 1 + Dispersant 1	Corrosion inhibitor 1 + Dispersant 2	Corrosion inhibitor 2 + Dispersant 1	Corrosion inhibitor 2 + Dispersant 2	Dispersant 1 + Dispersant 2
Cu 2p_{3/2}	Cu / Cu₂S / CuS / Cu₂O	932.56	932.85	932.57	932.85	932.43	932.27	932.55	932.44	932.32	932.55
	CuO	934.53	934.98	934.41	934.53		934.61		934.73	934.64	934.20
	CuSO₄		936.05	935.63	935.77						935.43
N 1s	NH₃ organic	399.63	399.69	399.05	399.89	399.65	399.48	399.66	399.42	399.85	399.07
	C-NH₂ organic			400.30			400.74		400.26		400.29
	Ammonium salt	401.95	401.66		402.57	401.67		402.09	401.12	402.26	402.10
O 1s	CuO		530.50		530.21		529.51				
	Cu₂O / CuO	530.77		530.87		530.78		530.32	531.16		530.13
	Cu(OH)₂ / CuCO₃	531.73	531.79	531.67	531.72	531.89	531.35	531.85	531.98	531.33	531.45
	Nitrate Organic C=O	533.33	533.37	533.31	533.55	533.46	532.90	533.41	533.26	532.93	533.19
S 2p_{3/2}	Cu₂S / CuS	162.58		161.90	162.07	162.60	162.32	162.59	161.64	161.84	161.90
	S	164.18				164.22	164.05	164.22			
	SO₂	167.96				167.82		167.51			
	CuSO₄		168.76	168.08	168.33		168.04		168.10	168.20	168.20

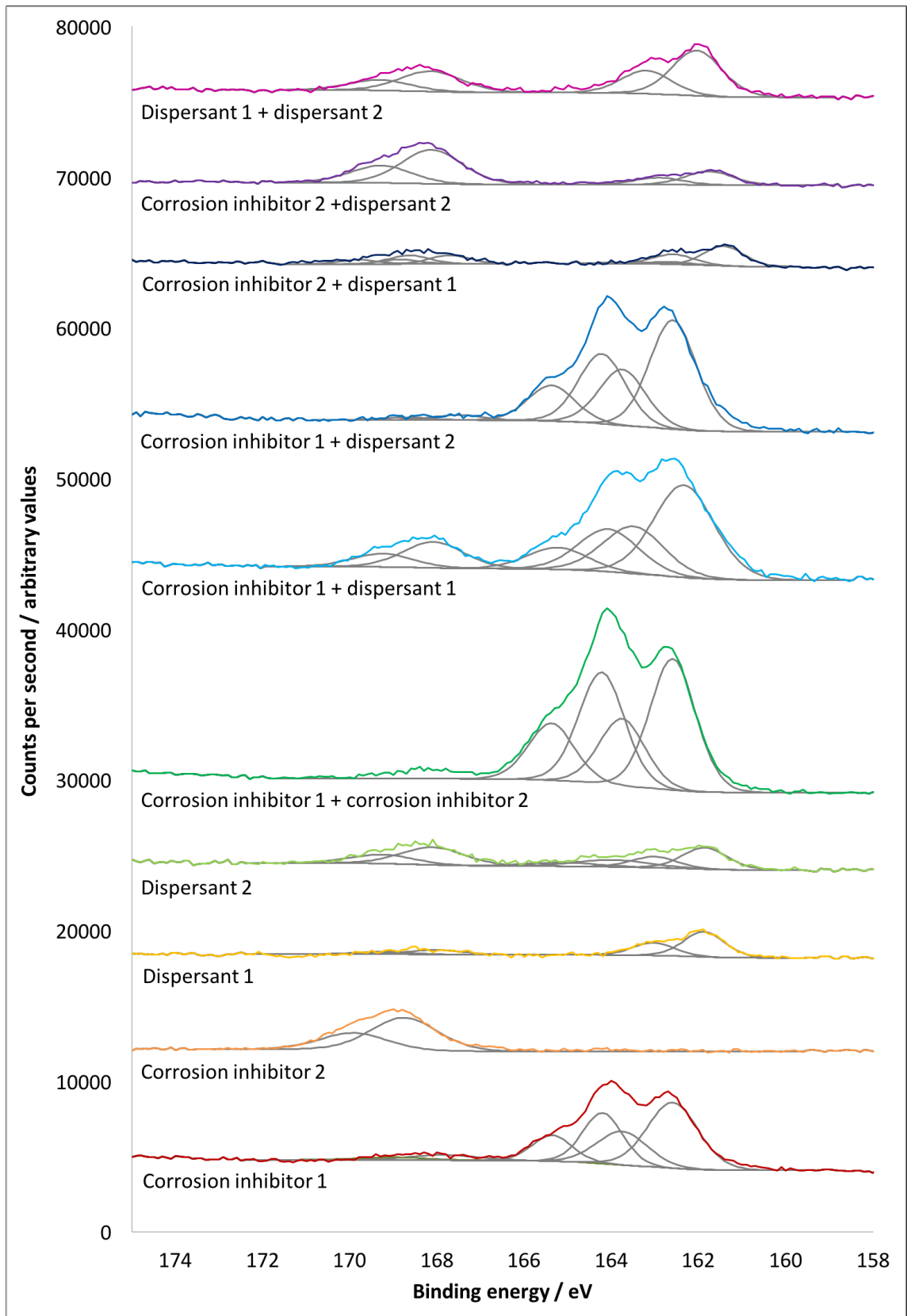
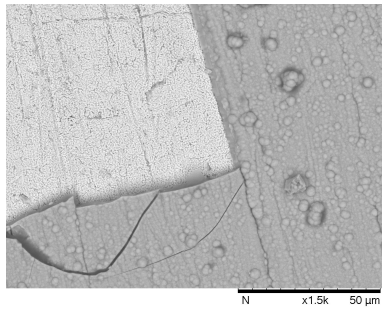
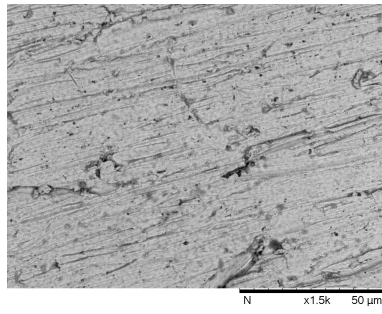


Figure 8.11: High resolution XPS sulfur scans for samples run at 150 °C containing corrosion inhibitor 1, corrosion inhibitor 2, dispersant 1, and dispersant 2

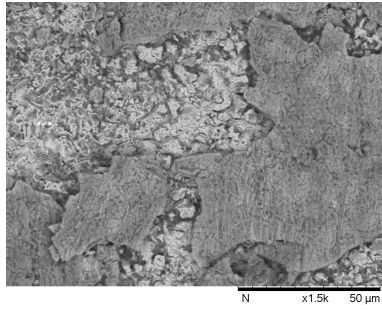
not appear to be a film formed on the surface but it does also not appear as corroded as when tested individually; if it is it has corroded more uniformly.



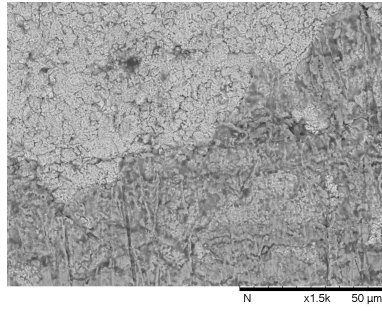
(a) Corrosion inhibitor 1



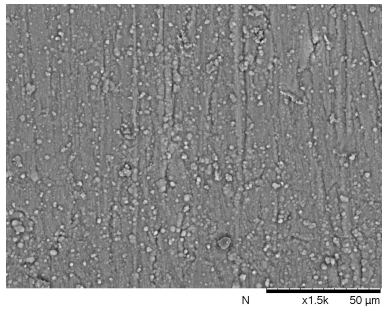
(b) Corrosion inhibitor 2



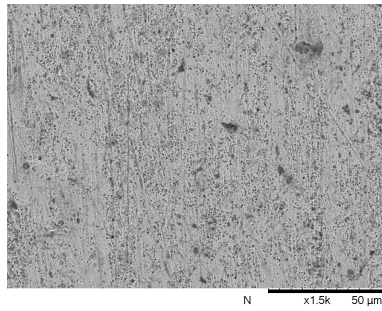
(c) Dispersant 1



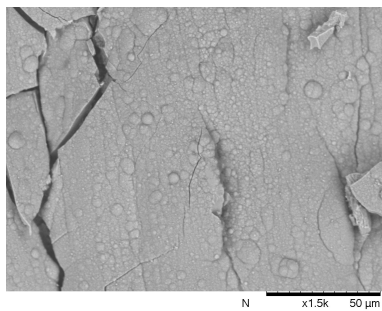
(d) Dispersant 2



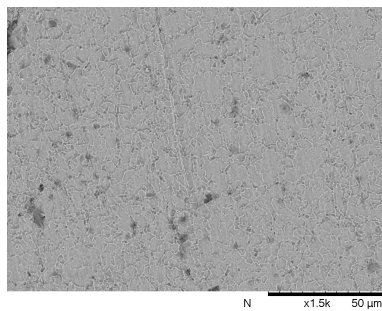
(e) Corrosion inhibitor 1 + corrosion inhibitor 2



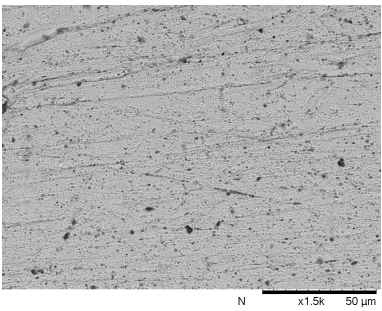
(f) Corrosion inhibitor 1 + dispersant 1



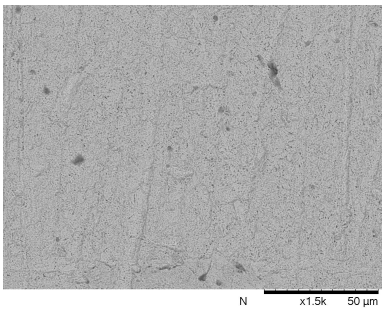
(g) Corrosion inhibitor 1 + dispersant 2



(h) Corrosion inhibitor 2 + dispersant 1



(i) Corrosion inhibitor 2 + dispersant 2



(j) Dispersant 1 + dispersant 2

Figure 8.12: SEM images of coupons tested at 150 °C in corrosion inhibitor 1, corrosion inhibitor 2, dispersant 1, dispersant 2, and their combinations

8.7 Summay

- All additive combinations have been tested and synergies and antagonisms identified for ASTM ratings, copper levels in the end of test fluid and the radius change of the copper wire; they were not the same in each of these tests. Copper levels and radius changes often showed only very small synergies, which made it questionable as to whether they were true synergies. Antagonisms were much clearer as they were generally significantly worse than either of the individual additives.
- Most tests were additive, with the results of the combinations sitting between those of the individual additives.
- XPS analysis of the individual corrosion inhibitor and dispersant samples were compared with combinations of these additives. Changes were identified primarily in the copper, nitrogen and sulfur spectra.
- SEM images of the corrosion inhibitor and dispersant samples showed that combinations containing dispersant showed less severe corrosion than when the dispersants were tested alone.

9: Film progression

Monitoring the change in radius of a thin copper wire has given good insight into how the interaction between an additive and the copper surface may be progressing. However for the individual additives and their combinations all fluid and coupon analysis has been carried out at the end of the test. How the copper surface evolves over time is unknown. For example do the films form at the start of the test and then get thicker with time; or are different surface structures seen as the experiment progresses? Knowing this is important, particularly for the combinations, as it should help to determine if multiple mechanisms are taking place.

As was determined when this experiment was first trialled on the full formulation fluids the wires cannot be disturbed during the test because they are sensitive to movement. For this reason the following tests have been carried out using the same equipment as the wire tests but using only coupons in the test beakers. The tests were conducted at 150 °C on the following fluids. Concentrations are the same as previously tested but are included for clarification, abbreviations have also been included as some tables required them due to size constraints:

- Corrosion inhibitor 1 (0.5 wt%)
- Corrosion inhibitor 2 (0.05 wt%)
- Dispersant 1 (5 wt%)
- Dispersant 2 (5 wt%)
- Corrosion inhibitor 1 (0.5 wt%) + Corrosion inhibitor 2 (0.05 wt%) (CI 1 + CI 2)
- Corrosion inhibitor 1 (0.5 wt%) + Dispersant 1 (5 wt%) (CI 1 + disp 1)
- Corrosion inhibitor 1 (0.5 wt%) + Dispersant 2 (5 wt%) (CI 1 + disp 2)
- Corrosion inhibitor 2 (0.05 wt%) + Dispersant 1 (5 wt%) (CI 2 + disp 1)
- Corrosion inhibitor 2 (0.05 wt%) + Dispersant 2 (5 wt%) (CI 2 + disp 2)

- Dispersant 1 (5 wt%) + Dispersant 2 (5 wt%) (Disp 1 + disp 2)

Images of each of the coupons was taken at the end of each test period and the amount of copper in the test fluid determined using ICP-AES. The surface of each of the coupons was analysed using BSE imaging with an accelerating voltage of 5 kV and 15 kV. The 15 kV beam energy penetrates slightly deeper into the surface film and it was found that, particularly at longer time spans, slightly different surface structures were seen, so for example a surface layer was being formed but underneath this layer there were more subtle changes. The images presented are the 15 kV images unless otherwise stated.

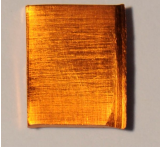
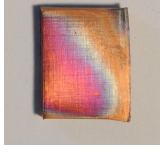
9.1 Surface changes of copper tested in individual additives

The corrosion inhibitors and dispersants were tested individually for periods up to 200 hours. Images of the coupon surface after 1, 3, 16, 100 and 200 hours are shown in Table 9.1. BSE images of the surfaces after the same time periods are shown in Table 9.2.

As explained in the methodology when the wire tests are conducted the first hour is considered to be a stabilisation period, allowing the wire and fluid to come to temperature. In order to make sure that no substantial change had occurred after this time coupons were tested for 1 hour and then analysed. As can be seen from Table 9.2 the BSE shows all samples are similar indicating no significant change to the surface. Interestingly despite no differences in the BSE images and no copper measured in the test fluid the ratings do differ. The samples tested in corrosion inhibitors are of a more orange hue than those tested in dispersants, which are pinker in colour, as can be seen in Table 9.1.

The standard test length for the ASTM D130 is 3 hours. Coupons tested in corrosion inhibitors and dispersants for 3 hours differ very little to those immersed for only 1 hour (Table 9.1). There is a slight difference in the BSE images of the corrosion inhibitors; after 3 hours there is the start of film formation, indicated by a fewer number of small black spots on the image, as seen in Table 9.2. There is still no copper measured in the test fluid so 3 hours is not long enough for corrosion to occur.

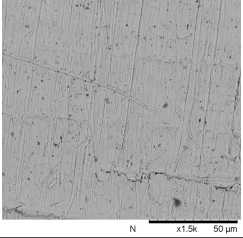
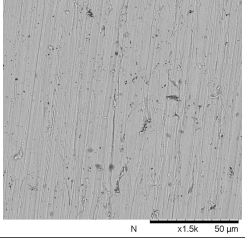
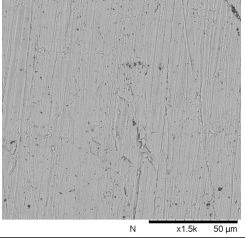
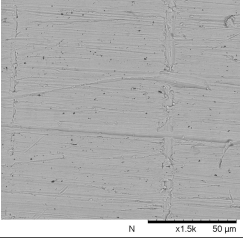
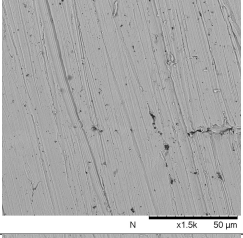
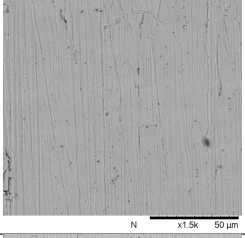
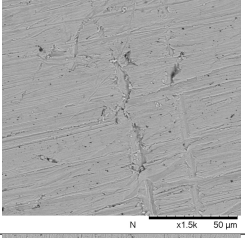
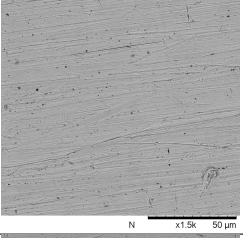
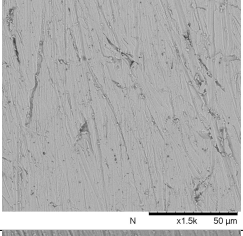
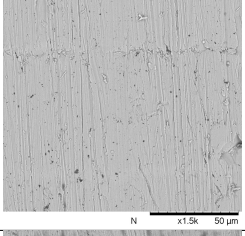
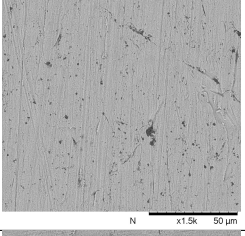
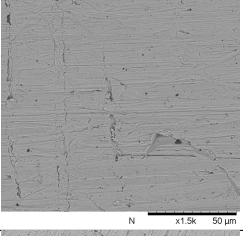
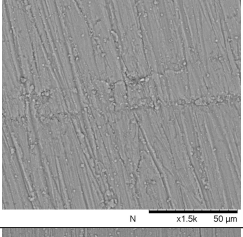
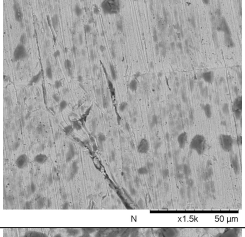
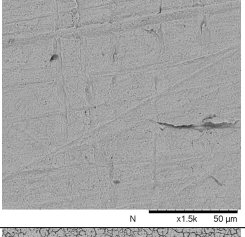
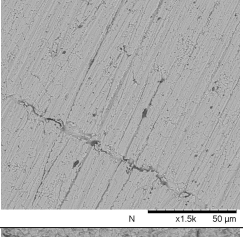
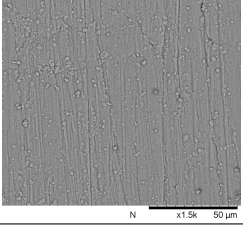
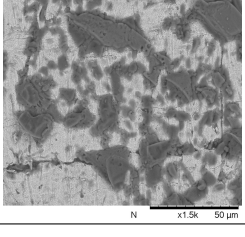
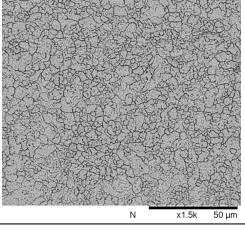
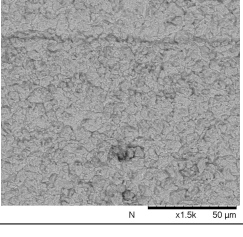
Table 9.1: Images and ratings of coupons after different immersion periods in specified additives

Time	Corrosion inhibitor 1	Corrosion inhibitor 2	Dispersant 1	Dispersant 2
1 hour	 1b	 1b	 1a	 1a
3 hours	 1a	 1b	 1a	 1a
16 hours	 3b	 2a	 1a	 3b
100 hours	 4a	 3a	 1b	 3b
200 hours	 4a	 1b	 2b	 2b

Significant changes to the surface begin to occur around 16 hours; this is also when the amount of copper in the fluid begins to rise for the dispersants. As can be seen in Table 9.2 there is clear film formation on the surface of the corrosion inhibitor samples, particularly corrosion inhibitor 1. A number of small holes are also seen on the surface of the dispersant samples. As seen in Table 9.1 a greater difference is seen in the ratings of the coupons.

The biggest visual changes begin to occur at 50 hours (not shown) but can be clearly seen at 100 hours. Table 9.2 shows the surface and BSE images for samples after 100 hours. The formation of a film on the corrosion inhibitor 1 sample is clearly seen with some small particles of other deposit on the surface. The corrosion inhibitor 2 sample shows

Table 9.2: BSE images of the coupon surfaces after immersion for different time periods in specified additives

Time	Corrosion inhibitor 1	Corrosion inhibitor 2	Dispersant 1	Dispersant 2
1 hour				
3 hours				
16 hours				
100 hours				
200 hours				

areas of large flat patches that do not come together to form a continuous layer. This was not seen in tests conducted with the wire also present. The sample in dispersant 1 shows the beginning of surface etching. The dispersant 2 sample is more difficult to describe with some signs of surface attack with the appearance of small holes but it is possibly the least changed from the 16 hour samples. Table 9.1 shows that at 100 hours there are significant differences between the coupons tested in the different additives and also between the previous time periods.

The change between 100 and 200 hours for the corrosion inhibitors is small in both

rating and BSE images. The rating of the corrosion inhibitor 2 sample changes, but the image looks very similar (Table 9.1). This is one difficulty of the ASTM rating, in that ratings of 1b and 3a are similar in colour with only slight differences, all samples are rated in a light box to keep lighting conditions constant and the images do not always capture the subtle differences between surface colours. The dispersant 2 sample is also interesting in this way. At 150 hours (not shown) the image is similar to that at 100 hours with a brightly coloured, shiny surface. Between 150 and 200 hours the surface becomes dull and loses any surface layer, as can be seen by the 200 hour image. Table 9.2 shows the dispersant 1 sample is more severely etched 200 hours. A similar surface, although slightly less severe is seen for the dispersant 2 sample.

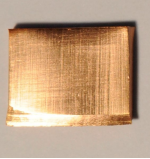
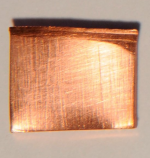
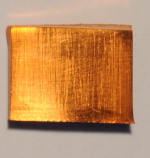
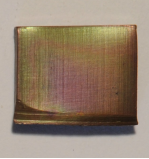
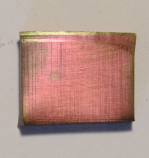
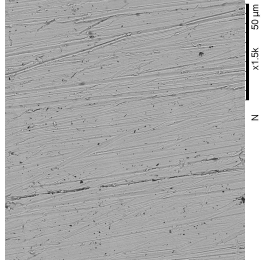
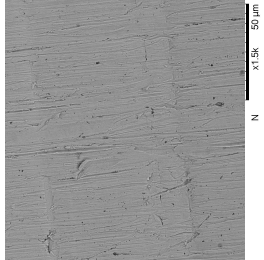
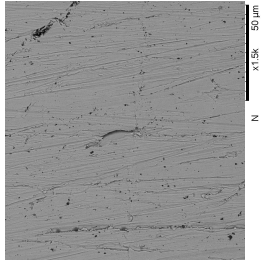
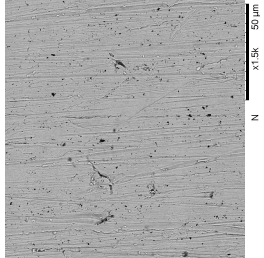
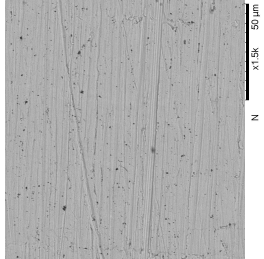
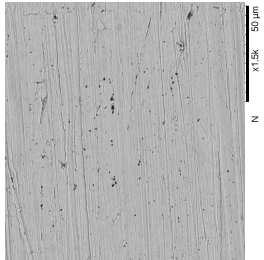
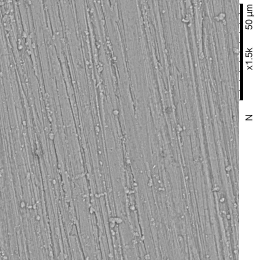
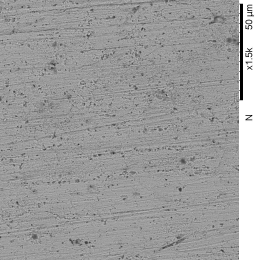
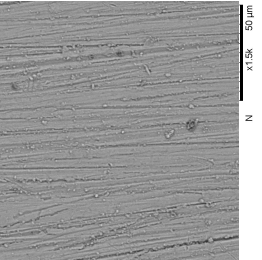
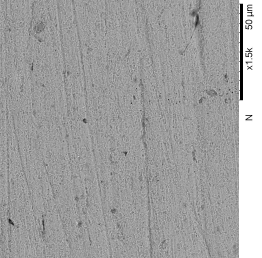
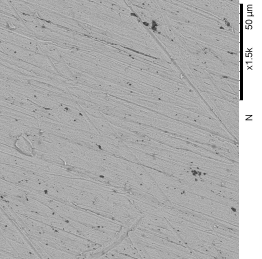
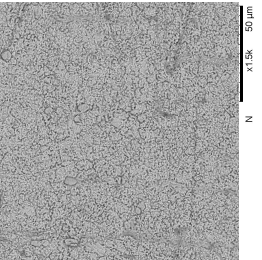
9.2 Surface changes of copper tested with simple additive mixtures

Having examined the additives individually the additive combinations were then tested. The samples tested for 3 hours, the standard length of the ASTM D130 test, are shown in Table 9.3. The ASTM D130 test is often run in order to try and distinguish between fluids. It may be the case that after 3 hours fully formulated fluid would show some differences but in the case of single additives or mixtures of two additives there is little to distinguish between the samples.

BSE images of the surface show that there is little interaction with the surface after 3 hours and measurement of the amount of copper in the end of test fluid by ICP showed no copper for any of the additive mixtures.

After 100 hours, the maximum time used for testing these fluid combinations, the samples tested in combinations of additives showed some interesting differences to those tested with single additives. Table 9.3 shows the results of the samples tested in mixtures of additives. Corrosion inhibitor 1 with corrosion inhibitor 2 or dispersant 2 showed a surface similar in both rating and BSE image to corrosion inhibitor 1 tested alone, with clear film formation on the surface and small deposit like structures on top. This suggests

Table 9.3: Images and ratings and BSE image of coupons after 3 hours and 100 hours immersion in specified additives

Time	CI 1+ CI 2	CI 1+ disp 1	CI 1+ disp 2	CI 2+ disp 1	CI 2+ disp 2	Disp 1+ disp 2
3 hours	 1b	 1a	 2b	 1a	 1b	 1a
100 hours	 4a	 2d	 3b	 3a	 3a	 3a
3 hours	 N x1.5K 50µm	 N x1.5K 50µm	 N x1.5K 50µm	 N x1.5K 50µm	 N x1.5K 50µm	 N x1.5K 50µm
100 hours	 N x1.5K 50µm	 N x1.5K 50µm	 N x1.5K 50µm	 N x1.5K 50µm	 N x1.5K 50µm	 N x1.5K 50µm

that corrosion inhibitor 1 interacts with the surface more prominently than corrosion inhibitor 2 or dispersant 2.

Corrosion inhibitor 1 with dispersant 1 was not like this, there is no clear sign of film formation, however there is also no sign of etching, as there was with dispersant 1 alone; albeit not too advanced at 100 hours, as seen in Table 9.2. This suggests that corrosion inhibitor 1 provides the surface with some protection, however the lack of clear film formation indicates that dispersant 1 either interferes with the interaction between corrosion inhibitor 1 and the surface to prevent film formation, or interacts with the film formed on the surface to remove it. Both of these provide protection to the copper surface but it is unclear which is likely to be the case.

When corrosion inhibitor 2 is present with corrosion inhibitor 1 we have already established that it does not have much impact on the surface. When it is combined with dispersant 1 or dispersant 2 it seems to protect the surface from etching as was seen at 100 hours with dispersant 1 and 2 alone (Table 9.2), however there does seem to be the presence of some small holes across the surface.

The sample tested in dispersant 1 combined with dispersant 2 after 100 hours shows more severe etching to the surface than either of the dispersants tested alone after this period of time. This suggests that there may be an antagonism occurring when both dispersants are combined.

9.3 Copper level in test fluids measured using ICP-AES

Understanding how the surface changes over time and how combining additives can impact the surface differently to individual additives is useful. For example if it can be seen that one additive which negatively affects the surface begins to show surface deterioration, after 20 hours say, but a surface protector is showing signs of film formation at 10 hours then it could be assumed that combining these additives would lead to film formation before surface deterioration. What may actually be seen is the the film is no longer formed because the additives interact in the fluid. The amount of copper in the

test fluid was measured to see if correlations could be drawn between the copper levels and visual differences on the surface.

Figure 9.1 shows how the copper level changes with time for fluids containing corrosion inhibitor 1. Corrosion inhibitor 1 rises very slowly with time showing very little change after 100 hours. When corrosion inhibitor 2 or dispersant 2 are combined with corrosion inhibitor 1 they follow the same trend, with almost identical values to corrosion inhibitor 1 alone. The levels are below 0.5 ppm and so it is possible that the test is not sensitive enough to differentiate between such small amounts, and it also means the levels are more susceptible to machine contamination.

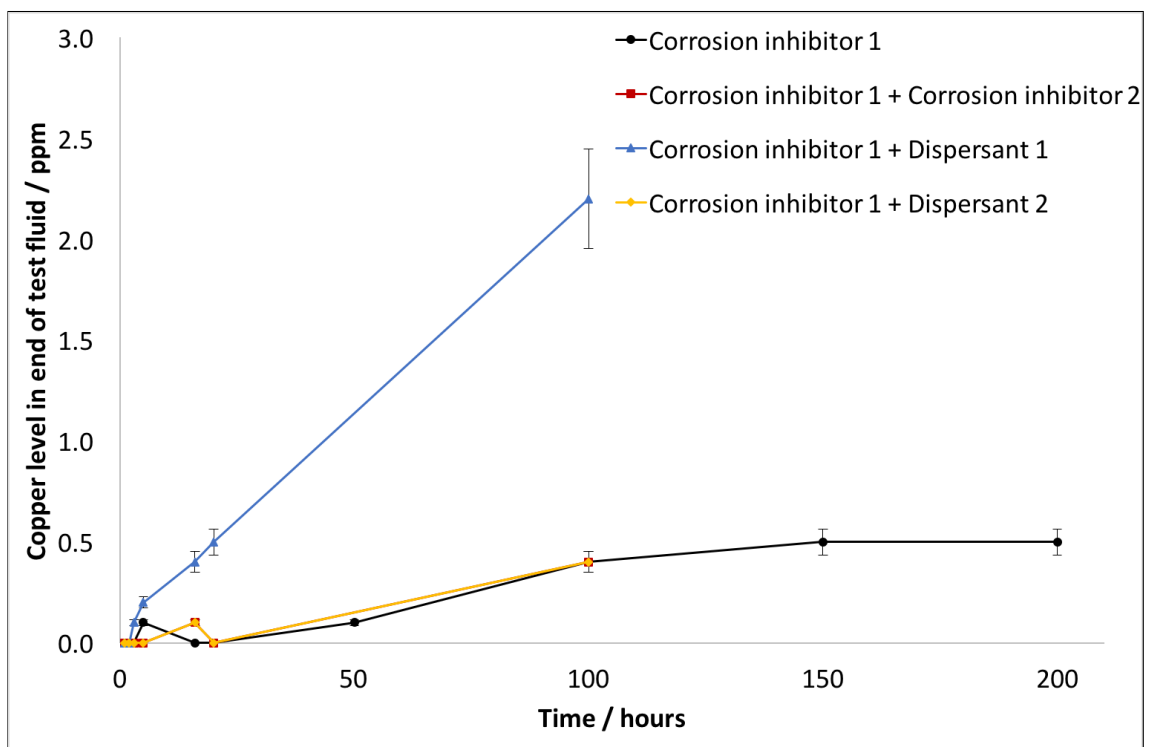


Figure 9.1: Amount of copper in end of test fluid after different time periods for fluids containing corrosion inhibitor 1

BSE images of the surfaces showed visible film formation on the surface of samples tested in corrosion inhibitor 1 alone and when in combination with dispersant 2 and corrosion inhibitor 2 from the 16 hour sample onwards. The fact that the amount of copper measured with time is almost the same for these three sample, along with the BSE images, suggests that corrosion inhibitor 1 interacts most strongly with the surface.

When corrosion inhibitor 1 is in combination with dispersant 1 the copper level measured in the fluid is greater than when corrosion inhibitor 1 is present alone. This

means that the dispersant is having an effect on the surface. The BSE images show that the dispersant interferes with the film forming process as no film formation is seen on the surface even after 100 hours (Table 9.3).

Corrosion inhibitor 2 does not appear as effective as corrosion inhibitor 1 at protecting the surface when another additive is present as when it is on its own. Tested alone corrosion inhibitor 2 had very low copper levels. When tested in combination with corrosion inhibitor 1 or dispersant 2 the amount of copper in the fluid increased, as can be seen in Figure 9.2. Despite the slight increase the overall level of copper is low and so corrosion inhibitor 2 is providing some protection to the copper surface.

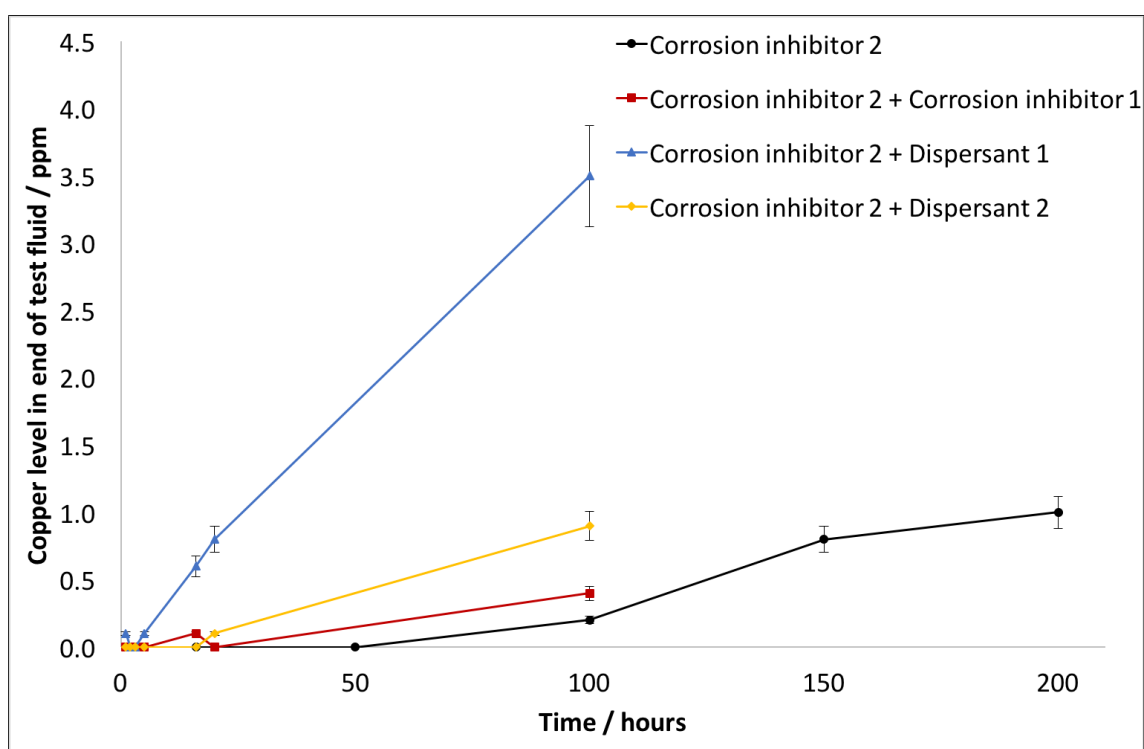


Figure 9.2: Amount of copper in end of test fluid after different time periods for fluids containing corrosion inhibitor 2

When tested in combination with dispersant 1 there is a greater increase in the amount of copper present in the fluid, which begins to rise significantly after 16 hours.

Figure 9.3 shows the level of copper measured with time for fluids containing dispersant 1. Tested alone dispersant 1 shows a steady increase in copper in the fluid throughout the test. When combined with either of the corrosion inhibitors it still rises but the overall level of copper is lower, with corrosion inhibitor 1 providing the better protection as it reduces the copper level more than corrosion inhibitor 2. The BSE images

for the 100 hour samples, Table 9.3, show a number of small holes on the surface for dispersant 1 combined either of the corrosion inhibitors but the corrosion inhibitor 1 sample is not noticeably better than the corrosion inhibitor 2 sample.

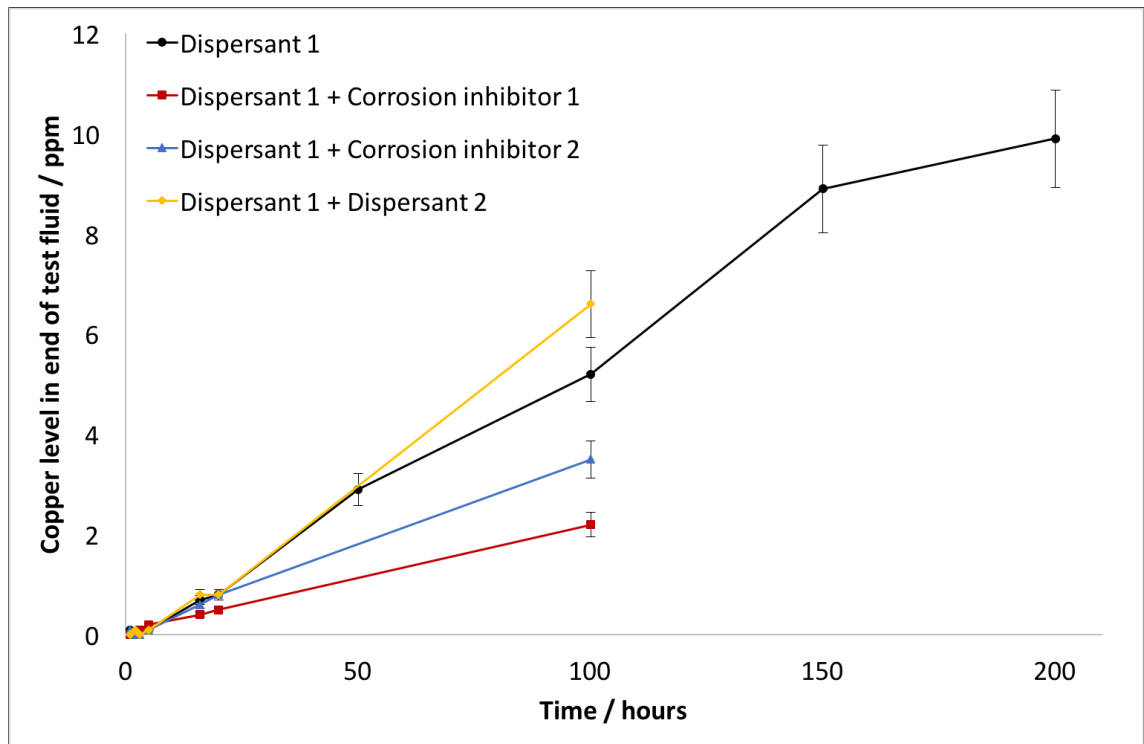


Figure 9.3: Amount of copper in end of test fluid after different time periods for fluids containing dispersant 1

When dispersant 1 is combined with dispersant 2 the amount of copper is higher than either of the dispersants alone, as seen in Figures 9.3 and 9.4. The mechanism of how the dispersants interact with the copper surface will be discussed in Chapter 11. This suggests the combination of dispersants is antagonistic. This is not immediately obvious from the sample images but when the samples are studied the etching seen for the combination at 100 hours is similar to that at 200 hours for dispersant 1 alone indicating that the combination causes etching to occur earlier.

Dispersant 2 tested in combination with either corrosion inhibitor shows a lower level of copper than when tested alone. This is the same trend as seen with dispersant 1. From this we can conclude that the addition of corrosion inhibitor to dispersant reduces the amount of copper seen in the test fluid when compared to the dispersant alone, however the level is higher than for the corrosion inhibitor alone.

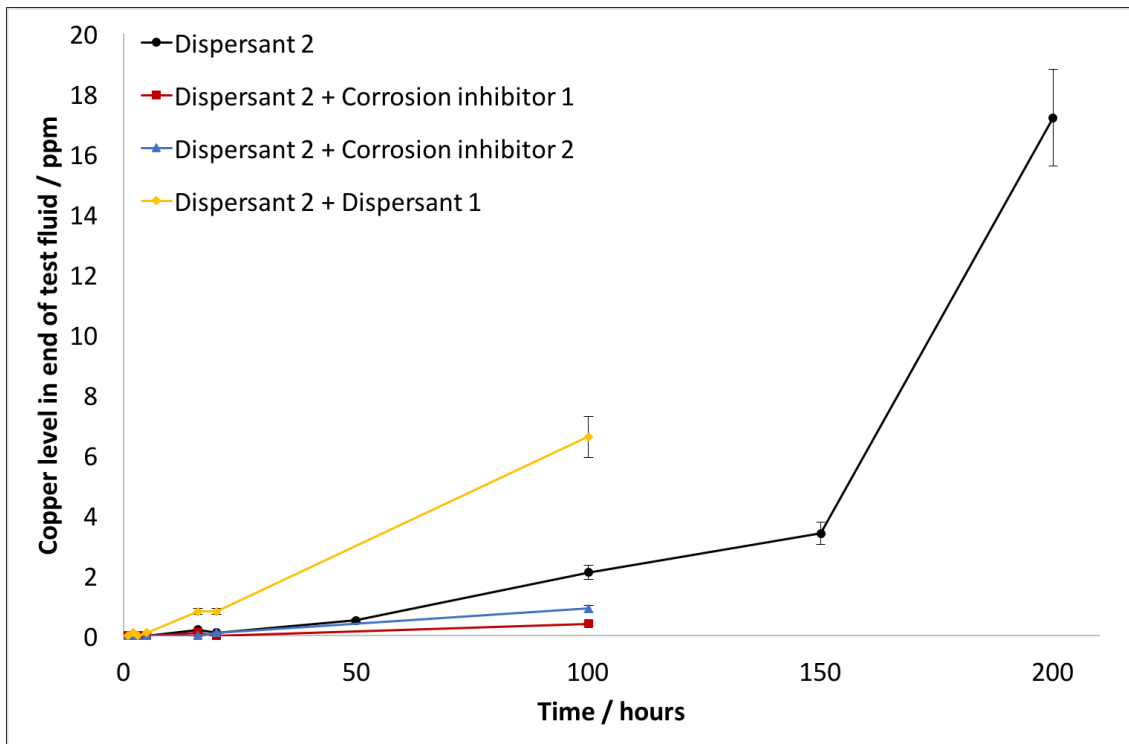


Figure 9.4: Amount of copper in end of test fluid after different time periods for fluids containing dispersant 2

9.4 Summary

- A 3 hour test period is not long enough to show differences between the fluids tested and BSE images of the surface show little film formation.
- Changes begin to be seen at around 16 hours testing. Increases in the level of copper in the fluids containing dispersant are seen. BSE images show film formation on the surfaces of coupons tested in corrosion inhibitor and greater differentiation in the ASTM rating is seen between samples.
- Progression through the ratings is seen with increasing time periods.
- Gradual changes in the level of copper in the end of test fluid give an idea of the rate of corrosion.

10: Predicting full formulation behaviour from simple additive mixture results

Having studied each of the additives individually and then in combination with each other a large amount of information has been collected; from the rating and SEM images of each surface, to the change in radius of copper wires and the copper level in the end of test fluid.

It was wondered if it would be possible to predict which additives were causing the behaviour seen in full formulation fluids by comparing the results of the individual and simple mixture additive tests with those of the full formulations. Considering the simple additive mixture tests were carried out at fixed concentrations and the full formulation fluids had additive levels that varied this will not be an exact comparison but is interesting to see if the simplified tests carried out could identify the properties of the full formulation behaviours.

Due to difference in the test methods between the initial full formulations tested and the simple additive mixtures the SEM images shall be compared initially, as they should be most comparable despite the difference in test length. As a reminder the full formulation tests were conducted in an oven, held at 120 °C for four weeks. The additive combination testing was carried out in oil baths at 120 °C for two weeks.

10.1 Comparison of results from full formulations and simple additive mixtures

The SEM images for the copper coupons tested in full formulation fluids and simple additive mixtures were inspected and matched. In some instances the full formulation surface could be matched to several similar additive combination surfaces, and in other instances no similarities were seen. Once all images had been examined the additives present in the formulation were checked to see if the matched additive combinations were present.

In Chapter 5 the surfaces of the coupons tested in full formulation fluids were grouped by similarity. One group showed clearly defined spheres on the surface of the coupon, Section 5.6.2. The additive combination of corrosion inhibitor 1 with the AO, AW, FM mix was the only combination to show spheres on the surface. For ease of reference the SEM images for each of the samples showing spheres is shown in Figure 10.1.

The additive formulation information for these samples are shown in Table 10.1. For clarity where no additive was present the space has been left blank.

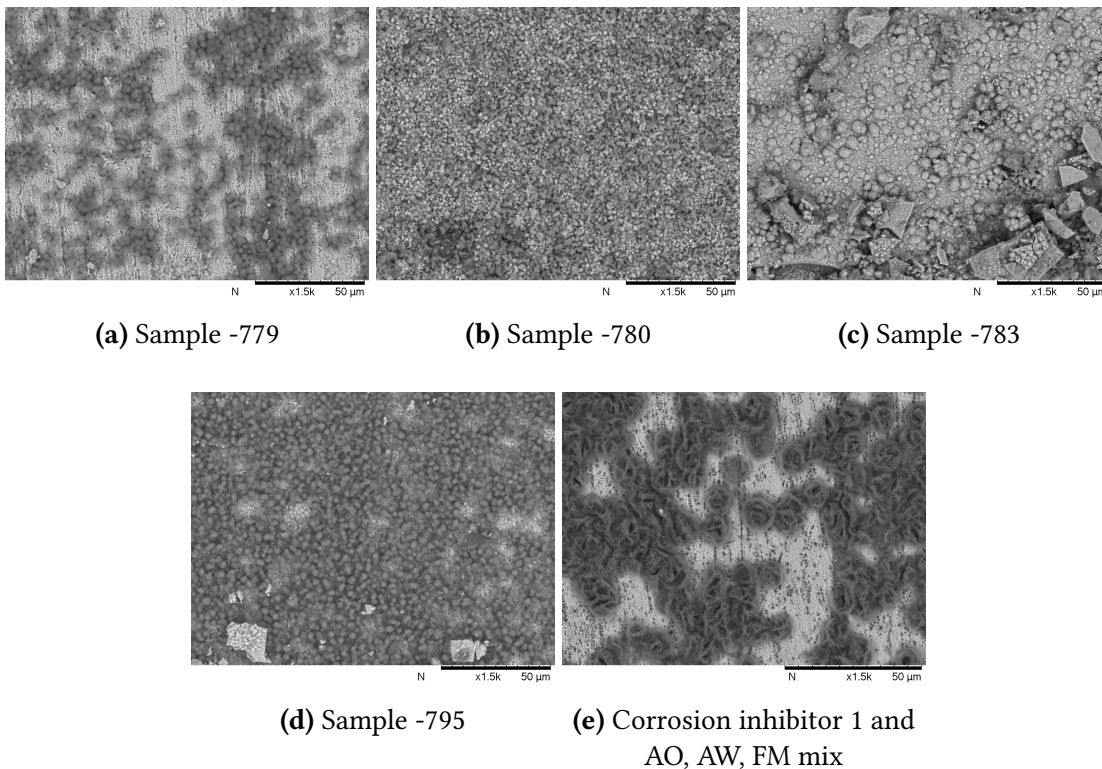


Figure 10.1: SEM images of full formulation samples showing spheres on the surface along with the corrosion inhibitor 1 and AO, AW, FM mix sample surface

Table 10.1: Full formulation additive levels for samples which showed spheres on their surface, along with the additive combination corrosion inhibitor 1 and the AO, AW, FM mix

Sample number	Corrosion inhibitor 1	Corrosion inhibitor 2	Dispersant 1	Dispersant 2	Detergent 1	Detergent 2	Antioxidant	Antiwear	Friction modifier
Corr inhib 1 & AO, AW, FM mix	0.5						0.33	0.165	0.65
-779	0.5	0.026					0.6	0.11	0.65
-795	0.5		2.5		0.2		0.6	0.22	1.2
-783	0.5			5	0.1	0.4	0.6	0.11	0.1
-780	0.5			2.5		0.4	0.06	0.22	1.2

It can be seen that all the formulations contained 0.5 wt% corrosion inhibitor 1 and antioxidant, antiwear and friction modifier at varying levels. Few other additives were present in the formulations and where they were present they were often in lower concentrations. It is likely that the spheres seen on the surface of the full formulation samples come from the interaction of corrosion inhibitor 1, antioxidant, antiwear and friction modifier.

The size and density of the spheres does vary between the samples and this is likely due to the presence of other additives. Sample -779 is most similar to that of the corrosion inhibitor 1 and AO, AW, FM mix; with particles spaced apart and a slightly porous surface underneath; the additives also deviate least from the simple additive combination.

Interestingly in this instance the amount of copper detected in the end of test fluid for each of these formulations appears to be explained by looking at the additives present. Table 10.2 shows the amount of copper measured in the end of test fluid for each of the formulations.

Table 10.2: Amount of copper in the end of test fluid for formulations which showed spheres on their surface

Additive combination or Formulation	Amount of copper / ppm
Corrosion inhibitor 1 & AO, AW, FM mix	14.8
-779	17.0
-783	11.3
-780	17.0
-795	55.7
Dispersant 1 & AO, AW, FM mix	56.0

In the case of -779, -783 and -780 the copper levels are 17 ppm, 11.3 ppm and 17 ppm respectively. These match quite well with the level of copper measured for the corrosion inhibitor 1 and AO, AW, FM mix combination, 14.8 ppm; bearing in mind that the full formulations tests ran for a longer period of time. Formulation -795 is different and has a much higher copper level of 55.7 ppm. Looking again at the additives present in the formulation of -795 it can be seen that dispersant 1 is present at 5 wt%. It has already been shown that the presence of dispersant increases the level of copper measured in the end of test fluid. Interestingly though the additive combination test of dispersant 1 with the AO, AW, FM mix the copper level was measured as 56 ppm, very similar to that of the -795 formulation.

As mentioned previously only one simple additive combination showed the formation of spheres on its surface; this made it simple to match with the full formulation samples showing spheres. Matching the other full formulation surfaces with those of simple additive mixtures was more complicated as many of them had similar surfaces. As the full formulation samples were able to be grouped by similarity (Chapter 5, Section 5.6) the surfaces of the simple additive mixtures were placed into the same groups.

This gave many samples with similar surfaces in the same group. This made it very difficult to match simple additive combination surface images with those of the full formulations as there were too many possibilities based on a visual inspection alone.

This meant that grouping the samples did not prove to be particularly useful as the groups had too many samples to be useful. Another method was therefore tried whereby a full formulation was picked and the additives present studied. The corresponding simple additive mixtures were then compared to see if the surfaces showed similarities. In some instances more than one simple additive mixture could be matched to the surface.

To try and simplify the analysis formulations containing the highest level of corrosion inhibitor 1, 0.5 wt%, were first looked at. Figure 10.2 shows these full formulation samples matched with the surfaces of simple additive mixtures. Their corresponding formulations can be seen in Table 10.3.

This proved to be a successful way to analyse the samples and almost all of the full formulation fluids containing 0.5 wt% corrosion inhibitor 1 were able to be matched

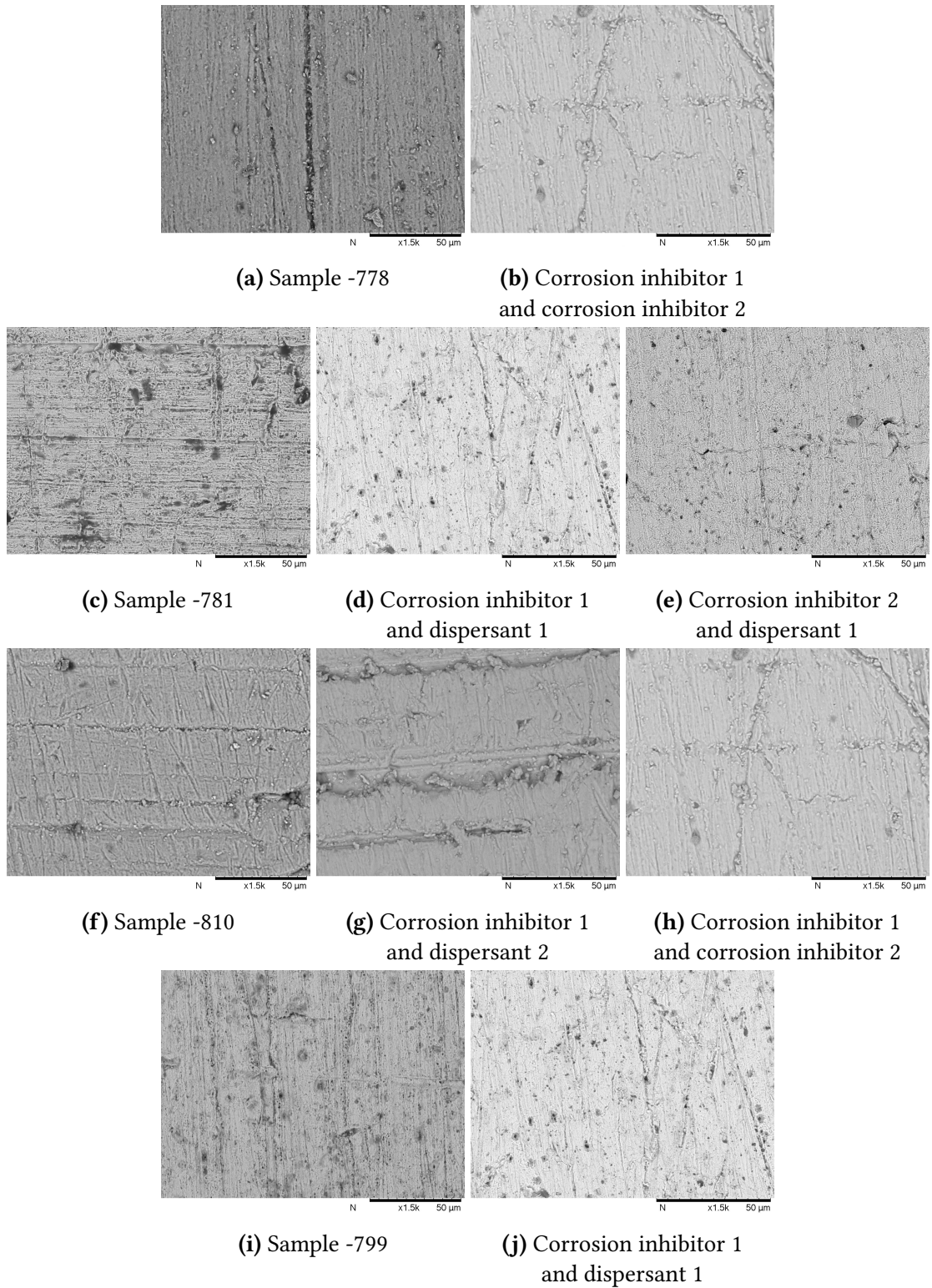


Figure 10.2: SEM images of the surfaces of full formulation samples and simple additive combination samples which contained corrosion inhibitor 1 at 0.5 wt%

with simple additive combinations containing corrosion inhibitor 1. This suggests that at high concentrations corrosion inhibitor 1 may be the dominant surface interaction in formulations.

Samples containing high levels of dispersants were next analysed, however they were

Table 10.3: Full formulation additive levels for samples with high levels of corrosion inhibitor 1 and the simple additive combinations they were matched with

Sample number	Corrosion inhibitor 1	Corrosion inhibitor 2	Dispersant 1	Dispersant 2	Detergent 1	Detergent 2	Antioxidant	Antiwear	Friction modifier
Corr inhib 1 & corr inhib 2	0.5	0.05							
-778	0.5	0.013	2.5	2.5			0.06	0.11	1.2
Corr inhib 1 & dispersant 1	0.5		5						
Corr inhib 2 & dispersant 1		0.05	5						
-781	0.5	0.026	5			0.4	0.33	0.22	0.1
Corr inhib 1 & dispersant 1	0.5		5						
-799	0.5		5		0.2	0.2	0.06	0.11	0.1
Corr inhib 1 & dispersant 2	0.5			5					
Corr inhib 1 & corr inhib 2	0.5	0.05							
-810	0.5	0.026		5	0.2		0.06	0.22	0.1

unable to be matched closely with any of the simple additive combination surfaces. The remaining samples were then examined to see if any could be matched with the simple additive combinations.

Sample -793 showed close matches with both corrosion inhibitor 1 with dispersant 1 and also dispersant 1 with dispersant 2. The SEM of these sample surfaces are shown in Figure 10.3, with the formulations shown in Table 10.4.

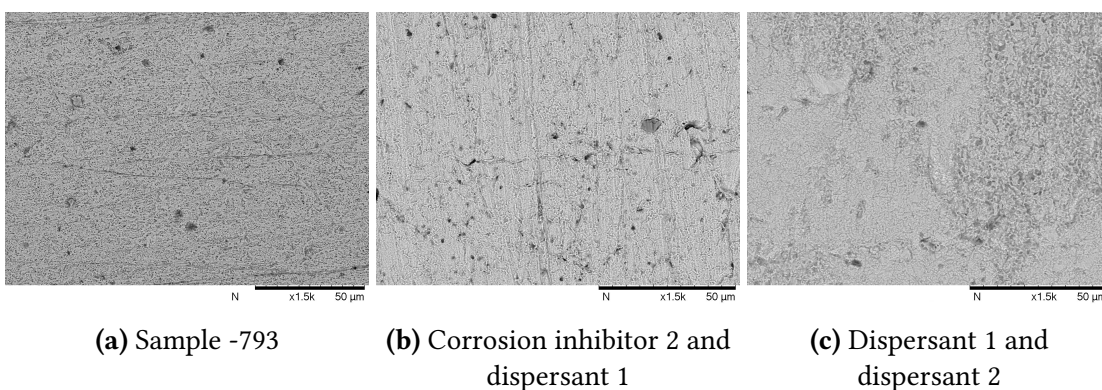


Figure 10.3: SEM images of sample -793 and the simple additive mixtures it was matched with

Table 10.4: Additive breakdown of formulation -793 and the simple additive combinations which matched the surface

Sample number	Corrosion inhibitor 1	Corrosion inhibitor 2	Dispersant 1	Dispersant 2	Detergent 1	Detergent 2	Antioxidant	Antiwear	Friction modifier
Corr inhib 2 & dispersant 1		0.05	5						
Dispersant 1 & dispersant 2			5	5					
-793	0.03	0.026	3.33	1.67	0.2		0.6	0.11	0.1

The images do not match as well as previous ones, however this is explained by looking at the formulation in more detail. Sample -793 has a high number of additives present in the formulation. None of the additives are at the same level as those tested in the simple additive combinations, consequently the match is not as good. However the surface does show enough of a match with the simple additive combinations stated, particularly dispersant 1 and dispersant 2.

Sample -796 could also be considered to match the simple combination of dispersant 1 and detergent 2. Again this is a poor match compared to previous samples, as seen in Figure 10.4.

Again the formulations contains many additives none of which are at the same level as the simple additive combination, as shown in Table 10.5.

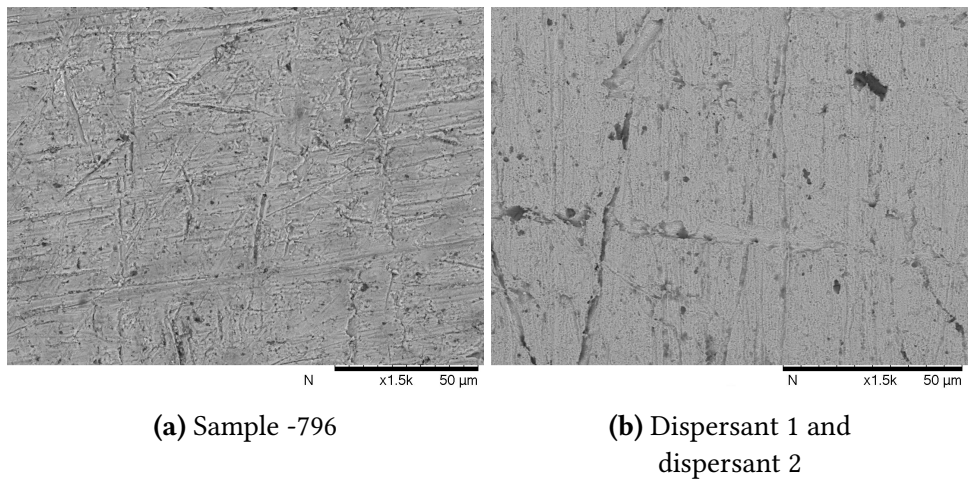


Figure 10.4: SEM images of sample -796 and the simple additive mixtures it was matched with

Table 10.5: Additive breakdown of formulation -793 and the simple additive combinations which matched the surface

Sample number	Corrosion inhibitor 1	Corrosion inhibitor 2	Dispersant 1	Dispersant 2	Detergent 1	Detergent 2	Antioxidant	Antiwear	Friction modifier
Dispersant 1 & dispersant 2		0.05	5						
-796	0.03		2.5	2.5	0.2	0.4	0.06	0.22	0.65

Sample -798 contains all of the additives tested in this study, but matches most closely with combinations containing corrosion inhibitor 1, as shown in Figure 10.5. Interestingly corrosion inhibitor 1 is not present at its highest level of 0.5 wt%, but at a reduced level of 0.265 wt%. The other additives present are also not present at their highest concentrations, with the exception of detergent 2. This could explain why the corrosion inhibitor 1 and dispersant 2 surface gives the best match to sample -798.

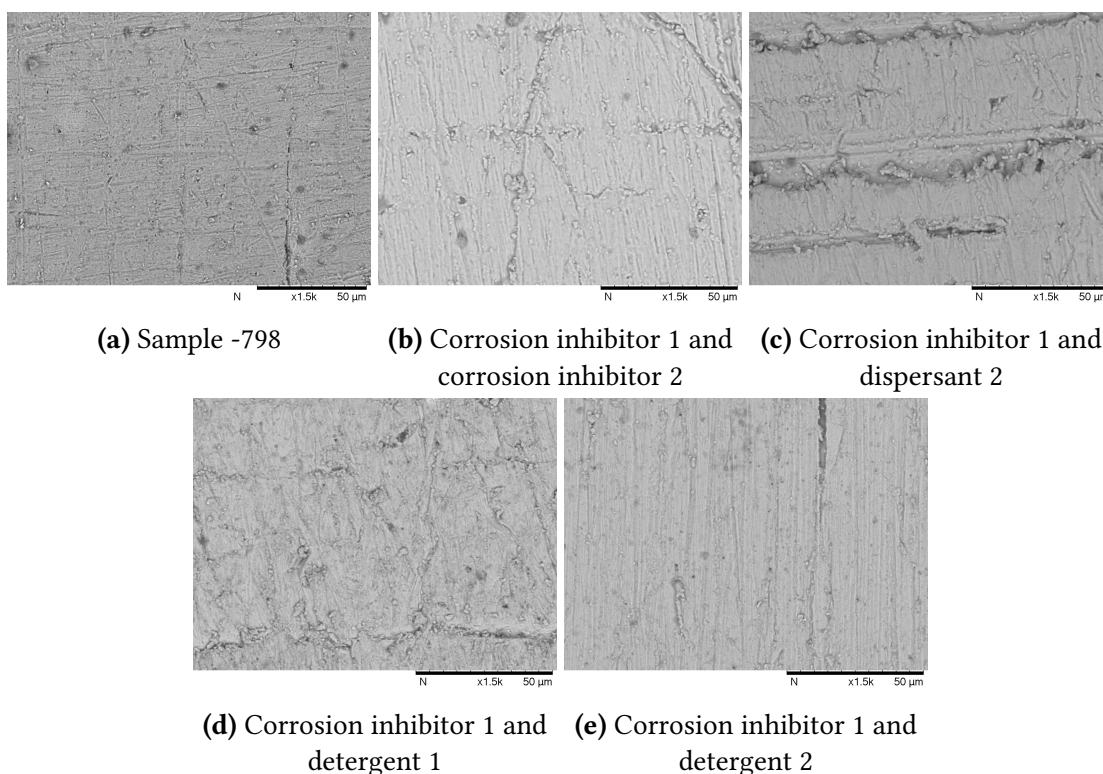


Figure 10.5: SEM images of sample -798 and all the simple additive mixtures it was matched with

A number of the full formulations samples could not be matched with simple additive combinations; their formulations are shown in Table 10.6. These formulations generally

have low levels of corrosion inhibitor 1 and the concentration of other additives vary from those tested in the simple additive combinations.

Table 10.6: Full formulations that did not show similarities in their SEM images with those of the simple additive combinations

Sample number	Corrosion inhibitor 1	Corrosion inhibitor 2	Dispersant 1	Dispersant 2	Detergent 1	Detergent 2	Antioxidant	Antiwear	Friction modifier
-776	0.03			5	0.2		0.33	0.11	1.2
-777	0.03	0.026	5		0.1		0.06	0.22	1.2
-782	0.03						0.06	0.165	0.1
-794	0.265	0.026			0.2	0.4	0.06	0.11	1.2
-797	0.5	0.026	2.5	2.5	0.2	0.4	0.6	0.165	1.2
-806	0.03		5			0.4	0.6	0.11	1.2
-807	0.03	0.013			0.2	0.4	0.6	0.22	0.1
-808	0.03	0.026		5		0.2	0.6	0.22	1.2
-809	0.03	0.026	1.67	3.33		0.4	0.06	0.11	0.1
-811		0.026	5			0.4	0.33	0.22	0.25

10.2 Summary

- Effects seen on the surface of full formulation samples can often be explained by looking at the surfaces of simple additive combination samples and visually matching them.
- Matches are generally seen for the additives which are present at the highest concentrations in the full formulation fluid.
- The best matches are seen when additives in the full formulation fluid are at the same concentration as the components in the simple additive mixtures.
- The more additives present in a combination the more difficult it is to match the surface with a simple additive combination.
- The greater the concentration deviation from the simple additive combination the more difficult it is to find a match for the full formulation sample.

11: Discussion

This section shall give a discussion on the main findings of the study. It shall start with an evaluation of the ASTM D130 standard test method, which is widely used in industry, with the wire resistance test used in this study. It will then go on to look at the other test methods used in this study and how the different results obtained from these compare; specifically whether they predict the same level, or order, of corrosion.

Focus will then be placed on the effect of temperature on the interaction between copper and the individual additives and simple additive mixtures. The corrosion rate of these fluids will also be examined.

More detailed analysis will then look at the behaviour of the individual additives and how they interact with the surface.

11.1 Evaluation of the ASTM D130 standard test method and the wire resistance test

The ASTM D130 [84] is an industry standard test which looks at the corrosiveness of petroleum products to copper. The scope of the test method covers a wide variety of fluids from aviation fuel to lubricating oil. The test was originally developed to look at the impact of any residual sulfur left in the fluid after the refining process. The problem is that nowadays many lubricating fluids, and in particular ATFs, have negligible amounts of sulfur yet the same test is used to determine their corrosiveness. The test places a clean copper coupon into a specified volume of fluid which is heated to 150 °C for 3 hours. At the end of this time the copper strip is removed, rinsed and rated against a set of corrosion standards. The standards are 13 lithographed strips which are reproductions

in full-colour of typical test strips encased in plastic to protect them. This makes comparison harder as corroded or tarnished test pieces are compared with what is essentially a photograph printed on metal. Each strip represents a degree of tarnish or corrosion and is allocated a specific number and letter, 1a through to 4c.

The 3 hour test duration can pose a question as to the usefulness of the test. The results shown in Chapter 9, Table 9.1, show that after 3 hours there is little differentiation between the samples tested in single additive fluids. This is not a particular problem as it is feasible that the fluids may all be non-corrosive over this time period. The greater worry is that the samples look very different after 200 hours compared to 3 hours. If a sample were to pass after 3 hours would it be representative of the sample after a longer period of time. Many of the wire experiments show minimal to no change in the first 3 hours, but corrosion can then be seen to occur later in the test. For example the wire radius data for dispersant 1, Figure 7.18, begins to show significant change after 25 hours. SEM images of the surfaces of samples tested in dispersant 1 show nothing of interest after 3 hours but severe etching after 200 hours, Figure 9.2. The short test duration of the ASTM D130 may therefore be giving results which are passable, but over longer exposure times could be problematic.

The rating is a visual inspection of the sample surface only, which means that the results can be subjective depending on the experience of the person and the light conditions used. Within a lab this is minimised as the same person will often carry out the rating under controlled conditions, such as in a light box. However there may be fluctuations between laboratories. The standards are printed to represent the tarnish seen, which means that there can be difficulties in matching the coupons with them. It has also been seen that it is possible to achieve some colours on the coupons which are not present on the standard strip ratings.

As the test is purely visual it does not give any information as to why the fluid may have failed [57]. It is possible that some fluids may form protective films on the copper surface after which there is no further change. If the film is dark it is likely to be rated poorly and fail, even though it may actually be providing protection to the copper surface. Alternately it is possible that the copper surface is constantly corroded

throughout the test leaving a bright shining surface which would be rated favourably. If this fluid was to be used in a real life situation it is possible that failure could occur due to the corrosion of the surface.

One such example of this in the literature is in a study conducted by Rathgeber et al. [11] in which copper strips are stored in different ATFs for 1000 hours. This study did not use the ASTM D130 test method but images of the test coupons are shown. After testing in ATF A the copper piece is dull and would receive a poor ASTM rating, as shown in Figure 11.1a. In ATF B, Figure 11.1b, the test piece is bright and would receive a much better rating.

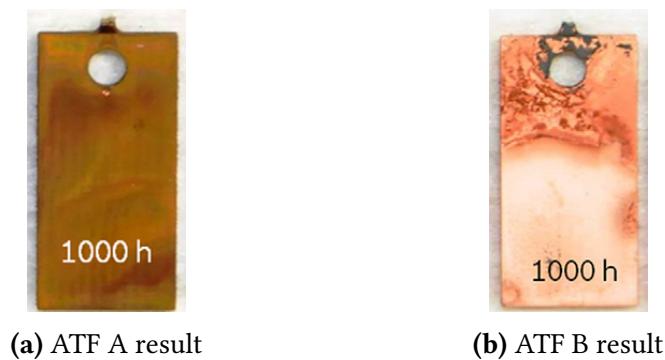


Figure 11.1: Coupons tested for 1000 hours in two different ATFs by Rathgeber et al. [11]

The study conducted by Rathgeber et al. showed that the dull looking test piece forms a robust reaction layer and prevents copper from leaching into the solution, the brighter piece however is unable to form this layer and the amount of solved copper is far higher (2000 mg/kg compared to 80 mg/kg).

Figure 11.2 plots the radius loss of the copper wires against the rating obtained on the equivalent coupon, both the wire and coupon were tested in the same beaker for the same length of time. Two points are not shown due to the scaling of the graph, these correspond to samples which gave ratings of 2e and 4b which had radius losses of 6.76 μm and 8.92 μm respectively.

As can be seen from this graph generally samples with lower ratings have lower radius loss. At higher ratings the spread of radius loss data is far greater. This shows that higher ratings do not always lead to high copper loss and so can be misleading with

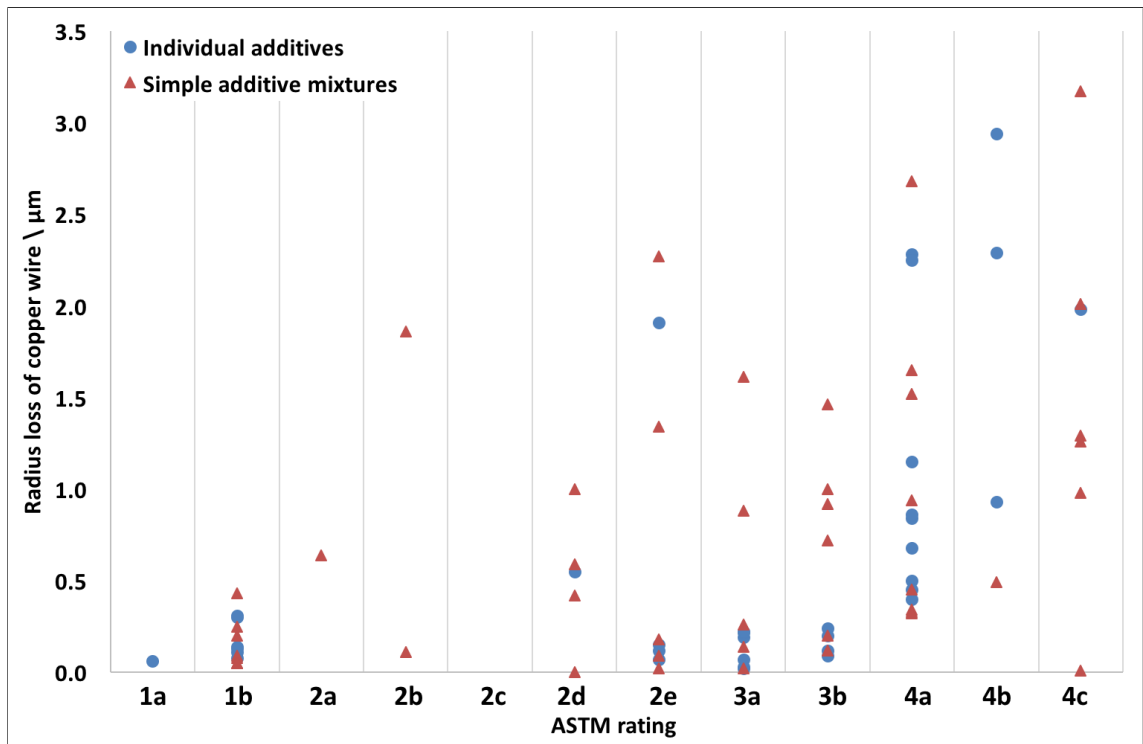


Figure 11.2: The radius loss of copper wires after approximately 300 hours plotted against the coupon rating for wire-coupon tests conducted in individual additives and simple additive mixtures across all temperatures

dull surfaces able to provide protection to the surface; the samples with ratings of 2e, 3a and 3b are examples of this with most of the radius loss clustered below $0.5 \mu\text{m}$.

The ASTM D130 test is also limited in that it provides information about only one time point, at one temperature. It is possible that in the 3 hours of the test a fluid behaves well but if the copper were to be immersed for longer periods of time the fluid may fail, due to the build up of corrosive degradation products in the fluid for example.

The $150 \text{ }^\circ\text{C}$ temperature at which the test is conducted is far higher than would normally be found in a transmission, running temperatures below $100 \text{ }^\circ\text{C}$ are more likely. It is thought that higher temperatures accelerate the rate at which a process occurs but this only applies if the mechanism does not change, as was also shown by Rathgeber et al. [11].

As the ASTM D130 test lasts for 3 hours it is a relatively quick test that could be used to screen fluids, however it is worth considering if there is any other useful data which could be gathered to give more information on the way that the fluid is interacting with the surface. The wire tests described in this study provide in-situ information on the interaction of the fluid with the copper surface. Although they take longer to run more

information is available, particularly when the copper coupons are also used allowing surface analysis to be more easily undertaken.

This duration of the wire tests used in this study varied from 10 days, when looking at the initial formulation fluids, to 14 days for the individual additives. Hunt et al. [116, 122, 123] have a number of papers which use this method with the test duration varying between 180 hours (7.5 days) and 10 days; however the data for many of the fluids begin to plateau earlier than this, which was also seen in this study. Depending on the information required from the test it may be possible to run the test for as little as 5 days. However, the longer the test is run the greater the differentiation between samples and the greater confidence that further change is unlikely.

One downside to the wire test method is the sensitivity of the test to external movement. Further investigation into unusual spikes seen in data found that the tests were disturbed by vibrations from the cleaners mopping the floor, drilling in an office adjacent to the fume cupboard as well as the opening and closing of the fume hood sash. Once identified these disturbances were able to be eliminated; no testing was carried out when drilling or other building work was ongoing and the fume cupboard sash was closed once the test was started and not opened again until the end of the test. The cleaners mopping only caused minor disturbances in the data acquisition and would occur only once during the test. Any fluctuations in the data appeared to return to expected levels in around an hour, it could however be problematic if disturbances were caused at the end of the test, however this was not seen for any of the samples in this study. The reason for this sensitivity is thought to be the size of the wires; very thin wires are used as pressure sensors as their sensitivity to pressure changes is greater than thicker wires [143]. Thin wires are used in this test so that the change in the radius is significant, compared to the overall size of the wire, and therefore easier to measure.

The wires can be difficult to handle due to their small size and care must be taken not to introduce strain; knotting is also a distinct possibility. Surface analysis can be difficult to conduct, not only due to the wires size but also its curvature. Many techniques, such as XPS, can be sensitive to changes in the height of surfaces, giving incorrect results. However the benefits of having in situ measurements for the corrosion of the copper is

far greater.

Although both the ASTM D130 and the wire test have their own problems combining them can give good results; the wire-coupon method did this. This allowed in situ measurements from the wire to be taken, giving an idea of the interaction between the fluid and the copper with time. The coupon was easier to handle and made surface analysis simpler. This combined test also gave more data; the rating could still be obtained from the coupon, as well as weight change measurements although these could be inaccurate depending on the deposits formed. ICP on the end of test fluid was also carried out to evaluate the amount of copper present. The radius change data from the wire is a good addition able to provide in situ information.

11.2 Correlation of full formulation results to the additives present in their formulations

In order to try and determine which additives were causing the effects seen during full formulation investigations the results were compared in a number of different ways, to see if samples which showed similar results had similar additives present in their formulations.

Table 11.1 shows the additives present in each formulation, grouped by ASTM rating. There are no definitive correlations between the rating and the additives present in the formulations.

At first it does seem that there may be similarities within each rating group, for example the samples with a 1a rating both contain 0.026 wt% of corrosion inhibitor 2, 5 wt% dispersant 1, no dispersant 2 and 0.22 wt% antiwear; however it is easy to find similarities in a set of two. The group containing samples with a 3a rating is more difficult to find similarities within.

Generally samples containing higher levels of corrosion inhibitor 1 have more severe ratings, particularly when corrosion inhibitor 2 is not present. However when this is scrutinised in more detail it is not always true, for example sample -799 contains 0.5 wt% of corrosion inhibitor 1, no corrosion inhibitor 2 and a low rating of 2b. The formulations

Table 11.1: Formulations grouped by rating for all full formulation coupons run

Sample number	Concentration of Additive (wt%)									Rating
	Corrosion inhibitor 1	Corrosion inhibitor 2	Dispersant 1	Dispersant 2	Detergent 1	Detergent 2	Antioxidant	Antiwear	Friction Modifier	
-777	0.03	0.026	5	0	0.1	0	0.06	0.22	1.2	1a
-811	0	0.026	5	0	0	0.4	0.33	0.22	0.25	1a
-806	0.03	0	5	0	0	0.4	0.6	0.11	1.2	1b
-794	0.265	0.026	0	0	0.2	0.4	0.06	0.11	1.2	2b
-792	0.265	0	2.5	2.5	0	0	0.6	0.22	0.1	2b
-799	0.5	0	5	0	0.2	0.2	0.06	0.11	0.1	2b
-782	0.03	0	0	0	0	0	0.06	0.165	0.1	2c
-796	0.03	0	2.5	2.5	0.2	0.4	0.06	0.22	0.65	2d
-807	0.03	0.013	0	0	0.2	0.4	0.6	0.22	0.1	2e
-778	0.5	0.013	2.5	2.5	0	0	0.06	0.11	1.2	3a
-810	0.5	0.026	0	5	0.2	0	0.06	0.22	0.1	3a
-798	0.265	0.013	2.5	2.5	0.1	0.2	0.33	0.165	0.65	3a
-797	0.5	0.026	2.5	2.5	0.2	0.4	0.6	0.165	1.2	3a
-808	0.03	0.026	0	5	0	0.2	0.6	0.22	1.2	3a
-809	0.03	0.026	1.67	3.33	0	0.4	0.06	0.11	0.1	3a
-779	0.5	0.026	0	0	0	0	0.6	0.11	0.65	3b
-781	0.5	0.026	5	0	0	0.4	0.33	0.22	0.1	3b
-783	0.5	0	0	5	0.1	0.4	0.6	0.11	0.1	3b
-793	0.03	0.026	3.33	1.67	0.2	0	0.6	0.11	0.1	3b
-776	0.03	0	0	5	0.2	0	0.33	0.11	1.2	4a
-795	0.5	0	2.5	0	0.2	0	0.6	0.22	1.2	4b
-780	0.5	0	0	2.5	0	0.4	0.06	0.22	1.2	4c

are complex so it is difficult to say with any certainty that the presence, or lack, of certain additives causes a specific rating.

FTIR spectra and SEM images were taken of the surface to provide further information on the sample surface. FTIR spectra grouped according to similarities in their peaks showed little correlation in the corresponding formulations, as shown in Chapter 5.5. When grouped by surface features, identified using SEM, correlations in the formulations again proved difficult to spot; however one correlation was found.

Three of the samples were seen to have flaking surfaces. Flaking is reported in literature when layers of copper sulfide are formed on the surface [26]. Demirkan et al. [50] found this corrosion product to become worse with longer exposure to the sulfur containing environment. The fully formulated fluids contain very little free sulfur; due

to the base oil having less than 0.03 % sulfur content. However sulfur is contained within the molecular structure of corrosion inhibitor 1, dispersant 2 and detergent 1.

Examining the formulations of the flaking samples showed none of them contained corrosion inhibitor 2, which is the benzotriazole based molecule. Looking at all other samples with no corrosion inhibitor 2 in their formulation it was found that the samples which flaked had higher levels of corrosion inhibitor 1 (thiadiazole) and dispersant 2 (quaternary amine). A schematic of this can be seen in Figure 11.3 where the SEM images of sample surfaces containing no corrosion inhibitor 2 have been plotted based on their levels of corrosion inhibitor 1 and dispersant 2. It is possible that there is an interaction which takes place between corrosion inhibitor 1 and dispersant 2 when corrosion inhibitor 2 is not present causing the formation of copper sulfide on the surface, which then causes the flaking seen on the surface.

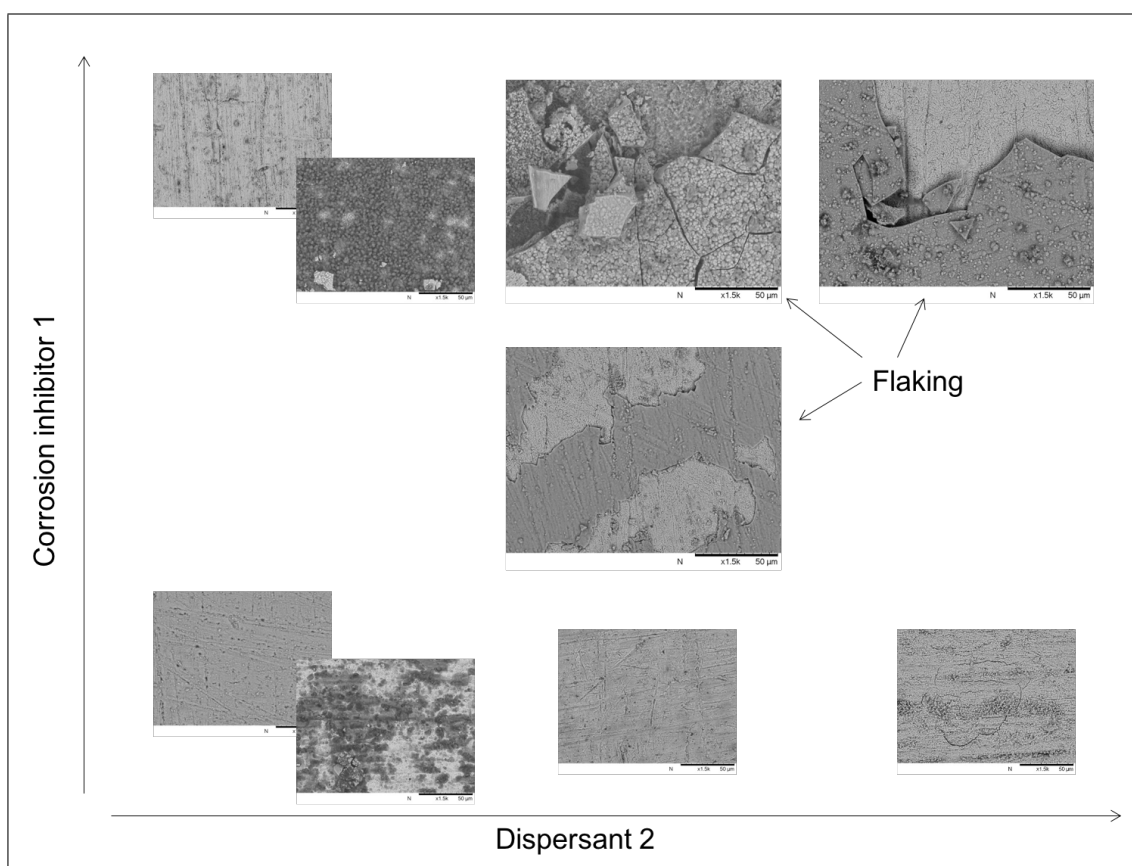


Figure 11.3: Schematic of samples containing no corrosion inhibitor 2 and their corresponding levels of corrosion inhibitor 1 and dispersant 2 showing that higher levels of corrosion inhibitor 1 and dispersant 2 lead to flaking of the surface film on the sample

Corrosion inhibitors and dispersants are the most surface active additives in the formulations and so should have the greatest effect on the surface. Dispersants are

designed to keep particles, such as soot, suspended in the fluid [147]. From the results it was thought that the dispersants may play a part in the amount of copper measured in the end of test fluid. To see if this were true modifications were made to the additive levels of a number of full formulations to vary the concentration of dispersant 1 and dispersant 2, as described in Chapter 5.

The addition or removal of dispersant from full formulation fluids has an impact on the amount of copper measured in the end of test fluid. Figure 11.4 shows the effect of dispersant on the amount of copper in the end of test fluid (A), and the ASTM rating (B). In almost all cases the presence of dispersant gives a higher amount of copper in the end of test fluid and a higher ASTM rating. With the greatest changes observed for variations of dispersant 2.

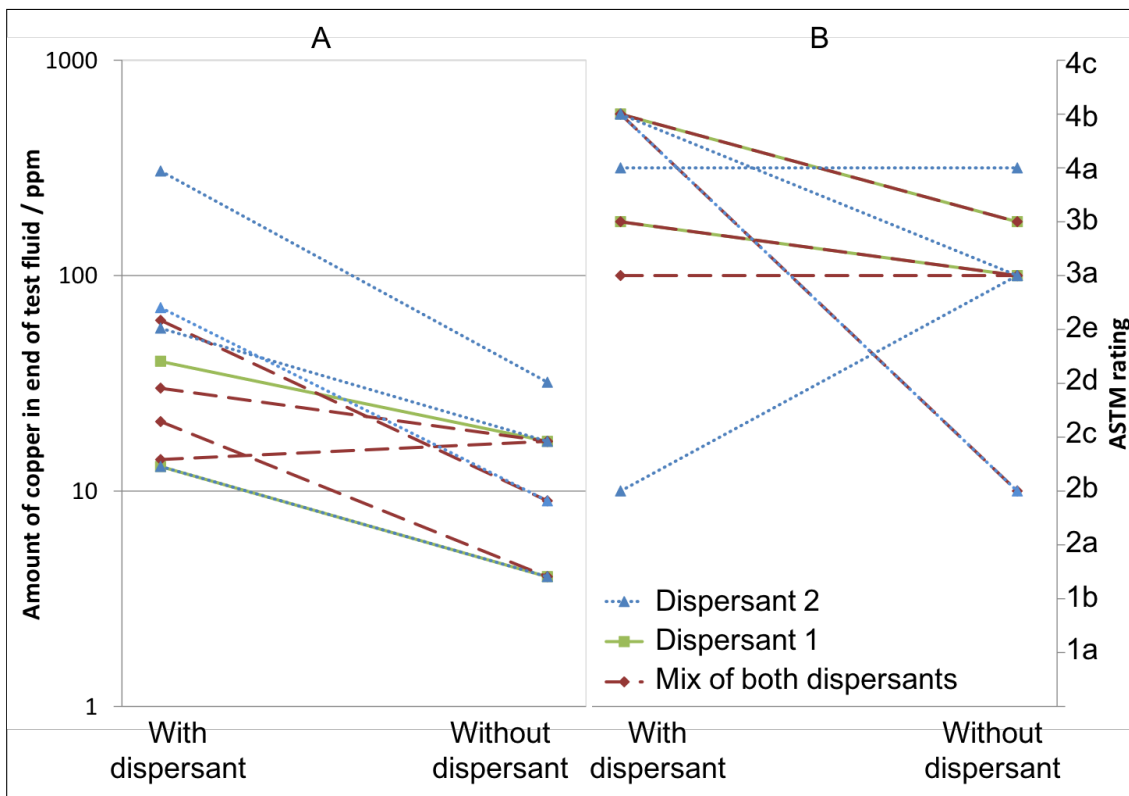


Figure 11.4: The effect of dispersant in fully formulated fluids on (A) the level of copper in the end of test fluid, and (B) the ASTM rating

Immersion tests on dispersants alone showed that they are only slightly corrosive towards copper with copper levels increasing from 4 ppm in the base oil alone to 13 ppm when dispersant was present, as seen in Figure 5.17, Section 5.7.1. The increased levels of copper in the other samples are likely as a result of other components in the formulation being corrosive.

The dispersant could act in a number of different ways to increase the copper level:

- Suspension of surface corrosion layer
- Suspension of degradation products
- Attack of exposed surface

If a copper containing corrosion layer is formed on the surface it is possible that the dispersant could be removing this layer, but this would only likely be the case if it was poorly adhered to the surface.

The dispersant may be suspending degradation products which would otherwise deposit on the surface and therefore could act as a passivating layer. Without these surface deposits the surface could be more exposed allowing more copper to be leached to the fluid.

Alternatively an unstable reaction layer could be produced which naturally flakes off the surface and exposes more copper, which is in turn attacked by the dispersant pulling more copper into solution. A similar effect was reported by Rathgeber et al. [11] who found that copper coupons tested in different ATFs could produce stable and unstable reaction layers, depending on the formulation. Unstable layers were liable to flake off the surface and consequently led to higher levels of copper in the end of test fluid.

SEM images of samples tested in formulations with no dispersant showed deposit like particles on the surface; when dispersant was present, these particles did not appear (Chapter 5, Figures 5.18–5.26). This makes the suspension of degradation products one of the more plausible options, the lack of deposit on the surface could in turn lead to greater leaching of the copper into the fluid.

Changes to the ASTM rating are not as clear but were generally seen to be lower when dispersant was not present. This shows a further limitation of the ASTM D130 test; the improvement in the copper level is not matched by an improvement in the rating.

The complexity of full formulation fluids and the lack of information provided by the ASTM D130 test meant another technique was needed to try and elucidate the interactions between ATF additives and the copper surface.

After individual additives and simple additive mixtures had been investigated the

SEM images of the coupon surface were compared to those tested in full formulations, as detailed in Chapter 10. It was found that effects seen on the surface of full formulation samples could often be explained by looking at the simple additive mixtures. The more additives present in a formulation and the greater the deviation in concentration from the simple additive mixture the more difficult it became to explain which additives were causing the effects seen on the surfaces. However generally the additives present in the formulation at the highest concentration had the greatest impact on the coupon surface.

11.3 Correlating the radius loss of copper wires to other test results

It was difficult to correlate the ASTM ratings with other results which could measure corrosion such as the amount of copper in the end of test fluid or the weight change of the coupons, as shown in Chapter 5, Sections 5.1–5.3; however the copper level and the weight change of the coupons were found to correlate well to each other (Section 5.3).

The radius change of a copper wire should give a better indication of corrosion than the ASTM D130 test and should also correlate to other results, such as weight change and amount of copper in the end of test fluid.

For the full formulations investigated, the amount of copper was measured in the end of test fluid after the coupon tests. Wire tests were conducted separately but the two measurements should correlate, assuming all the copper that is measured as a decrease in the radius is removed; as opposed to being incorporated into a corrosion layer which remains on the surface but is not conductive and therefore not measured in the wire test.

Figure 11.5 shows the radius loss of the copper wires plotted against the amount of copper measured in the end of test fluid after the full formulation coupon immersion tests.

Two correlations were identified and have been plotted as red squares and blue circles, each with a line of best fit, in Figure 11.5. One sample, indicated with the green triangle, was not seen to fit with either correlation and so has not been included with the best fit lines but has been kept on the plot for completeness.

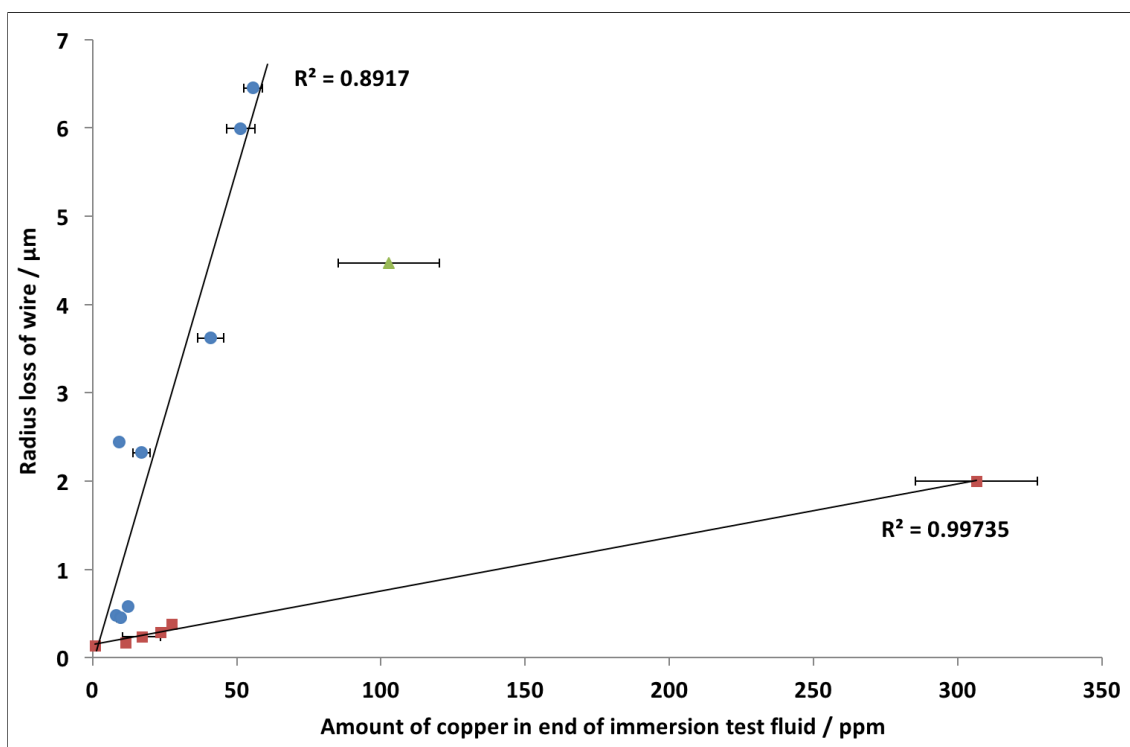


Figure 11.5: Radius loss of copper wire plotted against the amount of copper measured at the end of the coupon immersion test for full formulation fluids

One sample seems to give a very high level of copper despite its low radius change. This sample, -776, gave an end of test copper level of 306 ppm and a radius loss of 2 µm. This sample fits with the correlation indicated by red squares, but has already been identified as different to other samples as SEM of its surface showed it to be very uneven, covered in lots of small particles but with cracks and holes present across the surface, as shown in Chapter 5.6.4. FIB was used to create a cross section and EDX showed copper and sulfur to be the main components of the surface layer. The exact chemical composition of this layer could not be determined but copper sulfide is known to be partially conductive [50, 66, 148]. If the corrosion layer is copper sulfide and able to conduct a charge then this could explain why the radius change of the copper is less than that suggested by the amount of copper in the end of test fluid.

The formulations for each of these samples are shown in Table 11.2 and coloured, red, blue or green to match. It is immediately obvious that the samples grouped in red have no dispersant 1 present and very little or no corrosion inhibitor 2. Within this grouping those which have higher levels of copper in their end of test fluid also have low levels of corrosion inhibitor 1.

All of these samples (highlighted in red) also show a radius loss of $2\mu\text{m}$ or below. This would suggest that dispersant 1 plays a role in increasing the radius loss of the wires, but the level of corrosion inhibitor also plays a part.

Table 11.2: Formulations grouped according to correlations seen in Figure 11.5

Sample number	Concentration of Additive (wt%)									ICP / ppm
	Corrosion inhibitor 1	Corrosion inhibitor 2	Dispersant 1	Dispersant 2	Detergent 1	Detergent 2	Antioxidant	Antiwear	Friction Modifier	
-795	0.5	0	2.5	0	0.2	0	0.6	0.22	1.2	56
-796	0.03	0	2.5	2.5	0.2	0.4	0.06	0.22	0.65	51
-811	0	0.026	5	0	0	0.4	0.33	0.22	0.25	41
-779	0.5	0.026	0	0	0	0	0.6	0.11	0.65	17
-778	0.5	0.013	2.5	2.5	0	0	0.06	0.11	1.2	12
-798	0.265	0.013	2.5	2.5	0.1	0.2	0.33	0.165	0.65	10
-794	0.265	0.026	0	0	0.2	0.4	0.06	0.11	1.2	9
-792	0.265	0	2.5	2.5	0	0	0.6	0.22	0.1	8
-776	0.03	0	0	5	0.2	0	0.33	0.11	1.2	306
-808	0.03	0.026	0	5	0	0.2	0.6	0.22	1.2	27
-782	0.03	0	0	0	0	0	0.06	0.165	0.1	24
-780	0.5	0	0	2.5	0	0.4	0.06	0.22	1.2	17
-783	0.5	0	0	5	0.1	0.4	0.6	0.11	0.1	11
-810	0.5	0.026	0	5	0.2	0	0.06	0.22	0.1	1
-806	0.03	0	5	0	0	0.4	0.6	0.11	1.2	103

From all the data collected so far it is clear that the corrosion inhibitors and dispersants have the biggest impact on the corrosion of the copper surface. The mechanisms involved are discussed in Section 11.5.

The change in radius of the copper wire can be correlated with the amount of copper in the end of test fluid. The copper level in the fluid, weight of a coupon and radius change of a wire were recorded at eight different time points for samples tested in formulations -806, -779, -780 and -811 to see how the results correlated over time. Figure 11.6 shows the weight change of the coupons as the experiment progresses; the radius of the copper wire at each point is also plotted. These results were initially shown individually in Section 6.

The weight change of the coupons is large for -811 and -806. The profile of the weight change appears similar to the change in radius of the wire for these samples. Coupons

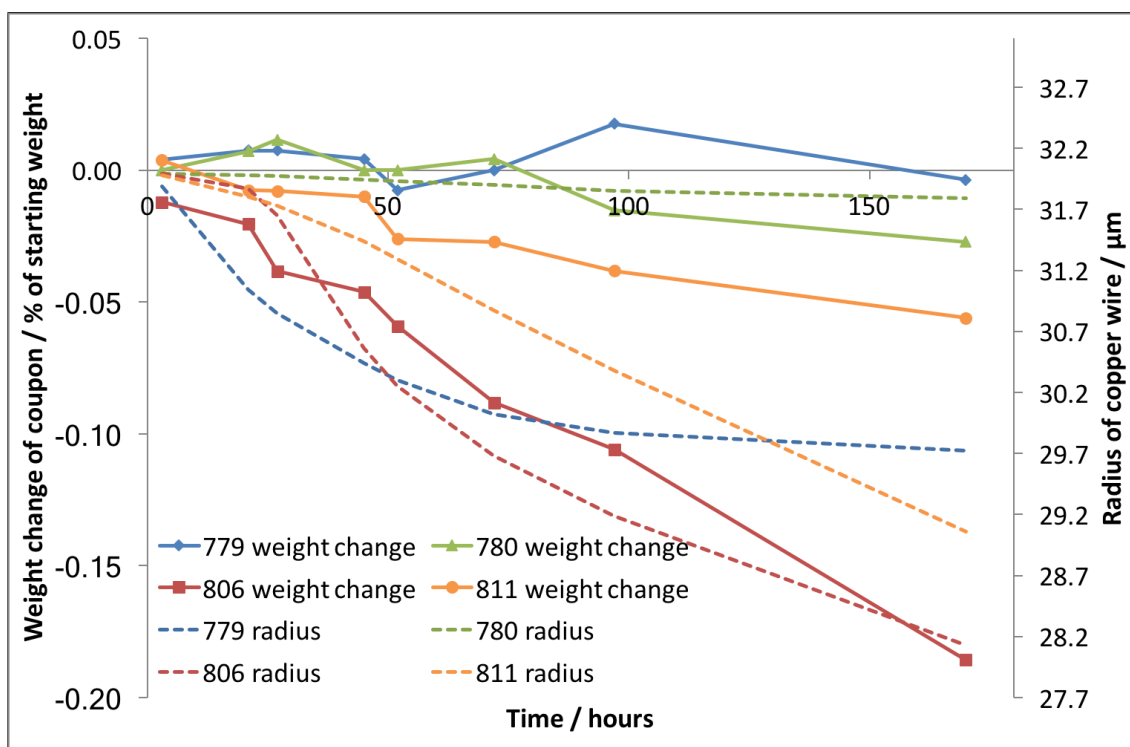


Figure 11.6: Weight change for the coupons at each specified time point in the experiment at 130 °C, recorded as a percentage of the start weight of the coupon

immersed in -811 show a constant steadily decreasing radius and weight change; although the two do not overlay this is due to the way the two graphs are scaled and overlaid.

Coupons immersed in -780 show little change in weight or radius. However coupons tested in -779 show very little weight change yet there is a fairly significant change in the radius of the copper wire over the course of the experiment. This suggests that a non-conductive film is likely to be being formed on the surface hence the weight is not decreasing in the same manner as the radius.

It is interesting to see that in some cases the trend in the radius change of the copper wire is mirrored by the trend in the weight change of the coupon. What is more interesting is when these changes are not the same as it tells us about possible film formation on the surface.

In Figure 11.7 the amount of copper in the fluid, measured by ICP is plotted, along with the radius of the copper wire, which overlay very well. This shows that in these formulations the decrease in radius of the wire is primarily due to loss of the copper to the fluid, rather than incorporation into a non-conductive layer. For sample -779 this is

in contrast to results seen with the weight change of the coupon which suggested the sample may have a non-conductive layer formed on the surface, as little weight loss was seen. As there is copper lost to the fluid it is then possible that the lack of weight change of the coupon is due to deposition of degradation products from the fluid.

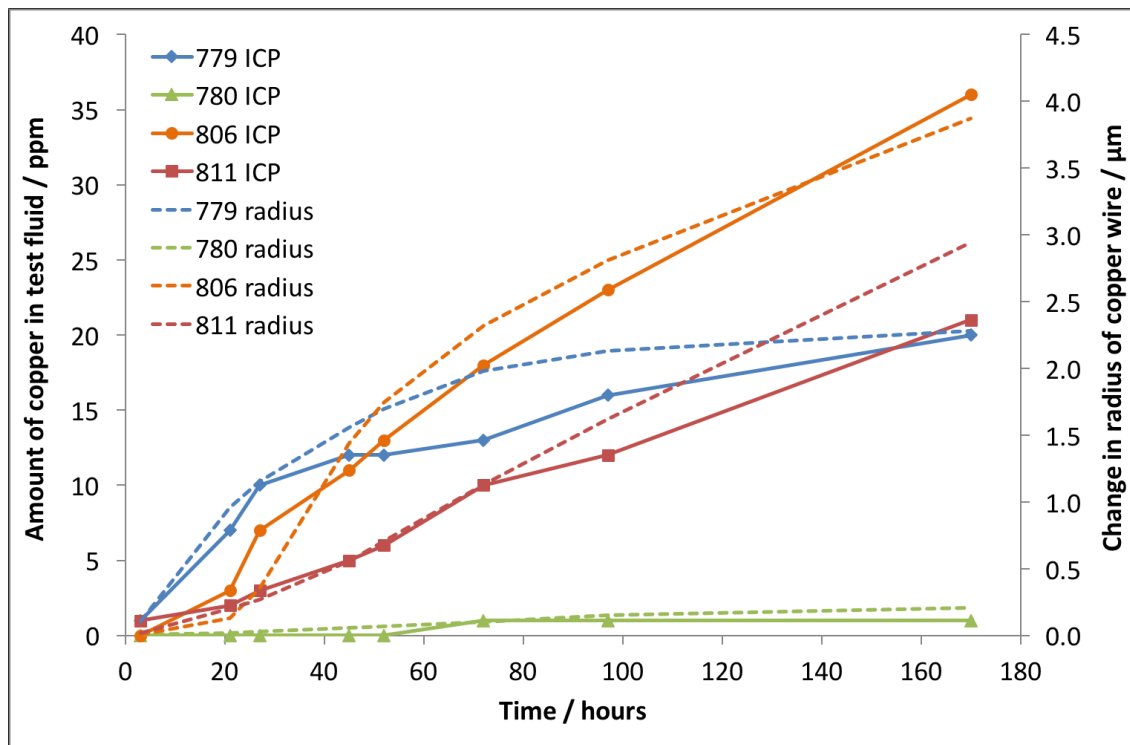


Figure 11.7: Similarities between the amount of copper in the test fluid and the changes in radius of the copper wire for the experiment carried out at 130 °C

It has been seen that the correlation between the radius change data and other corrosion results is fairly good in full formulation fluids. To see if the correlation between radius change and copper level was also true for individual additives and simple combinations relevant data from all of the wire-square tests were plotted.

Figure 11.8 plots the data for individual additives across all temperatures tested. It shows that there is a very good correlation between the amount of copper in the end of test fluid and the radius loss of the copper wire; however there are two outliers to this trend from the data tested at 120 °C. These correspond to the friction modifier and antioxidant additives tested alone. as is seen with most of the samples the radius loss of the wire should be directly related to the amount of copper in the solution, because as copper is removed from the wire it should be taken into solution. In the instance of the friction modifier and antioxidant additives the amount of copper is higher than would

be expected from the given radius. For the copper level to be greater than expected for a given radius loss the copper being removed from the wire would have to be replaced by a conductive layer. This is likely to result in unusual wire radius data, but the results show nothing out of the ordinary. The results for the antioxidant and friction modifier additives can be seen in Figure 7.44 and Figure 7.47 in Chapter 7. This makes it more likely that there was contamination of the ICP when the fluids were run. Further tests would need to be run to confirm this.

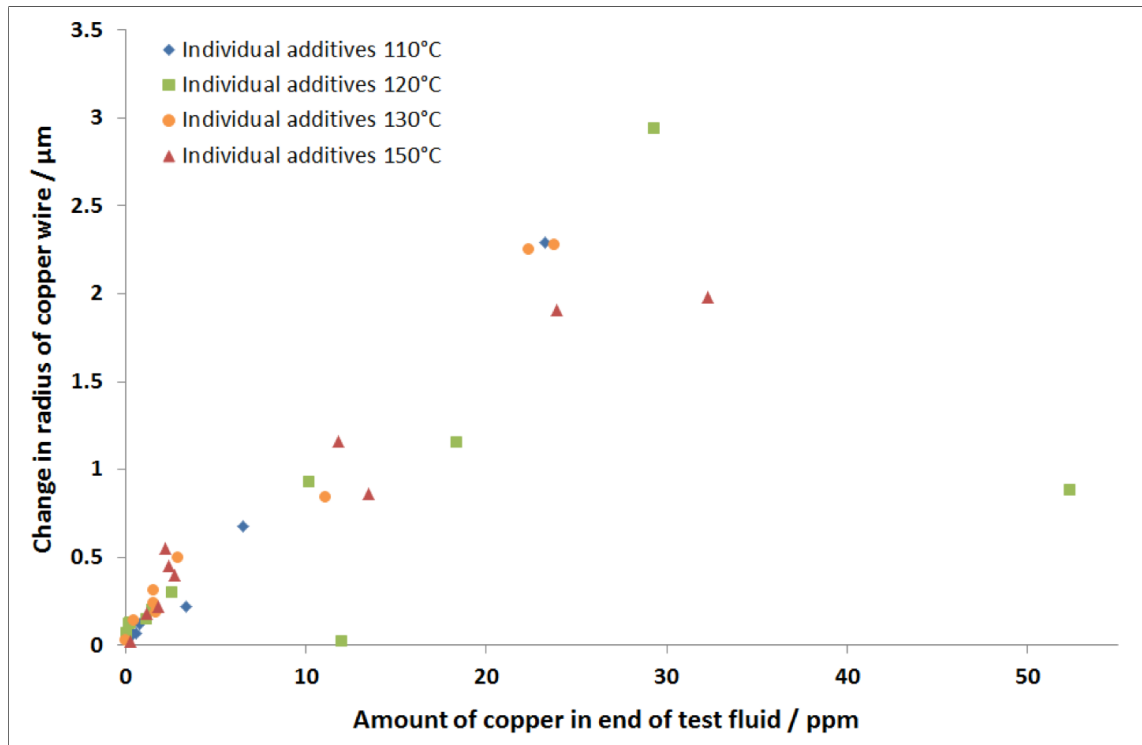


Figure 11.8: Amount of copper in the end of test fluid and the change in radius of the copper wire for all individual additives tested at temperatures between 110 °C and 150 °C

A correlation between the radius change of the wire and the amount of copper in the end of test fluid is also seen for additive combinations, as shown in Figure 11.9. There is one combination which lies far outside of the trend-line; with a high level of copper, 57 ppm, in the end of test fluid but a very small change in the radius of the wire. This corresponds to a sample tested in dispersant 1 and the AO, AW, FM mix at 150 °C. It is possible that the result is anomalous and there was an error in the wire; the copper level results were repeated and found to be the same, but due to time constraints it was not possible to repeat the entire wire test. However if the radius change is correct then the surface of the copper must have a conducting film build up at the same rate

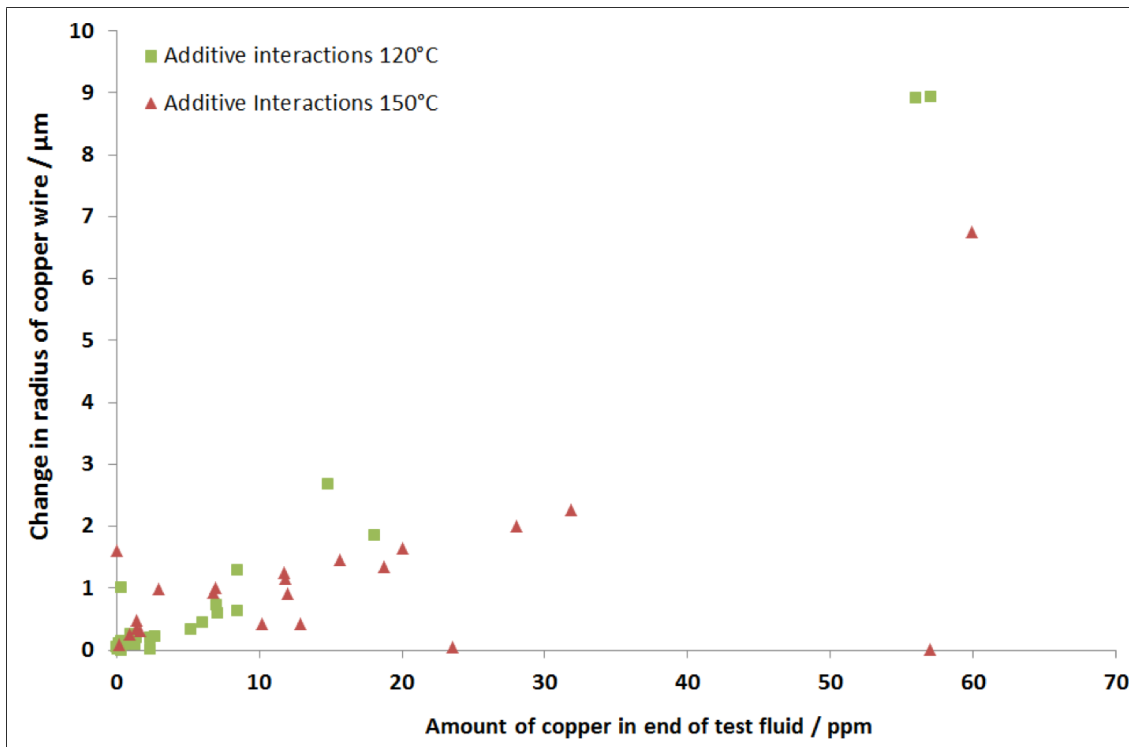


Figure 11.9: Amount of copper in the end of test fluid and the change in radius of the copper wire for all additive combinations tested at temperatures of 120 °C and 150 °C

that copper was removed. The film on the surface was poorly adhered and removed on rinsing making this unlikely and so the result is more likely to be anomalous.

11.3.1 Comparing the amount of copper lost to the amount measured in the end of test fluid

The amount of copper lost from the wire can be calculated by determining the volume of the wire at the start and end of the test and assuming that change is uniform. The concentration of copper in the solution can be calculated as the weight loss of the wire, calculated from radius change, plus the weight loss of the coupon. The total weight loss can be used to determine the concentration of copper in the solution (ppm) using Equation 11.1, where $mass_{solute}$ is the total mass loss of copper (g) and $mass_{solution}$ is the mass of the oil used for testing (g).

$$\text{Concentration} = \frac{1 \times 10^6 \times mass_{solute}}{mass_{solution} + mass_{solute}} \quad (11.1)$$

The concentration of copper in solution has been calculated for each of the individual

additives and additive combinations run and this has been plotted against the amount of copper measured in the fluid at the end of the test using ICP-AES. The two should correlate perfectly if all copper lost from the wire goes into solution.

The results can be seen in Figure 11.10, along with a line which shows very good correlation, the measured copper level appears to be only slightly higher than the calculated copper level and this could be due to the placement of the trend-line. Deviations from this line are likely to be caused by the fact that not all coupons measure a weight loss. Some coupons show weight gain which is most likely through formation of a surface film. This weight gain has been used to calculate the total weight change for the combined wire and coupon and hence some calculated copper levels are negative, this would not be possible in real life.

There are only two major outliers in this data, both of which show higher measured copper levels than calculated levels. The ICP measurements were repeated in order to check these results and were consistent each time; which makes it unlikely that there was contamination from the machine. On further cross-referencing these two samples are the friction modifier tested alone at 120 °C and dispersant 1 and the AO, AW, FM mix at 150 °C previously highlighted as outliers in Figure 11.8 and 11.9.

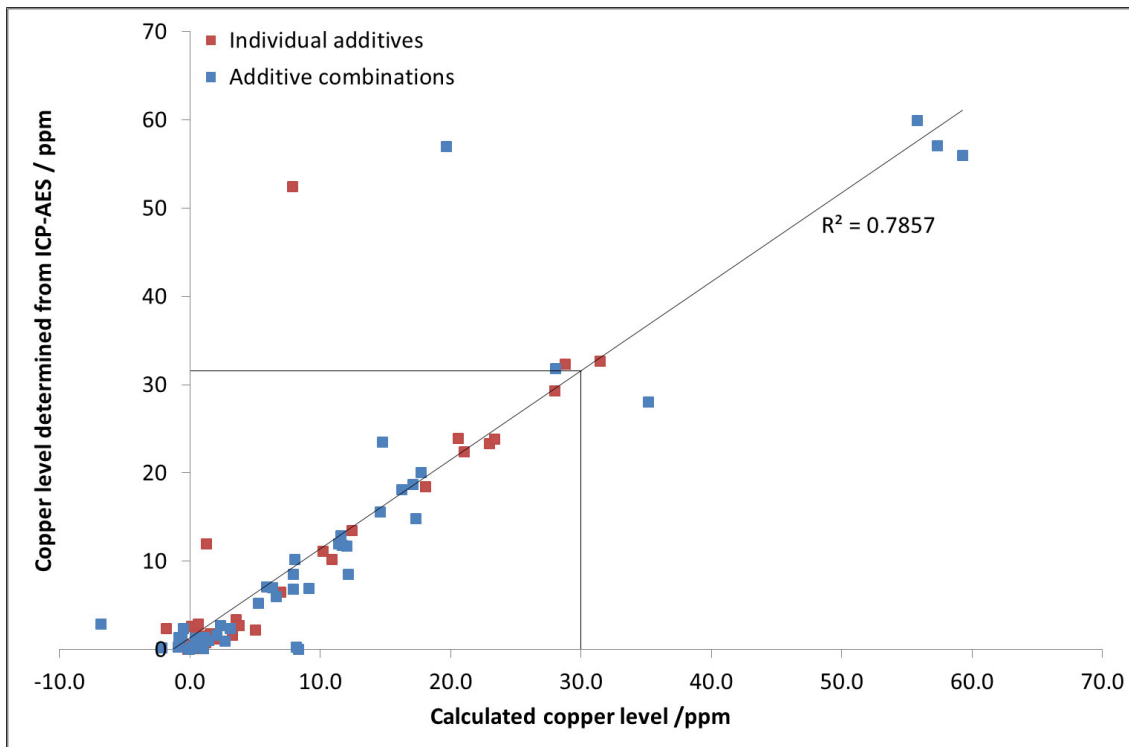


Figure 11.10: Copper levels in end of test fluids determined by ICP-AES against the calculated level of copper determined form weight loss of coupons and radius loss of wire

11.4 Effect of temperature

The ASTM D130 test is most often run at 150 °C as this is thought to accelerate the corrosion process, however most transmissions would not get this hot, so it is not true to life. One element of this study looked at how the additives interacted with copper at different temperatures.

The wire-coupons test used individual additives run at 110 °C, 120 °C 130 °C and 150 °C to determine the effect of temperature on the corrosion of copper; by monitoring the change in radius, rating and amount of copper in the end of test fluid.

Images and ratings of the surfaces did not show a uniform trend. In some cases the rating got worse with increasing temperature, some did not change and in the case of the AO, AW, FM mix the rating improved with increasing temperature, these results are shown in full in Chapter 7.

Figure 11.11 plots the amount of copper measured in the end of test fluid for each additive at each temperature. The amount of copper generally increases with temperature, but not proportionally; that is the difference in the amount of copper between 110 °C

and 120 °C is not the same as the difference seen between 120 °C and 130 °C.

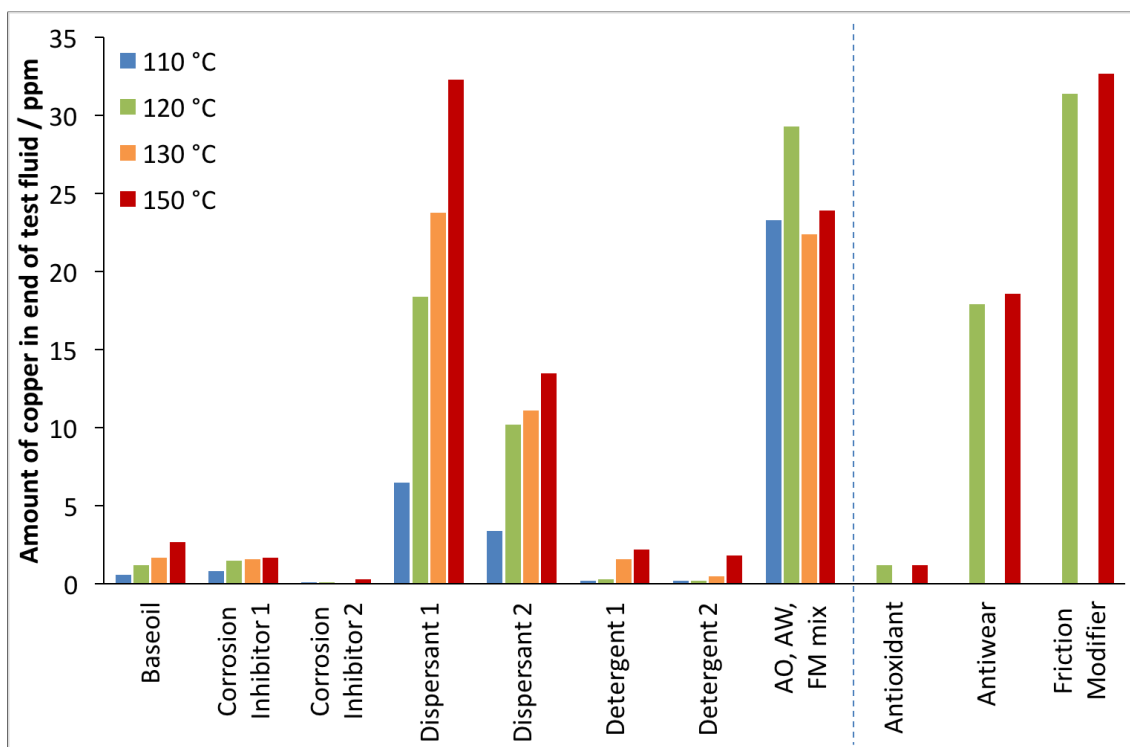


Figure 11.11: Copper in end of test fluid for tests carried out in fluids containing individual additives

Dispersant 1 appears to have a big impact on the amount of copper measured in the end of test fluid, dispersant 2 does not seem to have as much impact. This effect of dispersants giving a large amount of copper in the end of test fluid was previously seen when the full formulation fluids were looked at in Section 11.3. The AO, AW, FM mix also gives a high amount of copper in the end of test fluid, looking at the individual additives of this mix it appear the antiwear and friction modifier are the main contributors to the amount of copper on the end of test fluid. This should be taken into account when looking at full formulation results as higher levels of antiwear and friction modifier could exacerbate the amount of copper leached into solution overall.

Figure 11.12 plots the radius loss of the 32 μm wire tested in individual additives. Data for corrosion inhibitor 1 at 150 °C was not plotted as the wire broke, giving a radius change of 32 μm , but the wire did not completely disintegrate so still had a radius, it was just unable to be measured. Results for the antiwear alone are also not shown as the wires broke in the gaseous phase, within a few hours, and so the results were not thought to be representative of the actual fluid interaction with the copper.

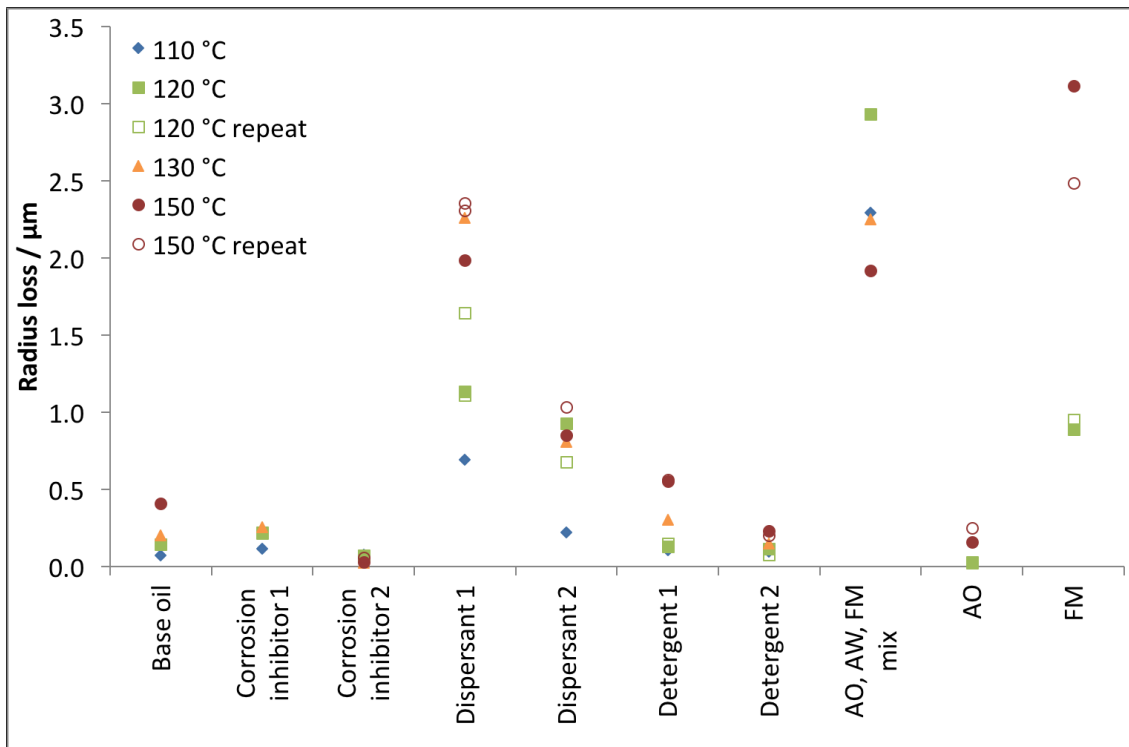


Figure 11.12: Radius loss of copper wire immersed in test fluids containing individual additives at different temperatures

In general it can be seen that the final radius loss measured increases with temperature, following the same trend as the amount of copper in the end of test fluid seen in Figure 11.11. This is generally what is expected and the reason that many experiments are conducted at elevated temperatures, to increase the rate, or amount of corrosion seen [11, 90, 149]. There is one exception to this; the AO, AW, FM mix showed a decrease in the radius loss with increasing temperature between 120 °C and 150 °C which is not as obviously seen in the amount of copper measured in the end of test fluid.

Figure 11.11 and Figure 11.12 generally agree with each other that increasing the temperature leads to more corrosion. Copper corrosion is generally reported to increase with increasing temperature [20, 69, 77]. However in cases where film formation occurs on the copper surface increasing the temperature can make the layer thicker [150] or can cause faster formation of the film [67]. Looking at the end point alone can only give so much information, the AO, AW, FM mix is an example of this.

If the radius change graph for the AO, AW, FM mix is examined, Figure 11.13, the shape of the graph would suggest that there are three stages of corrosion. An initial period

where little happens, the length of time this period lasts decreases with increasing temperature. There is then a period where corrosion is consistent and rapid; interestingly the slope of the graph during this period is almost the same at all temperatures suggesting that this corrosion rate is not influenced by temperature. However the length of time this period lasts for decreases with increasing temperature. The third stage is a plateau in the corrosion rate. The mechanism behind these different stages of corrosion is discussed later in Section 11.5.6.

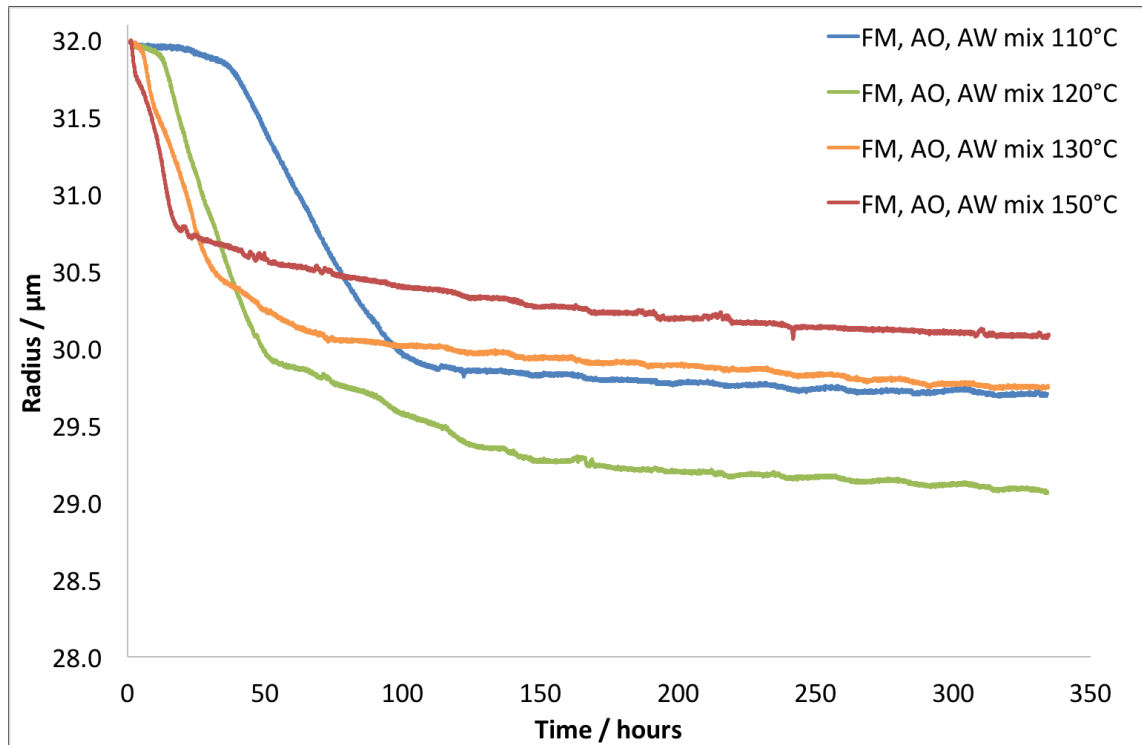


Figure 11.13: Graph showing how the temperature effects the change in radius of wire tested in the AO, AW, FM mix

Melchers [151] reported that a large scale study on the corrosion of copper-nickel alloys in seawater could give results showing that increasing temperature increased corrosion, but in other cases an increase in temperature decreased corrosion. The parameters of the experiment were partly causing the differences seen but he states that, the total amount of corrosion seen is influenced by the degree of corrosion caused during the initial stages of exposure. Figure 11.14 shows the initial stages of corrosion of copper-nickel alloys in seawater at different temperatures. The lower the temperature the greater the corrosion. Although obtained over different time periods this figure is very similar to that obtained for the AO, AW, FM wire radius change graph in this study.

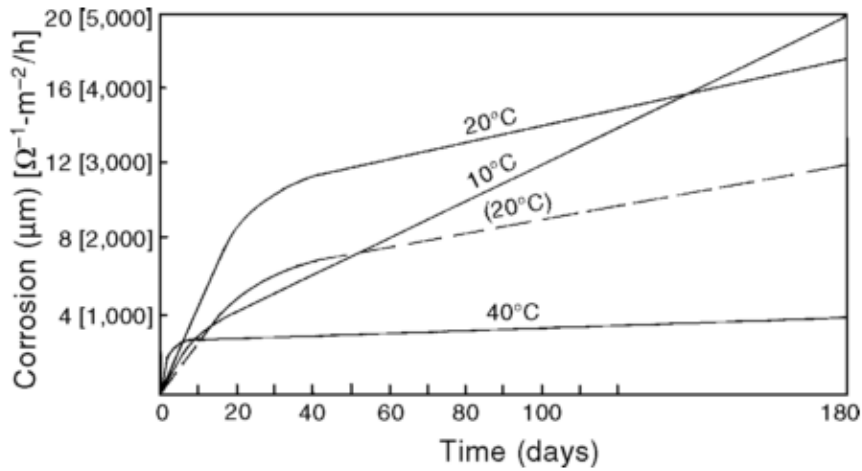


Figure 11.14: Graph showing estimation of corrosion with time at different temperatures [151]

It is most likely that in the case of the AO, AW, FM mix film formation is occurring at the surface, the growth of which increases with increasing temperature, therefore decreasing the overall amount of corrosion measured.

The ASTM D130 test is carried out at 150 °C because it is thought to accelerate the rate of corrosion. It assumes that the corrosion occurring at 150 °C will be the same as that occurring at 110 °C. This is also the premise of the Arrhenius equation which states that as a general rule of thumb for every 10 K increase in temperature the rate of a reaction will double [123]. Several papers have used the Arrhenius equation to predict the activation energy of a corrosion reaction [60, 94, 141].

Arrhenius proposed that if a reaction is temperature dependant and the mechanism is the same [11] then it should obey Equation 11.2; where k = rate constant, A = pre-exponential factor, E_a = activation energy (J mol^{-1}), R = Universal gas constant ($8.314 \text{ J K}^{-1} \text{ mol}^{-1}$), and T = temperature (K).

$$k = Ae^{-E_a/RT} \quad (11.2)$$

From the data presented in Figure 11.11 and Figure 11.12 changes to radius and the amount of copper in the end of test fluid do not follow the Arrhenius equation, although this assumes a linear reaction rate between the start and end of the test; that is, the radius change of the wire occurs at a constant rate over the duration of the test. Looking at the raw data which shows how the radius of the wire changes with time, Appendix B,

the lines do not always follow the same shape and so this suggests that many of the additives on reacting with a copper surface do not follow the Arrhenius equation and the mechanism of interaction will be different at different temperatures.

Whilst it is possible to fit models to these lines, and therefore also determine a rate of corrosion, this is not entirely helpful as the model can only be fitted across the time period of the experiment (approximately 350 hours), after which it is possible that the corrosion could deviate from the model. As the model fitting is not linear but often takes the form of a complex polynomial or logarithmic equation it is easier to compare the raw data of two different additives rather than determine their position at a given time using a model. As polynomials have inflection points, after which they begin to rise again, it is not feasible to extend the model as the radius of the wire would not be able to increase. Therefore comparisons between additives will be done using the raw data obtained from the wire tests.

11.5 Mechanisms of surface interactions

In order to try and understand the mechanisms of interaction each additive will be analysed in turn. A summary of the additive will be followed by a suggested mechanism with which it is thought to interact with the copper surface and whether this mechanism changes with temperature. The interaction of the additive with other additives will also be discussed.

As each of the additives were tested in base oil an understanding of how the base oil interacts with the surface is also desirable. The radius change of the wires tested in base oil alone showed very little change at 110 °C, a slight decrease at 120 °C and 130 °C and more of a decrease at 150 °C which can be seen in Section 7.1, Figure 7.3.

From the radius plots it can be seen that the rate of corrosion decreases with time, which is shown in the fact that the lines level out. Norouzi et al. [20] found that the corrosion of copper in biodiesel decreased with time, as seen here with base oil alone at higher temperatures. This was attributed to the formation of a passive layer and a protective film on the surface of the copper. Degradation of the base oil leads to an increase in polar organic compounds, such as ketones, alcohols, carboxylic acids and

esters, according to Tripathi and Vinu [80]. More polar compounds are likely to have a greater affinity for the surface and so migrate to it and interact, either to corrode it or to form deposits.

From SEM images taken of the surface of coupons tested in base oil (Section 7.1, Figure 7.1) the surface of the 110 °C sample had no distinguishing features, whereas at higher temperatures small particles could be seen on the surface which grew in size as the temperature increased. These particles are thought to be degradation products from the oil but which also act as a barrier between the fluid and the surface, through which newly formed corrosive species would need to migrate, thereby slowing the rate of corrosion.

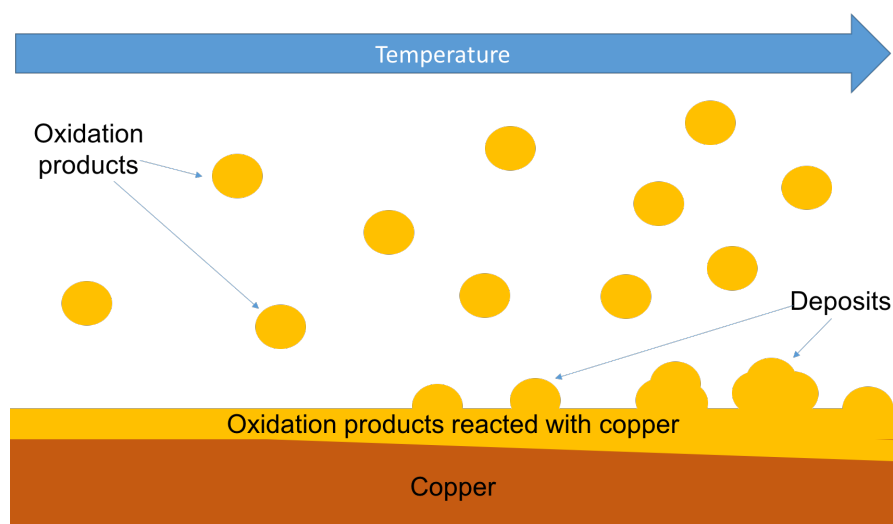


Figure 11.15: Schematic diagram showing base oil interaction with copper surface as temperature increases

The natural degradation of base oil causes the formation of compounds which are mildly corrosive to the copper. The number of these compounds increase with temperature hence greater corrosion is seen. These particles also result in the formation of deposits on the surface, and as they are more abundant at higher temperatures, the amount of deposit seen on the surface is also greater. This is shown schematically in Figure 11.15.

As all of the additives investigated were dissolved in base oil they will be compared against the results obtained for base oil alone, in order to try and determine the impact the additive has on the copper surface. In order to aid the discussion and to act as a reference point Figures 11.16–11.19 show the radius change of each individual additive

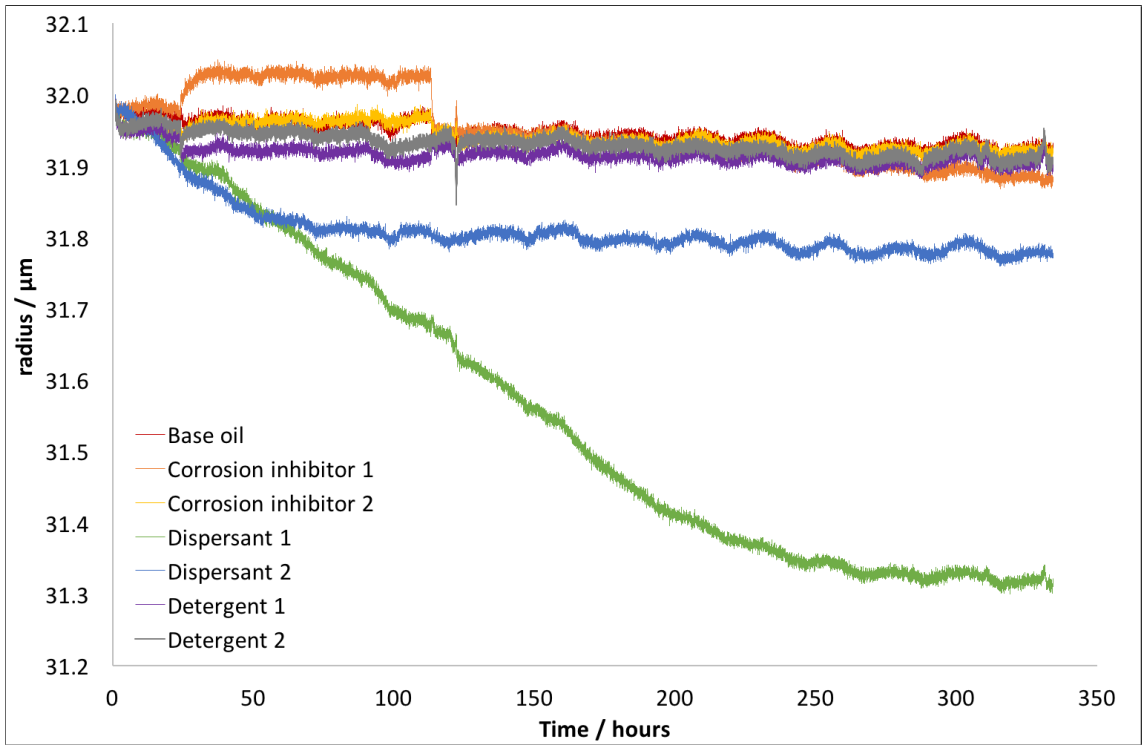


Figure 11.16: Radius change of copper wires tested at 110 °C

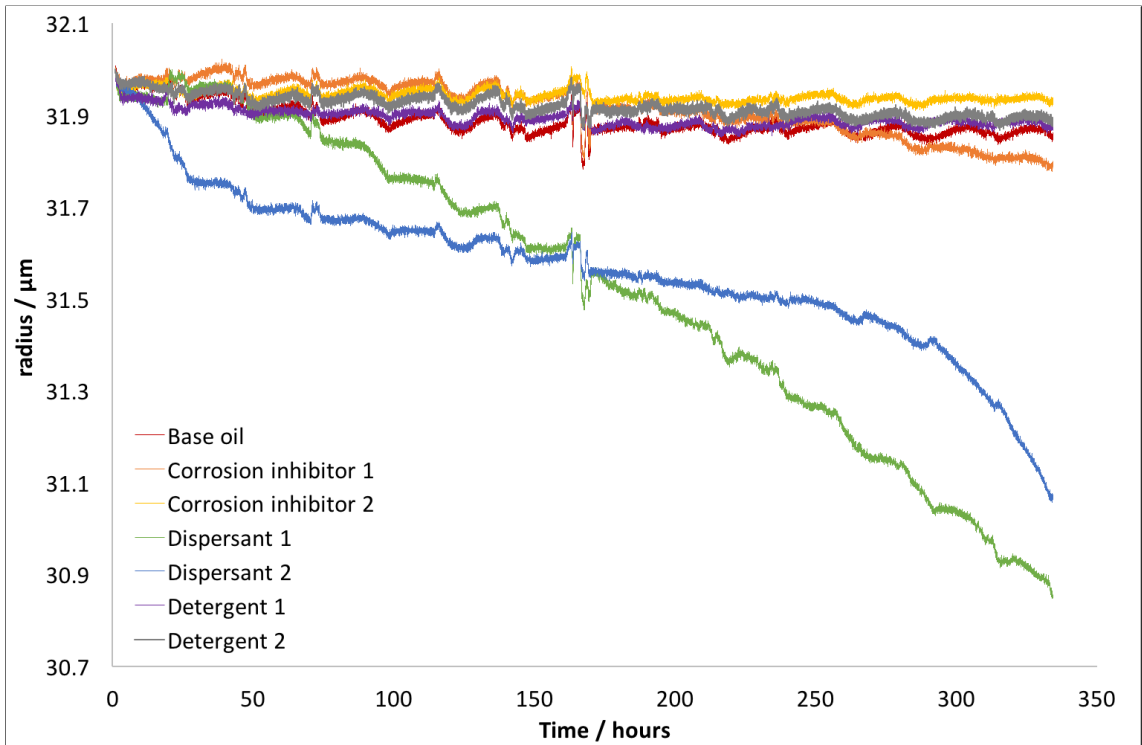


Figure 11.17: Radius change of copper wires tested at 120 °C

grouped by temperature, allowing the radius change of an additive to be compared to that of the base oil alone. Graphs which are grouped by additive can be found in Chapter 7.

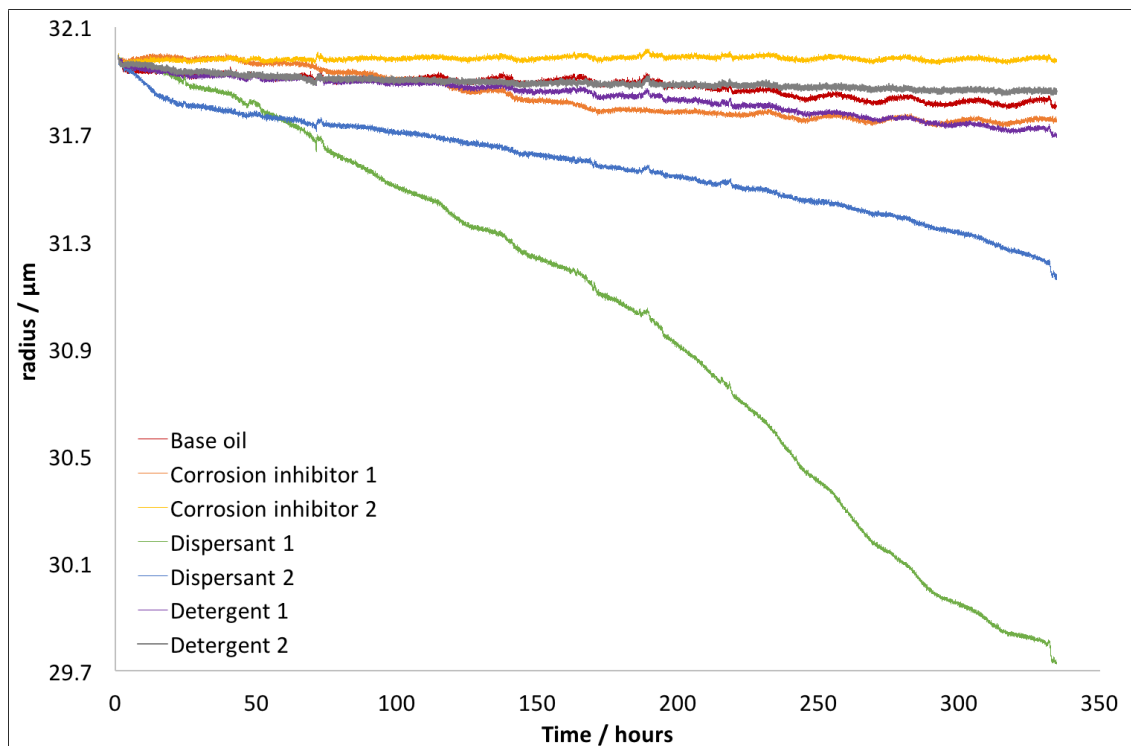


Figure 11.18: Radius change of copper wires tested at 130 °C

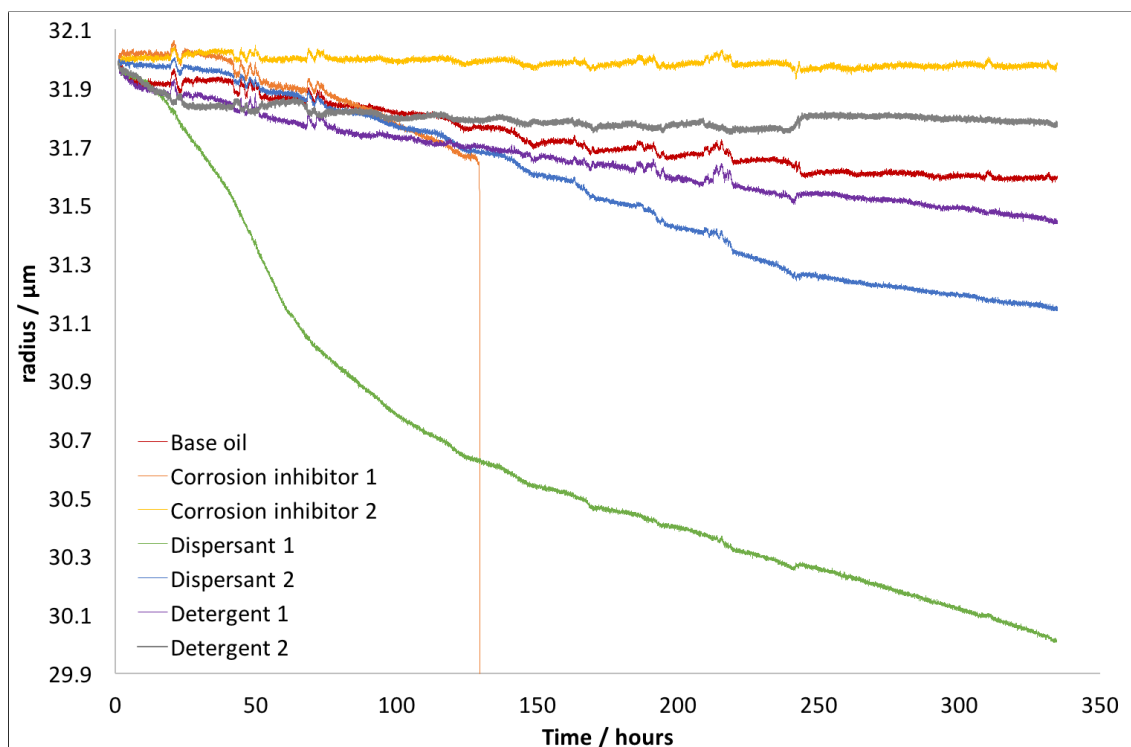


Figure 11.19: Radius change of copper wires tested at 150 °C

11.5.1 Corrosion inhibitor 1

Corrosion inhibitor 1 is a dimercaptodiathiazole (DMTD) inhibitor which is a well known corrosion inhibitor, thought to function by adsorbing onto the surface and preventing

corrosion via the formation of a protective surface film [49, 112, 113].

At temperatures below 130 °C the amount of corrosion was equal to or slightly greater than that of the base oil alone. However SEM images of the surface of the coupons tested in corrosion inhibitor 1 showed clear formation of a surface film. This is in line with other studies which show that DMTD forms a surface film. The exact orientation of adsorption cannot be determined from this study but a number of other studies have looked at the mechanism of adsorption.

Ling et al. [111] suggest that DMTD can form a one-dimensional polymer chain on the copper surface with the proposed mechanism shown in Figure 11.20.

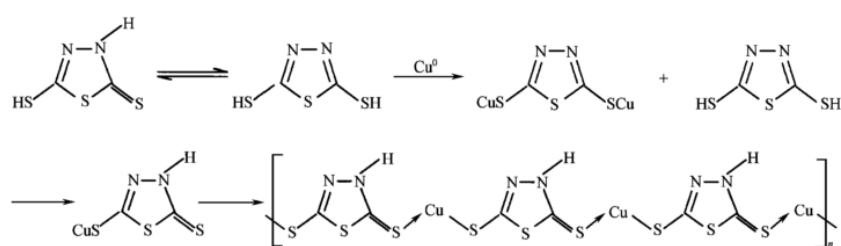


Figure 11.20: Proposed mechanism, by Ling et al., of the interaction of DMTD with a copper surface [111]

They state that this would give the copper a +1 state. The XPS carried out in this study at 120 °C showed the copper to be in a +2 state and so this is unlikely to be the binding mechanism occurring. The relevant XPS results are shown and discussed in Section 8.5, Figure 8.5.

Hipler et al. [113] studied the adsorption of similar thiadiazole molecules onto gold surfaces. They concluded that 2,5-dimercapto-1,3,4-thiadiazole was likely to bond to the surface with one thiol group whilst the other pointed away from the surface and so was able to form bonds with other thiadiazole molecules, forming sulfide linked multilayers, as shown in Figure 11.21.

Loto et al. [27] state that generally, coordinative bond strength increases in the order of $O < N < S < P$. This would suggest that the thiadiazole molecules are more likely to coordinate to the copper through the sulfur atoms than the nitrogen atoms, which is also suggested in the mechanisms proposed above.

A number of studies, summarised by Loto et al. [27] concluded that the efficiency of the inhibitor increased with concentration, which was also reported by Xiong et al. [115].

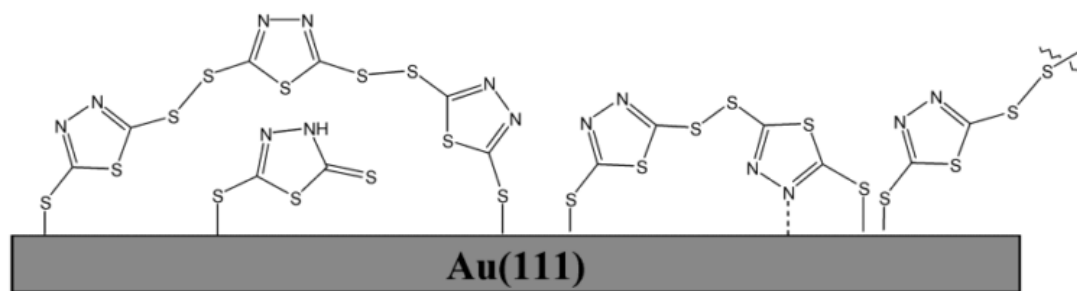


Figure 11.21: Mechanism proposed by Hipler et al. of the interaction of DMTD with a gold surface [113]

This has been seen in the full formulation fluids; where formulations containing higher levels of corrosion inhibitor 1 often gave lower levels of corrosion. This has already been discussed in Section 11.3.

Tomi et al. [94] tested a number of different thiadiazole based inhibitors and found that inhibition decreased with increasing temperature. With this in mind the behaviour of corrosion inhibitor 1 changes significantly at 150 °C. Pitting was found on the copper coupon surface (Figure 11.22), and in the case of the wires several breakages were seen along its length.

A very rapid radius change followed by a break in the wire was seen only for corrosion inhibitor 1 alone when tested at 150 °C, as seen in Section 7.2 Figure 7.8. The wire broke after 130 hours and at the end of the test localised pitting was seen on the surface. The behaviour was found to be repeatable, with the rapid decrease in radius beginning within 5 hours of each other and taking almost exactly 2 hours to break in both cases.

White light interferometry images of two pits found on the surface of a coupon tested in corrosion inhibitor 1 at 150 °C can be seen in Figure 11.22. The pit depths were measured as being between 45 µm and 60 µm deep. The copper wires are 64 µm in diameter at the start of the test. It is therefore feasible that pits formed on the surface of the wire would be similar in size to the diameter and cause the wire to break.

Corrosion inhibitor 1 is an alkyl dimercaptiothiadiazole and so has sulfur side chains of varying lengths. It is well known that sulfur, particularly elemental sulfur and short mercaptans, can be highly corrosive to copper [26, 69, 85, 87, 89]. If these sulfur side chains were to break down it is possible that the resulting sulfur compounds could cause

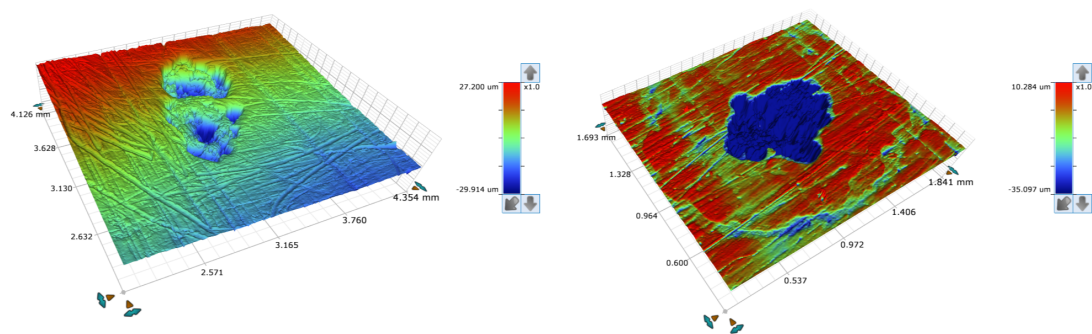


Figure 11.22: White light interferometry images of two pits found on the surface of a coupon tested in corrosion inhibitor 1 at 150 °C

corrosion.

A thermogravimetric study was carried out to look at the temperature that corrosion inhibitor 1 breaks down with and without the presence of copper. Plots of the first derivative against temperature are shown in Figure 11.23 for corrosion inhibitor 1 alone, corrosion inhibitor 1 which was pre-mixed with two different amounts of copper and allowed to stand for 24 hours before testing, and one where copper was measured into the pan and then corrosion inhibitor was added. Where copper was pre-mixed in solution the samples were shaken before testing.

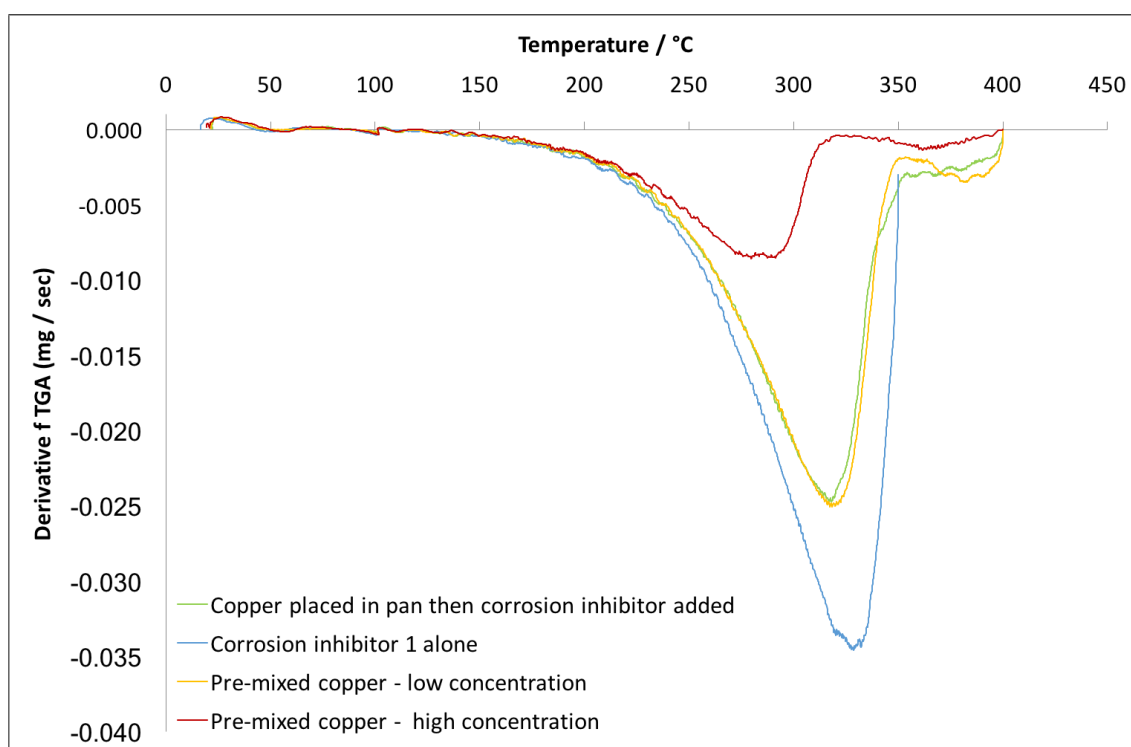


Figure 11.23: First derivative of TGA against temperature for corrosion inhibitor 1 with and without the presence of copper

As can be seen from Figure 11.23 the solution containing only corrosion inhibitor broke down at a higher temperature than the solutions which contained copper. A high concentration of copper made the corrosion inhibitor break down at a significantly lower temperature whilst lower concentrations lowered the breakdown by only a small amount. The onset of deterioration is at 150 °C, the temperature at which corrosion inhibitor 1 was seen to cause pitting.

At 150 °C corrosion inhibitor 1 was found to form a relatively thick black layer on the surface of the coupons that visibly flaked, this was shown in the results Section 7.2, Table 7.2. Reid and Smith [26] reported something similar when studying the effect of elemental sulfur on copper during the ASTM D130 test. They reported that it formed a film comprised of Cu – S which eventually spalled away from the surface.

Sulfur spectra of the corrosion inhibitor 1 sample can be seen in Figure 11.24. The sulfur spectrum at 120 °C has a large peak around 168 eV. It is possible that this peak corresponds to CuSO₄ [152], however whilst trying to identify this peak a number of larger organic molecules containing S were also seen to fall around this binding energy. This peak could therefore be indicative of the corrosion inhibitor binding with the copper surface, a copper-thiadiazole bond.

At 150 °C the spectrum does not show a peak at 168 eV. As this peak was attributed to the binding of the corrosion inhibitor with the copper surface it could be assumed that the corrosion inhibitor is no longer in the same form, and has potentially broken down to form sulfur or thiols. The peaks around 162 eV and 164 eV are slightly enhanced and correspond to Cu₂S and S (or thiols) supporting the idea of corrosion inhibitor breakdown. The flaking nature of the film at 150 °C coupled with the XPS makes Cu₂S likely and this was also seen by Reid and Smith [26] when testing copper immersed in elemental sulfur.

Comparison of the copper XPS spectra of corrosion inhibitor 1 samples run at 120 °C and 150 °C show a difference in oxidation state, Figure 11.25. At 150 °C the copper is in a Cu (I) or Cu (0) state whereas at 120 °C it is in a Cu (II) state [146]. Both SO₄²⁻ and the interaction of the corrosion inhibitor with the surface would give rise to copper in the 2+ state, but it is not possible to determine which, or indeed if both, are present on the

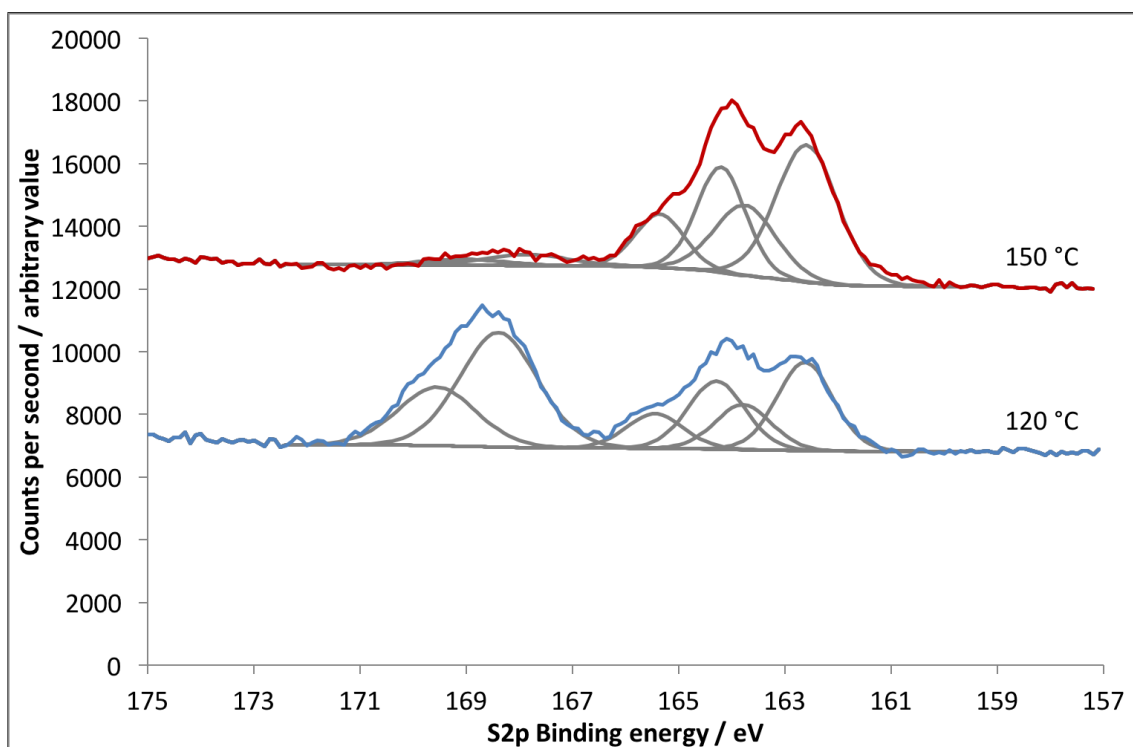


Figure 11.24: Corrosion inhibitor 1 sulfur XPS spectra at 120 °C and 150 °C

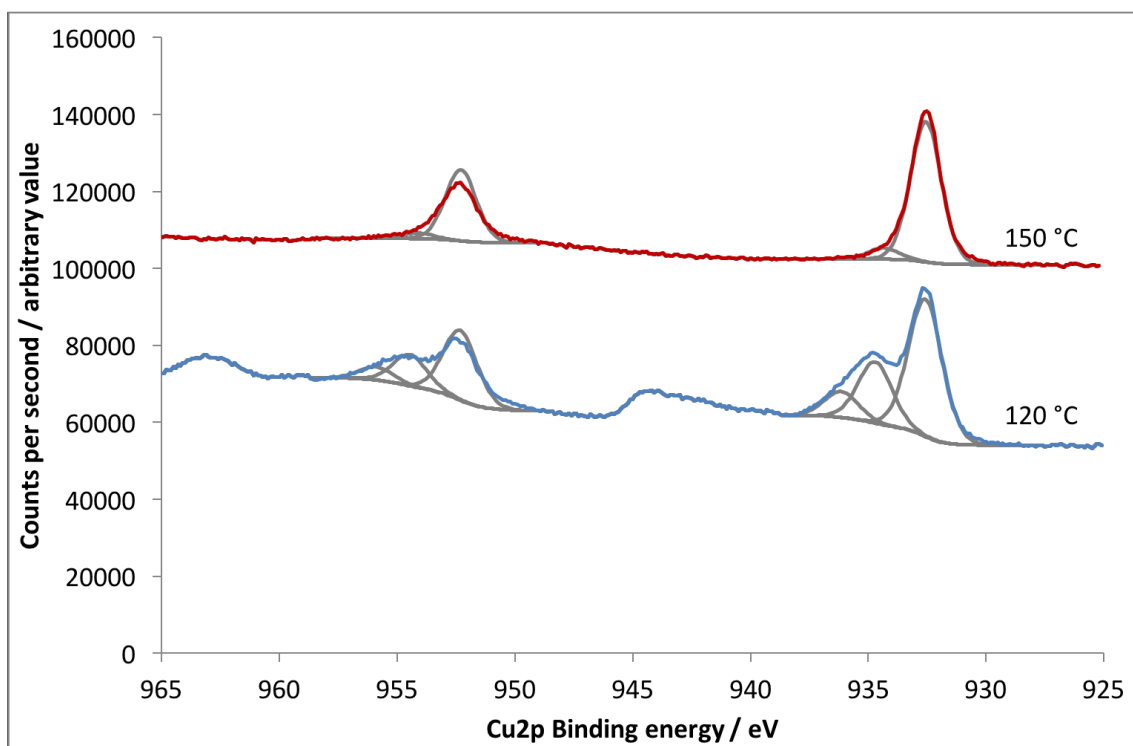


Figure 11.25: Corrosion inhibitor 1 copper XPS spectra at 120 °C and 150 °C

surface.

The amount of oxygen detected on the surface is significantly lower at 150 °C than at 120 °C suggesting that the film on the surface is predominantly Cu–S at higher temperatures.

It is surprising to see that corrosion inhibitor 1 shows a greater loss of the wire radius than base oil alone. This is most likely due to the inhibitor molecules attaching themselves to the surface and converting the outer layer of copper into a non-conductive copper-inhibitor complex, therefore decreasing the radius of the wire.

A schematic diagram showing how corrosion inhibitor 1 bonds to the copper surface at temperatures above and below 150 °C can be seen in Figure 11.26.

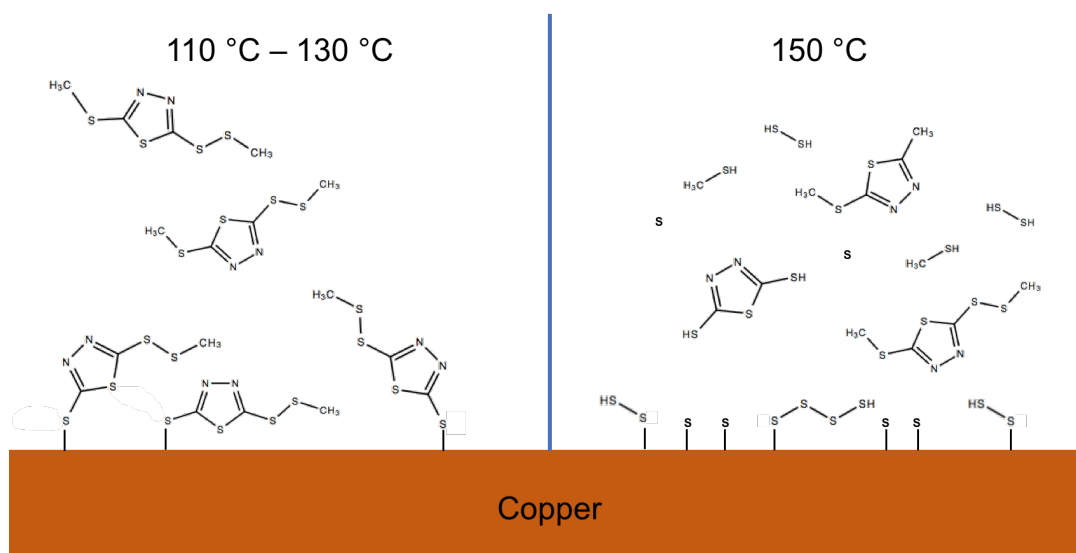


Figure 11.26: Schematic diagram of corrosion inhibitor 1 interaction with copper surface above and below 150 °C

11.5.1.1 Corrosion inhibitor 1 with other additives

We now have an idea as to how corrosion inhibitor 1 interacts with a copper surface when alone in base oil.

At 120 °C corrosion inhibitor 1 was combined with the other additives to various effect. The coupon ratings were generally very similar to that of corrosion inhibitor 1 tested alone (Table 8.1) and the amount of copper in the end of test fluid was reduced in the case of the dispersant and the AO, W, FM mix, and similar to that of corrosion inhibitor 1 tested alone in most other cases (Table 8.3).

The wire radius change for samples tested in combinations containing corrosion inhibitor 1 were generally similar to when corrosion inhibitor 1 was tested alone (Table 8.6). Coupled with the coupon and ICP copper level results this suggests that when corrosion inhibitor 1 is present as part of a combination it is the additive most likely

to interact with the surface. SEM images seem to confirm this as the surface takes the appearance of the corrosion inhibitor 1 coupon surface over the other additive when in combination with any other additive.

When corrosion inhibitor 1 is combined with any of the other additives at 150 °C it is very interesting to see that no breakages of the wire occur and no pitting was observed on the coupon surfaces. In addition to this the amount of corrosion measured by wire radius loss was not dramatically increased compared to the other additive alone (Table 8.6). However the surface of the coupons were poorly rated in all cases, most with with black layers which were poorly adhered (Table 8.2).

It is thought that at 150 °C there is initially some interaction of the inhibitor molecule with the surface. The corrosion inhibitor then breaks down into corrosive species, as when alone, but these species are prevented from interacting with the surface due to the presence of the other additives. In the case of corrosion inhibitor 2 a protective barrier is formed on the surface; the dispersants keep the corrosive species in solution; the detergents neutralise the acidic species formed; in all cases the corrosive species are prevented from attacking the surface, hence no pitting is seen. There is one exception to this, when corrosion inhibitor 1 is combined with the AO, AW, FM mixture.

Initially there is a surface film formed and the wire is protected from corrosion from the mix. After 130 hours, the time at which the wire broke, and the time it is thought to take for corrosive species to occur there is a drop in the wire radius which decreases to almost the same level as the AO, AW, FM mix alone. This can be seen in Figure 11.27.

There is nothing in this combination able to adsorb the corrosive sulfur species created by the breakdown of corrosion inhibitor 1. It is not clear why the corrosion should plateau out rather than continue to pit but it is thought it is due to corrosion products being formed on the surface which are able to offer some protection.

From studying corrosion inhibitor 1 alone and in combination with other additives it is clear that at temperatures below 150 °C it prevents corrosion by formation of a surface film. The nature of the interaction between the corrosion inhibitor molecules and the surface is thought to be due to adsorption of the sulfur atoms in the corrosion inhibitor molecule with the copper surface.

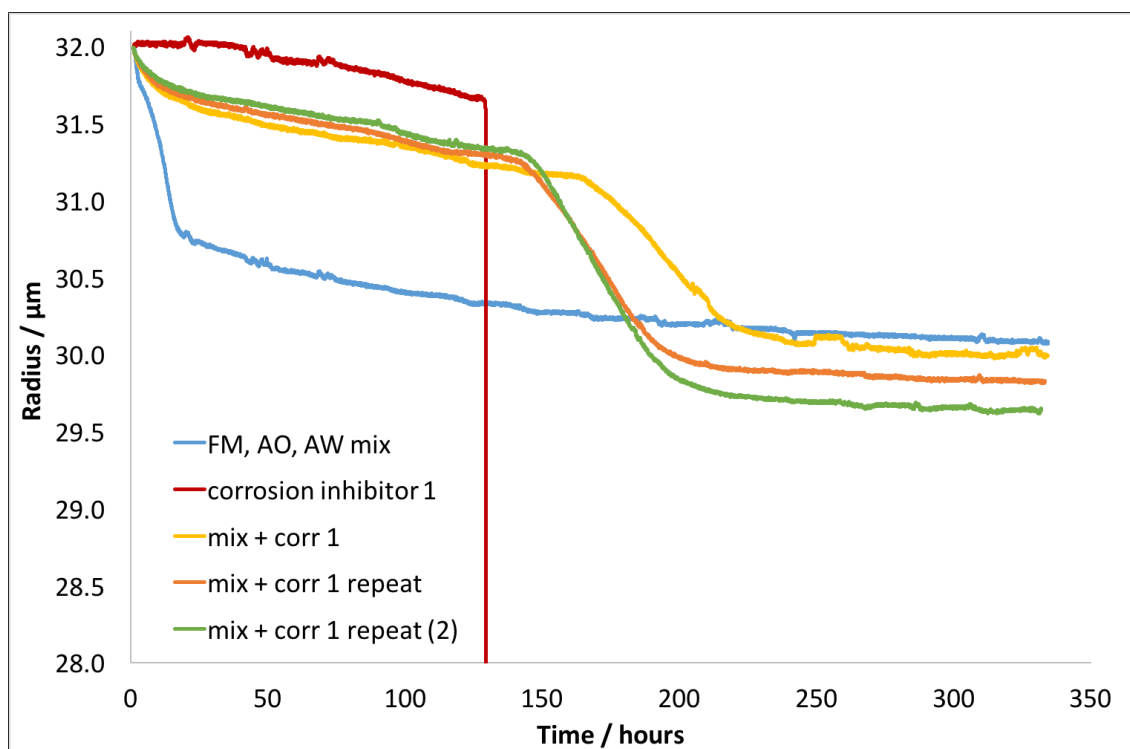


Figure 11.27: Radius change of copper wires tested at 150 °C in corrosion inhibitor 1 alone, the AO, AW, FM mix alone, and a combination of both, with repeats

At 150 °C a film initially forms on the surface but this is followed by the breakdown of the molecule leading to the formation of corrosive sulfur species which attack the copper surface causing pitting. When other additives are present they are able to prevent those corrosive species from attacking the surface, either by formation of a protective layer on the surface or through neutralisation and suspension in the bulk fluid.

11.5.2 Corrosion inhibitor 2

Corrosion inhibitor 2 is oil soluble benzotriazole, which is a well known copper corrosion inhibitor molecule [34, 142]. The mechanism of interaction is still debated [75] but it is known that the benzotriazole molecules react with the surface to form a copper-benzotriazole complex which acts as a protective layer [93]. Most of the work looking at the mechanism of benzotriazole has been conducted in aqueous media.

It is reported in literature that benzotriazole prevents the copper surface from becoming discoloured [93] and this has been seen throughout this study as the coupons tested in corrosion inhibitor 2 at all temperatures were a similar colour after a 2 week test period. These images can be seen in Table 7.3, in Section 7.3.

Corrosion inhibitor 2 was found to be an effective inhibitor at all temperatures tested. The radius change of the wires was minimal, with very little copper measured in the end of test fluid, below 0.5 ppm in all cases. SEM images of the surface also show few signs of corrosion, all of these results can be found in Section 7.3.

XPS analysis of surfaces tested in the presence of corrosion inhibitor 2 show the presence of Cu(I) and Cu(II), these results were shown in Figures 8.5 and 8.9. Although the mechanism by which benzotriazole and copper interact is not completely understood [75, 93] the general consensus is that copper forms a complex with benzotriazole [107]; this complex can be Cu(I)-BTA or Cu(II)-BTAH. The complex covers the surface to produce a film which acts as a physical barrier to corrosive products [96, 106, 110]. Some studies have shown that the Cu(I) species oxidises to Cu(II) on removal from the liquid phase [105] and so it is not possible to draw conclusions as to which species formed initially in this study as XPS was carried out on coupons which had been exposed to air for significant periods of time.

The radius change for copper wires tested in corrosion inhibitor 2 at all temperatures were shown in Section 7.3, Figure 7.13. The radius change was found to be the same at all temperatures with negligible increase in the amount of copper in the end of test solution. It can be seen from Figures 11.16–11.19 that corrosion inhibitor 2 is the least corrosive additive to copper. The suggested mechanism of bonding is through the nitrogen in the ring, however this study did not investigate through which nitrogens the bonding took place. Drawing on literature [75, 76] it is thought that the molecules packed closely together to cover the surface. The fact that the layer was able to prevent corrosion across a range of temperatures suggest that a chemical bond may be formed as suggested by Cotton and Scholes [39]. Corrosion is then prevented as the benzotriazole forms a physical barrier to corrosive species, as depicted in Figure 11.28.

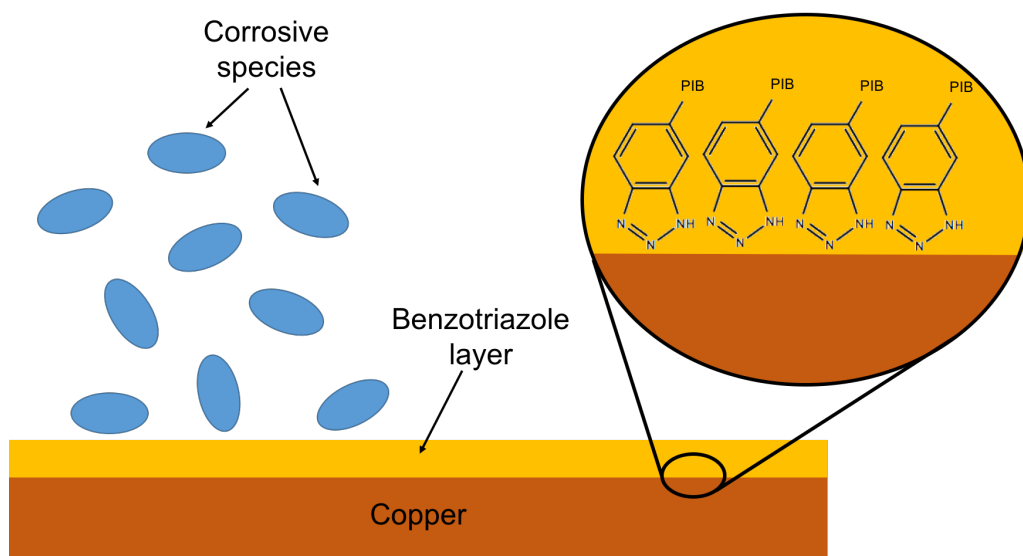


Figure 11.28: Schematic diagram of corrosion inhibitor 2 interaction with copper surface

11.5.2.1 Corrosion inhibitor 2 with other additives

The addition of corrosion inhibitor 2 to other additives was also found to improve the rating, compared to the rating given when the other additive was tested alone; however it does not completely prevent the colour change as reported in some literature [93]. Images of the coupons tested in corrosion inhibitor 2 with another additive present can be seen in Chapter 8, Tables 8.1 and 8.2.

When corrosion inhibitor 2 was combined with other additives at 120 °C and 150 °C there was a reduction in the radius change compared to the other additive alone, but an increase compared to corrosion inhibitor 2 alone, see results in Table 8.6. The same was seen for the amount of copper in the end of test fluid, Tables 8.3 and 8.4.

From these results it can be concluded that corrosion inhibitor 2 helps to reduce the corrosion caused by other additives, this is easiest to see in the wire radius results shown in full in Appendix B, Figures B.2 and B.9. One example in more detail is the combination of corrosion inhibitor 2 with dispersant 1. Figure 11.29 shows the radius changes for wires tested in corrosion inhibitor 2 and dispersant 1 both alone and combined at 120 °C and 150 °C. When combined the radius change is improved over the dispersant alone.

SEM images of the surface show a more dramatic change; dispersant 1 alone shows etching but when combined with corrosion inhibitor 2 this is no longer seen, as shown in Figure 11.30.

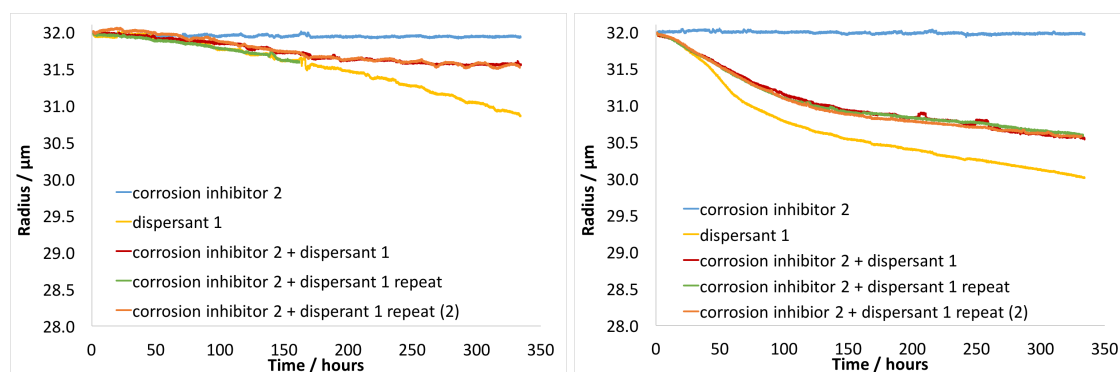


Figure 11.29: Radius changes of copper wires immersed in corrosion inhibitor 2 and dispersant 1 alone and combined, at 120 °C (left) and 150 °C (right)

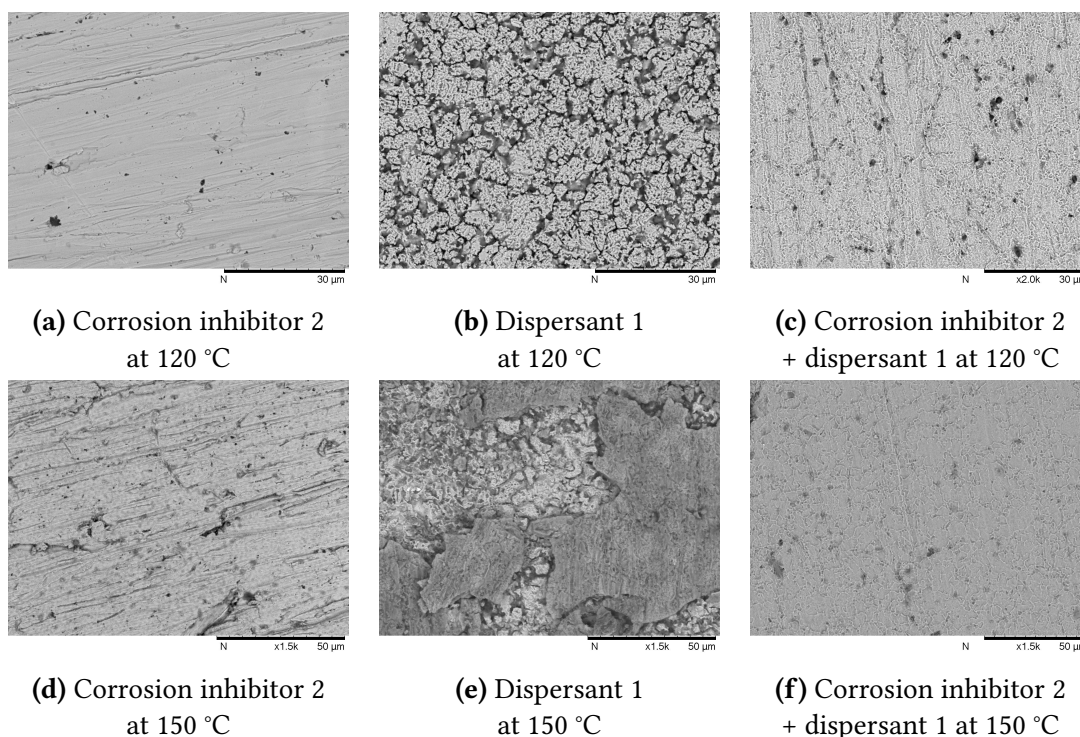


Figure 11.30: SEM images showing improvement of surface when corrosion inhibitor 2 is combined with dispersant 1 at 120 °C (top line) and 150 °C (bottom line)

Cotton and Scholes [39] reported that the benzotriazole film formed under aqueous conditions resisted washing water and many other organic degreasants, suggesting a chemical bond is formed with the surface, as opposed to physisorption. A number of papers state that an adsorbed layer of benzotriazole is initially formed on the copper surface [105, 153]. It is possible that at 150 °C the dispersant prevents the benzotriazole from interacting with the surface long enough to form a chemical bond and instead an adsorbed layer is constantly being removed and replaced by the dispersants, therefore although it prevents some corrosion from occurring it cannot prevent all corrosion.

When corrosion inhibitor 2 is present in combination with other additives it is thought

that the mechanism is the formation of a surface film as described above for corrosion inhibitor 2 alone. However the addition of other additives can cause competing reactions at the surface and so the film is not built up as quickly or is unable to pack as closely therefore allowing some corrosion of the copper surface. It should be noted that when corrosion inhibitor 2 is present it is at a very low concentration, 0.05 wt%, this is the lowest level of any additive in the formulation; and is put into perspective when compared to the 5 wt% of dispersant in the formulation. It is possible that increasing the level of corrosion inhibitor 2 may provide even greater protection to the copper surface when other additives are present although at higher levels solubility can become problematic.

11.5.3 Dispersant 1

Dispersant 1 consists of a long chain amine backbone with amide and succinimide side groups, as a reminder Figure 11.31 shows the structure of dispersant 1. In the bulk fluid the dispersant is thought to function via the interaction of oxygen side groups with polar molecules in the oil, that may be produced as a result of degradation, stabilising them and keeping them suspended in the fluid.

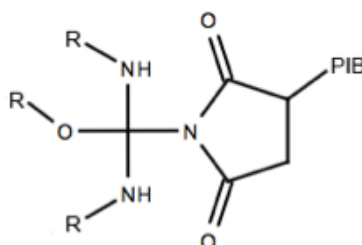


Figure 11.31: Structure of dispersant 1

In this study we are interested in how the dispersant molecule interacts with the copper surface rather than how it behaves in the bulk fluid.

Dispersant 1 was found to negatively interact with the copper surface across all temperatures, with the greatest corrosion seen for any individual additive as shown in Figures 11.16–11.19. An increase in the amount of copper in the end of test fluid was also seen as the temperature increased. At 120 °C and above SEM images showed etching on the surface of the copper, as shown in Chapter 7, Figure 7.16. Images presented by Gahagan and Hunt [116] showed similar results with etching or pitting seen on

the surface of wires when dispersant was present at 130 °C. They used two variants of polyisobutenyl succinimide combined in different quantities, the greatest amount of etching was seen with a combination of both dispersants.

The radius change data collected from wires tested in dispersant 1 have different shapes at the different temperatures tested. Although these results were shown in Section 7.4, for ease of reference they are presented again in Figure 11.32.

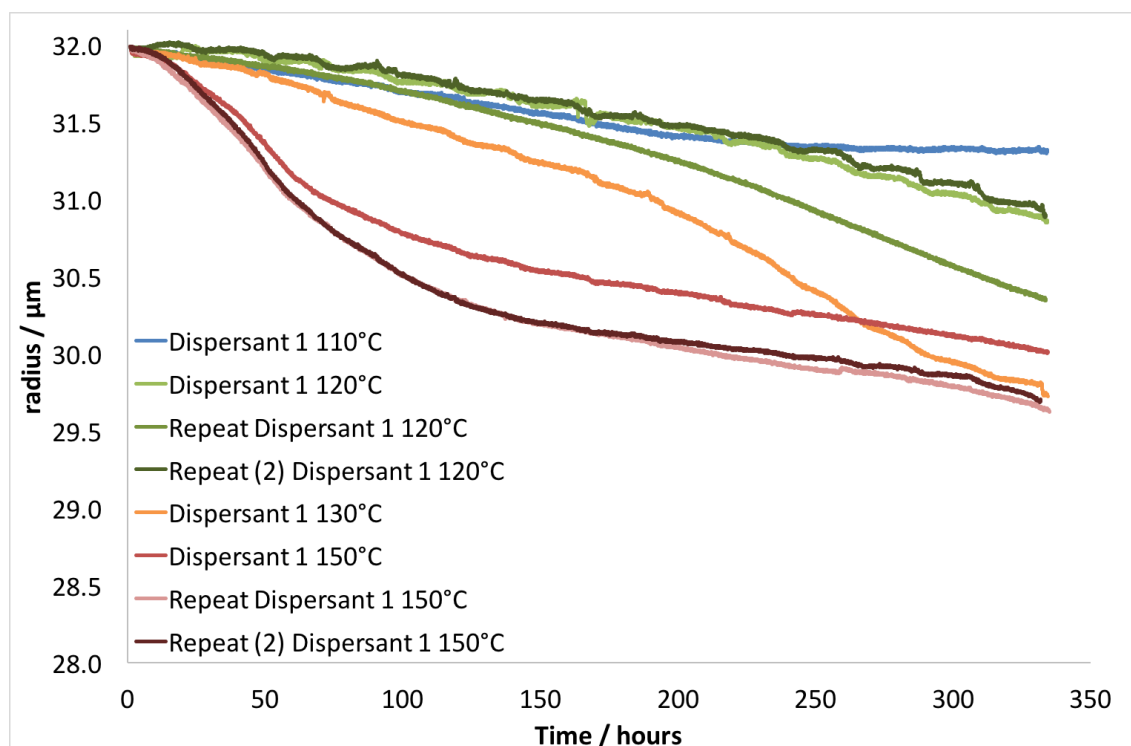


Figure 11.32: Radius change of wire immersed in dispersant 1 at various temperatures

At 110 °C the corrosion is constant, with a steady rate of change for the initial 200 hours, after which the corrosion begins to slow and levels off until the end of the test. This suggests that the dispersant is initially corrosive but over time something prevents it from continuing to attack the surface. The SEM image of the surface at 110 °C, Section 7.4, Figure 7.16, shows very small pits on the surface. There is nothing to suggest the formation of a protective film on the surface, which would be the most likely scenario given how the radius change flattens out. There is no corrosion caused by the base oil alone at 110 °C and so the presence of the dispersant must be the cause of the corrosion.

It is possible that initially the dispersant removes copper oxide, which would naturally be present on the surface, after this has been removed it is unable to remove the

copper itself and the temperature is too low to create any degradation products in the time frame of the experiment and so corrosion stops.

At 120 °C a different shape is seen. Initially the radius change seems similar to that at 110 °C but the graph has a slight downwards inflection, that is that the corrosion occurring speeds up as the test progresses. Over the length of the experiment no plateau or change in this shape is seen, suggesting that the corrosion would continue to speed up if the test were extended. At 130 °C this downwards inflection is also seen but the rate of change is greater. At around 300 hours the radius change begins to flatten out, meaning that there is a decrease in the rate of change at this point. Given this information it is likely that if the test at 120 °C were to be extended it would reach a point at which the corrosion would slow. SEM images of the coupon surfaces tested at 120 °C and 130 °C are very similar suggesting that the same mechanism is taking place and etching the surface.

At 150 °C the shape of the graph looks different again to those at 120 °C and 130 °C. However closer inspection shows that the initial portion of the graph, up to around 60 hours has the same downwards inflection seen at the lower temperatures. After 60 hours the rate of change slows and becomes linear with no signs of changing by the end of the test, although that is not to say that it would continue at this rate indefinitely.

The radius change data and the SEM images of the surfaces, Section 7.4, Figure 7.16, suggests that the mechanism occurring at the surface at 150 °C is similar to that at 120 °C and 130°C.

XPS analysis of the surface showed very little nitrogen was present, which would be expected if dispersant 1 were to remain on the surface. This means that the dispersant interacts with the surface without forming any permanent bonds.

Dispersants are designed to keep corrosion products suspended in the fluid [2, 10, 154], rather than depositing on the surface [155] or forming sludge [147]. It is thought that the dispersant is approaching the surface and removing the copper, possibly in the form Cu-O, as there is likely to be an oxide layer on the surface as the coupons are exposed to air before they are placed into the test fluids. At 110 °C once the initial Cu-O layer has been removed corrosion stops as no degradation products are being

formed and interacting with the surface. Above 120 °C degradation products do form in the oil and as they interact with the surface the dispersant interacts with them to remove them leading to greater corrosion of the copper surface.

11.5.3.1 Dispersant 1 with other additives

It was found that the addition of dispersant 1 to any other additive negatively affected the performance of the other additive, compared to when it was tested alone. Although it could be said that the addition of any additive to dispersant 1 minimised the effect it had on the copper surface, particularly in respect to the amount of copper measured in the end of test fluid, Chapter 8, Figures 8.3 and 8.4.

The changes in wire radius with time are shown in full in Appendix B, Figures B.3 and B.10. The summary of final radius changes is shown in Table 8.6, Chapter 8. At 120 °C antagonisms are seen between dispersant 1 and dispersant 2 and also the AO, AW, FM mix. It is unclear why the AO, AW, FM mix with dispersant 1 gives such bad corrosion. As there are four additives present it is more difficult to ascertain what may be happening but it is thought that the dispersant could be removing film formed by the other additives. When antiwear was tested alone it was found to form a poorly adhered film and so it is possible that the dispersant is able to readily remove this.

Interestingly when synergies and antagonisms were looked at for the ratings and copper levels it was found that they did not show the same results; this shows how the ASTM D130 test does not give a very good understanding of corrosion occurring at the surface. The radius change recorded from the wires gives more information regarding how corrosion proceeds. This test gives far more potential to understand the corrosion taking place at the surface however more in depth work would need to be done before the changes in the wire radius could be fully understood. As it stands at the moment in this study it is possible to see that combining additives is beneficial when dispersant 1 is involved as other additives generally prevent some of the corrosion seen with dispersant 1 alone.

11.5.4 Dispersant 2

Dispersant 2 is a quaternary amine compound, stabilised with a sulfate group. In the bulk fluid the dispersant should suspend any polar degradation products through interaction with the amine head group.

In literature there is little information on the use of quaternary amine compounds as dispersants but interestingly Hegazy et al. [139] studied the effect of copper corrosion inhibition by two different quaternary amine compounds in nitric acid, between 25 °C and 55 °C and found that they were effective as inhibitors but efficiency decreased with increasing temperature as the molecules were only physisorbed to the surface. The use of quaternary amines as corrosion inhibitors is also mentioned by Dariva and Gailo [92].

In this study dispersant 2 was not found to be a corrosion inhibitor however it was not as corrosive as dispersant 1. Interestingly the radius changes seen with dispersant 2 were similar in shape, if not magnitude to that seen with dispersant 1.

At 110 °C there is an initial decrease in the radius which slows significantly after 50 hours. At 120 °C and 130 °C there is a downwards inflection to the radius change graph, showing the corrosion increases in rate as time goes on. At 150 °C there is a slight downwards inflection to the data which then begins to plateau near the end of the experiment. These results can be seen in Section 7.5, Figure 7.23. The similarity in the shape of the radius change graphs suggests that both dispersants interact with the copper surface in similar ways even though they are different in chemistry and structure.

As sulfur is known to be corrosive to copper it was wondered if the sulfate group interacted with the surface and whether this would lead to increased corrosion. Sulfur XPS spectra, shown in Figures 8.7 and 8.11, Section 8.4, for the dispersant 2 samples show only a small sulfate peak, suggesting that the sulfate group does not bond to the copper surface at either 120 °C or 150 °C. The fact that dispersant 2 does not show particularly aggressive corrosion makes it unlikely that the sulfate group is causing further corrosion to the surface.

The mechanism of interaction of the dispersants with the surface will be slightly different for each but is likely to consist of an approach to the surface, interaction with

the copper or other oxidation or degradation products that may have formed at the surface, then movement back to the bulk with copper. A schematic of this is shown in Figure 11.33.

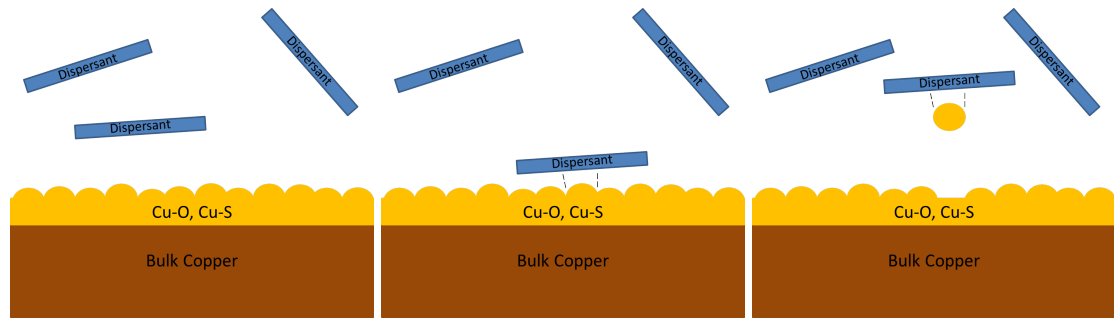


Figure 11.33: Schematic of dispersant interaction with surface

11.5.4.1 Dispersant 2 with other additives

When combined with other additives dispersant 2 generally gave additive results. The main exceptions to this are when it is in combination with corrosion inhibitor 1 or dispersant 1.

When corrosion inhibitor 1 was present the radius change generally followed the same line as the inhibitor alone. It has already been discussed that corrosion inhibitor 1 is generally the more dominant species to attach to the surface when in a combination.

When combined with dispersant 1 at 120 °C an antagonism is seen in the wire radius results. It is thought that the poor result is due to both dispersants attacking the surface to exacerbate the corrosion seen by either of them alone; essentially the amount of dispersant has been doubled. With this in mind it is surprising that even more corrosion is not seen. The amount of copper in the end of test fluid is no more than when dispersant 1 is present alone. SEM images of the surface show less etching than dispersant 1 alone, as if the entire surface has been more evenly corroded. This can be seen in Figure 11.34 where SEM images of coupons tested in dispersant 1 alone, dispersant 2 alone and in a combination of both dispersants are shown.

It is thought that each dispersant has slightly different affinities for the oxidation and degradation products on the surface of the copper. When both are present more are removed from the surface giving a more even corrosion and a slightly greater radius change.

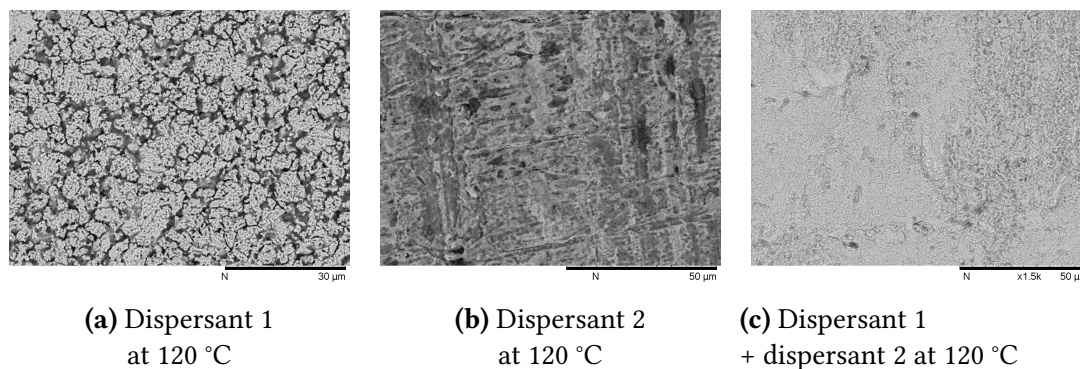


Figure 11.34: Copper coupons tested at 120 °C in dispersant 1, dispersant 2 and a combination of both

11.5.5 Detergent 1 and detergent 2

Both detergent 1 and detergent 2 have been grouped together as their behaviour was similar. The detergents showed little interaction with the copper surface and at high temperatures seemed to be beneficial. At 150 °C, for example, SEM images, Figure 11.35, of base oil tested alone showed a large amount of deposit on the surface. When either of the detergents was present this deposit was not seen; this was also the case at 130 °C.

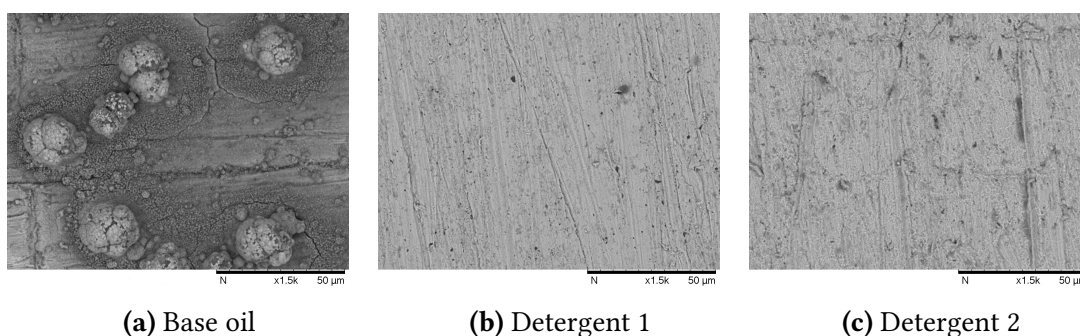


Figure 11.35: Copper coupons tested at 150 °C in base oil alone or with the presence of detergent

The rating of tests carried out with detergent 1 were better than tests conducted only in base oil. At 120 °C and above an improvement was also seen when detergent 2 was used. The amount of copper measured in the end of test fluid was also better for the detergents than for base oil alone.

When we consider the function of the detergents this is not unsurprising. The detergents used in this study are over-based with calcium carbonate and should interact with acidic species, neutralising them. This could explain why the amount of copper in the end of test fluid is slightly better than the base oil alone. If acidic components cause

some corrosion of the copper, allowing it to be dissolved into solution, then when the detergents are present these compounds are neutralised and so this corrosion would take place to a lesser extent. The side chains which keep the calcium carbonate suspended in solution are also able to keep other particulates suspended. This would explain why the rating of the samples tested in the presence of detergent are better than those tested in base oil alone: they do not have deposits on the surface.

Interaction with the copper surface is not seen because the detergents do not interact with the surface. Instead they interact with acid and small particulates in the oil, neutralising them, preventing corrosion and stopping them from depositing on the surface.

11.5.6 Antioxidant, Antiwear and Friction Modifier

In the initial stages of this study the antioxidant, antiwear and friction modifier molecules were grouped together as they were not expected to have a big impact on the surface. After an initial period of testing it was found that this mixture had one of the biggest impacts on the surface and so it was broken down into its component parts.

Figures 11.36 and 11.37 show graphs of the radius change of the AO, AW, mix and each of the components individually at 120 °C and 150 °C respectively.

When tested alone at either temperature the antiwear was found to be highly corrosive to copper and in three of the four tests run the wire broke in the gas phase. Due to this it can be assumed that the antiwear evaporates out of the oil and reacts with the wire in the gas phase. It is interesting that the AO, AW, FM mix at both 120 °C and 150 °C follow almost the same line as the antiwear alone up to the point where it would break. The fact that it does not break when in the AO, AW, FM mix is likely due to the presence of the other additives but it is not entirely certain whether they offer some protection in the gaseous phase or if they prevent the antiwear from evaporating.

The antioxidant does not initially appear to interact with the surface. It shows minimal to no loss of radius of the copper wire, the amount of copper in the end of test fluid is very low and although it gives a 2e rating the surface is clean and bright. However XPS analysis of the surface showed higher nitrogen levels compared to the base oil alone and so it is possible that when alone the antioxidant does interact with the surface.

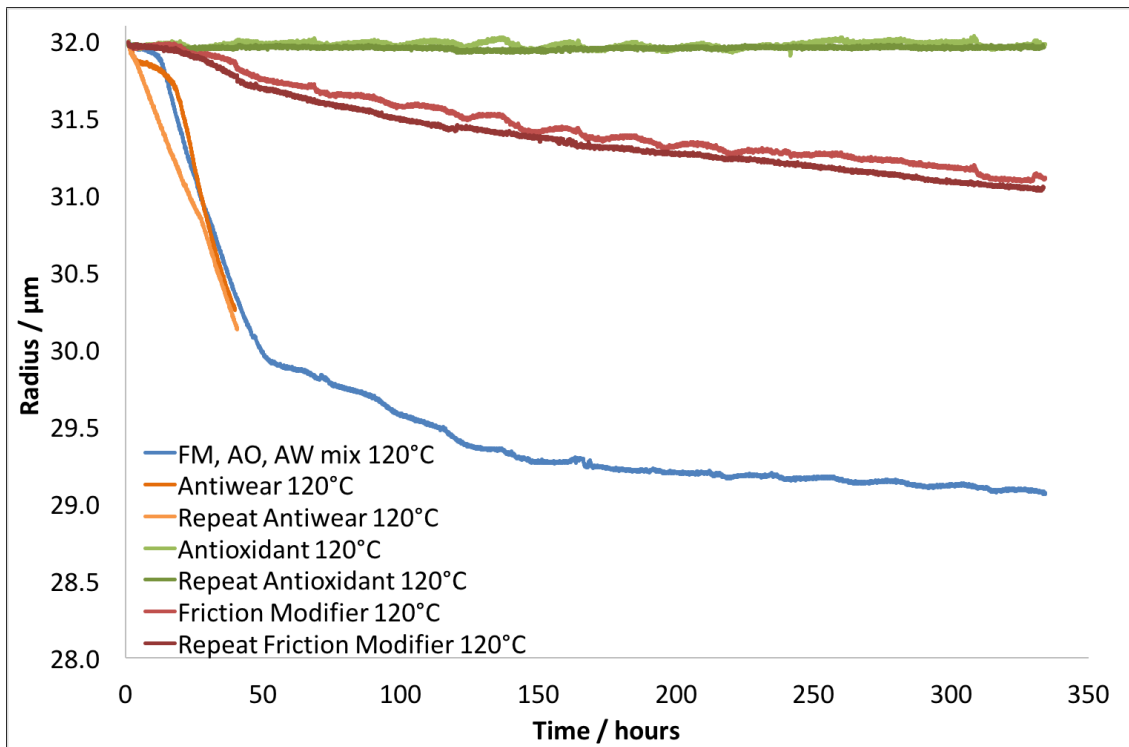


Figure 11.36: Radius change for AO, AW, FM mix and antioxidant, antiwear, and friction modifier independently at 120°C

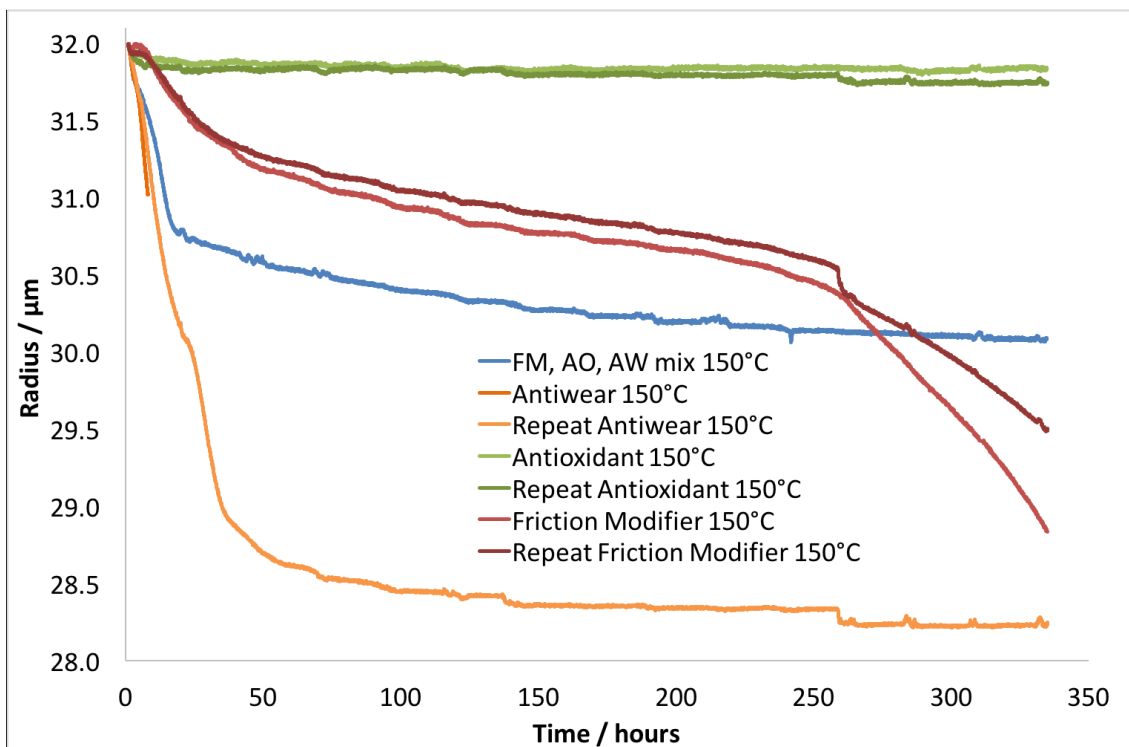


Figure 11.37: Radius change for AO, AW, FM mix and antioxidant, antiwear, and friction modifier independently at 150°C

The friction modifier was found to corrode the copper surface after an initial period, which decreased in time with an increase in temperature. Friction modifier molecules are designed to interact with the surface and form a layer which helps to prevent friction by

keeping surfaces apart. The SEM images and XPS spectra taken show that the friction modifier interacts with the surface however it does not form a uniform film and it is possible that the film is poorly adhered, looking at the surface images. This means that it is possible that the film peels away from the surface removing some of the copper with it. The fact it is not a uniform film means that any corrosive species formed in the oil can still attack the exposed surface areas.

11.6 Interactions in full formulations

The basic mechanisms by which the additives are thought to interact with the surface have been discussed. In full formulations these same mechanisms are thought to occur in much the same way however due to the greater complexity involved with more additives it is more difficult to tell.

It has been seen that generally additives which are in the greatest concentration in a formulation are more likely to interact with the surface. This is logical when you consider that an additive has a greater possibility of reacting with the surface if there is more of it in the fluid. Due to the time constraints of this study it was not possible to carry out concentration studies but it would be interesting to see if combinations of two additives, conducted at various concentrations were able to predict which additive is most likely to react with the copper surface in a more complex fluid.

From the simple additive interactions corrosion inhibitor 1 seemed most likely to react with the surface when in combination with any other additive. This also seemed to hold true for the full formulations where those containing high levels of corrosion inhibitor 1 seemed to form surface films which when analysed with SEM were similar to that of corrosion inhibitor 1 alone, as shown in Chapter 10.

Formulations which were unable to be matched had the greatest difference in concentration from the additives tested alone or in combination.

Having looked at how a number of different additives interact with copper surfaces alone, in simple combinations and in full formulations there are several points to consider.

The ASTM D130 test has several downsides;

- It is a visual test and the ratings can be subjective depending on the person rating
- The original test was developed to evaluate the level of corrosion caused by residual sulfur compounds. In modern ATF fluids the corrosive sulfur is often negligible and when sulfur is present it is in the form of large molecules in which it causes no corrosion
- The rating given to the coupons does not correlate to other measures of corrosion, such as weight loss of a coupon, or level of copper in the end of test fluid
- The temperature at which the ASTM D130 is conducted (150 °C) is higher than would be expected in a transmission
- No information is obtained as to why a given fluid passes or fails

On the other hand the test is simple and quick to run with results able to be obtained in around 3 hours.

As fluids are becoming more complex, allowing greater protection for longer periods of time, new tests may be required for better evaluation of test fluids. The copper wire test is a good example of such a test. In situ data is able to be obtained showing how the radius of the wire changes with time. Rather than relying on the colour of a test piece more valuable data can be acquired, showing how quickly corrosion is occurring at the surface of the wire and whether the corrosion is continuous. The wire test does take longer to run than the coupon test but results are not subjective and have been shown to be repeatable.

Admittedly there are still flaws in the copper wire test as there are with any bench-top test. The material used for testing is pure copper and whilst this may be representative of the wires present in a transmission other components are copper alloys. If the alloys present are however, able to be drawn into a wire which conducts a current there is no

reason the copper wire test could not be conducted using these alloys.

Finding an ATF which works well is not just dependant on corrosion results and other tests, such as friction, wear and deposit testing would also need to be conducted, however having a more robust corrosion test would help to identify fluids that may otherwise have been discarded due to a poor visual rating with the ASTM D130 test.

12: Conclusions and Future Work

12.1 Conclusions

Copper wires and coupons were tested in several common ATF additives to see how the fluids interacted with the copper surface. Individual additives, simple mixtures and fully formulated fluids were all used to try and determine how the additives interacted with the copper surface when alone and in combination with each other. The key findings of the study are summarised below.

12.1.1 ASTM D130 standard test method and wire resistance tests

- The elevated temperatures used in the ASTM D130 standard test method are not representative of what would happen at real transmission temperatures, with the mechanism of corrosion found to change in some instances.
- Wire tests proved to be a good way to monitor the interaction of additives with the copper surface in situ, rather than coupons which only gave information at the time at which the test was stopped.
- The amount of current used was found to have no effect on the interaction between the fluid and the wire, up to 20 mA, and no ohmic heating was detected for the currents used.
- Visual ratings of the surface often do not correlate with other methods of corrosion indication, for example the amount of copper in the end of test fluid, the weight change of test coupons, the radius change of copper wires or inspection of the surface using SEM.

- The wire-tests were found to correlate well with the amount of copper in the end of test fluid, but not with the weight change of the coupons; although these were weighed with any surface films still intact.
- Wire-tests were successfully used to measure the interaction of copper with both fully formulated fluids and single additives dissolved in base oil.

12.1.2 Effect of temperature

- When additives were tested individually the amount of corrosion measured increased with temperature. When additives were combined the amount of corrosion did not always increase with temperature, which is why the ASTM D130 test is not always representative to real life applications; higher temperatures can sometimes give lower corrosion levels.
- The additives tested do not follow Arrhenius behaviour and changing temperature can change the reaction mechanism taking place at the surface. Corrosion inhibitor 1 is the best example of significantly different mechanisms taking place at different temperatures.
 - At temperatures of 130 °C or lower corrosion inhibitor 1 absorbs to the surface and forms a protective film.
 - At 150 °C corrosion inhibitor 1 broke down, forming corrosive sulfur compounds, which then caused localised pitting on the copper surface. The pits found on the coupon surface were of a depth similar to that of the radius of the wire, explaining why the wire broke.
 - XPS analysis of the surface at 120 °C showed the presence of SO_4^{2-} or bonding between the copper and corrosion inhibitor 1. At 150 °C this peak was no longer present and the surface consisted of Cu – S and thiols.
 - A thermogravimetric study showed that it was possible for corrosion inhibitor 1 to begin to break down at 150 °C in the presence of copper.

12.1.3 Mechanisms of surface interactions

- Corrosion inhibitor 1 and corrosion inhibitor 2 were found to form protective films on copper surfaces at temperatures of 130 °C or lower.
- At 150 °C corrosion inhibitor 1 breaks down to form corrosive sulfur species and causes pitting on the copper surface. Corrosion inhibitor 2 continues to function as an inhibitor and forms a protective layer.
- When placed in combination with other additives corrosion inhibitor 1 appears to show dominant interaction with the surface.
- At 150 °C the addition of any other additive to corrosion inhibitor 1 prevented the pitting seen when it was tested alone. It is thought that the sulfur species may be kept suspended by the dispersants and detergents and when corrosion inhibitor 2 is present it is able to help form a protective layer on the surface.
- The dispersants are thought to interact with the copper surface and draw it into solution, slowly removing any Cu – O before reaching the bulk. The similarity in the chemistry between the dispersants and the friction modifier means that it is thought that the friction modifier behaves in the same way, when present alone.
- Detergents are thought not to interact with the surface but instead interact with any acidic species in the fluid, preventing them from interacting with the surface and causing corrosion.
- The behaviour of some full formulation fluids could be explained by comparing them to the behaviour of the simple combinations, when the concentrations were at similar levels

12.2 Future research

There are a number of tests that would be interesting to carry out to obtain further information on the interaction of ATF additives with copper surfaces.

12.2.1 Concentration effects

The effect of concentration was not studied due to the volume of additives to be tested. This study used individual additives at the highest concentration they were likely to be found in a fully formulated fluid. It would be interesting to look at the concentration at which the effects of the individual additives are observed.

Where more than one additive is present varying the concentration of each additive to look at when each appears to be the dominant interaction with the surface could give information regarding how to improve formulations.

12.2.2 Static versus non-static testing

All of the tests were carried out under static conditions. In a transmission the fluid would be circulated. Circulating the fluid during testing would be interesting, primarily because some of the films formed on the copper surface are poorly adhered and it is possible that they may be removed by the circulating fluid. This could lead to further corrosion being seen for those fluids.

There is also evidence to suggest that pits are more likely to propagate under static conditions and so it would be interesting to see if a circulating fluid prevented the pitting seen with corrosion inhibitor 1 at 150 °C.

The sensitivity of the wires could be problematic as it was found that if tests were disturbed then large spikes were observed in the data sets.

12.2.3 Multiple interactions

The majority of tests conducted for this study looked at individual additives and combinations of two of those additives. The exception was the antiwear, antioxidant, friction modifier mix which was used as a single entity for combination purposes. The combinations with the mix gave some of the more interesting radius change graphs and as such it was more difficult to understand what was occurring at the surface.

Having studied combinations of two additives adding a third would be interesting and may provide more information on how the additives are likely to react when in a fully formulated fluid.

12.2.4 Alloying effects

All tests carried out in this study were conducted on copper that was 99.9% pure. Alloying effects have a big impact on the corrosion of metals. The metal washers and other components found in a transmission are not pure copper but are copper alloys. Repeating the tests with wires and coupons of different alloys could give an idea of if the components in the transmission would react very differently to the tests conducted with pure copper.

A: XPS analysis of coupons tested in individual additives

One coupon tested in each individual additive was sent to NEXUS for XPS analysis. Survey spectra were taken at three different areas on the surface of the coupon.

The raw spectra for each of the coupons are shown in this appendix. The elements of interest identified in each spectrum are listed in a table superimposed onto the graph and give details of the element, the position of the peak, the full width half maximum (FWHM) value, the area of the peak and the atomic percentage concentration.

The values for the atomic percentage concentrations across the three different areas surveyed were averaged and the results presented in Chapter 7.

A.1 Base oil

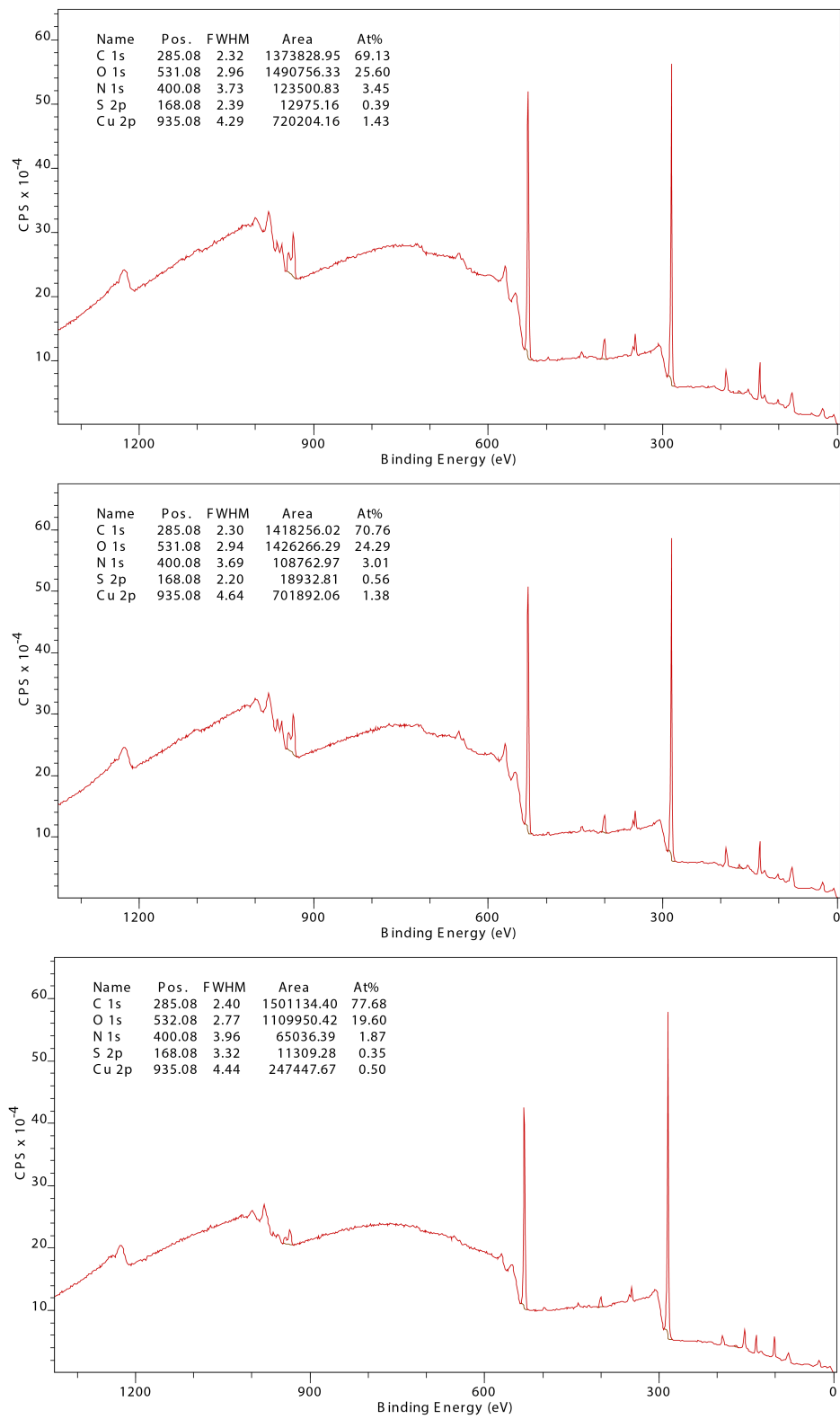


Figure A.1: XPS analysis of three different areas of a coupon tested in base oil at 120 °C

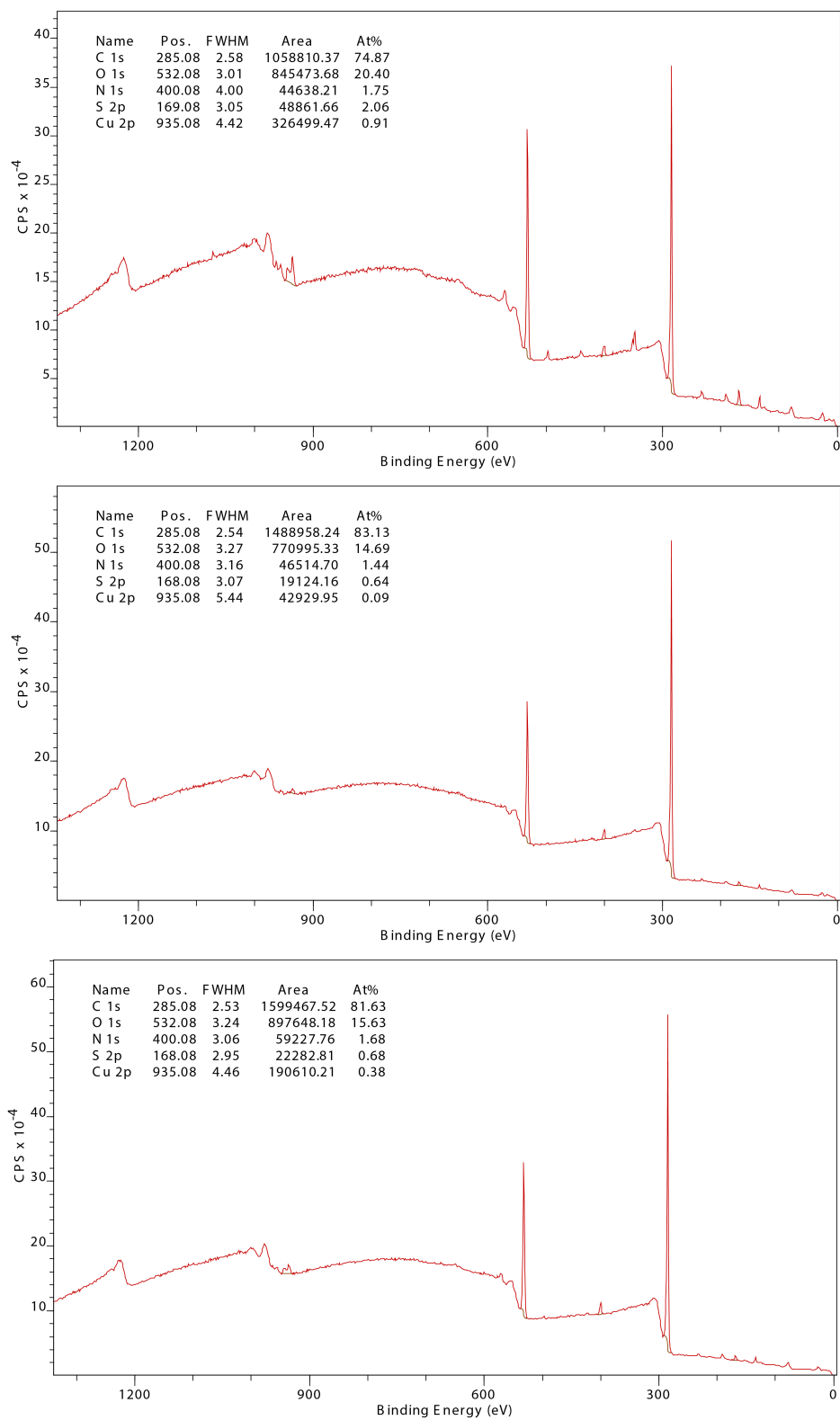


Figure A.2: XPS analysis of three different areas of a coupon tested in base oil at 150 °C

A.2 Corrosion inhibitor 1

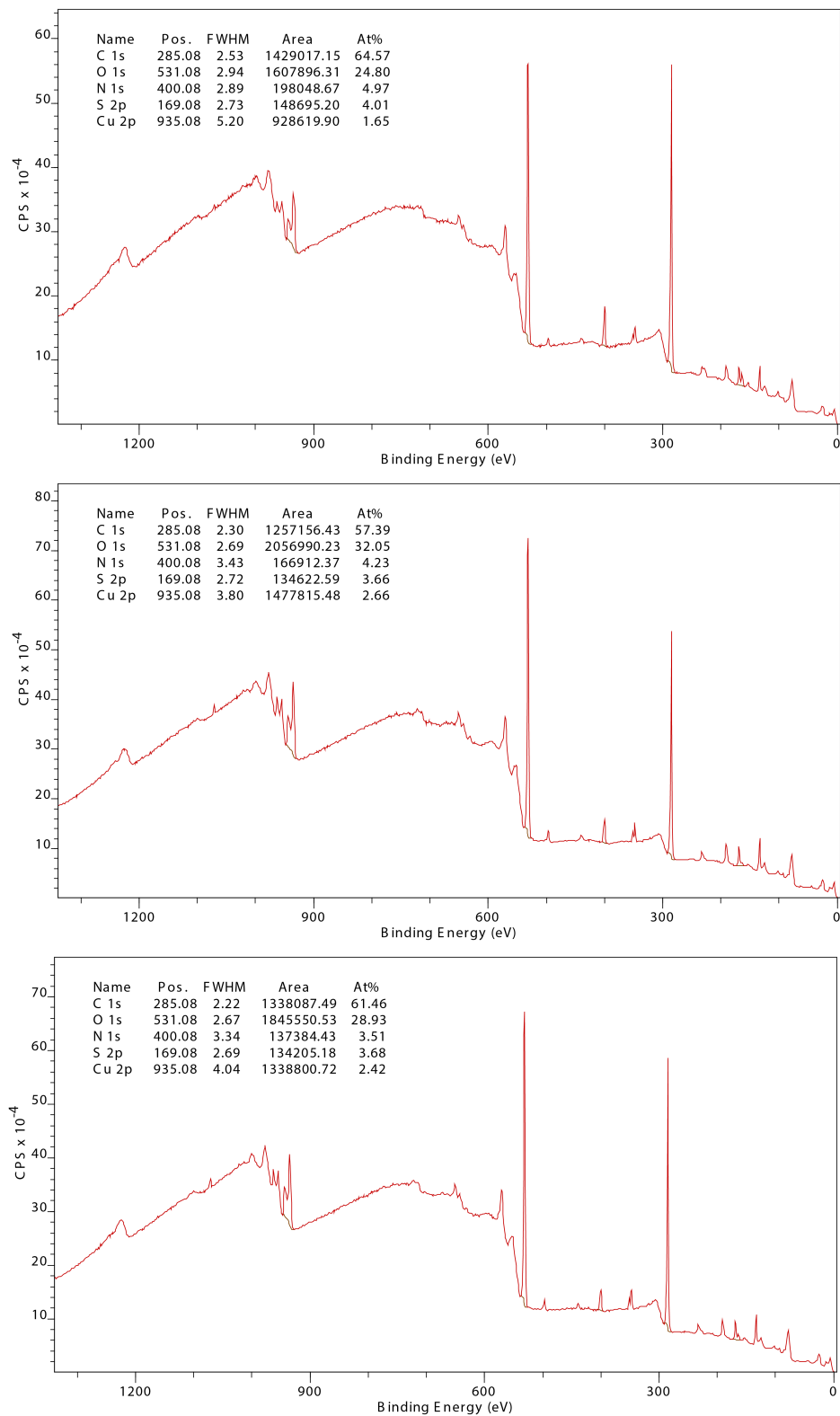


Figure A.3: XPS analysis of three different areas of a coupon tested in corrosion inhibitor 1 at 120 °C

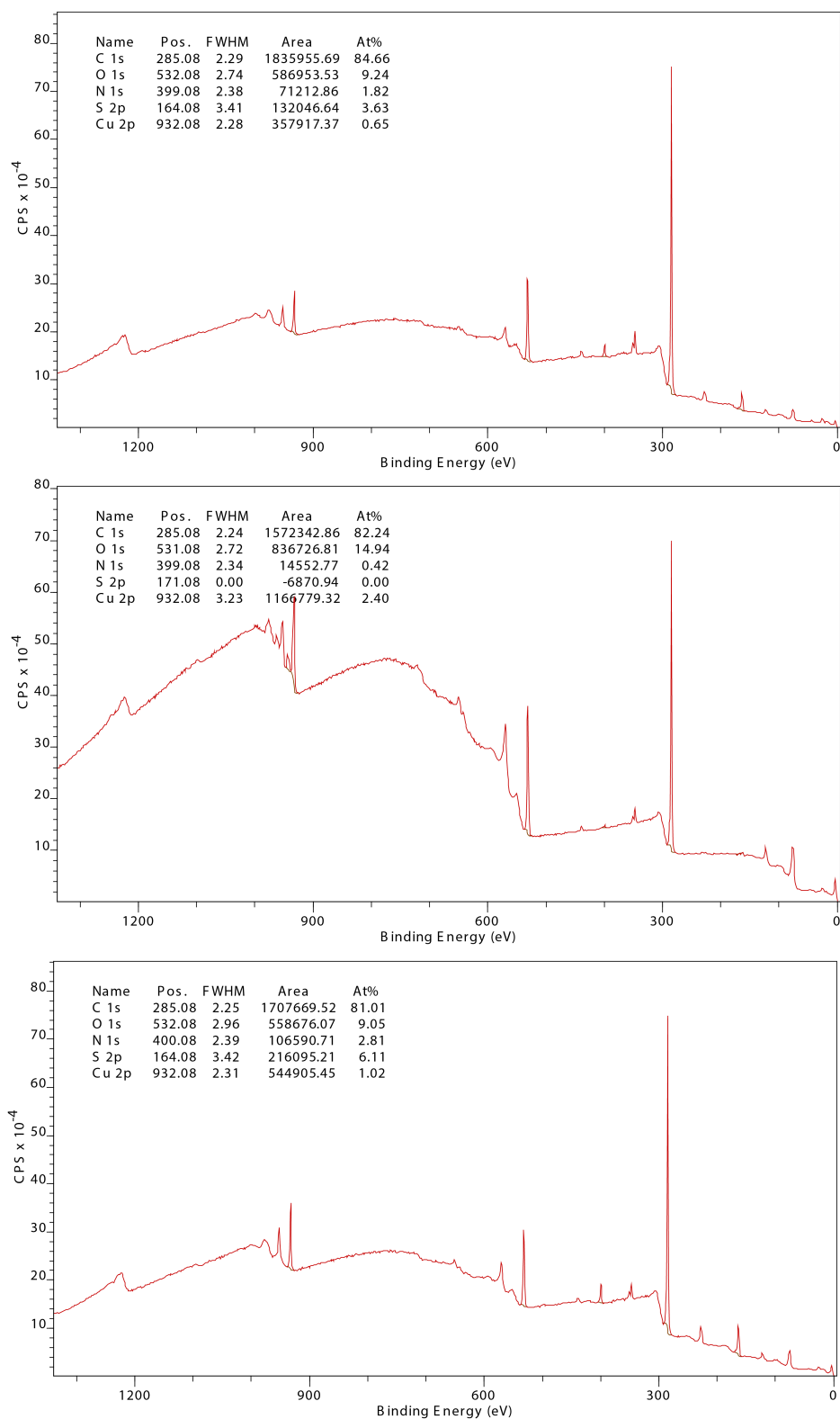


Figure A.4: XPS analysis of three different areas of a coupon tested in corrosion inhibitor 1 at 150 °C

A.3 Corrosion inhibitor 2

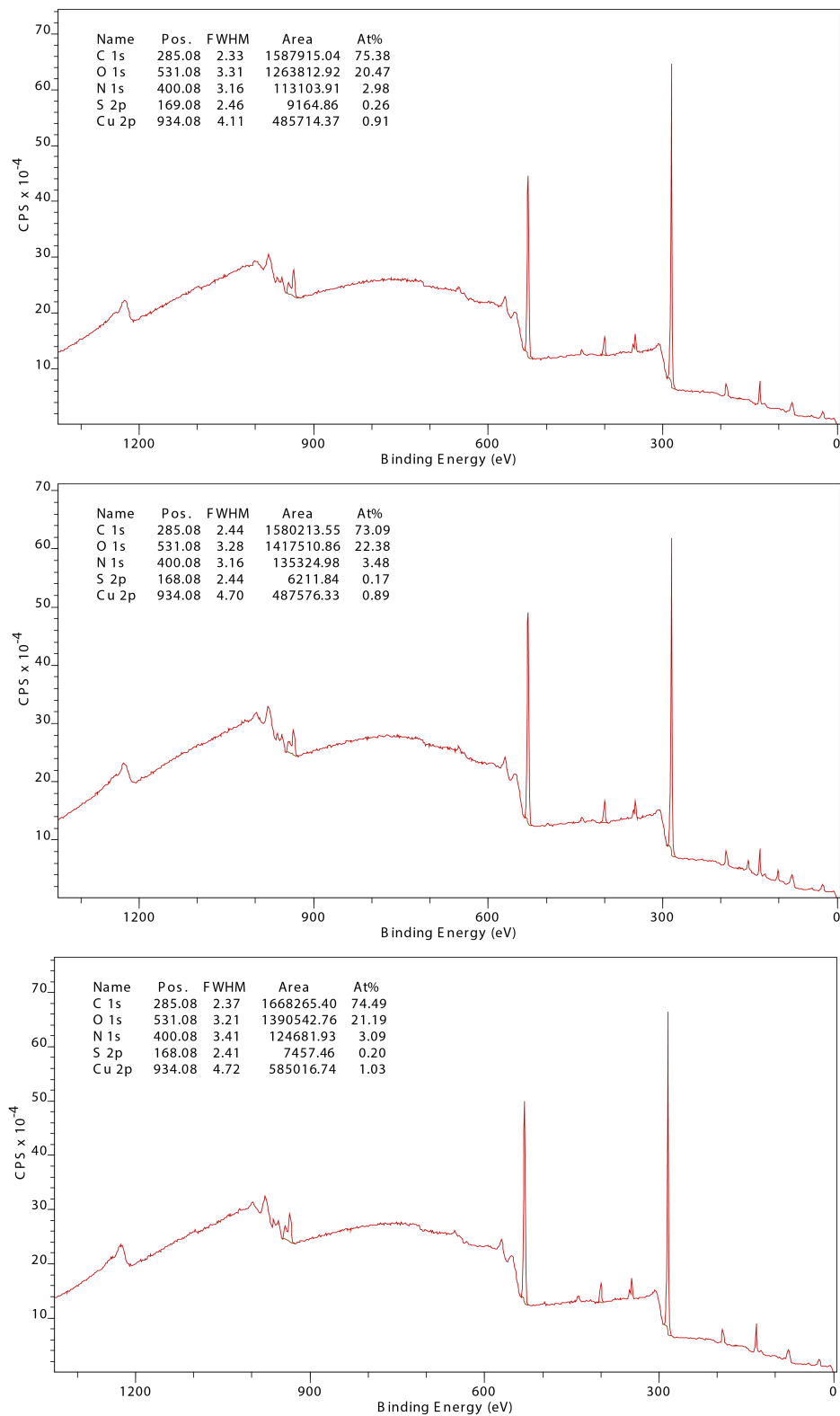


Figure A.5: XPS analysis of three different areas of a coupon tested in corrosion inhibitor 2 at 120 °C

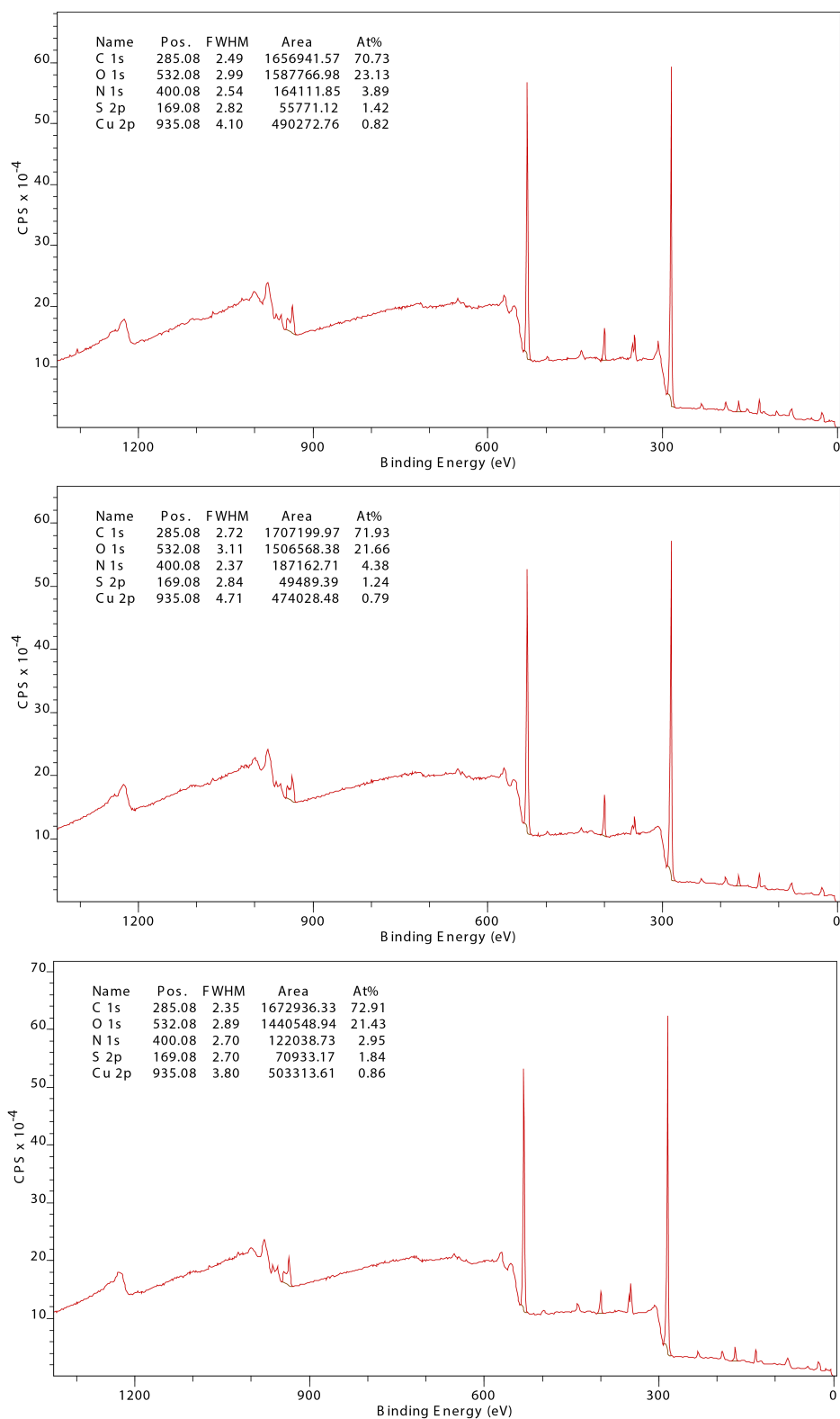


Figure A.6: XPS analysis of three different areas of a coupon tested in corrosion inhibitor 2 at 150 °C

A.4 Dispersant 1

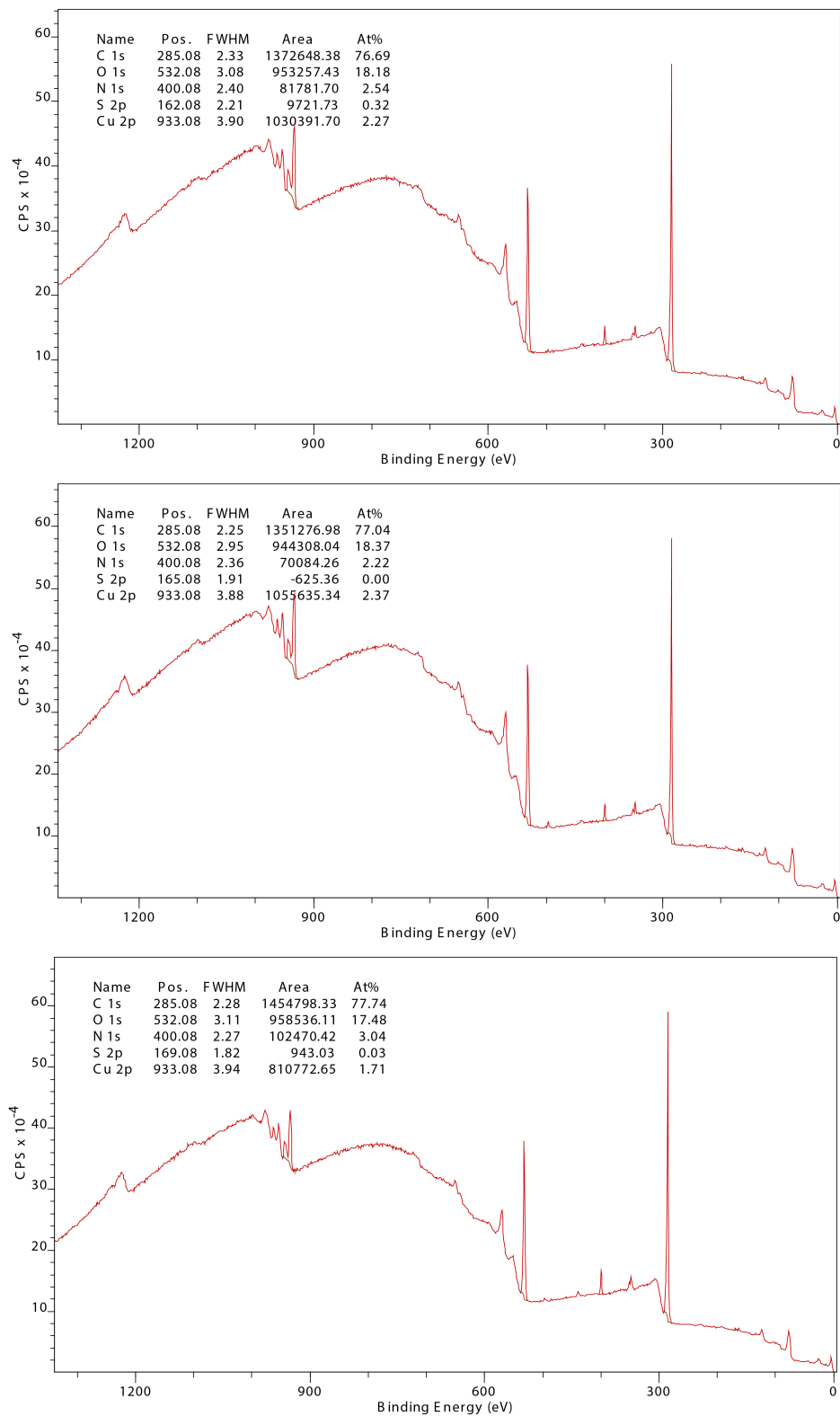


Figure A.7: XPS analysis of three different areas of a coupon tested in dispersant 1 at 120 °C

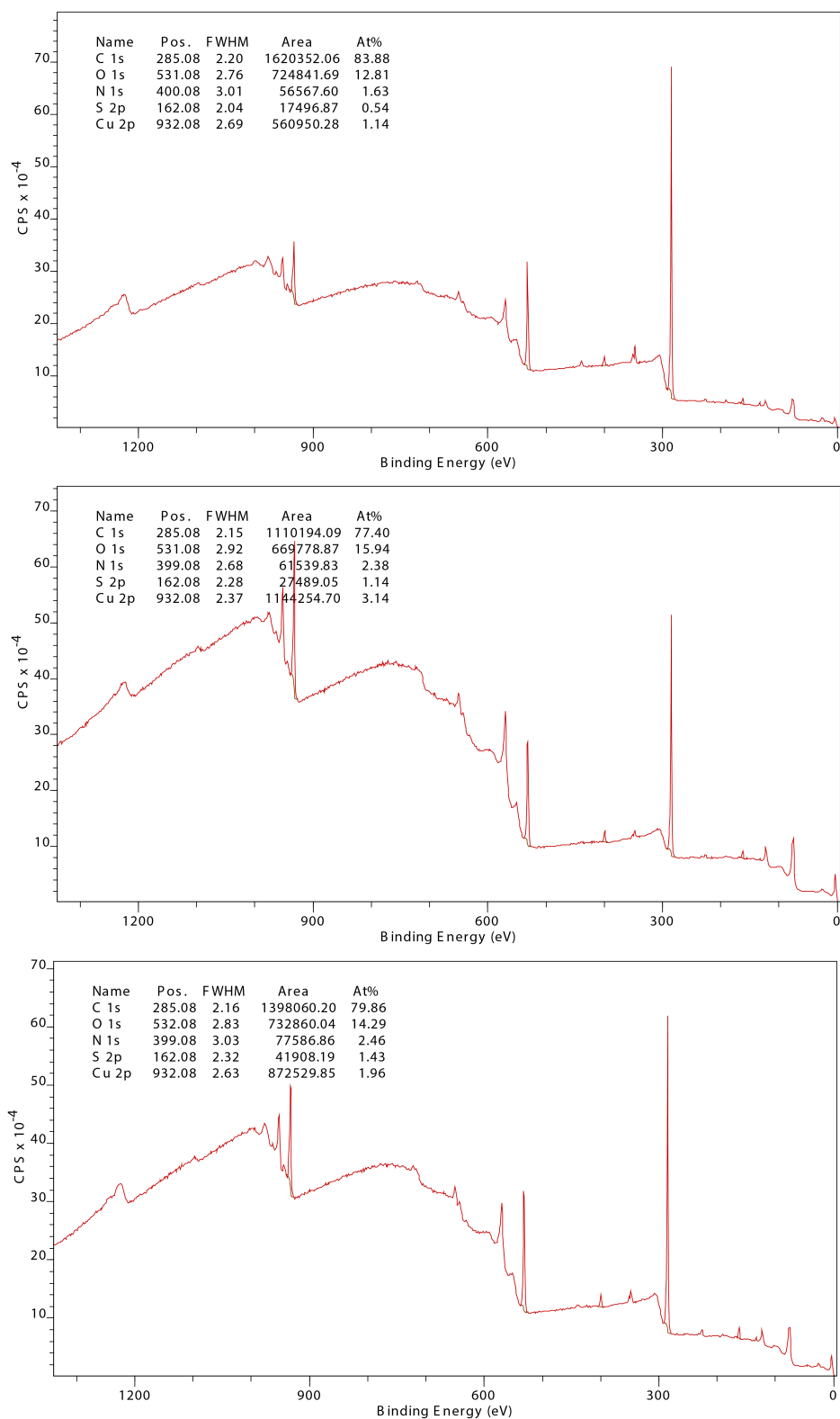


Figure A.8: XPS analysis of three different areas of a coupon tested in dispersant 1 at 150 °C

A.5 Dispersant 2

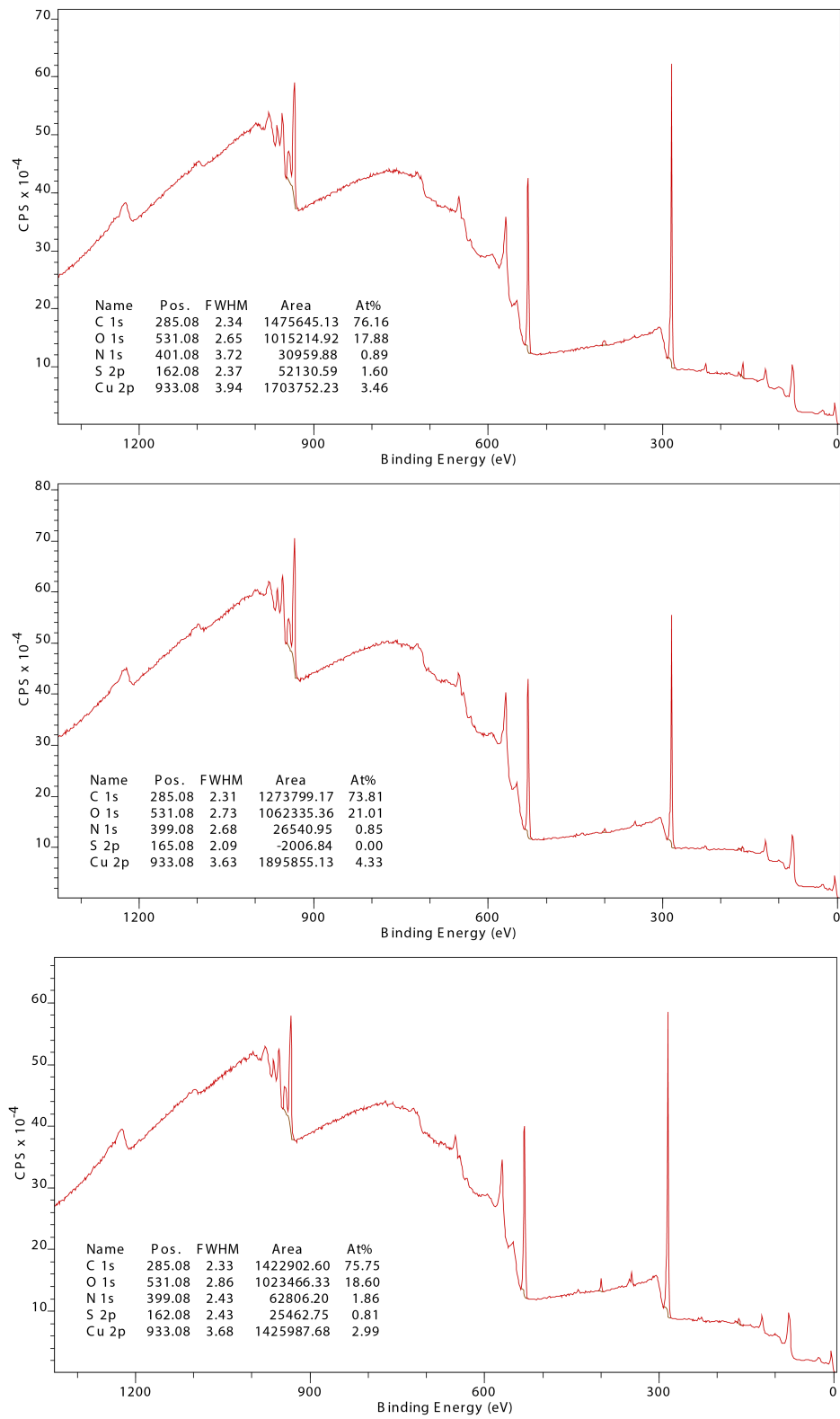


Figure A.9: XPS analysis of three different areas of a coupon tested in dispersant 2 at 120 °C

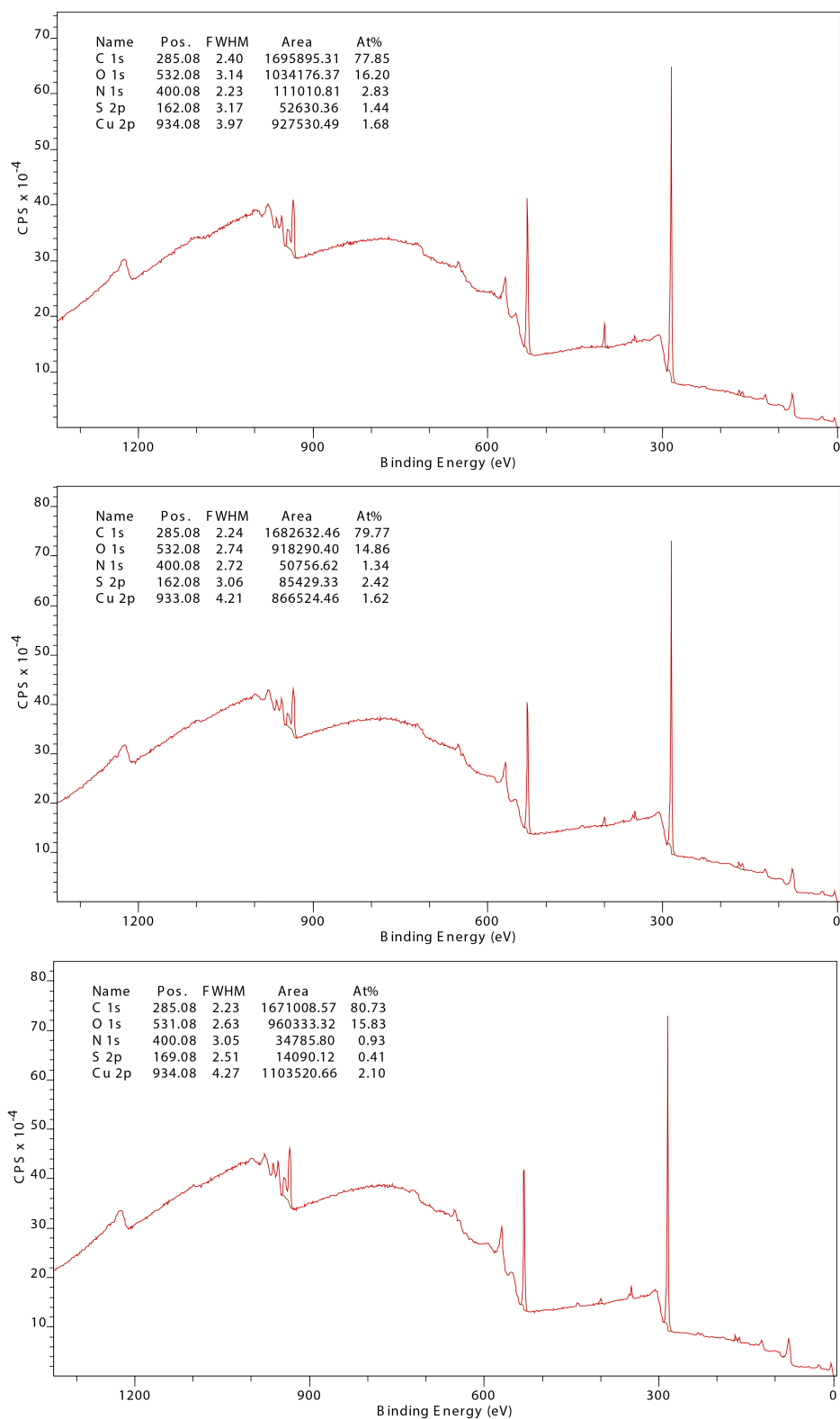


Figure A.10: XPS analysis of three different areas of a coupon tested in dispersant 2 at 150 °C

A.6 Detergent 1

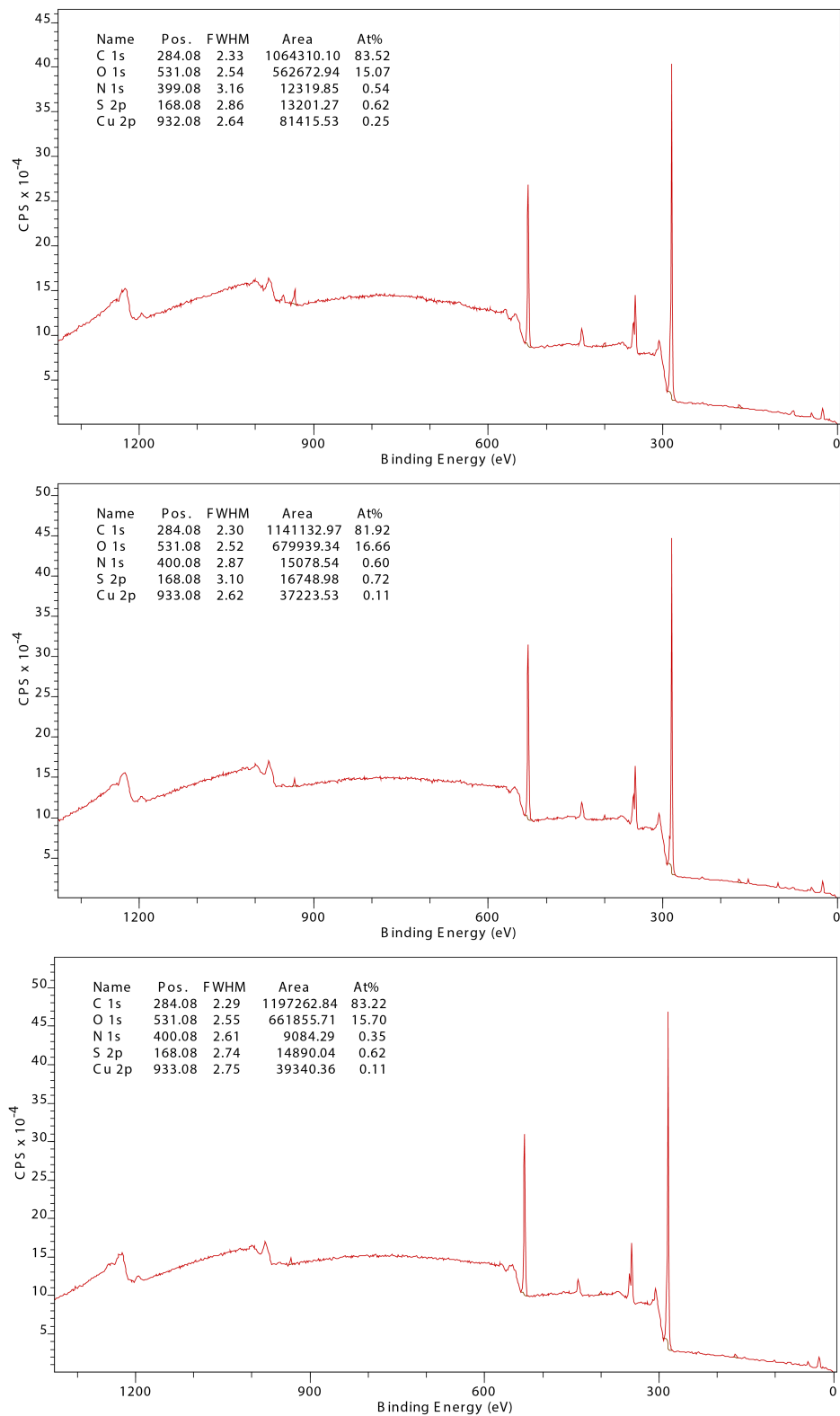


Figure A.11: XPS analysis of three different areas of a coupon tested in detergent 1 at 120 °C

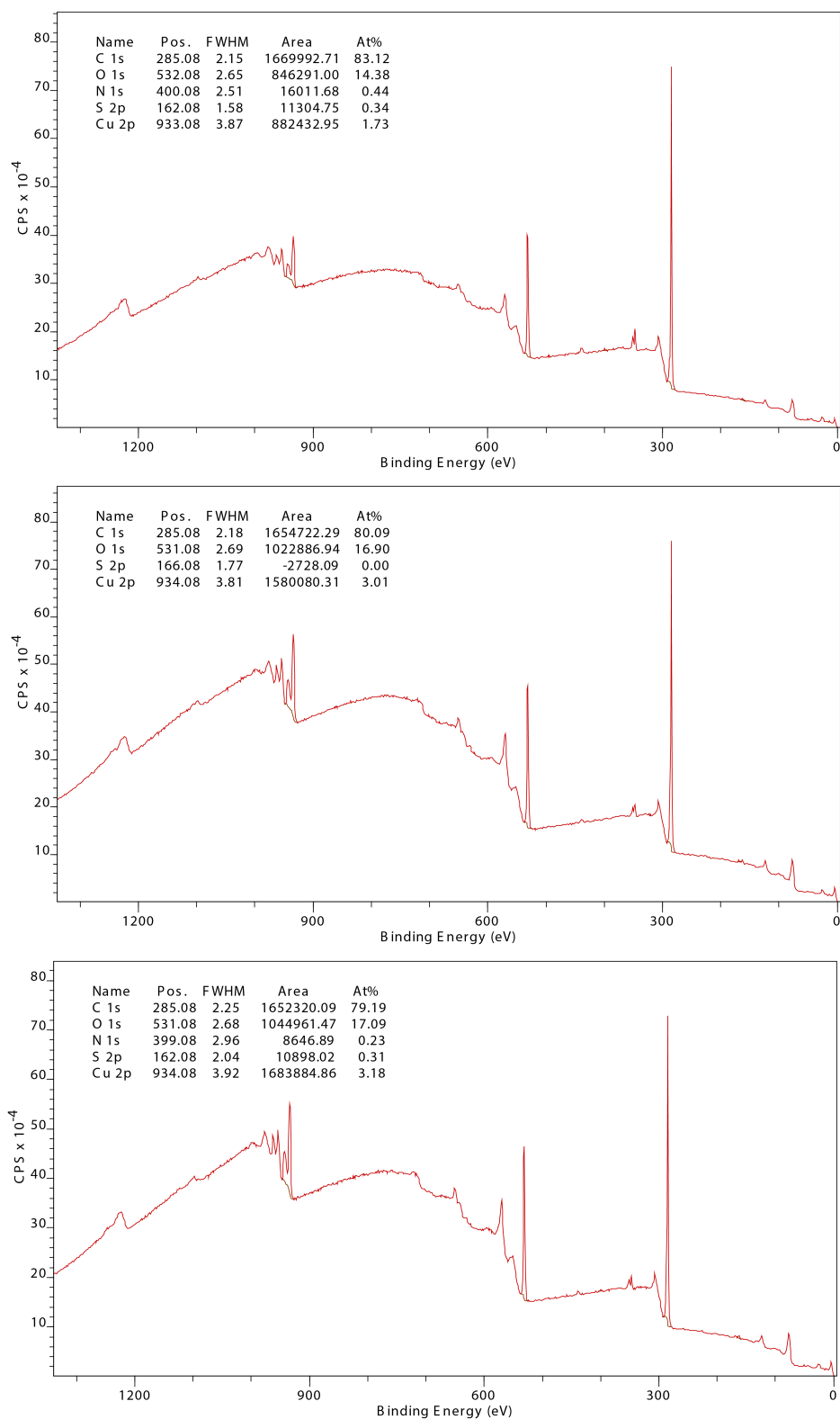


Figure A.12: XPS analysis of three different areas of a coupon tested in detergent 1 at 150 °C

A.7 Detergent 2

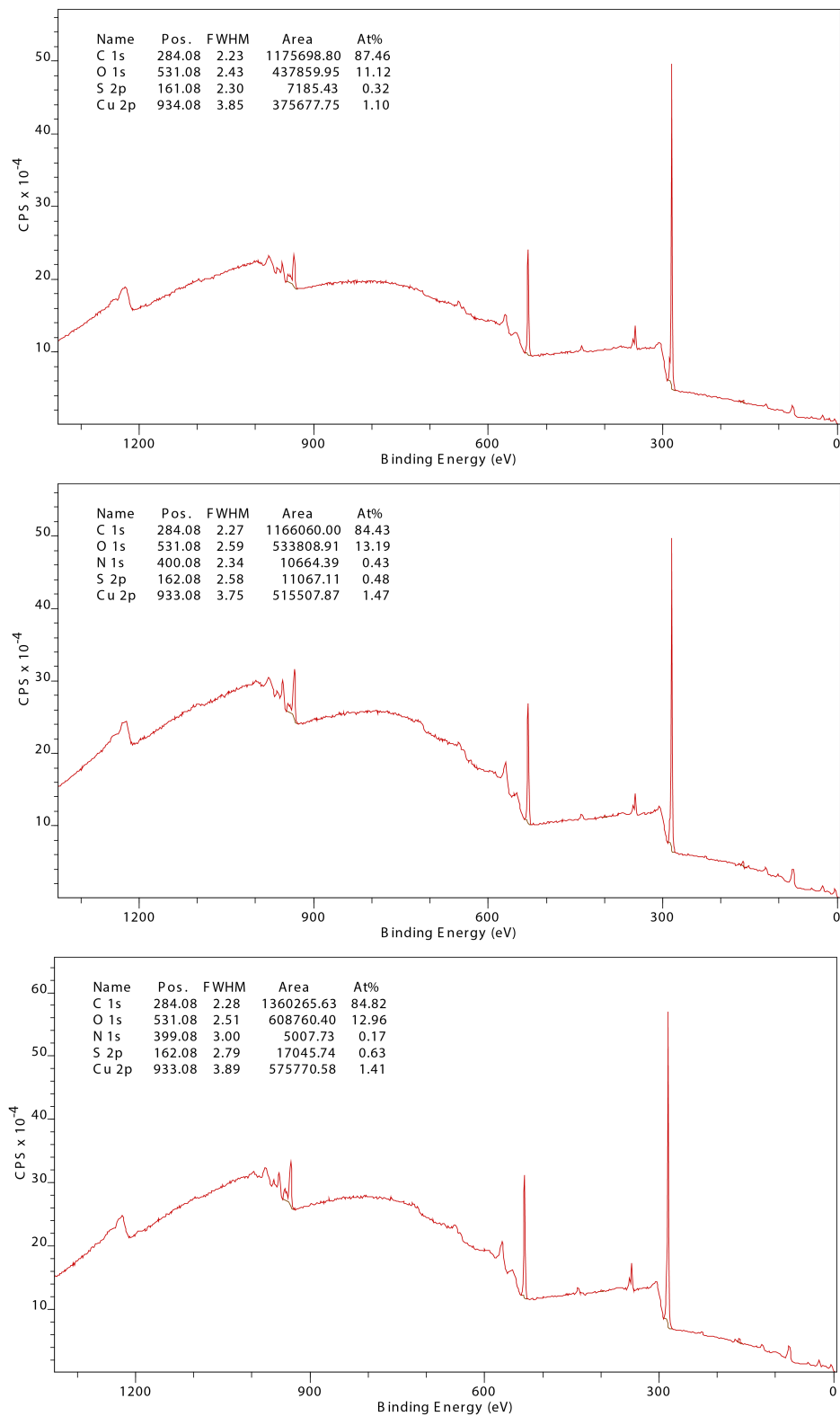


Figure A.13: XPS analysis of three different areas of a coupon tested in detergent 2 at 120 °C

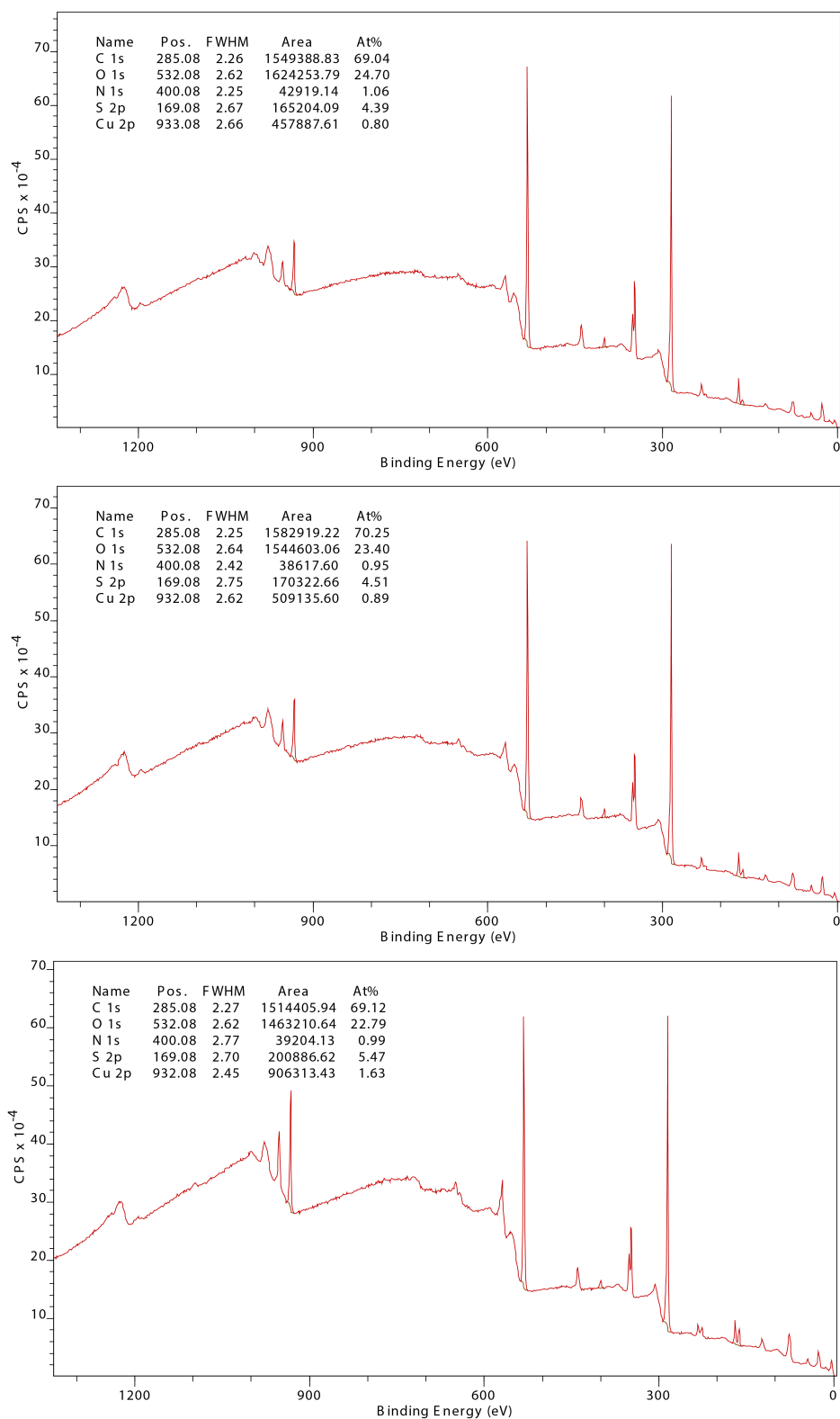


Figure A.14: XPS analysis of three different areas of a coupon tested in detergent 2 at 150 °C

A.8 Antioxidant, antiwear, friction modifier mixture

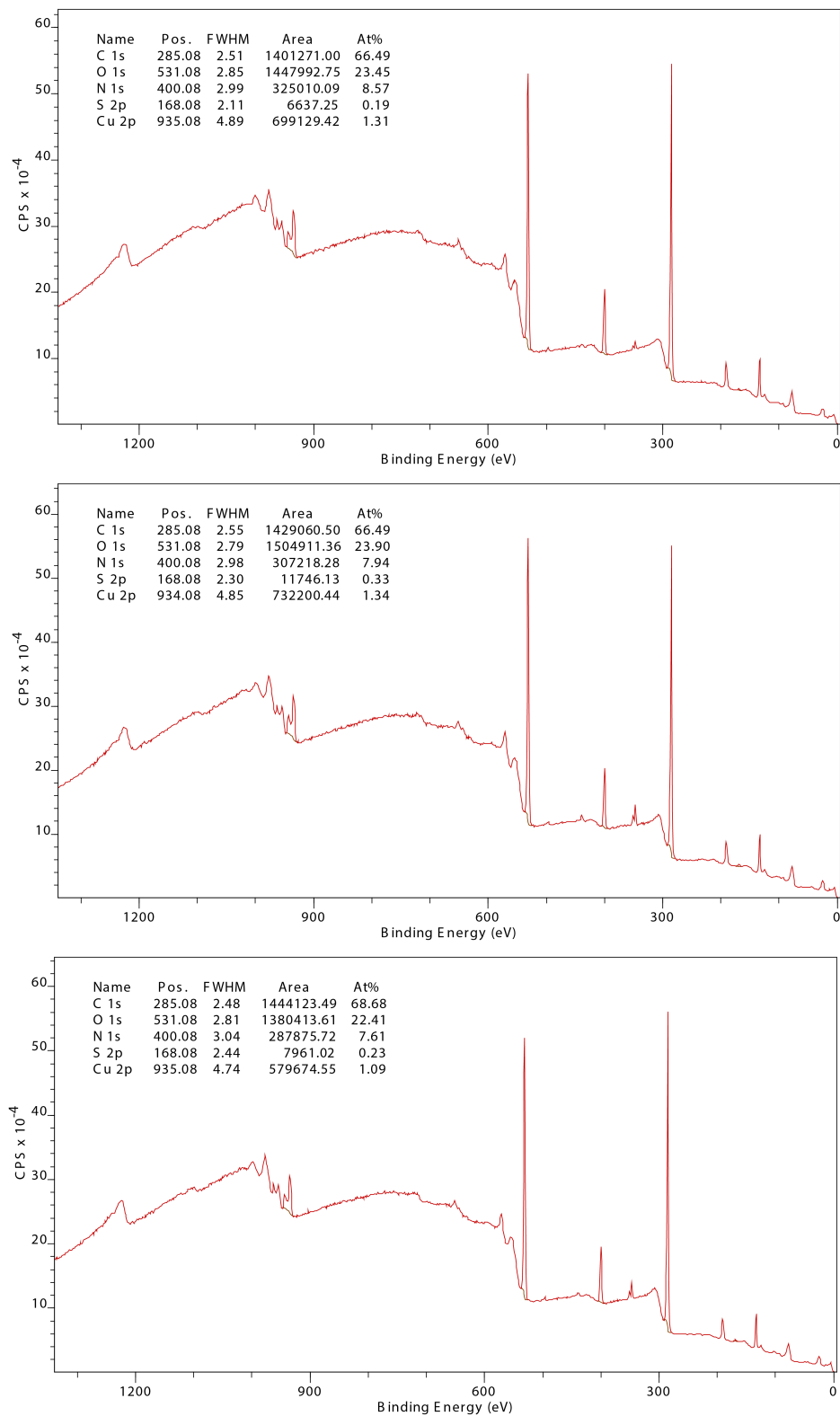


Figure A.15: XPS analysis of three different areas of a coupon tested in the antioxidant, antiwear, friction modifier mixture at 120 °C

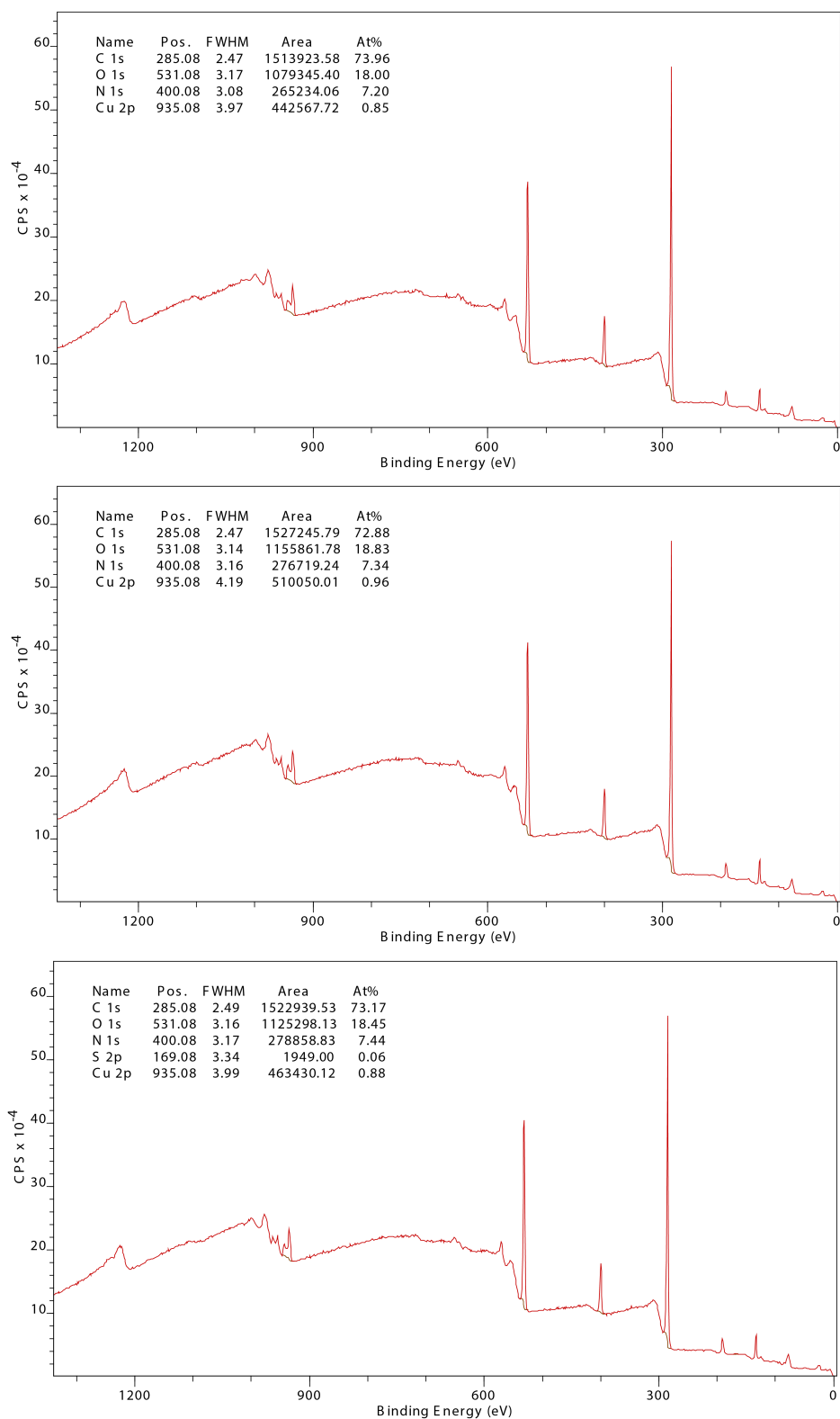


Figure A.16: XPS analysis of three different areas of a coupon tested in the antioxidant, antiwear, friction modifier mixture at 150 °C

A.9 Corrosion inhibitor 2 + antiwear

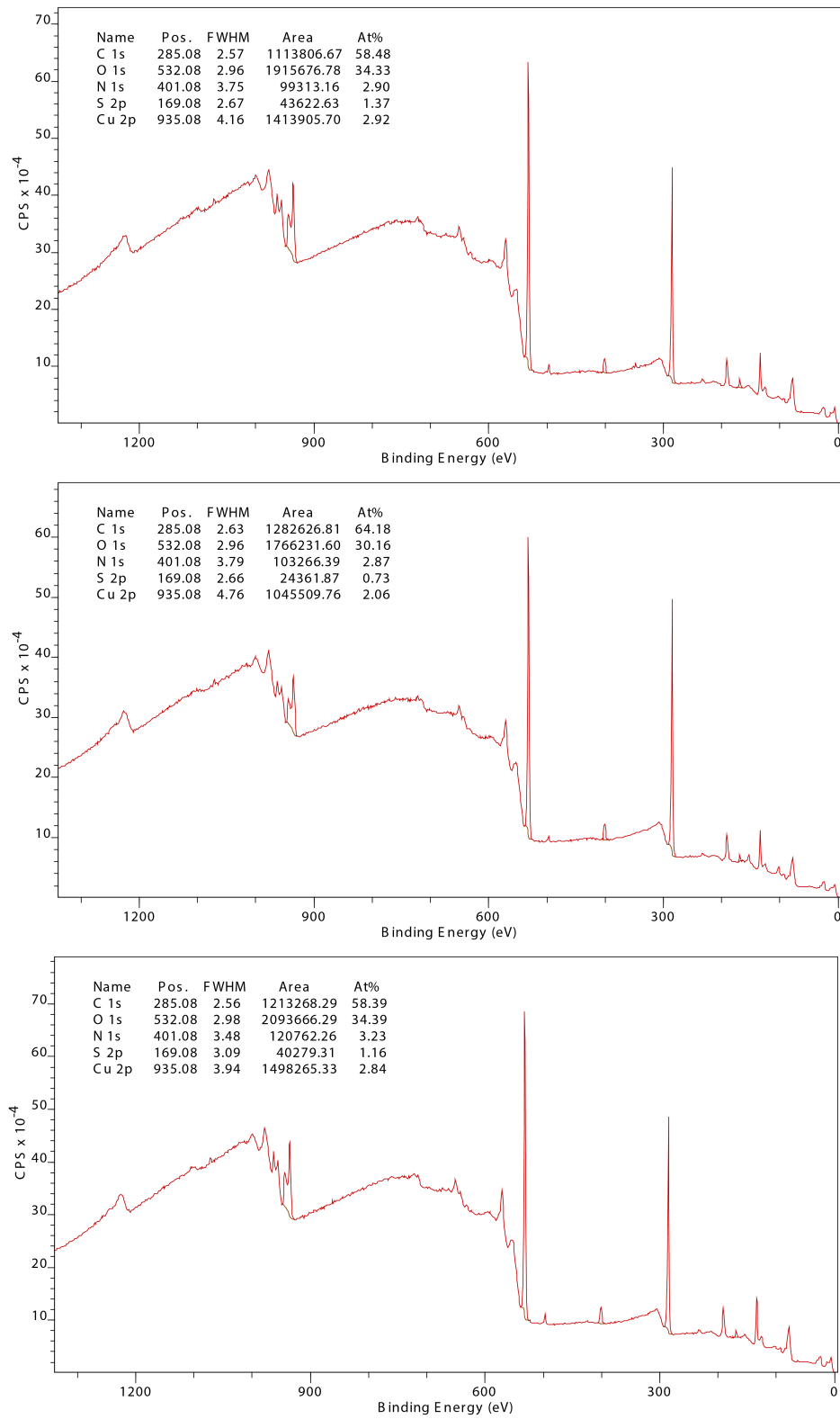


Figure A.17: XPS analysis of three different areas of a coupon tested in corrosion inhibitor 2 + antiwear at 120 °C

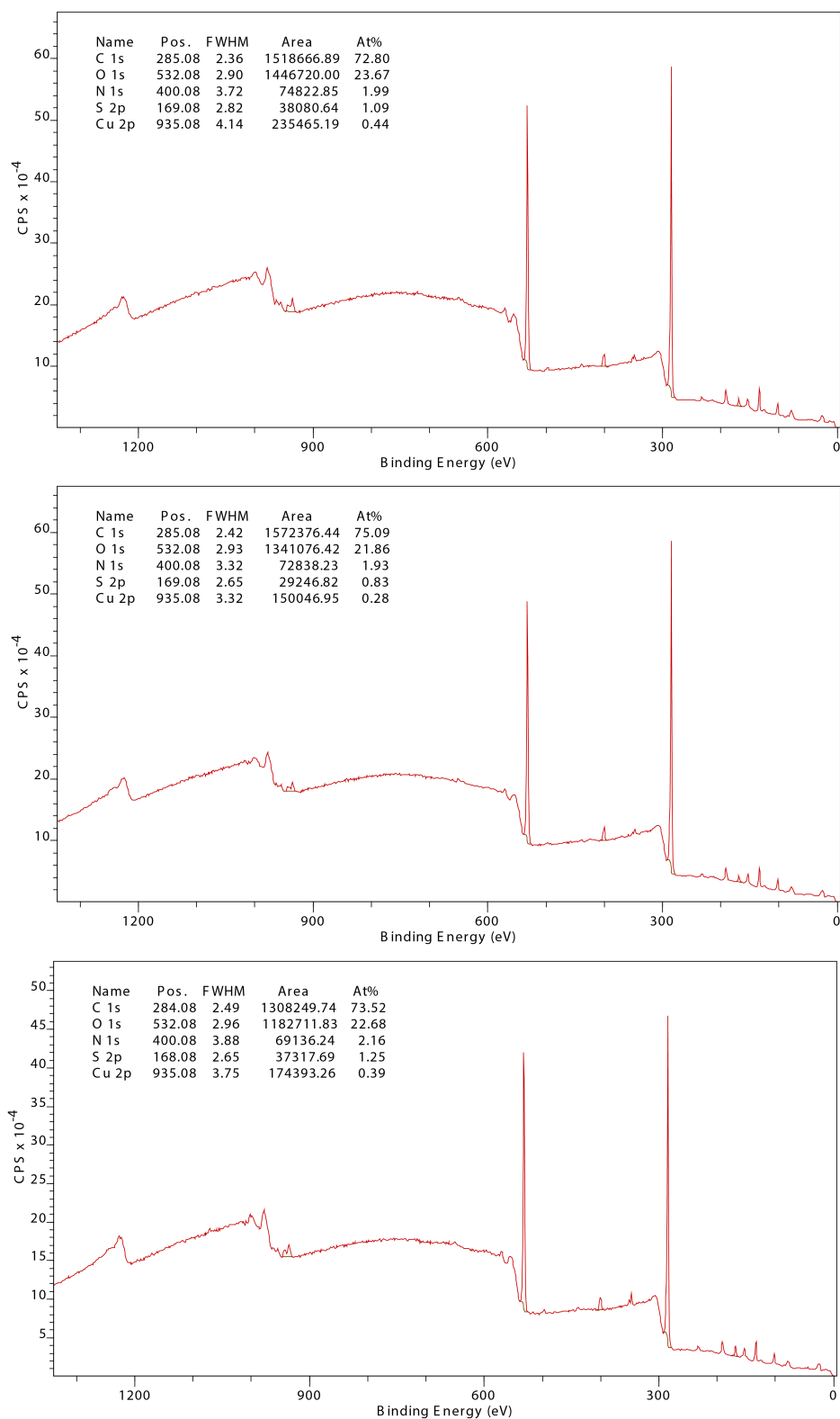


Figure A.18: XPS analysis of three different areas of a coupon tested in corrosion inhibitor 2 + antiwear at 150 °C

A.10 Antioxidant

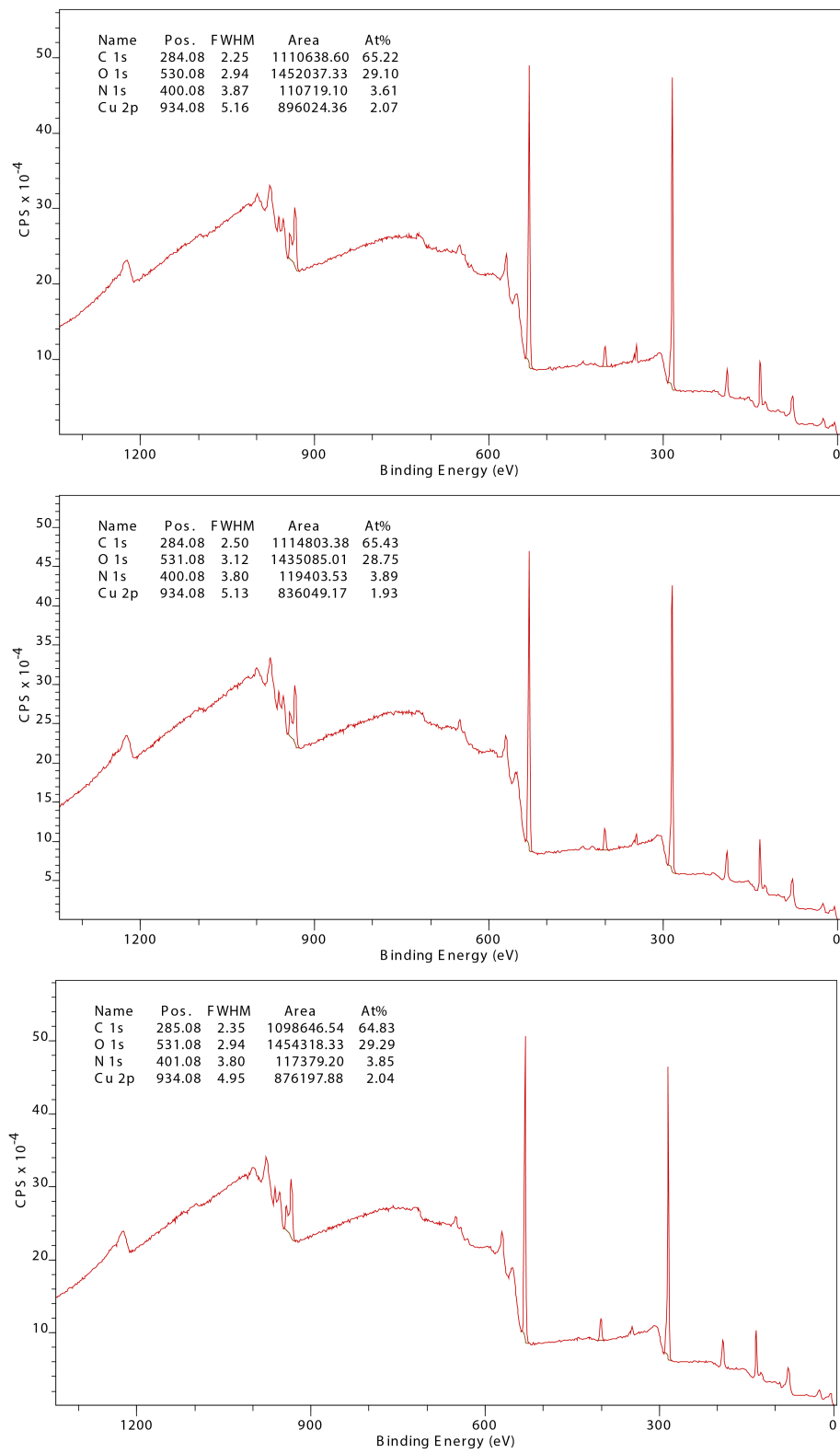


Figure A.19: XPS analysis of three different areas of a coupon tested in antioxidant at 120 °C

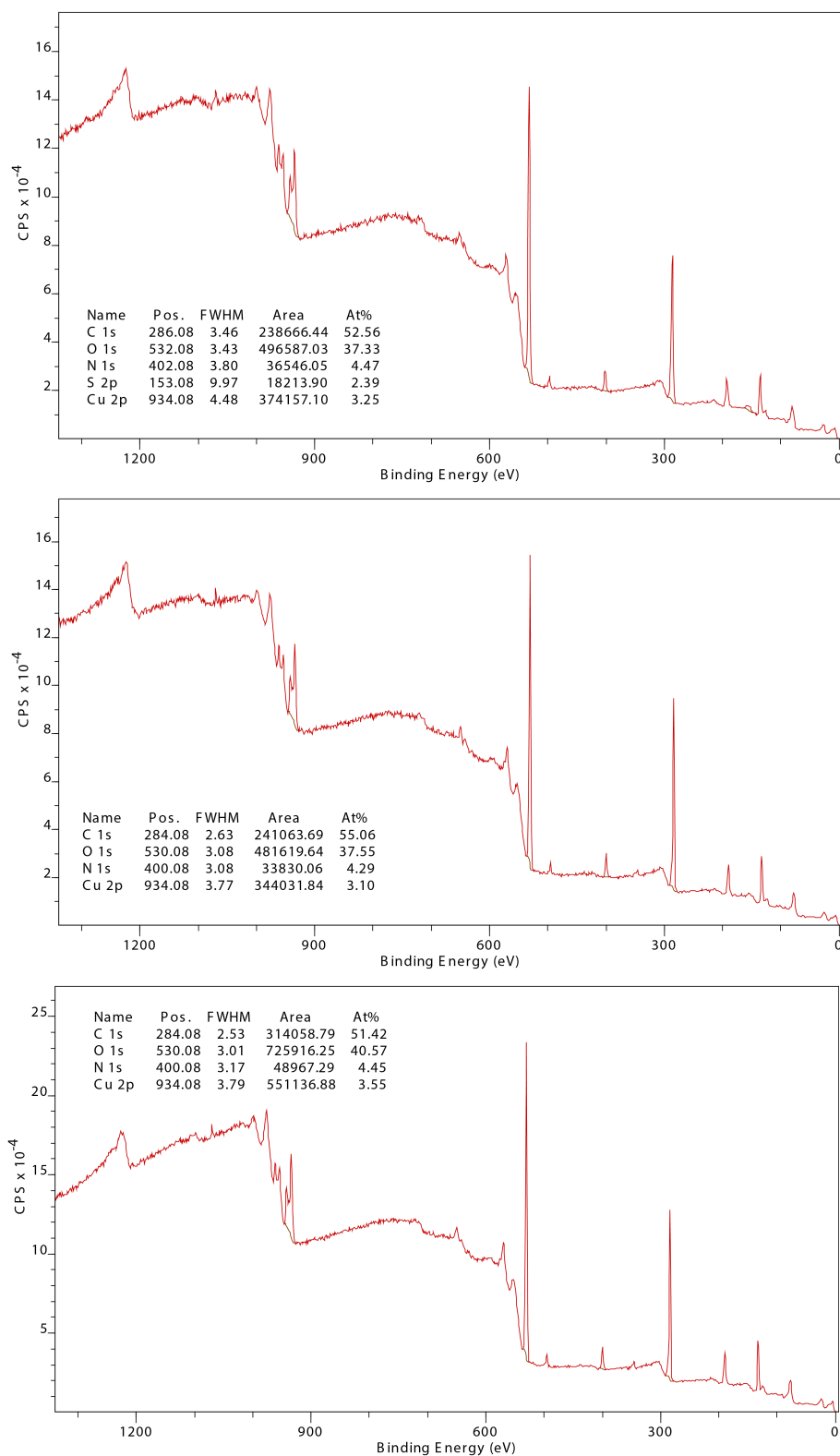


Figure A.20: XPS analysis of three different areas of a coupon tested in antioxidant at 150 °C

A.11 Antiwear

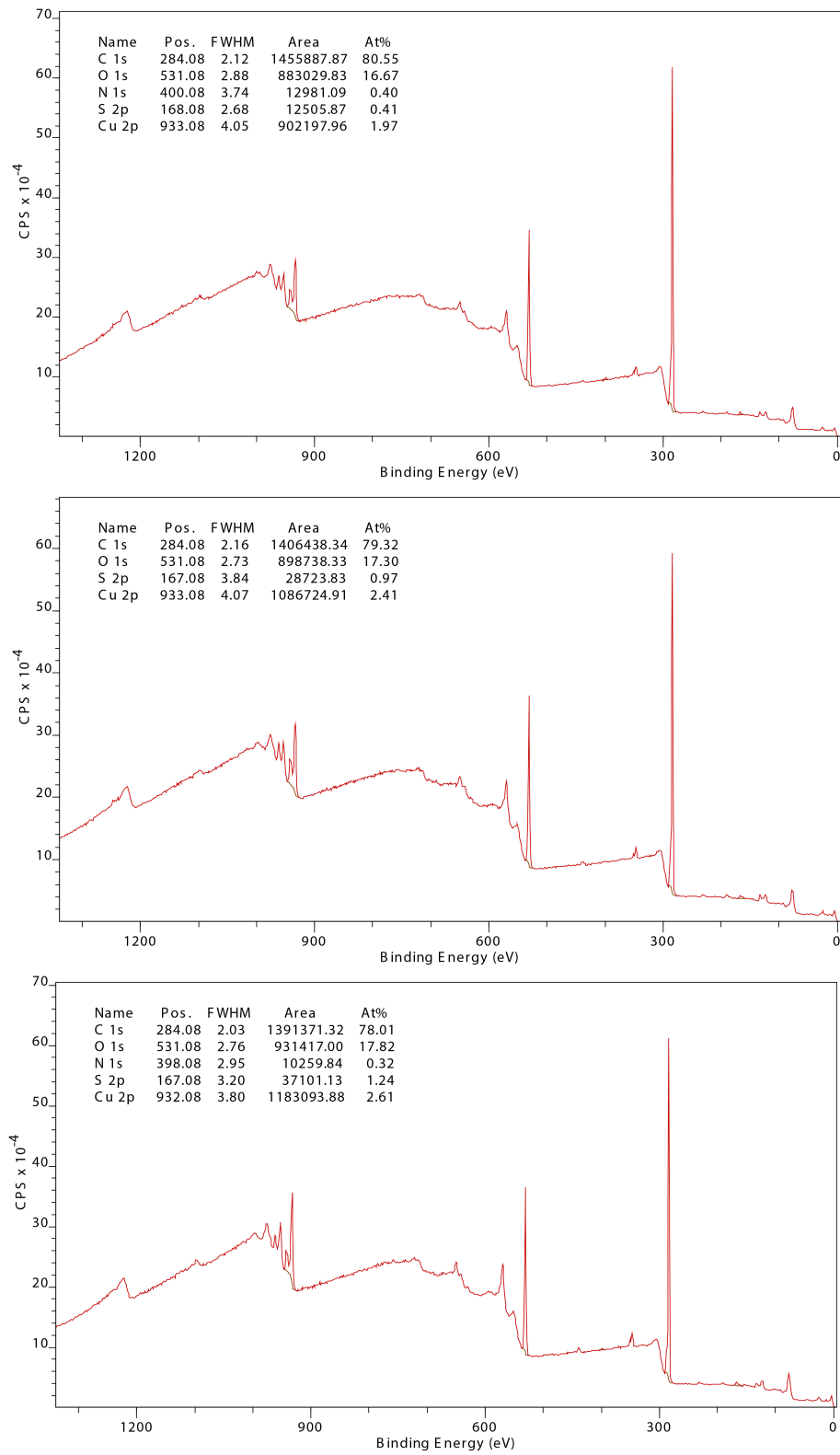


Figure A.21: XPS analysis of three different areas of a coupon tested in antiwear at 120 °C

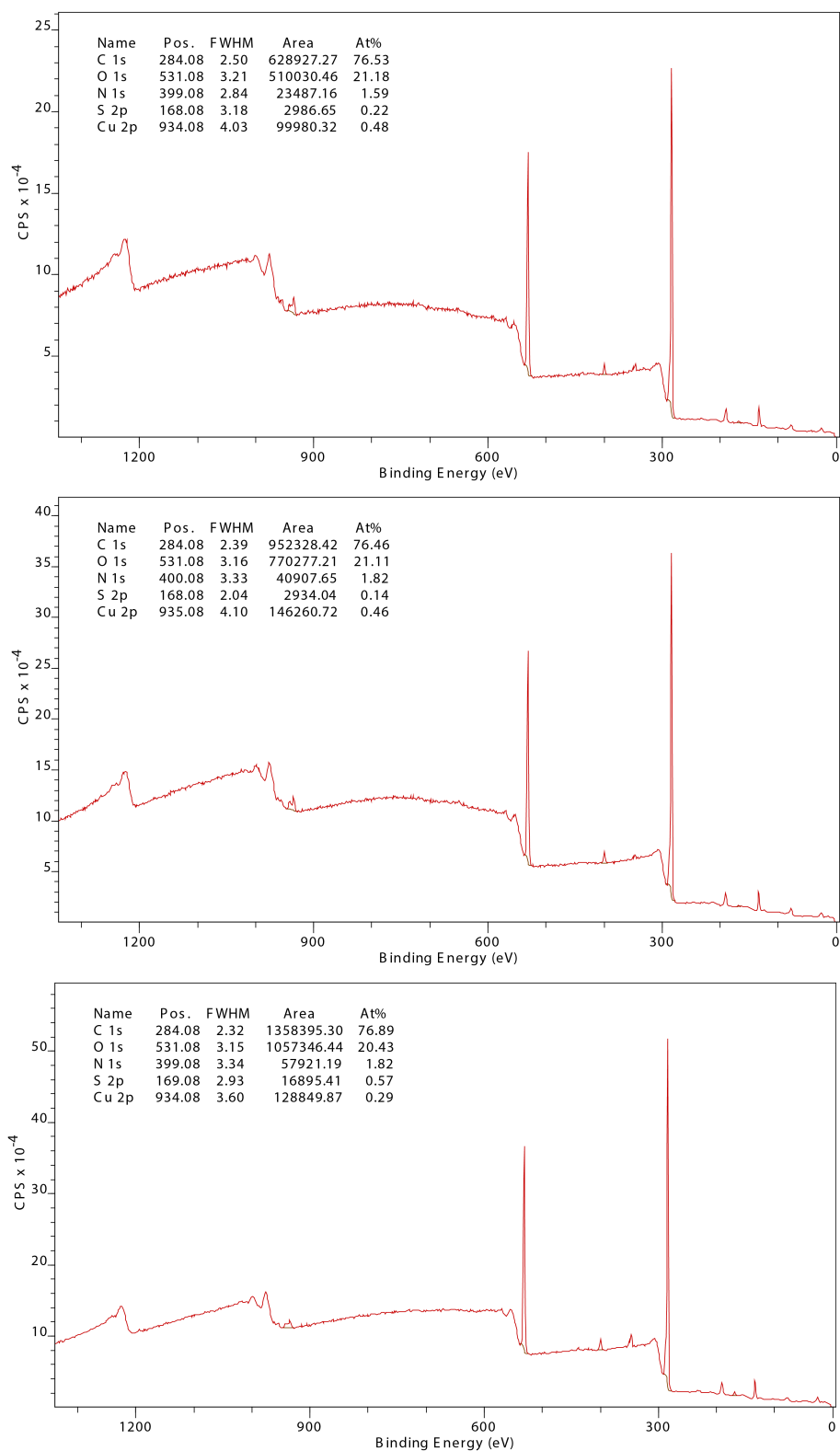


Figure A.22: XPS analysis of three different areas of a coupon tested in antiwear at 150 °C

A.12 Friction modifier

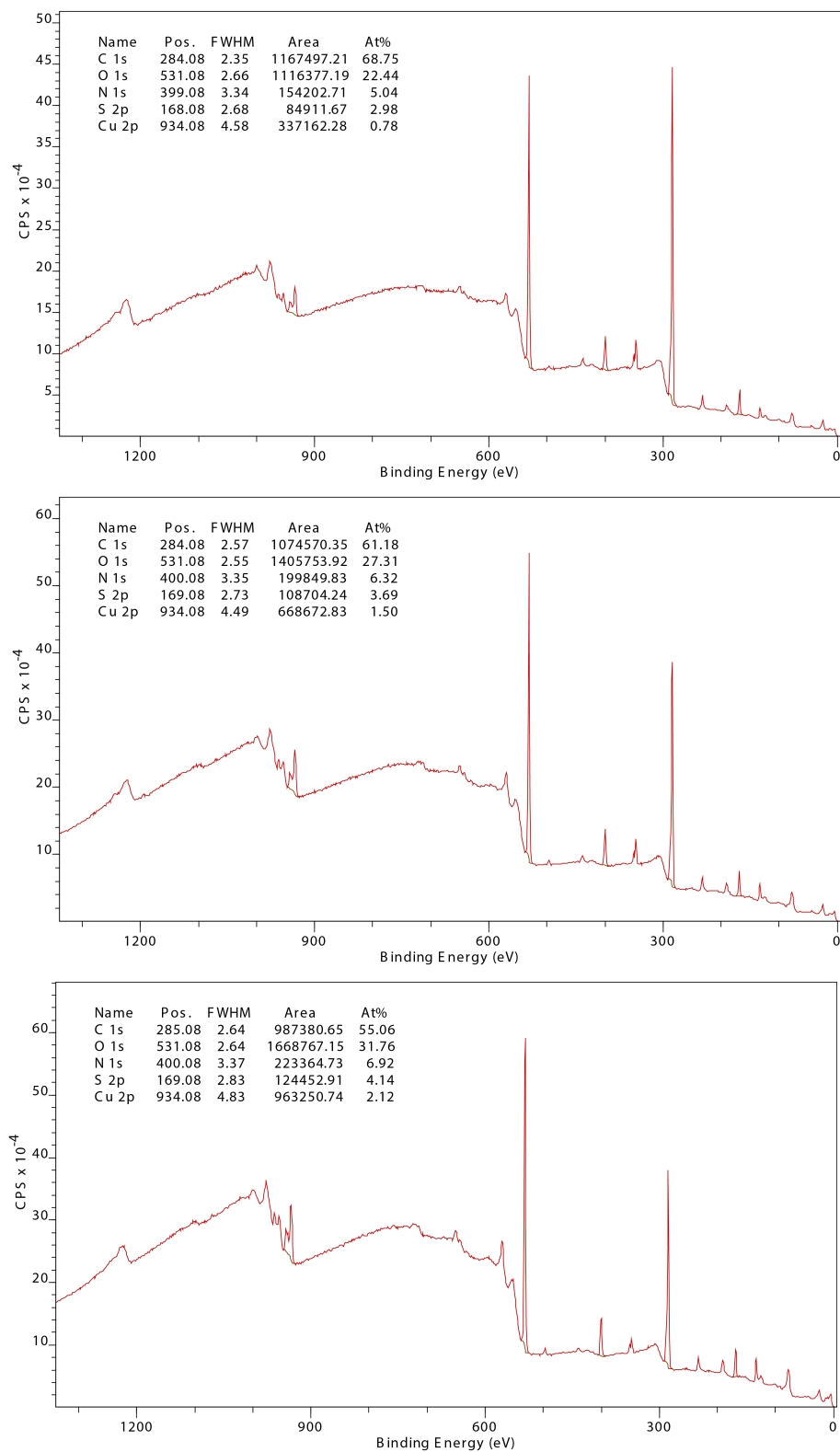


Figure A.23: XPS analysis of three different areas of a coupon tested in friction modifier at 120 °C

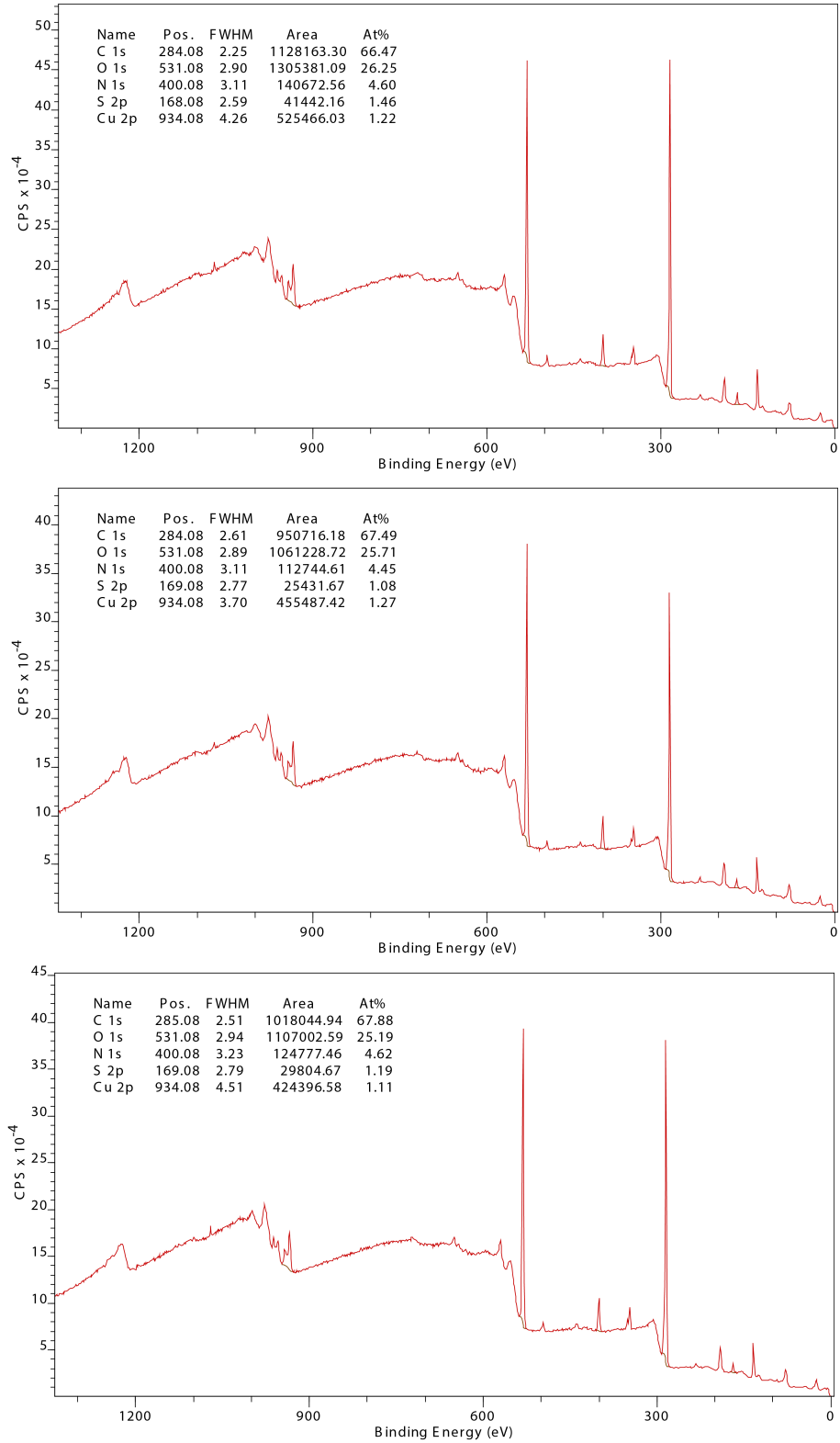


Figure A.24: XPS analysis of three different areas of a coupon tested in friction modifier at 150 °C

B: Radius changes

All of the results from the combined additive testing is shown in this appendix, which is split into two sections. The first section gives the results of testing carried out at 120 °C whilst the second section gives the results from 150 °C.

We shall take Figure B.1 as an example. This figure shows graphs displaying radius change data for all of the results of additives combined with corrosion inhibitor 1. Each graph has a key clearly identifying which additives are being shown. The radius change of the wire tested in the combination is shown along with the results of its component additives alone. The results of the individual additives are shown in blue and yellow. The combinations are shown in red; where run, repeats of the combinations are shown in green and orange. The results are duplicated in order to provide a more complete picture for each additive and to make comparison easier.

Results in both sections are shown in the order of combinations with:

- Corrosion inhibitor 1
- Corrosion inhibitor 2
- Dispersant 1
- Dispersant 2
- Detergent 1
- Detergent 2
- AO, AW, FM mix

B.1 Additives at 120 °C

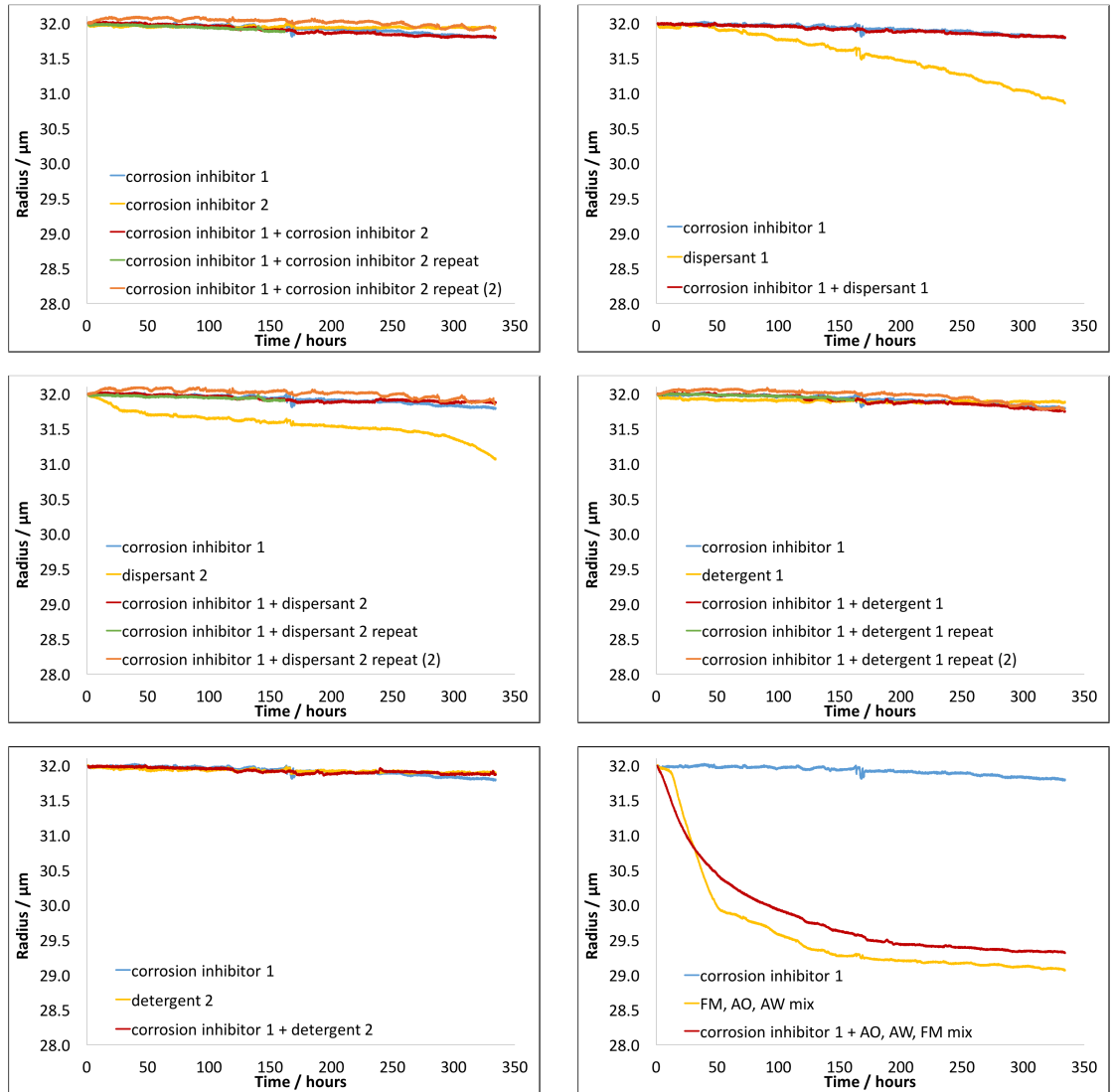


Figure B.1: Radius change data for additive combinations, and their individual additives at 120 °C for fluids containing corrosion inhibitor 1, with repeats where they were carried out

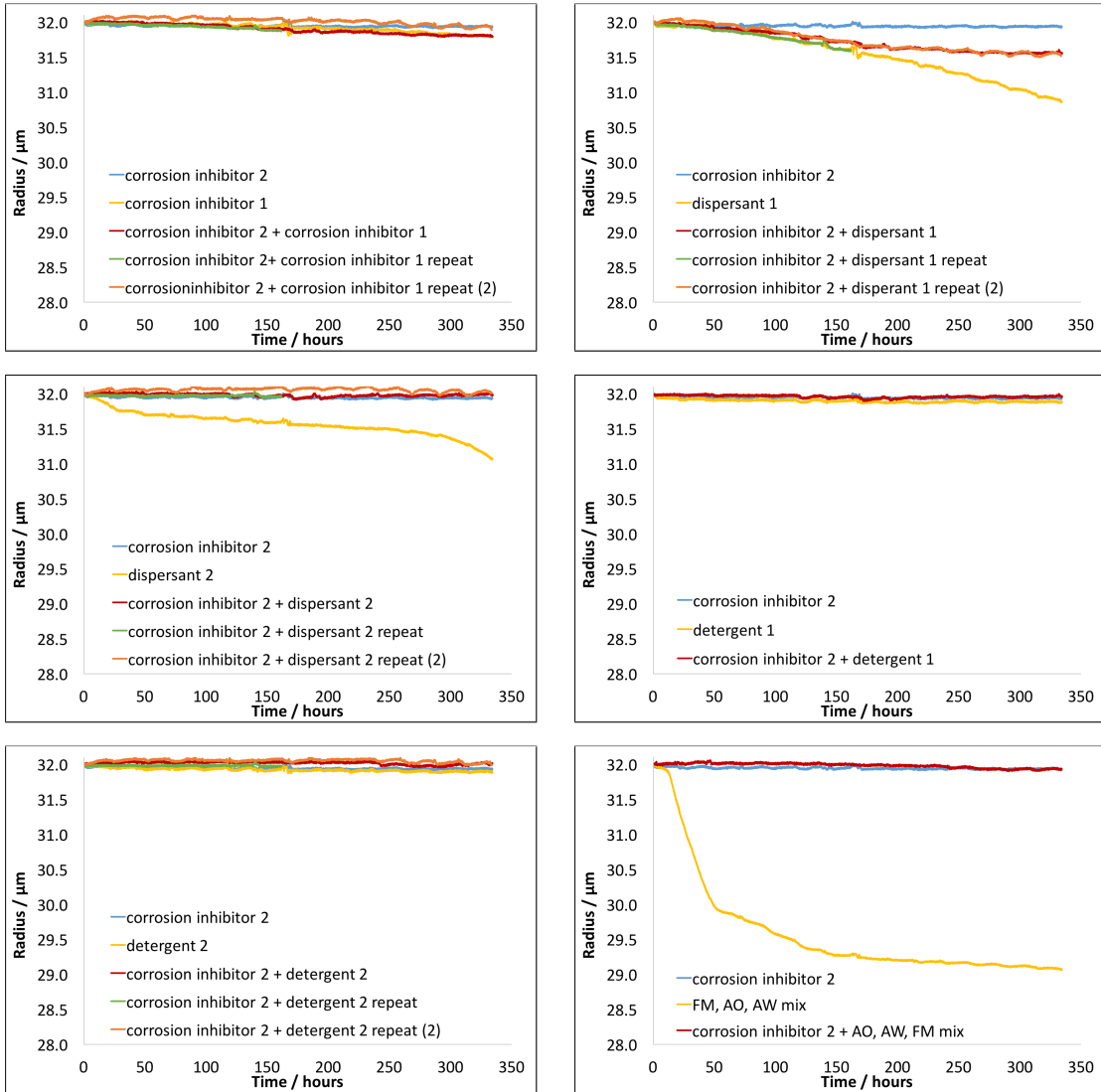


Figure B.2: Radius change data for additive combinations, and their individual additives at 120 °C for fluids containing corrosion inhibitor 2, with repeats where they were carried out

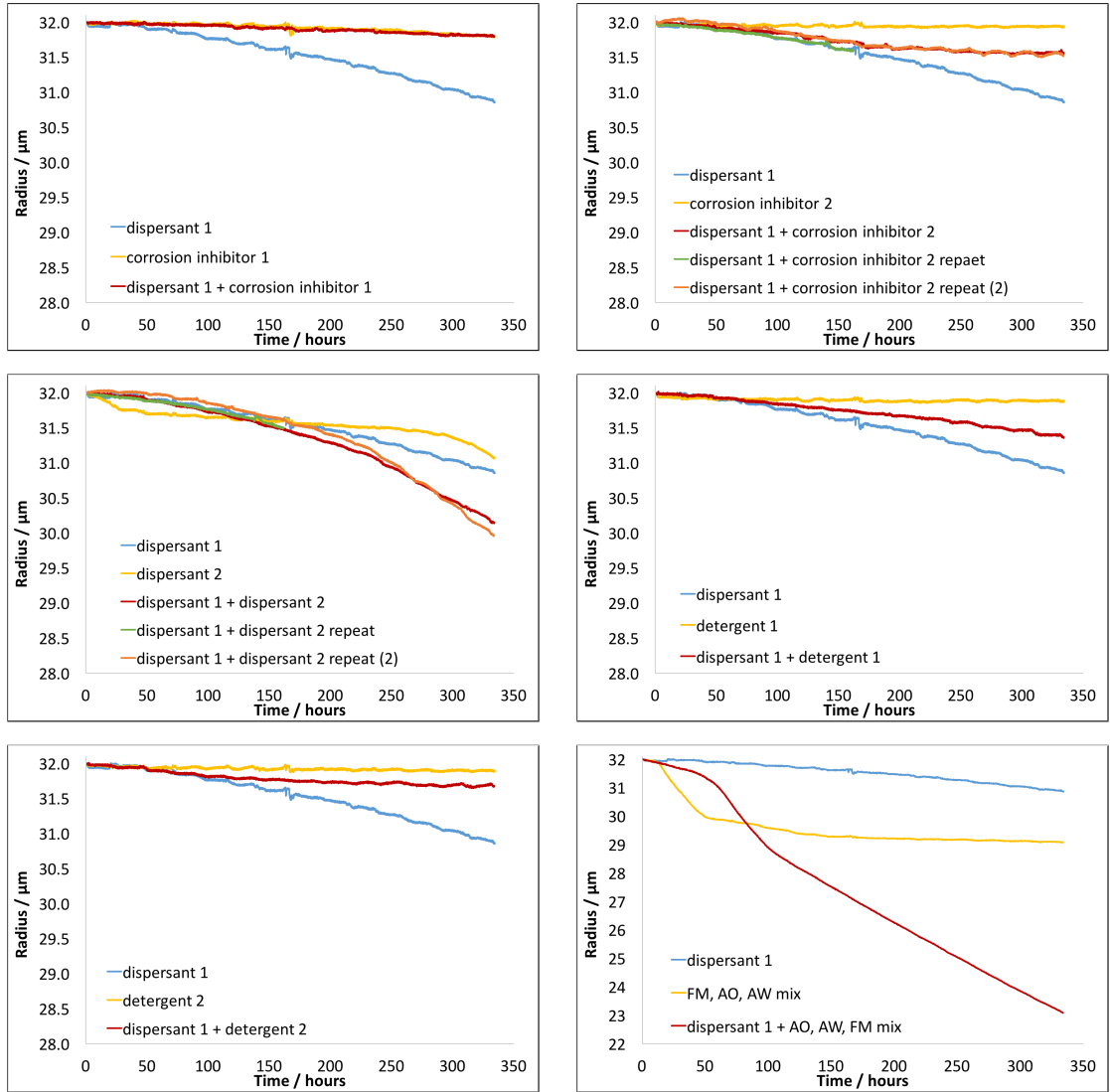


Figure B.3: Radius change data for additive combinations, and their individual additives at $120\text{ }^\circ\text{C}$ for fluids containing dispersant 1, with repeats where they were carried out

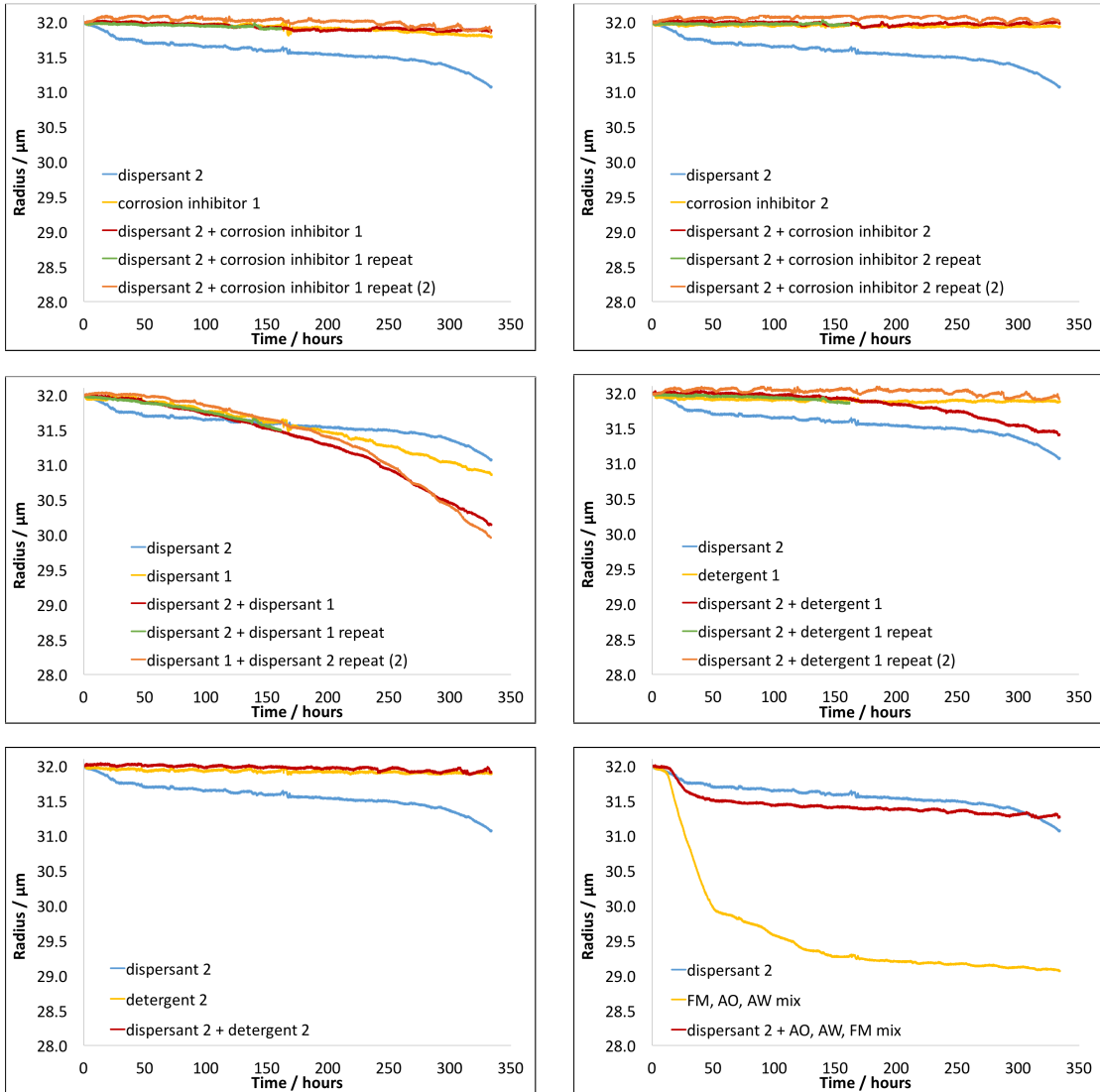


Figure B.4: Radius change data for additive combinations, and their individual additives at $120\text{ }^\circ\text{C}$ for fluids containing dispersant 2, with repeats where they were carried out

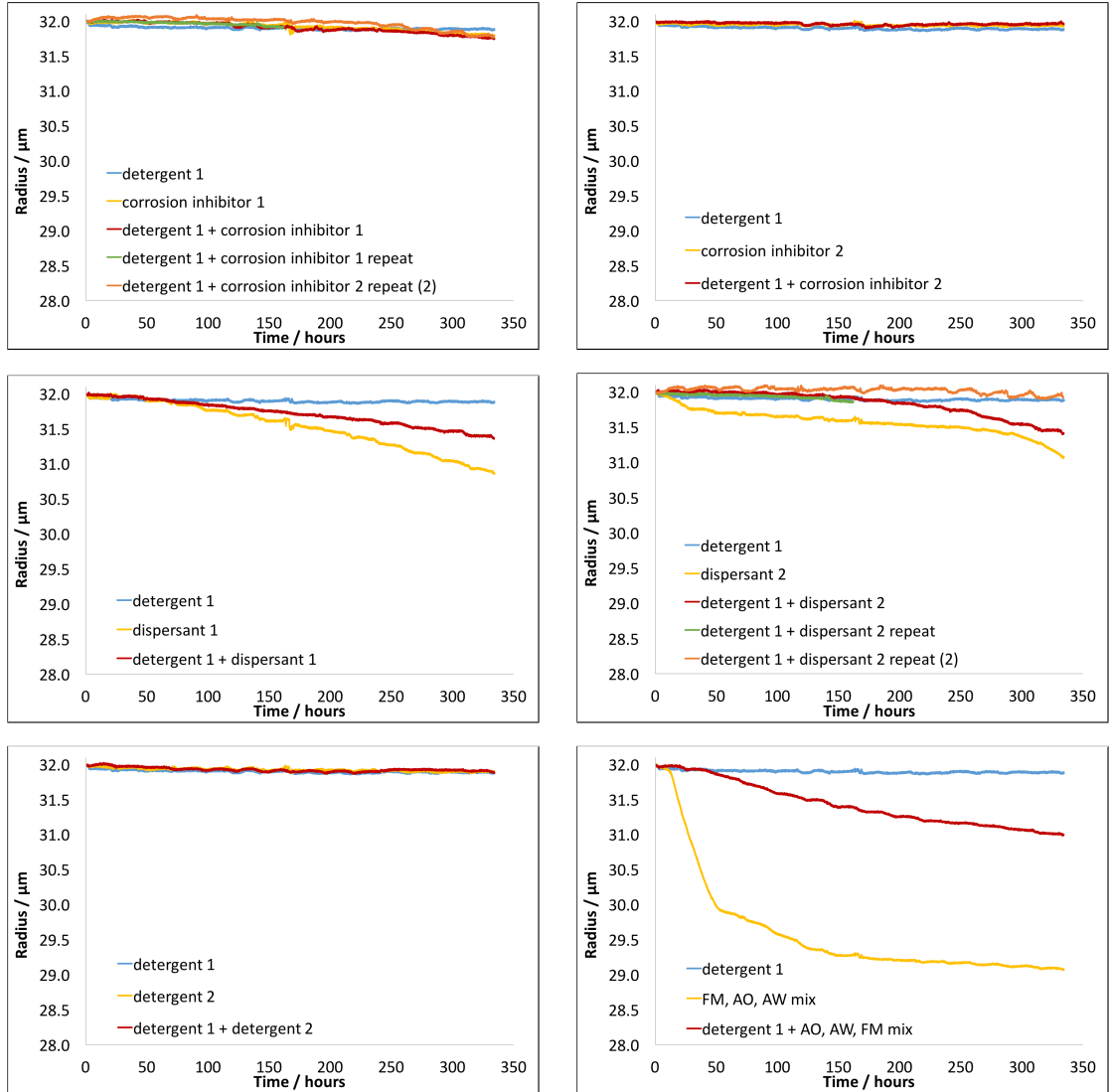


Figure B.5: Radius change data for additive combinations, and their individual additives at 120 °C for fluids containing detergent 1, with repeats where they were carried out

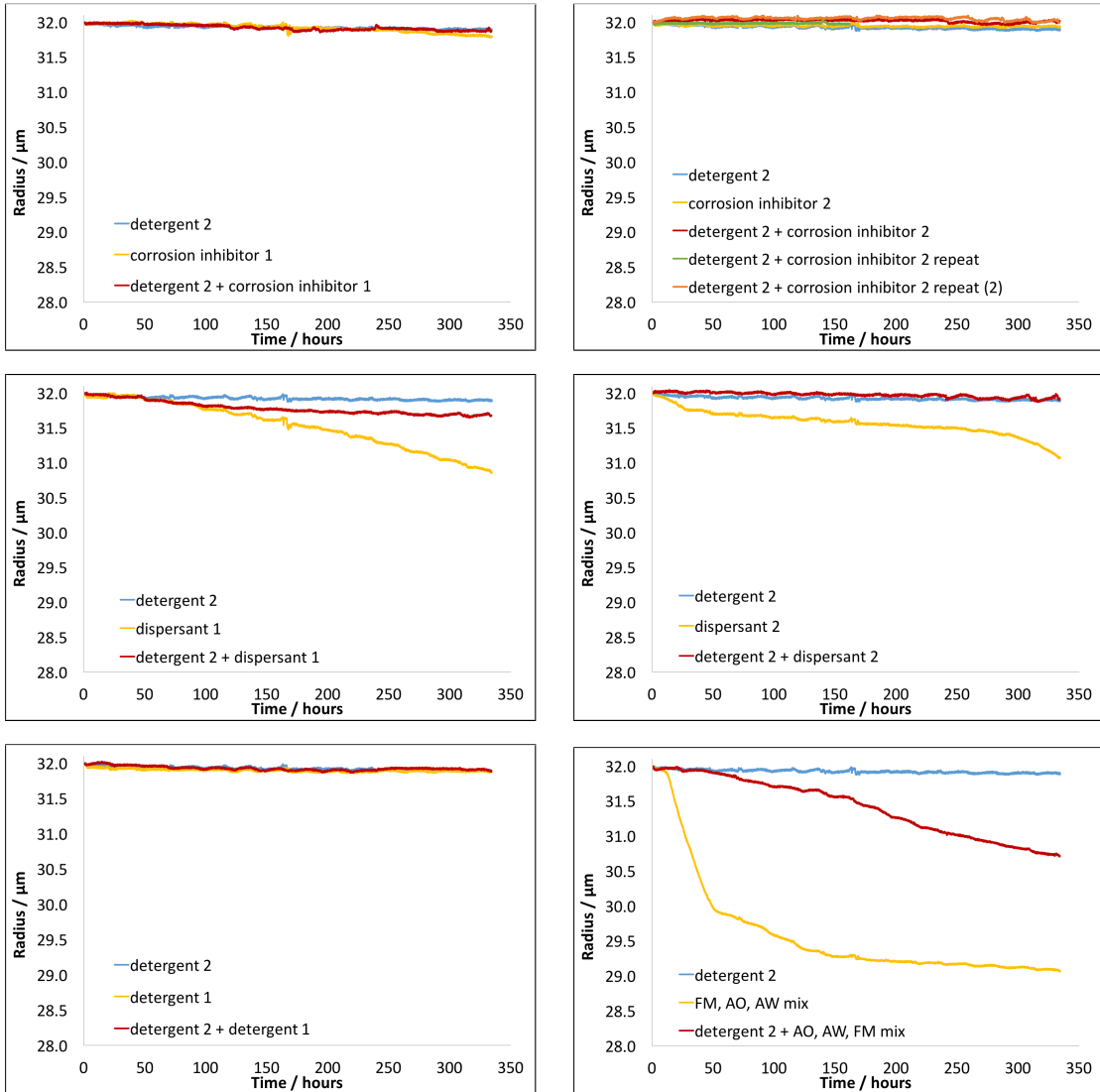


Figure B.6: Radius change data for additive combinations, and their individual additives at 120 °C for fluids containing detergent 2, with repeats where they were carried out

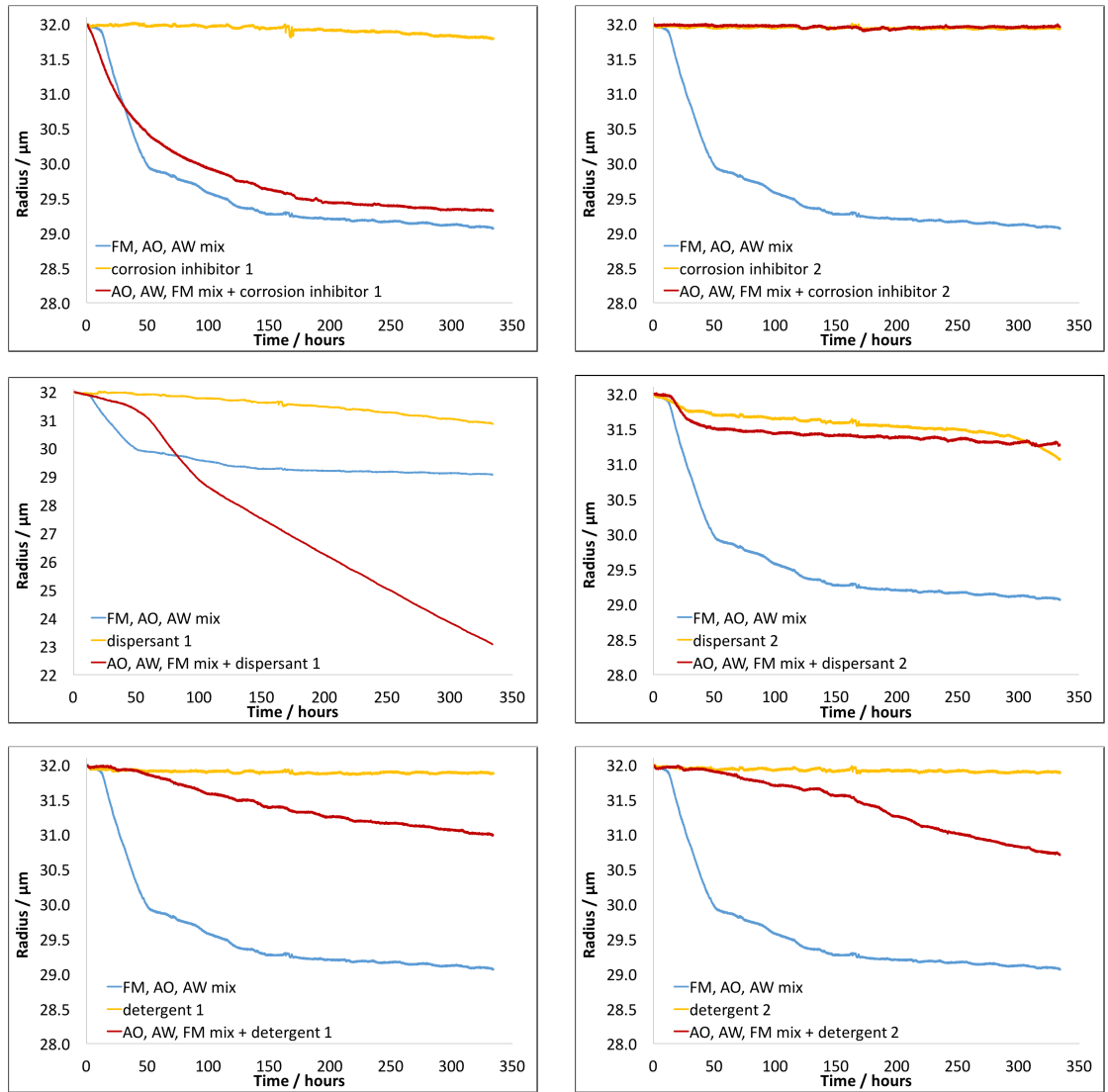


Figure B.7: Radius change data for additive combinations, and their individual additives at 120 °C for fluids containing the AO, AW, FM mix, with repeats where they were carried out

B.2 Additives at 150 °C

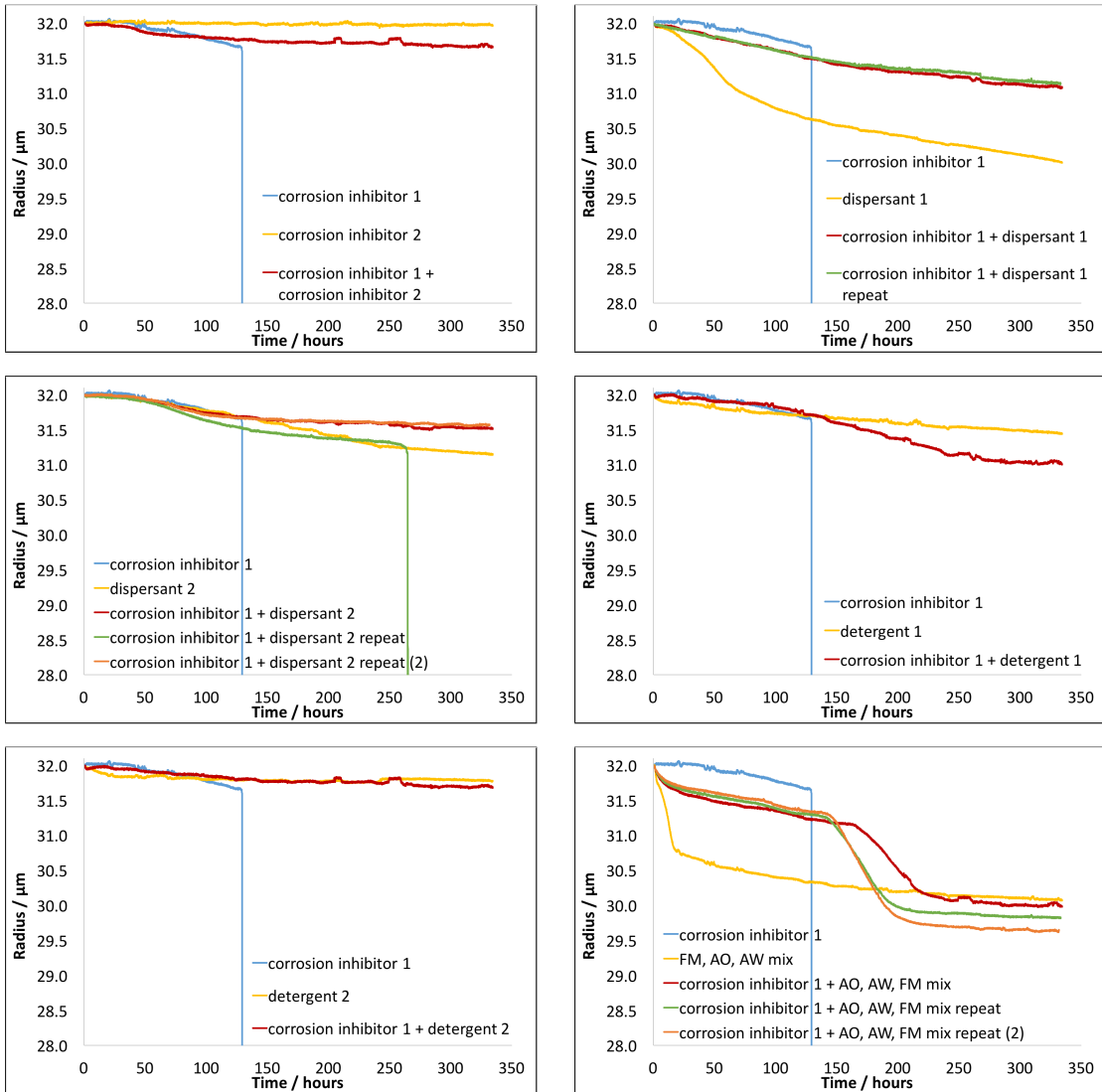


Figure B.8: Radius change data for additive combinations, and their individual additives at 150 °C for fluids containing corrosion inhibitor 1, with repeats where they were carried out

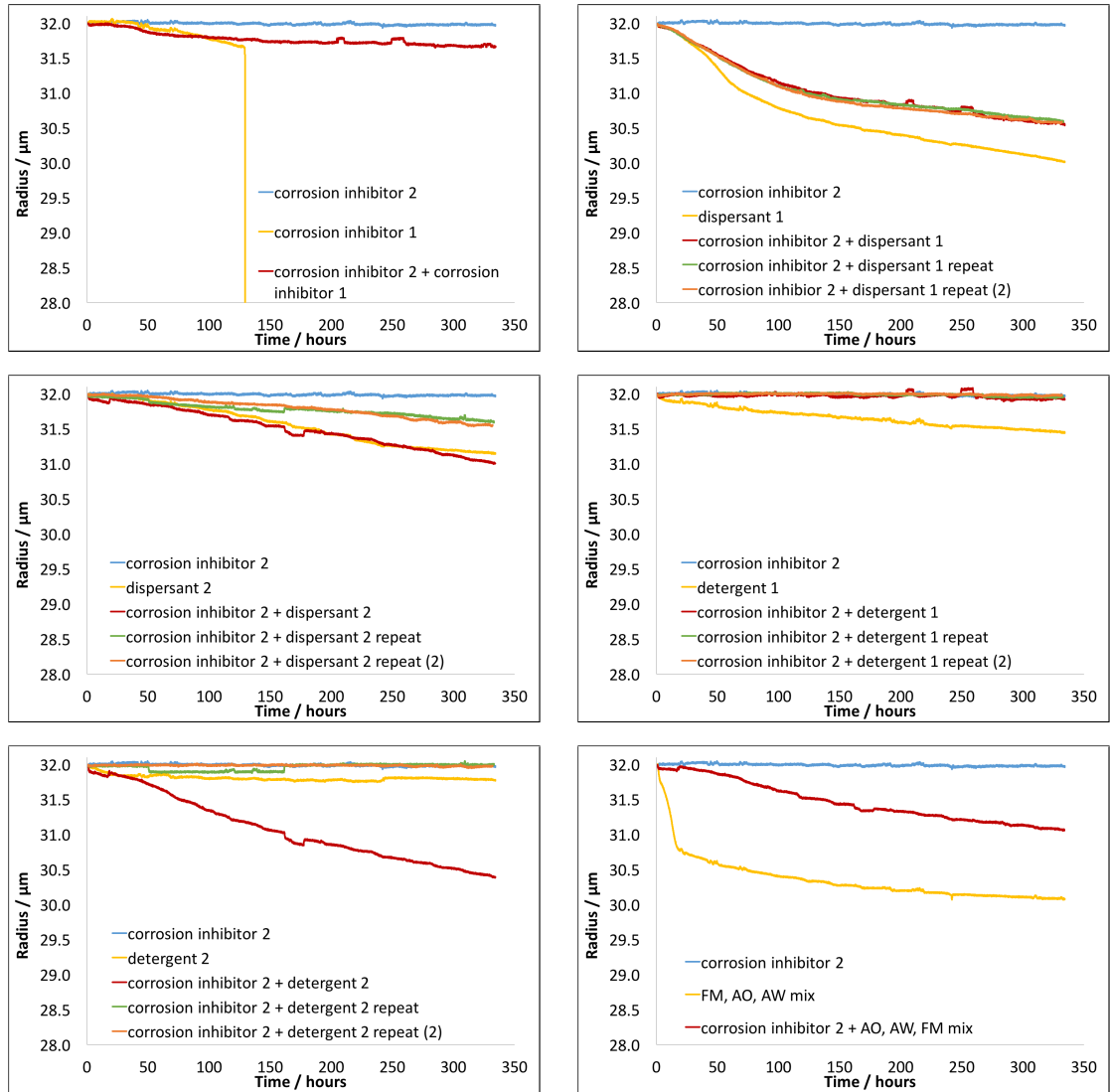


Figure B.9: Radius change data for additive combinations, and their individual additives at 150°C for fluids containing corrosion inhibitor 2, with repeats where they were carried out

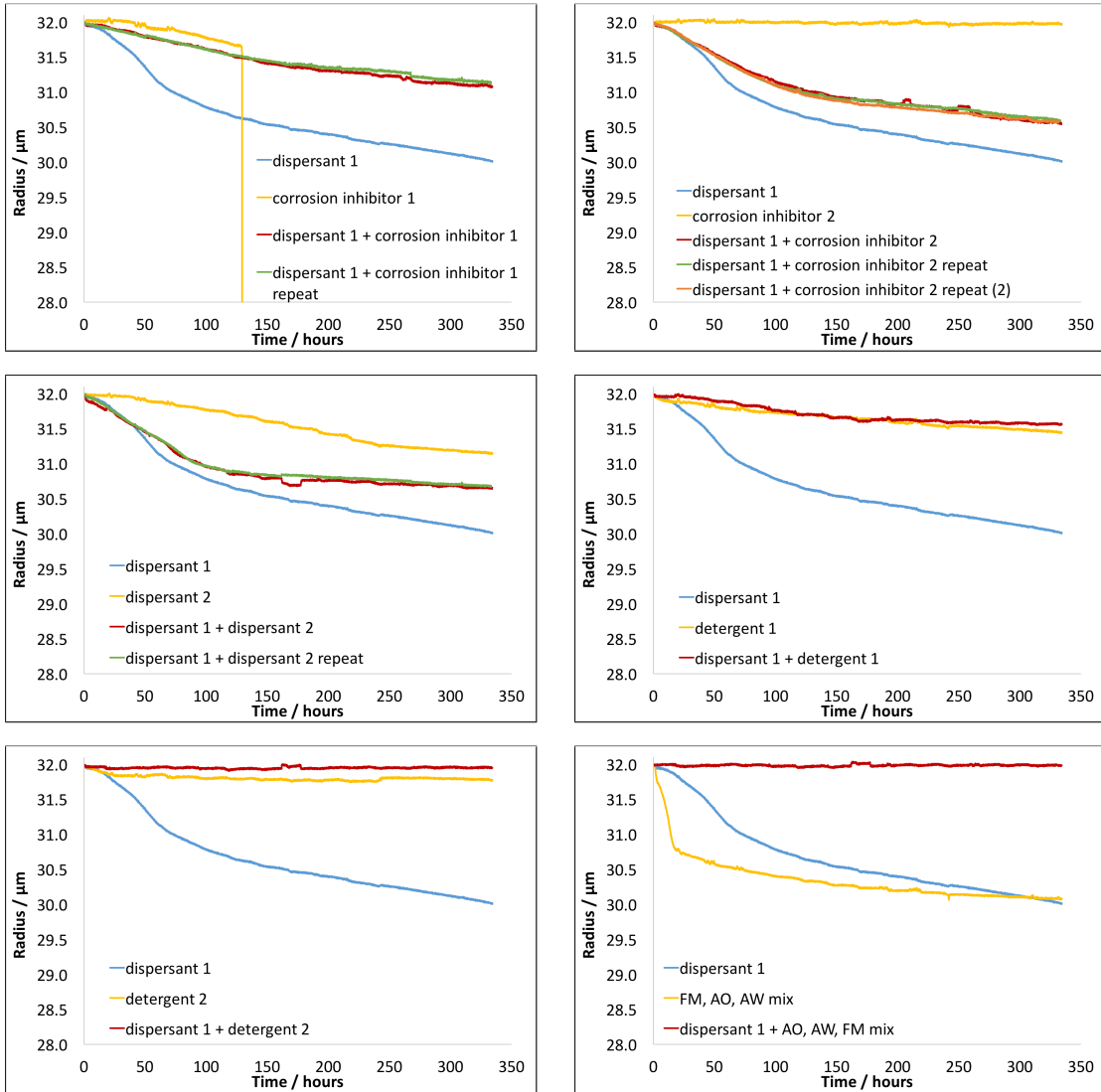


Figure B.10: Radius change data for additive combinations, and their individual additives at 150 °C for fluids containing dispersant 1, with repeats where they were carried out

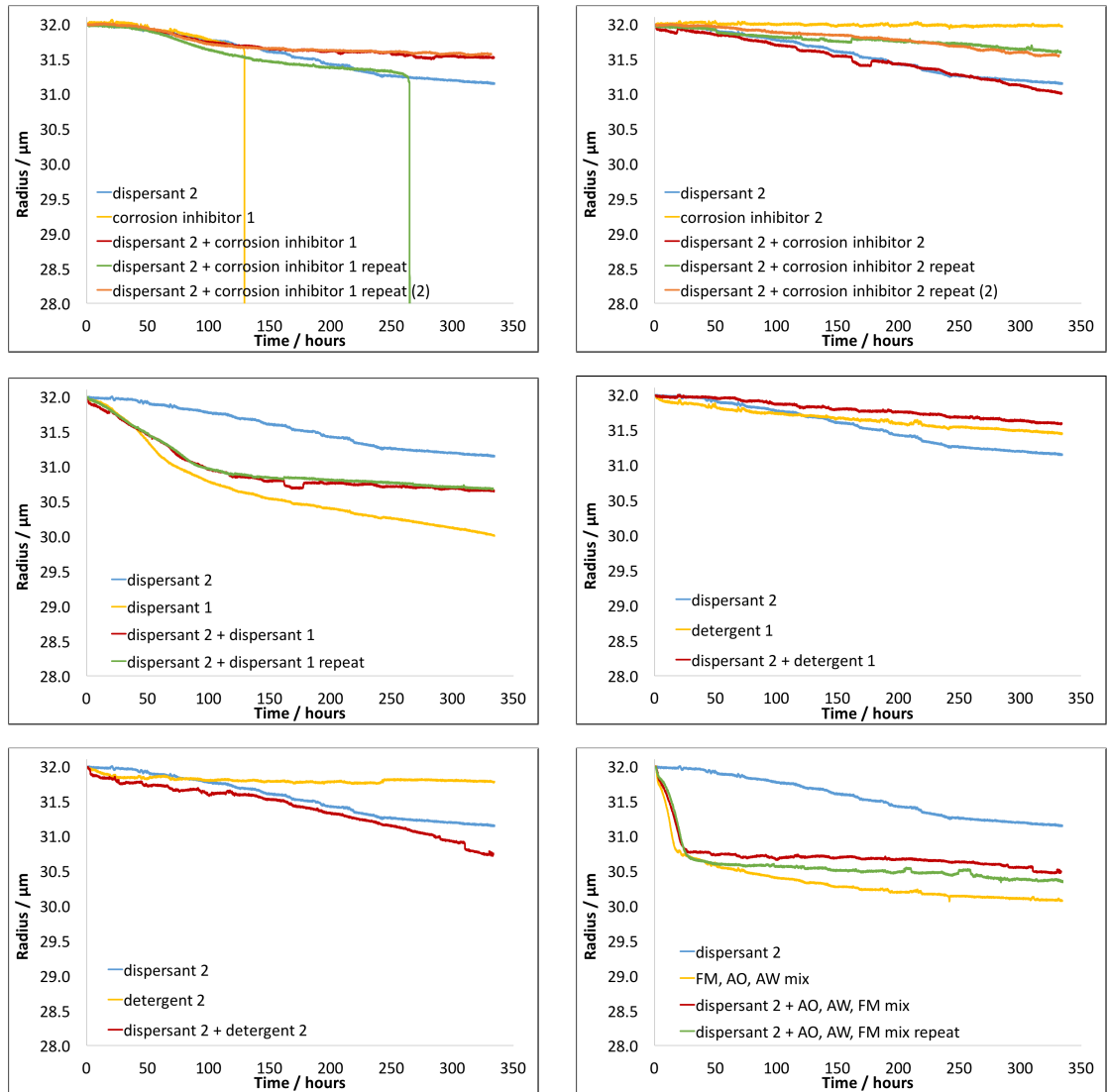


Figure B.11: Radius change data for additive combinations, and their individual additives at $150\text{ }^\circ\text{C}$ for fluids containing dispersant 2, with repeats where they were carried out

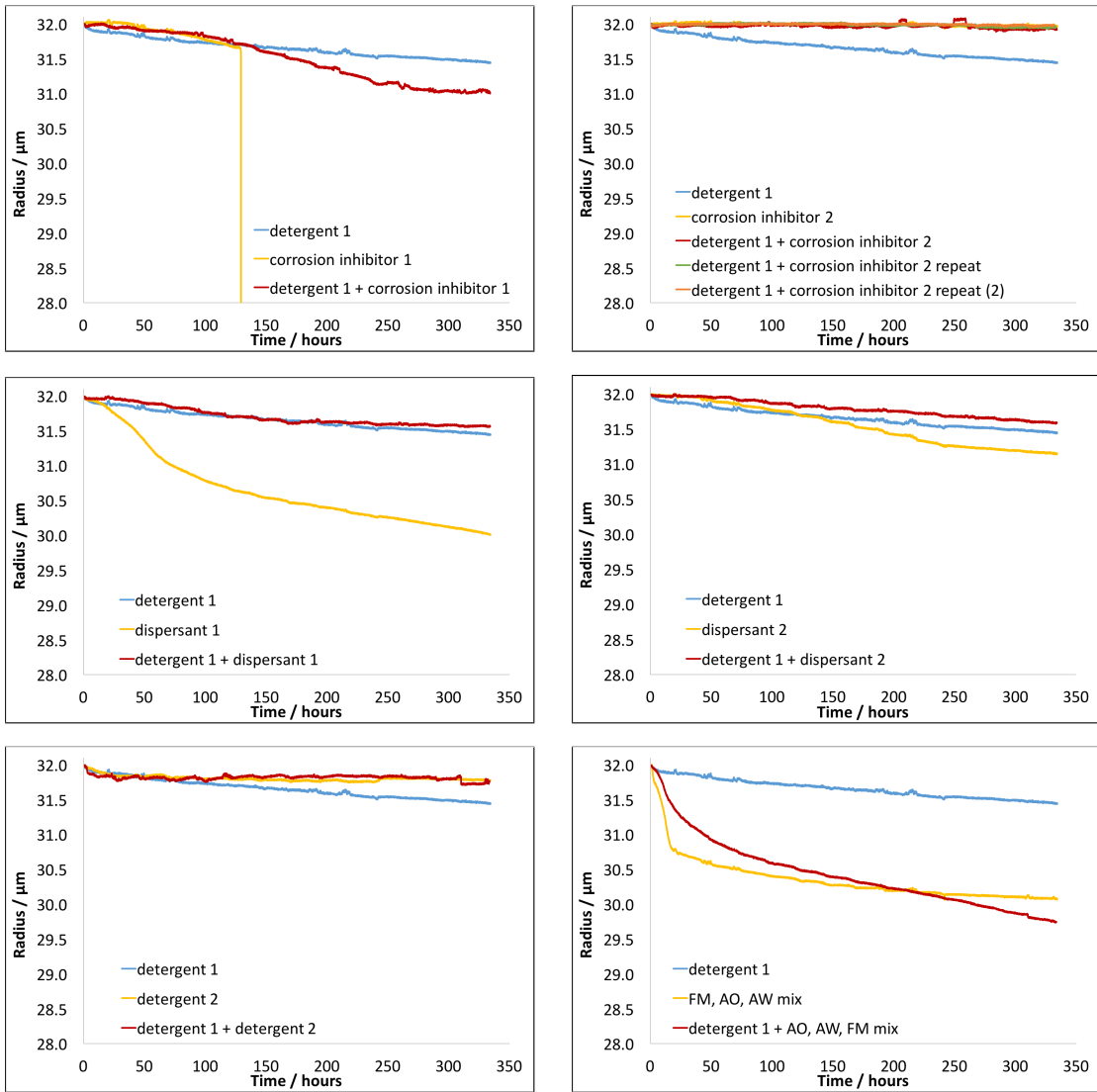


Figure B.12: Radius change data for additive combinations, and their individual additives at $150\text{ }^\circ\text{C}$ for fluids containing detergent 1, with repeats where they were carried out

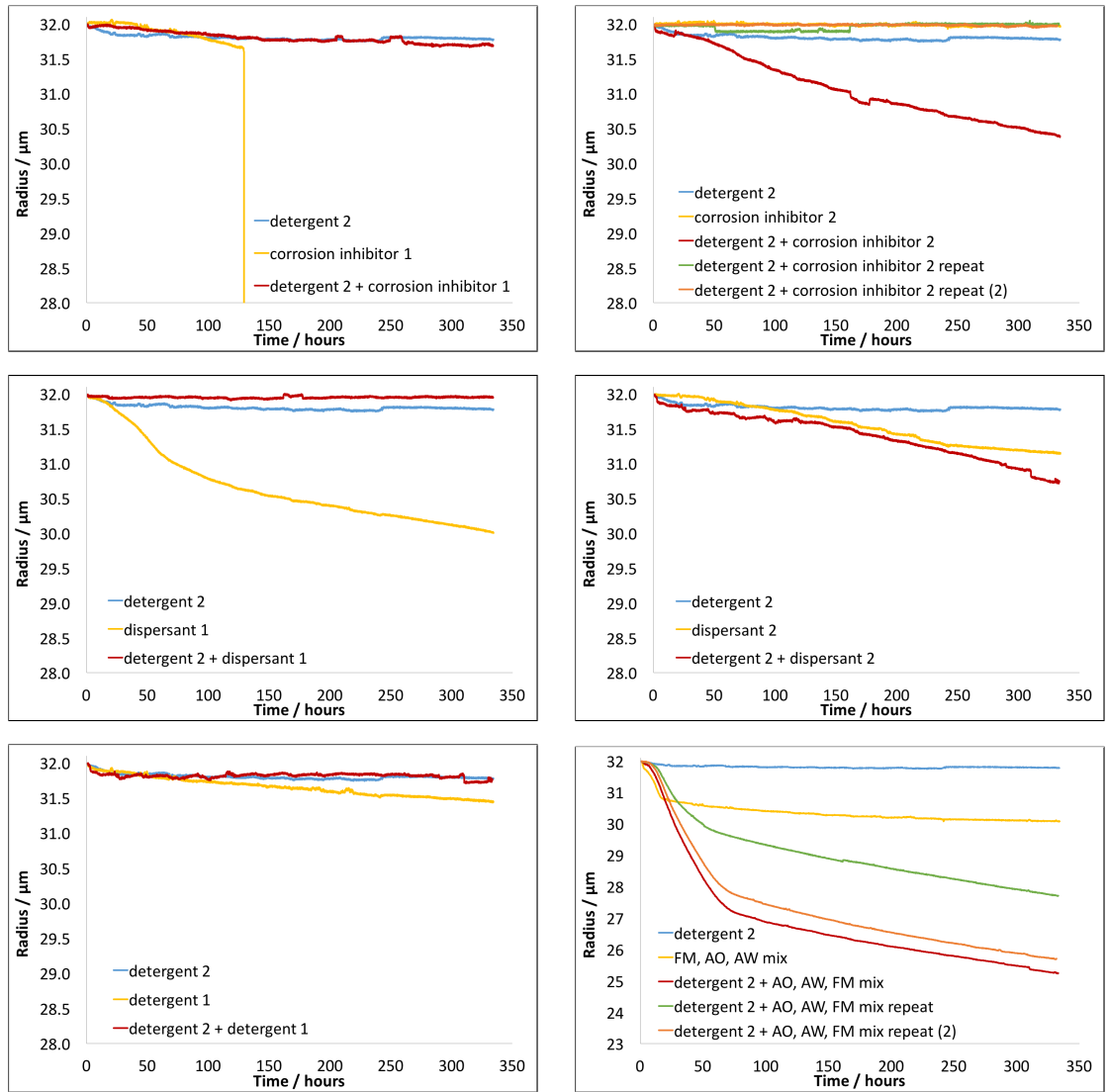


Figure B.13: Radius change data for additive combinations, and their individual additives at 150 °C for fluids containing detergent 2, with repeats where they were carried out

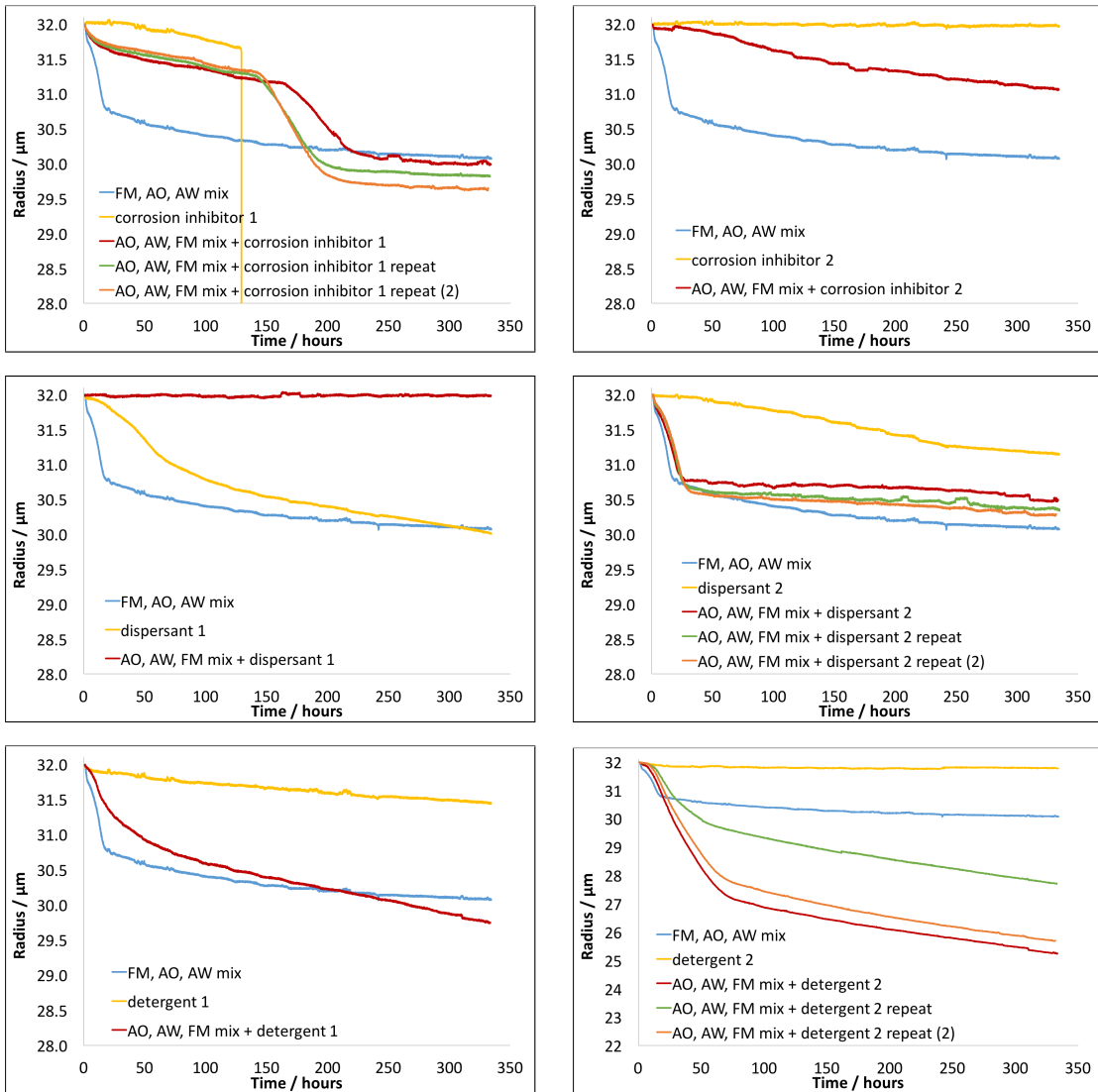


Figure B.14: Radius change data for additive combinations, and their individual additives at $150\text{ }^\circ\text{C}$ for fluids containing the AO, AW, FM mix, with repeats where they were carried out

Bibliography

- [1] S. Rathgeber, R. Bauer, A. Otto, E. Peter, and J. Wilde, “Harsh environment application of electronics - Reliability of copper wiring and testability thereof,” *Microelectronics Reliability*, vol. 52, no. 9-10, pp. 2452–2456, 2012.
- [2] T. Ishii, N. Tsuyuno, T. Sato, and M. Masuda, “Corrosion studies of copper and aluminum interconnects exposed to automotive oils,” *IEEE Transaction on components and packaging technologies*, vol. 29, no. 1, pp. 213–221, 2006.
- [3] S. Halley and R. Vickerman, “Types of Driveline Fluids and Their Characteristics,” tech. rep., The Lubrizol Corporation, 2014.
- [4] A. G. Papay, “Effect of Chemistry on Performance of Automatic Transmission Fluids,” *Lubrication Engineering*, vol. 46, no. 8, pp. 511–518, 1990.
- [5] S. Halley and R. Vickerman, “Transmissions and Transmission Fluids,” in *Synthetics, Mineral Oils and Bio-Based Lubricants* (L. Rudnick, ed.), pp. 449–458, CRC press, second ed., 2013.
- [6] J. Dong and C. A. Migdal, “Antioxidants,” in *Lubricant Additives: Chemistry and Applications, Second Edition* (L. R. Rudnick, ed.), ch. 1, pp. 3–50, CRC Press, 2 ed., 2009.
- [7] ASTM International, “Standard Test Method for Corrosiveness to Copper from Petroleum Products by Copper Strip Test,” in *ASTM Volume 05.01 Petroleum Products, Liquid Fuels, and Lubricants (I): C1234fD3709*, West Conshohocken, PA: ASTM International, 2012.
- [8] J. García-Antón, J. Monzó, J. L. Guiñón, D. Gómez, and J. Costa, “Study of corrosion on copper strips by petroleum naphtha in the ASTM D-130 test by means of electronic microscopy (SEM) and energy dispersive X-ray (EDX),” *Fresenius’ Journal of Analytical Chemistry*, vol. 337, no. 4, pp. 382–388, 1990.
- [9] G. A. Cragolino, “Corrosion fundamentals and characterization techniques,” in *Techniques for corrosion monitoring* (L. Yang, ed.), pp. 6–45, Woodhead Publishing, 2008.
- [10] C. R. Brundle, C. A. J. Evans, and S. Wilson, “Introduction and Summaries,” in *Encyclopedia of Materials Characterization - Surfaces, Interfaces, Thin Films* (L. E. Fitzpatrick, ed.), ch. 1, pp. 1–56, Elsevier, 1992.
- [11] H. A. Spikes, “Additive-Additive and Additive-Surface Interactions in Lubrication,” *Lubrication Science*, vol. 2, no. 1, pp. 3–23, 1989.
- [12] P. R. Roberge, “Corrosion Detectability,” in *Corrosion Inspection and Monitoring*, ch. 2, pp. 27–52, John Wiley & Sons, 2007.

- [13] V. Burt, "Pitting Corrosion," in *Corrosion in the Petrochemical Industry (2nd Edition)*, ch. 6, pp. 33–38, ASTM International, 2 ed., 2015.
- [14] P. Zhou, *An in situ kinetic investigation of the selective mechanism of Cu alloys*. PhD thesis, Universite Pierre at Marie Curie, 2018.
- [15] A. Morina and M. Bryant, "ATF interaction with the copper-based alloy," tech. rep., University of Leeds, 2014.
- [16] A. Agoston, N. Dorr, and B. Jakoby, "Corrosion sensors for engine oils - laboratory evaluation and field tests," *Sensors and Actuators B: Chemical*, vol. 127, pp. 15–21, oct 2007.
- [17] D. G. Reid and G. C. Smith, "The X-ray Photoelectron Spectroscopy of Surface Films Formed During the ASTM D-130/ISO 2160 Copper Corrosion Test," *Petroleum Science and Technology*, vol. 32, pp. 387–394, 2014.
- [18] J. Monzó, J. García-Antón, and J. L. Guñón, "Influence of elemental sulfur and mercaptans on corrosion of copper strips in the ASTM D-130 test by means of electronic microscopy (SEM) and energy dispersive X-ray (EDX)," *Fresenius' Journal of Analytical Chemistry*, vol. 341, no. 10, pp. 606–610, 1991.
- [19] J. A. Schreifels, J. J. Weers, and T. Bagwell, "Time dependent formation of sulfidic films on copper substrates when exposed to hydrocarbons containing elemental sulfur," *Fuel Science and Technology International*, vol. 9, no. 10, pp. 1223–1244, 1991.
- [20] C. G. Dariva and A. F. Gailo, "Corrosion Inhibitors fi?? Principles, Mechanisms and Applications," in *Developments in Corrosion Protection*, InTech, feb 2014.
- [21] F. M. Bayoumi, A. M. Abdullah, and B. Attia, "Kinetics of corrosion inhibition of benzotriazole to copper in 3.5% NaCl," *Materials and Corrosion*, vol. 59, no. 8, pp. 691–696, 2008.
- [22] H. Ling, S. Jian, R. Jun, M. Qingjin, and Y. Tsing, "The adsorption of 2,5-dimercapto-1,3,4-thiadiazole (DMTD) on copper surface and its binding behavior," *Chinese Science Bulletin*, vol. 46, no. 5, pp. 387–389, 2001.
- [23] F. Hipler, S. Gil Girol, W. Azzam, R. A. Fischer, and C. Woll, "Interaction of thiadiazole additives with metal surfaces: Reactions and thin-film formation on gold as a model surface," *Langmuir*, vol. 19, pp. 6072–6080, 2003.
- [24] B. M. Thethwayo and A. M. Garbers-Craig, "Laboratory scale investigation into the corrosion of copper in a sulphur-containing environment," *Corrosion Science*, vol. 53, no. 10, pp. 3068–3074, 2011.
- [25] JEOL, *Scanning Electron Microscope A To Z*. JEOL, 2006.
- [26] D.-c. Kong, C.-f. Dong, K. Xiao, and X.-g. Li, "Effect of temperature on copper corrosion in high-level nuclear waste environment," *Transactions of Nonferrous Metals Society of China*, vol. 27, no. 6, pp. 1431–1438, 2017.
- [27] P. Larkin, *Basic Principles*. Elsevier, 2011.
- [28] R. E. Melchers, "Temperature Effect on Seawater Immersion Corrosion of 90 : 10 Copper-Nickel Alloy," *Corrosion*, no. May, pp. 440–451, 2001.

- [29] HM Government, “2050 Pathways Analysis,” *Analysis*, no. July, pp. 1–252, 2010.
- [30] R. D. Whitby, “Automotive Trends in Europe,” in *Synthetics, Mineral Oils and Bio-Based Lubricants* (L. Rudnick, ed.), pp. 781–812, CRC press, second ed., 2013.
- [31] B. Kamchev, “Europe’s Transmission of the Future,” *Lubes’N’Greases Europe-Middle East-Africa*, no. 26, 2011.
- [32] S. Halley, “How to Read Representative ATF / CVTF Test Data,” tech. rep., The Lubrizol Corporation, 2014.
- [33] H.-S. Hong, “Designing Automotive Gear Oils for the New Millennium,” *Lubrication Science*, vol. 14, no. 4, pp. 435–453, 2002.
- [34] N. S. Ahmed and A. M. Nassar, “Lubricating Oil Additives,” in *Tribology-Lubricants and Lubrication* (C.-H. Kuo, ed.), ch. 10, pp. 249–268, InTech, 2009.
- [35] S. Q. A. Rizvi, “Mineral Base Oils,” in *A Comprehensive Review of Lubricant Chemistry, Technology, Selection, and Design* (S. Q. A. Rizvi, ed.), ch. 2, pp. 23–46, 100 Barr Harbor Drive, PO Box C700, West Conshohocken, PA 19428-2959: ASTM International, jan 2009.
- [36] R. W. Wilson and L. L. Shreir, “Corrosion Prevention in Lubricant Systems,” in *Corrosion* (L. L. Shreir, ed.), ch. 2.11, pp. 2:143–2:154, Newnew-Butterworths, second ed., 1976.
- [37] N. Canter, “Use of antioxidants in automotive lubricants,” *Tribology and Lubrication Technology*, pp. 12–19, sep 2008.
- [38] M. L. Free, “Introduction to Surfactants,” in *Surfactants in Tribology* (G. Biresaw and K. L. Mittal, eds.), pp. 3–10, CRC press, 2008.
- [39] A. G. Hopkins, “Surface analysis,” in *Corrosion Tests and Standards: Application and Interpretation* (R. Baboian, ed.), ch. 4, pp. 76–82, ASTM International, second ed., 2005.
- [40] S. Norouzi, K. Hazeri, M. L. Wyszynski, and A. Tsolakis, “Investigation on the effects of temperature, dissolved oxygen and water on corrosion behaviour of aluminium and copper exposed to diesel-type liquid fuels,” *Fuel Processing Technology*, vol. 128, pp. 220–231, 2014.
- [41] G. Light, “Nondestructive evaluation technologies for monitoring corrosion,” in *Techniques for corrosion monitoring* (L. Yang, ed.), ch. 12, pp. 293–312, Woodhead Publishing, 2008.
- [42] W. Li and D. Y. Li, “Influence of surface morphology on corrosion and electronic behavior,” *Acta Materialia*, no. 54, pp. 445–452, 2006.
- [43] L. L. Shreir, R. A. Jarman, and G. T. Burstein, “Principles of Corrosion and Oxidation,” in *Corrosion*, ch. 1, Elsevier, 1994.
- [44] A. Kalantar and M. Levin, “Factors affecting the dissolution of copper in transformer oils,” *Lubrication Science*, vol. 20, pp. 223–240, jul 2008.

- [45] R. T. Loto, C. A. Loto, and A. P. I. Popoola, "Corrosion inhibition of thiourea and thiadiazole derivatives: A review," *Journal of Materials and Environmental Science*, vol. 3, no. 5, pp. 885–894, 2012.
- [46] L. Garverick, "Forms of Corrosion in the Petrochemical Industry," in *Corrosion in the Petrochemical Industry*, ch. 1, pp. 3–39, ASTM International, 1994.
- [47] P. R. Roberge, "Corrosion Monitoring," in *Corrosion Inspection and Monitoring*, ch. 4, pp. 189–213, John Wiley & Sons, 2007.
- [48] A. Rajasekar, L. Rajendran, S. Maruthamuthu, N. Palaniswamy, and A. Rajendran, "Prediction of corrosion rate of steel AP5LX using curve fitting method," *Zastita Materijala*, vol. 47, pp. 47–50, 2006.
- [49] J. J. Santana Rodríguez, F. J. Santana Hernández, and J. E. González González, "The effect of environmental and meteorological variables on atmospheric corrosion of carbon steel, copper, zinc and aluminium in a limited geographic zone with different types of environment," *Corrosion Science*, vol. 45, no. 4, pp. 799–815, 2003.
- [50] A. Fateh, M. Aliofkhaezai, and A. R. Rezvanian, "Review of corrosive environments for copper and its corrosion inhibitors," *Arabian Journal of Chemistry*, 2017.
- [51] G. T. Burstein, C. Liu, R. M. Souto, and S. P. Vines, "Origins of pitting corrosion," *Corrosion Engineering, Science and Technology*, vol. 39, no. 1, pp. 25–30, 2004.
- [52] G. S. Frankel, "Pitting Corrosion of Metals," *Journal of The Electrochemical Society*, vol. 145, no. 6, p. 2186, 1998.
- [53] D. Vasquez Moll, M. R. G. De Chialvo, R. C. Salvarezza, and A. J. Arvia, "Corrosion and passivity of copper in solutions containing sodium sulphide. Analysis of potentiostatic transients," *Electrochimica Acta*, vol. 30, no. 8, pp. 1011–1016, 1985.
- [54] N. R. T. Bharucha and Baker, "Working With Copper: Benzotriazole: An effective corrosion inhibitor for copper alloys," *Copper Development Association International Copper Research Association*, 1964.
- [55] J. B. Cotton and I. R. Scholes, "Benzotriazole and Related Compounds as Corrosion Inhibitors For Copper," *British Corrosion Journal*, vol. 2, pp. 1–5, jan 1967.
- [56] G. S. Frankel and N. Sridhar, "Understanding localized corrosion," *Materials Today*, vol. 11, no. 10, pp. 38–44, 2008.
- [57] V. Burt, "Crevice Corrosion," in *Corrosion in the Petrochemical Industry (2nd Edition)*, ch. 7, pp. 39–44, ASTM International, 2015.
- [58] NACE International, "Intergranular Corrosion."
- [59] L. L. Shreir, R. A. Jarman, and G. T. Burstein, "Corrosion Testing, Monitoring and Inspection," in *Corrosion*, ch. 19, pp. 19:1–19:30, Elsevier, 1994.
- [60] X. Zhu and T. Lei, "Characteristics and formation of corrosion product films of 70Cu-30Ni alloy in seawater," *Corrosion Science*, vol. 44, pp. 67–79, jan 2002.
- [61] A. J. Forty, "Corrosion micromorphology of noble metal alloys and depletion gilding," *Nature*, vol. 282, no. 6, pp. 597–598, 1979.

- [62] N. Sato, "Basics of Corrosion Chemistry," in *Green Corrosion Chemistry and Engineering*, pp. 1–32, Weinheim, Germany: Wiley-VCH Verlag GmbH & Co. KGaA, nov 2011.
- [63] S. Virtanen, H. Wojtas, P. Schmuki, and H. Bohni, "Passivity of High Corrosion Resistant Cu-Al-Sn Alloys," *Journal of The Electrochemical Society*, vol. 140, no. 10, pp. 2786–2790, 1993.
- [64] M. M. Antonijevic and M. B. Radovanovic, "Methods for Characterization of Protective Films on the Copper Surface - A Review," *Zastita Materijala*, vol. 51, pp. 111–122, 2010.
- [65] K. Demirkan, G. E. Derkits, D. A. Fleming, J. P. Franey, K. Hannigan, R. L. Opila, J. Punch, W. D. Reents, M. Reid, B. Wright, and C. Xu, "Corrosion of Cu under Highly Corrosive Environments," *Journal of the Electrochemical Society*, vol. 157, pp. C30–C35, 2010.
- [66] G. Fonder, F. Laffineur, J. Delhalle, and Z. Mekhalif, "Alkanethiol-oxidized copper interface: The critical influence of concentration," *Journal of Colloid and Interface Science*, 2008.
- [67] R. Procaccini, W. H. Schreiner, M. Vázquez, and S. Ceré, "Surface study of films formed on copper and brass at open circuit potential," *Applied Surface Science*, 2013.
- [68] H. Y. H. Chan, C. G. Takoudis, and M. J. Weaver, "Oxide Film Formation and Oxygen Adsorption on Copper in Aqueous Media As Probed by Surface-Enhanced Raman Spectroscopy," *The Journal of Physical Chemistry B*, vol. 103, no. 2, pp. 357–365, 1999.
- [69] C. A. Melendres, G. A. Bowmaker, J. M. Leger, and B. Beden, "In-situ synchrotron far infrared spectroscopy of surface films on a copper electrode in aqueous solutions," *Journal of Electroanalytical Chemistry*, vol. 449, pp. 215–218, 1998.
- [70] J. C. Hamilton, "In Situ Raman Spectroscopy of Anodic Films Formed on Copper and Silver in Sodium Hydroxide Solution," *Journal of The Electrochemical Society*, vol. 133, no. 4, pp. 739–745, 1986.
- [71] N. K. Allam and E. A. Ashour, "Promoting effect of low concentration of benzotriazole on the corrosion of Cu10Ni alloy in sulfide polluted salt water," *Applied Surface Science*, 2008.
- [72] R. Holm, D. Holtkamp, R. Kleinstuck, H. J. Rother, and S. Storp, "Surface analysis methods in the investigation of corrosion inhibitor performance," *Fresenius' Zeitschrift fur Analytische Chemie*, vol. 333, no. 4-5, pp. 546–554, 1989.
- [73] D. Q. Zhang, L. X. Gao, and G. D. Zhou, "Inhibition of copper corrosion in aerated hydrochloric acid solution by heterocyclic compounds containing a mercapto group," *Corrosion Science*, vol. 46, pp. 3031–3040, 2004.
- [74] J. Chen, Z. Qin, and D. W. Shoesmith, "Kinetics of Corrosion Film Growth on Copper in Neutral Chloride Solutions Containing Small Concentrations of Sulfide," *Journal of The Electrochemical Society*, 2010.

- [75] Y. Zhi Hu, R. Sharangpani, and S.-P. Tay, "Kinetic investigation of copper film oxidation by spectroscopic ellipsometry and reflectometry Studies of metallic multilayer structures, optical properties, and oxidation using in situ spectroscopic ellipsometry Morphology and phase of tin oxide thin fil," *Journal of Vacuum Science & Technology A*, vol. 18, no. 5, pp. 2527–2532, 2000.
- [76] P. Keil, D. Lützenkirchen-Hecht, and R. Frahm, "Investigation of room temperature oxidation of Cu in air by Yoneda-XAFS," in *AIP Conference Proceedings*, 2007.
- [77] A. C. Ohajianya and O. E. Abumere, "Effect Of Cuprous Oxide (Cu₂O) Film Thickness On The Efficiency Of The Copper-Cuprous Oxide (Cu₂O/Cu) Solar Cell," *The International Journal Of Engineering And Science*, vol. 2, no. 5, pp. 2319–1805, 2013.
- [78] D. Persson and C. Leygraf, "In Situ Infrared Reflection Absorption Spectroscopy for Studies of Atmospheric Corrosion," *Journal of The Electrochemical Society*, vol. 140, no. 5, pp. 1256–1260, 1993.
- [79] S. K. Chawla, B. I. Rickett, N. Sankarraman, and J. H. Payer, "An X-ray photoelectron spectroscopic investigation of the air-formed film on copper," *Corrosion Science*, vol. 33, no. 10, pp. 1617–1631, 1992.
- [80] S. Degeratu, P. Rotaru, S. Rizescu, S. Danoiu, N. G. Bizdoaca, L. I. Alboteanu, and H. O. Manolea, "Condition monitoring of transformer oil using thermal analysis and other techniques," *Journal of Thermal Analysis and Calorimetry*, no. 119, pp. 1679–1692, 2015.
- [81] T. Wan, H. Qian, Z. Zhou, S. K. Gong, X. Hu, and B. Feng, "Suppressive mechanism of the passivator irgamet 39 on the corrosion of copper conductors in transformers," *IEEE Transactions on Dielectrics and Electrical Insulation*, vol. 19, no. 2, pp. 454–459, 2012.
- [82] G. A. Oweimreen, A. M. Y. Jaber, A. M. Abulkibash, and N. A. Mehanna, "The depletion of dibenzyl disulfide from a mineral transformer insulating oil," *IEEE Transactions on Dielectrics and Electrical Insulation*, vol. 19, no. 6, pp. 1962–1970, 2012.
- [83] N. A. Mehanna, A. M. Y. Jaber, G. A. Oweimreen, and A. M. Abulkibash, "Assessment of Dibenzyl Disulfide and Other Oxidation Inhibitors in Transformer Mineral Oils," *IEEE Transactions on Dielectrics and Electrical Insulation*, vol. 21, no. 3, pp. 1095–1099, 2014.
- [84] Y. Qian and W. Su, "Research on influencing factors of corrosive sulfur attacking copper in insulating oil and prevention," *IEEE Transactions on Electrical and Electronic Engineering*, vol. 8, no. 6, pp. 546–549, 2013.
- [85] C. Fiaud, M. Safavi, and J. Vedel, "Identification of the corrosion products formed on copper in sulfur containing environments," *Materials and Corrosion*, vol. 35, pp. 361–366, 1984.
- [86] R. Schlesinger, H. Klewe-Nebenius, and M. Bruns, "Characterization of artificially produced copper and bronze patina by XPS," *Surface and Interface Analysis*, vol. 30, no. 1, pp. 135–139, 2000.

- [87] J. G. Cowie, "Surface Resistance Changes Due to Heat Aging of Copper and Coated Copper Alloys in Transmission and Brake Fluids," *SAE Technical Paper*, apr 2007.
- [88] J. Li, J. W. Mayer, and E. G. Colgan, "Oxidation and protection in copper and copper alloy thin films Layered Cu-based electrode for high-dielectric constant oxide thin film-based devices Oxidation and protection in copper and copper alloy thin films," *Journal of Applied Physics*, vol. 70, no. 75, pp. 2820–2518, 1991.
- [89] N. Cabrera and N. F. Mott, "Theory of the oxidation of metals," *Reports on Progress in Physics*, vol. 12, pp. 163–184, 1949.
- [90] F. Grillo, D. W. Tee, S. M. Francis, H. A. Früchtl, and N. V. Richardson, "Passivation of copper: Benzotriazole films on Cu(111)," *Journal of Physical Chemistry C*, vol. 118, no. 16, pp. 8667–8675, 2014.
- [91] F. Grillo, D. W. Tee, S. M. Francis, H. A. Früchtl, and N. V. Richardson, "Initial stages of benzotriazole adsorption on the Cu(111) surface," *Nanoscale*, vol. 5, no. 12, pp. 5269–5273, 2013.
- [92] D. Reza khani, "The effects of temperature, dissolved oxygen and the velocity of seawater, on the corrosion behavior of condenser alloys," *Anti - Corrosion Methods and Materials*, vol. 58, no. 2, pp. 90–94, 2011.
- [93] M. Gahagan, "Dual Clutch Transmission Fluids," Tech. Rep. 1, The Lubrizol Corporation, 2014.
- [94] S. Toyama, J. Tanimura, N. Yamada, E. Nagao, and T. Amimoto, "Highly Sensitive Detection Method of Dibenzyl Disulfide and the Elucidation of the Mechanism of Copper Sulfide Generation in Insulating Oil," *IEEE Transactions on Dielectrics and Electrical Insulation*, vol. 16, no. 2, 2009.
- [95] A. Tripathi and R. Vinu, "Characterization of Thermal Stability of Synthetic and Semi-Synthetic Engine Oils," *Lubricants*, vol. 3, pp. 54–79, mar 2015.
- [96] G. W. Poling, "Films of Oil Oxidation Products on Copper," *Journal of the Electrochemical Society: Solid State Science*, vol. 117, no. 4, pp. 520–524, 1970.
- [97] J. J. Melchiorre and I. W. Mills, "The role of copper during the oxidation of transformer oils," *Journal of the Electrochemical Society*, vol. 112, no. 4, pp. 390–395, 1965.
- [98] J. Monzó, J. García-Antón, and J. L. Guñón, "Study of corrosion on copper strips by mixtures of mercaptans, sulphides and disulphides with elemental sulphur in the ASTM D-130 test by means of electron microscopy (SEM) and energy dispersive X-ray (EDX)," *Fresenius' Journal of Analytical Chemistry*, vol. 343, no. 7, pp. 593–596, 1992.
- [99] M. Kashima and Y. Nose, "An Electron Diffraction Investigation on the ASTM Copper Strip Corrosion Test," *Bulletin of The Japan Petroleum Institute*, vol. 1, pp. 33–45, 1959.
- [100] M. Facciotti, P. S. Amaro, A. F. Holt, R. C. D. Brown, P. L. Lewin, J. A. Pilgrim, G. Wilson, and P. N. Jarman, "Contact-based corrosion mechanism leading to copper sulphide deposition on insulating paper used in oil-immersed electrical power equipment," *Corrosion Science*, vol. 84, pp. 172–179, 2014.

- [101] J. A. Schreifels, T. Bagwell, and J. J. Weers, "Copper Corrosion Inhibition in Sour Hydrocarbon Fuels," *Corrosion Engineering*, vol. 45, no. 1, pp. 84–91, 1989.
- [102] M. Finšgar and I. Milošev, "Inhibition of copper corrosion by 1,2,3-benzotriazole: A review," *Corrosion Science*, vol. 52, no. 9, pp. 2737–2749, 2010.
- [103] I. H. R. Tomi, A. H. Al-Daraji, and S. A. Aziz, "Synthesis, characterization, and study the inhibitory effect of thiazole and thiadiazole derivatives toward the corrosion of copper in acidic media," *Synthesis and Reactivity in Inorganic, Metal-Organic and Nano-Metal Chemistry*, vol. 45, pp. 605–613, 2015.
- [104] R. Youda, H. Nishihara, and K. Aramaki, "A SERS study on inhibition mechanisms of benzotriazole and its derivatives for copper corrosion in sulphate solutions," *Corrosion Science*, vol. 28, no. 1, pp. 87–96, 1988.
- [105] J. J. Kester, T. E. Furtak, and A. J. Bevolo, "Surface Enhanced Raman Scattering in Corrosion Science : Benzotriazole on Copper," *Electrochemical Science and Technology*, vol. 129, no. 8, pp. 1716–1719, 1982.
- [106] V. Brusic, M. A. Frisch, B. N. Eldridge, F. P. Novak, F. B. Kaufman, B. M. Rush, and G. S. Frankel, "Copper Corrosion With and Without Inhibitors," *Journal of The Electrochemical Society*, vol. 133, no. 8, pp. 2253–2259, 1991.
- [107] M. Finšgar, "2-Mercaptobenzimidazole as a copper corrosion inhibitor: Part I. Long-term immersion, 3D-profilometry, and electrochemistry," *Corrosion Science*, vol. 72, pp. 90–98, 2013.
- [108] M. R. Vogt, W. Polewska, O. M. Magnussen, and R. J. Behm, "In Situ STM Study of (100) Cu Electrodes in Sulfuric Acid Solution in the Presence of Benzotriazole Adsorption," *Journal of Electrochemical Society*, vol. 144, no. 5, pp. L113–L116, 1997.
- [109] W. Polewska, M. R. Vogt, O. M. Magnussen, and R. J. Behm, "In Situ STM Study of Cu(111) Surface Structure and Corrosion in Pure and Benzotriazole-Containing Sulfuric Acid Solution," *The Journal of Physical Chemistry B*, 1999.
- [110] N. Huynh, S. E. Bottle, T. Notoya, and D. P. Schweinsberg, "Inhibitive action of the octyl esters of 4- and 5-carboxybenzotriazole for copper corrosion in sulphate solutions," *Corrosion Science*, 2000.
- [111] C. Tornkvist, D. Thierry, J. Bergman, B. Liedberg, and C. Leygraf, "Methyl Substitution in Benzotriazole and Its Influence on Surface Structure and Corrosion Inhibition," *Journal of Electrochemical Society*, vol. 136, no. 1, pp. 58–64, 1989.
- [112] M. R. Vogt, R. J. Nichols, O. M. Magnussen, and R. J. Behm, "Benzotriazole Adsorption and Inhibition of Cu(100) Corrosion in HCl: A Combined in Situ STM and in Situ FTIR Spectroscopy Study," *The Journal of Physical Chemistry B*, vol. 102, pp. 5859–5865, 1998.
- [113] D. Chadwick and T. Hashemi, "Adsorbed corrosion inhibitors studied by electron spectroscopy: Benzotriazole on copper and copper alloys," *Corrosion Science*, vol. 18, no. 1, pp. 39–51, 1978.
- [114] P. G. Fox, G. Lewis, and P. J. Boden, "Some chemical aspects of the corrosion inhibition of copper by benzotriazole," *Corrosion Science*, vol. 19, no. 7, pp. 457–467, 1979.

- [115] K. Cho, J. Kishimoto, T. Hashizume, H. W. Pickering, and T. Sakurai, "Adsorption and film growth of BTA on clean and oxygen adsorbed Cu(110) surfaces," *Applied Surface Science*, 1995.
- [116] K. Cho, J. Kishimoto, T. Hashizume, and T. Sakurai, "An Observation of Benzotriazole (BTA) Adsorption on Cu(110) by the Ultra High Vacuum (UHV)-Scanning Tunneling Microscope (STM) and Low Energy Electron Diffraction (LEED)," *Japanese Journal of Applied Physics*, vol. 33, pp. L125–L128, jan 1994.
- [117] B. S. Fang, C. G. Olson, and D. W. Lynch, "A photoemission study of benzotriazole on clean copper and cuprous oxide," *Surface Science*, vol. 176, no. 3, pp. 476–490, 1986.
- [118] G. W. Poling, "Reflection infra-red studies of films formed by benzotriazole on Cu," *Corrosion Science*, vol. 10, pp. 359–370, 1970.
- [119] Y.-H. Luo, B.-Y. Zhong, and J.-C. Zhang, "The Mechanism of Copper-Corrosion inhibition by Thiadiazole Derivatives," *Lubrication Engineering*, vol. 51, no. 4, pp. 293–296, 1994.
- [120] E.-S. M. Sherif, A. M. El Shamy, M. M. Ramla, and A. O. H. El Nazhawy, "5-(Phenyl)-4H-1,2,4-triazole-3-thiol as a corrosion inhibitor for Cu in 3.5% NaCl solution," *Materials Chemistry and Physics*, no. 102, pp. 231–239, 2007.
- [121] S. Xiong, J. Sun, X. Yan, and Y. Xu, "Inhibition effect of azole derivate on corrosion activity of copper in rolling oil," *Surface and Interface Analysis*, vol. 48, no. 2, pp. 88–98, 2016.
- [122] M. P. Gahagan and G. J. Hunt, "New Insights on the Impact of Automatic Transmission Fluid (ATF) Additives on Corrosion of Copper – The Application of a Wire Electrical Resistance Method," *International Journal of Automotive Engineering*, vol. 7, pp. 115–120, 2016.
- [123] K. Chiang and T. Mintz, "Gravimetric techniques," in *Techniques for corrosion monitoring* (L. Yang, ed.), ch. 9, pp. 247–264, Woodhead Publishing, 2008.
- [124] R. H. Hausler, "Corrosion Inhibitors," in *Corrosion tests and standards* (R. Baboian, ed.), ch. 41, pp. 480–499, ASTM International, 2 ed., 2005.
- [125] P. C. Hamblin, U. Kristen, and D. Chasan, "Ashless antioxidants, copper deactivators and corrosion inhibitors: Their use in lubricating oils," *Lubrication Science*, vol. 2, pp. 287–318, jul 1990.
- [126] J. A. Waynick, "The Development and Use of Metal Deactivators in the Petroleum Industry: A Review," *Energy & Fuels*, vol. 15, pp. 1325–1340, nov 2001.
- [127] C. Brossia, "Electrical resistance techniques," in *Techniques for corrosion monitoring* (L. Yang, ed.), pp. 277–292, Woodhead Publishing, 2008.
- [128] G. J. Hunt, M. P. Gahagan, and M. A. Peplow, "Wire resistance method for measuring the corrosion of copper by lubricating fluids," *Lubrication Science*, vol. 29, no. 4, pp. 279–290, 2017.
- [129] G. J. Hunt, "New perspectives on the temperature dependence of lubricant additives on copper corrosion," *SAE International Journal of Fuels and Lubricants*, vol. 10, no. 2, 2017.

- [130] ASTM International, "ASTM D89:1921 Copper Corrosion by Petroleum Products."
- [131] K. Asami and K. Hashimoto, "X-ray Photoelectron Spectroscopy for Corrosion Studies," *Langmuir*, vol. 3, no. 6, pp. 897–904, 1987.
- [132] C. R. Brundle, C. A. J. Evans, and S. Wilson, "Imaging Techniques (Microscopy)," in *Encyclopedia of Materials Characterization* (L. E. Fitzpatrick, ed.), ch. 2, pp. 57–84, Elsevier, 1992.
- [133] A. M. Beccaria, Y. Z. Wang, and G. Poggi, "Study of Passive Film Formation on Cu-Ni 70/30 Alloy in Seawater at High Temperature," *SURFACE AND INTERFACE ANALYSIS*, vol. 21, pp. 442–446, 1994.
- [134] N. Huynh, S. E. Bottle, T. Notoya, and D. P. Schweinsberg, "Inhibition of copper corrosion by coatings of alkyl esters of carboxybenzotriazole," *Corrosion Science*, no. 44, pp. 2583–2596, 2002.
- [135] B. H. Loo, A. Ibrahim, and M. T. Emerson, "Analysis of surface coverage of benzotriazole and 6-tolyltriazole mixtures on copper electrodes from surface-enhanced Raman spectra," *Chemical Physics Letters*, vol. 287, pp. 449–454, 1998.
- [136] J. Oelichmann, "Surface and depth-profile analysis using FTIR spectroscopy," *Fresenius Z Anal Chem*, vol. 333, pp. 353–359, 1989.
- [137] A. Bonyar, T. Hurtony, and S. David, "Investigation of the oxidation process at the copper-solder interface with atomic force microscopy," in *2012 IEEE 18th International Symposium for Design and Technology in Electronic Packaging (SIITME)*, pp. 317–320, IEEE, oct 2012.
- [138] D. E. Newbury, "Mistakes encountered during automatic peak identification of minor and trace constituents in electron-excited energy dispersive X-ray microanalysis," *Scanning*, vol. 31, no. 3, pp. 91–101, 2009.
- [139] C. R. Brundle, C. A. J. Evans, and S. Wilson, "Vibrational Spectroscopies and NMR," in *Encyclopedia of Materials Characterization* (L. E. Fitzpatrick, ed.), pp. 413–441, Elsevier, 1992.
- [140] M. A. Hegazy, A. A. Nazeer, and K. Shalabi, "Electrochemical studies on the inhibition behavior of copper corrosion in pickling acid using quaternary ammonium salts," *Journal of Molecular Liquids*, vol. 209, pp. 419–427, 2015.
- [141] M. Fonsati, F. Zucchi, and G. Trabaneli, "Study of corrosion inhibition of copper in 0.1 M NaCl using the EQCM technique," *Electrochimica Acta*, vol. 44, pp. 311–322, sep 1998.
- [142] R. C. Rabelo Neto, D. O. Lima, T. D. S. Pinheiro, R. F. Almeida, T. N. Castro Dantas, M. S. G. Dantas, M. A. S. Araújo, C. L. Cavalcante, and D. C. S. Azevedo, "Thermo-Oxidative Stability of Mineral Naphthenic Insulating Oils: Combined Effect of Antioxidants and Metal Passivator," *Industrial & Engineering Chemistry Research*, vol. 43, pp. 7428–7434, nov 2004.
- [143] J. Rubim, I. G. R. Gutz, and W. J. Orville-thomas, "Surface enhanced Raman spectra of benzotriazole adsorbed on a copper electrode," *Journal of Molecular Structure*, vol. 100, pp. 571–583, 1983.

- [144] J. Fraden, *Handbook of Modern Sensors*. New York, NY: Springer New York, fourth ed., 2010.
- [145] F. T. Barcroft, "A technique for investigating reactions between E.P. additives and metal surfaces at high temperatures," *Wear*, vol. 3, no. 6, pp. 440–453, 1960.
- [146] P. Cool and M. Ockendon, "Repeatability and Reproducibility."
- [147] M. C. Biesinger, L. W. M. Lau, A. R. Gerson, and R. S. C. Smart, "Resolving surface chemical states in XPS analysis of first row transition metals, oxides and hydroxides : Sc, Ti, V, Cu and Zn," *Applied Surface Science*, vol. 257, no. 3, pp. 887–898, 2010.
- [148] N. S. Ahmed, A. M. Nassar, and A.-A. A. Abdel-Azim, "Synthesis and evaluation of some detergent/dispersant additives for lube oil," *International Journal of Polymeric Materials and Polymeric Biomaterials*, no. 57, pp. 114–124, 2008.
- [149] I. Grozdanov and M. Najdoski, "Optical and electrical properties of copper sulfide films of variable composition," 1995.
- [150] S. K. Fasogbon and O. R. Olagoke, "Influence of Temperature on Corrosion Characteristics of Metals in Used Cooking Oil Methyl Ester," *The International Journal Of Engineering And Science*, vol. 5, no. 4, pp. 71–75, 2016.
- [151] R. D. Armstrong and C. A. Hall, "The corrosion of metals in contact with ester oils at temperatures up to 200C," *Corrosion Science*, vol. 36, no. 3, pp. 463–477, 1994.
- [152] A. V. Naumkin, A. Kraut-Vass, S. W. Gaarenstroom, and C. J. Powell, "NIST X-ray Photoelectron Spectroscopy Database."
- [153] S. Pizzini, K. J. Roberts, I. S. Dring, R. J. Oldman, and D. C. Cupertino, "Application of X-ray absorption spectroscopy to the structural characterisation of monodispersed benzotriazole coatings on partly oxidised copper thin films," *Journal of Materials Chemistry*, vol. 3, no. 8, pp. 811–819, 1993.
- [154] A. Miller, "The chemistry of lubricating oil additives," *Journal of Chemical Education*, vol. 33, pp. 308–312, jul 1956.
- [155] L. Rudnick, "Lubricant Additives," *Lubricant Additives*, vol. 20093578, pp. 251–279, 2009.